

**Investigation of Resolvin E1 as a metabolite of
eicosapentaenoic acid with anti-colorectal cancer activity**

John Michael Hutchinson

Submitted in accordance with the requirements for the
degree of Doctor of Philosophy

The University of Leeds
School of Medicine

Submitted June 2016

The candidate confirms that the work submitted is his own and that appropriate credit has been given where reference has been made to the work of others.

This copy has been supplied on the understanding that it is copyright material and that no quotation from the thesis may be published without proper acknowledgment.

©2016 The University of Leeds, John Michael Hutchinson

Acknowledgments

The author would like to thank the following people:

Supervisors: Professor Mark A Hull, Professor Anna Nicolaou, Dr. Milène Volpato and Dr. Paul Loadman for their scientific guidance over the course of this PhD degree.

Dr. Louise Coletta, whose weekly feedback on my studies was supportive, valuable and educational.

Dr. Nick West whose assistance with the immunohistochemistry scoring was greatly appreciated.

Laboratory colleagues: Ms. Sarah Perry, Dr. Gemma Marston and Dr. James L Thorne.

The team at the University of Bradford where the mass spectrometry studies were performed: Dr. Karen Massey and Dr. Paula Urquhart.

Cancer Research UK for funding the clinical research fellowship.

Finally, last but not the least, my wife Danielle whose support and encouragement whilst looking after our children Phoebe, Martha and Alex has been the keystone in allowing me to complete this thesis.

Experimental Acknowledgments

All experiments detailed in this thesis were carried out by the candidate apart from:

Sample injection and programming of the LC/ESI-MS/MS, performed either by Dr. Karen Massey or Dr. Paula Urquhart for results sections 4.5.1; 4.5.3; 4.5.5; 4.5.6; 4.5.7; 4.5.8; 5.5.1; 5.5.2 & 5.5.3. Chromatographs were provided directly to the candidate by Dr. Karen Massey for results sections 4.5.3 & 4.5.5.

The RAW264.7 PGE₂ time course experiment; Dr. Paul Loadman analysed the samples by mass spectrometry and provided the raw data to the candidate for analysis.

Professor Beech for allowing the candidate to use his laboratory facilities at the University of Leeds, for the calcium influx assays detailed in section 5.5.8.

Abstract

Eicosapentaenoic acid (EPA) is an omega (ω)-3 polyunsaturated fatty acid (PUFA) found at high levels in oily fish such as salmon and mackerel. EPA has been shown to have anti-colorectal cancer (CRC) effects in two clinical studies where it was shown to reduce polyp burden in familial adenomatous polyposis (FAP) patients, and possibly improve overall survival in patients following liver resection for CRC liver metastases. At present, it is unknown how EPA exerts its anti-CRC effects.

Resolvin E1 (RvE1) is a lipid with anti-inflammatory and pro-resolving activities derived from EPA. RvE1 biosynthesis requires three enzymes; aspirin acetylated cyclooxygenase-2 (COX-2), 5-lipoxygenase (5-LOX) and leukotriene A₄ hydrolase (LTA₄H). RvE1 has been shown to mediate its anti-inflammatory effects through two different G-protein coupled receptors, ChemR23 and BLT1. The hypothesis was that RvE1 synthesised within CRC could induce CRC cell apoptosis through either or both ChemR23 and BLT1 receptor signaling.

ChemR23 and BLT1 protein were found to be expressed by human CRC clinical samples. ChemR23 and BLT1 were expressed at lower levels in histologically normal colorectal epithelium when compared to CRC, a relationship also seen with the associated stroma. No RvE1 mediated effect on CRC survival or apoptosis was identified on ChemR23 expressing human CRC cell lines *in vitro*. There was no BLT1 expression by human CRC cells *in vitro*.

Human polymorphonuclear leukocytes (PMNs) treated directly with 18-hydroxyeicosapentaenoic acid (18-HEPE) generated RvE1. *In vitro* CRC cells and macrophages alone and in a transcellular synthesis model failed to produce RvE1.

In conclusion, ChemR23 and BLT1 receptors were found to be expressed by human CRC clinical samples. RvE1 was not synthesised by a CRC model *in vitro*. The candidate identified no *in vitro* RvE1 biological activity. Further research could look to establish whether RvE1 can be detected in human CRC samples.

Contents Page

1	Introduction.....	1
1.1	The clinical problem.....	1
1.2	Epidemiology of colorectal cancer	1
1.3	Colorectal cancer staging	1
1.4	Aetiology of colorectal cancer	2
1.5	Molecular pathogenesis of colorectal cancer	3
1.5.1	Colorectal anatomy and histology.....	3
1.5.2	The adenoma-carcinoma sequence.....	4
1.5.3	Epithelial-mesenchymal transition	4
1.5.4	Inflammation and colorectal cancer	7
1.6	Eicosanoids and colorectal carcinogenesis.....	8
1.6.1	Eicosanoid biosynthesis	8
1.6.2	Lipidomic analysis of eicosanoids.....	15
1.6.3	Eicosanoids metabolism and colorectal cancer.....	15
1.7	Aspirin and colorectal cancer.....	17
1.8	Eicosapentaenoic acid and colorectal cancer	19
1.9	Resolvin E1	20
1.9.1	Resolvin E1 biosynthesis.....	20
1.9.2	Biological effects of Resolvin E1	23
1.9.3	The receptors for Resolvin E1	24
2	Aims and Hypotheses to be tested	28
2.1	A potential role for Resolvin E1 in colorectal cancer treatment	28
2.2	Hypothesis.....	29
2.3	Aims	29
3	Characterisation of BLT1 and ChemR23 expression in human colorectal cancer samples and <i>in vitro</i> models	30
3.1	Introduction.....	30

3.1.1	Aims	31
3.2	Materials and Methods	31
3.2.1	Cell culture	31
3.2.2	Gene expression analysis.....	32
3.2.3	Western blotting.....	36
3.2.4	Immunofluorescence	39
3.2.5	Immunohistochemistry.....	41
3.3	Results (BLT1).....	44
3.3.1	BLT1 expression by human colorectal cancer epithelial cell lines	44
3.3.2	BLT1 expression by human colorectal cancer tissue	48
3.4	Results (ChemR23)	59
3.4.2	ChemR23 expression by human colorectal cancer tissue.....	70
3.5	Discussion	79
3.5.1	The <i>in vitro</i> expression of BLT1 and ChemR23 by human colorectal cancer cells.....	79
3.5.2	Expression of BLT1 and ChemR23 by human clinical colorectal cancer tissue.....	83
3.6	Summary	85
4	Development of an <i>in vitro</i> model for investigation of Resolvin E1 synthesis by colorectal cancer cells	87
4.1	Introduction.....	87
4.2	Hypothesis.....	87
4.3	Aims	88
4.4	Materials and Methods	88
4.4.1	Experimental solutions.....	88
4.4.2	Cell culture	90
4.4.3	Western blotting.....	90
4.4.4	High performance liquid chromatography electrospray ionisation tandem mass spectrometry analysis of lipid mediators	91

4.4.5	Cell viability assay	98
4.4.6	Human polymorphonuclear leukocyte isolation from whole blood samples and treatment with 18-HEPE for Resolvin E1 synthesis.....	99
4.5	Results	100
4.5.1	Resolvin E1 synthesis by human polymorphonuclear leukocytes	100
4.5.2	COX-2 protein expression in human colorectal cancer cell lines.....	101
4.5.3	COX derived lipid mediators synthesis by human colorectal cancer cell lines.....	101
4.5.4	Western blot analysis of 5-LOX protein expression in a panel of seven human colorectal cancer cell lines	106
4.5.5	Lipidomic analysis for 5-LOX derived 5-HETE synthesis in a panel of seven different human colorectal cancer cell lines	106
4.5.6	Synthesis of the acetylated COX-2 derived lipid mediator 15R-HETE in aspirin treated HCA7 human colorectal cancer cells.....	110
4.5.7	Lipidomic analysis for RvE1 and 18-HEPE synthesis by HCA7 human colorectal cancer cells	114
4.5.8	Lipidomic analysis for 18-HEPE and Resolvin E1 synthesis by MC38 mouse colorectal cancer cells and RAW264.7 mouse macrophage cells.	123
4.6	Discussion	146
4.6.1	Resolvin E1 synthesis by human polymorphonuclear leukocytes	146
4.6.2	Human HCA7 colorectal cancer cell lipidomic experiments	147
4.6.3	Murine transcellular metabolism experiments	149
4.7	Summary	152
5	Effect of Resolvin E1 on human colorectal cancer cell viability and apoptosis	153
5.1	Introduction.....	153
5.2	Hypothesis.....	153
5.3	Aims	153
5.4	Materials and Methods	154
5.4.1	Experimental solutions.....	154

5.4.2	Western blotting.....	154
5.4.3	Cytotoxicity assay.....	154
5.4.4	Apoptosis assay	155
5.4.5	Gene expression analysis.....	157
5.4.6	Intracellular calcium influx assay	158
5.4.7	High performance liquid chromatography electrospray ionisation tandem mass spectrometry analysis of Resolvin E1 standard	160
5.5	Results	162
5.5.1	Mass spectrometry analysis of the Resolvin E1 Cayman Chemical standard and stability at 37°C.....	162
5.5.2	Does the Cayman Chemical Resolvin E1 product contain chemically recognisable Resolvin E1?	162
5.5.3	Does synthetic Resolvin E1 remain stable in aqueous solution?.....	162
5.5.4	Effect of Resolvin E1 on human colorectal cancer apoptosis.....	165
	167
5.5.5	Effect of Resolvin E1 on human colorectal cancer cell viability	180
5.5.6	Measurement of intestinal alkaline phosphatase expression in Resolvin E1 treated human colorectal cancer cells.....	182
5.5.7	Measurement of CD55 (decay accelerating factor) expression in Resolvin E1 treated human colorectal cancer cells.....	185
5.5.8	Investigation of Resolvin E1 mediated induction of intracellular calcium in human peripheral blood monocytes and the THP-1 human acute monocytic leukaemia cells.....	193
5.6	Discussion	196
5.7	Summary	199
6	Final discussion and future work.....	200
7	References	205
8	Appendices.....	235

List of Figures

Figure 1. Diagram showing the proposed pathways for CRC development from normal colorectal epithelium.	6
Figure 2. The chemical structures of AA and EPA.	9
Figure 3. Schematic overview of AA metabolism.	13
Figure 4. Schematic overview of EPA metabolism.	14
Figure 5. The chemical structure of RvE1.	21
Figure 6. Proposed biosynthesis for pathway for EPA derived RvE1.	22
Figure 7. The biological effects of RvE1.	27
Figure 8. Immunostaining scoring system for BLT1 and ChemR23 protein expression in human CRC epithelium.	43
Figure 9. BLT1 mRNA expression in a panel of human CRC cell lines.	45
Figure 10. BLT1 protein expression as measured by western blot in a panel of human CRC cell lines.	47
Figure 11. Inter-observer agreement for BLT1 expression in human CRC tissue.	51
Figure 12. Cytoplasmic BLT expression in human CRC epithelium	52
Figure 13. BLT expression in human CRC epithelium.	53
Figure 14. BLT1 expression between matched histologically normal CR epithelium and CRC epithelium.	54
Figure 15 BLT1 expression in human CRC epithelium associated stroma	56
Figure 16. BLT1 expression between matched histologically normal CR epithelium associated stroma and CRC epithelium associated stroma	57
Figure 17. BLT1 expression in CRC epithelium associated stroma and cancer location in relation to splenic flexure	58
Figure 18. ChemR23 mRNA expression in a panel of human CRC cell lines.	61
Figure 19. ChemR23 protein expression in a panel of human CRC cell lines.	63
Figure 20. Semi-quantitative analysis of ChemR23 expression in a panel of human CRC cell lines.	64
Figure 21. ChemR23 protein expression in the membrane protein fraction of Caco2 human CRC cells.	65

Figure 22. ChemR23 protein expression by Caco2 human CRC cells at increasing cell confluency.	66
Figure 23. Immunofluorescence detection of ChemR23 by Caco2 human CRC cells at differing cell confluencies.	67
Figure 24. Western blot detection of ChemR23 by human CRC cell lines at differing cell confluencies.	68
Figure 25. BLT1 protein expression by human CRC cell lines at differing cell confluencies.	69
Figure 26. Cytoplasmic ChemR23 expression in human CRC epithelium	72
Figure 27. ChemR23 expression in human CRC cancer epithelium.	74
Figure 28. ChemR23 expression between matched histologically normal CR epithelium and CRC epithelium.	75
Figure 29. ChemR23 protein expression by histologically normal CR epithelium	76
Figure 30 ChemR23 expression in human CRC epithelium associated stroma.	77
Figure 31. ChemR23 expression between matched histologically normal human CR epithelium associated stroma and CRC epithelium associated stroma.	78
Figure 32. Experimental design for CRC and macrophages RvE1 biosynthesis experimentation.	94
Figure 33. LC/ESI-MS/MS data analysis example.	97
Figure 34. RvE1 biosynthesis by human polymorphonuclear leukocytes.	100
Figure 35. COX-2 protein expression by human CRC cell lines.	102
Figure 36. COX derived lipid mediator synthesis by human CRC cell lines.	103
Figure 37. COX derived lipid mediator synthesis by AA treated human CRC cells lines.	104
Figure 38. COX derived AA lipid mediators from the HCA7 human CRC cell line.	105
Figure 39. 5-lipoxygenase protein expression in human cell lines.	107
Figure 40. LC/ESI-MS/MS analysis for 5-HETE in the cell conditioned medium from LoVo human CRC cells.	108
Figure 41. 5-lipoxygenase activating protein expression in human CRC cell lines.	109
Figure 42. Determination of the aspirin cytotoxicity in the HCA7 human CRC cancer cell line.	111

Figure 43. 15R/S-HETE, and PGE ₂ synthesis by HCA7 human CRC cells.	112
Figure 44. 15R and 15S-HETE chromatograms.....	113
Figure 45. Determination of the cytotoxicity of EPA on HCA7 human CRC cell lines.	114
Figure 46. RvE1 chromatograms (HCA7 cells).	115
Figure 47. Analysis of HCA7 cell conditioned medium for 18-HEPE, PGE ₂ , PGE ₃ and 15-HETE.....	117
Figure 48. 18-HEPE chromatograms (HCA7 cells).	118
Figure 49. 15-HETE chromatograms (HCA7 cells).....	119
Figure 50. 5-HETE chromatograms (HCA7 cells).....	120
Figure 51. Leukotriene B ₄ chromatograms (HCA7 cells).	121
Figure 52. Aspirin triggered-LXA ₄ chromatograms (HCA7 cells).	122
Figure 53. Analysis of LPS stimulated RAW264.7 cell conditioned medium for PGE ₂ over 24 hours.	123
Figure 54. Assessment of MC38 and RAW264.7 cell viability over a range of aspirin dosages.	124
Figure 55. Assessment of MC38 and RAW264.7 cell viability over a range of EPA doses.	125
Figure 56. Analysis of MC38 cell conditioned medium for RvE1.	126
Figure 57. Analysis of LPS stimulated RAW264.7 cell conditioned medium for RvE1.	127
Figure 58. Analysis of MC38 cell conditioned medium for 18-HEPE.	129
Figure 59. Analysis of LPS stimulated RAW264.7 cell conditioned medium for 18-HEPE.	130
Figure 60. Analysis of MC38 cell conditioned medium for 18-HEPE, PGE ₂ , PGE ₃ and 15-HETE.....	131
Figure 61. Analysis of LPS stimulated RAW26.7 cell conditioned medium for 18-HEPE, PGE ₂ , PGE ₃ and 15-HETE.	132
Figure 62. Analysis of MC38 cell conditioned medium for 15-HETE.....	134
Figure 63. Analysis of LPS stimulated RAW264.7 cell conditioned medium for 15-HETE.	135
Figure 64. Analysis of MC38 cell conditioned medium for LTB ₄	136

Figure 65. Analysis of LPS stimulated RAW264.7 cell conditioned medium for LTB ₄	137
Figure 66. Analysis of LPS stimulated RAW264.7 cell conditioned medium for LTB ₅	138
Figure 67. Analysis of MC38 cell conditioned medium for aspirin triggered-LXA ₄	139
Figure 68. Aspirin triggered-LXA ₄ biosynthesis by mouse macrophage RAW264.7 cells.	140
Figure 69. Analysis of the transcellular model (MC38/ RAW264.7) cell conditioned medium for RvE1.	141
Figure 70. Analysis of the transcellular model (MC38/ RAW264.7) cell conditioned medium for 18-HEPE.	142
Figure 71. Analysis of the cell cultured medium from the transcellular synthesis model for 18-HEPE, and 15-HETE.	143
Figure 72. Analysis of the cell cultured medium from the transcellular synthesis model for PGE ₂ and PGE ₃	144
Figure 73. Analysis of the cell conditioned medium from the transcellular synthesis model for aspirin triggered-LXA ₄	145
Figure 74. Electrospray ionization product ion spectrum for RvE1.	163
Figure 75. RvE1 identification and stability when incubated at 37°C for 24 hours.	164
Figure 76. Flow cytometry forward and side scatter dot plot for the analysis of the Caco2 human CRC cell line.	167
Figure 77. Flow cytometry forward and side scatter dot plot for the analysis of the HCA7 human CRC cell line.	168
Figure 78. Apoptosis in etoposide treated Caco2 human CRC cells (flow cytometry scatter plots).....	170
Figure 79. Apoptosis in etoposide treated HCA7 human CRC cells (flow cytometry scatter plots).....	172
Figure 80. Apoptosis in RvE1 treated Caco2 human CRC cells.	174
Figure 81. Apoptosis in RvE1 treated Caco2 human CRC (flow cytometry scatter plots).	175
Figure 82. Apoptosis in RvE1 treated HCA7 human CRC cells.	176
Figure 83. Apoptosis in RvE1 treated HCA7 human CRC cells (flow cytometry scatter plots).....	177

Figure 84. Apoptosis in etoposide treated Caco2 human CRC cells.	178
Figure 85. Apoptosis in etoposide treated HCA7 human CRC cells.	179
Figure 86. Determination of the cytotoxicity of RvE1 by MTT assay in the human CRC cell lines Caco2 and HCA7.	181
Figure 87. Time dependent expression of ALPI mRNA expression in RvE1 treated Caco2 human CRC cells.	182
Figure 88. Dose dependent expression of ALPI mRNA in RvE1 treated Caco2 human CRC cells.	183
Figure 89. CD55 mRNA expression in RvE1 treated Caco2 human CRC cells.	185
Figure 90. CD55 mRNA expression in RvE1 treated Caco2 human CRC cells.	186
Figure 91. CD55 mRNA expression in RvE1 treated T84 human CRC cells (100nM, 24 hours).	189
Figure 92. CD55 mRNA expression in RvE1 treated T84 human CRC cells (0-500 nM, 6 hours).	191
Figure 93. Measurement of intracellular calcium levels in RvE1 treated human PBMCs.	194
Figure 94. Measurement of intracellular calcium levels in RvE1 treated human THP-1 acute monocytic leukaemia cells.	195

List of Tables

Table 1. TaqMan gene expression assay details	35
Table 2. TaqMan gene expression assay reaction contents.....	36
Table 3. Antibody details for western blotting and immunohistochemistry studies.....	40
Table 4. Mean cycle threshold (Ct) values for BLT1 and β -actin in the screened panel of human cell lines.....	46
Table 5. Clinical characteristics of the BLT1 study population.....	48
Table 6. Mean cycle threshold values (Ct) for ChemR23 and β -actin in a panel of human cell lines.....	62
Table 7. Clinical characteristics of the ChemR23 study population	70
Table 8. Summary of both the expression and functional status of COX (-2) and 5-LOX in a panel of seven human CRC cell lines.	110
Table 9. TaqMan gene expression assay reaction contents for the ALPI and CD55 studies	158
Table 10. Caco2 human CRC cell viability in gated cell population 1 on flow cytometry.	165
Table 11. HCA7 human CRC cell viability in gated cell population 1 on flow cytometry..	165
Table 12. Caco2 human CRC cell viability in gated cell population 2 on flow cytometry.	166
Table 13. HCA7 human CRC cell viability in gated cell population 2 on flow cytometry..	166
Table 14. Caco2 human CRC cell apoptosis secondary to etoposide.	169
Table 15. HCA7 human CRC cell apoptosis secondary to etoposide.....	171
Table 16. Cycle threshold (Ct) values for β -actin and ALPI for the RvE1 treated Caco2 time course experiment.....	184
Table 17. Cycle threshold (Ct) values for β -actin and ALPI for the RvE1 treated Caco2 dose response experiment.....	184
Table 18. Cycle threshold (Ct) values for the time course CD55 RvE1 treated Caco2 cells experiments.....	187
Table 19. Cycle threshold (Ct) values for CD55 in RvE1 treated Caco2 dose response experiments.....	187
Table 20. Cycle threshold (Ct) values for β -actin and CD55 for RvE1 treated T84 cells over 24 hours.....	190

Table 21. Cycle threshold (Ct) values for β -actin and CD55 for the RvE1 treated T84 dose response experiment. 192

List of Appendices

Appendix 1. Research ethics committee approval letter.....	236
Appendix 2. BLT antibody optimisation for immunohistochemistry.....	239
Appendix 3. Membranous BLT1 protein expression by human immune type cell.....	240
Appendix 4. No primary control images between different BLT1 immunohistochemistry runs.....	241
Appendix 5. BLT1 immunohistochemistry inter-run variability in a human CRC tissue sample.....	242
Appendix 6. BLT1 human CR epithelial and associated stromal expression by immunohistochemistry in two different human CRC tissue samples.....	243
Appendix 7. Correlation of BLT1 expression in human CRC epithelium with age, cancer location, cancer size, cancer cell differentiation, pT, pN stage and vascular invasion status.....	244
Appendix 8. Correlation of BLT1 expression in human histologically normal colorectal epithelium with age, cancer location, cancer size, cancer cell differentiation, pT, pN stage and vascular invasion status.....	245
Appendix 9. Correlation of BLT1 expression in human CRC associated stroma with age, cancer size, cancer cell differentiation, pT, pN stages and vascular invasion status.....	246
Appendix 10. Correlation of BLT1 expression in human histologically normal CR epithelium associated stroma with age, cancer location, cancer size, cancer cell differentiation, pT, pN stages and vascular invasion status.....	247
Appendix 11. Correlation of BLT1 expression between human CRC associated stroma and CRC epithelium.....	248
Appendix 12. Correlation of BLT1 expression between histologically normal human CR epithelium associated stroma and CR epithelium.....	249
Appendix 13. Western blot analysis of ChemR23 receptor protein expression by three different commercially available anti-ChemR23 antibodies in a panel of seven different human CRC cell lines.....	250
Appendix 14. ChemR23 antibody optimisation for immunohistochemistry.....	251
Appendix 15. No primary control images between different ChemR23 immunohistochemistry runs.....	252
Appendix 16. ChemR23 immunohistochemistry inter-run variability in a human CRC tissue sample.....	253

Appendix 17. Bioss anti-ChemR23 antibody sensitivity and specificity consistency between four different vials of antibody (bs-2530R.LOT 130320).....	254
Appendix 18. Bioss anti-ChemR23 antibody sensitivity and specificity inconsistency between different LOTS (example shown BS2530R. lot YE1027W).....	255
Appendix 19. ChemR23 expression in human CRC between two different batches of the same Bioss anti-ChemR23 antibody.	256
Appendix 20. Correlation of ChemR23 expression in human CRC epithelium with age, cancer location, cancer size, cancer cell differentiation, pT, pN stage and vascular invasion status.....	257
Appendix 21. Correlation of ChemR23 expression in histologically normal human CRC epithelium with age, cancer location, cancer size, cancer cell differentiation, pT, pN stage and vascular invasion status.	258
Appendix 22. Correlation of ChemR23 expression in human CRC epithelium associated stroma with age, cancer location, cancer size, cancer cell differentiation, pT, pN stage and vascular invasion status.....	259
Appendix 23. Correlation of ChemR23 expression in histologically normal human CR epithelium associated stroma with age, cancer location, cancer size, cancer cell differentiation, pT, pN stage and vascular invasion status.....	260
Appendix 24. Correlation of ChemR23 expression in human CRC associated stroma with matched CRC epithelium.	261
Appendix 25. Correlation of ChemR23 expression between matched histologically normal human CR epithelium associated stroma and CR epithelium.....	262
Appendix 26. Correlation of BLT1 and ChemR23 expression in matched human CRC epithelial samples.	263
Appendix 27. Correlation of BLT1 and ChemR23 expression in matched histologically normal human CR epithelium samples.	264
Appendix 28. Correlation of BLT1 and ChemR23 expression in matched human CRC epithelium associated stromal samples.....	265
Appendix 29. Correlation of BLT1 and ChemR23 expression in matched histologically normal human CR epithelium associated stromal samples.	266
Appendix 30. Nucleotide sequence for BLT1 with TaqMan assay target.....	267
Appendix 31. Nucleotide sequence for ChemR23 with TaqMan assay target.	268
Appendix 32. ChemR23 mRNA expression in Caco2 human CRC cells at increasing cell confluency.	269

Appendix 33. The migration of two commercially available protein standards through a 12% SDS-PAGE gel.	270
Appendix 34. Detailed experimental schematic for the CRC and macrophage RvE1 biosynthesis experiment.	271
Appendix 35. COX derived DGLA and EPA lipid mediators from the HCA7 human CRC cell line.	272
Appendix 36. COX derived AA/ DGLA and EPA lipid mediator synthesis by HCA7 human CRC cells.....	273
Appendix 37. COX derived AA/ DGLA and EPA lipid mediator synthesis by LoVo human CRC cells.....	274
Appendix 38. COX derived AA/ DGLA and EPA lipid mediator synthesis by T84 human CRC cells.....	275
Appendix 39. COX derived AA/ DGLA and EPA lipid mediator synthesis by HRT18 human CRC cells.....	276
Appendix 40. COX derived AA/ DGLA and EPA lipid mediator synthesis by HT29 human CRC cells.....	277
Appendix 41. COX derived AA/ DGLA and EPA lipid mediator synthesis by Caco2 human CRC cells.....	278
Appendix 42. COX derived AA/ DGLA and EPA lipid mediator synthesis by HCT116 human CRC cells.....	279
Appendix 43. Apoptosis in etoposide treated HCA7 human CRC cells.	280
Appendix 44. ALPI mRNA expression in RvE1 treated T84 human CRC cells over 24 hours.	281
Appendix 45. ALPI mRNA expression in T84 human CRC cells treated for six hours with range of RvE1 doses (0-500 nM).....	282
Appendix 46. The effect of the cytotoxicity of EPA on cells <i>in vitro</i> when made up in cell culture medium with and without 10% FBS.....	283

List of Abbreviations

AA	Arachidonic acid
AChE	Acetylcholinesterase
ADP	Adenosine diphosphate
AICR	American Institute of Cancer Research
ALA	Alpha- linolenic acid
ALPI	Intestinal alkaline phosphatase
AM	Acetoxymethyl ester
APC	Adenomatous polyposis coli
ATCC	American Type Culture Collection
ATP	Adenosine triphosphate
BSA	Bovine serum albumin
C	Carbon
CaCl₂	Calcium chloride
CAF	Carcinoma-associated fibroblast

CD	Crohn's disease
cDNA	Complementary deoxyribonucleic acid
CIMP	CpG Island Methylator Phenotype
CIP	Chromosomal instability pathway
cm	Centimeter
CMKLR	Chemokine like receptor
COX	Cyclooxygenase
CRC	Colorectal cancer
CRUK	Cancer Research UK
Ct	Cycle threshold
CYP	Cytochrome P450
d	Deuterated
Da	Dalton
DAB	Diaminobenzidine
DAPI	4,6-diamidino-2-phenylindole
DC	Dendritic cell

DEN	diethylnitrosamine
DEPC	Diethylpyrocarbonate
DGLA	Dihomo-gamma-linolenic acid
DHA	Docosahexaenoic acid
DHET	Dihydroxyeicosatetraenoic acid
DMSO	Dimethyl sulfoxide
DNA	Deoxyribonucleic acid
DPBS	Dulbecco's Phosphate Buffered Saline
DPX	Diphenylxylene
DSS	Dextran sodium sulphate
ECACC	European Collection of Cell Cultures
E.coli	Escherichia coli
EDTA	Ethylenediaminetetraacetic acid
EET	Epoxyeicosatrienoic acid
EFA	Essential fatty acid
EIA	Enzyme immunoassay

ELISA	Enzyme-linked immunosorbent assay
EMT	Epithelial mesenchymal transition
EPA	Eicosapentaenoic acid
ERK	Extracellular signal-regulated kinase
ESI	Electrospray ionisation
FA	Fatty acids
FAP	Familial adenomatous polyposis
FBS	Foetal bovine serum
FFA	Free fatty acid
FFPE	Formalin fixed, paraffin embedded
FITC	Fluorescein isothiocyanate
FLAP	5-Lipoxygenase activating protein
G	Gauge
g	Gram
g	Gravitational force
GPCR	G-protein coupled receptor

H	Hydrogen
HCl	Hydrochloric acid
HEK	Human embryonic kidney
HEPE	Hydroxyeicosapentaenoic acid
HETE	Hydroxyeicosatetraenoic acid
HNPCC	Hereditary non-polyposis colorectal cancer
HP	High performance
HRP	Horseradish peroxidase
IF	Immunofluorescence
IFN	Interferon
IHC	Immunohistochemistry
IL	Interleukin
IS	Internal standard
k	Kilo
KCl	Potassium chloride
K_m	Michaelis constant

KRAS	Kirsten rat sarcoma viral oncogene
L	Litre
LA	Linoleic acid
LC	Liquid chromatography
LDS	Lithium dodecyl sulfate
LOD	Limit of detection
LOQ	Limit of quantification
LOX	Lipoxygenase
LPS	Lipopolysaccharide
LT	Leukotriene
LTA₄H	LTA ₄ hydrolase
LX	Lipoxin
m	milli
M	Molar
MCTS	Multi-cellular tumour spheroid
MgCl₂	Magnesium chloride

MAPK	Mitogen-activated protein kinase
mm	Millimeter
MMP	Metalloproteinase
MMR	Mismatch repair
MRM	Multiple reaction monitoring
mRNA	Messenger ribonucleic acid
MS	Mass spectrum
MSC	Mesenchymal stem cells
MSI	Microsatellite instability
MTT	3-(4,5-Dimethylthiazol-2-yl)-2,5-diphenyltetrazolium bromide
MW	Molecular weight
n	Nano
NaCl	Sodium chloride
NaOH	Sodium hydroxide
NFκB	Nuclear factor kappa-light-chain-enhancer of activated B cells
nm	Nanometer

NPW	Independent histopathologist
NSAID	Non-steriodal anti-inflammatory drug
O	Oxygen
OD	Optical density
p	Pico
P	Calculated probability
PAGE	Polyacrylamide gel electrophoresis
PBMCs	Peripheral Blood Monocytes
PBS	Phosphate Buffered Saline
PCR	Polymerase chain reaction
PFA	Paraformaldehyde
PG	Prostaglandin
PGDH	Prostaglandin dehydrogenase
PGI2	Prostacyclin
PI	Propidium iodide
PMN	Polymorphonuclear leukocyte

pM	Pathological metastasis
pN	Pathological nodal
PS	Phospholipid phosphatidylserine
pT	Pathological tumour
PUFA	Polyunsaturated fatty acid
PVDF	Polyvinylidene difluoride membrane
qPCR	Quantitative polymerase chain reaction
RIPA	Radio-immunoprecipitation assay
RNA	Ribonucleic acid
RNase	Ribonuclease
RPMI	Roswell Park Memorial Institute
RT	Reverse transcriptase
RvE1	5S,12R,18R-trihydroxy-6Z,8E,10E,14Z,16E-eicosapentaenoic acid (Resolvin E1)
SBS	Standard Bath Solution
SDS	Sodium dodecyl sulfate

STR	Short tandem repeat
TAM	Tumour-associated macrophage
TBS	Tris-buffered saline
TLR	Toll-like receptor
TNF	Tumour necrosis factor
TP53	Tumour protein 53
Tw	Tween
TX	Thromboxane
UC	Ulcerative colitis
UK	United Kingdom
UNG	Uracil N-glycosylase
UTR	Untranslated region
UV	Ultraviolet
μ	Micro
v	Volume
VEGF	Vascular endothelial growth factor

w	Weight
WB	Western blotting
WCRF	World Cancer Research Fund
α	Alpha
β	Beta
δ	Delta
γ	Gamma
k	Kappa
ω	Omega

1 Introduction

1.1 The clinical problem

There has been a steady rise in human colorectal cancer (CRC) incidence globally and the increasing healthcare costs associated with CRC screening, diagnosis, treatment and surveillance, mean there is still an unmet need to identify novel, safe and well tolerated anti-CRC agents. At present there is considerable pre-clinical evidence that omega (ω)-3 polyunsaturated fatty acids (PUFAs) have anti- CRC activity. However it is unclear how ω -PUFAs exert this activity. The candidate aimed to establish whether a novel ω -3 PUFA derived lipid mediator could explain in part their anti-CRC activity.

1.2 Epidemiology of colorectal cancer

CRC is a common and significant health problem in the United Kingdom (UK), and is currently the third most common malignancy with 40,695 new cases registered in 2010 (Cancer Research UK, 2013). Across Europe, around 334,000 new cases of CRC were diagnosed in 2008 (Ferlay *et al.*, 2010a). Worldwide, CRC is the third most common cancer after lung cancer and breast cancer, with an estimated 1.24 million new cases diagnosed in 2008 (Ferlay *et al.*, 2010b). Arnold *et al* (2016) estimate that the global burden of CRC is likely to reach in excess of two million new cases by 2030. Eastern countries, such as Japan, have undergone a 'westernisation' of the diet over the last fifty years and have subsequently seen a marked increase in the number of new cases of CRC (Koyama & Kotake, 1997, Toyoda *et al.*, 2009).

Despite the increased incidence, the overall CRC mortality rate has steadily fallen over the last twenty years in the United Kingdom (UK), with earlier detection and improved treatment being the key reasons for this (Cancer Research (CR) UK., 2014; www.cancerresearchuk.org). However, the disease continues to carry a high mortality when compared to many other solid organ malignancies, and is the second most common cause of cancer-related mortality in the UK with 16,187 cancer-related deaths occurring in 2012 (CRUK., 2014).

1.3 Colorectal cancer staging

There are four stages of primary tumour determined by pathology (pT) based on the depth of invasion, with pT1 representing tumour contained within the submucosa, pT2 where tumour has invaded into the muscularis propria of the colon wall, pT3 where the tumour has grown into the subserosal fat and pT4 representing tumour that has spread

through the peritoneum or involves adjacent organs. There are also three stages of lymph node (pathological nodal; pN) spread, with pN0 showing no lymph nodes containing tumour cells, pN1 where one to three regional lymph nodes contain cancer cells, and pN2 where four or more lymph nodes contain tumour cells. Finally there are two stages of tumour metastasis spread (pathological metastasis; pM), pM0 means that the tumour has not spread to distant organs and pM1 represents a tumour that has spread to other parts of the body (Sobin & Wittekind, 1997).

1.4 Aetiology of colorectal cancer

The vast majority of CRCs (75% of cases) are believed to develop sporadically, with 20% of cases having familial aggregation with more than two-first degree relatives affected, whereas 5% of cases occur due to Mendelian inheritance in the context of a hereditary syndrome (Lynch *et al.*, 2003).

Familial adenomatous polyposis (FAP) is an autosomal dominant inherited disease caused by mutations in the adenomatous polyposis coli (*APC*) gene on chromosome 5 (Kinzler *et al.*, 1991). This results in multiple colorectal adenomas at a very early age (Grodin *et al.*, 1991). Invariably, at least one of these adenomas will develop into an invasive cancer in the second or third decade of life. Lynch syndrome, previously known as Hereditary non-polyposis colorectal cancer (HNPCC), is associated with a germline mutation in one of the deoxyribonucleic acid (DNA) mismatch repair (MMR) genes and results in early onset cancers of the large bowel and other organs (Bellizzi & Frankel, 2009). Both FAP and Lynch syndrome patients usually undergo intensive colonoscopic surveillance to detect polyps and cancers at an early stage, and may undergo prophylactic removal of the large intestine.

There are several established risk factors that contribute to CRC development. The main risk factor associated with CRC is advancing patient age with more than 90% of cases occurring in those aged 50 years or older (Surveillance, Epidemiology and end Results Program Cancer Statistic Review, 1975-2002; www.seer.cancer.gov). Obesity has been shown to increase CRC incidence in both men and woman (Renehan *et al.*, 2008), as has smoking (Botteri *et al.*, 2008). Diet may also play a role in CRC with consumption of high amounts of red and processed meat, and low consumption of fibre and fish as exposable risk factors for CRC development (Vargas *et al.*, 2012).

There have been several studies looking at the relationship between fish consumption and risk of CRC, with most reporting a reduction in CRC risk, albeit small, with higher dietary fish consumption (Geelen *et al.*, 2007, World Cancer Research Fund, 2007, Wu *et al.*, 2012, Pham *et al.*, 2013). Recently a Phase II double-blind, randomised, placebo

controlled trial showed a possible overall survival benefit post liver resection surgery (for CRC liver metastases) in those patients who took eicosapentaenoic acid (EPA) compared with placebo (Cockbain *et al.*, 2014).

Chronic inflammation is also associated with an increased risk of CRC. Idiopathic inflammatory bowel disease, of which there are two main types, ulcerative colitis (UC) and Crohn's disease (CD), both predispose the individual to CRC development which is also known as colitis-associated cancer. In UC patients who have active disease, the risk of CRC is 2% after 10 years, 8% after 20 years and 18% after 30 years (Eaden *et al.*, 2001). CD is associated with a two fold relative risk of developing CRC (Canavan *et al.*, 2006).

1.5 Molecular pathogenesis of colorectal cancer

1.5.1 Colorectal anatomy and histology

The colorectum in humans is made up of the colon and the rectum. The caecum is the proximal part of the large intestine that lies in the right iliac fossa that is joined to the ascending colon, which ascends to the right hypochondrium and then becomes the transverse colon. The transverse colon then passes horizontally to the left hypochondrium and then descends to form the descending colon. At the left iliac fossa the descending colon becomes the sigmoid colon. The sigmoid colon then becomes the rectum (Christensen, 1991).

The colorectum histologically is made up of four layers. These four layers are the mucosa, submucosa, muscularis propria and the adventitia. The mucosa is made up of epithelial cells supported by the lamina propria. The epithelium is arranged in straight tubular glands referred to as 'crypts of Lieberkühn'. These crypts pass from the central lumen of the colorectum towards the submucosa and are made up of two cell types, simple columnar epithelial cells, which have a microvillus apical border and the basally located goblet cells. Stem cells within the base of the crypts proliferate to form daughter cells, which as they ascend up the crypt mature into their differentiated phenotype, before shedding into the colorectal lumen at the apical surface of the crypt (Wong & Wright, 1999, Winton., 2001). The dysregulation of this cell proliferation and migration has long been thought to lead to CRC development (Lipkin, 1974). Supporting the epithelium of the mucosa is the lamina propria which contains immune cells such as T-cells, macrophages and myofibroblasts along with blood and lymphatic vessels within a connective tissue matrix. The muscularis mucosa separates the mucous from the submucosa, which is a denser layer of connective tissue, blood and lymphatic vessels and nerves which support the mucosa. Outwards from the colorectal

lumen the submucosa is surrounded by the muscularis propria which is made up of two layers of smooth muscle. The inner layer is circular and the outer layer is longitudinally orientated muscle. The adventitia then surrounds the muscularis propria and is made up of loose connective tissue with an epithelial squamous lining, and then the peritoneum or fascia (Christensen, 1991).

1.5.2 The adenoma-carcinoma sequence

CRC typically develops over a ten to fifteen years period (Muto *et al.*, 1975). Benign adenomatous polyps are the most common form of precursor lesion leading to CRC development (Jass., 2007). Adenomas increase in frequency with age and are thought to be present in around 30% to 40% of individuals in western populations (Midgley & Kerr., 1999). However, only a small proportion of adenomas will develop into invasive CRCs. High risk factors for malignant transformation of adenoma include size equal or greater than ten millimeters, three or more adenomas, villous architecture and adenomas with high grade dysplasia (Muto *et al.*, 1975, Winawer *et al.*, 2006).

Around 85% of CRCs are believed to develop through the classical chromosomal instability pathway (CIP), a stepwise accumulation of genetic mutations that develop as the lesion progresses from a benign adenoma through to an invasive carcinoma (Vogelstein *et al.*, 1988). *APC* gene mutations occur early in colorectal carcinogenesis being present in over 70% of colorectal adenomas (Kinzler *et al.*, 1996). Mutations that activate the kirsten rat sarcoma (*KRAS*) oncogene and mutations that inactivate tumour protein (*TP*)53 tumour suppressor gene further promotes progression to carcinoma (Lengauer *et al.*, 1997).

However CRC is a heterogeneous disease and there is no single mechanism for CRC carcinogenesis, and in addition to the CIP there are other pathways such as the CpG island methylator phenotype (CIMP) pathway (Toyota *et al.*, 1999, Samowitz *et al.*, 2005), microsatellite instability (MSI) pathway (Vilar & Gruber, 2010) and the serrated pathway (Legget & Whitehall, 2010) which have been shown to cause CRC development (Figure 1).

1.5.3 Epithelial-mesenchymal transition

The differentiation of epithelial cells to motile cells with mesenchymal characteristics is a process called epithelial mesenchymal transition (EMT). Whilst EMT is fundamental in embryological development and wound healing, it is also thought to be involved in cancer progression. EMT is typically characterised by a loss of cell-cell adhesion, loss of apical-basal cell polarity and increased motility, serving to promote migration away

from the primary tumour (Thiery, 2002). Epithelial cell-cell protein junctions serve to maintain epithelial integrity via tight junctions, adherens junctions, desmosomes and tight junctions (Huang *et al.*, 2012). As there is loss of expression of junctional proteins there is loss of cell apical-basal polarity (Huang *et al.*, 2012). During EMT initiation these junctions are degraded or repositioned and typically associated with a loss of E-cadherin expression secondary to transcriptional repressors such as SNAIL, ZEB2, and Twist. Such transcriptional repressors have been shown to be involved in cancer invasion and metastasis (Peinado *et al.*, 2007). Transforming growth factor- β is also involved in EMT through the suppression of genes such as E-cadherin (Xie *et al.*, 2004).

Interestingly the proteins that are involved in the regulation of cell polarity also play an important role in asymmetric cell division an event that plays a role in cell renewal and differentiation two vital properties of stem cells (Kong, *et al.*, 2011). Mani and colleagues have shown that EMT can form cells with stem cell like properties (Mani *et al.*, 2008). Mesenchymal stem cells (MSCs) which are thought to be non haematopoietic multipotent stem cells are thought to migrate to tumours such as CRC, integrating in the tumour architecture as carcinoma-associated fibroblasts (CAFs). CAFs have been implicated in CRC invasiveness, with CAFs being associated with increased migration and invasion of CRC epithelial cells in three-dimensional culture (Tommelein *et al.*, 2015). The interaction between the cancer epithelium and its associated stroma in the progression of cancer is a greatly complex, but rapidly developing field of scientific interest.

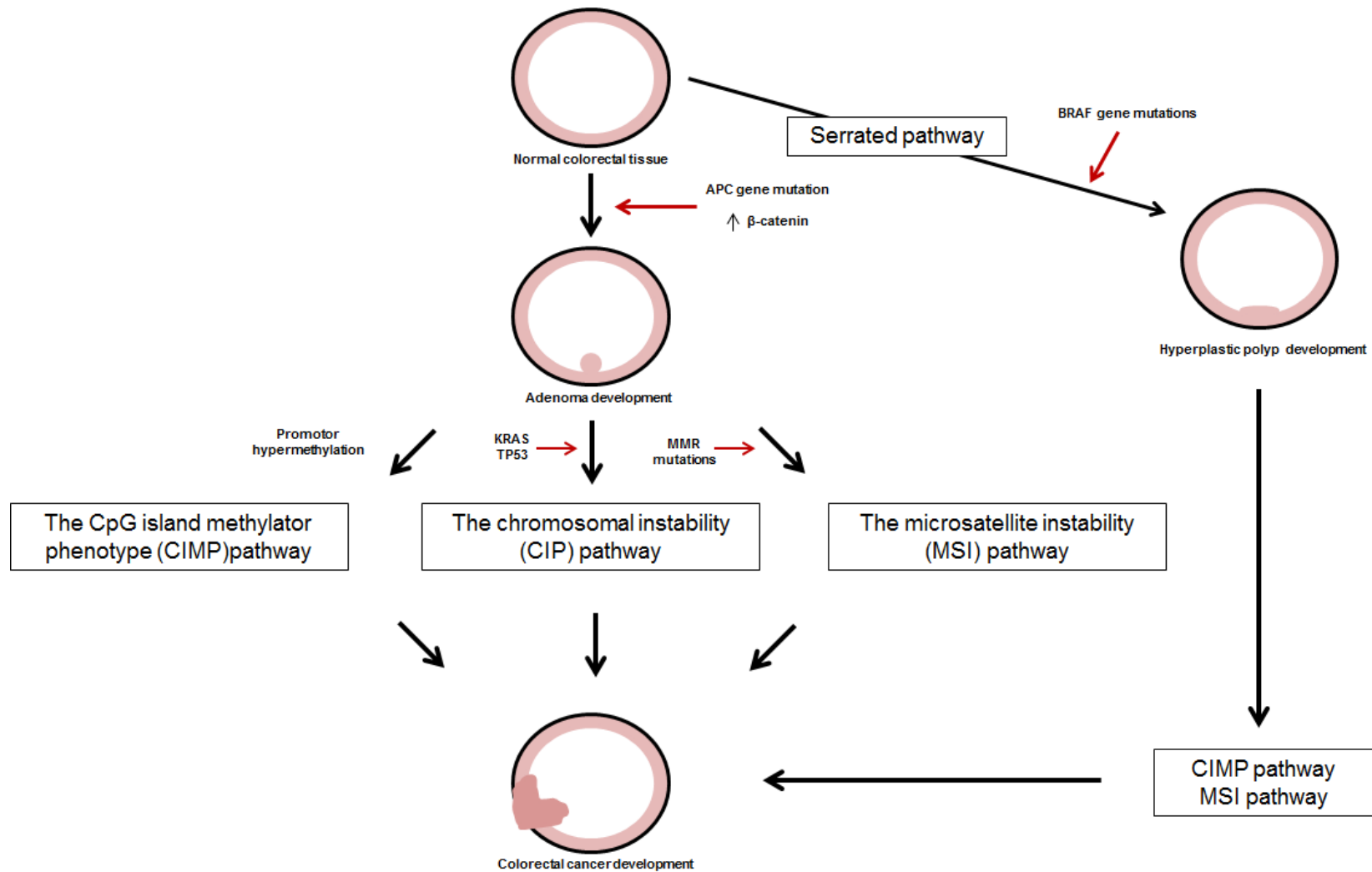


Figure 1. Diagram showing the proposed pathways for CRC development from normal colorectal epithelium.

CRC is a heterogeneous disease that is postulated currently to arise via four different molecular pathways. The CpG island methylator phenotype (CIMP) pathway, the chromosomal instability (CIP) pathway, the microsatellite instability (MSI) pathway (associated with Mismatch repair mutations-MMR) and the serrated pathway. Diagram adapted from Harrison & Benziger, 2011.

1.5.4 Inflammation and colorectal cancer

There are six fundamental hallmarks that are essential for carcinogenesis (Hanahan & Weinberg, 2000), which are:

1. Self-sufficient growth.
2. Resistance to growth inhibitory signals.
3. Evasion of programmed cell death (apoptosis).
4. Sustained angiogenesis.
5. Replicative immortality.
6. Activation of invasion and metastasis.

Advancement in the understanding of cancer over the last decade has led to the presence of two further emerging hallmarks, which includes the ability to elude immune destruction and the capability to alter cellular metabolism and thus support continued cancer cell proliferation (Hanahan & Weinberg, 2011).

There is also increasing evidence that implicates the role of inflammation in the development and progression of CRC (Terzić *et al.*, 2010). Inflammation is recognised as an emerging hallmark of cancer (Colotta *et al.*, 2009; Hanahan & Weinberg, 2011). The production of pro-inflammatory signals within tumours is thought to drive cell transformation via DNA damage and consequent tumour growth (Shacter *et al.*, 2002). Tumour cells and other cells recruited to the tumour microenvironment produce cytokines and chemokines that drive inflammation, such as tumour necrosis factor (TNF)- α , interleukin (IL)-6 and IL-1 β . TNF- α is a potent pro-inflammatory cytokine that is thought to play a role in the pathogenesis of CRC (Popivanova *et al.*, 2008). IL-6 is a multifunctional cytokine that has been shown to be increased in the plasma of CRC patients and levels have been shown to correlate with tumour stage, size, metastasis and patient survival (Knüpfer *et al.*, 2010). IL-1 β is another pro-inflammatory cytokine that is produced by activated macrophages, that has been shown to stimulate the expression of TNF- α , IL-6 and prostaglandin (PG)E₂ all of which are implicated in CRC development (Duque *et al.*, 2006).

Immune cells such as macrophages are present in tumours, located principally in the tumour stroma, which is made up of blood vessels, fibroblasts and immune cells (Mantovani *et al.*, 2002). Macrophages play a vital role in resolving acute inflammation (Serhan & Savill, 2005). Macrophages within the tumour microenvironment are known as tumour-associated macrophages (TAMs). TAMs with anti-inflammatory properties are thought to suppress tumour progression whilst those with pro-inflammatory properties promote tumour progression. This difference in TAM phenotype may explain

why some have correlated increased TAM density with improved CRC prognosis (Forsell *et al.*, 2007), and others have associated increased density with poorer prognosis (Bailey *et al.*, 2007, Kang *et al.*, 2010). Ong *et al.*, (2012) found that TAMs in their human co-culture multi-cellular tumour spheroid (MCTS) model were pro-inflammatory (increased synthesis of IL-6/8, interferon (IFN)- γ) and inhibited tumour cell proliferation (Human HT29 CRC cell line and primary human monocytes). TAMs have also been shown to increase expression tumour growth factor (TGF)- β which promote epithelial mesenchymal transition and also matrix metalloproteinases (MMP), which promotes cell invasion through E-cadherin disruption (Thuault *et al.*, 2006, Illemann *et al.*, 2006). The role of TAMs in CRC remains complex and controversial and their phenotype is likely to be influenced by cell to cell interactions within the tumour microenvironment.

NF- κ B is a transcription factor activated by certain cytokines and chemokines (Lin *et al.*, 2007). NF- κ B is involved in regulating the expression of genes involved in cell proliferation, angiogenesis and metastasis (Naugler *et al.*, 2008). Inhibition of NF- κ B activation (IKK β knockout mice) reduced the incidence of CRC (Greten *et al.*, 2004).

In addition to the cytokine and chemokine production in the tumour microenvironment there has been a growing body of published evidence examining the role of lipids in CRC pathogenesis, such as eicosanoids (discussed below in section 1.6).

COX-2 is one of three isoforms (-1 and -3), (Chandrasekharan *et al.*, 2002), which act on the substrate arachidonic acid (AA) to produce the precursor for PGs and thromboxanes (TXs), which play a role in a number of cellular processes such as proliferation, inflammation and angiogenesis. COX-2 was first shown to be over-expressed in CRC in the 1990's (Eberhart *et al.*, 1994), and its overexpression is associated with worse survival in CRC patients (Ogino *et al.*, 2008), (see section 1.6.1 for COX-2 discussion).

1.6 Eicosanoids and colorectal carcinogenesis

1.6.1 Eicosanoid biosynthesis

Fatty acids (FAs) are long chain aliphatic compounds made up of carbon and hydrogen chains with a carboxylic (-COOH) group at one end (start of the chain also known as 'alpha') and a methyl group (CH₃) at the other end (end of the chain also known as 'omega'). FAs containing only single bonds between carbons are called saturated FAs whereas unsaturated fatty acids contain at least one (monounsaturated) or more (polyunsaturated carbon-carbon double bonds. Omega-3 and ω -6 PUFAs are so named because of the position of the first double bond from the methyl end (third [n-3] and sixth [n-6] carbon respectively). The parent ω -6 PUFA is linoleic acid (LA) and the

parent ω -3 PUFA is alpha-linolenic acid (ALA). LA and ALA are essential fatty acids (EFA), as mammals must consume them as they are unable to directly synthesise them, as the desaturase enzyme required in order to place the double bond in either the n-3 or n-6 position is not present. LA and ALA are both found in vegetable oils. LA and ALA can be further metabolized into AA (20:4n-6) and eicosapentaenoic acid (EPA, 20:5n-3) respectively through the action of delta (Δ)-6 desaturase and Δ 5 desaturase enzymes, however the conversion of EPA from ALA in humans is not very efficient and is likely due to several factors such as genetic variations and substrate preferences for the desaturases (Pawlosky *et al.*, 2001; Burdge, 2006, Glaser *et al.*, 2010). The main ω -3 PUFAs are EPA and docosahexaenoic acid (DHA, 22:6n-3), which are present in oily fish such as salmon and mackerel. The main PUFAs in the western diet are the ω -6 PUFAs.

Twenty-carbon PUFAs such as AA and EPA (Figure 2A/ B) are biologically important, with roles in phospholipid membrane structure and function, as well as cellular signaling and lipid metabolism (Ricciotti & FitzGerald., 2011, Gorjão *et al.*, 2009).

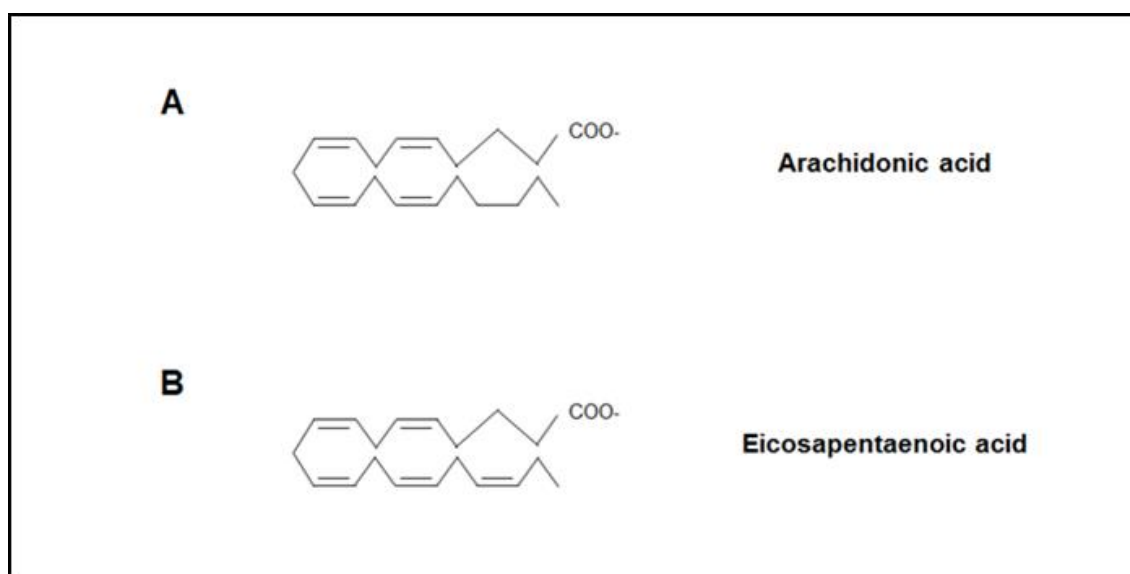


Figure 2. The chemical structures of AA and EPA.

AA and EPA are present in the phospholipid membrane of cells and is released by the phospholipase A2 family of enzymes and in this free form is then oxidized by three main enzymatic pathways:

1. Cyclooxygenase (COX) pathway (COX-1 and COX-2).
2. Lipoygenase (LOX) pathway (5-LOX, 12-LOX and 15-LOX).
3. Cytochrome (CYP) P450 pathway (superfamily of monooxygenase enzymes).

These three pathways synthesise a wide variety of metabolites from 20-carbon FAs such as AA, collectively known as eicosanoids. Eicosanoids are made up of five families, PGs, prostacyclins (PGI), TXs, leukotrienes (LT), and lipoxins (LX). Prostanoids are a sub-group of eicosanoids including PGs, TXs, and PGIs (Figure 3; AA derived eicosanoids).

There are three different isoforms of COX (COX-1,-2, and -3), COX-3 is not functional in humans. The COX-1 gene is constitutively expressed in tissues (Fitzpatrick *et al.*, 2004, Topper *et al.*, 1996), and is highly expressed in platelets and gastric epithelial cells where it activates platelets through TXA₂ production and cytoprotects the gastric epithelial cells through PGE₂ synthesis (Capone *et al.*, 2007). COX-2 is an immediate-early gene which can be induced by various cytokines and growth factors; however COX-2 can also be expressed constitutively in some cells such as endothelial cells where PGI₂ directs anti-thrombotic and vasoprotective actions (Di Franscesco *et al.*, 2009).

COX-1 and-2 generates PGH₂ from AA through the bis-oxygenation and cyclisation of AA to PGG₂ then the peroxidation of PGG₂ to PGH₂ (Smith *et al.*, 2000). The COXs are made up of 72 kilodaltons (kDa) homodimers (Smith *et al.*, 2000). Each of the monomers can bind to AA, but each can act as a regulatory allosteric subunit on the other, which allows the other subunit to convert AA into PGG₂, before the peroxidation of PGG₂ to PGH₂. The PGH₂ is then acted upon by a series of tissue or cell-specific synthases and isomerases to produce a number of biologically active prostanoids (Ueno *et al.*, 2005). PGE₂ one of the most abundant human prostanoids is synthesised by PGE synthase. PGE₂ is involved in the classical signs of inflammation; redness, swelling and pain, via increased vascular dilatation, permeability, and activation of sensory neurons (Funk, 2001). PGE₂ also has a diverse array of gastrointestinal functions from control of gastric acid secretion, gastrointestinal motility, and mucus production, through its membrane receptors EP. PGE₂ is thought to play a role in CRC as differential expression of its EP receptors has been shown in CR carcinogenesis (Shoji *et al.*, 2004; Kawamori *et al.*, 2005). In addition to the prostanoids the COXs can also synthesise further AA oxygenated products such as 11(R)-hydroxyeicosatetraenoic acid (HETE), and 15S-HETE, in less abundance than the prostanoids, with product formation differing in their individual Km values (Michaelis constant), (Thuresson *et al.*, 2000).

The lipoxygenases (LOXs) are a family of iron containing dioxygenases that insert molecular oxygen into PUFAs with at least one five carbon chain with two double bonds known as a pentadiene. These enzymes have been shown to be expressed in mammalian tissue. LOXs are classified according to their positional specificity of AA

oxygenation as 5-, 12- and 15-LOX. AA is initially oxygenated to 5-, 8-, 12- and 15-hydroperoxyeicosatetraenoic acids (HPETEs) by their respective lipoxygenases which then reduce to the appropriate hydroxyeicosatetraenoic acids (HETEs), (Pidgeon *et al.*, 2007), (Figure 3). LOXs are involved in the metabolism of eicosanoids.

5-HPETE is formed from the oxygenation of AA by 5-LOX and an 18kDa 5-LOX activating protein (FLAP). In its active state 5-LOX translocates to the nuclear membrane and associates with FLAP. FLAP then allows AA to interact with the nuclear membrane bound 5-LOX to produce 5-HPETE (Mancini *et al.*, 1993). The 5-HPETE is either reduced to 5-HETE or dehydrated to the unstable metabolite leukotriene A₄ (LTA₄). LTA₄ can then be either converted to the cysteinyl leukotrienes (LTC₄, LTD₄ and LTE₄) through glutathione conjugation, hydrolysed to LTB₄, or utilised for LX synthesis. LXs are trihydroxyeicosatetraenoic acids derived from AA, formed by transcellular synthesis. They are formed by two different pathways, (Bannenberg *et al.*, 2010):

1. Platelet-leukocyte interaction. LTA₄ produced by polymorphonuclear leukocytes (PMNs) is converted to LXA₄ and LXB₄ by platelet 12-LOX (Chiang *et al.*, 2005).
2. Epithelial-immune cell interaction. 15-HETE produced by epithelial cells is oxygenated by 5-LOX to generate LXA₄ and LXB₄.

LTB₄ is a potent chemoattractant mainly produced by PMNs, whilst the cysteinyl leukotrienes are bronchoconstrictors and vasodilators (Lewis *et al.*, 1990). LXs differ from most other eicosanoids in that they have potent anti-inflammatory activities. Examples include; inhibition of neutrophil chemotaxis, up regulation of monocyte chemotaxis and up regulation of monocyte ingestion of apoptotic neutrophils (Serhan, 1997 & 2002).

The CYPs are a family of diverse enzymes that catalyse the oxidation of organic matter. CYPs are present not only in animals but also in fungi, bacteria, viruses and plants. In humans, CYPs are found on the membrane of endoplasmic reticulum and the inner mitochondrial membrane. The human genome contains 57 CYP genes (Nelson, 2009). Human CYP enzymes oxidise both xenobiotics and endogenous compounds such as hormones, cholesterol and vitamin D. CYP enzymes can also metabolise PUFAs through hydrolysis or epoxygenation. AA epoxygenation by CYP mono-oxygenases can result in four different epoxyeicosatrienoic acids (EET), which can undergo hydroxylation to biologically inactive dihydroeicosatetraenoic acid (DHET), or AA oxidation to synthesise several different HETEs (Konkel *et al.*, 2011).

Whilst the COXs, LOXs and the CYP enzymatic system can metabolise AA they can also metabolise EPA to generate less active eicosanoids (Calder *et al.*, 2006). EPA is

present within the phospholipid membrane of cells and is released and metabolised like AA to generate eicosanoids. EPA incorporation into mammalian cells membranes has been shown (Miles *et al.*, 2003, Kew *et al.*, 2004, Browning *et al.*, 2012). EPA metabolism via COXs produces the three series prostanoids, including PGE₃ (Figure 4). COX-1 oxygenates EPA with only about 10% potency of that of AA, and COX-2 oxygenates EPA at about 30% of that of AA (Wada *et al.*, 2007). PGE₃ has been shown to be less efficient in up regulating COX-2 than PGE₂, and induces synthesis of less IL-6 in macrophages when compared to PGE₂ (Bagga *et al.*, 2003). EPA derived 5-series LTs are synthesised via the 5-LOX pathway and 5-, 12-, 15-hydroxyeicosapentaenoic acids (HEPEs) by the respective LOXs. The CYP system can also metabolise EPA to form various (HEPEs) and epoxyeicosatetraenoic acids (EEQs), (Figure 4; EPA derived eicosanoids).

Colonic mucosa AA and EPA levels in healthy controls have been shown to be around 8% and 1% of the main total mucosal fatty acids (Courtney *et al.*, 2007). In respect to human colonic mucosa it has been shown that ω -3 PUFA supplementation is associated with an increase in mucosal EPA content and decrease in AA content (Anti *et al.*, 1993, Courtney *et al.*, 2007, West *et al.*, 2009, West *et al.*, 2010). The majority of eicosanoids that are generated in humans are derived from AA, principally as the western diet contains higher levels of LA than ALA.

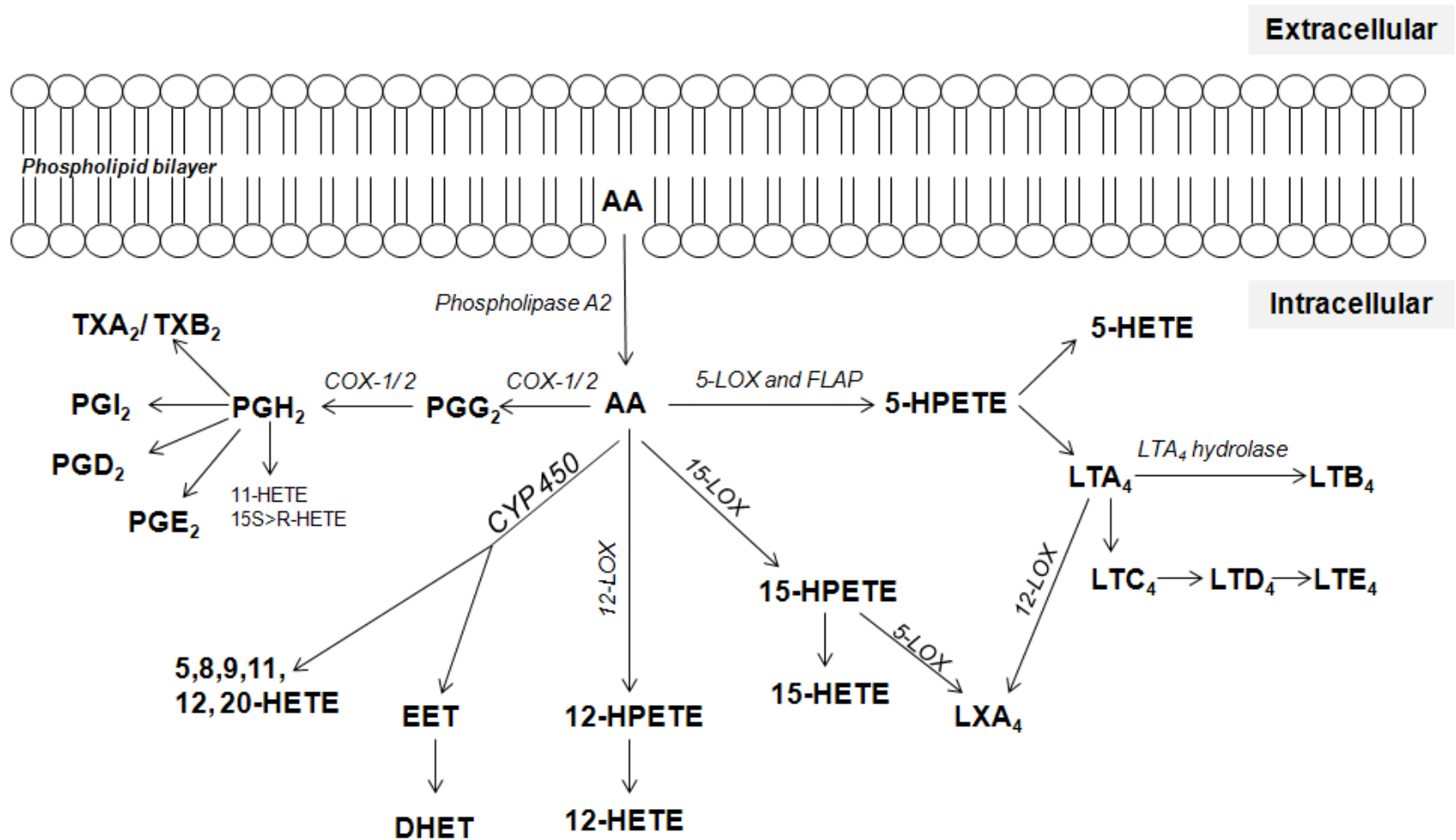


Figure 3. Schematic overview of AA metabolism.

Arachidonic acid (AA) is metabolised to eicosanoids by the actions of three different enzyme systems: the cyclooxygenase (COX), the lipoxygenase (LOX) and the cytochrome P450 monooxygenase system.

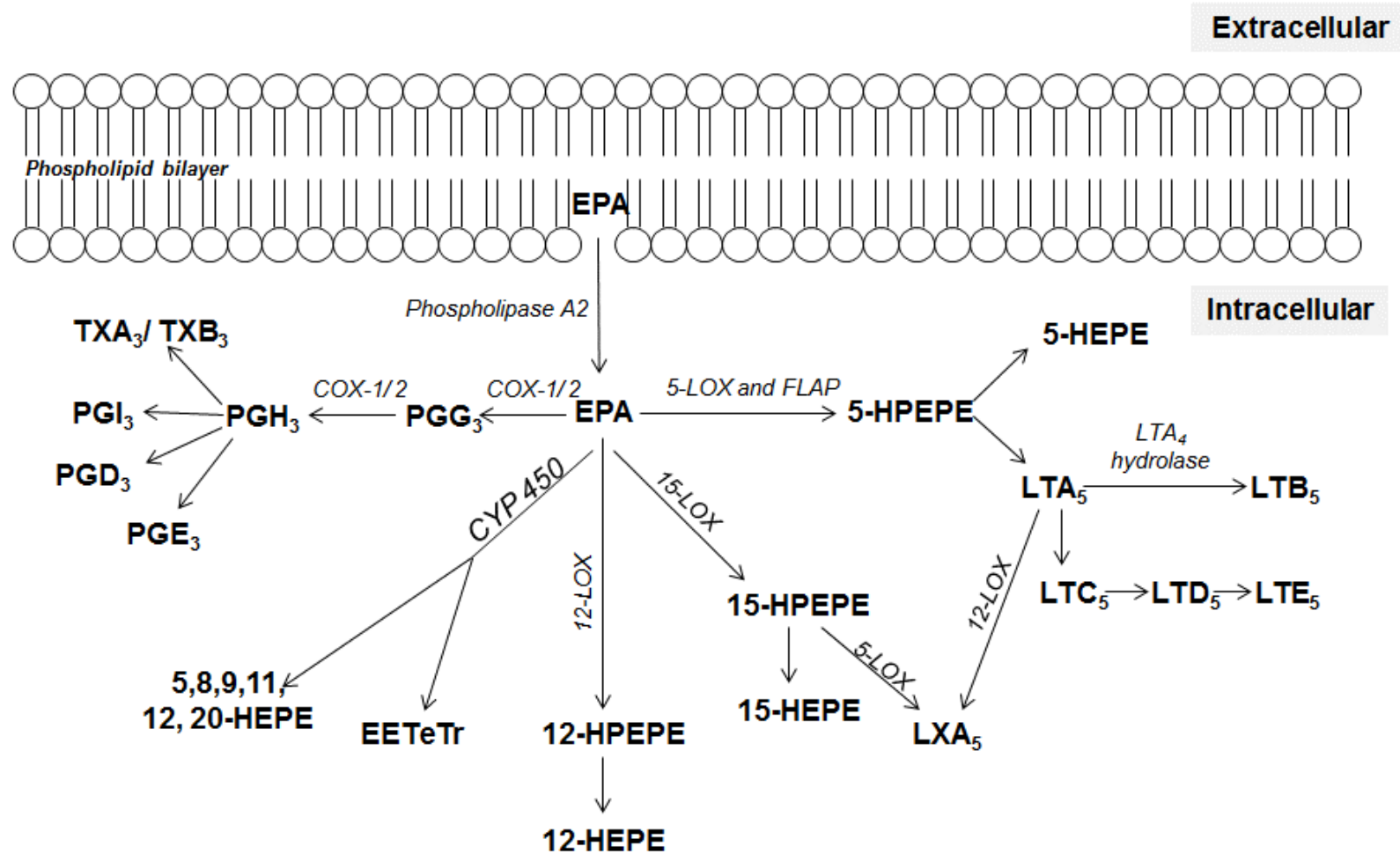


Figure 4. Schematic overview of EPA metabolism.

Eicosapentaenoic acid (EPA) is metabolised to eicosanoids by the actions of three different enzyme systems: the cyclooxygenase (COX), the lipoxygenase (LOX) and the cytochrome P450 monooxygenase system.

1.6.2 Lipidomic analysis of eicosanoids

Methods currently used to analyse lipids such as eicosanoids include enzyme immunoassays (EIA) (Nicosia *et al.*, 1992), gas chromatography (GC) mass spectrometry (MS) (Hubbard *et al.*, 1986, Tsukamoto *et al.*, 2002). EIA whilst readily available has low specificity and is affected by cross-reactivity, and cannot simultaneously detect more than one lipid. GC/MS is sensitive but requires sample derivatisation prior to analysis. Liquid chromatography (LC) coupled to MS has allowed the simultaneous qualitative and quantitative assessment of several lipid mediators in one biological sample (Masoodi & Nicolaou, 2006, Masoodi *et al.*, 2008). The use of electrospray ionisation (ESI) has permitted the ionisation of compounds such as lipids, so that the metabolites can form either positive or negative ion species. The separation ability of liquid LC through high performance-LC can easily be coupled to MS. Quantitation of mediators can be met through the coupling of LC-ESI to a tandem MS (MS/MS) on a multiple reaction monitoring mode (MRM). Calibration lines constructed using synthetically prepared internal lipid standards allow the absolute quantification of the mediator of interest (Masoodi & Nicolaou, 2006). LC-ESI-MS/MS analysis was used in the candidate's experimentation for lipidomic profiling, and is discussed further in Chapter 4.

1.6.3 Eicosanoids metabolism and colorectal cancer

The COX, LOX, and CYP450 systems have been implicated in the development of cancer (Wang & Dubois, 2010, Panigrahy *et al.*, 2010). COX-2 is up-regulated in colorectal adenomas and cancer with approximately half of all adenomas and over 85% of CRC having elevated COX-2 levels (Eberhart *et al.*, 1994, Sano *et al.*, 1995, Shao *et al.*, 2000, Soslow *et al.*, 2000). It is considered that COX-2 plays an important role in CRC progression as it has been shown that increased COX-2 levels correlate with larger tumour size, advanced stage, risk of recurrence and poorer survival in human CRC (Sheehan *et al.*, 1999, Tomozawa *et al.*, 2000, Zhang *et al.*, 2002, Soumaoro *et al.*, 2004, Ogino *et al.*, 2008). COX-2 driven tumorigenic activity is believed, at least in part, to be due PGE₂ which is abundantly expressed in human CRC (Rigas *et al.*, 1993) and has been shown to play a role in early colorectal carcinogenesis (Wang & Dubois., 2010, Hernandez *et al.*, 2010). Whilst COX-2 has been thought to be the principal isoenzyme involved in CRC carcinogenesis, there is evidence indicating the role played by COX-1 (Sano *et al.*, 1995). The Apc mouse model (murine model of FAP), has shown that COX-1 is expressed in all polyps whilst COX-2 is only induced in those polyps greater than one millimetre in size. Such evidence supports the role of COX-1 in generating basal PGE₂ levels supporting early polyp growth followed by an induction in COX-2 expression to further increase growth

in the polyp (Takeda *et al.*, 2003). The induction in COX expression found in CRC leads to increased PGE₂ synthesis. Increased PGE₂ is associated with a poorer prognosis in CRC (Rigas *et al.*, 1993). PGE₂ has been shown to promote CR cell proliferation, survival and angiogenesis through prostaglandin receptor (EP) signalling, and activation of *Wnt* signalling (Castellone *et al.*, 2006, Dorsam *et al.*, 2007, Cherukuri *et al.*, 2007). PGE₂ has also been associated with the promotion of CRC development in several mouse models (Wang *et al.*, 2004, Wang & Dubois, 2006, Cha & Dubois, 2007). Fibroblasts and macrophages present within the cancer also express COX-2, thus may have a role in CRC development via COX-2 (Bamba *et al.*, 1999, Ota *et al.*, 2002).

5-LOX protein over-expression has been implicated in murine CRC development (Ye *et al.*, 2004), Melstrom *et al.*, (2008) using human CRC cell lines in a mouse xenograft model, found that the 5-LOX inhibitor α -pentyl-3-(2-quinolinylmethoxy)-benzene methanol reduced tumour growth. A role of 5-LOX in CRC in angiogenesis has also been proposed (Barresi *et al.*, 2007). Over-expression of 5-LOX was shown to correlate with the presence of typical high-risk factors for malignant transformation in adenomatous polyps such as high grade intraepithelial neoplasia, polyp size and villous and tubulovillous adenoma (Wasilewicz *et al.*, 2010), furthermore this was supported by Soumaoro *et al.*, 2006 who demonstrated that 5-LOX over-expression was associated with advanced cancer stage, size and vessel invasion. AA derived 5-LOX mediator LTB₄ has been shown to promote cell survival and proliferation in human CRC cells *in vitro* (Ihara *et al.*, 2007).

LXs have been shown to reduce cell proliferation *in vitro* in lung cancer cells (Clària *et al.*, 1996) and reduce the expression of the pro-inflammatory cytokines TNF- α and IL-8 in a co-culture model using a CRC cell line (Caco2) and mouse macrophage cell line (Kure *et al.*, 2010). LXA₄ has been identified *in vivo* in several experimental models (Munger *et al.*, 1999, Chiang *et al.*, 1999, Bandeira-Melo *et al.*, 2000, Aliberti *et al.*, 2002a, 2002b, Bellenger *et al.*, 2010) and in human samples (Pouliot *et al.*, 2000, Bonnans, *et al.*, 2002, Karp *et al.*, 2004, Levy *et al.*, 2005, Planagumà *et al.*, 2008). At present there has been no study looking for a potential role of LXs as potential anti-CRC agents.

The use of combined COX-2 and 5-LOX inhibitors such as licofelone as chemopreventative agents for CRC have been shown *in vitro* (Tavolari *et al.*, 2008, 2012) and *in vivo* (Mohammed *et al.*, 2009). The effect of licofelone has not only been shown on the malignant epithelial cells but also on H-ras transformed rat fibroblasts where licofelone induced apoptosis in these transformed carcinogenic fibroblasts (Kabadere *et al.*, 2014). Furthermore the safety and tolerability of licofelone in human

subjects was confirmed in a phase III clinical trial for osteoporosis (Alvaro-Gracia, 2004). At present there has been no published literature on the use and effects of licofelone in human cancer patients.

The CYP ω -hydroxylases of the 4A and 4F families generate HETEs whilst the epoxygenase pathway driven by the 2C and 2J genes generates the EETs. CYP derived 20-HETE has been shown *in vitro* to stimulate cell proliferation in a glioblastoma cell line, and also increase tumour growth when these cells were implanted into a rodent model (Jiang *et al.*, 2005). 10-HETE increased expression of vascular endothelial growth factor (VEGF) and metalloproteinase (MMP)-9 in non-small cell lung cancer cells *in vitro* with associated promotion of invasion. This same group also showed that non-small lung cell tumour burden was increased in a mouse model in 20-HETE pre-treated cells, with the tumour size reduced when the cells were pre-treated with a CYP ω -hydroxylase inhibitor (HET0016) or a 20-HETE antagonist (WIT002), (Yu *et al.*, 2011). Jiang *et al.*, 2005 identified CYP2J2 as potential target in cancer, they showed that when CYP2J2 was over-expressed in several human cancer cell lines there was an induction of cell proliferation and increased tumour burden when injected into a murine model. Data such as this suggest a potential role for EETs in cancer development. The gut microflora is most abundant and diversely functioning microbial population in the human body, comprising around ten times the number of human cells (Savage, 1977, Peterson *et al.*, 2009). Whilst there are a few studies that have looked at the gut microbial content of CRC and the difference in makeup compared to normal subjects (Shen *et al.*, 2010, Sobhani *et al.*, 2011), there has been no study to date looking at CYP gut microbiota CYP metabolism of PUFAs and CRC.

1.7 Aspirin and colorectal cancer

Aspirin (acetylsalicylic acid) is an analgesic and anti-inflammatory agent that inhibits the generation of prostanoids, through the inhibition of the activity of both COX-1 and COX-2 (Capone *et al.*, 2007). Aspirin acetylates either serine 529 on COX-1 or serine 516 on COX-2, this irreversibly inhibits the cyclooxygenase activity of COXs. The acetylated COXs are therefore unable to form PGG₂, but acetylated COX-2 retains some catalytic activity and metabolises AA into 15R-HETE (Lecomte *et al.*, 1994). 15R-HETE is a substrate for 5-LOX producing aspirin triggered-LXs (ATL). ATLs, like LXs, have been shown to have potent anti-inflammatory actions such as the non-phylogistic engulfment of apoptotic PMNs, (Clària *et al.*, 1995, Serhan *et al.*, 2005), and inhibition of PMN chemotaxis in a zymosan induced peritonitis murine model (Chiang *et al.*, 2005). ATLs have also been identified in experimental *in vivo* models (Chiang *et al.*, 1998, Peretti *et al.*, 2002, Titos *et al.*, 1999, Fiorucci *et al.*, 2002), in human blood samples treated once a day with 81 mg of aspirin for eight weeks (Chiang *et al.*, 2004),

in human gastric mucosa (Fiorucci *et al.*, 2003). Aspirin-triggered LXA₄ has been shown to have *in vitro* anti-neoplastic effects in lung cancer (Clària *et al.*, 1996). To date the presence of ATLs in CRC has not yet been commented upon.

Evidence supporting the use of aspirin as an agent that can reduce the risk of CRC is becoming well established (Flossman & Rothwell, 2007, Rothwell *et al.*, 2010, Bosetti *et al.*, 2012). Daily intake of aspirin for at least five years reduced the 20 year risk of CRC by 32% (Rothwell *et al.*, 2010). Furthermore a meta-analysis of four separate RCTs showed a risk reduction of colorectal adenoma development by 17% and a risk reduction of 28% in advanced adenomas, in patients that took aspirin daily (75-325 mg) for three years (Cole *et al.*, 2009). There are several proposed mechanisms to explain the anti-CRC activity for aspirin. The most widely studied is the ability of aspirin to block the metabolism of AA through the COXs. The acetylation of COX-1 by aspirin causes complete loss of COX activity. Aspirin has been shown *in vitro* to be between 50 and 100-fold more potent at inhibiting platelet's COX-1 activity than monocyte's COX-2 activity and has a short half-life in the human circulation (15-20 minutes), (Dovizio *et al.*, 2012, Ferrández *et al.*, 2012). As COX-2 expressing cells are able to resynthesize COX-2, high doses of aspirin are required to inhibit it (Patrono *et al.*, 2004). The loss of COX-1 enzymatic activity and consequent inhibition of TXA₂ dependent platelet function therefore may play a significant part in the anti-cancer effect of aspirin. It is postulated that activated platelets play a role in cancer progression through the release of several factors involved in cell growth and angiogenesis (Gay & Felding-Habermann, 2011). An *in vitro* study showed that human CRC cells grown in co-culture with platelets stimulated TXA₂ platelet synthesis that was inhibited by aspirin (Dovizio *et al.*, 2012). Increased TXA₂ synthesis by colon-26 adenocarcinoma cells was shown to result in increased tumour growth when inoculated into a syngeneic mouse model (Pradono *et al.*, 2002). Therefore the prevention of platelet aggregation may offer an explanation for the anti-CRC effects of aspirin.

Interestingly, aspirin and other non-steroidal anti-inflammatory drugs (NSAIDs) have been shown to have anti-proliferative effects on COX negative cells (Hanif *et al.*, 1996; Yu *et al.*, 2002), thus supporting COX independent anti-CRC actions. Aspirin has been shown to have effects on the anti-apoptotic gene *BCL2L1* (Zhang *et al.*, 2000) and the pro-apoptotic gene *PAWR* (Zhang & Dubois., 2000), increase MMR protein expression and promote apoptosis in COX negative cell lines (Goel *et al.*, 2003).

At the present time the relative contribution of COX dependent and independent anti-neoplastic mechanisms of aspirin are not clear (Wang *et al.*, 2006, Baron *et al.*, 2006, Chan A.T *et al.*, 2007, Borthwick *et al.*, 2006, Deng *et al.*, 2009).

1.8 Eicosapentaenoic acid and colorectal cancer

Observational studies have reported a relationship between fish intake and CRC risk. Systematic reviews of observational studies have stated limited supporting evidence for an association between ω -3 PUFAs intake and CRC prevention (Gerber *et al.*, 2012). This relationship is supported by the updated interim report of the second expert report of the World Cancer Research Fund (WCRF) and American Institute for Cancer Research (AICR), (WCRF/ AICR, 2007 and 2011). There have been several *in vitro* studies that have supported the role as EPA as anti-CRC agent, through reduced cell proliferation and increased apoptosis (Meneaud *et al.*, 1992, Tsai *et al.*, 1998, Clarke *et al.*, 1999, Palozza *et al.*, 2000, Boudreau *et al.*, 2001, Calviello *et al.*, 2004, Hawcroft *et al.*, 2010). However it remains that there is only limited evidence for the beneficial effects of fish consumption and CRC risk, (WCRF/AICR., 2011).

There is strong pre-clinical evidence that the ω -3 PUFA EPA has anti-CRC activity (Calviello *et al.*, 2007). EPA was shown to suppress polyp number in APC (Min/+) mice (Fini *et al.*, 2010), which is a mouse model of FAP. Leading on from this study a double-blind randomised controlled trial showed that the use of EPA in patients with FAP was associated with a significant reduction in polyp burden, both in size and number, which suggests that EPA may have a potential chemopreventative effect in CRC (West *et al.*, 2010). There was reduced liver tumour burden in a diethylnitrosamine (DEN)-induced liver tumour model using the fat-1 transgenic mouse model (endogenously converts ω -6 PUFAs to ω -3 PUFAs such as EPA), (Weylandt *et al.*, 2011). A recent phase II double-blind, randomized controlled study of daily EPA use in patients undergoing surgery for CRC liver metastasis reported a 40% increase in EPA in the tumour tissue (Cockbain *et al.*, 2014).

The proposed mechanisms behind EPA's anti-CRC activity include:

1. Induction of cellular oxidative stress.
2. Effects on membrane dynamics and cell surface receptors.
3. Alternative substrate for COX/ LOX enzymatic activity.

Altered cellular redox status and amplified cellular oxidative stress due to increased reactive oxygen species in colonocytes of EPA/ DHA supplemented rats has been shown to induce colonocyte apoptosis in a rat CRC model with ROS levels inversely related to DNA damage (Hong, *et al.*, 2002, Sanders *et al.*, 2004).

Disruption of lipid rafts by ω -3 PUFAs in the cell phospholipid cell membrane has been shown (Wassall *et al.*, 2009). Omega-3 PUFA supplementation to breast cancer cells *in vitro* reduced expression of the chemokine receptor CXCR4 which is a marker of breast

cancer metastasis (Altenburg & Siddiqui., 2009). Altenburg & Siddiqui (2009) showed that ω -3 PUFAs displaced CXCR4 an effect that was not seen with the saturated FA stearic acid. EPA incorporation into the lipid rafts of mammalian breast cancer cells has also been shown to alter epidermal growth factor receptor (EGFR) signaling and subsequent tumour growth *in vitro* (Schley *et al.*, 2007). Both ω -3 and ω -6 PUFAs can bind and activate the G-protein coupled receptor (GPCR) GPR120. GPR120 has been shown to be expressed in the *in vitro* human CRC cell line Caco2 and human colonic samples (Mobraten *et al.*, 2013). Mobraten *et al* (2013) found that EPA inhibited NF- κ B activation via GPR120 signaling. Further work is needed looking at GPR120 expression in CRC clinical samples and the possible influence that EPA signaling may have.

EPA can act as an alternative substrate for the COXs and LOXs. Instead of AA acting as a substrate for the COXs and producing the pro-tumorigenic 2-series PGs such as PGE₂, EPA is converted to the less inflammatory 3-series PGs (e.g. PGE₃) (Hawcroft *et al.*, 2010), in human CRC cells. However to date there has been no evidence showing a PGE₂ to PGE₃ switch in human CRC tissue, with no switch identified by Cockbain *et al* (2014). At present there has also been no published work looking at whether the 5 series LTs such as LTB₅ have a role to play in EPA directed anti-CRC effects, but it is established that LTB₅ is less pro-inflammatory than LTB₄ (Terano *et al.*, 1984, Tatsuno *et al.*, 1990). Resolvins of the E series are novel anti-inflammatory and pro-resolving lipid mediators derived from EPA. At present there are three different Resolvins of the E series, known as Resolvin E1 (RvE1), (Serhan *et al*, 2000, Arita *et al.*, 2005), RvE2 (Tjonahen *et al.*, 2006) and RvE3 (Isobe *et al.*, 2012). The work presented by the candidate focuses on RvE1 as a potential novel anti-CRC agent.

1.9 Resolvin E1

1.9.1 Resolvin E1 biosynthesis

EPA is the precursor for the resolution phase interaction product known as RvE1. RvE1 was initially identified through lipidomic profiling of exudates collected during the resolution phase of inflammation in mice treated with aspirin and EPA, using LC-MS/MS, (Serhan *et al.*, 2000). Aspirin-acetylated COX-2 metabolises EPA to a lipid intermediate called 18-hydroxyeicosapentaenoic acid (18R-HEPE), which when acted upon by two further enzymes, 5-LOX and LTA₄ hydrolase (LTA₄H), produces RvE1 (Oh *et al.*, 2011), (Figure 5; chemical structure of RvE1). The chirality of the hydroxyl group on carbon 18 of 18-HEPE is important as the hydroxyl group in the R position is required to synthesise RvE1. RvE1 have also been shown to be synthesised from EPA via the CYP system (Haas-Stapleton *et al.*, 2007). Figure 6 summarises the current

proposed cellular pathway for RvE1. RvE1 exerts its biological actions *in vitro* in the nanogram (ng) range and has been shown to be rapidly enzymatically inactivated (Arita *et al.*, 2006).

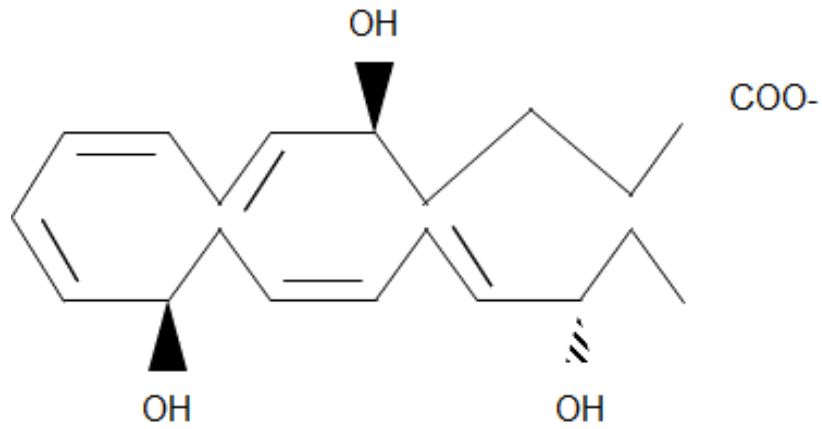


Figure 5. The chemical structure of RvE1.

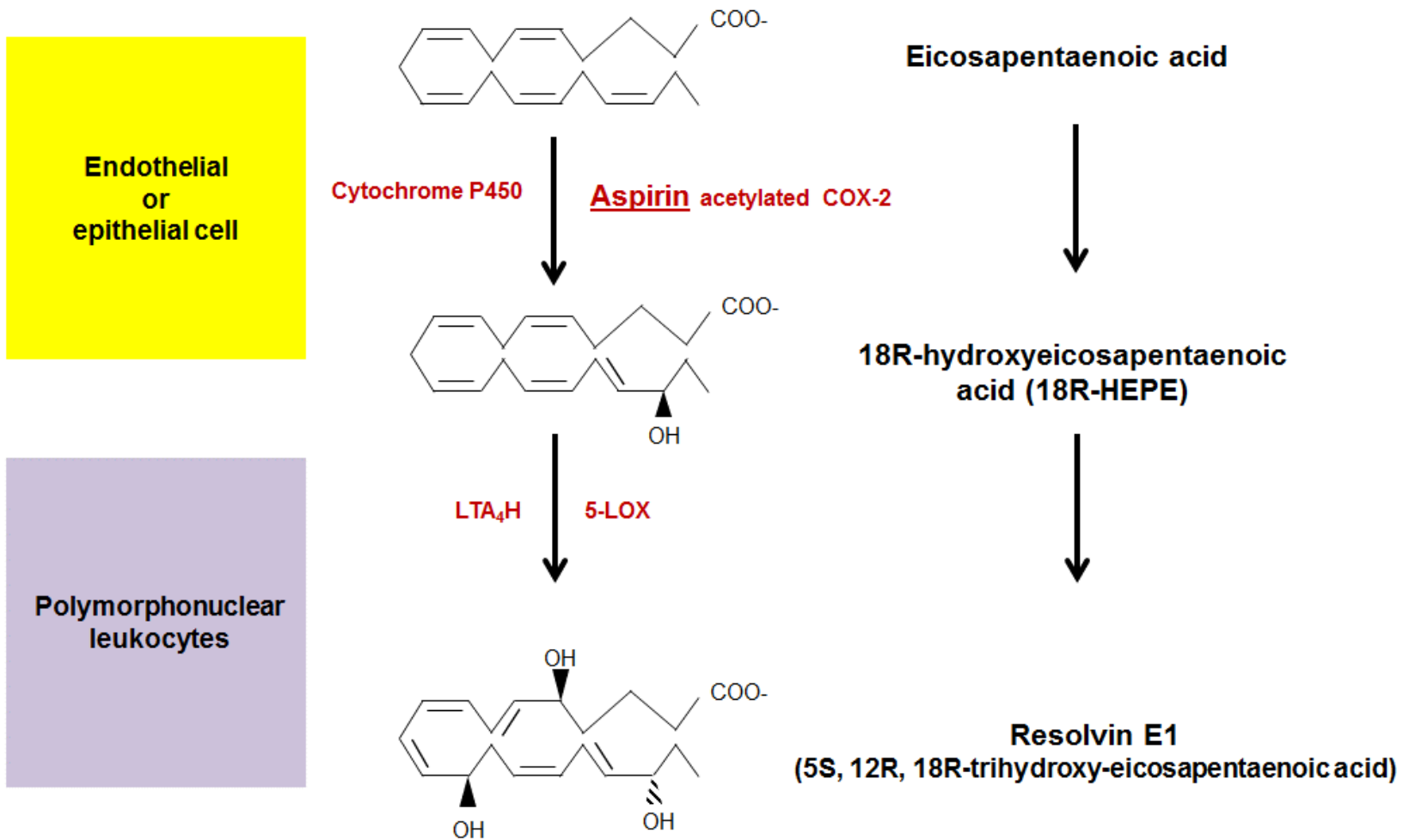


Figure 6. Proposed biosynthesis for pathway for EPA derived RvE1.

Eicosapentaenoic acid (EPA) within an epithelial cell or endothelial cell is converted to 18R-HEPE via acetylated COX-2 or by the CYP450 system. The 18R-HEPE then leaves the cell (by an unknown cellular mechanism) and is taken up (by an unknown cellular mechanism) by a polymorphonuclear leukocyte (PMN) such as a neutrophil. The neutrophil then converts the 18R-HEPE to RvE1 through the actions of two different enzymes 5-LOX and LTA₄ hydrolase (LTA₄H).

The RvE1 intermediate 18R-HEPE has been produced by EPA and aspirin treated human vascular cells *in vitro* (Serhan *et al.*, 2000). 18R-HEPE has been shown to be present in the plasma of EPA alone and EPA/aspirin supplemented healthy volunteers (Oh *et al.*, 2011), (aspirin 81 mg at 0 hour, then 81 mg aspirin and fish oil capsule containing 1 g EPA at 12 hours, then plasma analysed by LS-MS/MS after 3 hours). RvE1 has been synthesised *in vitro* by human PMNs when exposed to human vascular endothelial cell line derived 18R-HEPE (Serhan *et al.*, 2000), and when synthetic 18-HEPE standard was treated with recombinant 5-LOX and LTA₄H (Oh *et al.*, 2011). RvE1 has also been identified *in vivo* in the colons of EPA treated *fat-1* transgenic mice with chemically induced colitis (Hudert *et al.*, 2006). The *fat-1* transgenic mice are genetically engineered to express the *Cenorhabditis elegans fat-1* gene which encodes a ω -3 FA desaturase enzyme, able to convert ω -6 PUFAs to ω -3 PUFAs (Kang *et al.*, 2004). RvE1 has also been identified in the plasma of EPA and aspirin treated healthy volunteers with a published range of 0.1 to 0.4 ng/ mL in the six participants (Arita *et al.*, 2005a), (1 g EPA/ 0.7 g DHA then 160 mg aspirin, three hours later, plasma then analysed four hours after EPA/DHA given by LS-MS/MS) and at plasma levels of around 0.2 ng/ mL in a cohort of healthy volunteers on a described 'normal' diet (Psychogios *et al.*, 2011). RvE1 is metabolised into several different lipid products via dehydrogenation through the enzyme 15-hydroxyprostaglandin dehydrogenase (15-PGDH). These metabolites include 18-oxo-RvE1 (Arita *et al.*, 2006), 20-carboxy-RvE1 (via 19 and 20-hydroxy-RvE1) and 10, 11-dihydro-RvE1. These lipid products were shown to display no or very little anti-inflammatory properties compared to RvE1 particularly in respect to leukocyte infiltration in the murine peritonitis model used (Hong *et al.*, 2008). Interestingly 15-PGDH has been shown to be down regulated in human CRC (Backlund *et al.*, 2004).

1.9.2 Biological effects of Resolvin E1

RvE1 stimulates the resolution of acute inflammation by reducing transmigration of human PMNs *in vivo* (Serhan *et al.*, 2000, Arita *et al.*, 2005, Campbell *et al.*, 2007) and increasing the clearance of PMNs through the induction of CD55 (or decay accelerating factor). CD55 is an anti-adhesive protein expressed at the epithelial surface and acts to facilitate PMN clearance (Louis *et al.*, 2005, Campbell *et al.*, 2007). Furthermore RvE1 increases mononuclear infiltrates *in vivo* into sites of inflammation (Schwab *et al.*, 2007, Kebir *et al.*, 2012), reduces IL-12 production by dendritic cells (Arita *et al.*, 2005) and stimulates macrophage phagocytosis (Schwab *et al.*, 2007, Hong *et al.*, 2008, Kebir *et al.*, 2012). Interestingly, 18-HEPE, the intermediate lipid product in the formation of RvE1 from EPA, has been shown to reduce PMN infiltration in the TNF- α induced inflammatory murine dorsal pouch model, but its potency was less than 50% of

that of RvE1 (Arita *et al.*, 2005). Platelet aggregation been shown to be inhibited by RvE1 (Dona *et al.*, 2008, Fredman *et al.*, 2009). RvE1 has also been shown to antagonise the effects of the pro-inflammatory eicosanoid LTB₄ (Arita *et al.*, 2007). RvE1 was shown to be protective in murine colitis (Arita *et al.*, 2005, Ishida *et al.*, 2010, Campbell *et al.*, 2010) and inhibited lipopolysaccharide (LPS) induced macrophage synthesis of TNF- α in mouse peritoneal macrophages (Ishida *et al.*, 2010). RvE1's protective actions in chemically induced murine colitis models are in part thought to be due to the induction in intestinal alkaline phosphatase (ALPI), which can detoxify bacteria endotoxins such as LPS (Campbell *et al.*, 2010).

Interestingly RvE1 has been shown to inhibit NF- κ B signaling (Arita *et al.*, 2005 & 2007). NF- κ B, as discussed previously, is a transcription factor that can regulate cancer cell proliferation through upregulation of Cyclin D1 expression (Guttridge *et al.*, 1999, Baldwin., 2001), apoptosis through the increased expression of anti-apoptotic proteins such as Bcl-x_L (Chen *et al.*, 2000) cancer angiogenesis through VEGF (Huang *et al.*, 2000), and cancer migration and invasion through MMP-9 (Choo *et al.*, 2008). NF- κ B has also been shown to be constitutively active in 40% of human CRC tissue (Sakamoto *et al.*, 2009). RvE1 inhibition of NF- κ B signaling therefore offers a potential novel approach towards cancer inhibition. The biological effects of RvE1 are summarised in Figure 7.

Importantly the stereochemistry of the hydroxyl group on carbon 18 (R or S) has been shown to alter the biological activity of RvE1. 18S-RvE1 has higher affinity for the RvE1 receptor than 18R-RvE1 (see section 1.9.3), but is more rapidly metabolised. Both stereoisomers were shown also to have slightly different potencies on macrophage phagocytosis *in vivo* (engulfment of *Escherichia coli* (*E.coli*), zymosan and apoptotic neutrophils), neutrophil infiltration and cytokine synthesis in the murine peritonitis model (Oh *et al.*, 2011).

1.9.3 The receptors for Resolvin E1

There are two known receptors of RvE1 named ChemR23 (Arita *et al.*, 2005) and BLT1 (Arita *et al.*, 2007). ChemR23 and BLT1 are both GPCRs. GPCRs are plasma membrane-bound glycoprotein receptors that interact with heterotrimeric guanine nucleotide binding proteins called G-proteins that are involved in the regulation of cellular processes through the transduction of extracellular stimuli to intracellular signals (Kroeze *et al.*, 2003).

1.9.3.1 ChemR23

ChemR23 (also known as chemokine-like receptor 1), is a receptor for both the chemoattractant adipokine chemerin and RvE1. ChemR23 has two isoforms A and B, (A: 373 amino acids, B: 371 amino acids) with predicted molecular weights (MWs) of 42.3 kDa and 42.0 kDa, respectively. Whether there is differing functions and expression patterns between the two isoforms of ChemR23 is unknown. ChemR23 has been shown to be expressed in human T lymphocytes and macrophages (Arita *et al.*, 2005), human skeletal muscle cells (Sell *et al.*, 2009), and human platelets (Dona *et al.*, 2008, Fredman *et al.*, 2010). Interestingly in murine macrophages ChemR23 messenger ribonucleic acid (mRNA) expression was increased after LPS stimulation. ChemR23 mRNA expression was shown to be increased in the colons of murine colitis models compared to control mice *in vivo* (Ishida *et al.*, 2010). When the ChemR23 transfected HEK293 were treated with pertussis toxin, the RvE1 mediated extracellular signal regulated kinase (ERK) phosphorylation was inhibited, this suggests ChemR23 coupling to Gai/o (Arita *et al.*, 2005). RvE1 has been shown to promote phosphorylation of (ERK) mitogen-activated protein kinase (MAPK) in human monocytes and ChemR23 transfected human embryonic kidney (HEK) 293 epithelial cells.

Chemerin was the initial ligand identified to bind to ChemR23. Chemerin promotes chemotaxis of all leukocyte populations that express ChemR23 (dendritic cells and macrophages), (Wittamer *et al.*, 2004, Luangsay *et al.*, 2009, Vermi *et al.*, 2005, Parolini *et al.*, 2007, Demoor *et al.*, 2011). In human models chemerin has been shown to promote the chemotaxis of immature dendritic cells (DC) and macrophages and inhibit PMN chemotaxis (Wittamer *et al.*, 2003, Vermi *et al.*, 2005). There is also evidence that chemerin functions as an adipokine regulating adipogenesis and adipocyte metabolism (Goralski *et al.*, 2007, Muruganandan *et al.*, 2011) via ChemR23 mediated pathways.

RvE1 binding to ChemR23 was demonstrated through tritium-labelled RvE1 ligand binding studies. EPA and 18R-HEPE did not specifically bind to ChemR23 (Arita *et al.*, 2005). Unlike chemerin, RvE1 was not able to evoke a change in extracellular acidification rate in ChemR23 transfected HEK293 cells, thus suggesting that RvE1 could induce a different signalling cascade upon binding to its receptor (Arita *et al.*, 2005). RvE1 also inhibited TNF- α stimulated NF- κ B activation via ChemR23 in ChemR23 transfected HEK293 cells (Arita *et al.*, 2005). Interestingly both RvE1 and chemerin have been shown to induce ALPI expression in the ChemR23 expressing human CRC cell line Caco2 (Campbell *et al.*, 2010). RvE1 induced epithelial expression of ALPI was shown to be protective against sodium dextran sulphate (DSS)

induced colitis in a mouse model, possibly through the detoxification of bacterial endotoxin. RvE1 and chemerin have also been shown to induce the expression of CD55 in the ChemR23 transfected KB oral epithelial cell line *in vitro*. This induction in CD55 expression was shown to promote the clearance of PMNs across the epithelial surface thus facilitating the resolution of inflammation (Campbell *et al.*, 2007).

1.9.3.2 BLT1

BLT1 (also known as LTB₄ receptor 1/ chemoattractant receptor like-1/ G-protein coupled receptor 16/ P2Y purinoceptor 7), is a receptor for the potent inflammatory lipid LTB₄. BLT1 is 352 amino acids long and has a predicted MW of 37.6 kDa. It has been shown to be expressed primarily in granulocytes (Pettersson *et al.*, 2000, Dasari *et al.*, 2000, Kebir *et al.*, 2012). The major function of LTB₄ is in the recruitment and activation of leukocytes (Ford-Hutchinson *et al.*, 1980). There are two different GPCRs for LTB₄ called BLT1 and BLT2. LTB₄ binds to BLT1 with greater affinity than BLT2 (Yokomizo *et al.*, 2000). However RvE1 does not interact with BLT2. RvE1 was shown to induce intracellular calcium levels in human peripheral blood monocytes (PBMCs) but at about one third that of LTB₄. Interestingly pre-treatment of human PBMCs with RvE1 inhibited the LTB₄ induced raised intracellular calcium. Furthermore RvE1 was shown in an *in vitro* cell model to block LTB₄ dependent NF-κB activation, (Arita *et al.*, 2007). These competitive substrate binding studies support RvE1 as a partial BLT1 agonist.

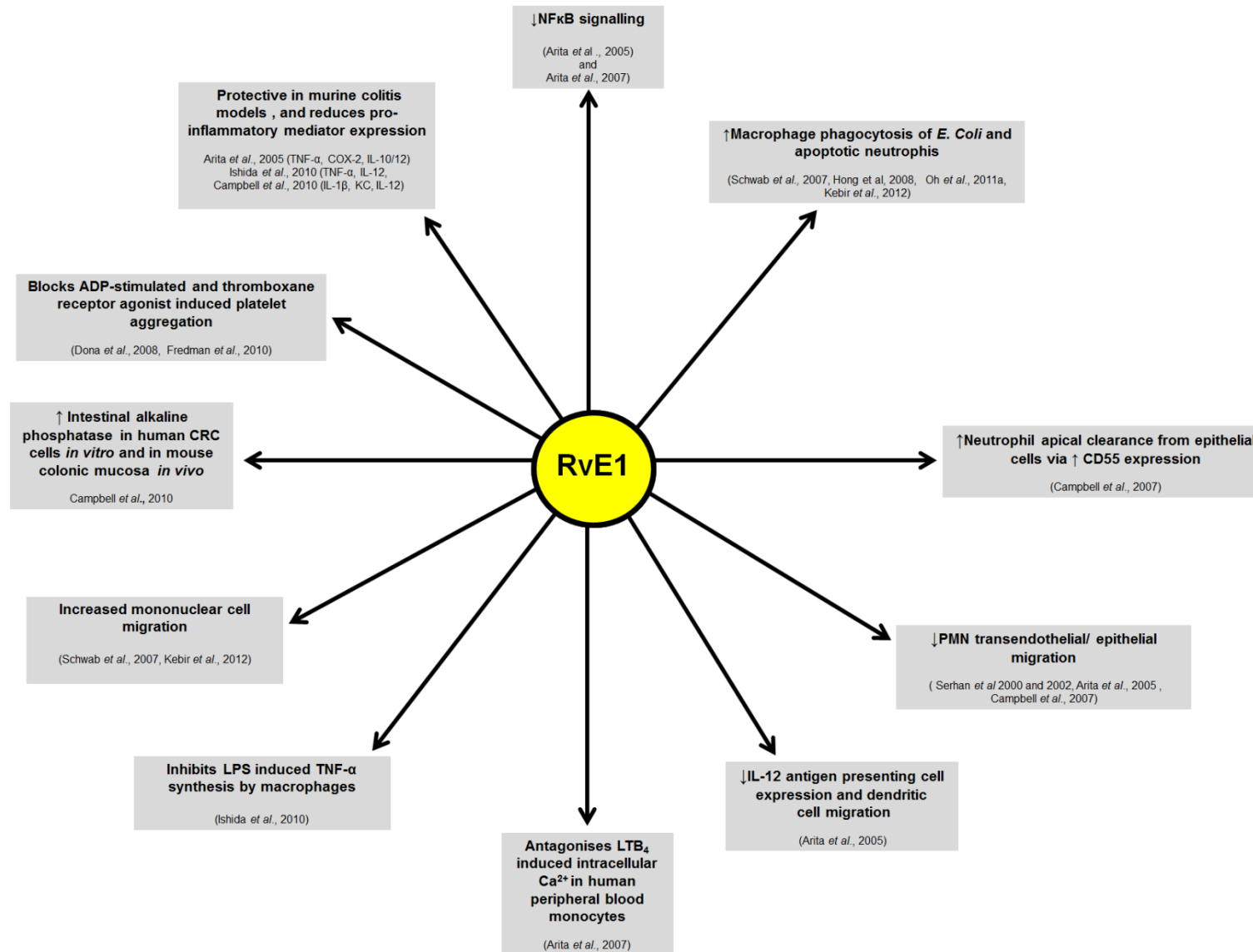


Figure 7. The biological effects of RvE1.

2 Aims and Hypotheses to be tested

2.1 A potential role for Resolvin E1 in colorectal cancer treatment

The mechanism of actions for EPA's anti-CRC activity are not completely known. The role of EPA derived RvE1 as a potential anti-CRC agent had not been previously investigated at the time of writing this thesis. Exogenous RvE1 has been shown to attenuate chemically induced colitis in several mouse models with concomitant reduction in the synthesis of pro-inflammatory cytokines such as TNF- α (Ishida *et al.*, 2010, Campbell *et al.*, 2010). Constitutively activated NF- κ B has been shown to be present over half of CRCs (Lind *et al.*, 2001) In the distal colon of a sodium dextran sulphate (DSS) murine colitis model, RvE1 inhibited the phosphorylation of NF- κ B at serine residue 276 (Ishida *et al.*, 2010), and up regulated the expression of ALPI (Campbell *et al.*, 2010). Such protective anti-inflammatory effects for RvE1 *in vivo*, support a possible beneficial role that requires investigating in an inflammatory environment like CRC. The RvE1 receptor ChemR23 has been identified to date in two different human CRC cell lines T84 and Caco2 in both cell lines (Campbell *et al.*, 2010). At the time of writing there has been no published work investigating ChemR23 expression in human clinical CRC samples.

BLT1 receptor expression was shown both *in vitro* by human CRC cell lines (Caco2 and HT29) and in clinical human CRC tissue samples (Ihara *et al.*, 2007). This group showed that there was BLT1 expression by both the malignant epithelium and the immune cell infiltrate (10 out of 10 different samples). They also showed that BLT1 was not present in normal human CR epithelium (ten cases), with expression present in eight out of the ten CR adenomas examined. There was reduced BLT1 expression in the adenomatous tissue compared to that of CRC. The ERK pathway also known as the MAPK pathway when activated is involved in several cellular function such as cell proliferation, survival and motility. Disturbance of this pathway has been shown in several cancers including CRC. Ihara *et al.*, (2007) showed LTB₄ induced activation of ERK signaling in the Caco2 cell line was blocked by the BLT1 antagonist U75302. One possibility is that RvE1 may act as a partial antagonist, blocking LTB₄-BLT1 signaling in CRC.

The RvE1 mediated effects on the inhibition of adenosine diphosphate (ADP) and TX mediated platelet aggregation could potentially influence colorectal carcinogenesis (Dona *et al.*, 2008, Fredman *et al.*, 2010). Interestingly recent findings have shown that

aspirin taken at a dose of at least 75 mg (anti-platelet dose) reduces the incidence and mortality of cancers such as CRC (Rothwell *et al.*, 2010 & 2011).

Two of the enzymes required for the synthesis of RvE1, COX-2 and 5-LOX have been shown to be over-expressed in human CRC tissue. However LTA₄H and its metabolite LTB₄ have not been directly investigated in human CRC tissue to date, but have been shown to be expressed *in vitro* by human CRC cells (Dias *et al.*, 1992, Jeong *et al.*, 2009, Guillen-Ahlers *et al.*, 2011). As human CRCs over- express COX-2 and 5-LOX, RvE1 could feasibly be synthesised from EPA in CRC tissue, or via the CYP pathway without the need for an aspirin acetylated COX-2 enzyme.

This work is the first looking to establish whether RvE1 could play a part in the anti-CRC effects of EPA.

2.2 Hypothesis

RvE1 synthesised within CRC (epithelium and/ or macrophages), can inhibit CRC cell proliferation, and induce cancer cell apoptosis, through ChemR23 and/ or BLT1 receptor signaling.

2.3 Aims

- i. To investigate whether the receptors for RvE1, ChemR23 and BLT1 are expressed in human CRC tissue.
- ii. To determine whether human CRC epithelial cells and /or macrophages alone or by transcellular synthesis, can synthesise RvE1 from EPA *in vitro*.
- iii. To develop and use an *in vitro* cell culture model to determine whether RvE1 can exert a direct effect on CRC cell proliferation and/ or apoptosis.

3 Characterisation of BLT1 and ChemR23 expression in human colorectal cancer samples and *in vitro* models

3.1 Introduction

BLT1 and ChemR23 receptor expression in human CRC needs investigating. *In vitro*, BLT1 and ChemR23 have been reported to be expressed by THP-1 cells (a human acute monocytic leukaemia cell lines), (Hashidate *et al.*, 2010) and Jurkat cells (human T-cell lymphoma cell line), (Novus Biologicals® NB100-92428 antibody data sheet) respectively, with neither receptor reported to be expressed by HEK293 cells (Chen *et al.*, 2004, Arita *et al.*, 2005). The candidate therefore used the THP-1 cells as a positive control for the *in vitro* BLT1 studies and Jurkat cells as positive controls for the ChemR23 *in vitro* studies. The HEK293 cells were used as a negative control for both BLT1 and ChemR23 *in vitro* studies.

In respect to BLT1 expression in CRC tissue, there has been one published study to date (Ihara *et al.*, 2007). The authors commented that BLT1 was expressed in immune cell infiltrates and by the CRC epithelium; however they only examined ten cases. The authors also commented that none of the normal colon tissues expressed BLT1 and that eight out of ten adenomas expressed BLT1, but the BLT1 expression was weaker than that seen in the CRC epithelium. There were no descriptions of heterogeneous expression of BLT1 in the CRC samples and no comment as which specific immune cell types were staining, and no discussion of whether there was any correlation between BLT1 expression and the clinicopathological details of the patients.

There is no published evidence demonstrating ChemR23 expression in human CRC tissue. In other cancer types, publications are limited to investigating its role in the recruitment of anti-tumour natural killer cells in a murine melanoma model, where ChemR23 expression was associated with tumour growth inhibition (Pachynski *et al.*, 2012). Murine ChemR23 expression by tumour infiltrating and peritoneal macrophages has been confirmed (Rama *et al.*, 2011). They also showed that ChemR23 expression was increased in J744A.1 monocyte/macrophage cells by both tumour cells (4T1 mammary cancer cells) and fibroblasts (3T3-L1), with an associated chemerin (ChemR23 agonist) induced expression of pro-inflammatory cytokines such as IL-1 β and TNF- α (Rama *et al.*, 2011). A study also described ChemR23 single-nucleotide polymorphism (SNPs) rs1878022 was associated with a worse overall survival in stage III or IV non-small lung cancer, however no examination of ChemR23 protein expression or function was explored by the authors (Wu *et al.*, 2011). ChemR23 protein

expression has been reported in two human CRC cell lines T84 and Caco2 to date (Campbell *et al*/ 2010), with BLT1 protein expression shown in the Caco2 and HT29 cell lines (Ihara *et al.*, 2007). At the time of writing this thesis there has been no published work investigating ChemR23 expression in human CRC.

In view of the limited data for both BLT1 and ChemR23 expression in human CRC, expression was examined for in a panel of seven human CRC cell lines at both the mRNA and protein level. On confirming the specificity of the antibodies used in the protein expression studies *in vitro*, an immunohistochemical study looking at BLT1 and ChemR23 protein expression and receptor localisation was carried out by the candidate in a series of human CRC tissue specimens.

3.1.1 Aims

Characterisation of ChemR23 and BLT1 expression in human CRC tissue and in a panel of human CRC cell lines *in vitro*. Identify an appropriate human CRC cell line(s) so that *in vitro* RvE1 biological activity could be investigated.

3.2 Materials and Methods

3.2.1 Cell culture

3.2.1.1 Media and growth requirements

Human CRC cell lines HCA7, LoVo, T84, HRT18, HT29, Caco2 and SW480, human lymphocyte cell lines Jurkat (T-cell) and Raji (Burkitt's lymphoma B lymphocyte) cell lines used for 5-LOX and FLAP studies in Chapter 4) and the HEK293 cell lines were obtained from the European Collection of Cell Cultures (ECACC), Porton Down, United Kingdom (UK). THP1 (human acute monocytic leukaemia cell line) cells were gifted by Dr. Peter Laslo (Myeloid differentiation group, Leeds Institute of Cancer & Pathology, University of Leeds). HCA7, HRT18, HT29, Caco2, SW480, Raji, Jurkat, THP-1, and HEK293 cell lines were cultured in sterile RPMI 1640 with GlutaMAX™-I (Gibco® by Life Technologies; Cat. No. 61870-010) and 10% (v/v) foetal bovine serum (FBS). LoVo cells were cultured in F-12 with GlutaMAX™-I nutrient mixture (Ham) 1X (Gibco® Life technologies; Cat. No.31765-027) and 10% (v/v) FBS. T84 cells were cultured in Dulbecco's modified eagle's medium nutrient mixture F-12 Ham (Sigma®, Life Science; Cat. No. D8437) and 10% (volume (v/v) FBS. Cells were grown on sterile tissue culture treated non-pyrogenic polystyrene culture flasks (Corning Incorporated costar®,

United Kingdom [UK]) at 37°C in the presence of 5% CO₂. Cells were passaged at 70 to 80% confluency.

3.2.1.2 Passaging of the cell lines

Cells were passaged by removing cell culture medium from cells, rinsing with sterile Dulbecco's phosphate buffered saline (DPBS), (Gibco® by Life Technologies™ without calcium and magnesium; Cat. No. 14190-094), three times, and incubating with 0.05% (w/v) trypsin and 500 micromolar (µM) ethylenediaminetetraacetic acid (EDTA), (Gibco® by Life Technologies™) in sterile PBS at 37°C for five to ten minutes. Detached cells in trypsin solution were then placed in an equal volume of cell type specific culture medium and centrifuged at 400 gravitational force (*g*) for five minutes at 25 degrees centigrade (°C) in a 50 millilitre (mL) non pyrogenic sterile 50 mL tube (Corning Incorporated costar®, UK; Cat. No.430828). Cell pellets were either used for ribonucleic acid (RNA) isolation, or re-suspended in cell specific medium and counted (section 3.2.1.3) for further analysis, or used directly for passaging. Raji and THP-1 cells were suspension growing cells, and were seeded at 1x10⁶ cells/ mL and passaged when at a cell density of 3x10⁶ cells/ mL. Cells were used for up to a maximum of ten passages.

3.2.1.3 Viable cell counting

Cells were harvested from tissue culture flasks as described (3.2.2.1). The cell pellet was re-suspended in cell specific medium. A volume of 100 microliters (µL) of a cell suspension was mixed with an equal volume of 0.4% (v/v) trypan blue (Sigma-Aldrich, Poole, UK) in sterile DPBS. Cell viability was assessed using an improved Neubauer haemocytometer and exclusion of 0.4% (v/v) trypan blue, with viable cells being unstained and non-viable being stained. Cells were counted in four large corners (X20 magnification) on each of the grids and an average number was calculated.

3.2.2 Gene expression analysis

3.2.2.1 Sample preparation

Human cell lines were grown to 70% confluence in sterile tissue culture treated non-pyrogenic six well plates. The cells were then washed three times with sterile DPBS (1X) before being trypsinised (see section 3.2.3.1).

3.2.2.2 Ribonucleic acid extraction

Cells were pelleted at <1 x 10⁷ cells/ mL and total RNA was extracted using an RNeasy® Mini Kit (Qiagen, Crawley, UK; Cat. No.74104.) using the manufacturer's protocol. The concentration of the extracted RNA was then automatically calculated by

the quantified NanoDrop spectrophotometer (ND-1000 with version 3.3 software) at 260nm and 280nm).

3.2.2.3 First strand complementary deoxyribonucleic acid synthesis

First strand complementary deoxyribonucleic acid (cDNA) synthesis was carried out using a Superscript™ III First-Strand Synthesis SuperMix (Invitrogen, Life Technologies, Paisley, UK; Cat No. 11752-050) using the manufacturer's protocol. Total RNA used in a transcription reaction was standardised at 500 ng across all samples. The samples were then stored at -20°C until use. Samples without reverse transcriptase (RT) were also prepared to serve as 'RT-' negative controls.

3.2.2.4 Detection of gene expression by quantitative polymerase chain reaction

Commercial TaqMan primers/ probes for the quantitative polymerase chain reaction (qPCR) were obtained from Life Technologies (UK). Target genes were ChemR23 and BLT1 and the housekeeping gene control was β -actin (Table 2). The nucleotide sequence region amplified by the TaqMan gene expression assays were searched within the NCBI BLAST® resource to confirm the specificity of the respective assay for the target gene (Table 1). All PCR reactions were carried out in a 10 μ L reaction volume, in a sample well of an optical 96-well reaction plate (Life technologies, Applied Biosystems, MicroAmp™; Cat.No.4306737).

A master PCR mixture was prepared. In brief this contained TaqMan Universal Master Mix (MM)II (2X) with uracil N-glycosylase (UNG) and TaqMan gene expression assay (20X) containing the primers (one in ten dilution, of TaqMan gene expression assay to TaqMan Universal MM with UNG, respectively). The candidate used a one in four dilution of BLT1 cDNA to nuclease free water (Severn Biotech Ltd, Cat.No. 20-9000-01) and a one in two dilution for the ChemR23 study. This dilution of cDNA to nuclease free water (for both BLT1 and ChemR23) achieved housekeeping gene (β -actin) cycle threshold (Ct) values that ranged between 15 and 20 (Ct discussed below).

Each qPCR 10 μ L reaction volume was made up of 5.5 μ L (Master PCR mixture) and 4.5 μ L (cDNA and Nuclease free water), (Table 2). The plate was covered with a MicroAmp™ optical adhesive film (Life technologies, Applied Biosystems, MicroAmp™; Cat.No.4306737), then loaded into the 7900HT Fast real time PCR system (Life Technologies, Applied Biosystems, UK). Each experiment began with heating to 50°C for two minutes followed by ten minutes at 95°C to begin denaturation. This was followed by 40 repeat amplification cycles of heating to 95°C for 15 seconds followed by cooling at 60°C for one minute for primer annealing and elongation. Each sample was run in triplicate. Negative controls included no template cDNA reactions as well as RT-samples to rule out reaction mixture and genomic DNA contamination respectively.

SDS software version 2.3 (Life Technologies, Applied Biosystems, UK) was used to analyse qPCR reaction.

A Ct value was obtained when there was exponential amplification in the linear phase of the DNA of interest. Delta (Δ) Ct values were calculated by subtracting the Ct value of the target gene (BLT1 or ChemR23) from that of the housekeeping gene, β -actin.

TaqMan assay details	Species	Context nucleotide sequence	Amplicon length	Nucleotide sequence searched	Cross-reactivity search
BLT1 Hs00175124_m1	Human	GCCAAAGCTTGTAGTC CTCCCGAC	76	ttggca cagctccaaccagttcct gccaaagcttgaagtcctccc gac ggccatgaacactac atctctgcagcaccctcacta ggtgtagagttcatctctg	BLT1 identified as match
CD55 Hs00892618_m1	Human	GCCAGAGTGCAGAGAA ATTTATTGT	98	ttattcaggcagctctgccagtgg agtgaccggt gccagagtcag agaaattattgt ccagcaccacc acaaattgacaatggaataattca ag	CD55 identified as match
ChemR23 Hs01081979_s1	Human	ATGCTTCTGGGAGGC CAGCCTTGA	73	ccatacagccttgactagcaattt atgcttctgggagccagcctt gactgactcaagcaaaaagg aagaa	ChemR23 identified as match
IAP Hs00357579_g1	Human	GAGAGCGAGAGCGGGA GCCCGATT	56	accagacgtgaat gagagcgag agcgggagccccgatt accag cagcaggcg	IAP identified as match

Table 1. TaqMan gene expression assay details

The context sequence is the nucleotide sequence around the TaqMan probe.

PCR reaction mix	Single 10 μ L reaction
20X Taqman gene expression assay	0.5
2X Taqman gene expression master mix	5
cDNA template	1.125-2.25
RNase-free water	2.25-3.375

Table 2. TaqMan gene expression assay reaction contents

3.2.3 Western blotting

3.2.3.1 Sample preparation and protein extraction

Human cell lines were grown to 70-80% confluence in T75 cm² culture flasks. Cells were washed twice with sterile PBS. Cells were lysed with 1 mL of radio-immunoprecipitation assay (RIPA) buffer (50 mL solution containing 50 mM Tris-HCl, pH 8.0, with 150 mM sodium chloride, 1.0% Igepal CA-630 (NP-40), 0.5% sodium deoxycholate, and 0.1% sodium dodecyl sulphate [SDS]) containing protease inhibitor (One Complete[®] protease inhibitor cocktail tablet; Boehringer Mannheim, Lewes, UK), for 10 minutes (on ice). Cells were scraped off and placed in a Qiashredder column (QIAGEN, Crawley, UK, Cat No. 79654) and centrifuged for two minutes at $\geq 8000 \times g$. The protein lysates were then stored at -80°C prior to protein quantification.

3.2.3.2 Quantification of protein in cell extract

Protein concentration was determined using the Bio-Rad DC protein assay (BIO-RAD Laboratories, Richmond, CA, USA), a modification of the Lowry assay (Lowry et al., 1951). Following the manufacturer's instructions, serial dilutions of Bovine Serum Albumin (BSA) ranging from 0 to 2.0 mg/ mL of protein were prepared to construct a standard curve. Three serial dilutions of human cell lysates were prepared (neat, 50% v/v with RIPA buffer and 20% v/v with RIPA buffer). Five microlitres of standard or sample were placed into a clean, dry microtiter plate. A volume of 25 μ L of reagent A' (25 μ L reagent S added to 1 mL reagent A) was added to each well (samples were analysed in duplicate). Then 200 μ L of reagent B was placed into each well. After 15 minutes the optical density (OD) was measured in each sample at a wavelength of 630 nm using a plate reader (Dynex Technologies OpsysMR). The Dynex Technologies Revelation QuickLink version 4.04 software was used to calculate a calibration curve and determine the protein concentration of the cell lysates. The western blotting (WB) studies on BLT1 and ChemR23 used 20 μ g and 30 μ g protein concentrations.

3.2.3.3 Sodium dodecyl sulfate polyacrylamide gel electrophoresis of proteins

Protein lysates were mixed one in four with NuPAGE lithium dodecyl sulphate (LDS) Sample Buffer 4X (4% [v/v] pH 8.4, glycerol [v/v] 40-70% and 1% [v/v] β -2 mercaptoethanol [Life Technologies]). Samples were denatured by heating to 102°C for five minutes and cooled on ice prior to polyacrylamide gel electrophoresis (PAGE) electrophoresis. A 12% SDS-PAGE gel (NuPAGE Novex 12% Bis-Tris Gel 1.0 mm, 10 well) was placed into the gel/buffer core assembly unit and loaded into an Invitrogen XCell SureLock™ Mini-Cell. A total of 500 mL of running buffer, containing 475 mL de-ionised water and 25 mL NuPAGE® MOPS SDS running buffer 20X (pH 7.7, 50 mM MOPS, 50 mM Tris Base, 0.1% SDS, 1 mM EDTA [Invitrogen, United States of America (USA), Cat. No. NP0001]) was placed in the Invitrogen Mini-Cell. The denatured samples, as well as the molecular weight (MW) standard (ColorPlus Pre-stained Protein Marker, Broad Range 7-175 kDa [New England Biolabs, Cat. No. P7709S] mixed 25% v/v with a second protein marker, MagicMark™ XP Western Protein Standard [Invitrogen, Cat. No. LC5602]) were then loaded (10 μ L volume) into individual sample wells (samples at equal protein amounts). The electrophoresis chamber was sealed and electrophoresed at 150 volts (V) for 90 minutes.

3.2.3.4 Transblotting of sodium dodecyl sulfate polyacrylamide gel electrophoresis separated proteins

Resolved proteins were then transferred onto a polyvinylidene difluoride (PVDF) membrane (Thermo SCIENTIFIC, Rockford, USA; Cat.No.88518) by wet electrophoretic transfer. A PVDF and four pieces of Trans-Blot® filter paper (BIO-RAD Laboratories, Richmond, CA, USA Mini; Cat.No.1703932) were cut to the size of the gel and soaked first in 100% methanol for 30 seconds and then transfer buffer containing 375 mL de-ionised water, 100 mL 100% methanol and 25 mL of NuPAGE® transfer buffer 20X (Glycerol 190 mM, Bis-Tris 500 mM, EDTA 20 mM, Serva Blue G250 0.75 mL 1% [v/v] solution, phenol red 0.25 mL 1% [v/v] solution, ultrapure water, pH 8.5 [Invitrogen, USA, Cat. No. NP0006-1] for ten minutes. The membrane and gel flanked on either side by two sheets of Trans-Blot® filter paper were then placed into the electrophoretic transfer cell (Invitrogen XCell II™ Blot Module) and the tank filled with transfer buffer 1X. The outside of the tank was filled with cold water. A constant current of 350 millamperes was applied for 60 minutes.

3.2.3.5 Immunoblotting of proteins

PVDF membranes were incubated in blocking buffer (0.05 % [v/v] PBS-NP40 [Fluka Analytical, USA] and 5% [w/v] dried skimmed milk) for one hour at room temperature. The primary antibodies (ChemR23 and BLT1 see Table 3) were diluted in 0.05% [v/v] PBS-NP40 and 1% [w/v] dried skimmed milk overnight at 4°C. The protein loading controls used were either anti- human β -actin or mouse anti-human α -tubulin antibodies which were incubated for one hour at room temperature. Primary antibody concentrations were used at a concentration recommended on the product data sheet. BLT1 antibody dilution used (1 in 1000), was that published by Ihara *et al.*, 2007. After incubation the membranes were washed three times in blocking buffer for five minutes, at room temperature. The membranes were then incubated for one hour at room temperature with an appropriate horseradish peroxidase (HRP)-conjugated secondary antibody (see Table 3) in 0.05% [v/v] PBS-NP40 and 1% [w/v] dried skimmed milk. The membrane was then washed three times in blocking buffer for five minutes at room temperature.

3.2.3.6 Visualisation of antibody-reactive proteins

Proteins of interest were visualised using chemiluminescent substrate from Thermo SCIENTIFIC (SuperSignal[®] West Pico Chemiluminescent Substrate [Cat No. 34079]), following the manufacturer's instructions (standard chemiluminescent) and then SuperSignal[®] West Femto Chemiluminescent Substrate [Cat.34094]) referred to as 'high sensitivity chemiluminescence' if no signal detected with the standard chemiluminescent.

3.2.3.7 Densitometric analysis

Resolved protein signal intensity for ChemR23 and BLT1 and the protein loading controls β -actin or α -tubulin were measured using BIO-RAD Image Lab 4.1 software. Adjusted volume intensity (sum of intensity of pixels multiplied by pixel area in millimeter (mm)²) were calculated for each ChemR23 and BLT1 resolved protein band for each individual cell line tested and divided into the corresponding resolved protein loading control band for that blot. This allowed semi-quantitation of the ChemR23 and BLT1 protein expressed in each cell line.

3.2.3.8 Transmembrane protein extraction

To extract the transmembrane proteins from the human cell lines (to determine for BLT1 and ChemR23 expression), the Novagen[®] ProteoExtract[®] Transmembrane Protein Extraction Kit was utilised (Cat. No. 71772-3). The extraction was performed according to manufacturer's instructions. In brief HEK293 cells and Caco2 cells were

grown to 70-80% confluency in a T75 cm² culture flask. The culture medium was removed from the cells. The cells were then washed twice DPBS at 4°C. DPBS was then added to the culture flask at a volume of 3 mL. The cells were then scraped off using a cell scraper, and placed into a 15 mL falcon tube. Next the cells were centrifuged at 1000 x g for five minutes (at 4°C). The cells were then placed in 1 mL of manufacturer's Extraction Buffer 1 and 5 µL of Protease Inhibitor Cocktail Set III. The resuspended cells were then incubated for ten minutes at 4°C with gentle agitation. Following this the cells were centrifuged for five minutes at 1000 x g (4°C). The supernatant was then carefully removed and stored on ice as the cytosolic protein fraction. The remaining cell pellet was resuspended in manufacturer's Extraction Buffer 2A and 5 µL of Protease Inhibitor Cocktail. The suspension was then incubated for 45 minutes at room temperature with gentle agitation, before centrifuging at 16,000 x g for 15 minutes at 4°C. The supernatant was then transferred to a fresh falcon tube and protein quantified and analysed for ChemR23 as discussed in this section.

3.2.4 Immunofluorescence

Caco2 CRC cells were grown on sterile glass cover slips in six well plate to either 50% or 100% cell confluency. The cells were then washed three times with sterile DPBS. The cells were then fixed in 4% paraformaldehyde (PFA) for 20 minutes at room temperature. The 4% PFA was then removed and the cell were washed with sterile PBS for five minutes. The cells were then used for immunofluorescence studies.

Immunofluorescence (IF) was performed using ChemR23 (Bioss Cat. No bs2530R). Cells were blocked with antibody diluent reagent solution (Invitrogen Cat no, 003218) which was tipped off immediately. The coverslips were then incubated with primary antibodies diluted in TBS for one hour at room temperature. Anti-ChemR23 was used at a dilution of 1 in 50. A no-primary control was included. The cells were then washed with TBS-Tween (TBLS-T) (2 x 5 minutes), then TBS (1 x 5 minutes). The cells were then incubated for 1 hour in the dark with fluorescein isothiocyanate (FITC)-conjugated secondary antibodies (donkey anti-rabbit, Alexa Fluor[®]488 (Invitrogen) diluted in TBS at a 1 in 300 dilution) at room temperature, under the cover of tinfoil, in order to block out all of the light. Cells were then washed with TBS-T (2 x 5 minutes), then TBS (1 x 5 minutes). The cells were then mounted in ProLong[®] Gold anti-fade with 4,6-diamidino-2-phenylindole (DAPI) (Cell signaling Technology Cat No 8961). IF was visualized using a Zeiss AxioScope microscope and images were processed using the Axiovision 4.4 software. Representative images were taken using the appropriate optimal exposure time settings, assessed on the positive control cells (100% confluent Caco2 cells). Establishing the settings this way meant that semi-quantitative differences between the human cell lines tested could be ascertained.

Antibody	Type	Dilution used	Manufacturer details	Laboratory technique used	Chapter
Anti- α -tubulin	Mouse monoclonal IgG	1/5000	Sigma-Aldrich Cat. No T5168	Western blotting	Chapters 3,4 and 5
Anti- β -actin	Mouse monoclonal IgG	1/5000	Sigma-Aldrich Cat. No A5441	Western blotting	Chapter 4 (5-LOX)
Anti-BLT1	Rabbit polyclonal IgG	1/1000 1/1500	Cayman Chemical Cat. No 120114	Western blotting Immunohistochemistry	Chapters 3 and 5
Anti- ChemR23	Rabbit polyclonal IgG	1/1000	Abcam Cat. No. ab64881	Western blotting	Chapter 3
Anti- ChemR23	Rabbit polyclonal IgG	1/500 1/25	Bioss Cat. No bs2530R	Western blotting Immunohistochemistry	Chapters 3 and 5
Anti-ChemR23	Rabbit polyclonal IgG	1/1000	Novus Biologicals Cat. No. NB100-92428	Western blotting	Chapter 3
Anti-COX-2	Goat polyclonal IgG	1/250	Santa- Cruz Cat.No. sc-1745	Western blotting	Chapter 4
Anti-FLAP	Rabbit monoclonal IgG	1/1000	Novus Biologicals Cat. No. NBP1-95197	Western blotting	Chapter 4
Anti-5-LOX	Rabbit polyclonal IgG	1/250	BD Transduction Lab Cat. No. 610695	Western blotting	Chapter 4
Anti-goat HRP	Rabbit anti-goat IgG	1/2000	Dako Cat. No. P0449	Western blotting	Chapter 4
Anti-mouse HRP	Rabbit anti-mouse IgG	1/2000	Dako Cat.No P0260	Western blotting	Chapters 3,4 and 5
Anti-rabbit HRP	Swine anti-rabbit IgG	1/2000	Dako Cat. No. P0217	Western blotting	Chapters 3,4 and 5

Table 3. Antibody details for western blotting and immunohistochemistry studies.

Antibody details including species antibody raised in, antibody dilution used in experimentation and manufacturers details.

3.2.5 Immunohistochemistry

3.2.5.1 Ethical approval

Ethical approval for the collection of clinicopathological data and archival formalin fixed paraffin embedded human CRC specimens was obtained from the National Research Ethics Service (NRES) Committee Yorkshire & The Humber- Leeds Central REC reference 11/YH/0157 (Appendix 1 for approval letter).

3.2.5.2 Specimen collection and clinicopathological data

Formalin-fixed, paraffin-embedded (FFPE) tissue blocks of human CRC were selected from the histopathology archives at St. James's University Hospital, Leeds, UK.

3.2.5.3 Clinicopathological data

The patients' age, size of cancer in centimeters (cm), site of cancer (proximal or distal to the splenic flexure), grade of differentiation (poor, moderate or well), pathological (p) tumour (T) and nodal (N) stages and whether there was histological vascular invasion present were obtained.

3.2.5.4 BLT1 and ChemR23 immunohistochemistry

3.2.5.4.1 BLT1

FFPE sections (5 µm) were mounted on Thermo Scientific™ Superfrost™ Plus microscope slides. Sections were dewaxed in xylene (3 x 5 minutes) and rehydrated through a series of ethanol washes (3 x 5 minutes). The sections were then rinsed in running tap water for five minutes before endogenous peroxidase activity was blocked with 0.3% (v/v) hydrogen peroxide in 100% methanol for ten minutes at room temperature. The sections were then rinsed in running tap water for five minutes. The sections were then blocked with antibody diluent reagent solution (Invitrogen Cat no, 003218) to block non-specific binding sites. This blocking agent was then removed after 30 seconds and the primary antibody anti-BLT1 (Cayman Chemical Cat. No 120114) was incubated at room temperature with the tissue at a 1 in 1500 dilution for one hour at room temperature. The sections were then washed in TBS- tween (TBS-T), (2 x 5 minutes) then TBS (1 x 5 minutes). Slides were incubated in anti-mouse horseradish peroxidase (HRP) conjugated polymer secondary antibody (Dako, Cat No. K4001) for 30 minutes. The slides were then washed with TBS-T (2 x 5 minutes) and then TBS (1 x 5 minutes). Then 100 µL of diaminobenzidine (DAB) solution was added to each slide for exactly ten minutes. The sections were then rinsed in tap water for five minutes, and stained with haematoxylin (Solmedia Laboratory Suppliers, Cat No. HST011) for 30 seconds, followed by a one minute rinse in tap water. This was followed

by a wash in Scott's tap water for one minute, and a subsequent one minute rinse in tap water. The slides were dehydrated with graded ethanol (1 x 2 minutes followed by 2 x 1 minute) and xylene (3 x 1 minute), and mounted in diphenylxylene (DPX). The BLT1 antibody was optimised over several antibody concentrations, to obtain the optimal receptor immunostaining in the fixed human CRC tissue.

3.2.5.4.2 ChemR23

ChemR23 immunohistochemistry was also performed on FFPE sections using a rabbit anti-ChemR23 (BIOSS, bs-2530R LOT 130320). The immunohistochemistry was carried out as above except that prior to the blocking for endogenous peroxidase activity, the sections were placed in 10 mM citrate buffer, pH 6.0, and heated to 80°C for ten minutes in a microwave oven and then cooled down for a further 20 minutes and rinsed with tap water.

The ChemR23 antibody was optimised over several antibody concentrations with antigen retrieval to obtain the optimal receptor immunostaining in the fixed human CRC tissue. There were issues with batch availability, sensitivity and specificity issues for the anti-ChemR23 (BIOSS, bs-2530R) which are described further in section 3.4.2.2.

3.2.5.4.3 Controls

A no primary antibody control was included in each IHC run. To address inter-run variability a control slide was included that was present in every independent IHC run.

3.2.5.4.4 Scoring of ChemR23 and BLT1 immunostaining

Immunostaining scores were given to tumour epithelium, tumour stroma, histologically normal epithelium and histologically normal stroma. Normal CR tissue was on the same FFPE block as the CRC; the candidate acknowledges that this was therefore not truly representative of normal CR tissue and that ideally separate matched CR tissue blocks would be required. Separate normal CR tissue blocks were not available to the candidate, so for the purposes of this thesis whilst the candidate makes reference to normal CR epithelium and stroma, the candidate was fully aware of the aforementioned limitation. Receptor expression staining within the cancer epithelium was scored on an intensity scale of 0 to 3 (0= negative, 1= weak, 2= moderate, 3 =strong expression) and a percentage cell population staining (P) scale (0= negative, 1= 1-33%, 2= 34-66%, 3= 67-100%). The intensity and percentage scores were then multiplied to give a total score out of nine (Figure 8). Cancer associated stroma and normal stroma were scored 0-3 (0= negative, 1= weak, 2= moderate, 3 =strong). In respect to the stroma, the % cell population scores were consistent throughout, with a value of 3, hence stroma scores are solely expressed as an intensity value.

Twenty two different sections were scored by two independent observers who were the candidate and a gastrointestinal pathologist Dr. Nicholas P West (NPW), University of Leeds (NPW) to evaluate inter-observer agreement of the scoring. Upon confirmation of at least a moderate strength of agreement for scoring by weighted kappa statistical analysis (a minimum of a moderate strength weighted kappa agreement is recognised to be needed for IHC scoring), the candidate scored the sections independently.

3.2.5.5 Statistical analysis

The statistical significance of observed differences in ChemR23 and BLT1 expression related to CRC location, grade of differentiation, patient age, pT and pN stages and vascular invasion status were tested using the Mann-Whitney U test and Kruskal-Wallis as appropriate. The relationship between ChemR23 and BLT1 stromal, epithelium, stroma-epithelium expression was analysed by Spearman rank correlation coefficient. The relationship between BLT1 and ChemR23 expression between normal and cancer epithelium and between normal and cancer epithelium associated stroma was analysed by the Wilcoxon signed-rank test. Inter-observer concordance between the two-observers for the IHC scoring was measured using the weighted Cohen's kappa (k) coefficient statistic. Statistical significance was assumed if the P value was less than 0.05.

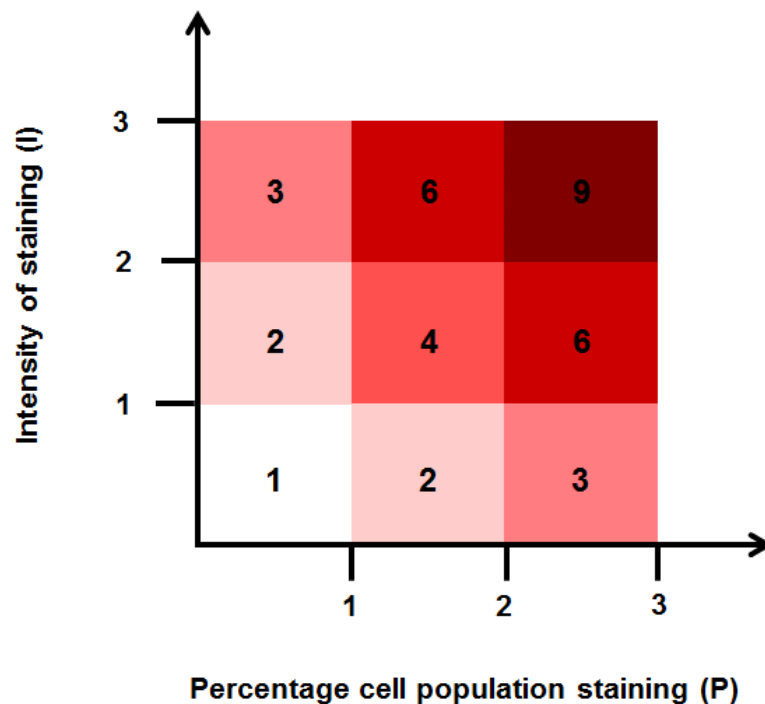


Figure 8. Immunostaining scoring system for BLT1 and ChemR23 protein expression in human CRC epithelium.

3.3 Results (BLT1)

3.3.1 BLT1 expression by human colorectal cancer epithelial cell lines

3.3.1.1 BLT1 mRNA detection in a panel of human colorectal cancer cell lines

BLT1 gene expression was measured by qPCR in seven human CRC cell lines. All cell lines screened expressed BLT1 receptor mRNA at detectable levels, including the cell line HEK293, which was hypothesized to be a negative control. As the negative control HEK293 cell line gave a delta (Δ)-Ct value of 11.5 (SEM 0.1) and the positive control cell line THP-1 gave a Δ -Ct value of 12.3 (SEM 0.4), this suggests that the negative control cell line contains more BLT1 than the positive control cell line. Furthermore the Ct values for BLT1 in all cell lines were greater than 30, and suggestive of only a small amount of BLT1. One possibility is that all cell lines have low BLT1 mRNA and/or the assay is not targeting BLT1 expression. Importantly the NTC and RT- controls gave no signal on the qPCR amplification plot. Mean Ct values for both BLT1 and β -actin with respective SEM are shown in Table 4. Figure 9 shows the small range of expression levels (Δ Ct values) detected in the cell lines.

3.3.1.2 BLT1 protein detection in a panel of human colorectal cancer cell lines

A single resolved protein band in keeping with the BLT1 receptor was confirmed in the positive control cell line THP1 (human acute monocytic leukaemia cell line) at 40kDa using the Cayman Chemicals anti-BLT1 antibody. No protein band was observed in the negative control HEK293 cells and no BLT1 protein band was seen in any of the human CRC cell lines screened under standard chemiluminescence (Figure 10A) or high sensitivity chemiluminescence (Figure 10B). Protein loading was confirmed by probing the PVDF membrane with mouse monoclonal α -tubulin antibody (see Figure 10C).

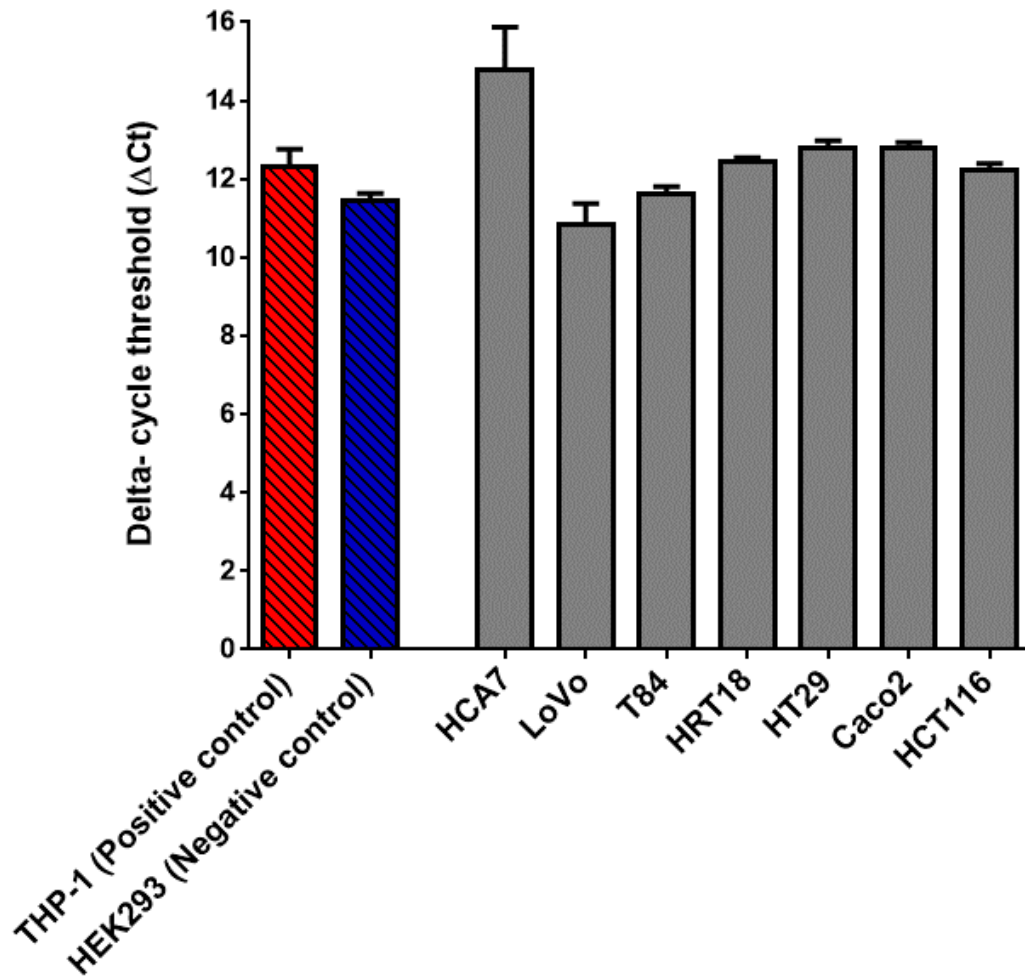


Figure 9. BLT1 mRNA expression in a panel of human CRC cell lines.

BLT1 receptor mRNA expression in a panel of human cell lines. Data collected from three individual independent cell cultures for each cell line, shown as mean delta-cycle threshold (Δ Ct) value with standard error of the mean.

Cell Line	BLT1 mean Ct value	BLT1 SEM	β -actin mean Ct value	β -actin SEM	Mean Δ -Ct value	Δ -Ct SEM
THP-1	31.4	0.2	19.7	1.0	12.3	0.4
HEK293	30.9	0.1	19.4	0.1	11.5	0.1
HCA7	35.0	0.5	20.2	0.7	14.8	0.6
LoVo	30.7	0.4	20.1	0.4	10.9	0.3
T84	31.2	0.2	19.6	0.3	11.6	0.1
HRT18	31.3	0.5	18.9	0.5	12.4	0.1
HT29	32.1	0.4	19.3	0.5	12.8	0.1
Caco2	32.2	0.2	19.4	0.3	12.8	0.1
HCT116	31.6	0.3	19.4	0.3	12.2	0.1

Table 4. Mean cycle threshold (Ct) values for BLT1 and β -actin in the screened panel of human cell lines.

Cycle threshold values were measured in three independently performed experiments for each of the nine human cell lines. Each individual experiment was performed in triplicate. Data shown as mean with standard error of the mean.

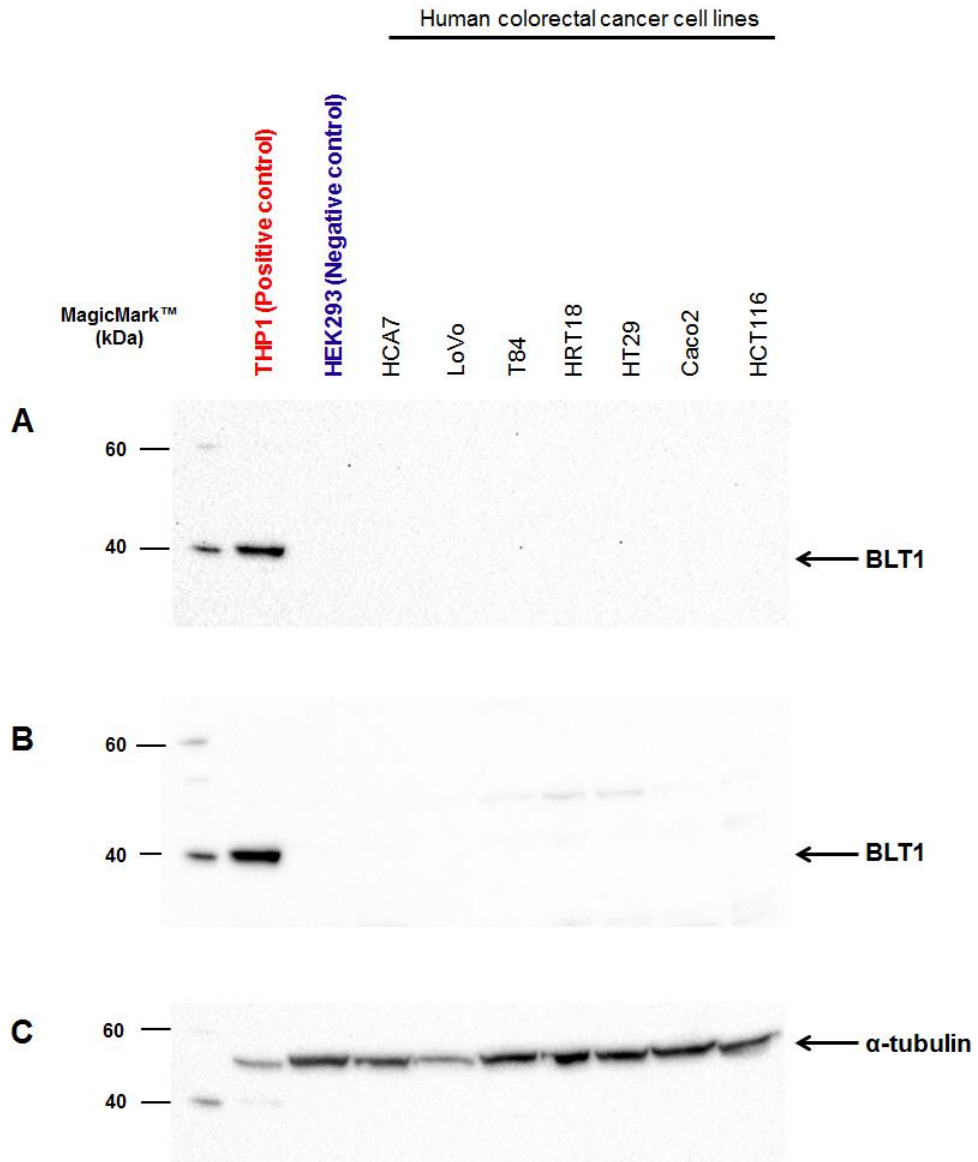


Figure 10. BLT1 protein expression as measured by western blot in a panel of human CRC cell lines.

BLT expression of human cell protein lysate was probed for in a panel of human cell lines. (A) The image was acquired after 180 seconds of standard chemiluminescence. (B) Image after two seconds of high sensitivity chemiluminescence. (C) Protein loading was assessed by probing with mouse monoclonal anti-human α -tubulin antibody (Sigma 1 in 5000), image acquired after one second of standard chemiluminescence. The first lane contains the (chemiluminescent protein ladder) MagicMark™.

3.3.2 BLT1 expression by human colorectal cancer tissue

3.3.2.1 Clinical characteristics of the study population

The clinical characteristics of the study population are summarized in Table 5. The median patient age at diagnosis was 74 years (range 37-93 years). Forty percent of patients had cancers proximal to the splenic flexure, and sixty percent of patients had cancers distal to the splenic flexure. Median size of the cancers was 3.5 cm (range 1.5-10 cm). Cancer differentiation was categorized as either well (3% of cases), moderate (79% of cases) and poor (18% of cases). The tumour stage distribution was pT1 in 4% of cases, pT2 in 9% of cases, pT3 in 56% of cases, and pT4 in 31% of cases. The nodal stage distribution was pN0 in 53% of cases, pN1 in 28% of cases and pN2 in 19% of cases. Presence or absence of vascular invasion was reported in 51% and 49% of cases respectively.

BLT1. Clinico-pathological details of patient cohort	
Characteristics	Number of cases n=78 (%)
Age	
Median age: 74 years	
Age range: 37-93 years	
Location of colorectal cancer	
Proximal to splenic flexure	31 (40%)
Distal to splenic flexure	47 (60%)
Colorectal cancer size	
Median size: 3.5cm	
Size range: 1.5-10cm	
Colorectal cancer cell grade	
Well	2 (3%)
Moderate	62 (79%)
Poor	14 (18%)
Pathological (p) tumour (T) stage	
pT1	3 (4%)
pT2	7 (9%)
pT3	44 (56%)
pT4	24 (31%)
Pathological (p) nodal (N) stage	
pN0	41 (53%)
pN1	22 (28%)
pN2	15 (19%)
Histological presence of vascular invasion	
Absent	38 (49%)
Present	40 (51%)

Table 5. Clinical characteristics of the BLT1 study population

3.3.2.2 BLT1 immunohistochemistry staining and scoring method optimisation

Optimisation of the BLT1 antibody on the human CRC tissue confirmed that a dilution of 1 in 1,500 with no antigen retrieval step gave specific staining in comparison to the no primary control (Appendix 2). There was no positive and negative tissue controls included. However BLT1 is expressed by PMNs and membranous staining was seen in immune type cells in CRC tissue samples (Appendix 3). Inter-observer agreement was confirmed by two independent observers, the candidate and NPW. Twenty-two different human CRC specimens were scored for BLT1 expression in the cancer epithelium and the cancer epithelium associated stroma. Moderate agreement (weighted kappa: 0.544; 95% confidence interval 0.318-0.890) was obtained between the candidate and NPW for the cancer epithelium (Figure 11A), with complete agreement in 14 of the 22 samples scored. It is accepted that moderate weighted Kappa agreement is an acceptable measure of inter-rater agreement.

There was strong agreement (weighted kappa: 0.605; 95% confidence interval 0.328-0.860) for the cancer associated stroma between the between the candidate and NPW (Figure 11B), with complete agreement in 16 of the 22 samples scored. The scoring system was therefore validated and applied to the full panel of samples. A no primary antibody control slide and a primary antibody control slide (positive staining slide from same tissue specimen in each IHC run) was included in each of the four runs required to complete the BLT1 IHC on 78 different CRC tissue samples (Appendix 4 for no primary antibody control images and Appendix 5 for the primary antibody control images, between the different IHC runs).

3.3.2.3 BLT1 expression in human CRC epithelium and histologically normal colorectal epithelium

BLT1 protein was detected in the cancer epithelium of all 78 of the 78 FFPE human CRC (Figure 12). Representative staining intensities from the cancer epithelium is shown (Figure 13). Positive staining was cytoplasmic. Thirty of the 31 samples containing histologically normal looking epithelium stained positively for BLT1, the staining appeared cytoplasmic (Figure 14B, further images see Appendix 6). It is important to note that whilst the candidate refers to this epithelium as being normal, the candidate accepts that this epithelium (and the later detailed normal CR associated stroma) was on the same tissue block as the CRC and therefore not a truly

independent normal CR (or associated stroma) sample. BLT1 staining was seen at the top of CR crypts but absent from the base of the crypt (Figure 14B). There was an increase in cytoplasmic BLT1 staining between matched histologically normal CR and CRC epithelial samples (Figure 14A; $P = 0.0051$). Representative staining for the increase in BLT1 expression between matched histologically normal colorectal and cancer epithelium is shown (Figure 14B and C).

There was no statistically significant correlation between BLT1 expression in either the human CRC epithelium or human histologically normal CR epithelium with the clinicopathological data including age, cancer location, cancer size, cancer cell differentiation, pT, pN or histological presence of vascular invasion (Appendix 7 for CRC epithelium and Appendix 8 for histologically normal CR epithelium data).

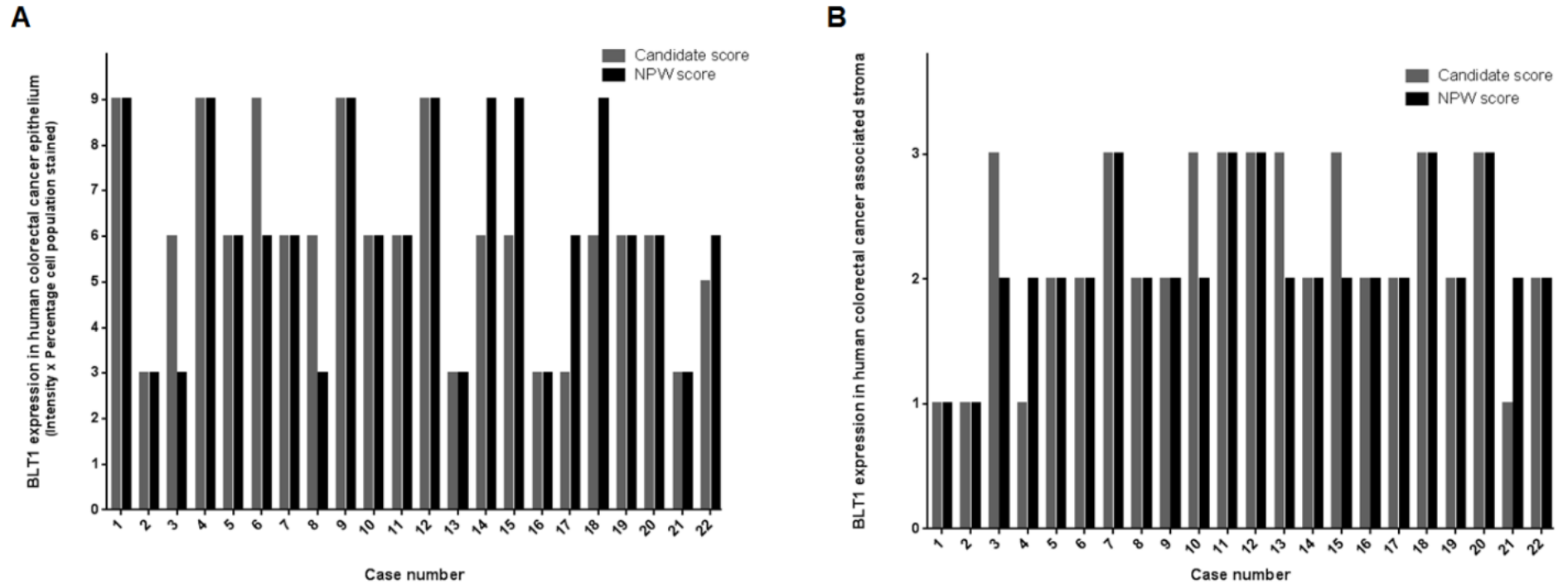


Figure 11. Inter-observer agreement for BLT1 expression in human CRC tissue.

Twenty- two different FFPE human CRC specimens where scored for BLT1 expression by two independent observers (myself and gastrointestinal histopathologist NPW). (A) Scores given to BLT1 expression levels in the CRC epithelium. (B) Scores given to BLT1 expression in the CRC epithelium associated stroma.

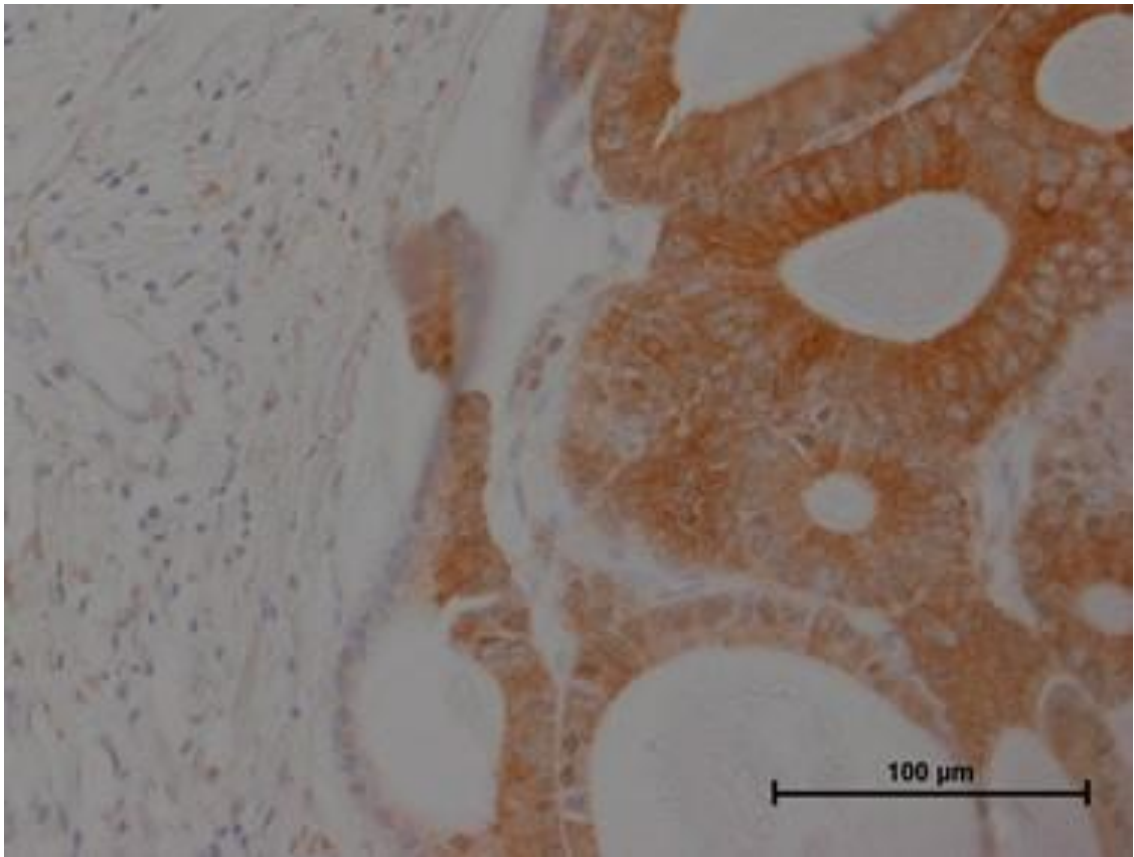


Figure 12. Cytoplasmic BLT expression in human CRC epithelium

Seventy-eight different FFPE human CRC samples were probed for BLT1 expression using a rabbit polyclonal anti-human BLT1 antibody (Cayman 1 in 1500 and probed with a secondary conjugated HRP antibody (anti-Rabbit envision kit) by IHC. Image shows the cytoplasmic BLT1 protein expression. (Scale bar 100 μm).

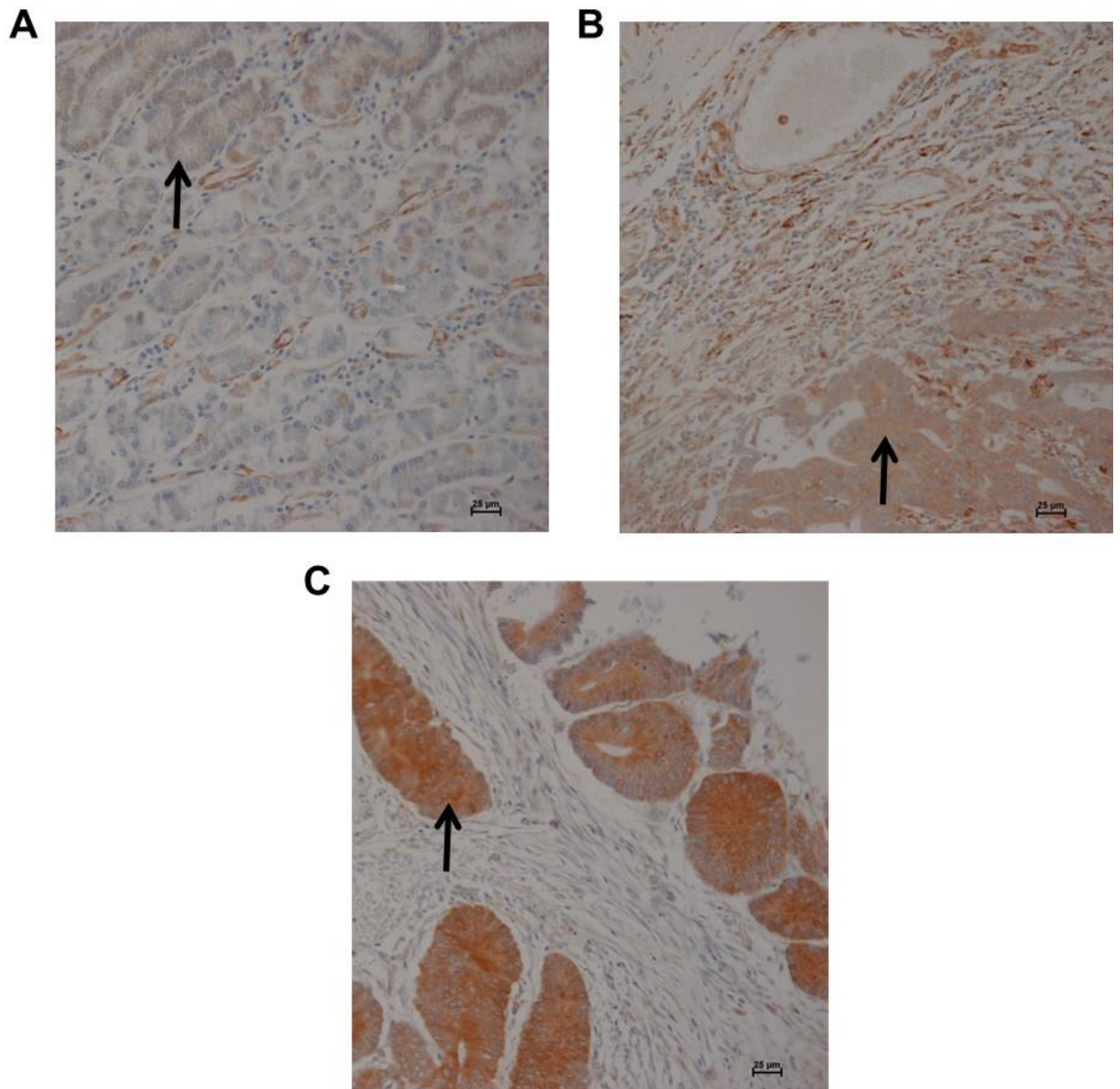


Figure 13. BLT expression in human CRC epithelium.

Illustrative images of different intensities of BLT1 protein expression as measured by immunohistochemistry. (A) Example of intensity score of 1. (B) Example of intensity score of 2. (C) Example of intensity score of 3. All samples had a cytoplasmic staining pattern for BLT1 with a spread of intensity scores between 0-3. Arrows indicate cancer epithelium. (Scale bars 25 μm).

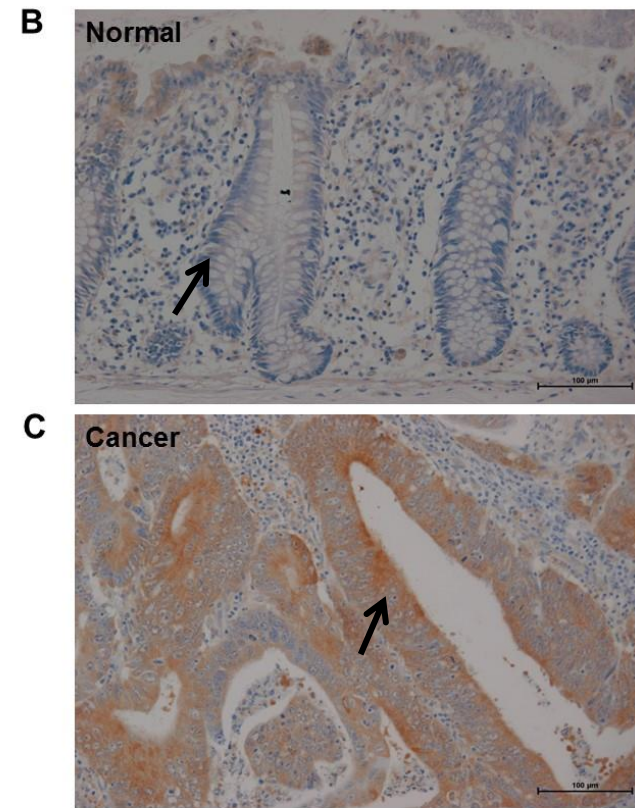
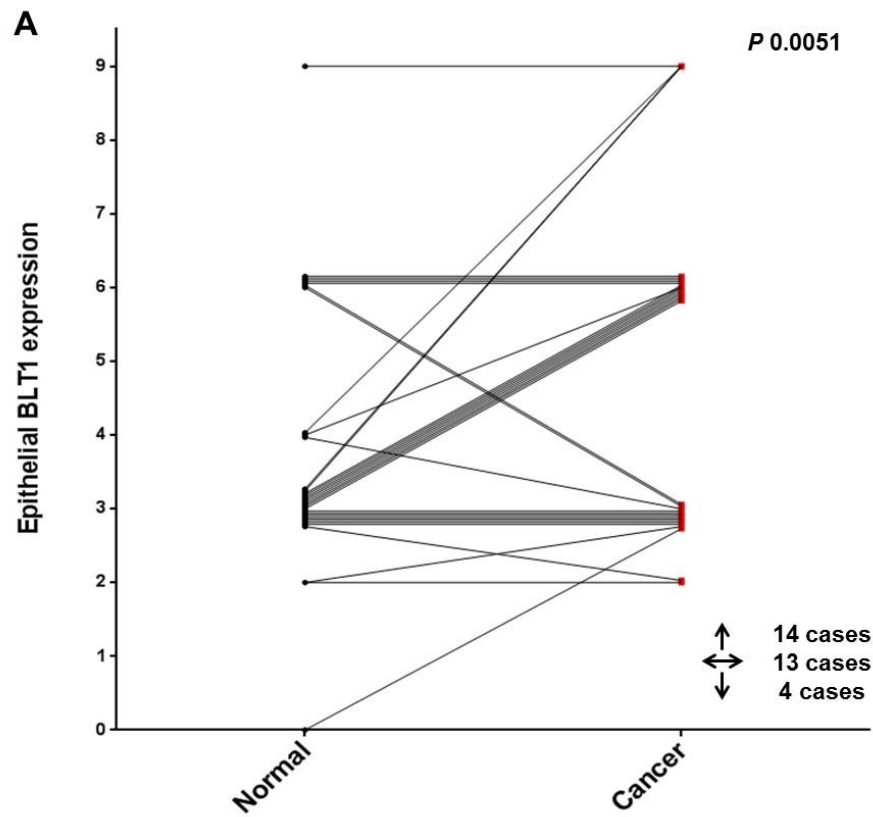


Figure 14. BLT1 expression between matched histologically normal CR epithelium and CRC epithelium.

There were 31 different FFPE human CRC samples with both histologically normal colorectal epithelium and CRC epithelium. (A) BLT1 expression in histologically normal colorectal epithelium and CRC epithelium, individual (I x P) scores for matched samples show statistical analysis performed using a Wilcoxon matched-pairs signed rank test ($P = 0.0051$). (B) BLT1 staining in histologically normal CR epithelium. (C) BLT1 staining in CRC cancer epithelium (sample matched to that of B). There was a significant increase found in BLT1 staining between matched CRC epithelium and histologically normal colorectal epithelium. Arrows indicate CR epithelium. (Scale bars 100 μm).

3.3.2.4 BLT1 expression in human colorectal cancer associated stroma and histologically normal colorectal epithelium associated stroma

BLT1 protein was detected in the stroma in all 78 of the 78 FFPE human CRC samples. Representative staining from the CRC epithelium associated stroma is shown (Figure 15A-C). All of the 31 samples containing histologically normal CR epithelium associated stroma stained positively for BLT1 (Appendix 6). Interestingly there was an increase in BLT1 staining between matched histologically normal CR associated stroma and CRC associated stroma samples (Figure 16A). Positive staining was not only seen by immune type cells, but also by spindle shaped cells (Figure 16B; further staining would be required to establish if these spindle shaped cells were myofibroblasts). There was a statistically significant correlation between BLT1 expression in the CRC associated stroma and cancer location, with higher expression being found in cancers distal to the splenic flexure (Figure 17). There were no other correlation found between CRC associated stroma and the remaining clinicopathological factors (Appendix 9 for graphical data). There was no statistically significant correlation found with histologically normal colorectal epithelium associated stroma and the clinicopathological data including age, cancer location, cancer size, cancer cell differentiation, pT, pN or histological presence of venous invasion, (Appendix 10 for graphical data).

No correlation was found between BLT1 staining in the CRC associated stroma and CRC epithelium on matched sample analysis (Appendix 11; Spearman r 0.117, 95% confidence interval -0.115-0.337, $P = 0.307$). There was no correlation found between BLT1 staining in the histologically normal CR epithelium associated stroma and CR epithelium on matched sample analysis (Appendix 12; Spearman r 0.032, 95% confidence interval -0.336-0.391, $P = 0.866$).

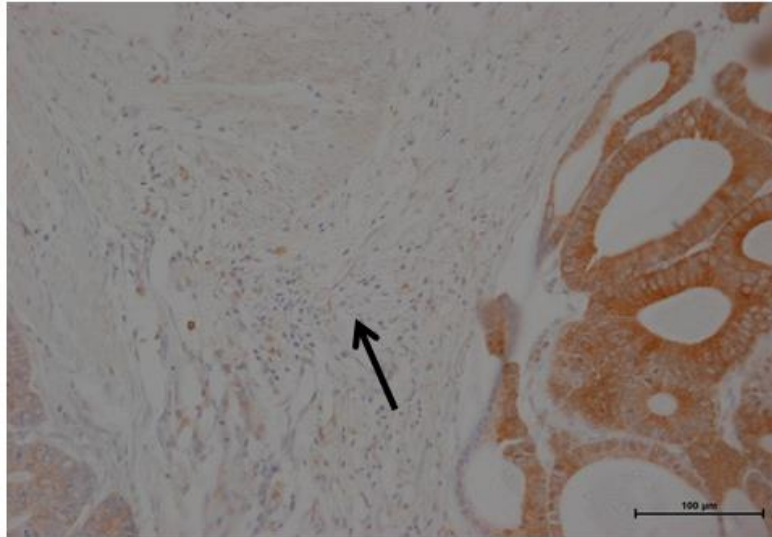
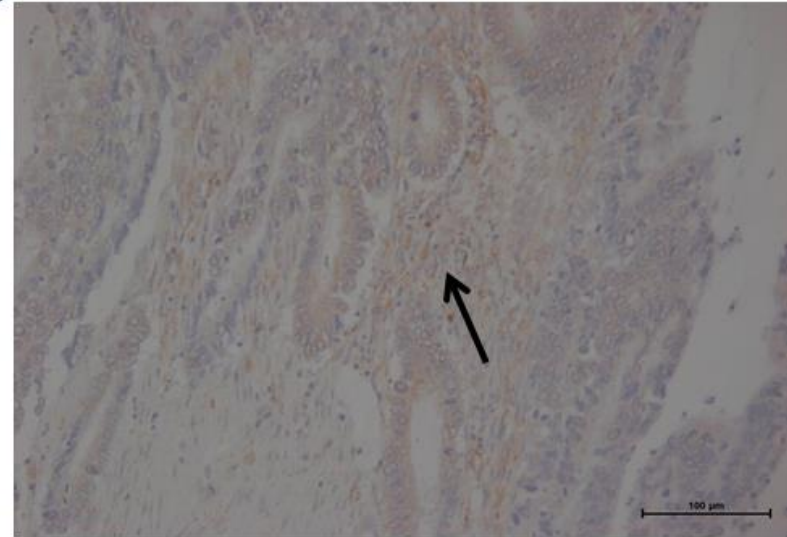
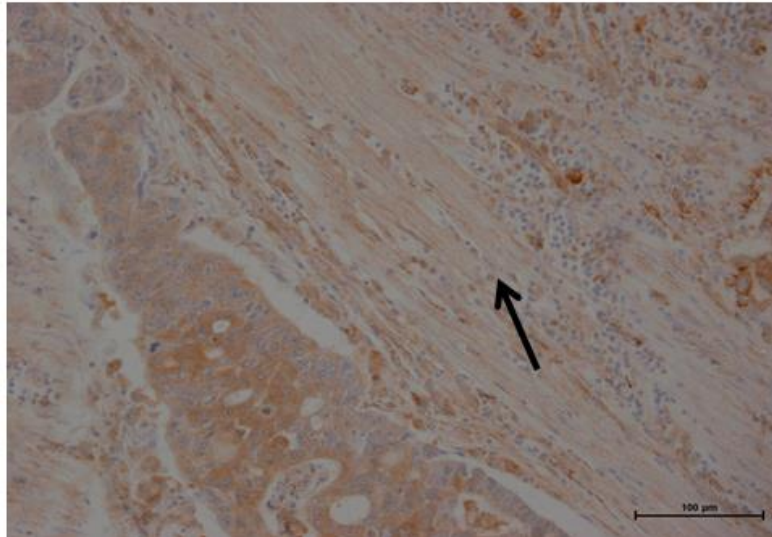
A**B****C**

Figure 15. BLT1 expression in human CRC epithelium associated stroma.

Illustrative images of different intensities of BLT1 protein expression as measured by immunohistochemistry. (A) Example of an intensity (I) score 1. (B) Example of an I score 2. (C) Example of an I score 3. Arrows indicate CRC epithelium associated stroma. (Scale bars 100 μm)

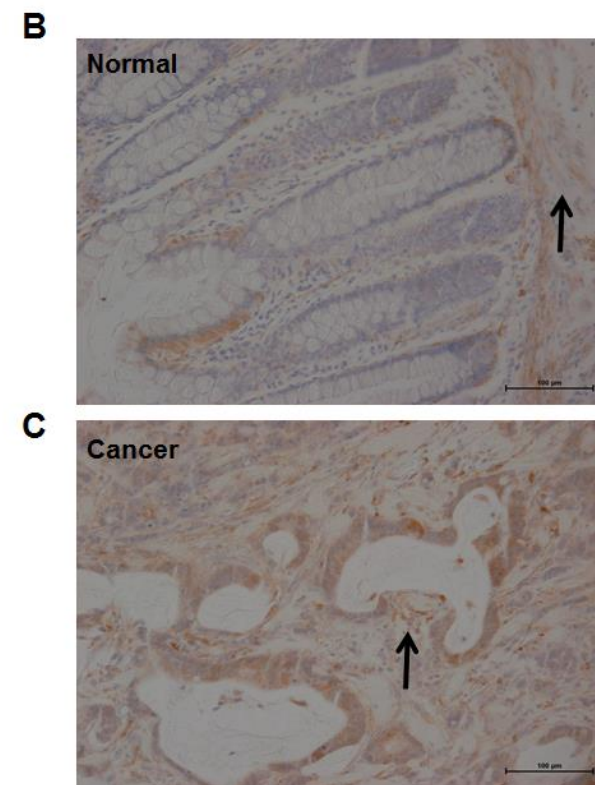
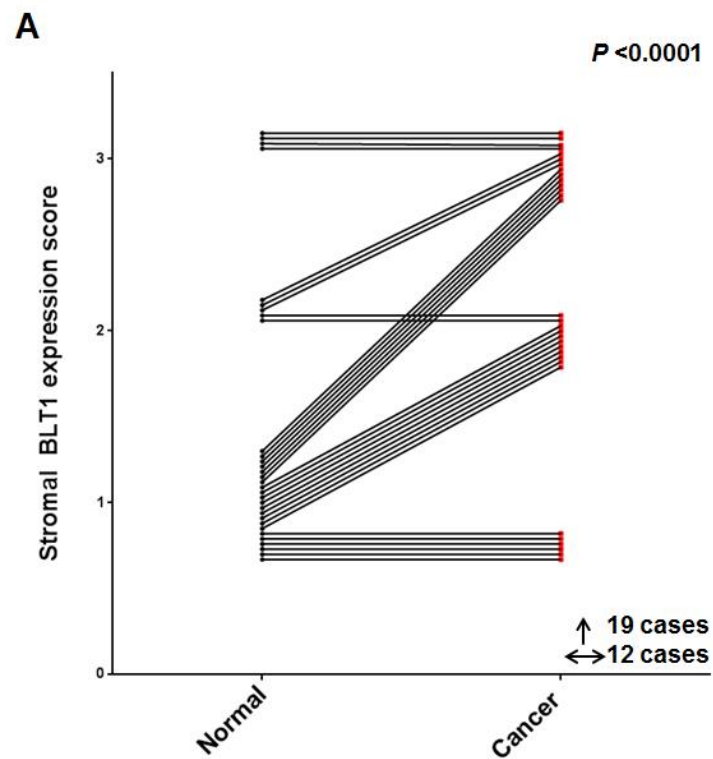


Figure 16. BLT1 expression between matched histologically normal CR epithelium associated stroma and CRC epithelium associated stroma

Thirty one different FFPE human CRC samples with both histologically normal colorectal epithelium and CRC epithelium were scored for BLT1 expression. (A) Graph illustrating the score for BLT1 expression in histologically normal colorectal epithelium associated stroma and CRC associated stroma. Statistical analysis was performed using a Wilcoxon matched-pairs signed rank test ($P = < 0.0001$). (B) BLT1 staining in histologically normal colorectal epithelium associated stroma. (C) BLT1 staining in CRC associated stroma epithelium (sample matched to that of B). Arrows indicate the epithelium associated stroma. (Scale bars 100 μm).

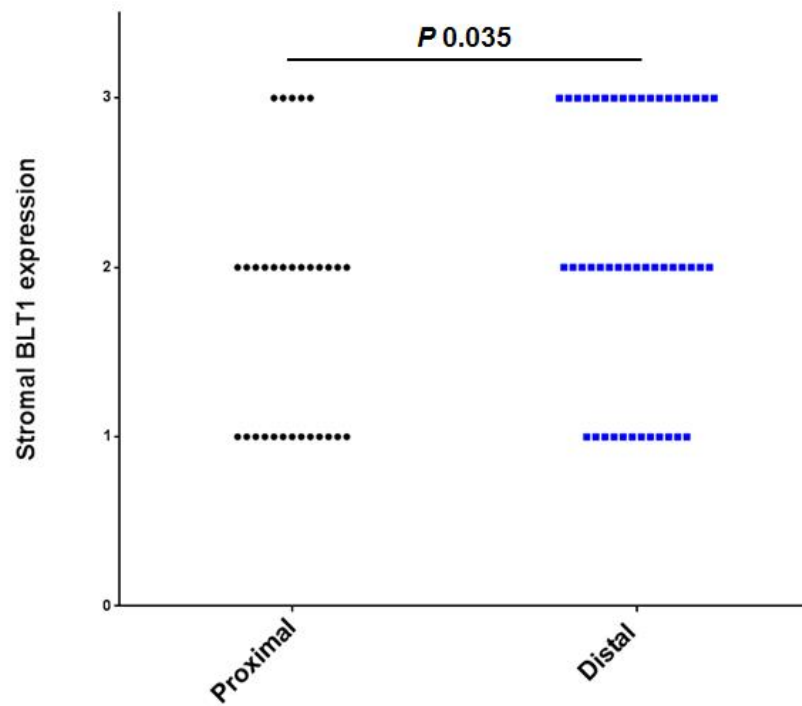
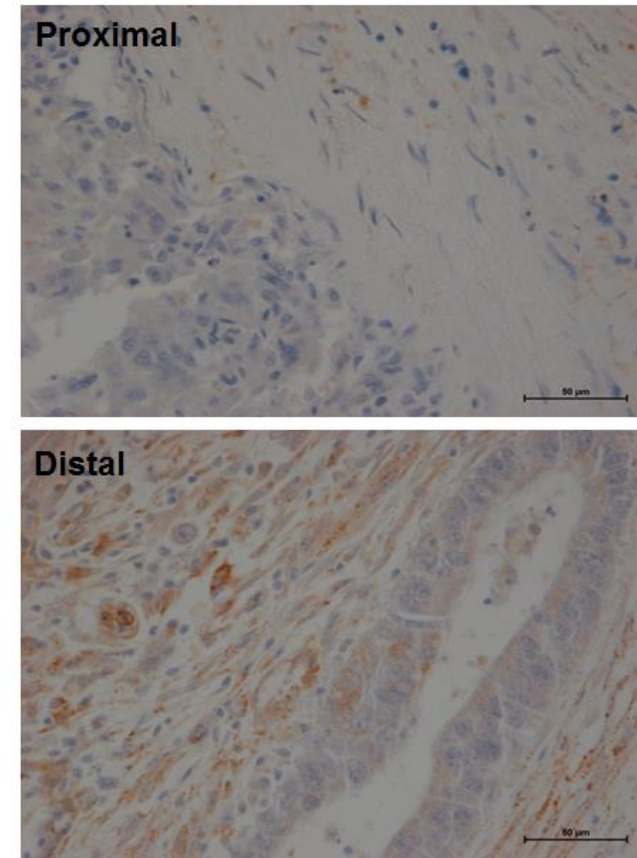
A**B**

Figure 17. BLT1 expression in CRC epithelium associated stroma and cancer location in relation to splenic flexure

Seventy-eight different FFPE human CRC epithelium samples were probed for BLT1. (A) Graph illustrating the score for BLT1 CRC associated stromal expression and cancer location (either distal or proximal to the splenic flexure, data analysed using a Mann-U Whitney test ($P = 0.035$)). (B) Representative images of the staining for BLT1 in CRC associated stroma in proximal to splenic flexure cancers. (C) Representative images of the staining for BLT1 in CRC associated stroma distal to splenic flexure. (Scale bars 50 μm).

3.4 Results (ChemR23)

3.4.1.1 ChemR23 mRNA detection in a panel of human colorectal cancer cell lines

Quantitative qPCR was utilised to characterise ChemR23 gene expression in seven human CRC cell lines. ChemR23 receptor mRNA was identified in all cell lines screened, including the negative control cell line HEK293. The NTC and RT- controls gave no signal on the qPCR amplification plot, ruling out DNA contamination. Whilst the Jurkat cell line (positive control) gave a ChemR23 mean Ct value of 27.8 and the HEK293 cell line a mean Ct value of 30.3 which implies a higher ChemR23 expression in the Jurkats. However when the β -actin mean Ct value was used for each cell line to calculate the Δ -Ct value there was no difference in ChemR23 mRNA expression between the cell lines, using this method. The results make conclusion on ChemR23 difficult as either all cells lines express low ChemR23 mRNA, or this method is not specific for ChemR23. Mean Ct values for both ChemR23 and β -actin with respective SEM are shown in Table 6. Figure 18 shows the small range of expression levels (Δ Ct values) detected in the cell lines.

3.4.1.2 ChemR23 protein detection in a panel of human CRC cell lines

Several commercially available anti-ChemR23 antibodies were tested to establish whether ChemR23 was expressed in human CRC cell lines. When Novus Biologicals, R&D systems and Abcam anti-ChemR23 antibodies were used several resolved protein bands at above and below the predicted MW expected for ChemR23 were seen, meaning these antibodies were not suitable for the ChemR23 studies (Appendix 13).

Using a high sensitivity chemiluminescent condition, a protein band at a MW of 45 kDa in keeping with that expected for the ChemR23 protein was seen in the positive control Jurkat cell line as well as the human CRC cell lines T84, HRT18, HT29, Caco2 and HCT116 (Figure 19A), when the Bioss anti-ChemR23 antibody was used. Using the Bioss anti-ChemR23 antibody the LoVo human CRC cell line did not give a resolved band at this MW under the chemiluminescent conditions used, with the HCA7 CRC cell line giving only a very faint resolved protein band. Resolved protein bands were also seen just above the 100 kDa standard marker in all cell lines, discussed later. Protein loading was monitored by probing for α -tubulin (Figure 19B). Figure 20 shows the ratio

of adjusted volume intensity of the ChemR23 resolved protein band against the α -tubulin loading control for each cell line. Caco2 human CRC cells were shown to have two fold more ChemR23 protein than HRT18 and HT29 CRC cells and five fold more protein than T84 and HCT116 human CRC cells under these conditions.

To confirm that the resolved protein band seen at 45 kDa was located at the membrane, and thus in keeping with that expected of a seven-transmembrane receptor such as ChemR23, the candidate probed the membrane protein lysate extracted from HEK293 (negative control) and Caco2 cells for ChemR23. The 45 kDa resolved protein band was identified in the membrane fraction in Caco2 cells, and absent in the HEK293 cells (Figure 21), thus adding further support to the identity of the 45 kDa resolved protein band being ChemR23.

An interesting finding was that ChemR23 protein expression increased in Caco2 human CRC at increasing cell confluency (Figure 22), with a four fold increase at 100% cell confluency. The IF study suggested that ChemR23 expression was more intense in confluent Caco2 cells compared to less confluent cells, with the NP controls giving no specific staining (Figure 23). This induction in ChemR23 protein expression with increased cell confluency was not seen in any of the other six human CRC cell lines investigated (Figure 24). As a result of this effect on ChemR23 with Caco2 cells, BLT1 protein was also investigated in the same panel of human CRC cell lines at either 50 or 100% cell confluency. No BLT1 expression was identified in either the 50% confluent cells or 100% confluent CRC cell lines (Figures 25). ChemR23 protein induction in confluent Caco2 human CRC cells was utilized in the cell viability/ apoptosis/ gene expression assays, and possible reasons for its increased expression discussed in Chapter 5.

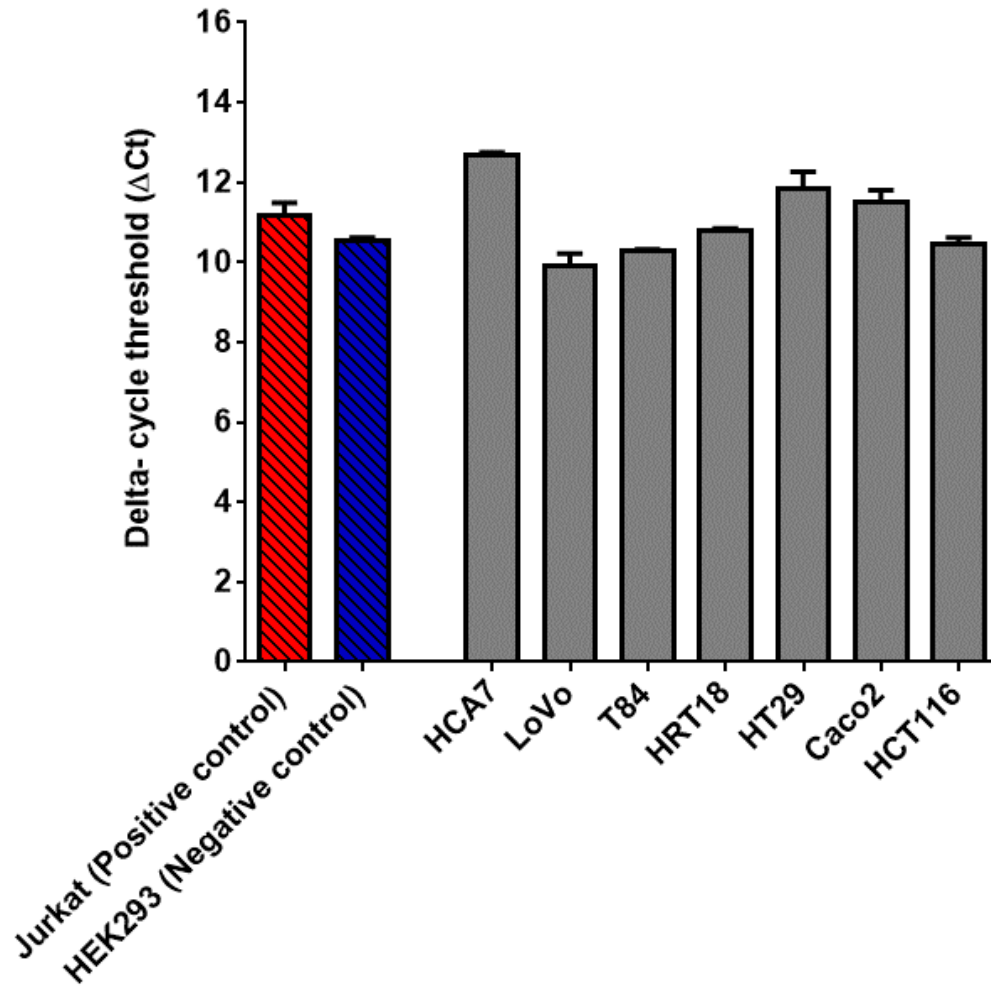


Figure 18. ChemR23 mRNA expression in a panel of human CRC cell lines.

ChemR23 receptor mRNA expression in a panel of human cell lines. Data collected from three individual independent cell cultures for each cell line, shown as mean delta-cycle threshold (Δ Ct) value with standard error of the mean.

Cell Line	ChemR23 mean Ct value	ChemR23 SEM	β -actin mean Ct value	β -actin SEM	Mean Δ -Ct value	Δ -Ct SEM
Jurkat	27.8	0.1	16.5	0.1	11.2	0.3
HEK293	30.3	0.2	19.7	0.1	10.6	0.1
HCA7	29.4	0.1	16.7	0.1	12.7	0.1
LoVo	28.2	0.1	18.3	0.2	9.9	0.3
T84	29.0	0.4	18.7	0.4	10.3	0.1
HRT18	27.8	0.1	17.0	0.1	10.8	0.1
HT29	29.1	0.2	17.3	0.2	11.9	0.4
Caco2	29.9	0.4	18.4	0.1	11.5	0.3
HCT116	28.8	0.1	18.3	0.2	10.5	0.2

Table 6. Mean cycle threshold values (Ct) for ChemR23 and β -actin in a panel of human cell lines.

Cycle threshold values were measured in three independently performed experiments for each of the nine human cell lines. Each individual experiment was performed in triplicate. Data shown as mean with standard error of the mean.

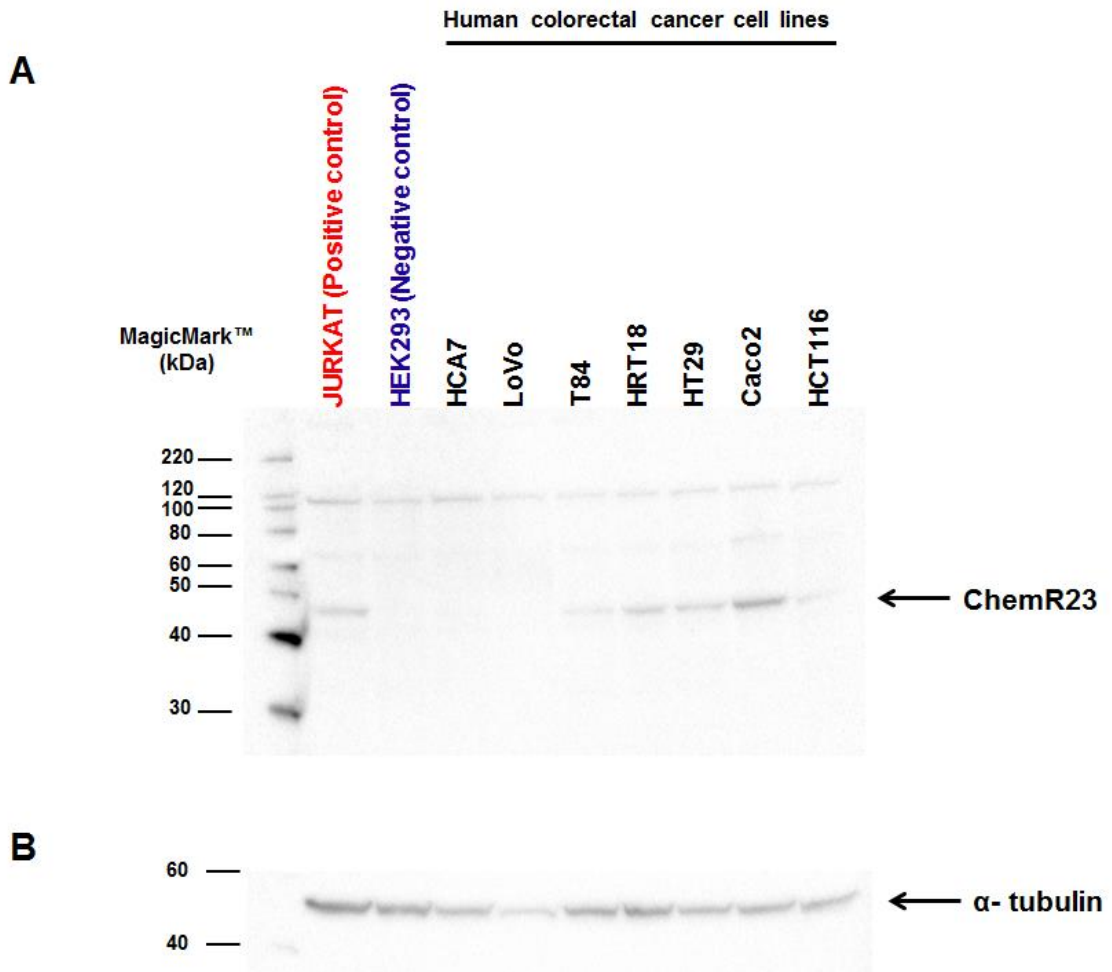


Figure 19. ChemR23 protein expression in a panel of human CRC cell lines.

Human CRC protein lysate was probed with anti-human ChemR23 antibody (Bioss) and probed with a secondary conjugated HRP antibody (1 in 2000), image from one second of high sensitivity chemiluminescence (A). A resolved protein band at a MW of 45 kDa in keeping with that expected for the ChemR23 protein was seen in the positive control Jurkat cell line as well as the human CRC cell lines T84, HRT18, HT29, Caco2 and HCT116 (see arrow). (B) Protein loading was confirmed by probing with mouse monoclonal anti-human α -tubulin antibody.

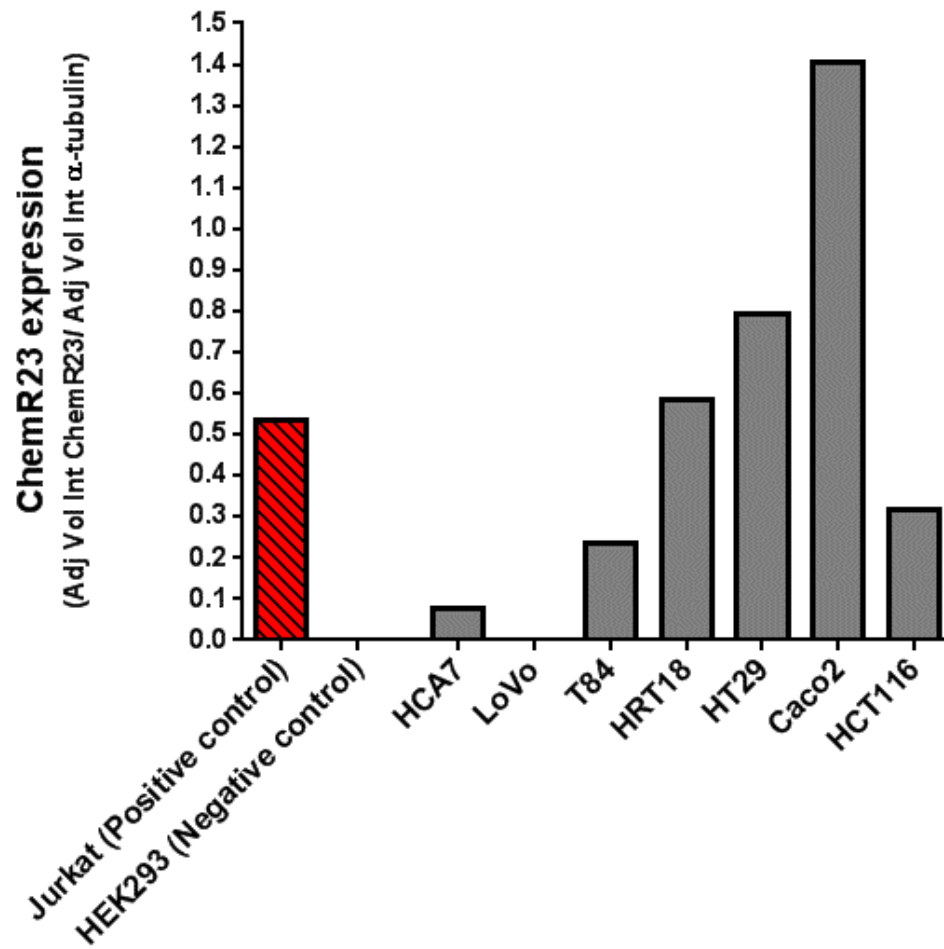


Figure 20. Semi-quantitative analysis of ChemR23 expression in a panel of human CRC cell lines.

The relative quantities of the ChemR23 protein expression for each cell line was calculated by dividing the adjusted volume intensity of the ChemR23 resolved band by that of the loading control (α -tubulin). The adjusted volume intensity values were calculated using the BIO-RAD Quantity One Software using the PVDF membrane image from Figure 18A (under standard chemiluminescence).

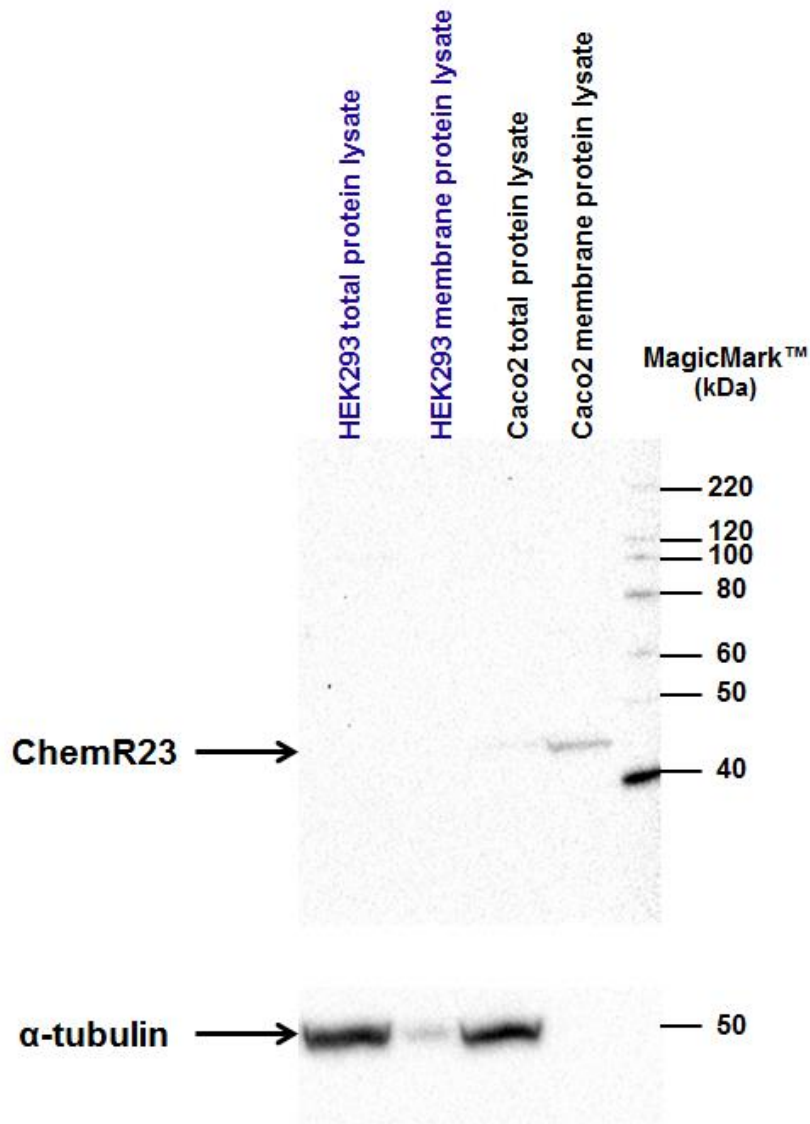


Figure 21. ChemR23 protein expression in the membrane protein fraction of Caco2 human CRC cells.

Human CRC protein lysate from membrane fraction was probed with affinity purified rabbit polyclonal anti-human ChemR23 antibody (Bioss, 1 in 1000), and probed with a secondary conjugated HRP antibody (1 in 2000), image from 15 seconds of standard chemiluminescence. A resolved protein band at a MW of 45 kDa in keeping with that expected for the ChemR23 protein was seen in membrane extracted fraction of Caco2 human CRC cells with none identified in the HEK293 cells. Protein loading was confirmed by probing with mouse monoclonal anti-human α -tubulin.

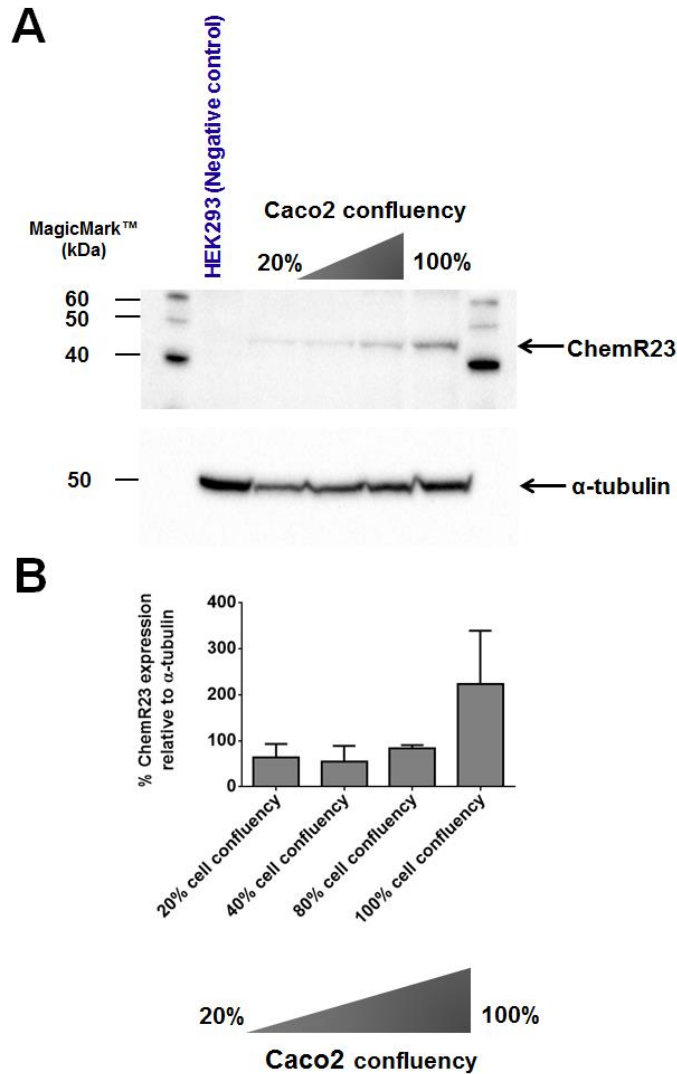


Figure 22. ChemR23 protein expression by Caco2 human CRC cells at increasing cell confluency.

Caco2 human CRC cells were grown to 20, 50, 80 or 100% cell confluency before the cells were lysed and the protein lysate collected. The protein lysates were then probed with a rabbit polyclonal anti-human ChemR23 antibody (Bioss 1 in 500), and probed with a secondary HRP1 swine anti-rabbit antibody (1 in 2000). (A) ChemR23 protein expression in 20, 50, 80, and 100% confluent Caco2 cells with α -tubulin protein loading. (B) Densitometric analysis of (A); data shown as percentage (%) ChemR23 resolved protein expression against the α -tubulin loading control for each protein lysate. Data analysis was carried out on three independent WB images.

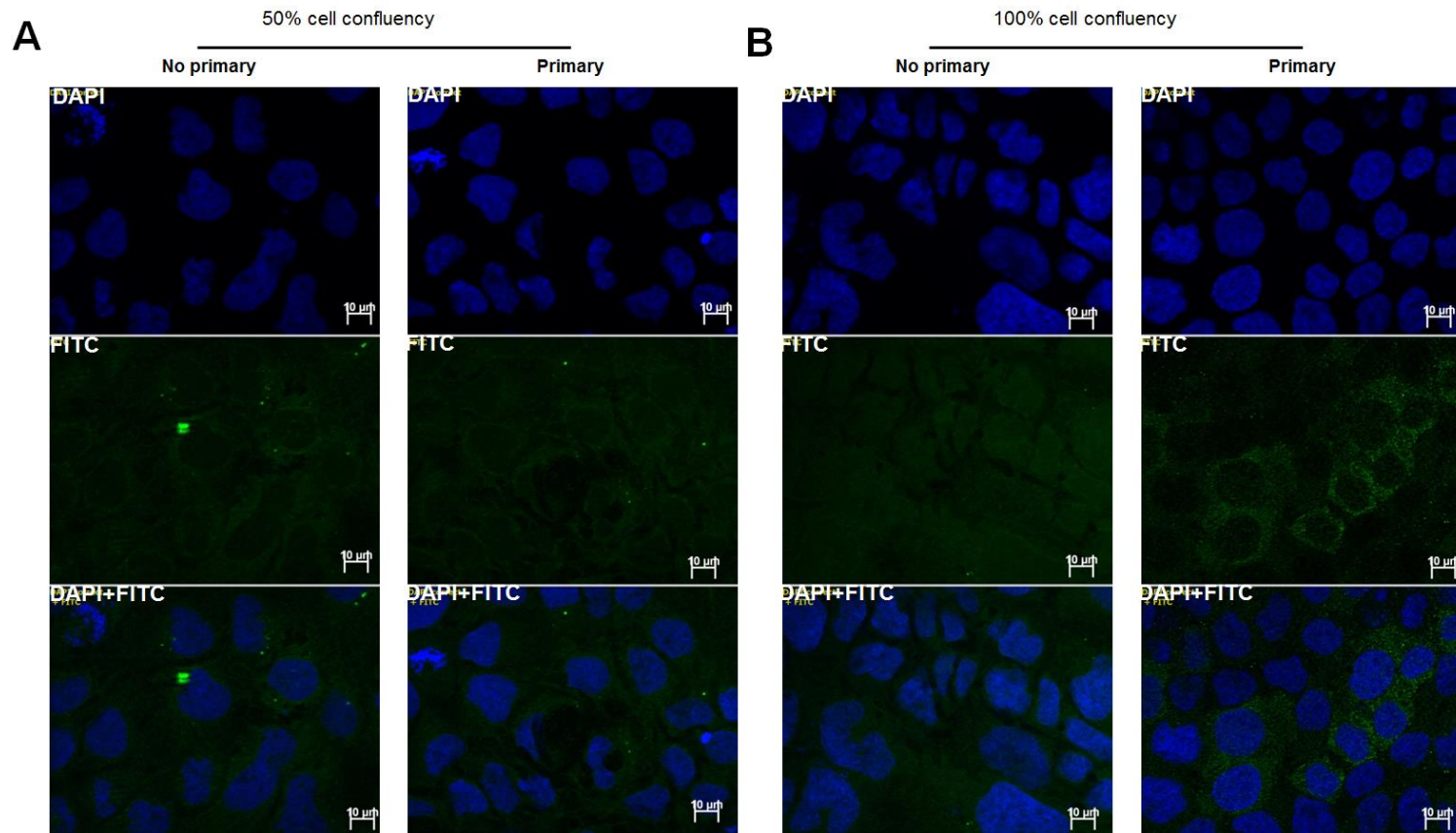


Figure 23. Immunofluorescence detection of ChemR23 by Caco2 human CRC cells at differing cell confluencies.

Caco2 human CRC cells were grown on sterile glass cover slides to either 50% or 100% cell confluency, before being fixed in 4% PFA. The cells were then probed with an affinity purified rabbit polyclonal anti-human ChemR23 antibody (Bioss 1 in 50), and probed with a secondary donkey anti-rabbit AlexaFluoro⁴⁸⁸ antibody (1 in 300). Cell nuclei were stained with DAPI (blue), ChemR23 receptor represented as FITC (green). The images were acquired using a Zeiss Axioscope microscope. (A) 50% confluent cells (at X63 magnification). (B) 100% confluent cells. (Scale bars 10 μm).

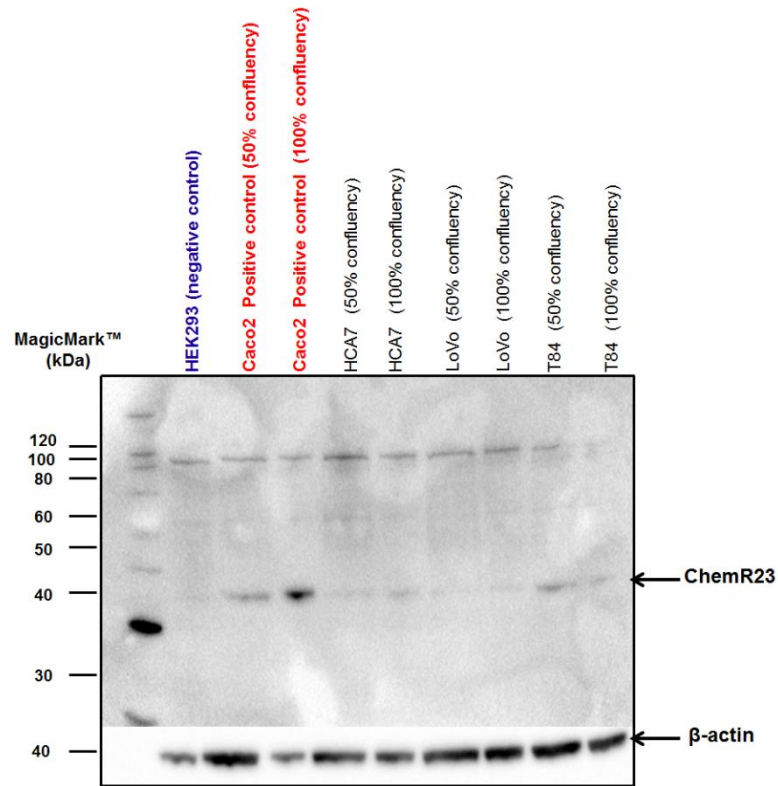
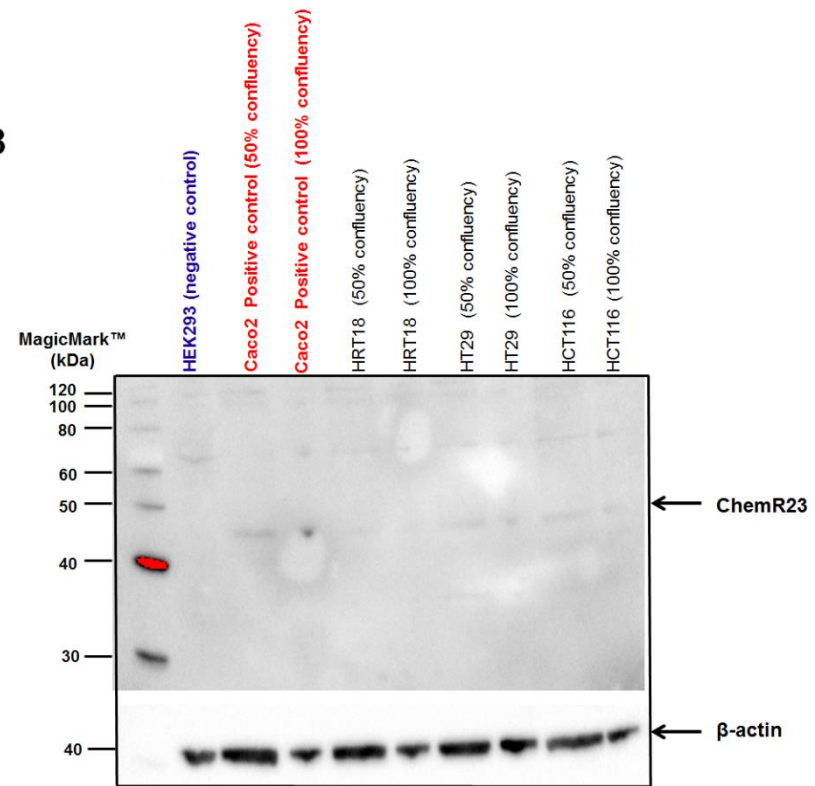
A**B**

Figure 24. Western blot detection of ChemR23 by human CRC cell lines at differing cell confluencies.

Human CRC protein lysates were probed with affinity purified rabbit polyclonal anti-human ChemR23 antibody (Bioss, 1 in 500), and probed with a secondary conjugated HRP antibody (1 in 2000). (A-B) ChemR23 protein expression in a panel of human CRC cell lines, using HEK293 cells as a negative control for ChemR23 expression, Image from one second of high sensitivity chemiluminescence, protein loading was monitored by probing with mouse monoclonal anti-human β -actin antibody.

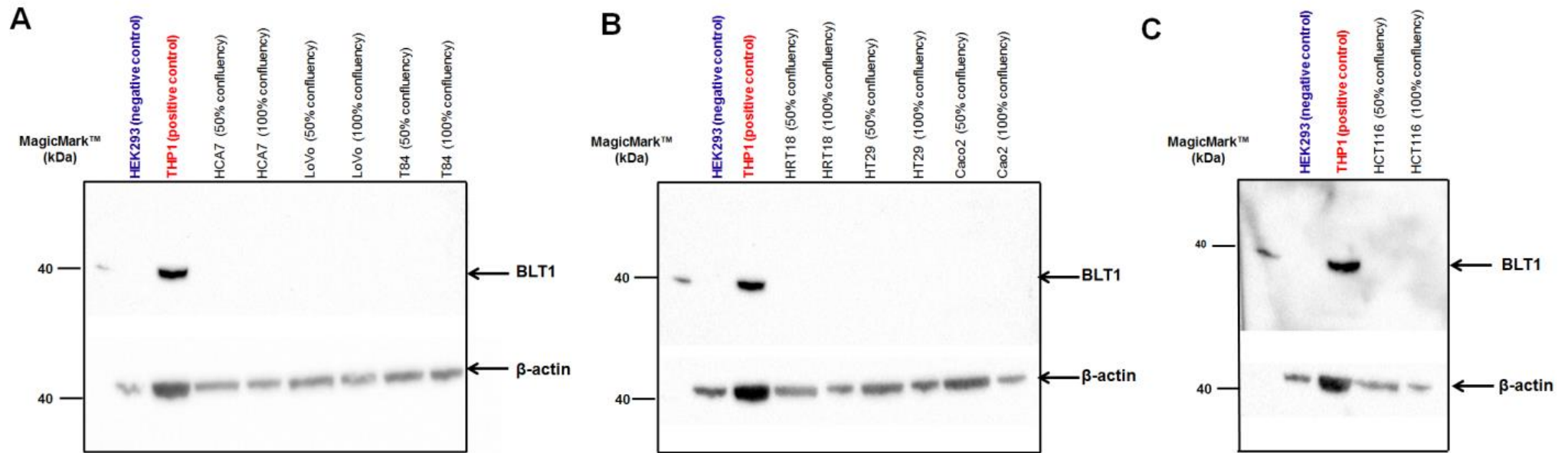


Figure 25. BLT1 protein expression by human CRC cell lines at differing cell confluencies.

Human protein lysates were probed with affinity purified rabbit polyclonal anti-human BLT1 antibody (Cayman Chemical, 1 in 1000), and probed with a secondary conjugated HRP antibody (1 in 2000), image from one second of high sensitivity chemiluminescence (A-C). Protein loading was monitored by probing with mouse monoclonal anti-human β -actin antibody (1 in 5000), image acquired from 15 seconds of standard chemiluminescence.

3.4.2 ChemR23 expression by human colorectal cancer tissue

3.4.2.1 Clinical characteristics of the study population

The clinical characteristics of the study population are summarized in Table 7. The median patient age at diagnosis was 73.5 years (range 45-93 years). Forty percent of patients had tumours proximal to the splenic flexure, and sixty percentage of patients had cancers distal to the splenic flexure. Median size of the cancers was 3.5 cm (range 1.5-10 cm). Cancer cell grade/differentiation was categorized as either well (3% of cases), moderate (79% of cases) and poor (18% of cases). The tumour stage distribution was pT1 in 3% of cases, pT2 in 8% of cases, pT3 in 56% of cases, and pT4 in 33% of cases. The pathological node (pN) was pN0 in 51% of cases, pN1 in 29% of cases and pN2 in 20% of cases. Histologically reported presence or absence of vascular invasion was reported in 52% and 48% of cases respectively. The number of cases is different to the BLT1 study as not all tissue blocks had enough tissue to allow ChemR23 analysis.

ChemR23. Clinicopathological details of patient cohort	
Characteristics	Number of cases n=73(%)
Age	
Median age: 74 years	
Age range: 45-93 years	
Location of colorectal cancer	
Proximal to splenic flexure	29 (40%)
Distal to splenic flexure	44 (60%)
Colorectal cancer size	
Median size: 3.5cm	
Size range: 1.5-10cm	
Colorectal cancer cell grade	
Well	2 (3%)
Moderate	58 (79%)
Poor	13 (17%)
Pathological (p) tumour (T) stage	
pT1	2 (3%)
pT2	6 (8%)
pT3	41 (56%)
pT4	24 (33%)
Pathological (p) nodal (N) stage	
pN0	37 (51%)
pN1	21 (29%)
pN2	15 (20%)
Histological presence of vasular invasion	
Absent	35 (48%)
Present	38 (52%)

Table 7. Clinical characteristics of the ChemR23 study population.

3.4.2.2 ChemR23 immunohistochemistry staining and scoring method

The scoring system was the same as that used in the BLT1 study, so the candidate scored all sections independently. All 73 specimens were scored for ChemR23 expression in cancer epithelium, histologically normal CR epithelium (as for the BLT this tissue was from the same CRC tissue sample, therefore not independent in location, as was also the case for the stroma), cancer epithelium associated stroma, and histologically normal CR epithelium associated stroma, ChemR23 expression. Optimisation of the ChemR23 antibody confirmed that a dilution of 1 in 1000 with an antigen retrieval step gave specific staining against the no primary control (Appendix 14). As for BLT1, a control no primary antibody slide and a primary antibody control slide was included in each of the four runs required to complete the ChemR23 IHC on the 73 different human CRC tissue samples (see Appendix 15 for no primary antibody control images and Appendix 16 for the primary antibody control images, between the different runs). Unfortunately Bioss were unable to supply the batch of antibody used to optimise the IHC. The candidate pooled together subsequent same lot numbers of the Bioss antibody after confirming their individual specificity via WB (Appendix 17). The candidate sought to confirm specificity initial as a previous lot of the Bioss antibody had very poor specificity making ChemR23 expression impossible (see Appendix 18 for example WB image). Initial optimisation of the Bioss antibody identified a 1 in 2000 dilution as optimal, however a 1 in 25 dilution was subsequently needed of the supplied antibody. Specificity between the two batches was similar as can be seen in their respective WB images (Figure 19 and Appendix 17, respectively), however their sensitivity differed markedly for the IHC, however there was comparable and good specificity on WB (Appendix 19).

3.4.2.3 ChemR23 expression in human colorectal cancer epithelium and histologically normal colorectal epithelium

The cancer epithelium of all 73 of the 73 FFPE human CRC samples expressed ChemR23. Typical staining from the cancer epithelium is shown (Figure 26 & 27) and appeared cytoplasmic. Twenty eight of the 28 samples containing histologically normal CR epithelium stained positively for ChemR23, with cytoplasmic expression. As seen with BLT1, ChemR23 expression was seen at the apex of the crypt (Figure 28). Additionally ChemR23 expression was shown to be increased in CRC epithelium when compared to matched histologically normal CR epithelial samples. The increase in

ChemR23 expression between matched histologically normal colorectal and cancer epithelium is shown in Figure 28.

As for BLT1 the candidate found no statistically significant correlation between ChemR23 expression in the human CRC epithelium with the clinico-pathological data including age, cancer location, cancer size, cancer cell grade, pT, pN or histological presence of venous invasion (Appendix 20 for graphical data). Neither was a statistically significant correlation found between ChemR23 expression in human histologically normal colorectal epithelium with the clinico-pathological data including age, cancer location, cancer size, cancer cell grade, pT, pN or histological presence of vascular invasion, (Appendix 21 for graphical data). Interestingly when the crypts were examined there appeared to be an induction in ChemR23 immunostaining at the apex of the crypt (Figure 29).

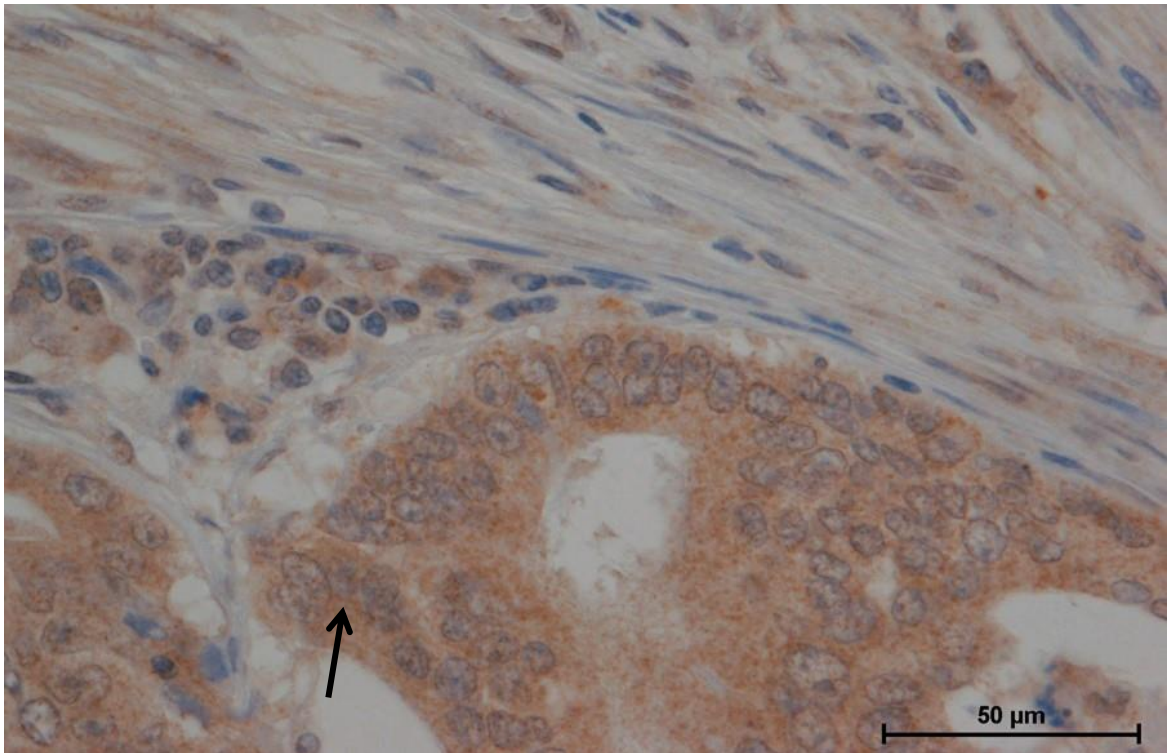


Figure 26. Cytoplasmic ChemR23 expression in human CRC epithelium

Seventy-three different FFPE human CRC samples were probed for ChemR23 expression using rabbit polyclonal anti-human ChemR23 antibody (Bioss 1 in 50 and probed with a secondary conjugated HRP antibody using anti-Rabbit envision kit). Illustrative image of the cytoplasmic (arrow) ChemR23 protein expression as measured by IHC (X40 magnification; scale bar 50 μ m).

3.4.2.4 ChemR23 expression in human colorectal cancer associated stroma and histologically normal colorectal epithelium associated stroma

Of the 73 human CRC samples investigated for ChemR23 expression, all were shown to express ChemR23 in the cancer-associated stroma. Figure 30 shows the stromal pattern of ChemR23 staining. Twenty-eight samples containing histologically normal CR epithelium associated stroma were all found to express ChemR23. ChemR23 staining was more pronounced in CRC associated stroma samples when compared with matched histologically normal CR associated stroma and (Figure 31). ChemR23 expression pattern was similar to that seen for BLT1 with expression by immune type and spindle shaped cells.

No statistically significant correlation found with human CRC epithelium associated stroma and the clinic-pathological data including age, cancer location, cancer size, cancer cell differentiation, pT, pN or histological presence of venous invasion, (Appendix 22 for graphical data). No statistically significant correlation was found with histologically normal CR epithelium associated stroma and the clinic-pathological data including age, cancer location, cancer size, cancer cell differentiation, pT, pN or histological presence of vascular invasion (Appendix 23 for graphical data).

There was a very weak correlation identified between ChemR23 expression in the CRC epithelium associated stroma and CRC epithelium (Appendix 24; Spearman r 0.237, 95% confidence interval 0.044-0.406, $P = 0.014$), with there being no correlation between histologically normal colorectal epithelium associated stroma and CR epithelium (Appendix 24; Spearman r -0.087, 95% confidence interval -0.455-0.30, $P = 0.660$).

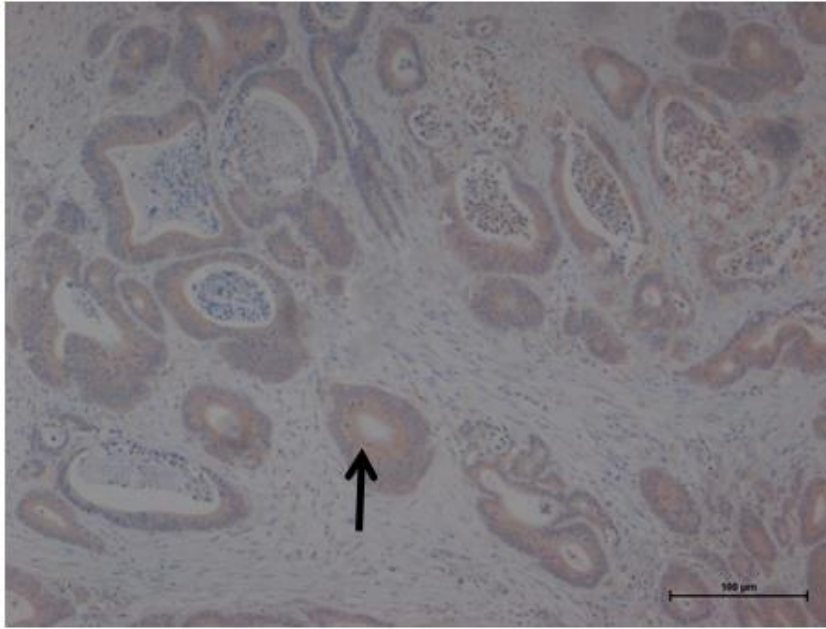
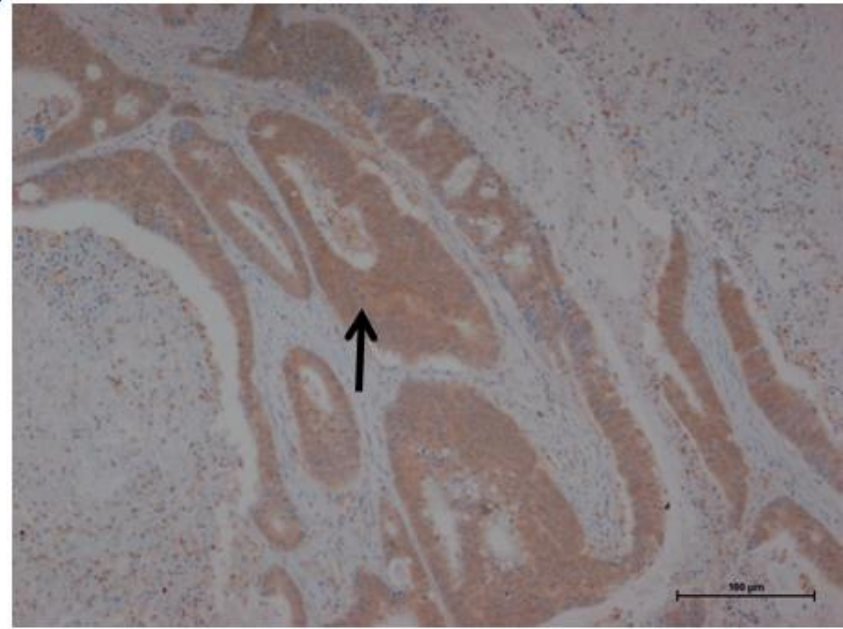
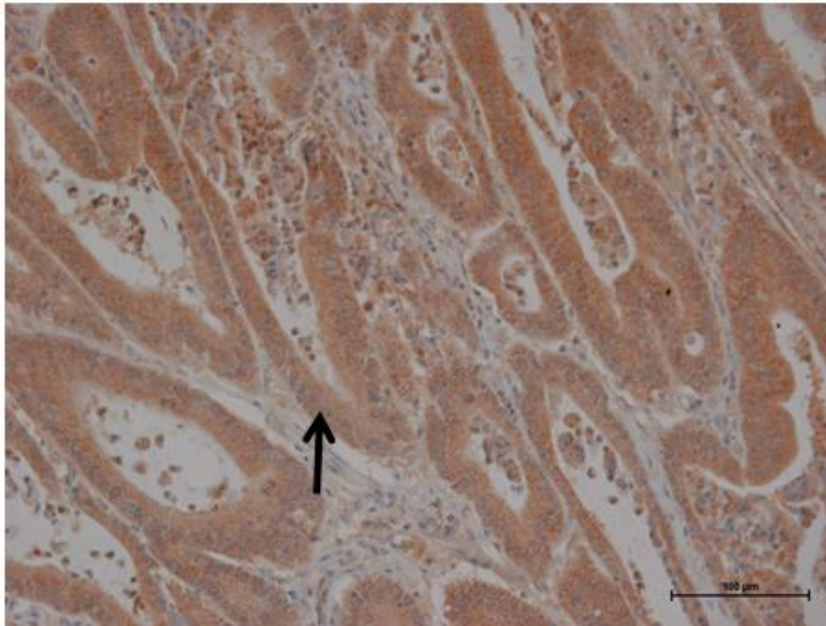
A**B****C**

Figure 27. ChemR23 expression in human CRC cancer epithelium.

Seventy-three different FFPE human CRC samples were probed for ChemR23 expression using rabbit polyclonal anti-human ChemR23 antibody (Bioss 1 in 50 and probed with a secondary conjugated HRP antibody (anti-Rabbit envision kit). The sections were scored for intensity (0-3) and percentage cell population staining (0-3). (A) Example of an I score of 1. (B) Example of an I score 2. (C) Example of an I score 3. All samples had a cytoplasmic staining pattern for ChemR23 with a spread of I scores between 0-3. All samples had 100% cell population staining of the cancer epithelium. Arrows indicate cancer epithelium. (Scale bars 100 µm).

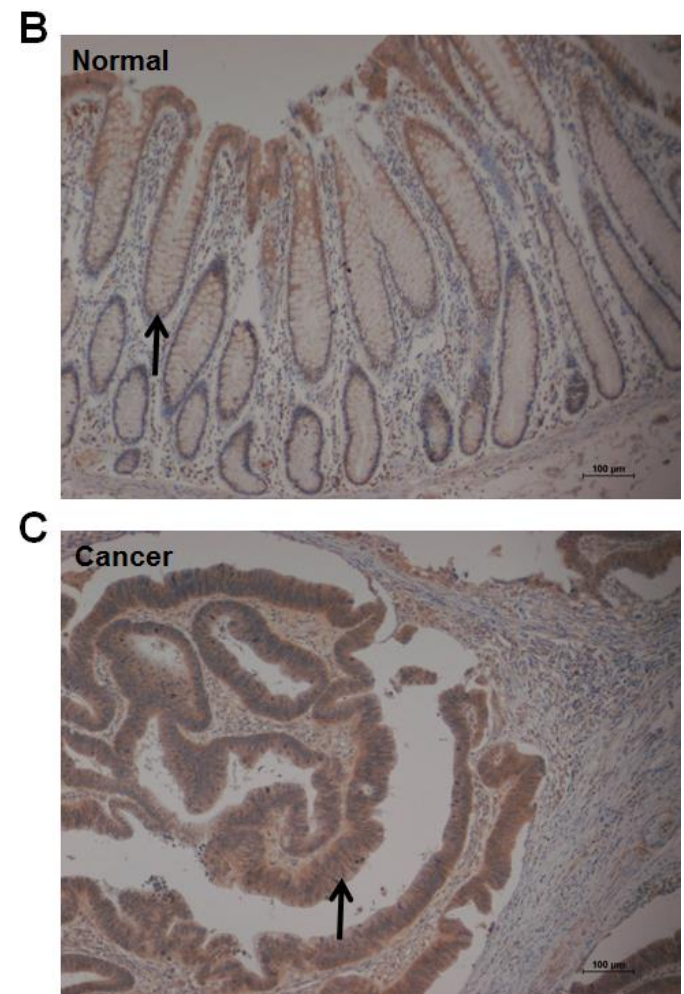
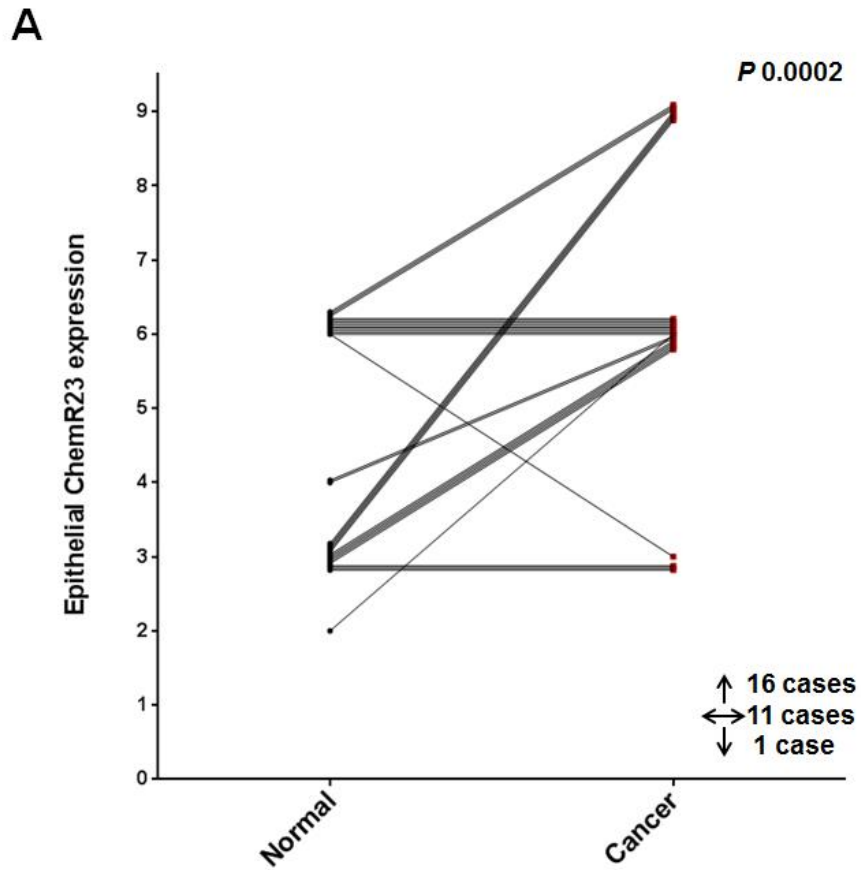


Figure 28. ChemR23 expression between matched histologically normal CR epithelium and CRC epithelium.

Twenty-eight different FFPE human CRC samples with both histologically normal colorectal epithelium and CRC epithelium. The sections had been scored for intensity (0-3) and percentage cell population staining (0-3). (A) Graph illustrating the score for ChemR23 expression in matched histologically normal colorectal epithelium and CRC epithelium. Statistical analysis was performed using a Wilcoxon matched-pairs signed rank test ($P = 0.003$). (B) ChemR23 staining in histologically normal colorectal epithelium. (C) ChemR23 staining in colorectal epithelium (sample matched to that of B). Arrows indicate epithelium. (Scale bars 100 µm).

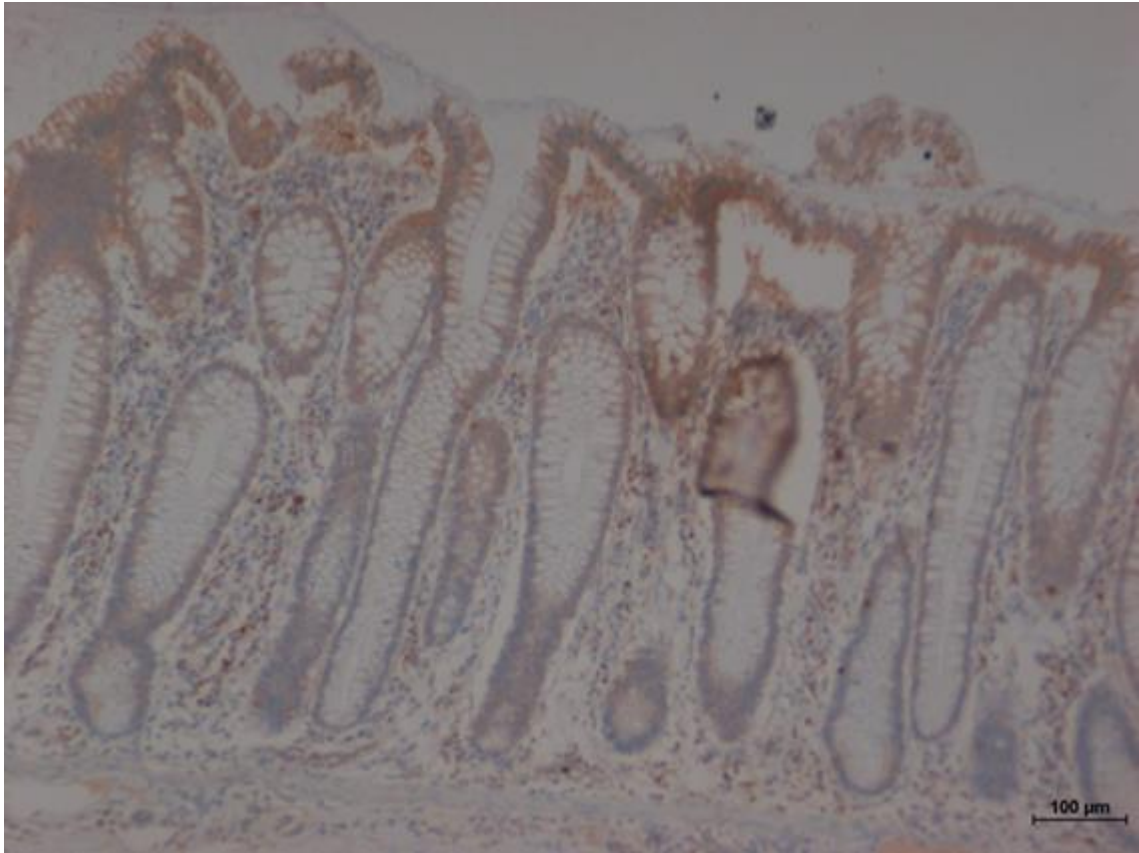


Figure 29. ChemR23 protein expression by histologically normal CR epithelium

Image taken from FFPE human CRC tissue specimen, used in the human CRC tissue study undertaken by the candidate. ChemR23 expression appears to be increased at the apical surface of the colonic crypt. (Scale bar 100 μm).

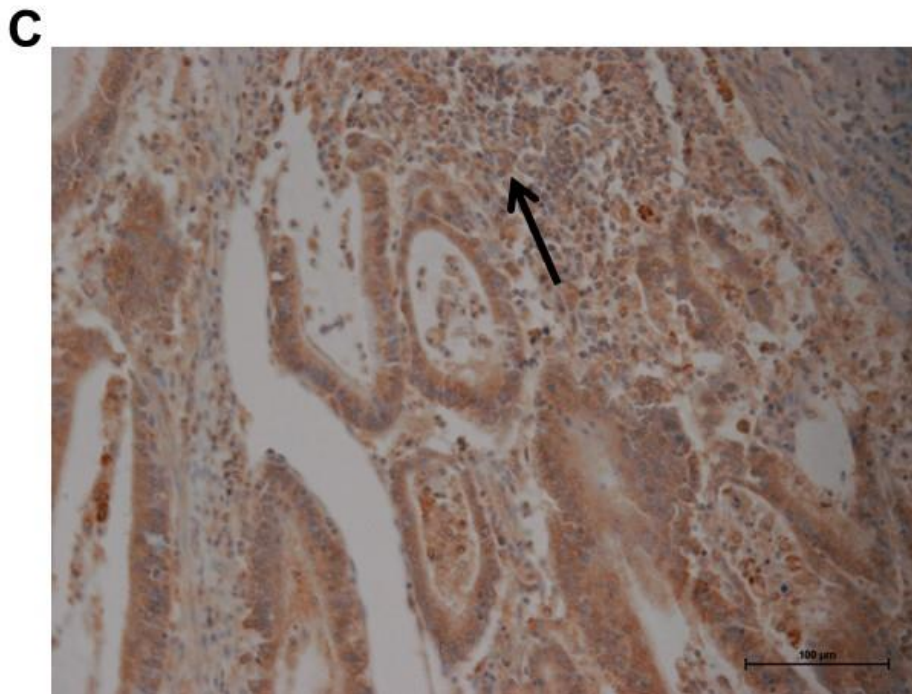
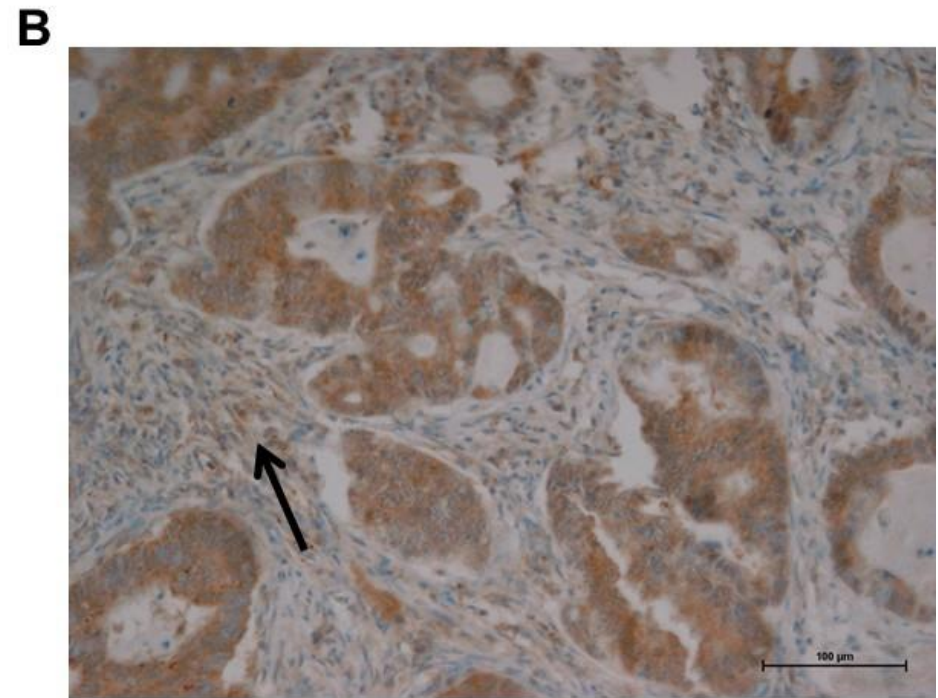
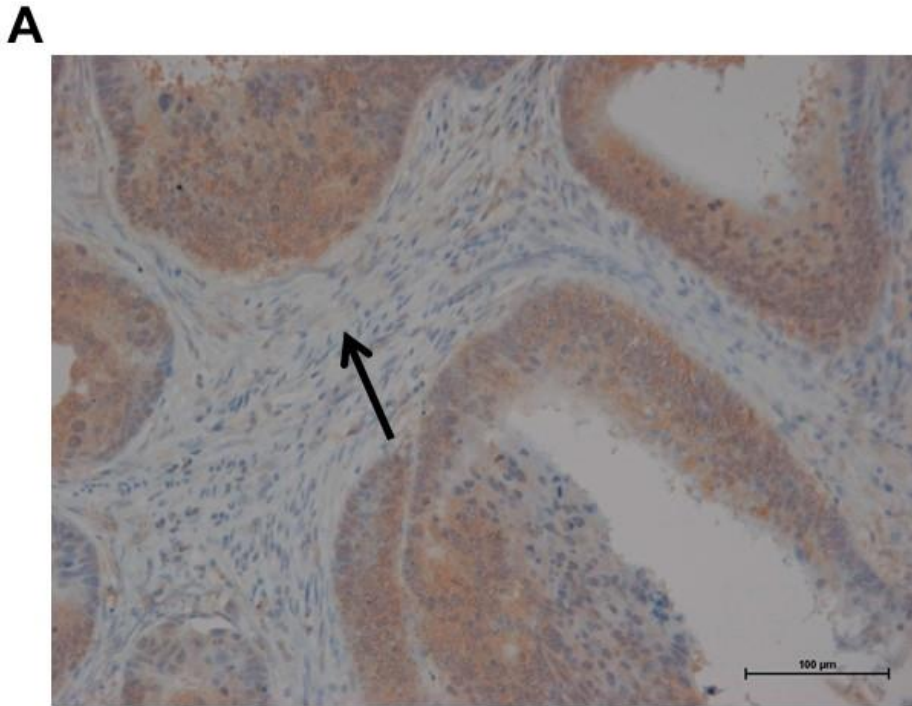


Figure 30 ChemR23 expression in human CRC epithelium associated stroma.

Seventy-three different formalin fixed paraffin embedded Human CRC samples were probed for ChemR23 expression using rabbit polyclonal anti-human ChemR23 antibody (BIOSS), and probed with a secondary conjugated HRP antibody (anti-Rabbit envision kit). The sections were scored for intensity (I) (0-3) and percentage cell population staining (0-3). (A) Example of an I score of 1. (B) Example of an I score 2. (C) Example of an I score 3. All samples had stromal staining pattern for BLT1 with a spread of I scores between 1-3. Arrows indicate cancer epithelium associated stroma. (Scale bars 100 μm).

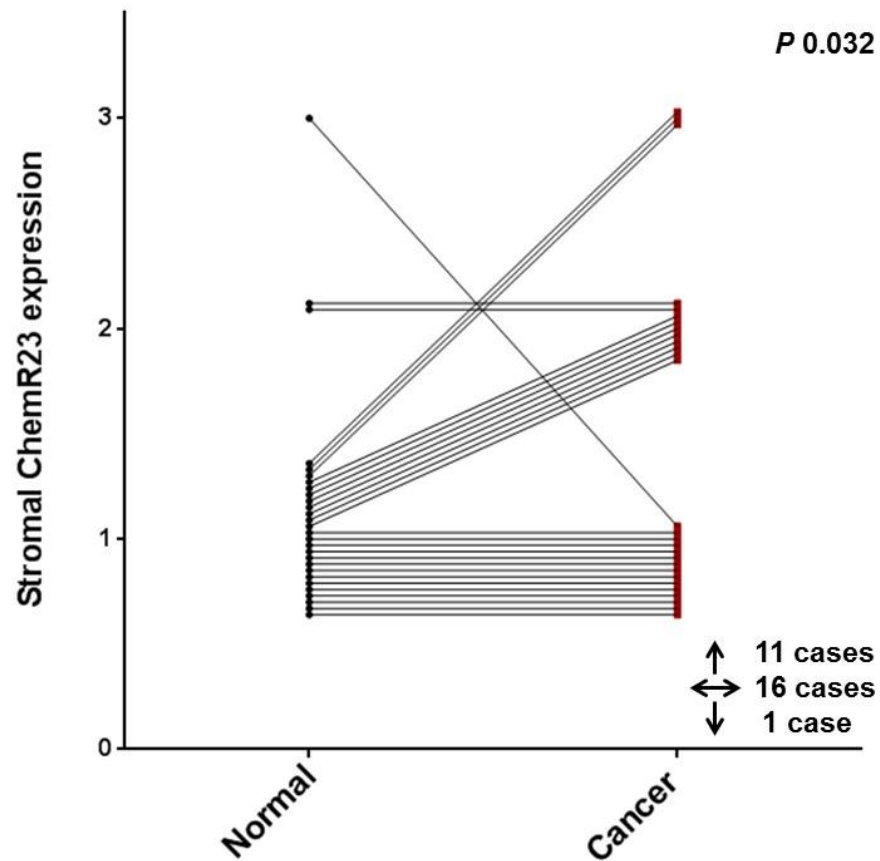
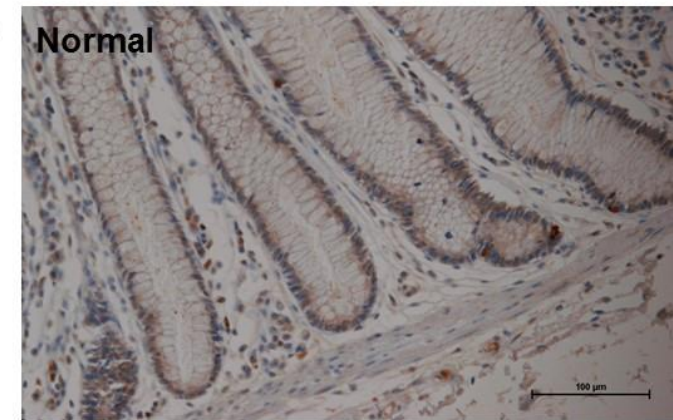
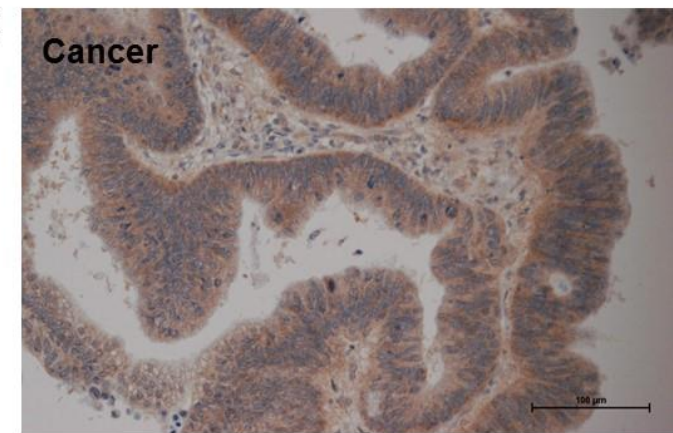
A**B****C**

Figure 31. ChemR23 expression between matched histologically normal human CR epithelium associated stroma and CRC epithelium associated stroma.

Twenty-eight different FFPE human CRC samples with both histologically normal CR epithelium associated stroma and CRC epithelium associated stroma. The sections had been scored for intensity (0-3) and percentage cell population staining (0-3). (A) Graph illustrating the score for ChemR23 expression in matched histologically normal CR epithelium associated stroma and CRC epithelium associated stroma. Statistical analysis was performed using a Wilcoxon matched-pairs signed rank test ($P = 0.032$). (B) ChemR23 staining in histologically normal CR epithelium associated stroma. (C) ChemR23 staining in CRC epithelium associated stroma (sample matched to that of B). There was an increase in ChemR23 expression between histologically normal human colorectal epithelium associated stroma and human CRC epithelium associated stroma. Arrows indicate stroma. (Scale bars 100 μ m).

3.4.2.5 Correlation between BLT1 and ChemR23 expression in human colorectal cancer tissue

There was no correlation found between 73 matched human CRC samples for BLT1 and ChemR23 expression in the CRC epithelium (Appendix 25; Spearman r 0.218, 95% confidence interval -0.019-0.433, $P = 0.064$). There was no correlation found between BLT1 and ChemR23 expression in the histologically normal colorectal epithelium in 19 matched samples (Appendix 26; Spearman r -0.358, 95% confidence interval -0.706-0.129, $P = 0.132$).

Furthermore no correlation was established between BLT1 and ChemR23 expression in the CRC epithelium from the matched 73 samples (Appendix 27; Spearman r -0.016, 95% confidence interval -0.252-0.221, $P = 0.891$), or in the 19 matched samples with histologically normal CR epithelium associated stroma expression (Appendix 28; Spearman r -0.279, 95% confidence interval -0.623-0.266, $P = 0.347$).

3.5 Discussion

Before examining whether RvE1 has any effects on CRC cell apoptosis or proliferation and whether CRC cells and or macrophages could synthesise RvE1, it was necessary to establish whether the GPCRs BLT1 and ChemR23 were expressed by CRC cells *in vitro*. Furthermore by establishing the BLT1 and ChemR23 expression profile of a panel of different human CRC cell lines *in vitro* would allow appropriate use of cellular models examining for RvE1 mediated effects on human CRC cell apoptosis and proliferation.

3.5.1 The *in vitro* expression of BLT1 and ChemR23 by human colorectal cancer cells

The qPCR screen of the human CRC cells confirmed expression of BLT1 receptor mRNA in all cell lines including the positive THP1 control cell line, and the negative HEK293 control cell line. ChemR23 expression was also seen in all cell lines including the supposedly negative HEK293 cells. These results must be interpreted with caution as the results are not in keeping with the literature, which casts doubt on the specificity of these assays for the receptors targeted by the candidate in this work.

Whilst HEK293 cells are reported to be negative for BLT1 gene expression (Chen *et al.*, 2004), this is not in keeping with the positive mRNA findings of the candidate's work. However the authors (Chen *et al.*, 2004) did not clarify which technique they used to confirm the absence of BLT1 in HEK293 cells, and did not show their data.

Recently HEK293 were shown to be positive for BLT1 mRNA qPCR, but the authors did not comment on BLT1 protein expression status in the HEK293 cells (Galet *et al.*, 2013). Using a Cayman Chemical anti-BLT1 antibody BLT1 protein expression was identified in the positive control cell line THP1 cell lines but not in any of the human CRC cell lines screened. A reason for the discrepancy between the qPCR and WB findings for BLT1 expression in human CRC cells could be that BLT1 mRNA is not translated into protein. Each cell line may be expressing extremely low levels of BLT1 mRNA. However as the THP-1 (positive) control cell line did not have a notably lower Δ Ct value than the HEK293 (negative control) cell line it is likely that the BLT1 primers were not effectively amplifying their target sequences. The Ct values across all cell lines for the target gene raises the possibility that the assay was not detecting BLT1 and thus the candidate is unable to comprehensively conclude on BLT1 mRNA expression, despite good expression in the β -actin housekeeping gene (Ct value less than 20).

As for BLT1 the qPCR screen of the human CRC cells confirmed expression of ChemR23 mRNA in all the human CRC cell lines including the positive control Jurkat cells and the negative control HEK293 cell line. The Jurkat (positive control) cell line however did not have a lower Δ Ct value than the HEK293 (negative control) cell line, which like the BLT1 primer, casts doubt on the primer specificity. ChemR23 protein expression was confirmed by WB in the positive control Jurkat cell line with ChemR23 detected in all the human CRC cell lines the under high sensitivity chemiluminescence. Furthermore the Caco2 human CRC cell line which had the highest level of endogenous ChemR23 protein expression did not have the highest expression of ChemR23 at the mRNA level.

However the lack of correlation between mRNA and protein findings for BLT1 and ChemR23 could also be genuine. For instance no correlation was found between gene and protein expression in the androgen treated prostate cell line LNCaP (Waghray *et al.*, 2001), and in a study comparing gene and protein expression in human lung adenocarcinomas, only 21% of genes had a significant correlation with the respective protein (Chen *et al.*, 2002). Another explanation for differences in protein translation between cell lines could be also due to differences in the untranslated regions (UTR) between different cell lines. Indeed both 5' and 3' UTR regions of mRNA contain motifs that can influence the stability of mRNA and subsequently the efficiency of its translation into protein (Pesole *et al.*, 2001). The ChemR23 TaqMan gene expression assay used was placed within the 3' UTR. Therefore gene amplification may be affected by variation in this region between cell lines and therefore account for the differences in between the mRNA and protein findings for ChemR23 (Appendix 30 and

Appendix 31, for BLT1 and ChemR23 respectively). Recent published work showed ChemR23 expression by M1 macrophages using qPCR that targeted the 5' region of the gene (Herová et al., 2010). Thus the primers used by the candidate may just not have worked. Indeed whilst there was ChemR23 protein induction in increasing confluent Caco2 cells this was not seen at the mRNA level (Appendix 32). Another reason for a lack of clear association between the mRNA and protein levels for both ChemR23 maybe down to the TaqMan assays being non-specific to the target gene. However a nucleotide sequence search of the probes used by TaqMan confirmed specificity for human BLT1 and ChemR23. Another reason could be secondary to an inherent difference between the cell lines used by the candidate and those of other group. Indeed short tandem repeat (STR) sequencing of the all the cell lines used in this work found allelic variation against that of published STRs (DNA sample collected by candidate for analysis but analysis performed by Leeds University cell line authentication service, data not shown). In summary the mRNA findings of both BLT1 and ChemR23 have to be interpreted with some caution as firm conclusions could not be made by the candidate.

Campbell *et al.*, (2010) reported that Caco2 and T84 human CRC cells express BLT1 protein and Ihara *et al.*, (2007) showed that both Caco2 and HT29 human CRC cells express BLT1 protein, which is not in keeping with the current negative findings of this work. An inherent difference between the group's cell lines may explain this. Indeed short tandem (STR) sequencing of the Caco2 and HT29 cells used showed that there was some allelic variation with published Caco2 and HT29 STR sequences. The authors also reported low expression of BLT1 protein in Caco2 and T84 cells using a Genetex anti-BLT1 antibody. Their published BLT1 WB included several other non-specific resolved protein bands and no clear protein MW marker, so firm conclusions on BLT1 protein status would be difficult to make. In respect to Ihara *et al.*, (2007) they used an anti-BLT1 antibody from Cayman Chemical (no more details provided), and did not publish a full WB image or define the MW of the BLT1 resolved protein detected. In respect to the 40 kDa size of the resolved protein band (Figure 10) and the predicted 38 kDa MW of BLT1, the difference could be explained by glycosylation of the BLT1 receptor. It is established that GPCRs are usually glycosylated, principally at their extracellular N-terminal domain. The candidate also confirmed a variation between different commercially available protein standards and the protein size may indeed be closer to 38 kDa. A similar size discrepancy was seen with the resolved ChemR23 protein band which may be contributed through glycosylation or discrepancy with the sizing of the standard protein bands.

In respect to ChemR23 there are several other resolved protein bands evident on the WB image, and this could be explained by the non-specificity of rabbit polyclonal identifying other related human proteins. Example human proteins that have amino acid residue coverage of 10 or greater with the immunogen used to raise the anti-ChemR23 antibody (amino acid sequence:YMACMVI WVLAFFLSS PSLVFRDTAN LHGKISCFNN F SLSTPGSSSW) includes probable G-protein coupled receptor 152, C3a anaphylatoxin chemotactic receptor, substance P receptor and Prostaglandin D2 receptor 2.

The candidate found that the protein ladder also could influence the interpretation of a resolved bands size, with two different protein standards migrating through a WB gel differently (see Appendix 33). The candidate used the MagicMark™ protein standard for all WB studies.

Campbell *et al.*, (2010) published that both T84 and Caco2 human CRC cells express ChemR23 mRNA and protein by flow RT-PCR and flow cytometry, respectively. Campbell *et al.*, (2010) also reported high cell population ChemR23 protein expression in Caco2 and T84 cells, with 83.7% cells staining positive for ChemR23 in the T84 cell population. This is different to the WB findings of this report where Caco2 protein expression was more than fivefold greater than for T84 cells. Reasons for this dissimilarity could be due to inherent variations between the cells, the type of anti-ChemR23 antibody used, a discrepancy in the growth conditions of the cells when analysed (e.g. cell confluency) and difference in the ChemR23 analytical technique used.

Interestingly the candidate's work has shown that Caco2 human CRC cells have an induction in ChemR23 protein expression at increased cell confluency. To date there has been no published literature on ChemR23 induction in human CRC cell lines; however there is literature describing ChemR23 protein expression in other cell types such as leukocytes of the monocytic lineage such as monocytes, macrophages, myeloid dendritic cells (mDC) and plasmacytoid dendritic cells (pDC), with ChemR23 downregulated in both mDC and pDC during differentiation (Vermi *et al.*, 2005). In macrophages ChemR23 has shown to be downregulated by proinflammatory cytokines (IFN- γ , TNF- α), TLR ligands (LPS) and increased by TGF- β (Zabel *et al.*, 2006). ChemR23 mRNA induction by TGF- β was also shown by Campbell *et al.* (2007) by oral epithelial cells (KB cells), however TGF- β did not change ChemR23 transcript levels in T84 and Caco2 human CRC cell lines (Campbell *et al.*, 2010). However Campbell *et al.* (2010) did not comment in their study on whether they measured ChemR23 mRNA transcript levels in the T84 and Caco2 cell lines tested, and whether or not they correlated with protein levels. Reasons for the ChemR23 induction in Caco2 cells may

be due to TGF- β levels or down to reduced nutrients or serum growth factors in the culture medium as the cells become more confluent. Heterogeneity between Caco2 cells for ChemR23 expression seen on the IF study suggests that there may be a cell confluency dependent effect, as staining appeared more intense on those Caco2 cells clustered closely together. Future work could look to investigate TGF- β levels in the conditioned medium from Caco2 cells over increasing confluency and measure ChemR23 expression in different serum depleted conditions. Human CRC cell confluency has been shown to effect protein expression previously, an example being CD26. CD26 is a dipeptidyl peptidase IV surface glycoprotein, the expression of which has been shown to increase in a confluency dependent manner in two different human CRC cell lines (HCT116 and HCT15) (Abe *et al.*, 2011). This group showed that CD26 induction was secondary to increased Cdx2 expression, related to a confluence-mediated cell cycle arrest. Future work should look to investigate the mechanism(s) involved in the confluence-dependent increase in ChemR23 expression in the Caco2 human CRC cell line, and the role that this receptor may have in CRC.

3.5.2 Expression of BLT1 and ChemR23 by human clinical colorectal cancer tissue

BLT1 protein expression was then examined in human CRC tissue. The anti-BLT1 antibody was the same as that used from the WB study. BLT1 expression was identified in all 78 cases of human CRC, with the immunostaining being cytoplasmic in the CRC epithelium. BLT1 expression was also examined in the histologically normal epithelium, and shown to be present in 30 of the 31 cases examined. There was a significant induction in BLT1 expression between matched histologically normal colorectal epithelium and CRC epithelium, which may be related to increased inflammation present in the CRC microenvironment. The reason why the staining for BLT1 a GPCR receptor appeared to be cytoplasmic could be due to the FFPE processing of the specimen, or intracellular cycling of the receptor. The cytoplasmic staining pattern of BLT1 in CRC epithelium and its increased expression in CRC epithelium compared to normal epithelium is in keeping with the study by Ihara *et al.* (2007), BLT1 was also showed to be cytoplasmic in human prostate cancer specimens (Galet, *et al.*, 2013). There is, however, evidence in the literature that other G protein coupled receptors such as GPR43 give a cytoplasmic staining pattern in normal colon and adenocarcinoma tissue (Tang *et al.*, 2010), as did GPR116 in normal breast and breast cancer tissue (Tang *et al.*, 2013). There was increased expression of BLT1 in the cells in the non-dividing, differentiated surface compartment (Figure 16B). Differential gene expression patterns between cells located in the basal crypts compared to cells at the top of the colonic crypts has been commented upon previously

(Kosinski, *et al.*, 2007), however differential BLT1 protein expression in colonic crypts has not been published to date.

BLT1 expression was seen in the stroma of the CRC samples, with expression not only by immune cells, in keeping with the published literature (Tager *et al.*, 2003), but also by spindle shaped cells (possibly myofibroblast cells). Fibroblasts (James *et al.*, 2006), and endothelial cells have both been shown to express BLT1 protein (Qiu *et al.*, 2006). Like with the cancer epithelium and histologically normal epithelium, there was a significant induction in BLT1 expression between histologically normal associated stroma and the cancer associated stroma. This increased expression in BLT1 between the normal and cancer for both the epithelium and stroma could present an increase in the inflammatory cellular environment associated with cancer.

BLT1 expression was increased in tumours distal to the splenic flexure, with the staining increased in spindle shaped cells (possibly myofibroblast) in those distal tumours. CRC pathogenesis is thought to be different between proximal colon and distal colon cancers, as these two sites originate embryologically from the midgut and hindgut (Langman, 1985). Differences in the genetic mechanisms between proximal and distal CRC initiation and progression is supported in the published literature (Delattre *et al.*, 1989; Breivik *et al.*, 1997; Konishi *et al.*, 1999). Therefore it may be that the difference in BLT1 expression between proximal and distal CRC may be being influenced by distinct genetic factors based on CRC location, such as *TP53* mutations, that have been predominantly found in distal CRCs (Konishi *et al.*, 1999).

The discrepancy between the negative *in vitro* findings for BLT1 expression in the human CRC cell lines and the positive cytoplasmic expression identified in the human CRC epithelium is interesting. The BLT1 expression in the stroma could be influencing the expression of BLT1 in the CRC epithelium through paracrine signaling, however this is speculative. Future *in vitro* cell modeling should take this into account and should incorporate a co-culture model including not only CRC epithelial cells but stromal cells such as myofibroblasts.

Interestingly, ChemR23 as with BLT1 protein expression was seen in the base of the crypts of the normal CR epithelium which could be due to expression by the colonic stem-like crypt cells. Furthermore, there was increased expression of ChemR23 in the cells in the non-dividing, differentiated surface cell compartment of the colonic crypt (as was seen with the BLT1 receptor). BLT1 and ChemR23 expression in colonic stem cells could be investigated. As intestinal stem cells are constantly replenishing the epithelium and there appears to be an induction in both BLT1 and ChemR23 expression in cells as they migrate up the colonic crypt then future studies should look to determine whether stem cells are expressing these receptors or whether more

differentiated crypt cells express these receptors. This could be studied in the first instance, through co-expression studies, using stem cell markers, such as the leucine-rich-repeat-containing G-protein coupled receptor 5, (Barker *et al.*, 2007).

BLT1 and ChemR23 expression by tumour associated myofibroblasts should be confirmed, particularly in regards to BLT1. The differences in CRC epithelium associated BLT1 expression between distal and proximal CRC appeared to be as a consequence of increased myofibroblast expression. Whether there are phenotypic differences between those myofibroblasts that are located proximal to the splenic flexures which are predominantly low expressors of BLT1 and those that are located distal to the splenic flexure which are higher BLT1, would be valuable to know. Establishing in the first instance whether the BLT1 expression in the myofibroblasts correlates with protease fibroblast activation protein- α expression, which is a protein that has been shown to be expressed by CAFs, (Henriksson *et al.*, 2011), and implicated as a negative prognostic factor in metastatic CRC patients, would be warranted (Henry *et al.*, 2007).

3.6 Summary

The candidate aimed to investigate whether ChemR23 and BLT1 are expressed in human CRC tissue. The candidate found that both human CRC epithelium and its associated stroma express both BLT1 and ChemR23.

BLT protein expression was not identified *in vitro* in the screened panel of human CRC cell lines, with ChemR23 protein expression identified in several of the cell lines screened. Consideration to whether human CRC cells need other cells such as fibroblasts or immune cells to express these receptors could be addressed through co-cultures. Future *in vitro* studies looking at a cell model to investigate RvE1 activity would need to address the fact that the human CRC cell lines screened by the candidate did not express detectable BLT1 protein. Therefore consideration to either screening further human CRC cell lines for BLT1 expression, or whether BLT1 expression could be promoted through cell co-cultures.

BLT1 and ChemR23 protein were shown to be expressed in human CRC tissue. BLT1 and ChemR23 expression was not only seen in the cancer epithelium but also in the associated stroma with immunostaining in immune like cells, endothelial and spindle shaped cells (possibly myofibroblasts). This work has shown an association between human colorectal epithelium BLT1 and ChemR23 protein expression and increased expression in CRC epithelium, which is likely secondary to the increased inflammatory microenvironment seen in CRC. There was a weak correlation between ChemR23 protein expression in the CRC epithelium and stroma. Furthermore there

was increased BLT1 protein expression identified in the CRC associated stroma distal to the splenic flexure. Human CRC tissue express increased amounts of BLT1 and ChemR23 and therefore offers a plausible pathway for any RvE1 mediated anti-CRC effect(s).

Future studies should look to examine for an association between ChemR23 and BLT1 with disease free and mortality outcomes as well as in adenomatous CRC precursor lesions.

4 Development of an *in vitro* model for investigation of Resolvin E1 synthesis by colorectal cancer cells

4.1 Introduction

The biosynthesis of RvE1 from EPA in the presence of aspirin was initially identified by liquid chromatography tandem mass spectrometry (LC-MS/MS) in TNF- α induced inflammatory exudates from murine air pouches (Serhan *et al.*, 2000). Subsequently Serhan and colleagues reported the presence of RvE1 in the colon of DSS-treated transgenic *fat-1* mice *in vivo* by LC-ultraviolet (UV)-MS/MS (Hudert *et al.*, 2006) and in human plasma samples by LC-MS/MS (Arita *et al.*, 2005).

As discussed in section 1.9.1, RvE1 is formed through the actions of aspirin acetylated COX-2, 5-LOX and LTA₄H enzymes on EPA. It is proposed that EPA within endothelial or epithelial cells is acted upon by aspirin acetylated COX-2 which acts like a peroxidase and adds a hydroxyl group (-OH) to C18 of EPA forming 18-HEPE. 18-HEPE is then converted to RvE1 by the actions of both 5-LOX and LTA₄H. Acetylation by aspirin on a serine residue in the channel of the COX enzyme causes COX-2 to lose one of its two catalytic activities, with the 15-lipoxygenase like activity remaining (Holtzman *et al.*, 1992), specifically in the R chiral form (Mancini *et al.*, 1994).

LC-ESI-MS/MS has the ability to simultaneously analyse multiple lipid mediators in a single biological sample (Masoodi *et al.*, 2008). This analytical method thus offers a distinct advantage over techniques such as enzyme-linked immunosorbent assay (ELISA), and the reason why it was used in this project for lipid mediator analysis.

No published study to date has investigated for the synthesis of RvE1 in cancer cells or tissues. There is well documented over-expression of COX-2 and overexpression of 5-LOX (Soumaoro *et al.*, 2006) in human CRC thus there is a theoretical pathway that would allow the synthesis of RvE1 synthesis in human CRC.

4.2 Hypothesis

RvE1 can be synthesised by CRC epithelium with or without macrophages present.

4.3 Aims

1. To confirm that RvE1 can be detected by the candidate using LC/ESI-MS/MS from human PMNs.
2. To investigate the COX-2 and 5-LOX protein status of a panel of seven human CRC cell lines.
3. To establish *in vitro* conditions that allow the successful acetylation of COX-2 by aspirin.
4. To determine whether human or mouse CRC cell lines or a mouse macrophage cell line (+/- aspirin treatment) can synthesise RvE1.
5. To determine whether a transcellular model (CRC cell line/ macrophage cell line) can synthesise RvE1.

4.4 Materials and Methods

4.4.1 Experimental solutions

4.4.1.1 Arachidonic Acid

AA (Cayman Chemical, Ann Arbor, MI, US; Cat. No 90010) was supplied as a solution in ethanol at 100 mg in 200 μ L. This stock solution was further dissolved in ethanol to make a 1 mM stock solution and was stored at -80°C . AA was added to culture medium to give experimental media containing AA at a concentration of 1 μ M at 0.1% (v/v) dilution. A working solution was freshly prepared to minimise degradation. Culture medium supplemented with 0.1% (v/v) ethanol served as negative control in each experiment.

4.4.1.2 Aspirin

Aspirin (Cayman Chemical, Ann Arbor, MI, US; Cat. No 70260) was dissolved in dimethyl sulfoxide (DMSO), (Sigma-Aldrich, Poole, UK; Cat. No. 472301) at 80 mg/mL. Aspirin was added to culture medium to give experimental media at a concentration of 500 μ M at 0.1% (v/v) dilution. Cell culture medium supplemented with DMSO served as negative control in each experiment.

4.4.1.3 Calcium Ionophore (A23187)

Calcium ionophore A21387 (SIGMA-ALDRICH, Missouri, US; Cat. No C7522) was dissolved in ethanol at 1 mg mL. Calcium ionophore A21387 was added to culture

medium to give experimental media at a concentration of 1 μM at 0.1% (v/v). Culture medium supplemented with ethanol served as negative control in each experiment.

4.4.1.4 Eicosapentaenoic acid

EPA free fatty acid (FFA) capsules were kindly provided by SLA Pharma (Watford, UK). EPA-FFA was extracted from a plastic capsule using a sterile 21 gauge (G) needle and diluted 1:100 in 95% (v/v) ethanol immediately before use. EPA was added to culture medium to give experimental media at a concentration of 50 μM at 0.1% (v/v) dilution. A working solution was freshly prepared to minimise degradation. Culture medium supplemented with ethanol served as negative control in each experiment.

4.4.1.5 18-hydroxyeicosapentaenoic acid

18-hydroxy-eicosapentaenoic acid (18-HEPE) standard (Cayman Chemical, Ann Arbor, MI, us; Cat.No 32840) was supplied as a solution in ethanol at 50 μg in 500 μL (314 μM). 18-HEPE was added to culture medium to give experimental media at concentration of 1 μM at 0.1% (v/v) dilution. A working solution was freshly prepared to minimise degradation. Culture medium supplemented with ethanol served as negative control in each experiment.

4.4.1.6 Ionomycin

Ionomycin calcium salt from *Streptomyces globatus* was supplied by (SIGMA-ALDRICH, Missouri, US; Cat. No I0634). Ionomycin was reconstituted in ethanol to make a stock one molar solution. Experimental solutions were made up to give a concentration of 1 μM at <0.1% (v/v).

4.4.1.7 Lipopolysaccharide

LPS from *Escherichia coli* 0128:B12 was supplied as a lyophilized powder (SIGMA-ALDRICH, Missouri, US; Cat. No L2887). LPS was reconstituted in sterile phosphate buffered saline (PBS) to make a stock 1 mM solution. LPS stock solution was added to culture medium at a 1 $\mu\text{g}/\text{mL}$ concentration.

4.4.1.8 Resolvin E1

RvE1 standard (Cayman Chemical, Ann Arbor, MI, US; Cat.No 10007848) was supplied as a stock solution in ethanol at 25 μg in 500 μL (143 μM) and stored in 20 μL aliquots at -80°C until use. During the course of the candidate's studies RvE1 was not readily available and permission was obtained from Cayman Chemical for supply.

4.4.2 Cell culture

4.4.2.1 Media and growth requirements

Cells were cultured as detailed in section 3.2.1.1.

4.4.2.2 Passaging of the cell lines

Seventy to eighty percent confluent cells were passaged and pelleted as outlined in section 3.2.1.2. Raji cells (B-lymphocytes), a suspension growing cell line were grown to a cell density of 3×10^6 cells/ mL before they were centrifuged to a cell pellet (400 x g for five minutes). Cells used to produce the conditioned medium for the lipidomic analysis, were passaged and pelleted immediately after the medium was collected so that viable cell counts could be performed. RAW264.7 cells were not trypsinised and were scraped off the culture flasks, before being pelleted by centrifugation (400 x g for five minutes). CRC, Raji and RAW264.7 cells used in the experiments were used for up to a maximum of ten passages.

4.4.2.3 Viable cell counting

Cells were harvested from tissue culture flasks as described and viable cell counts taken as in section 3.2.1.3. Lipid mediators could therefore be quantified as picograms (pg) per million cells.

4.4.3 Western blotting

4.4.3.1 Sample preparation and protein extraction

See section 3.2.3.1. HCA7 were used as a positive control cell line for COX-2 expression (Tavolari *et al.*, 2008). Raji cells were used as a positive control cell line for both 5-LOX and 5-LOX activating protein (FLAP) protein expression (Boudreau *et al.*, 2011).

4.4.3.2 Quantification of protein in cell extract

See section 3.2.3.2.

4.4.3.3 Sodium dodecyl sulphate polyacrylamide gel electrophoresis of proteins

See section 3.2.3.3.

4.4.3.4 Transblotting of sodium dodecyl sulphate polyacrylamide gel electrophoresis separated proteins

See section 3.2.3.4.

4.4.3.5 Immunoblotting of proteins

See section 3.2.3.5. Anti-COX-2 was used at a dilution of 1 in 250, anti-5-LOX at a dilution of 1 in 250, and anti-FLAP was used at a dilution of 1 in 1000. See Table 3 for antibody details.

4.4.3.6 Visualisation of antibody reactive proteins

See section 3.2.3.6.

4.4.4 High performance liquid chromatography electrospray ionisation tandem mass spectrometry analysis of lipid mediators

4.4.4.1 Preparation of cells for eicosanoid analysis

Human CRC cells were grown to 70-80% confluency in T75 cm² flasks in culture medium containing FBS (see section 3.2.1).

The experimental solutions prior to cell supernatant collection for LC/ESI-MS/MS analysis were made up in FBS-free medium, as lipids present in the FBS would prevent accurate analysis of the lipid mediators synthesised by human CRC cells when analysed by LC/ESI-MS/MS.

Cells were either treated with culture medium with control carrier or with 1 µM of AA for 24 hours, before cell conditioned medium collection. Each cell line had two biological replicates (i.e. two control and two AA supplemented samples; different passage numbered cells with experiments performed on different days). The cell conditioned media was then collected in 15 mL collection tubes placed on ice prior to immediate transfer to -80°C storage.

Cell viability counts were performed on the adherent cells so individual eicosanoid levels could be quantified against cell number.

Twenty three different COX derived eicosanoids and one 5-LOX derived eicosanoid 5-HETE was analysed by LC/ESI-MS/MS. The COX derived eicosanoids were (Figure 3):

1. AA COX derived series-2 prostanoids.
2. Dihomo-gamma-linolenic acid (DGLA) COX derived series-1 prostanoids.
3. EPA COX derived series-3 prostanoids and TBX₃.

4.4.4.2 COX-2 acetylation by aspirin in human colorectal cancer cells

HCA7 human CRC cells were grown in cell culture specific medium T75 cm² flasks to 70-80% confluency. HCA7 cells were treated with 500 µM aspirin (or control carrier) for 30 minutes, before the medium was removed and replaced with a 1 µM AA solution (or

control carrier) for three hours. The assay (cell conditioned) medium was collected, stored and prepared as discussed above prior to 15R/S-HETE chiral LC/ESI-MS/MS analysis. Each condition was performed in duplicate (different passage numbered cells with experiments performed on different days). PGE₂ was included in the analysis to confirm successful COX acetylation.

Carrier control (ethanol) treated HCA7 cells were included as a control. Cell viability counts were performed on the adherent cells so individual lipid mediator amounts could be quantified against cell number.

4.4.4.3 HCA7 human CRC, MC38 mouse colorectal cancer and RAW264.7 mouse macrophage cell preparation for the synthesis of Resolvin E1

HCA7 human CRC cells and MC38 mouse CRC cells were grown in cell culture specific medium to 70-80% confluency, and the mouse macrophage cell line RAW264.7 was grown to 50% confluency. MC38 cell conditioned medium was collected and used both for LC/ESI-MS/MS and indirect co-culture with RAW264.7 cells in section 4.4.4.4. This allowed direct comparison between the samples pre and post placement on the RAW264.7 cells.

The HCA7, MC38 CRC cells were treated for 30 minutes with 500 µM aspirin (or equivalent DMSO control carrier) before the cell conditioned medium was removed, and 50µM of EPA was then added to the cells (or ethanol) for a further three hours. RAW264.7 cells were also included to investigate whether these cells could synthesise RvE1. The 50% confluent RAW264.7 macrophage cells were treated with 1µg/mL lipopolysaccharide (LPS) for 12 hours in order to induce COX activity before aspirin treatment (the dose and duration of LPS stimulation had been established prior to performing the experiment: 1 µg/ mL LPS treatment, 0 to 48 hour time period; samples analysed by Dr.Paul Loadman, University of Bradford).

Further control conditions included AA in culture medium (1 µM, 3 hours), EPA in culture medium (50µM, three hours) and aspirin in culture medium (500 µM, 30 minutes), AA treated cells (1 µM, 3 hours), EPA treated cells (50 µM, 3 hours) and 18-HEPE treated cells (1 µM, 3 hours). No cell controls were also included.

The cell conditioned medium/ or culture medium was then collected and stored at -80°C prior to LC/ESI-MS/MS analysis for RvE1, 18-HEPE, PGE₂, PGE₃, 15-HETE, LTB₄, LTB₅, 5-HETE lipid mediators. Each condition was performed in triplicate (different passage numbered cells with experiments performed on different days) apart from the AA alone oxidation control where only one sample was analysed. Note that

the aspirin and EPA treated MC38 cells (and aspirin and AA treated cells) were used at 20 mL reaction volumes in T150 cm² flasks, whereas all remaining samples were carried out in 10mL reaction volumes in T75 cm² flasks. This meant that 10 mL of cell conditioned medium from the aspirin and AA treated MC38 cells and 10 mL of the cell conditioned medium from the aspirin and EPA treated MC38 cells could be used for the transcellular synthesis cell model (see section 4.5.8) whilst the remaining 10 mL could be analysed separately (see section 4.5.7). All experimental solutions dosed on the cells were free of FBS. Cell viability counts were performed on the adherent cells so individual lipid mediator amounts could be quantified against cell number. Experimental protocol summarised in Figure 30 (more detailed see Appendix 34).

4.4.4.4 Preparation of the transcellular synthesis cell model for the synthesis of RvE1

MC38 mouse CRC cells were grown in cell culture specific medium in T150cm² flasks to 70-80% confluency, and the mouse macrophage cell line RAW264.7 was grown to 70% confluency in T75 cm² flasks. The MC38 cells were treated for 30 minutes with 500 µM aspirin before the cell conditioned medium was removed, and 50 µM of EPA was then supplemented to the cells (or ethanol) for a further three hours. The cell conditioned medium from the MC38 mouse CRC cells treated with aspirin/EPA and aspirin/AA was then placed on 70% confluent mouse RAW24.7 macrophage cells for 3 hours at 37°C. The last 10 minutes of the experimental incubation involved each of the RAW264.7 samples being treated with ionomycin (1 µM) in order to increase intracellular calcium and activate 5-LOX. The cell conditioned medium/ or culture medium was then collected, stored at -80°C prior to LC/ESI-MS/MS analysis for RvE1, 18-HEPE, PGE_{2/3}, 15-HETE, LTB_{4/5}, 5-HETE lipid mediators. Each condition was performed in triplicate (different passage numbered cells with experiments performed on different days). Cell viability counts were performed on the adherent cells so individual lipid mediator amounts could be quantified against cell number. All experimental solutions dosed on the cells were free of FBS. The experimental protocol is summarised in Figure 30 (more detailed see Appendix 34).

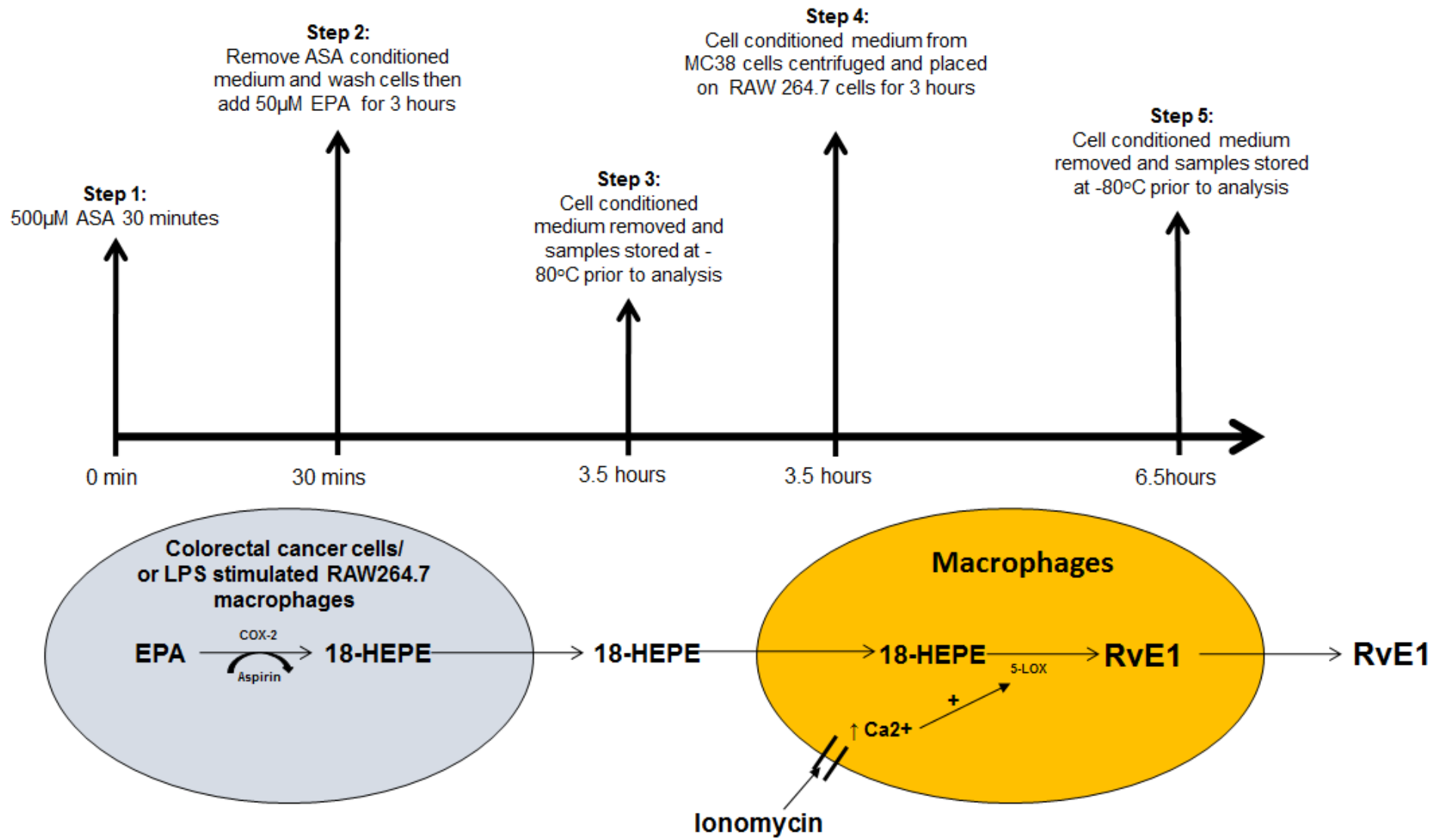


Figure 32. Experimental design for CRC and macrophages RvE1 biosynthesis experimentation.

4.4.4.5 Solid-phase extraction of lipid mediators

Prior to lipid extraction samples were thawed on ice and adjusted to 15% (v/v) methanol solution by adding 100% methanol (HPLC-grade, Fisher Scientific, Cat. No. M/4056/17). The internal standards (IS) PGB₂-*d4* (Cayman Chemical Co Ann Arbor, MI, USA, Cat. No. 311210), and 12-HETE-*d8* were added to each sample. The samples were acidified with 0.1 M hydrochloric acid (HCl; ACS reagent; Cat.No 320331) to pH 3.0 and applied to individual activated solid-phase extraction cartridges (SPE) cartridges C18-E (500 mg, 6 mL; Cat. No 8B-S001-HCH) as below.

The SPE cartridges were preconditioned with 20 mL of methanol followed by 20mL of de-ionised water. The extraction procedure was performed using a vacuum manifold (Phenomenex). After the samples were applied, the cartridges were washed with 20 mL 15% Methanol, 20 mL de-ionised water (ELGA system, 18.2 MΩ-cm purity, Model Ultra Ionic, Part No.PRIPLB0450, High Wycombe, UK) and 10mL Hexane (HPLC-grade, Fisher Scientific, Cat. No. H/0406/17), in succession. The lipid mediators were then eluted in 15 mL methyl formate (HPLC-grade, Fisher Scientific, Cat. No.12682-0025). The fraction was collected in a clean test tube and the solvent was evaporated under a stream of nitrogen. The residue was dissolved in 100 µL ethanol and stored at -20°C prior to analysis.

4.4.4.6 LC/ESI-MS/MS analysis

The analyses were performed on a Waters Alliance 2695 high performance liquid chromatography (HPLC) pump coupled to an ESI triple quadrupole Quattro Ultima mass spectrometer (MS) (Waters, Elstree, Hertsfordshire, UK), (LC/ESI-MS/MS). Instrument control and data acquisition were performed using the MassLynx™ version 4.0 software. The LC/ESI-MS/MS and chiral LC/ESI-MS/MS analyses were performed by the Nicolaou group. The candidate performed all the lipid mediator data analysis using chromatograms for lipid mediator specific MRMs supplied by the Nicolaou group from sections 4.4.4.1 and 4.4.4.2. The candidate acquired all chromatograms from lipid mediator appropriate MRMs for 4.4.4.3 and 4.4.4.4 under the supervision of the Nicolaou group.

In brief, stock solutions for all lipid mediators analysed were mixed and diluted to provide appropriate stock solutions between 2 and 100 pg/ µL final concentrations. For section 4.4.4.1 stock solutions of 2, 10, 20, 50 and 100 pg/ µL were used. For section 4.4.4.2; 10, 20, 50 and 100 pg/ µL stock solutions were used. For sections 4.4.4.3 and 4.4.4.4; 4, 10, 20, 50 and pg/ µL stock solutions were used. The internal standards PGB₂-*d4* and 12-HETE-*d8* were prepared in ethanol (2 ng/ µL) and added to all composite standards at a final concentration of 800 pg/ µL. Each individual lipid

mediator chromatogram had an x-axis (retention time, minutes) and a y-axis (% signal intensity), (Figure 31A) for the appropriate MRM mass to charge ratio (m/z), and a calculated peak area for the lipid mediator of interest (area calculated by MassLynx™ V4.0 software). The limit of detection (LoD) was calculated by using a signal-to-noise ratio (S/N) of 3 (ICH harmonised tripartite guidelines (2005)). The limit of quantitation (LoQ) was determined if the quantity of sample lipid mediator fell within the range of the standard calibration curve. Peak integrations and calculations of S/N ratios were performed using the MassLynx™ V4.0 software (Waters). The candidate constructed all lipid mediator standard calibration lines from chromatograms provided by the Bradford group for 4.4.4.1 and 4.4.4.2 (example shown in Figure 31B). Data acquisition and analysis were carried out by the candidate with supervision from Professor Nicolaou for 4.4.4.3 and 4.4.4.3. The peak-area ratios of the appropriate analyte, either to $\text{PGB}_2\text{-}d4$ or $12\text{-HETE-}d8$ (IS), were calculated or plotted against the concentration of the calibration standards. This serves to normalise analyte values to a known standard. Calibration line equations were calculated by the least-squares linear regression method. In order to calculate the concentration of a particular analyte the peak-area ratio of the analyte area against corresponding IS area was calculated and this area was quantified using the appropriate calibration line for said analyte (Figure 31C). Figure 31 summarises this method of lipid mediator analysis by the candidate, using PGE_2 synthesis by HCA7 cells as an example.

All cell conditioned media samples for lipidomic analysis were immediately stored at -80°C after collection. All samples were transported on dry ice to Bradford University. All samples immediately underwent solid-phase lipid extraction once they had defrosted. After solid-phase extraction the lipid samples were then immediately placed at -20°C storage ahead of sample analysis by LC/ESI-MS/MS.

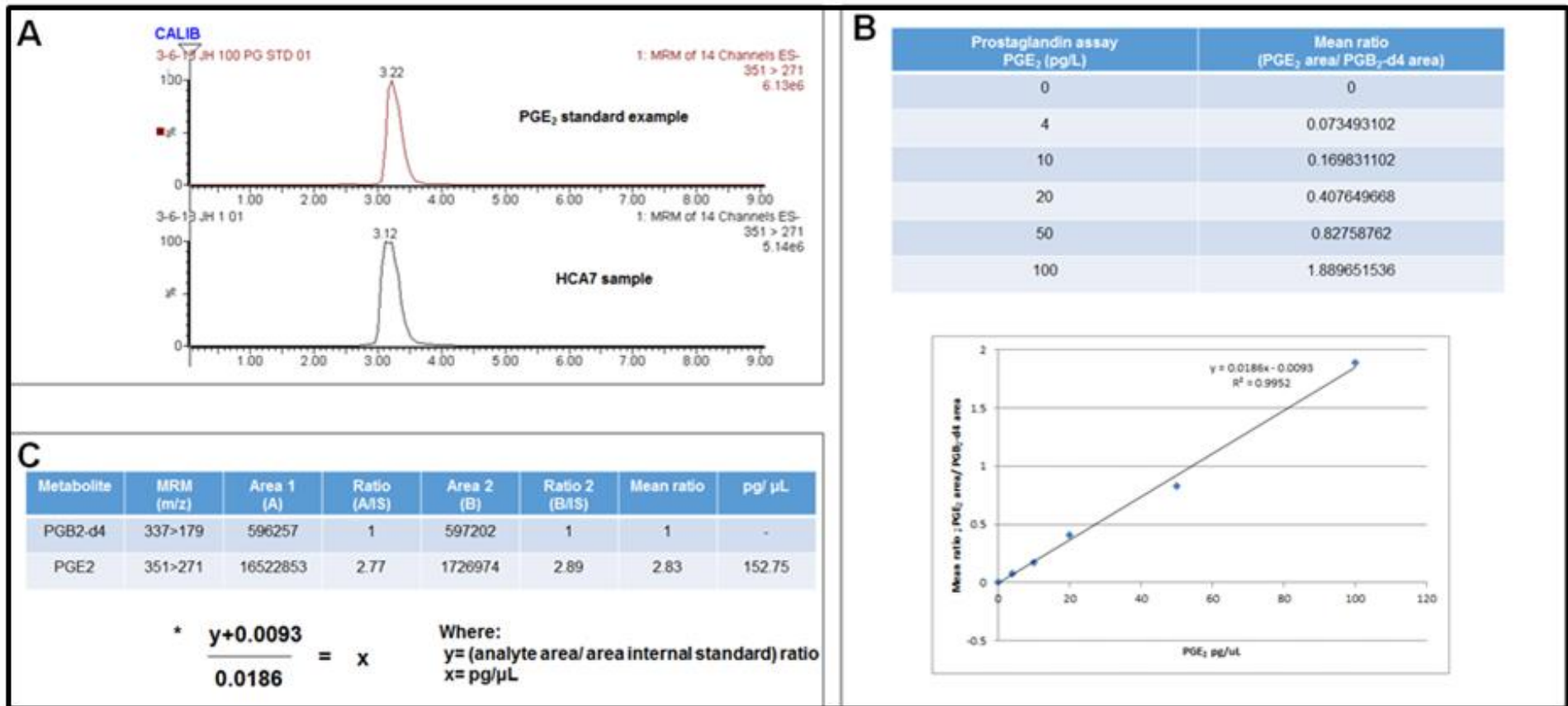


Figure 33. LC/ESI-MS/MS data analysis example.

The data analysis of the MRM allows the identification of the analyte of interest against a known m/z ratio(s). Construction of calibration lines from known amounts of lipid mediator allowed quantification of the lipid against that of the internal standard which was added in a known amount to the biological sample prior to analysis. (A) PGE₂ chromatogram example for the PG standard and from a HCA7 human CRC cell line sample at a MRM of 351> 271 (m/z). (B) Construction of PGE₂ calibration line from the 0-100 pg/ μ L standard data analysis; x-axis shows PGE₂ pg/ μ L and y-axis shows mass ratio; PGE₂ area/ PGB₂-d4 area. (C) Tabulated analyte (PGE₂) calculation example showing how the analyte is semi-quantified against the internal standard initially as an area ratio, before quantification using the least-squares linear regression method obtained for the specific lipid mediator standard calibration curve.

4.4.5 Cell viability assay

HCA7 human CRC cells, MC38 mouse CRC cells and RAW264.7 mouse macrophage cells were seeded into a 96 well plate at a cell concentration of 2000 cells per well for HCA7 and MC38 CRC cells and 3000 cells per well for the RAW264.7 macrophage cells. After 24 hours of incubation at 37°C, (each condition had eight wells) of a range of doses; 0 to 200 µM for EPA (3 hours 37°C) and 0 to 1600 µM (30 minutes, 37°C) for aspirin (culture medium was free of FBS). Controls included cells cultured in medium containing carrier control (eight replicates per plate) and culture medium alone (8 replicates per plate). The experimental solutions were made up in 50 mL sterile solution basins (Scientific Laboratory Supplies, UK; Cat.No.746180-2) to facilitate dosing of the cells by a multi-channel pipet. Seventy two hours after either EPA or aspirin treatment, 20 µL of 3-(4,5-Dimethylthiazol-2-yl)-2,5-diphenyltetrazolium bromide (MTT), (Sigma-Aldrich, Poole, UK; Cat.No M2128-1G) at a prepared concentration of 5 mg/ mL (in sterile DPBS) was added to each well and left in the dark at a temperature of 37°C for three hours. The culture medium solution was then aspirated, and DMSO added to the formazan precipitate left in the wells. The plate was then read at 570 nm using a microplate reader (Opsys MR™ Dynex technologies Ltd, UK) to give an optical density (OD) value for each well. The mean OD of a minimum of six wells was taken and a percentage cell viability value calculated by dividing the mean OD value for each individual experimental condition by the mean OD control value for each plate. Results were obtained from three independent experiments.

4.4.6 Human polymorphonuclear leukocyte isolation from whole blood samples and treatment with 18-HEPE for Resolvin E1 synthesis

The experimental protocol was developed by the candidate using information detailed in the previous publications in which RvE1 was synthesised by PMNs (Tjonahen *et al.*, 2006; Oh *et al.*, 2011).

Human plasma samples were collected from healthy volunteers who had not taken medication for at least two weeks prior to the samples being taken. Approval for the blood sampling was provided by the Leeds Multidisciplinary Research Tissue Bank, University of Leeds.

A total of 150 mL of blood was taken from two different volunteers in 6 mL VACUTTE[®] coagulation sodium citrate 3.2% tubes. Then 12 mL of HISTOPAQUE[®]-1119 was added to a 50mL plastic falcon tube. 12 mL of HISTOPAQUE[®]-1077 was then carefully layered onto the HISTOPAQUE[®]-1119. A volume of 24 mL of whole blood was then placed on top of the HISTOPAQUE[®] gradient. The 50 mL falcon tube(s) were then centrifuged at 700 x g for 30 minutes at room temperature (18-26°C). After centrifugation two distinct layers were seen, with the lower layer just above the red coloured erythrocytes containing the PMNs. The PMN layer was then carefully aspirated using a sterile 3mL Pasteur pipette. The PMNs were then washed by the addition of 10 mL isotonic PBS without calcium chloride (CaCl₂) and magnesium chloride (MgCl₂) (SIGMA-ALDRICH, US; Cat. No D8537). The cells were then centrifuged at 200 x g for 10 minutes. The supernatant was then removed and discarded. The PMNs were then re-suspended in 10 mL isotonic DPBS (without CaCl₂ and MgCl₂) and then centrifuged at 200 x g for 10 minutes. The cells were then washed re-suspended and centrifuged once more. The cells were then placed in sterile DPBS and a viability count was performed using trypan blue exclusion (see section 3.2.1.3).

Two samples were then prepared of 50 x 10⁶/ mL PMNs in sterile isotonic DPBS with CaCl₂ and MgCl₂ (Sigma-Aldrich, US; Cat. No D8662). One sample was treated with carrier control (ethanol, three minutes, 37°C) then with further carrier control (ethanol, 45 minutes, 37°C, v/v less than 0.1%) and the second sample was treated with 5 µM calcium ionophore A21387 (three minutes, 37°C) and then 50 µM of 18-HEPE (v/v 0.1%) for 45 minutes at 37°C. The incubations were stopped by adding two volumes of cold methanol. The samples were then immediately stored at -80°C until extraction and LC-ESI-MS/MS analysis (Nicolaou group).

4.5 Results

4.5.1 Resolvin E1 synthesis by human polymorphonuclear leukocytes

Human PMNs not treated with 18-HEPE did not synthesise detectable RvE1 (Figure 34A). Calcium ionophore stimulated human derived PMNs treated with 18-HEPE synthesised detectable RvE1 (Figure 34B). The MRM and retention time was directly comparable to that of the Cayman Chemical RvE1 (Figure 34C).

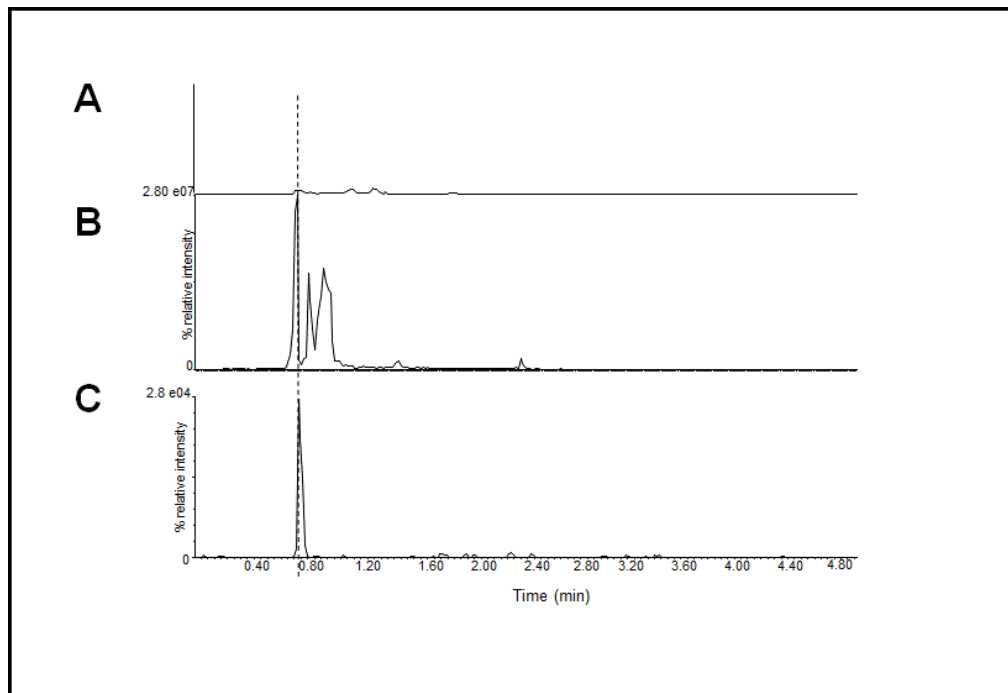


Figure 34. RvE1 biosynthesis by human polymorphonuclear leukocytes.

Samples were analysed using LC/ESI-MS/MS. (A) RvE1 chromatogram from the carrier control (ethanol) treated PMN sample. (B) RvE1 chromatogram from 18-HEPE treated, ionophore stimulated PMN sample. (C) RvE1 chromatogram from the RvE1 control Cayman Chemical RvE1. The dotted line represents the expected retention time for RvE1 (MRM 349>195).

4.5.2 COX-2 protein expression in human colorectal cancer cell lines

COX-2 protein expression in human CRC cells was analysed by WB. A band in keeping with its predicted MW of 72 kDa was detected by standard chemiluminescence in the HCA7 cell line, alone (Figure 35A). Under high sensitivity conditions several protein bands of varying MWs were seen in the remaining cell lines making conclusions on COX-2 status in the cell lines difficult, with possible low level expression in the HRT18, HT29 and Caco2 cell lines (Figure 35B). Protein loading was confirmed by probing the PVDF membrane with mouse monoclonal α -tubulin antibody (Figure 35C).

4.5.3 COX derived lipid mediators synthesis by human colorectal cancer cell lines

The lipid mediators synthesised by each human CRC cell line was analysed by LC/ESI-MS/MS in both AA supplemented and un-supplemented conditions. All of the human CRC cell lines synthesised quantifiable levels of COX derived lipid mediators from AA, DGLA and EPA, as shown in the heat map (Figure 36). There was no clear difference in the amounts of lipid mediators synthesised between the un-supplemented and AA supplemented cell lines (AA 1 μ M, 3 hours), on comparison of the heat maps of Figures 36 and 37, respectively, with individual AA/ DGLA/ EPA COX-derived lipid mediators shown in Figure 38. The HCA7 human CRC cells synthesised the largest amounts of AA derived COX derived lipid mediator PGE₂. Individual human CRC cell line lipid mediator synthesis data is tabulated in Appendix 35 and 36 (HCA7), Appendix 37 (LoVo), Appendix 38 (T84), Appendix 39 (HRT18), Appendix 40 (HT29), Appendix 41 (Caco2), and Appendix 42 (HCT116).

As the HCA7 cell line showed the highest level of COX enzymatic activity, with confirmed expression of COX-2 protein expression. This cell line was chosen to establish the *in vitro* conditions that would permit synthesis of the AA derived acetylated COX-2 product 15R-HETE.

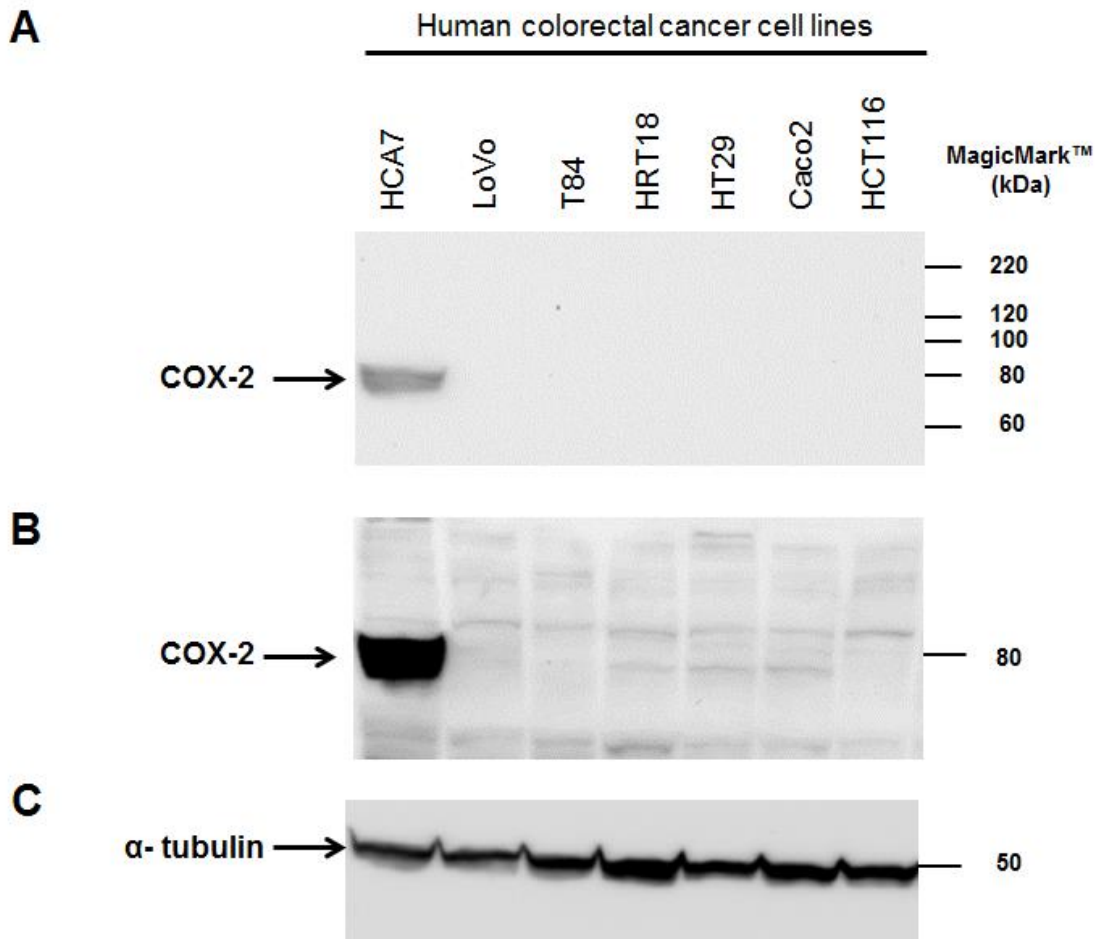


Figure 35. COX-2 protein expression by human CRC cell lines.

Human CRC cell lysate was loaded in each lane and probed with a goat anti-human COX-2 polyclonal antibody (1 in 250) and probed with a secondary conjugated HRP antibody (1 in 2000). (A) Image acquired using standard chemiluminescence. (B) Image acquired using high sensitivity chemiluminescence. (C) Protein loading was confirmed by probing for α -tubulin (50 kDa) with a mouse monoclonal anti-human α -tubulin antibody (1 in 5000), using standard chemiluminescence.

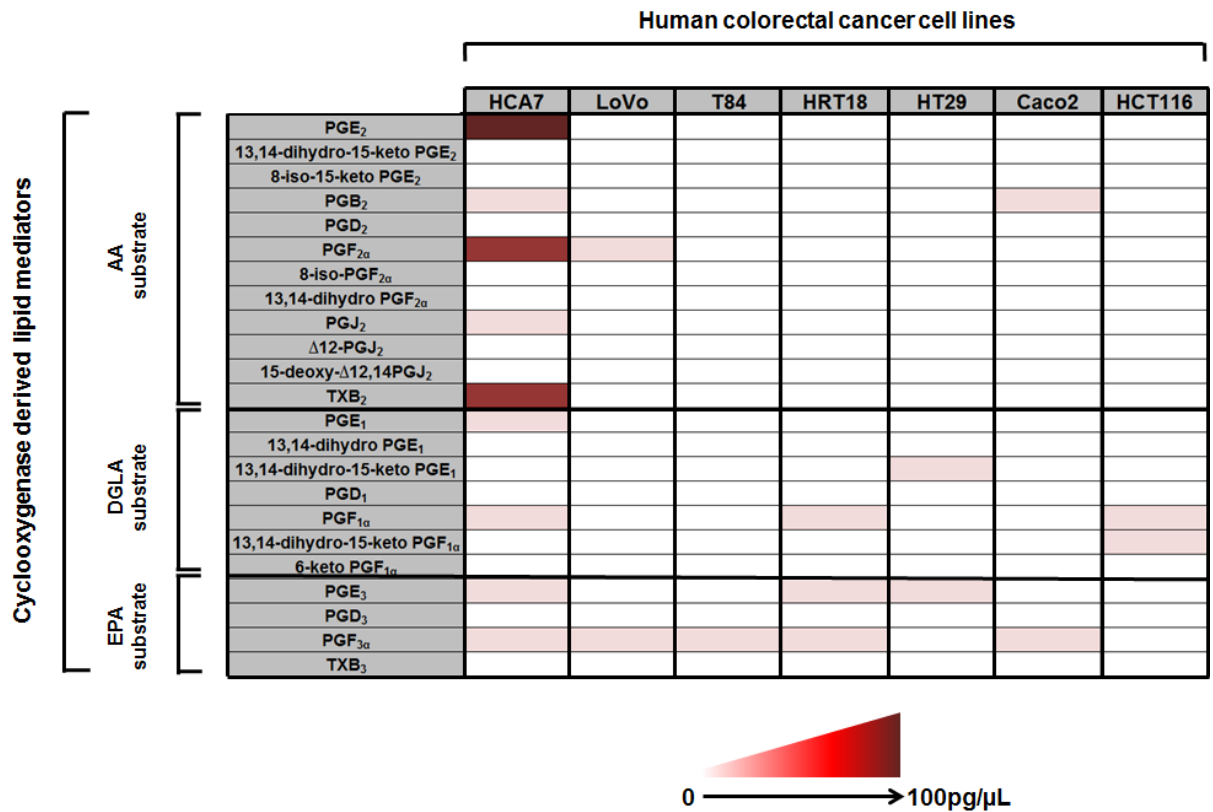


Figure 36. COX derived lipid mediator synthesis by human CRC cell lines.

Heat map illustrating the COX derived lipid mediators detected by LC/ESI-MS/MS analysis of the cell conditioned medium from control (no AA) human CRC cells. Coloured values represent picograms (pg)/ μL. Data acquired from two independently cultured experiments, using individual chromatograms, supplied by the Nicolaou group (appropriate standard calibration lines constructed and individual lipid mediator data analysed by the candidate). PGE₂ levels exceeded the 100 pg/ μL upper limit of quantification for the HCA7 human CRC cell line.

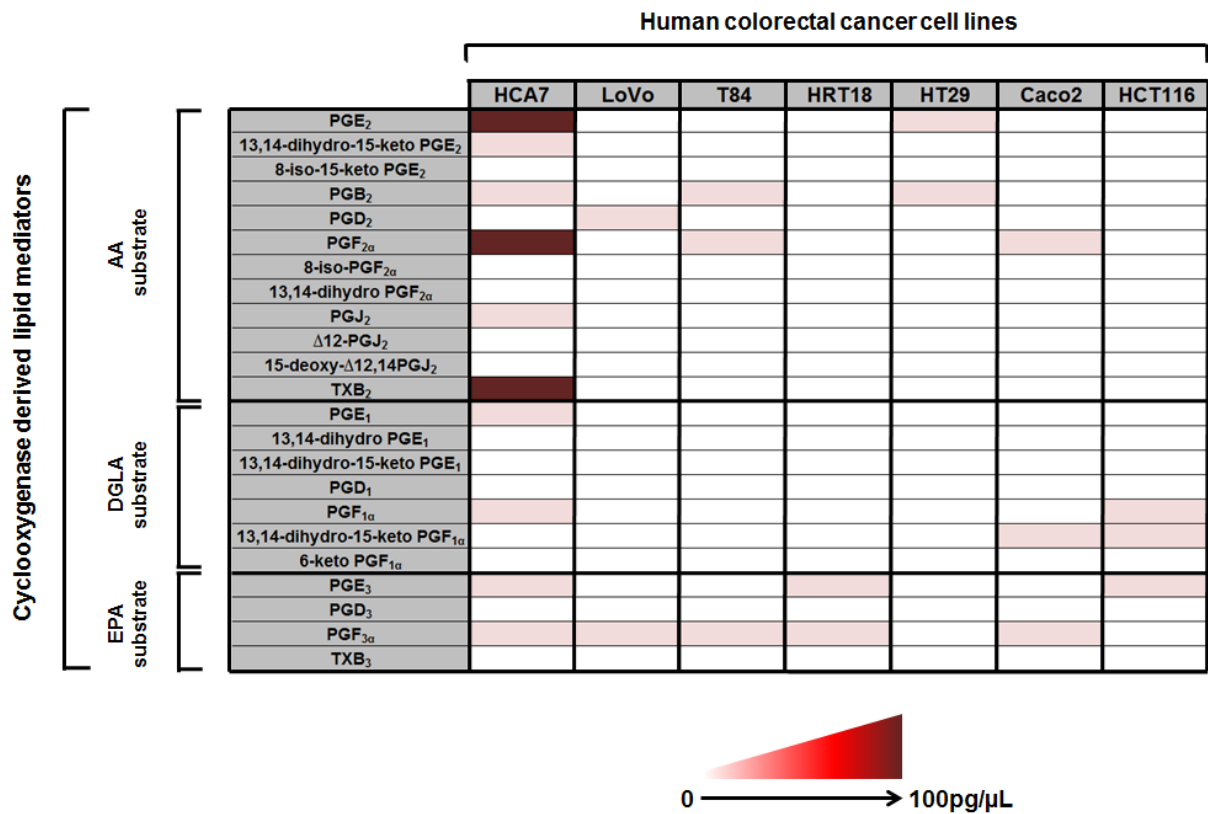


Figure 37. COX derived lipid mediator synthesis by AA treated human CRC cells lines.

Heat map illustrating the COX derived lipid mediators detected by LC/ESI-MS/MS analysis of the supernatant taken from AA supplemented (1 μM, 24 hours) human CRC cells. Coloured values pg/ μL. Data acquired from two independently cultured experiments, using individual chromatograms, supplied by the Nicolaou group (appropriate standard calibration lines constructed and individual lipid mediator data analysed by the candidate). PGE₂, PGF_{2α} and TXB₂ levels exceeded the 100 pg/ μL upper limit of quantification in the HCA7 human CRC cell line.

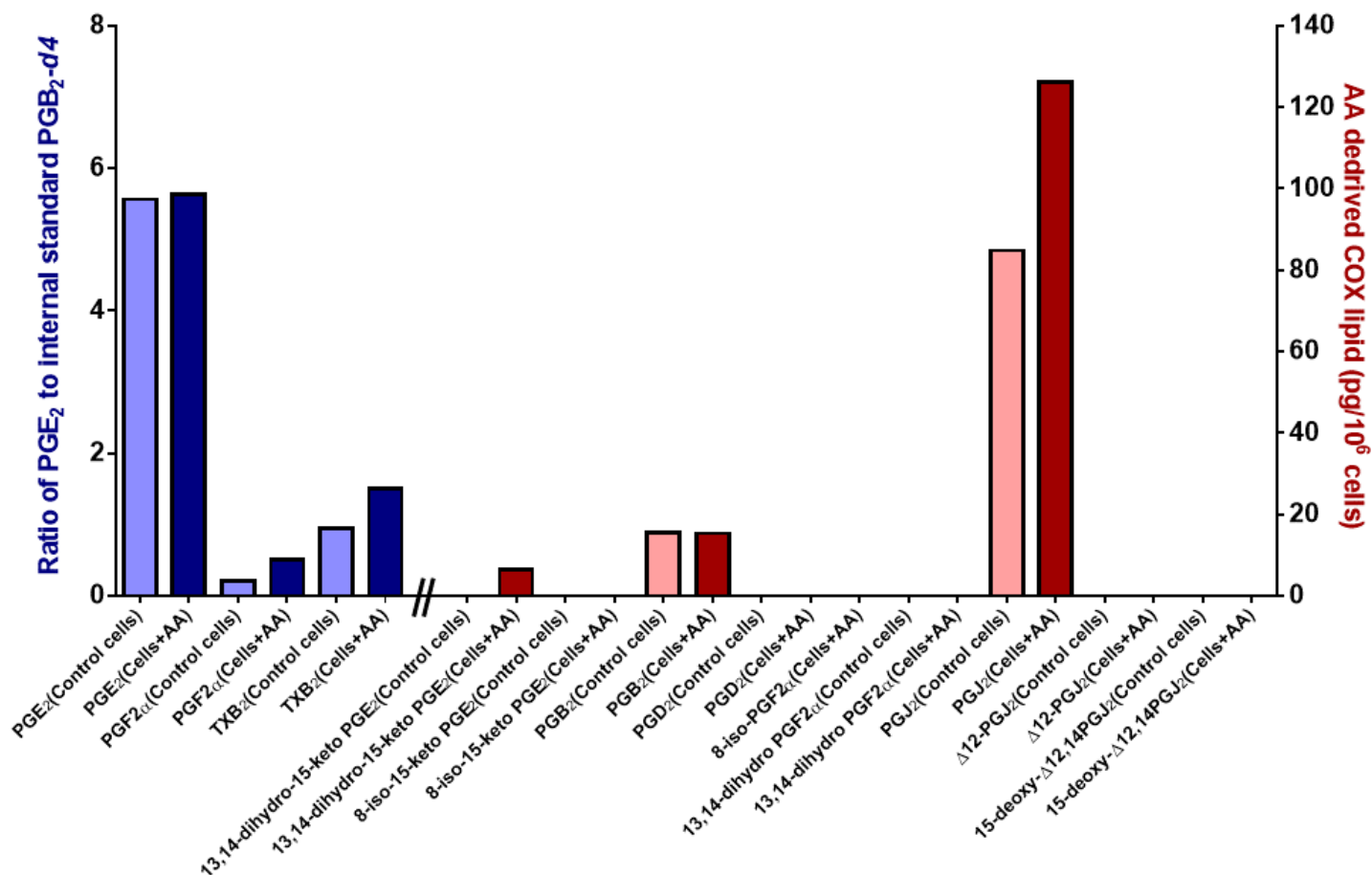


Figure 38. COX derived AA lipid mediators from the HCA7 human CRC cell line.

HCA7 cell conditioned medium was analysed for 12 different COX derived AA derived lipid mediators by LC/ESI-MS/MS, in the presence and absence of supplementary AA treatment. PGE₂, PGF_{2α} and TXB₂ levels exceeded the upper limit of the calibration curve for both control and AA samples and are shown as a ratio against the internal standard, (coloured blue). The remaining quantifiable lipid mediators are shown as pg per million (x10⁶ cells), (coloured red). The lighter coloured bars are the control samples and the darker coloured bars are the AA treated cell samples. Data shown as mean (two independent cell cultured experiments).

4.5.4 Western blot analysis of 5-LOX protein expression in a panel of seven human colorectal cancer cell lines

Expression of 5-LOX protein was investigated by WB using Raji cell lysate as a positive control (Boudreau *et al.*, 2011). Caco2 and HCA7 cells have also been shown to be positive for 5-lipoxygenase protein expression by WB using a BD Transduction Laboratories anti-5-LOX antibody (Tavolari *et al.*, 2008). WB revealed numerous protein bands so the presence of a 5-LOX protein could not be confirmed. Protein loading was confirmed by probing the PVDF membrane with mouse monoclonal β -actin antibody (Figure 39). As several protein bands of differing MWs were seen on the WB firm conclusions as to whether 5-LOX was indeed being detected under these experimental conditions could not be concluded upon.

4.5.5 Lipidomic analysis for 5-LOX derived 5-HETE synthesis in a panel of seven different human colorectal cancer cell lines

Production of the 5-LOX derived lipid mediator 5-HETE synthesised from AA was analysed by LC-ESI-MS/MS, in both AA supplemented and un-supplemented conditions. Only one of the human CRC cell line supernatant samples contained detectable levels of 5-HETE but not at levels that allowed quantification by LC-ESI-MS/MS (Figure 40). The 5-HETE peak in both the AA treated LoVo samples was above the baseline of the chromatogram, however this peak was not of sufficient magnitude for accurate quantification on analysis with the values obtained being <1 pg/ μ L, which is below the lowest concentration of 5-HETE used to construct the calibration line (2 pg/ μ L).

To investigate whether the lack of quantifiable 5-HETE was due to an absence of five lipoxygenase activating protein (FLAP), the panel of seven human CRC cell lines were screened for FLAP expression by WB. The Raji cells have been shown to be positive for FLAP expression (Bonizzi *et al.*, 1999), and were used as a positive control. Western blotting revealed the presence of a protein band in all human CRC cell lysates and Raji cells, in keeping with the predicted MW of FLAP which is 18 kDa (Figure 41).

In summary COX activity with COX-2 expression was seen in the HCA7 cell line, however 5-LOX expression/ enzymatic activity could not be established in any of the human CRC cell lines screened (Table 8).

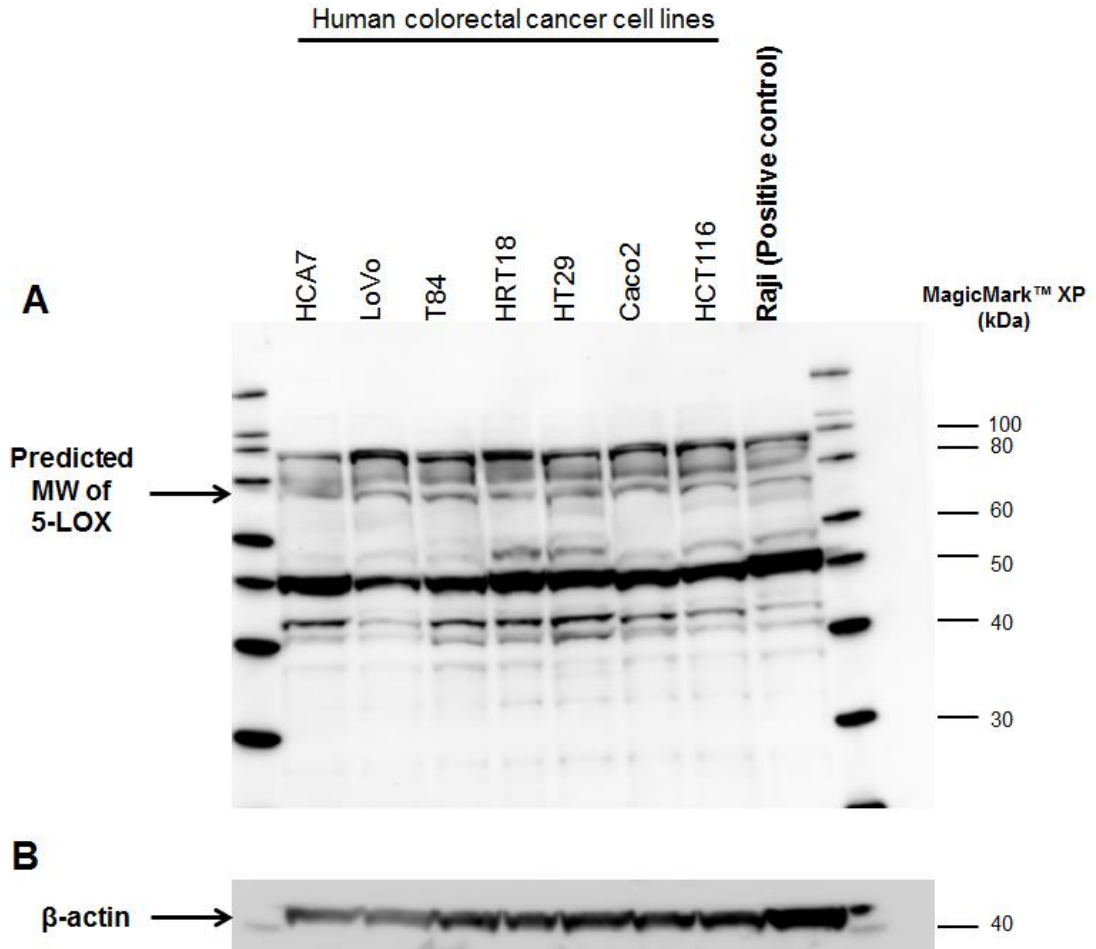


Figure 39. 5-lipoxygenase protein expression in human cell lines.

Human cell line lysate was probed with a rabbit anti-human 5-LOX polyclonal antibody (1 in 250) and probed with a secondary HRP (1 in 2000). (A) Image acquired after 45 seconds of high sensitivity chemiluminescence. (B) Protein loading was confirmed by probing for β -actin with a mouse monoclonal anti-human β -actin antibody (1 in 5000) using standard chemiluminescence. The presence of protein bands both above and below the predicted molecular weight (MW) of 5-LOX which is 78 kDa makes determination of the 5-LOX protein status of these cell lines under these conditions not possible.

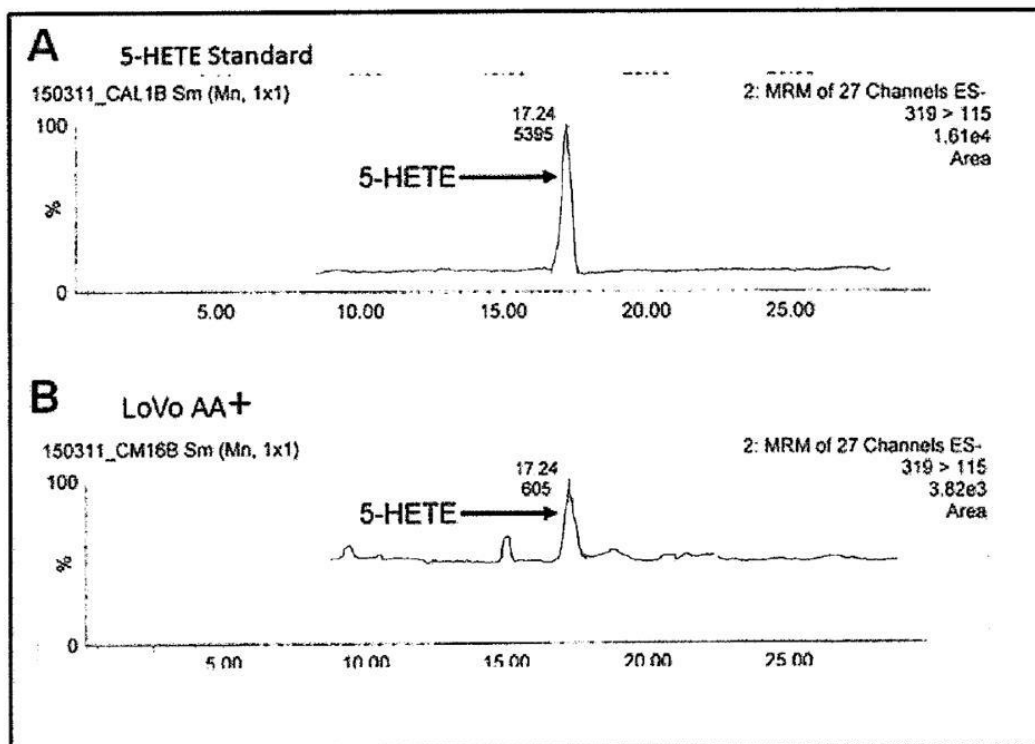


Figure 40. LC/ESI-MS/MS analysis for 5-HETE in the cell conditioned medium from LoVo human CRC cells.

Chromatograms obtained from LC/ESI-MS/MS analysis of the cell conditioned medium taken from AA treated LoVo cells (1 μ M, 24 hours) (A). 5-HETE internal standard chromatogram. (B). 5-HETE chromatogram The 5-HETE detected in the AA treated LoVo cells is just above the baseline of the chromatogram, and was not of sufficient magnitude for accurate quantification. No 5-HETE was detected in any of the other six human CRC cell line samples. The above original chromatograms provided by the Nicolaou group were very faint so the candidate has strengthened these peaks so that they can be visualised more clearly for the illustrative purposes of this thesis.

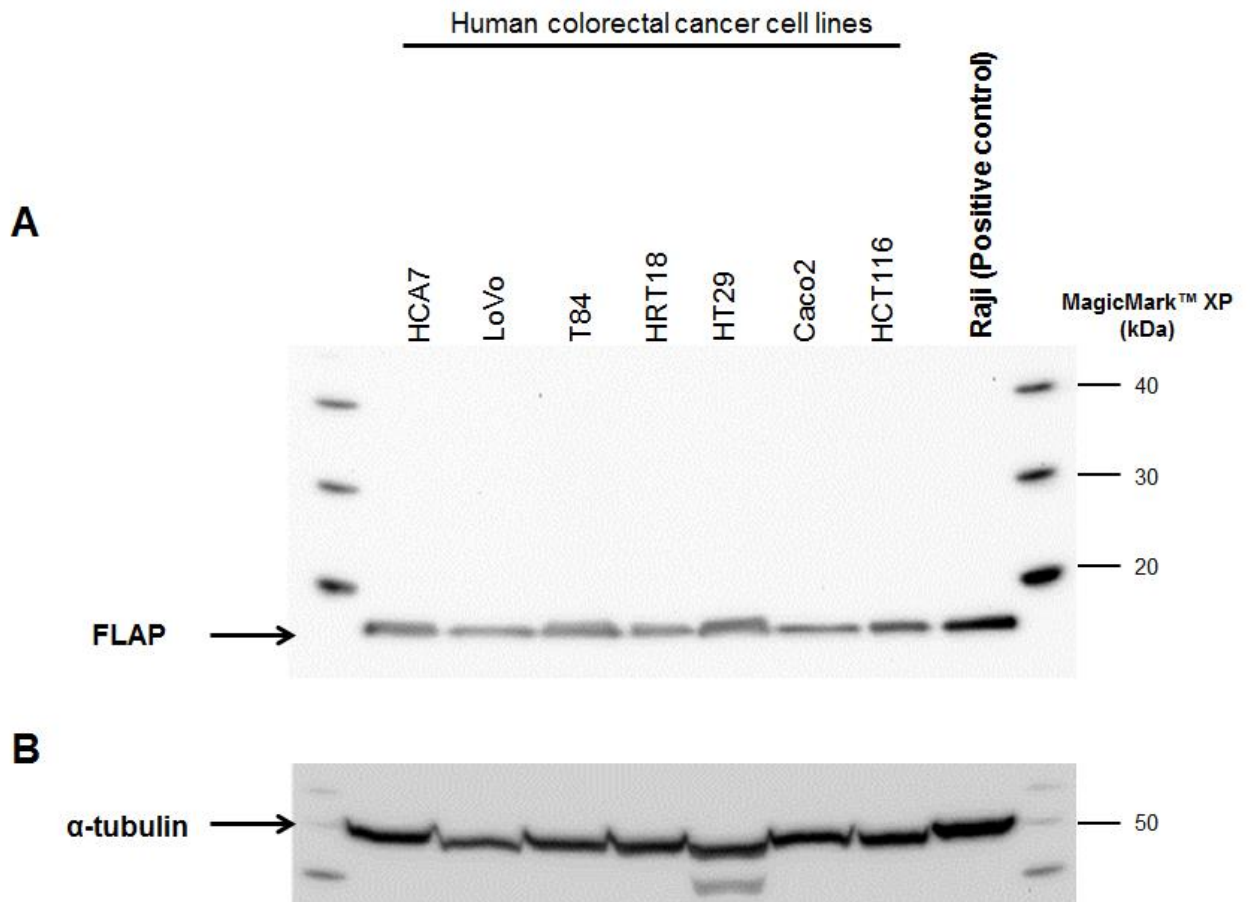


Figure 41. 5-lipoxygenase activating protein expression in human CRC cell lines.

Thirty micrograms of human cell lysates were probed with affinity purified rabbit monoclonal anti-human 5-lipoxygenase activating protein (FLAP) antibody (1 in 1000) and probed with a secondary HRP (1 in 2000). (A) Image acquired after 30 seconds of standard chemiluminescence, shows a single resolved protein band in each cell line at a molecular weight in keeping with that expected for FLAP (18 kDa). (B) Protein loading was confirmed by probing for α -tubulin with a mouse monoclonal anti-human α -tubulin antibody (1 in 5000), image acquired after 15 seconds of standard chemiluminescence. FLAP was found in all human CRC cell lines screened, including the positive control Raji cell line, under standard chemiluminescence (see arrow).

Human CRC cell line	COX-2 protein expression (Western Blotting)	COX lipid mediator synthesis (LC/ESI-MS/MS)	5-LOX mediator synthesis (LC/ESI-MS/MS)
HCA7	Positive	Quantifiable COX derived lipid mediators	None detected
LoVo	Negative	Detectable COX derived lipid mediators	Detected with AA supplementation only
T84	Negative	Detectable COX derived lipid mediators	None detected
HRT18	Weak positive	Detectable COX derived lipid mediators	None detected
HT29	Weak positive	Detectable COX derived lipid mediators	None detected
Caco2	Weak positive	Detectable COX derived lipid mediators	None detected
HCT116	Negative	Detectable COX derived lipid mediators	None detected

Table 8. Summary of both the expression and functional status of COX (-2) and 5-LOX in a panel of seven human CRC cell lines.

4.5.6 Synthesis of the acetylated COX-2 derived lipid mediator 15R-HETE in aspirin treated HCA7 human colorectal cancer cells

Due to the high COX-2 expression and proven COX activity the HCA7 human CRC cell line was chosen as the cell model for determining the *in vitro* conditions required for successful COX acetylation. The dose of aspirin used and length of duration of treatment on the cells were taken from published evidence (Serhan *et al.*, 2002) alongside cell viability data that determined that these aspirin conditions were not cytotoxic to HCA7 human CRC cells (Figure 42). 15-R-HETE synthesis was detected in aspirin treated conditions with levels further increased when HCA7 cells were treated with AA (Figure 43). Successful acetylation of COX-2 was also confirmed by the absence of 15S-HETE and the reduction of PGE₂ levels in the aspirin treated HCA7 cell conditioned medium (Figure 43). Interestingly, 15S-HETE production was found in the cell conditioned medium of HCA7 cells when exogenous AA was present (without aspirin). This is in keeping with the understanding whereby COX can produce 15S-HETE from AA (Hamberg & Samuleson, 1967). The chiral LS/ESI-MS/MS analysis confirmed that 15R-HETE was only synthesised by HCA7 cells when treated with

aspirin. Figure 44 illustrates representative chromatograms obtained from the chiral 15R- and 15S- HETE analysis.

In conclusion treating HCA7 human CRC cells with 500 μM of aspirin for 30 minutes acetylated COX-2 sufficiently to allow synthesis of 15R-HETE, an acetylated COX-2 AA derived lipid mediator.

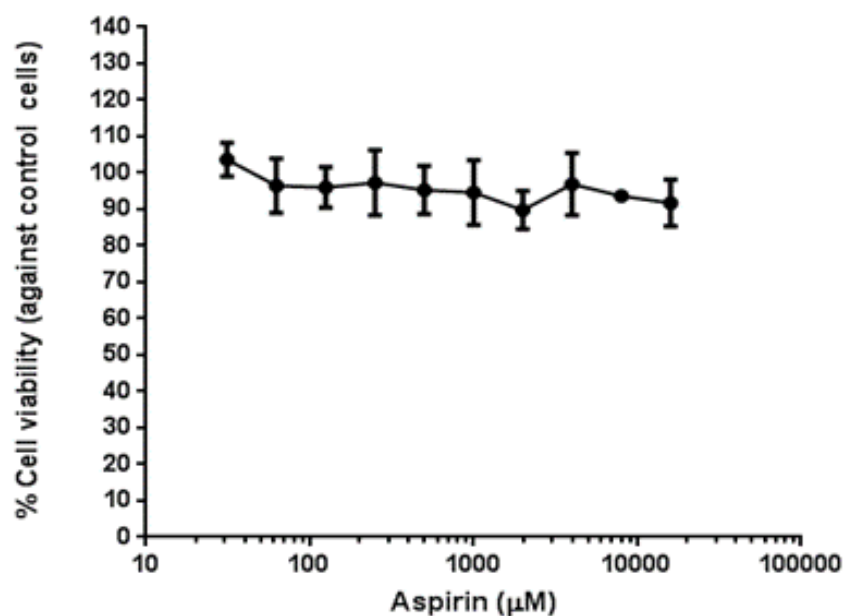


Figure 42. Determination of the aspirin cytotoxicity in the HCA7 human CRC cancer cell line.

HCA7 human CRC were exposed to a range of aspirin doses (0-16 mM) in cell medium free of fetal bovine serum (FBS) for 30 minutes (reflecting the FBS free conditions the cells will be in prior to LC/ESI-MS/MS analysis). Data collected from three independent cell experiments, shown as mean with standard error of the mean.

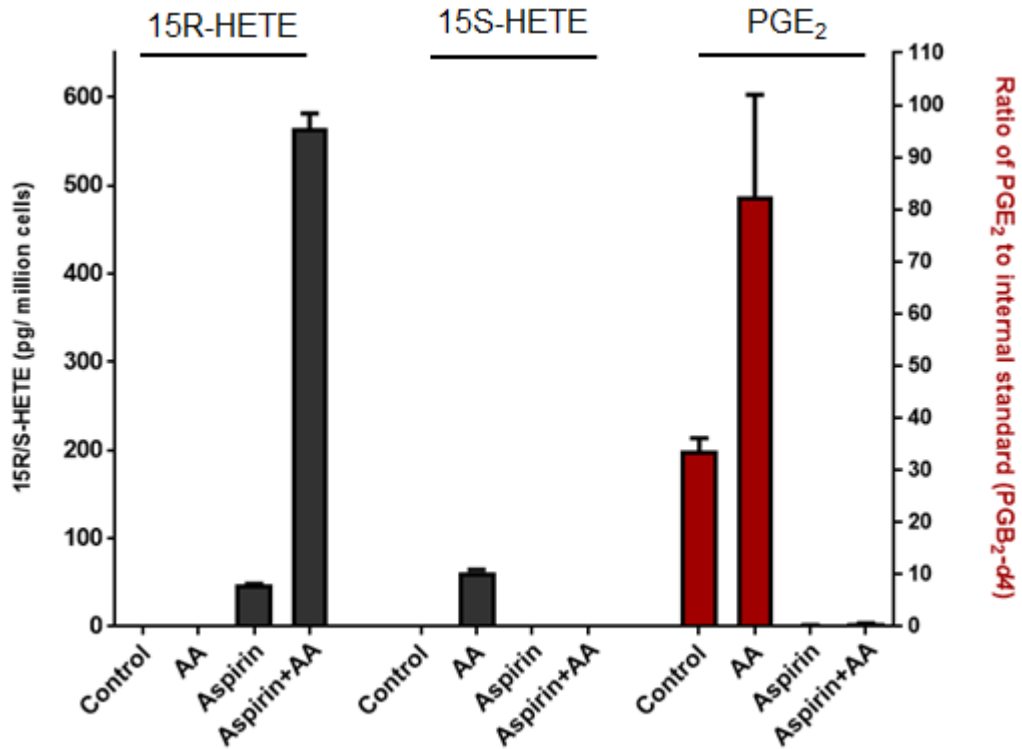


Figure 43. 15R/S-HETE, and PGE₂ synthesis by HCA7 human CRC cells.

15R/S-HETE and PGE₂ synthesis by HCA7 human CRC cells. In brief 500 μ M of aspirin was treated on the HCA7 cells for 30 minutes (or carrier control), followed by AA (1 μ M for three hours), or carrier control treatment. Data shown as mean, from two independent cell samples. Data acquired by candidate using individual chromatograms and appropriate standard calibration lines supplied by the Nicolaou group. 15R-HETE and 15S-HETE use left y-axis; PGE₂ data use the right y-axis). Where the lipid mediator exceeded the upper limit of the standard calibration curve the data is shown as a ratio against the internal standard, otherwise the data is shown as pg per 10⁶ cells.

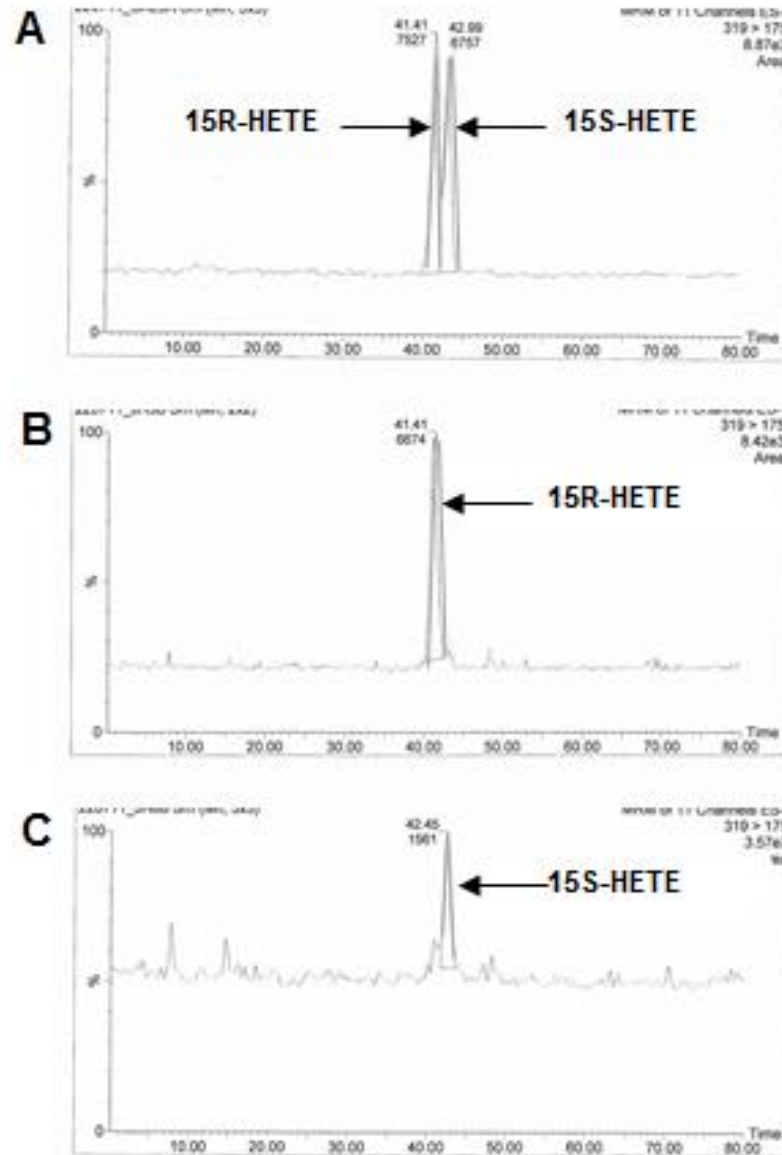


Figure 44. 15R and 15S-HETE chromatograms.

HCA7 human CRC cells were treated with and without aspirin. The AA derived COX product 15S-HETE and the AA acetylated COX-2 derived product 15R-HETE were analysed by chiral LC/ESI-MS/MS. (A) 15R and 15S-HETE internal standard chromatogram obtained from the chiral LC/ESI-MS/MS analysis: retention time 41.41 (R-) and 42.99 (S-). (B) 15R-HETE chromatogram obtained from the chiral LC/ESI-MS/MS analysis of the supernatant from aspirin treated (500 μ M, 30 minutes) HCA7 cells; retention time 41.41. (C) 15S-HETE chromatogram obtained from chiral LC/ESI-MS/MS analysis of the supernatant from AA (1 μ M, three hours) supplemented HCA7 cells: retention time 42.45. The original chromatograms (MRM 319>175) provided by the Nicolaou group were very faint, so the candidate strengthened these peaks so they could be visualised for the purposes of this thesis .

4.5.7 Lipidomic analysis for RvE1 and 18-HEPE synthesis by HCA7 human colorectal cancer cells

The HCA7 cell line was found to express COX-2 protein and synthesise the greatest amounts of COX derived lipid mediators. It was also shown capable of generating an acetylated COX-2 lipid, therefore this cell line was examined to see if it could synthesise RvE1.

Cell viability assays were completed to confirm that exposure to 50 μM EPA for three hours was not cytotoxic to the HCA7 (Figure 45).

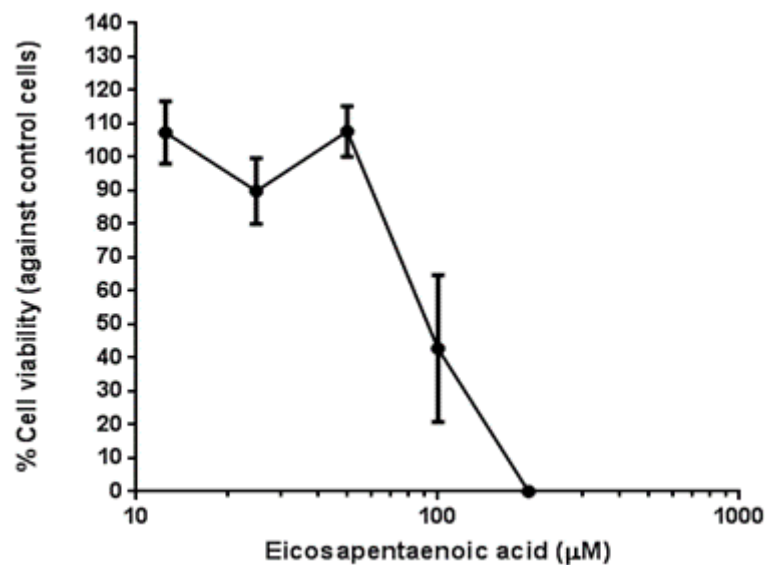


Figure 45. Determination of the cytotoxicity of EPA on HCA7 human CRC cell lines.

HCA7 human CRC cells were exposed to a range of EPA doses (0-200 μM) in cell medium free of FBS for three hours (reflecting the FBS free conditions the cells will be in prior to LC-ESI-MS/MS analysis), before removing and incubating the cells in cell medium plus FBS for 96 hours at 37°C. Data collected from three independent cell cultured experiments, shown as mean with standard error of the mean.

HCA7 cells supplemented with EPA with and without pre-treatment with aspirin did not synthesise detectable RvE1 under the experimental conditions used. No peak is seen within the chromatogram at the expected retention time of RvE1, as is shown in the representative chromatograms for RvE1 (Figure 46).

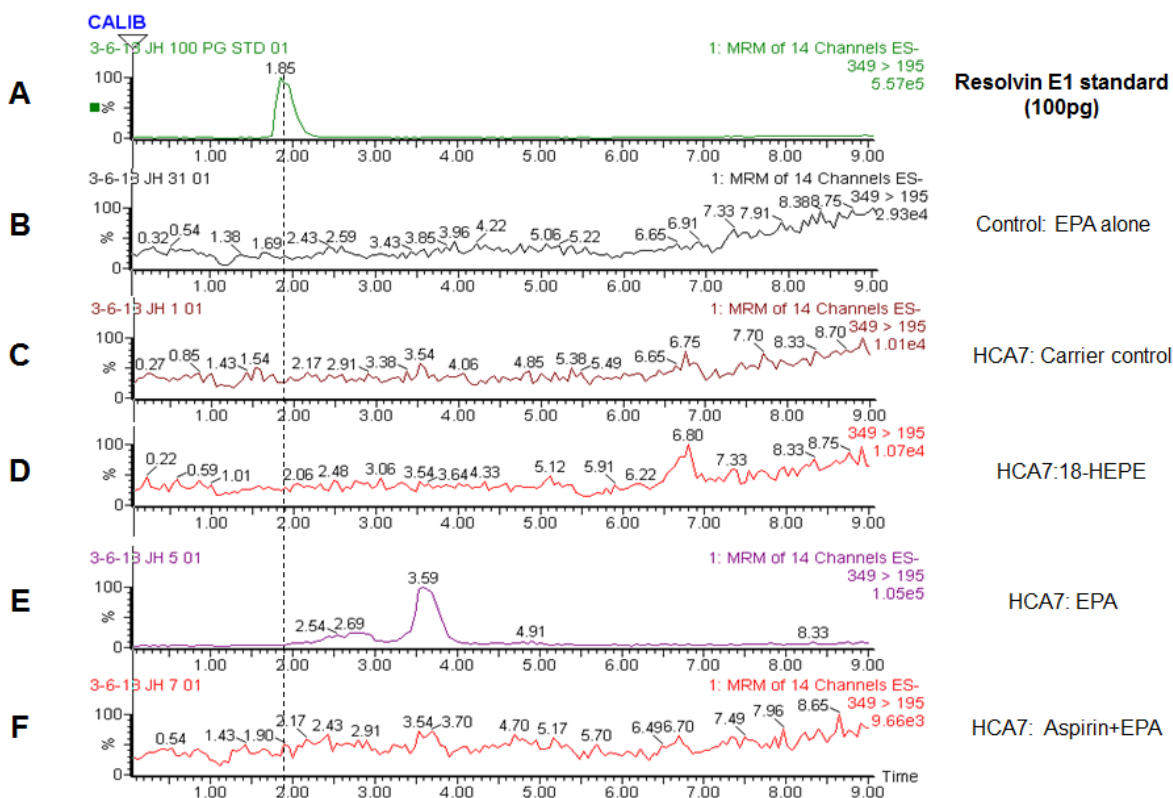


Figure 46. RvE1 chromatograms (HCA7 cells).

HCA7 human CRC cell condition medium was analysed for RvE1 by LC-ESI-MS/MS analysis. (A) Chromatogram for RvE1 standard (Cayman Chemical). (B) RvE1 chromatogram from control EPA (50 μ M, three hours). (C) RvE1 chromatogram for the cell conditioned medium from HCA7 carrier control treated cells. (D) RvE1 chromatogram for the cell conditioned medium from HCA7 18-HEPE (1 μ M, three hours) treated cells. (E) RvE1 chromatogram for the cell conditioned medium from HCA7 EPA treated (50 μ M, three hours) treated cells. (F) RvE1 chromatogram for the cell conditioned medium from HCA7 aspirin (500 μ M, 30 minutes) and EPA (50 μ M, three hours) treated cells. The dotted line represents the expected retention time for RvE1.

18-HEPE was detected in the EPA treated HCA7 cells, with 18-HEPE levels decreasing when the cells were pre-treated with aspirin (Figure 47A). However 18-HEPE was also detected in the control EPA samples in the absence of cells, suggesting a level of non-cellular EPA oxidation to 18-HEPE (Figure 47A). Representative 18-HEPE chromatograms are shown in Figure 48. The 18-HEPE levels detected in the control EPA alone samples were outside the range of the calibration curve (>100 pg/ μ L).

Successful acetylation of COX by aspirin was confirmed by the decrease in PGE₂ and PGE₃, in AA and EPA supplemented HCA7 cells respectively (Figures 47B/C), as well as the increase in 15-HETE levels in the aspirin treated cells (Figure 45D). Representative 15-HETE chromatograms are shown in Figure 49. However 15-HETE was detected in the no cell AA control likely secondary to non cellular driven AA oxidation to 15-HETE. However there was a clear increase in 15-HETE detected in the aspirin and AA treated cells when compared to AA treated cells, indicating that there may be 15-HETE synthesis above AA oxidation via non-cellular mechanisms. The levels for both PGE₃ and PGE₂ exceeded the upper limit of quantification and are consequently presented as ratio values of lipid mediator to internal standard (PGB_{2-d4}).

In addition to acetylated COX-2 activity on EPA, RvE1 synthesis requires 5-LOX and LTA₄ hydrolase enzymatic activity. In order to establish 5-LOX and LTA₄ hydrolase activity in the HCA7 cells, 5-HETE and 5-HEPE and LTB_{4/5} synthesis was analysed in the cell conditioned medium. 5-HETE is formed through the activity of 5-LOX on AA. LTB₄ and LTB₅ are formed through the activity of both 5-LOX and LTA₄H on AA and EPA, respectively (Figure 2, AA pathway summary; Figure 3, EPA pathway summary). A lipid mediator in keeping with 5-HETE was detected in all AA treated HCA7 cell conditioned medium samples. However this lipid mediator was also found in the AA alone control sample (Figure 50), indicating 5-HETE synthesis via a non cellular route. No quantification could be performed as no 5-HETE standard was included, however the amounts were still below the limits of quantification. No cell mediated 5-HETE synthesis could therefore be concluded upon. No LTB₄ (Figure 51), or LTB₅ (data not shown) was detected in AA or EPA supplemented HCA7 cells, respectively.

Aspirin triggered-LXA₄ is derived through the enzymatic activity of acetylated-COX-2 on AA which produces 15R-HETE, which is then oxygenated by 5-LOX to aspirin triggered-LXA₄, and thus represents the same enzymatic pathway involved in RvE1 synthesis. As was the case with RvE1 the HCA7 cell line was unable to synthesise detectable aspirin triggered-LXA₄ (Figure 52).

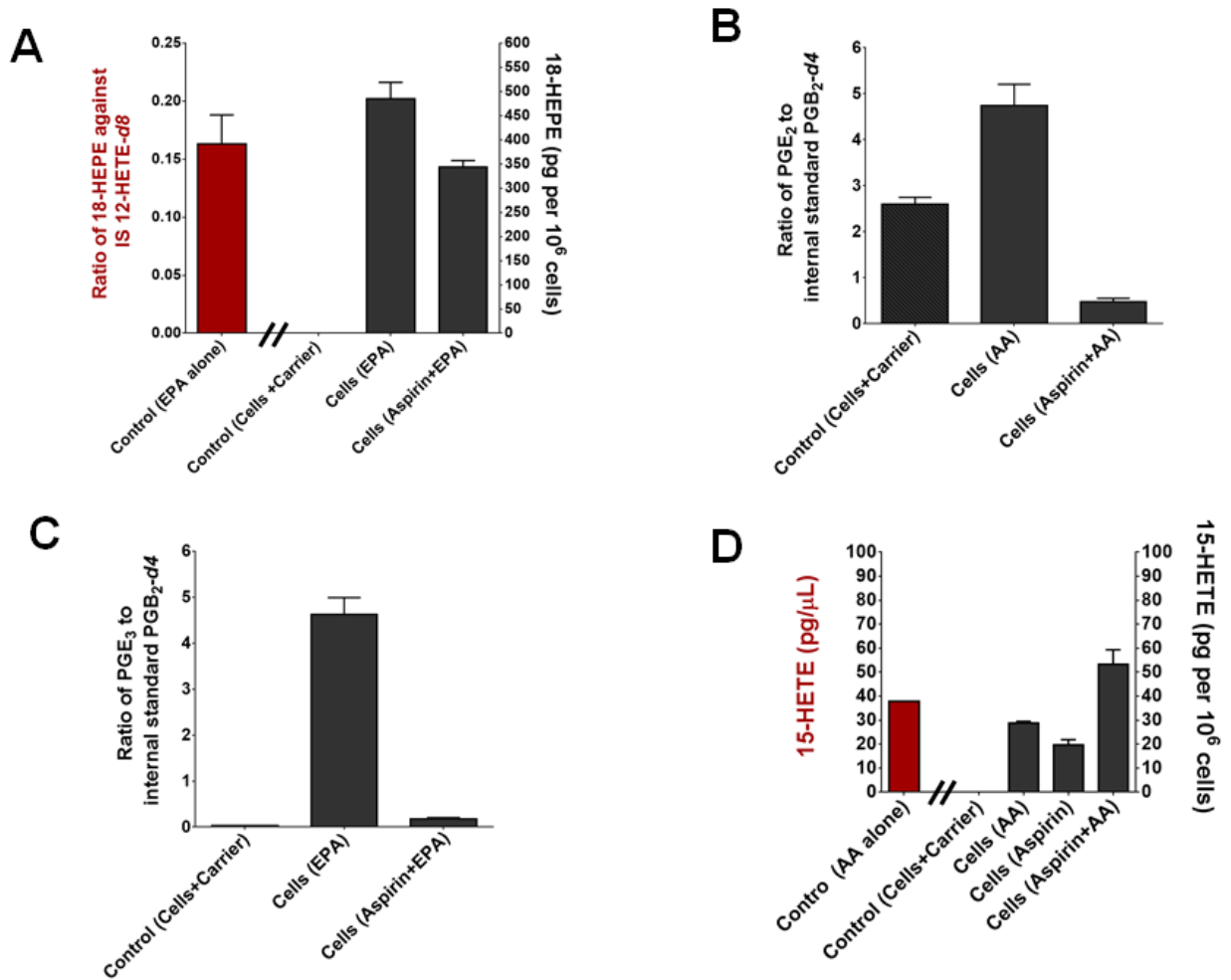


Figure 47. Analysis of HCA7 cell conditioned medium for 18-HEPE, PGE₂, PGE₃ and 15-HETE.

The cell conditioned medium from HCA7 human CRC cells was analysed by LC-ESI-MS/MS. (A) 18-HEPE biosynthesis by HCA7 cells (control no cell EPA sample use left y-axis; remaining samples use right y-axis). (B) PGE₂ biosynthesis by HCA7 cells. (C) PGE₃ synthesis by HCA7 cells. (D) 15-HETE synthesis by HCA7 cells (Control AA alone sample use left y-axis; remaining samples use right y-axis). Results from three independent experiments and shown as mean with standard error of the mean, the control AA alone sample represents data from one experiment. Where the lipid mediator exceeded the upper limit of the standard calibration curve the data are shown as a ratio against the internal standard, otherwise the data is shown as pg per 10⁶ cells. The control AA alone sample is shown as pg/ μL, as this was a cell free control sample.

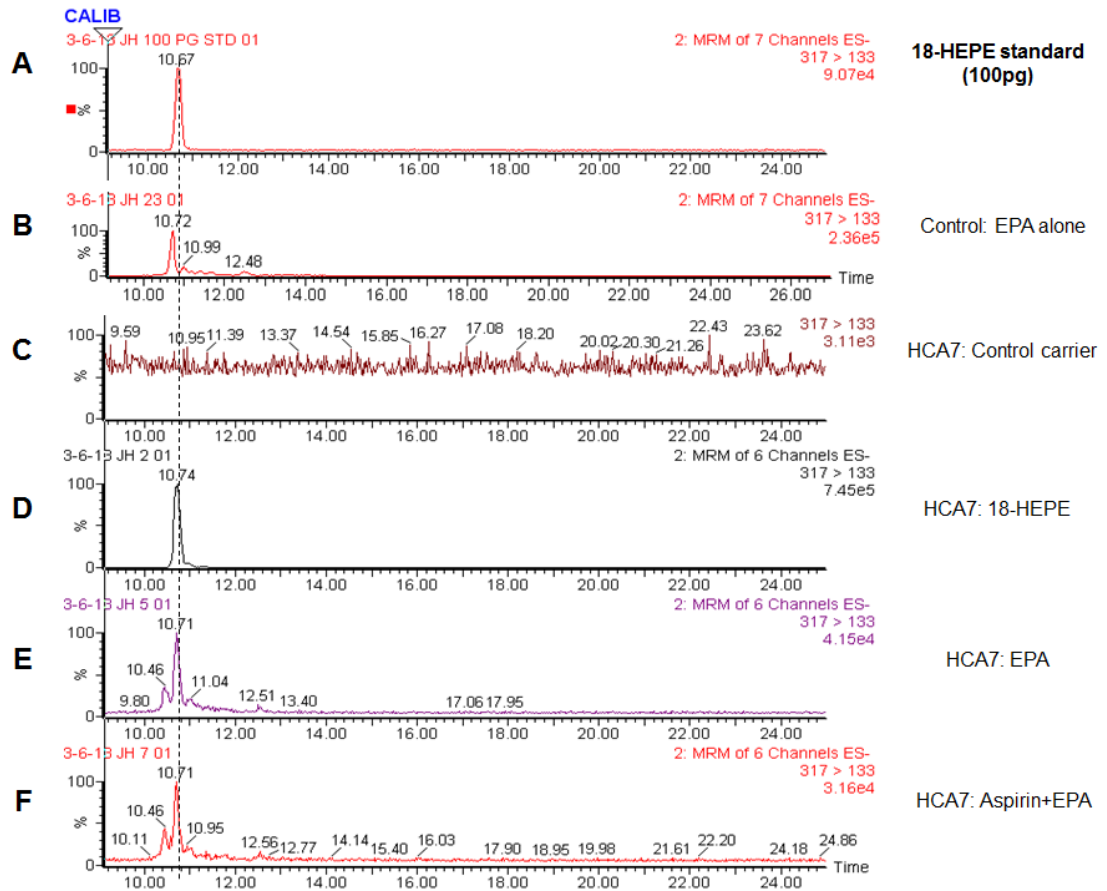


Figure 48. 18-HEPE chromatograms (HCA7 cells).

HCA7 human CRC cell conditioned medium was analysed for 18-HEPE by LC-ESI-MS/MS analysis (A) Chromatogram for 18-HEPE standard (Cayman Chemical). (B) 18-HEPE chromatogram for control EPA (50 μ M, three hours). (C) 18-HEPE chromatogram for the cell conditioned medium from HCA7 carrier control cells. (D) 18-HEPE chromatogram for the cell conditioned medium from HCA7 18-HEPE (1 μ M, three hours) treated cells. (E) 18-HEPE chromatogram for the cell conditioned medium from HCA7 EPA (50 μ M, three hours) treated cells. (F) 18-HEPE chromatogram for the cell conditioned medium from HCA7 aspirin (500 μ M, 30 minutes) and EPA (50 μ M, three hours) treated cells. The dotted line represents the expected retention time for 18-HEPE.

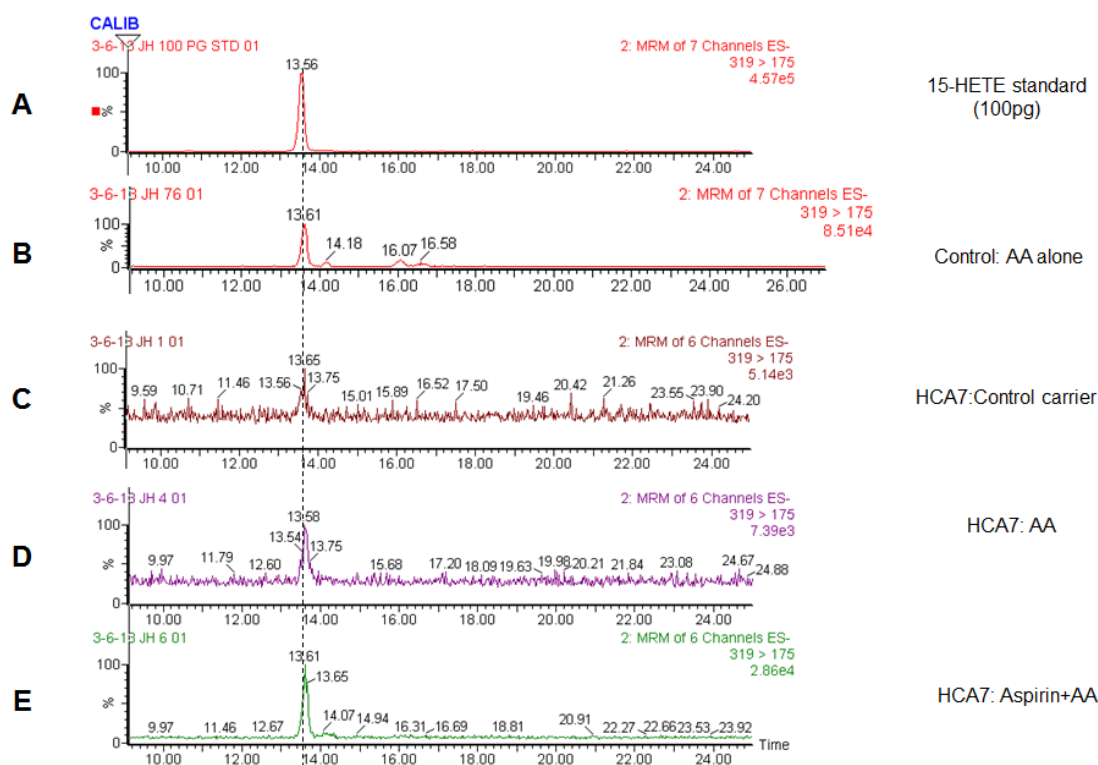


Figure 49. 15-HETE chromatograms (HCA7 cells).

HCA7 human CRC cell conditioned medium was analysed for 15-HETE by LC/ESI-MS/MS. (A) 15-HETE chromatogram for the standard (Cayman Chemical). (B) 15-HETE Chromatogram for the control no cell, AA (1 μ M, three hours culture medium). (C) 15-HETE chromatogram for HCA7 control carrier conditioned medium (two of the three samples detected 15-HETE but were below the limit of quantification (<4 pg/ μ L)). (D) 15-HETE chromatogram for HCA7 AA (1 μ M, three hours) treated cell conditioned medium. (E) 15-HETE chromatogram for HCA7 aspirin (500 μ M, 30 minutes) and AA (1 μ M, three hours) treated cell conditioned medium. The dotted line represents the expected retention time for 15-HETE.

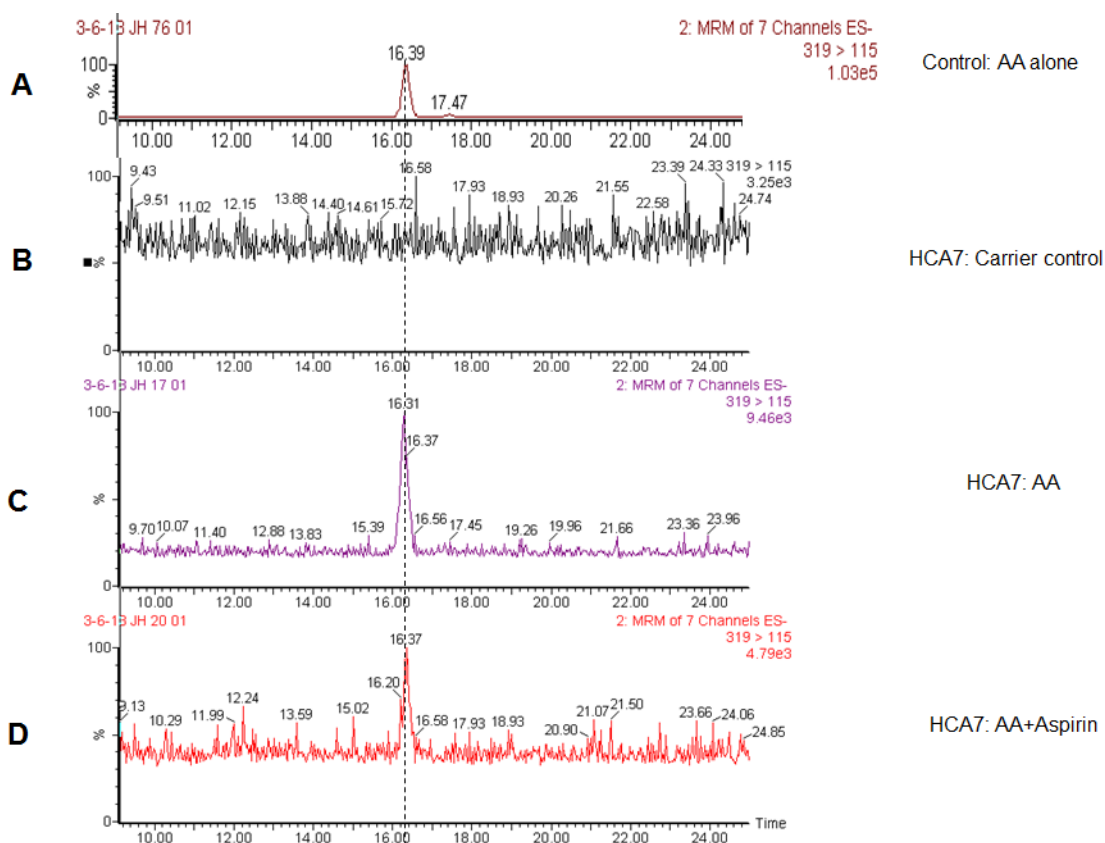


Figure 50. 5-HETE chromatograms (HCA7 cells).

The cell conditioned medium from HCA7 human CRC cells was analysed by LC-ESI-MS/MS. (A) Chromatogram from control AA (1 μ M, three hours) conditioned medium alone. (B) HCA7 carrier control treated cell conditioned medium. (C) HCA7 AA (1 μ M, three hours) treated cell conditioned medium. (D) HCA7 aspirin (500 μ M, 30 minutes) and AA (1 μ M, three hours) treated cell conditioned medium. The dotted line represents the expected retention time for 5-HETE.

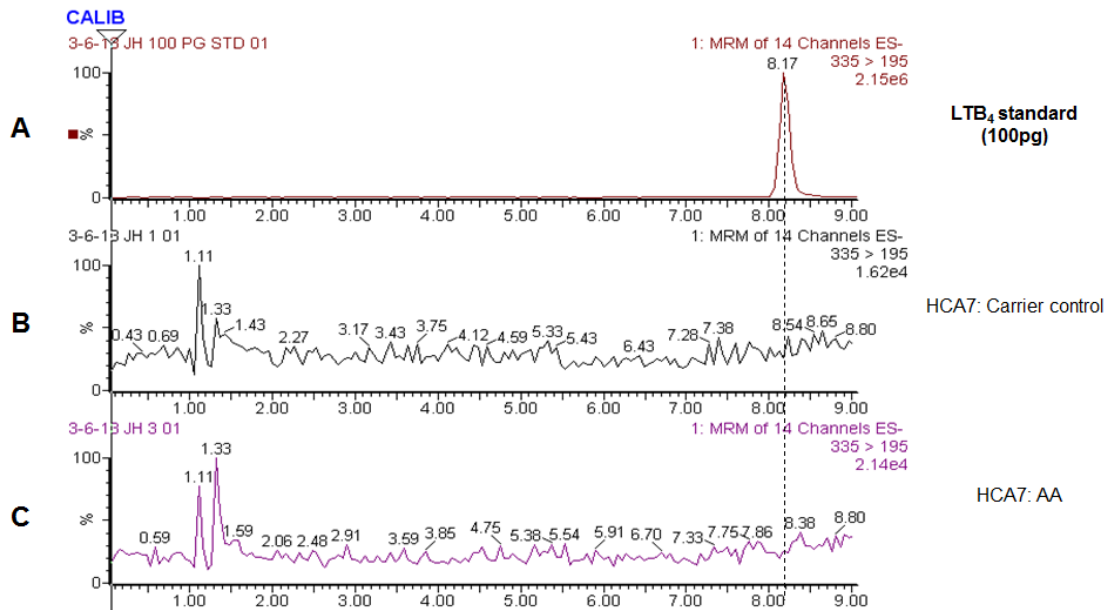


Figure 51. Leukotriene B₄ chromatograms (HCA7 cells).

The cell conditioned medium from HCA7 cells was analysed by LC-ESI-MS/MS. (A) Leukotriene B₄ (LTB₄) standard (Cayman Chemicals). (B) HCA7 carrier control treated cell conditioned medium. (C) HCA7 AA (1 μ M, three hours) treated cell conditioned medium. The dotted line represents the expected retention time for LTB₄.

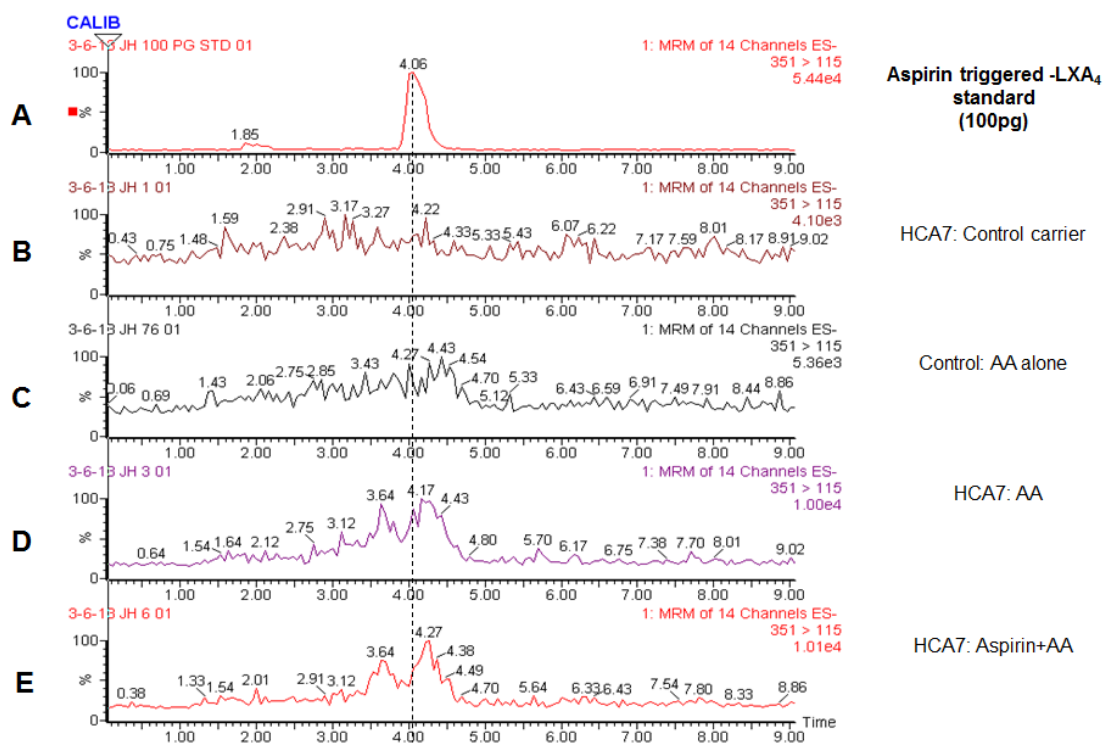


Figure 52. Aspirin triggered-LXA₄ chromatograms (HCA7 cells).

The cell conditioned medium from HCA7 cells was analysed by LC-ESI-MS/MS. (A) Chromatogram for aspirin triggered-LXA₄ standard (Cayman Chemical). (B) Chromatogram from control no cell AA (1 μ M, three hours) medium alone. (C) Chromatogram for HCA7 carrier control treated cell conditioned medium. (D) Chromatogram for HCA7 AA (1 μ M, three hours) treated cell conditioned medium. (E) HCA7 aspirin (500 μ M, 30 minutes) and AA (1 μ M, three hours) treated cell conditioned medium. The dotted line represents the expected retention time for aspirin triggered-LXA₄.

4.5.8 Lipidomic analysis for 18-HEPE and Resolvin E1 synthesis by MC38 mouse colorectal cancer cells and RAW264.7 mouse macrophage cells.

As the human CRC cell lines described previously were unable to synthesise detectable RvE1, likely due to a lack of functional 5-LOX/ LTA₄H enzymatic activity, a transcellular *in vitro* transcellular synthesis model was developed. To avoid species cross-reactivity in the model, two mouse cell lines were used. The MC38 mouse CRC cell line has established COX functional activity, and the RAW 264.7 mouse macrophage cell line, has COX and 5-LOX functional activity (Revermann *et al.*, 2011, Hofmann *et al.*, 2012, Norris *et al.*, 2012). RAW26.7 macrophage cells require LPS treatment in order to induce COX-2 activity. LPS stimulation of the RAW264.7 cell line to show COX activity was confirmed over a 48 hour time period. This also served to establish an appropriate duration of LPS treatment required to stimulate COX derived PGE₂ synthesis, prior to using the cells in aspirin/ AA/ EPA experiments (Figure 53). LPS (1 µg/ mL) for 12 hours was subsequently used, as this time point produced high levels of PGE₂. Cell viability assays were completed to confirm that 30 minutes of 500 µM aspirin (Figure 54) and three hours of 50 µM EPA treatment (Figure 55) would not be cytotoxic to either the MC38 mouse CRC, or the RAW264.7 mouse macrophage cell lines.

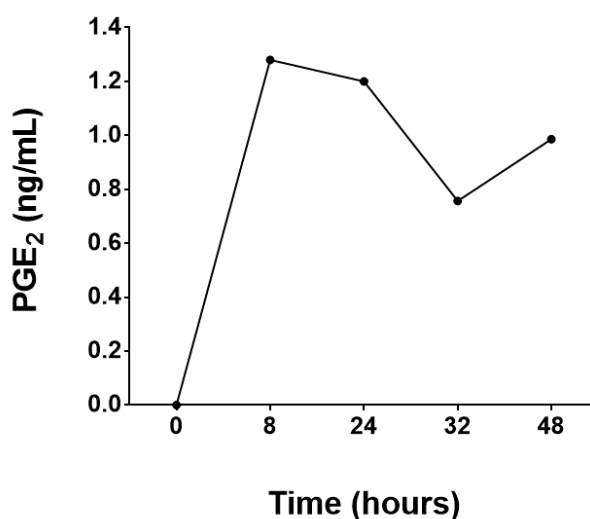


Figure 53. Analysis of LPS stimulated RAW264.7 cell conditioned medium for PGE₂ over 24 hours.

LPS stimulated mouse macrophage RAW264.7 cells were analysed for PGE₂ in the cell conditioned medium over a 48 hour period, by LS/ESI-MS/MS. Data represents one independent experiment. The samples were collected by the candidate; PGE₂ data provided by the Dr. Loadman.

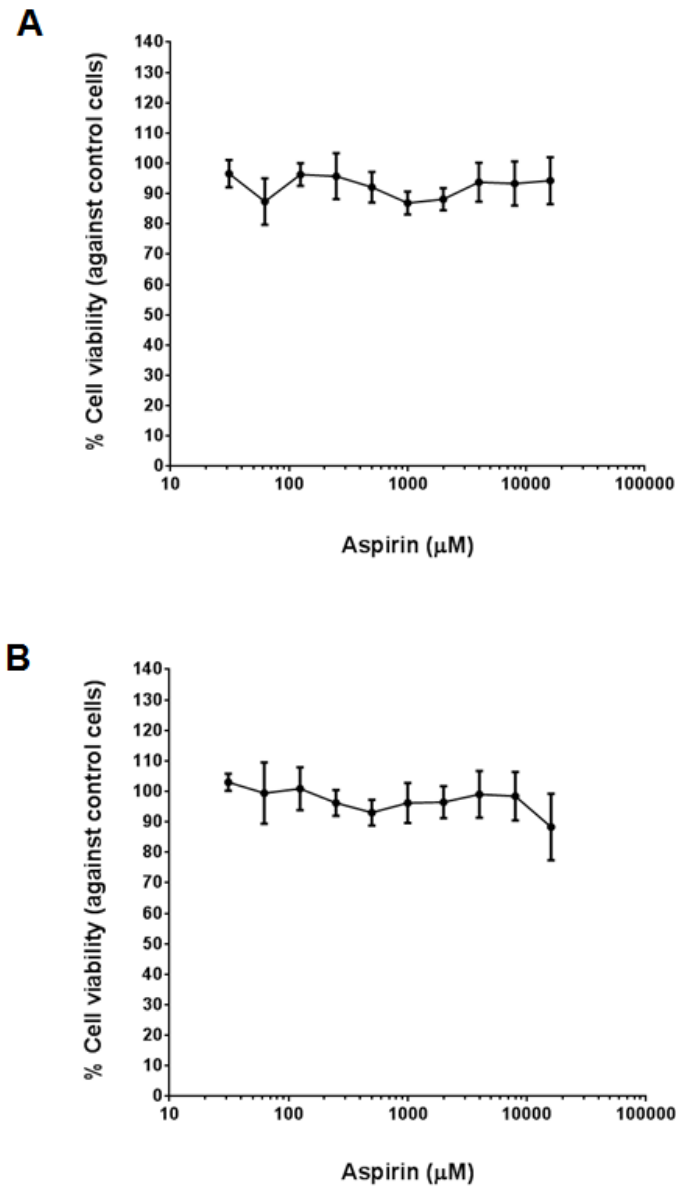


Figure 54. Assessment of MC38 and RAW264.7 cell viability over a range of aspirin dosages.

MC38 or RAW264.7 cells were grown in a T25 flask to 80% confluency before being seeded into a 96 well plate (1000 cells/ well) for 24 hours (in triplicate). (A) MC38 cells. (B) RAW264.7 cells were exposed to a range of either aspirin concentrations (0-100 mM) for 30 minutes in cell medium free of FBS for three hours (reflecting the FBS free conditions the cells will be in prior to LC-ESI-MS/MS analysis) before removing and incubating the cells in cell medium plus FBS for 96 hours at 37°C. Data collected from three independent cell experiments, shown as mean with standard error of the mean.

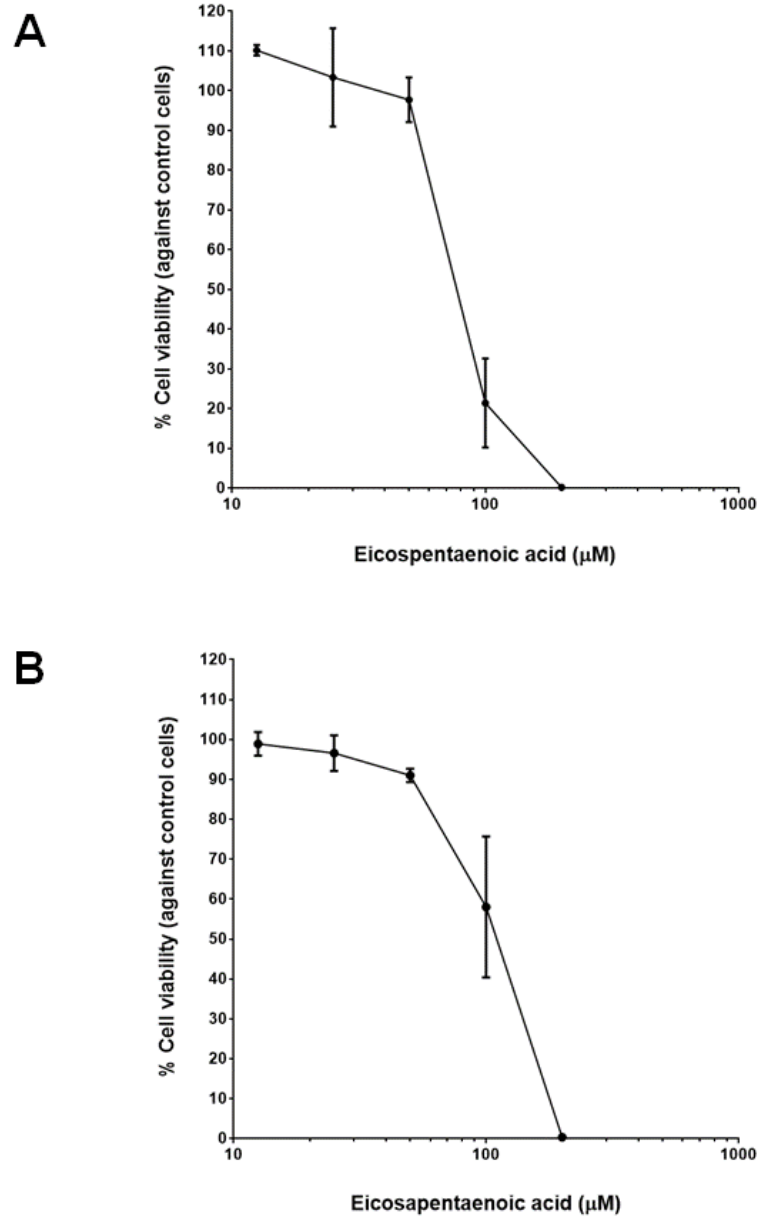


Figure 55. Assessment of MC38 and RAW264.7 cell viability over a range of EPA doses.

MC38 or RAW264.7 cells were grown in a T25 flask to 80% confluency before being seeded into a 96 well plate (1000 cells/ well) for 24 hours (in triplicate). (A) MC38 cells. (B) RAW264.7 cells were exposed to a range of eicosapentaenoic acid (EPA) doses (0-200 μM) in cell medium free of FBS for three hours (reflecting the FBS free conditions the cells will be in prior to LC-ESI-MS/MS analysis) before removing and incubating the cells in cell medium plus FBS for 96 hours at 37°C. Data collected from three independent cell experiments, shown as mean with standard error of the mean.

Initially it was examined whether either or both of the cell lines alone, could synthesise 18-HEPE or RvE1. The LC/ESI-MS/MS analysis confirmed that no RvE1 was detected in either the MC38 (Figure 56) or the RAW264.7 (Figure 57) cell conditioned medium samples treated with EPA and aspirin or with EPA alone or 18-HEPE directly. No peak was seen within the respective chromatograms at the expected retention time of RvE1.

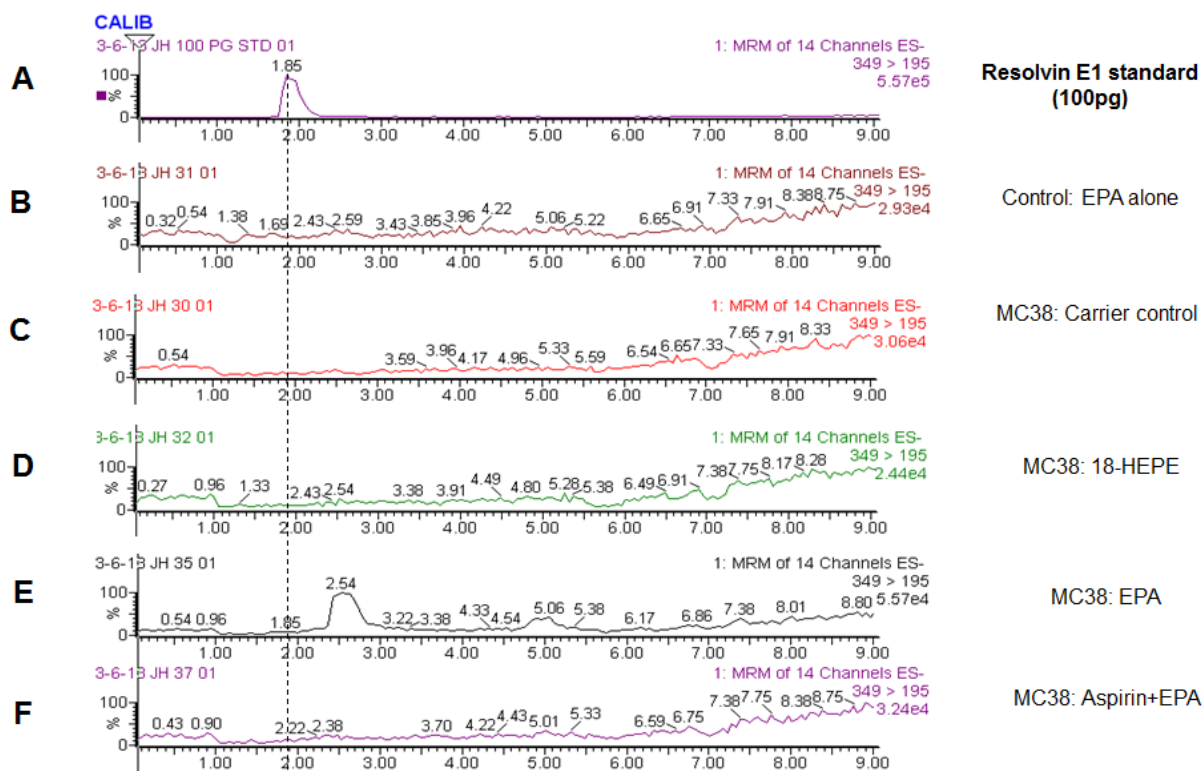


Figure 56. Analysis of MC38 cell conditioned medium for RvE1.

MC38 cell conditioned medium was collected and RvE1 analysed for by LC/ESI-MS/MS. (A) Chromatogram for RvE1 standard (Cayman Chemical). (B) RvE1 chromatogram for the control EPA (50 μ M, three hours) medium alone. (C) RvE1 chromatogram for the cell conditioned medium from MC38 carrier control cells. (D) RvE1 chromatogram for the cell conditioned medium from MC38 18-HEPE (1 μ M, three hours) treated cells. (E) RvE1 chromatogram for the conditioned medium from MC38 eicosapentaenoic acid treated (50 μ M, three hours) treated cells. (F) RvE1 chromatogram for the conditioned medium from MC38 aspirin (500 μ M, 30 minutes) and eicosapentaenoic acid (50 μ M, three hours) treated cells. The dotted line represents the expected retention time for RvE1.

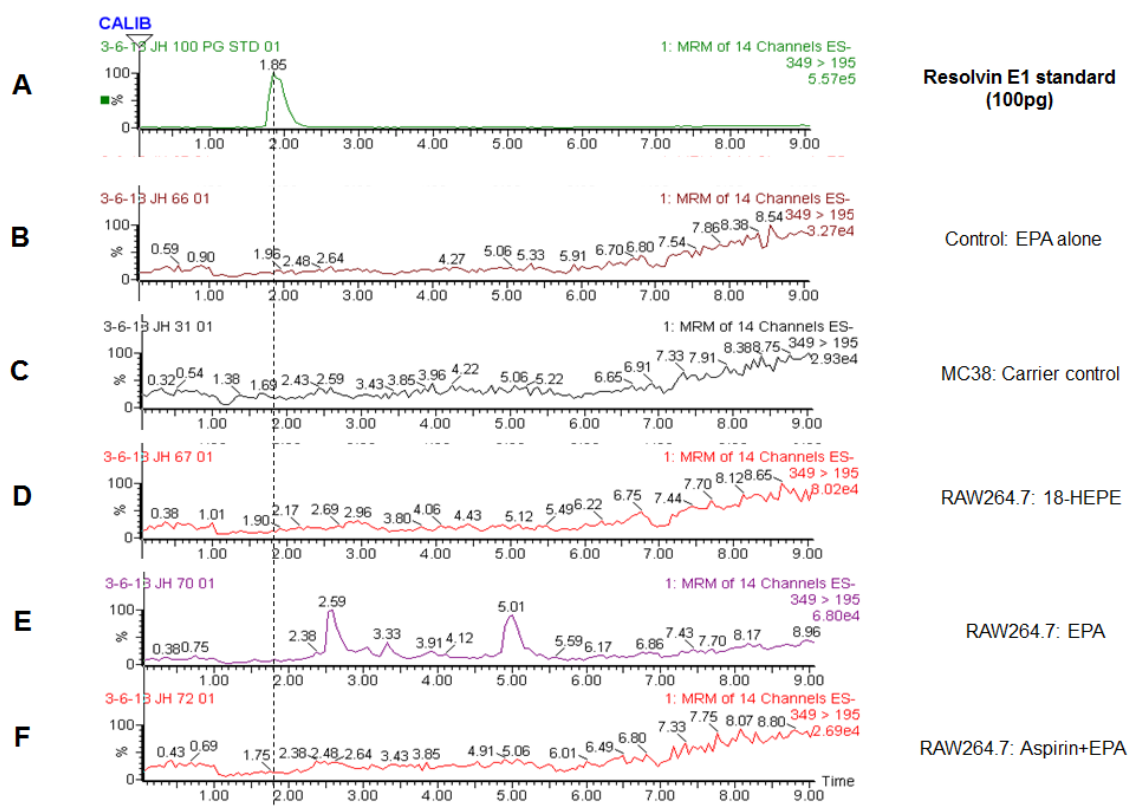


Figure 57. Analysis of LPS stimulated RAW264.7 cell conditioned medium for RvE1.

RAW264.7 cells were stimulated with LPS for 12 hours before being treated as appropriate. The cell condition was then collected and analysed for RvE1 by LC/ESI-MS/MS analysis. (A) Chromatogram for RvE1 standard (Cayman Chemical). (B) RvE1 chromatogram for the control EPA (50 μ M, three hours) medium alone. (C) RvE1 chromatogram for the cell conditioned medium from RAW264.7 carrier control cells. (D) RvE1 chromatogram for the conditioned medium from RAW26.4 18-HEPE (1 μ M, three hours) treated cells. (E) RvE1 chromatogram for the conditioned medium from RAW264.7 EPA treated (50 μ M, three hours) treated cells. (F) RvE1 chromatogram for the conditioned medium from RAW264.7 aspirin (500 μ M, 30 minutes) and EPA (50 μ M, three hours) treated cells. The dotted line represents the expected retention time for RvE1.

18-HEPE was detected in all samples where cells were treated with EPA (Figure 58; MC38 and Figure 59; RAW264.7) with 18-HEPE levels increasing when EPA supplemented cells were pre-treated with aspirin (Figure 60A; MC38 and Figure 61A; RAW264.7). However as discussed earlier 18-HEPE was also detected in the EPA oxidation control samples. The 18-HEPE levels detected in the samples were outside the range of the calibration curve (100 pg/ μL) for the oxidation control and the EPA treated MC38 CRC and RAW264.7 macrophage cells, both with and without aspirin treatment. Therefore the results are shown as a ratio of the 18-HEPE peak area against the internal standard peak area (12-HETE-*d8*), (Figure 60A; MC38 and Figure 61A; RAW264.7).

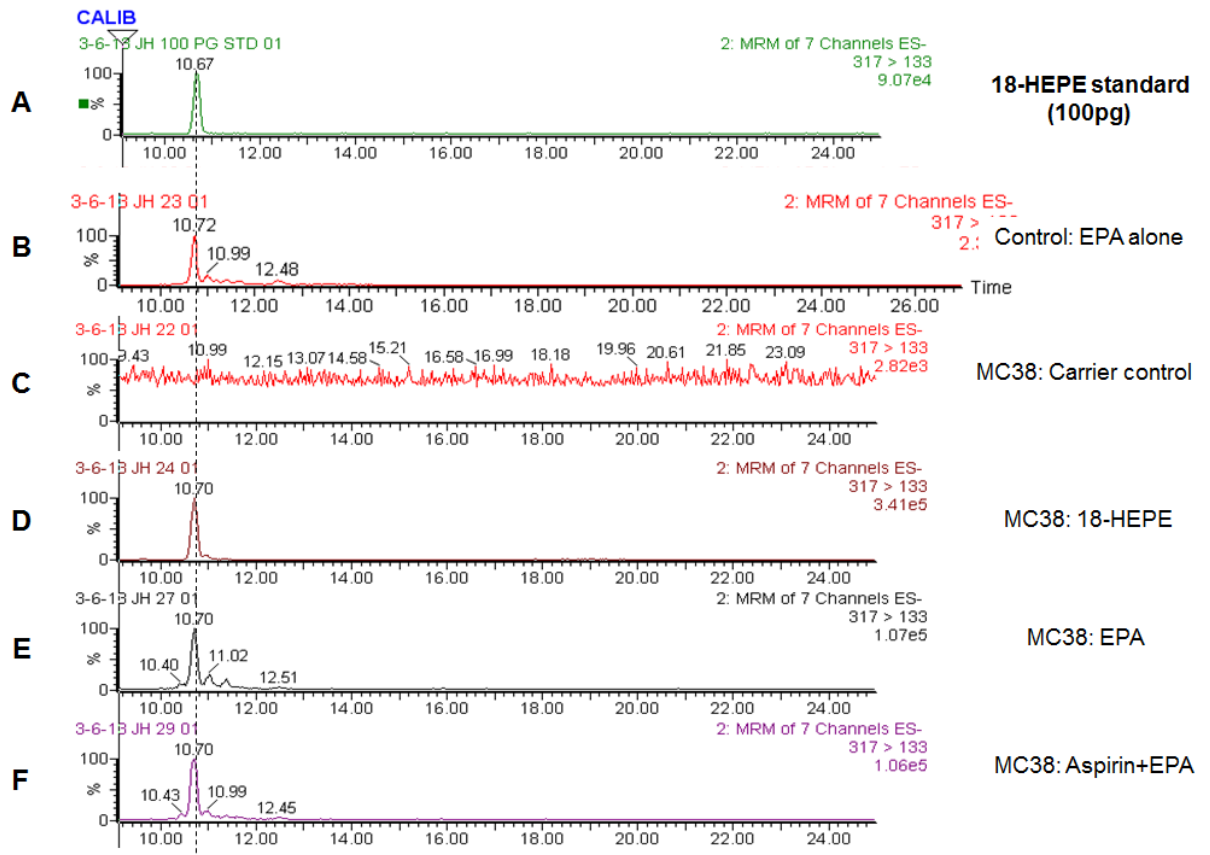


Figure 58. Analysis of MC38 cell conditioned medium for 18-HEPE.

MC38 mouse CRC cell conditioned medium was analysed for 18-HEPE by LC-ESI-MS/MS. (A) Chromatogram for 18-HEPE standard (Cayman Chemical). (B) 18-HEPE chromatogram for control EPA (50 μ M, three hours) medium alone. (C) 18-HEPE chromatogram for the carrier control MC38 cell conditioned medium. (D) 18-HEPE chromatogram for the cell conditioned medium from MC38 18-HEPE (1 μ M, three hours) treated cells. (E) 18-HEPE chromatogram for the cell conditioned medium from MC38 EPA (50 μ M, three hours) treated cells. (F) 18-HEPE chromatogram for the cell conditioned medium from MC38 aspirin (500 μ M, 30 minutes) and eicosapentaenoic acid (50 μ M, three hours) treated cells. The dotted line represents the expected retention time for 18-HEPE.

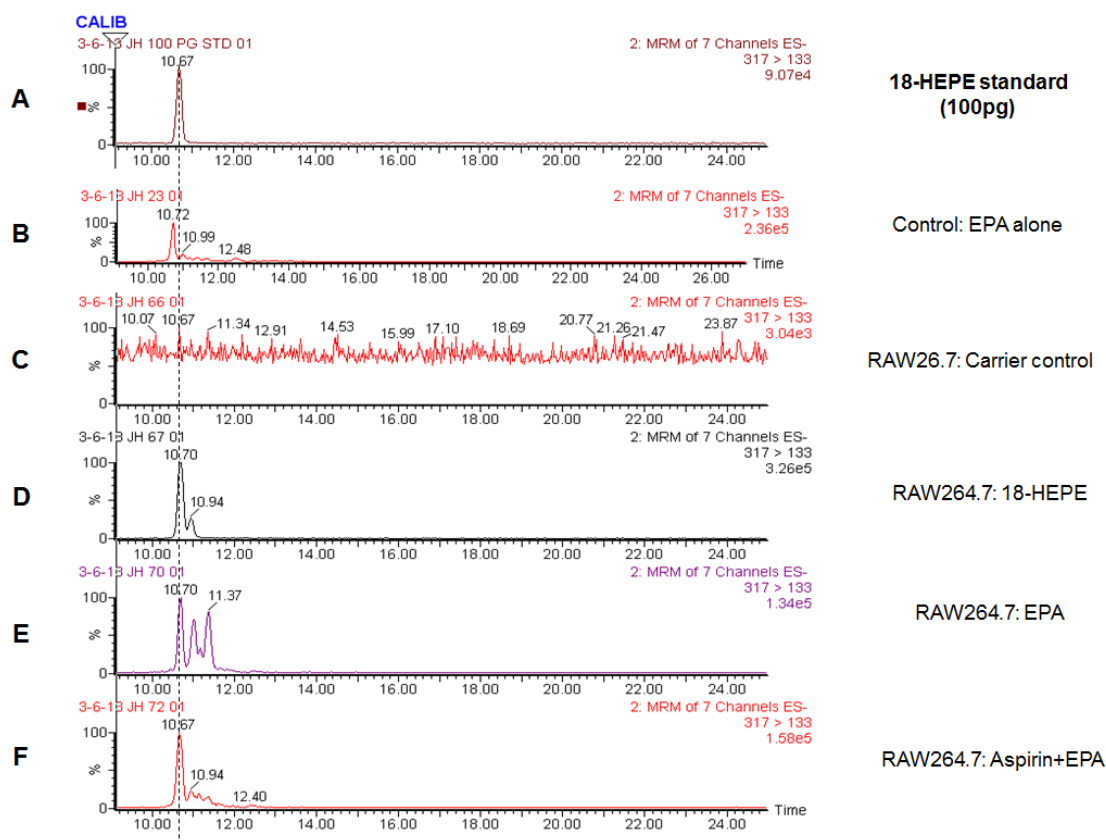


Figure 59. Analysis of LPS stimulated RAW264.7 cell conditioned medium for 18-HEPE.

LPS stimulated RAW264.7 cell conditioned medium was analysed for 18-HEPE by LC-ESI-MS/MS analysis. (A) Chromatogram for 18-HEPE standard (Cayman Chemical). (B) 18-HEPE chromatogram for the control EPA (50 μ M, three hours) medium alone. (C) 18-HEPE chromatogram from RAW264.7 control carrier cell conditioned medium. (D) 18-HEPE chromatogram for the cell conditioned medium from MC38 18-HEPE (1 μ M, three hours) treated cells. (E) 18-HEPE chromatogram for the cell conditioned medium from RAW264.7 EPA (50 μ M, three hours) treated cells. (F) 18-HEPE chromatogram for the cell conditioned medium from RAW264.7 aspirin (500 μ M, 30 minutes) and EPA (50 μ M, three hours) treated cells. The dotted line represents the expected retention time for 18-HEPE.

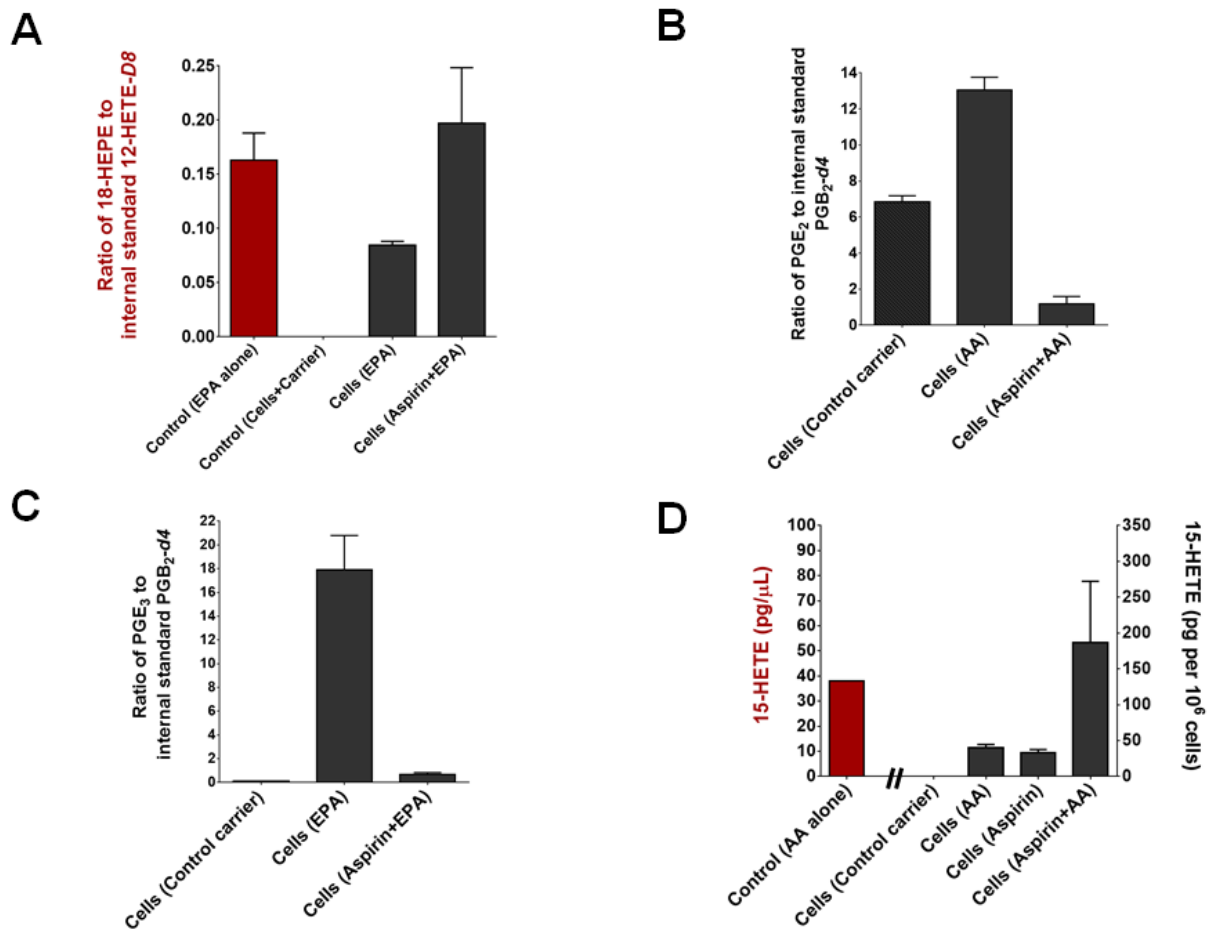


Figure 60. Analysis of MC38 cell conditioned medium for 18-HEPE, PGE₂, PGE₃ and 15-HETE.

The cell conditioned medium from MC38 mouse CRC cells was analysed by LC-ESI-MS/MS. (A). 18-HEPE biosynthesis by MC38 cells. (B) PGE₂ biosynthesis by MC38 cells. (C) PGE₃ synthesis by MC38 cells. (D) 15-HETE synthesis by MC38 cells (Control AA alone sample use left y-axis; remaining samples use the right y-axis). Results from three independent experiments and shown as mean with standard error of the mean, the control AA alone sample represents data from one experiment. Where the lipid mediator exceeded the upper limit of the standard calibration curve the data is shown as a ratio against the internal standard, otherwise the data are shown as pg per 10⁶ cells. The control AA alone sample is shown as pg/ μ L.

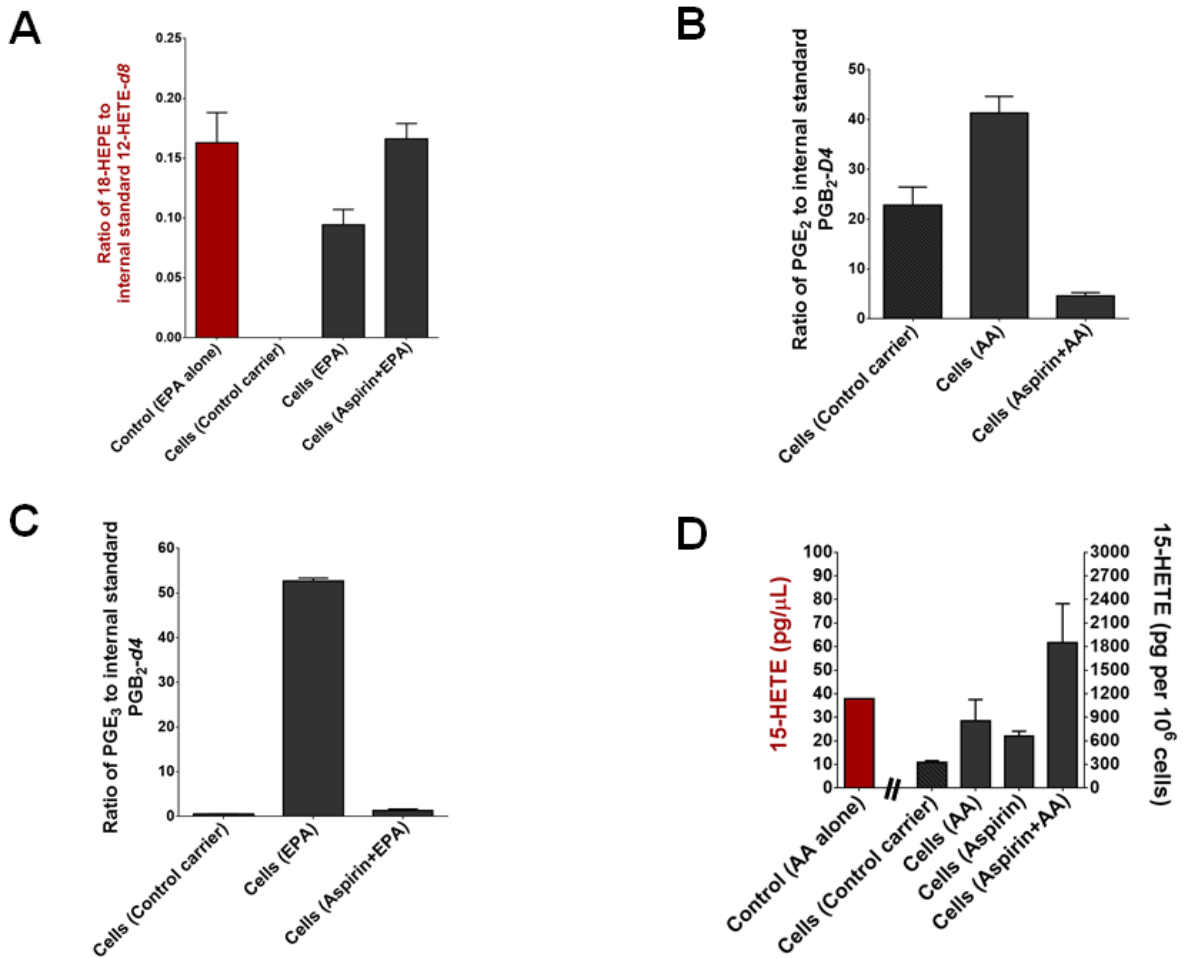


Figure 61. Analysis of LPS stimulated RAW26.7 cell conditioned medium for 18-HEPE, PGE₂, PGE₃ and 15-HETE.

The cell conditioned medium from LPS stimulated RAW264.7 cells was analysed by LC-ESI-MS/MS. (A) 18-HEPE biosynthesis by RAW264.7 cells. (B) PGE₂ biosynthesis by RAW264.7 cells. (C) PGE₃ synthesis by RAW264.7 cells. (D) 15-HETE synthesis by RAW264.7 cells (Control AA alone sample use left y-axis; remaining samples use the right y-axis). Results from three independent experiments and shown as mean with standard error of the mean, the control AA alone sample represents data from one experiment. Where the lipid mediator exceeded the upper limit of the standard calibration curve the data is shown as a ratio against the internal standard, otherwise the data are shown as pg per 10⁶ cells. The control AA alone sample is shown as pg/ μ L.

Acetylation of COX by aspirin was confirmed by the decrease in PGE₂ and PGE₃ (Figure 60C/D; MC38 and Figure 61C/D; RAW264.7) in the AA and EPA experimental conditions respectively. However the levels for both exceeded the upper limit of quantification and are consequently presented as ratio values of lipid mediator to internal standard (PGB₂-*d4*). Evidence for successful COX acetylation is also supported by the increase in 15-HETE levels in aspirin treated cells (Figure 60D; MC38 and Figure 61D; RAW264.7). However as discussed in section 4.5.7, 15-HETE was also detected in the no cell AA control, indicating that there may be an uncertain degree of 15-HETE synthesis secondary to non-cellular AA oxidation. 15-HETE chromatograms are shown for the MC38 and RAW264.7 cell samples in Figures 62 and 63, respectively. An increase in 15-HETE detected in the aspirin and AA treated cells compared to AA treated cells, (Figure 60D; MC38 and Figure 61D; RAW264.7), indicates a possible cell driven synthesis of 15-HETE beyond AA oxidation via non-cellular mechanisms.

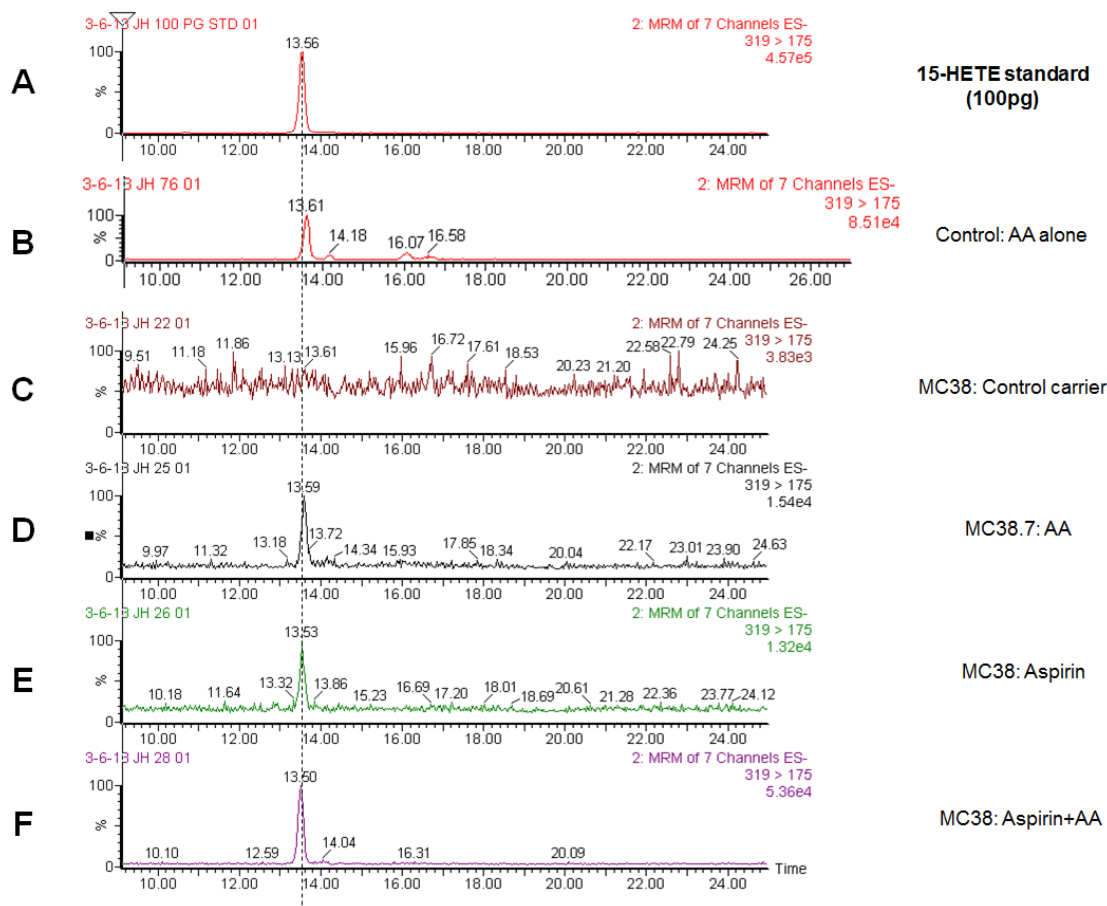


Figure 62. Analysis of MC38 cell conditioned medium for 15-HETE.

MC38 human CRC cell conditioned medium was analysed for 15-HETE by LC/ESI-MS/MS. (A) 15-HETE chromatogram for the standard (Cayman Chemical). (B) 15-HETE Chromatogram for the control AA (1 μ M, three hours) culture medium. (C) 15-HETE chromatogram for MC38 control carrier conditioned medium. (D) 15-HETE chromatogram for MC38 AA (1 μ M, three hours) treated cell conditioned medium. (E) 15-HETE chromatogram for MC38 aspirin (500 μ M, 30 minutes) and AA (1 μ M, three hours) treated cell conditioned medium. The dotted line represents the expected retention time for 15-HETE.

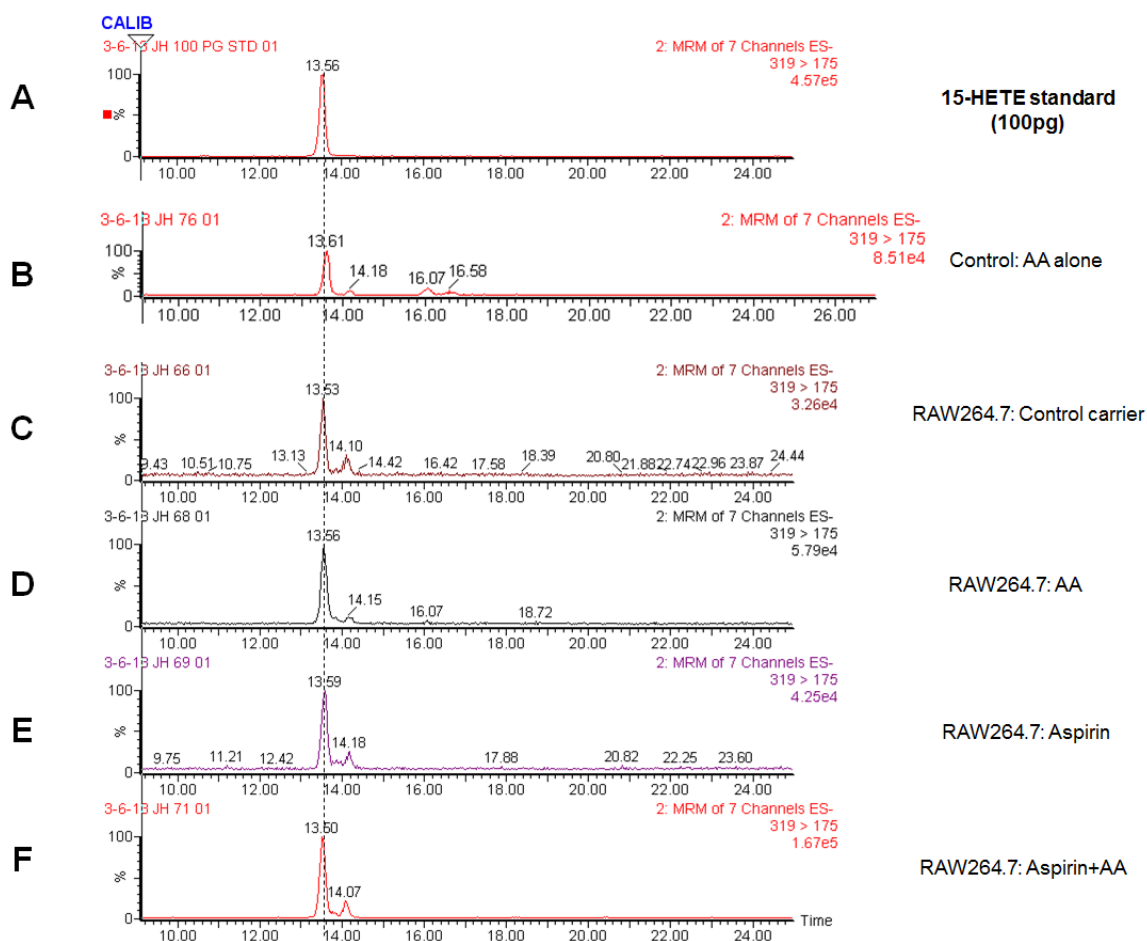


Figure 63. Analysis of LPS stimulated RAW264.7 cell conditioned medium for 15-HETE.

LPS stimulated RAW264.7 mouse macrophage cell conditioned medium was analysed for 15-HETE by LC/ESI-MS/MS. (A) 15-HETE chromatogram for the standard (Cayman Chemical). (B) 15-HETE Chromatogram for the control AA (1 μ M, three hours) no cell culture medium. (C) 15-HETE chromatogram for RAW264.7 control carrier conditioned medium. (D) 15-HETE chromatogram for RAW264.7 AA (1 μ M, three hours) treated cell conditioned medium. (E) 15-HETE chromatogram for RAW264.7 aspirin (500 μ M, 30 minutes) and AA (1 μ M, three hours) treated cell conditioned medium. The dotted line represents the expected retention time for 15-HETE.

No LTB₄ (Figure 64; MC38 and Figure 65; RAW264.7) or LTB₅ (Figure 66; RAW264.7) was detected, and whilst 5-HETE was detected in all AA treated cell conditioned medium samples, 5-HETE was found in the AA alone control sample. Consequently no cell driven 5-HETE could therefore be established. Despite treatment with a calcium ionophore RAW264.7 cells were unable to produce a detectable 5-LOX/ LTA₄H, AA or EPA derived lipid mediator. Therefore no 5-LOX enzymatic activity was identified in either MC38 or RAW264.7 cells under these *in vitro* conditions.

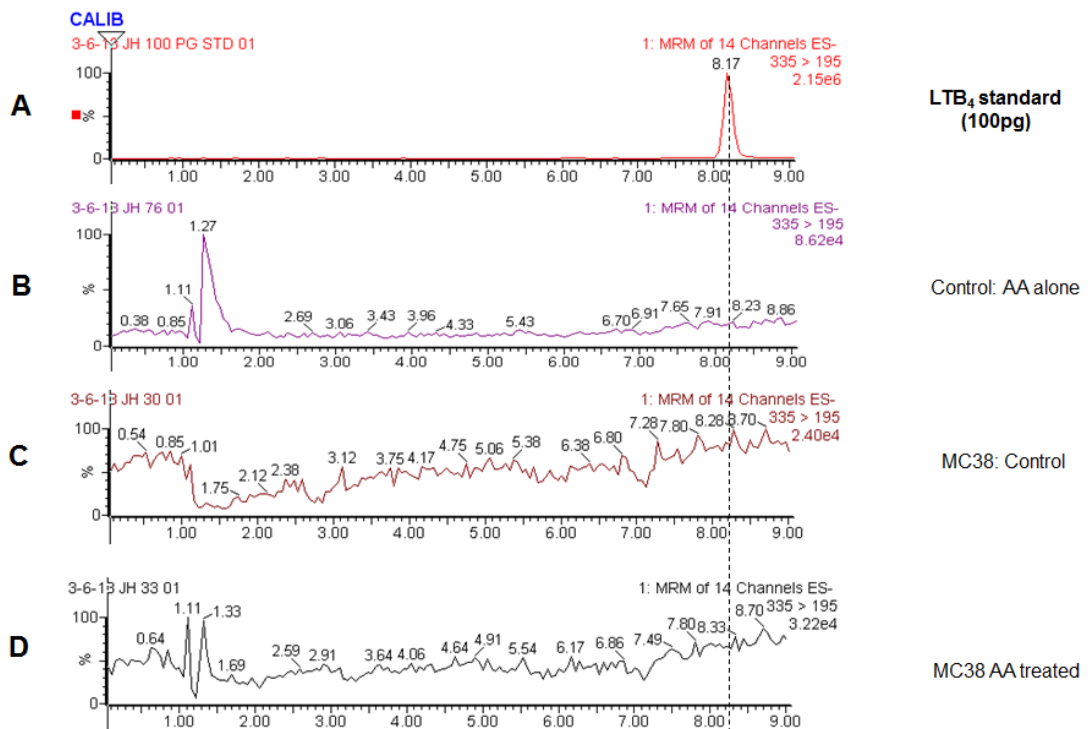


Figure 64. Analysis of MC38 cell conditioned medium for LTB₄.

MC38 cell conditioned medium was analysed for LTB₄ by LC-ESI-MS/MS. (A) LTB₄ chromatogram for the standard (Cayman Chemical). LTB₄ chromatogram. (B) LTB₄ chromatogram for control AA (1 μ M, three hours) medium. (C) LTB₄ chromatogram for MC38 carrier control treated cell conditioned medium. (D) LTB₄ chromatogram AA treated MC38 cells (1 μ M, three hours). The dotted line represents the expected retention time for LTB₄.

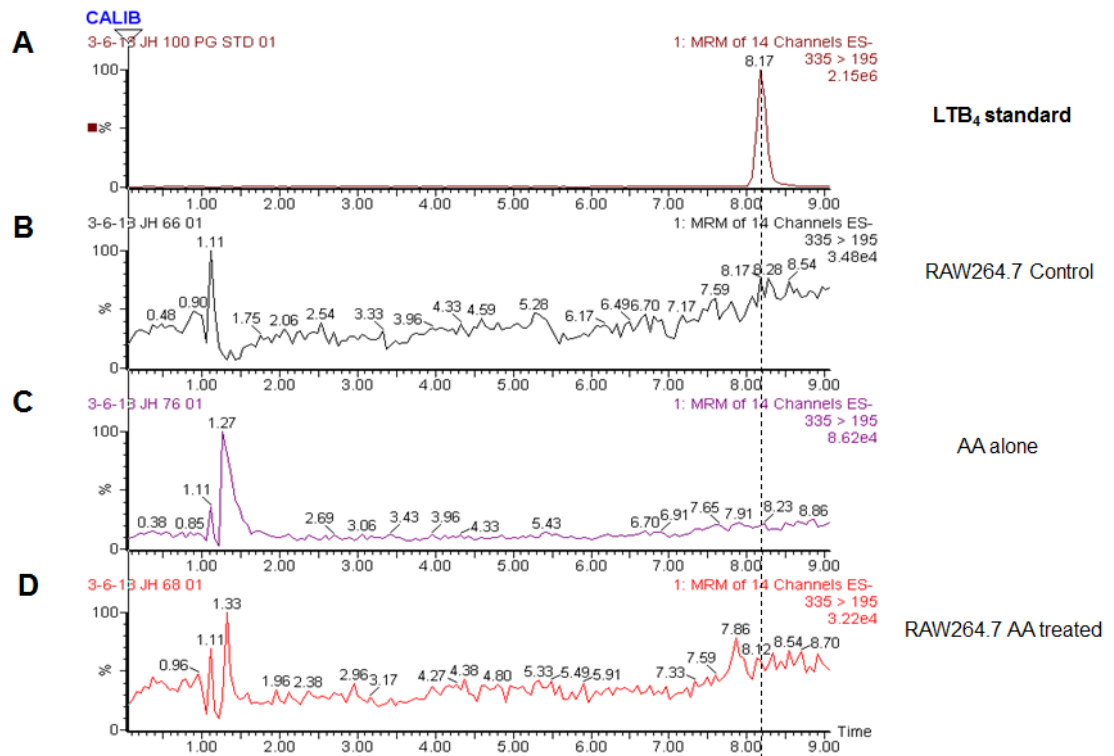


Figure 65. Analysis of LPS stimulated RAW264.7 cell conditioned medium for LTB₄.

RAW264.7 cell conditioned medium was analysed for LTB₄ by LC/ESI-MS/MS. (A) LTB₄ chromatogram for standard (Cayman Chemical). (B) LTB₄ chromatogram for control AA (1 μ M, three hours) medium. (C) LTB₄ chromatogram for RAW264.7 carrier control treated cell conditioned medium. (D) Chromatogram for AA (1 μ M, three hours) treated culture medium. The dotted line represents the expected retention time for LTB₄.

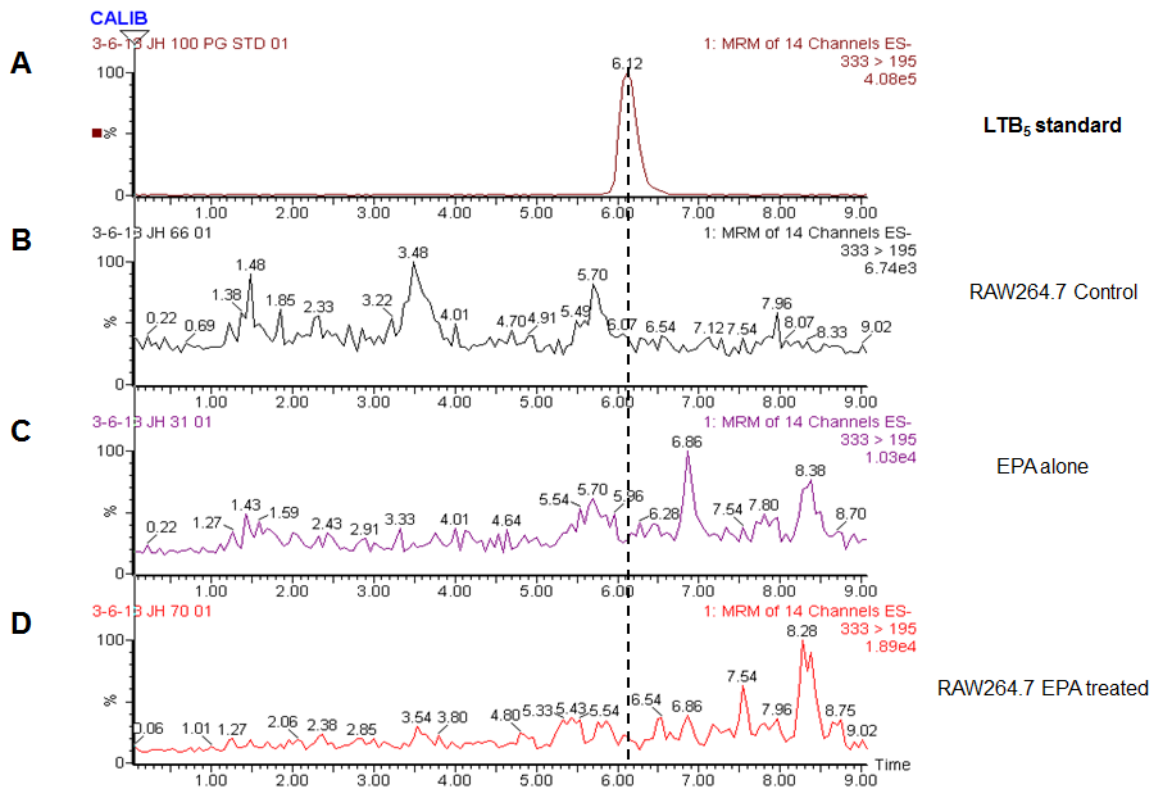


Figure 66. Analysis of LPS stimulated RAW264.7 cell conditioned medium for LTB₅.

RAW264.7 cell conditioned medium was analysed for LTB₅ by LC/ESI-MS/MS. (A) LTB₅ chromatogram for standard (Cayman Chemical). (B) LTB₅ chromatogram for control EPA (1 μ M, three hours) medium. (C) LTB₅ chromatogram for RAW264.7 carrier control treated cell conditioned medium. (D) Chromatogram for EPA (50 μ M, three hours) treated RAW26.7 cells. The dotted line represents the expected retention time for LTB₅.

As aspirin triggered-LXA₄ requires acetylated COX-2 and 5-LOX with AA as the substrate, which is directly comparable to RvE1 synthesis from EPA, aspirin triggered-LXA₄ was analysed for. The question being whether the substrate was the issue and not the enzymatic machinery in RvE1 synthesis. The candidate found that neither MC38 nor RAW26.7 cells could synthesise detectable aspirin triggered-LXA₄ (Figure 67; MC38 and Figure 68; RAW264.7).

In conclusion neither MC38 mouse CRC cells nor RAW264.7 mouse macrophage cells could cells synthesised detectable RvE1 or a comparable AA derived lipid mediator under the *in vitro* conditions used by the candidate.

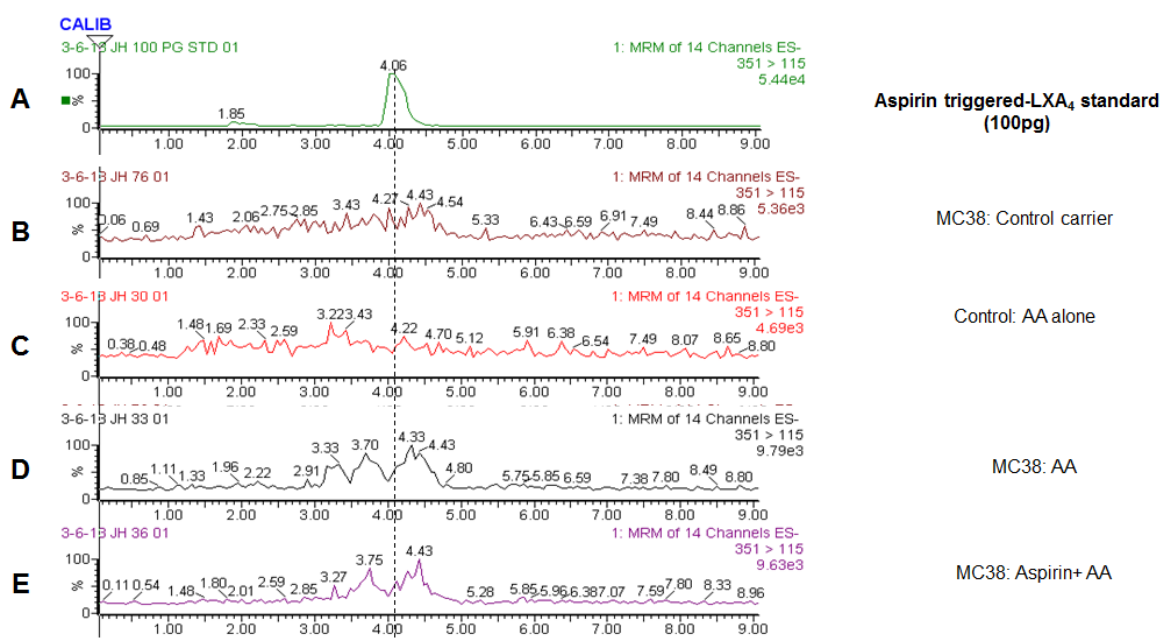


Figure 67. Analysis of MC38 cell conditioned medium for aspirin triggered-LXA₄.

MC38 cell conditioned medium was analysed for aspirin triggered-LXA₄ by LC-ESI-MS/MS. (A) Chromatogram for aspirin-triggered LXA₄ standard (Cayman Chemical). (B) Aspirin-triggered LXA₄ chromatogram from control (AA 1 μ M, three hours) medium. (C) Aspirin-triggered LXA₄ chromatogram for MC38 carrier control treated cell conditioned medium. (D) Aspirin-triggered LXA₄ chromatogram from MC38 AA (1 μ M, three hours) treated cell conditioned medium. (E) Aspirin-triggered LXA₄ chromatogram for MC38 aspirin (500 μ M, 30 minutes) and AA (1 μ M, three hours) treated cell conditioned medium. The dotted line represents the expected retention time for aspirin triggered-LXA₄.

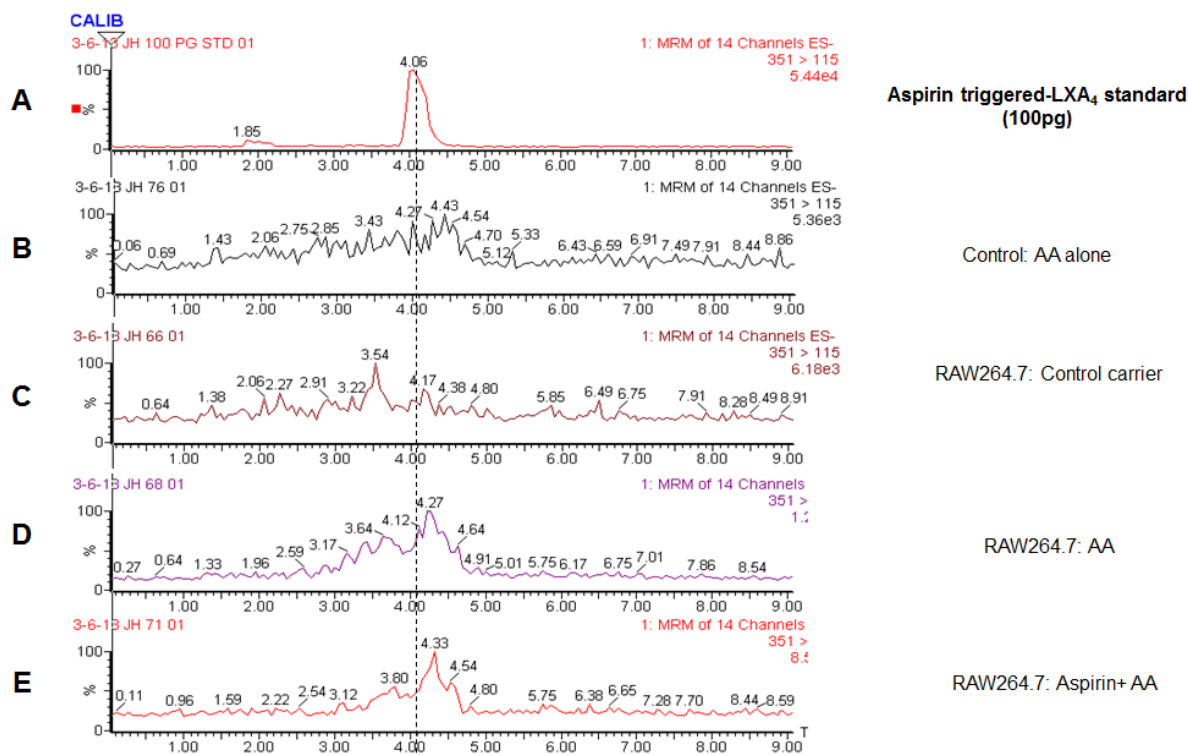


Figure 68. Aspirin triggered-LXA₄ biosynthesis by mouse macrophage RAW264.7 cells.

LPS stimulated RAW264.7 cell conditioned medium was analysed for aspirin triggered LXA₄ by LC-ESI-MS/MS analysis. (A) Aspirin triggered-LXA₄ chromatogram for the standard (Cayman Chemical). (B) Aspirin triggered-LXA₄ chromatogram for AA control (1 μM, three hours) no cell medium. (C) Aspirin triggered-LXA₄ chromatogram for RAW264.7 carrier control treated cell conditioned medium. (D) Aspirin triggered-LXA₄ chromatogram for RAW264.7 AA (1 μM, three hours) treated cell conditioned medium alone. (E) Aspirin triggered-LXA₄ chromatogram for RAW264.7 aspirin (500 μM, 30 minutes) and AA (1 μM, three hours) treated cell conditioned medium. The dotted line represents the expected retention time for aspirin triggered-LXA₄.

As no RvE1 synthesis was identified in the *in vitro* mouse cell model a transcellular model was developed. In this model cell conditioned medium from ASA and EPA treated MC38 cells was placed on RAW264.7 cells. The LC/ESI-MS/MS analysis confirmed that no RvE1 was detected in any of the cell conditioned medium samples from the transcellular synthesis models, as shown by the chromatograms showing the transition time expected for RvE1 (Figure 69). 18-HEPE was detected in the transcellular synthesis model (Figure 70).

The amount of 18-HEPE identified was lower, than that identified in MC38 (ASA+EPA) samples (Figure 71A). This was also seen for 15-HETE (Figure 71B).

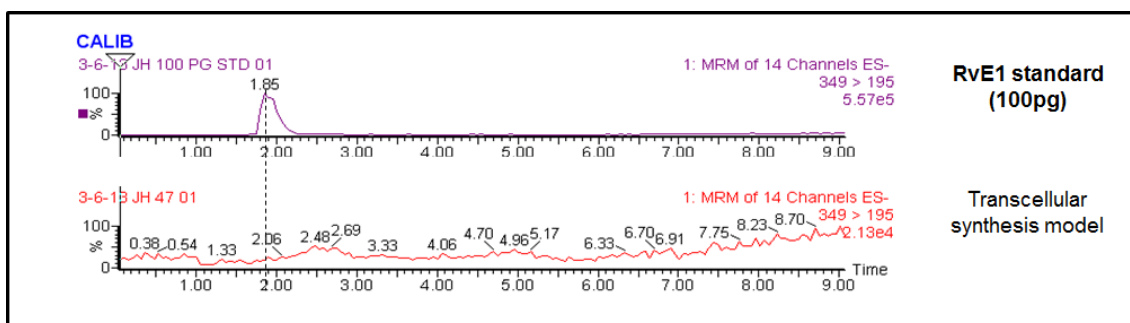


Figure 69. Analysis of the transcellular model (MC38/ RAW264.7) cell conditioned medium for RvE1.

MC38 cells were treated with aspirin and EPA, the cell conditioned medium was then placed on RAW264.7 cells for three hours. The cell conditioned medium was then analysed for RvE1 by LC-ESI-MS/MS analysis. RvE1 chromatograms for the standard (Cayman Chemical) and below for the transcellular synthesis model. The dotted line represents the expected retention time for RvE1.

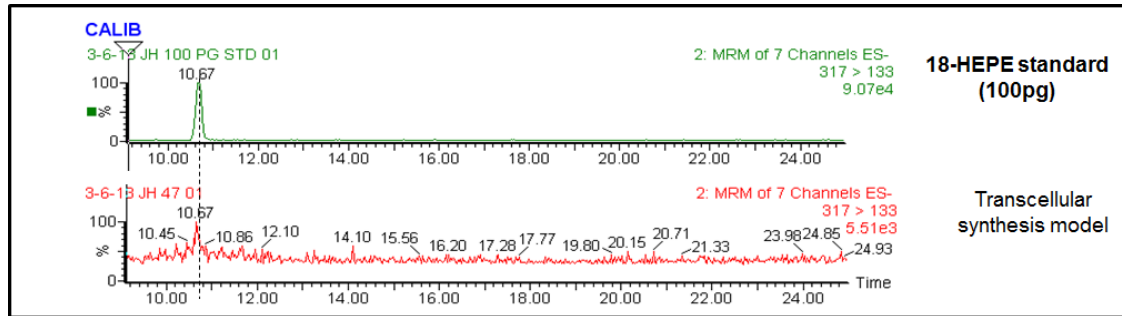


Figure 70. Analysis of the transcellular model (MC38/ RAW264.7) cell conditioned medium for 18-HEPE.

MC38 cells were treated with aspirin and EPA. The cell conditioned medium was then placed on RAW264.7 cells for three hours. The cell conditioned medium was then analysed for 18-HEPE by LC-ESI-MS/MS analysis. 18-HEPE chromatogram for the standard (Cayman Chemical) and below for the transcellular synthesis model. The dotted line represents the expected retention time for 18-HEPE.

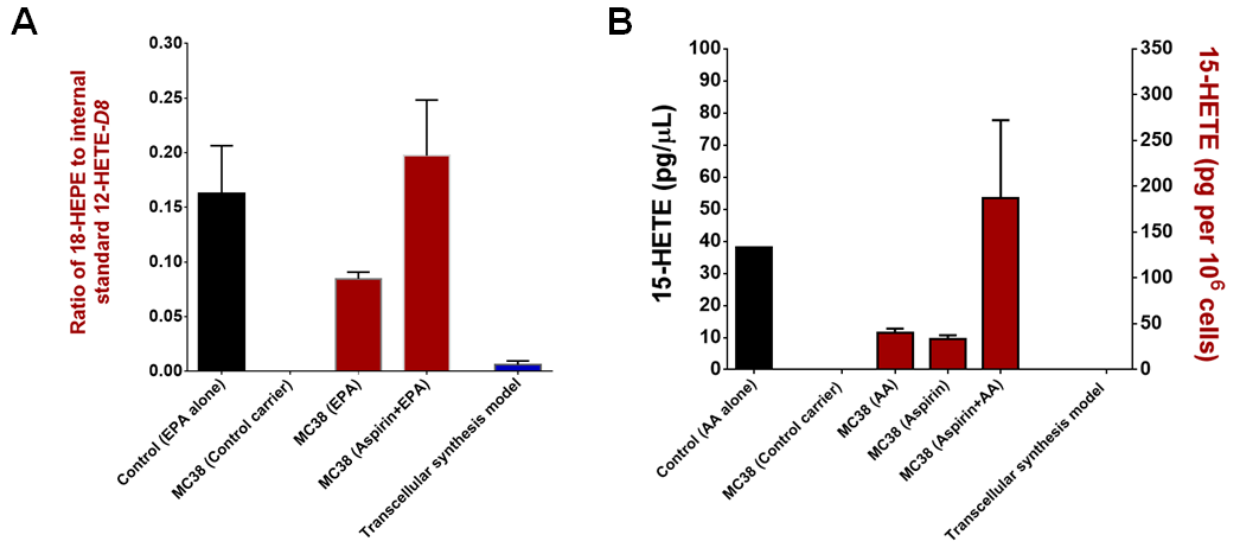


Figure 71. Analysis of the cell cultured medium from the transcellular synthesis model for 18-HEPE, and 15-HETE.

MC38 cells were treated with aspirin and EPA (or aspirin and AA), as appropriate. The cell conditioned medium was then placed on RAW264.7 cells for three hours. The cell conditioned medium was then analysed for 18-HEPE and 15-HETE by LC-ESI-MS/MS analysis. (A) 18-HEPE production. (B) 15-HETE production (control AA alone use right y-axis; MC38 and transcellular synthesis model data use left y-axis). Results from three independent experiments and shown as mean with standard error of the mean, the control AA alone sample represents data from one experiment. Where the lipid mediator exceeded the upper limit of the standard calibration curve the data are shown as a ratio against the internal standard, otherwise the data are shown as pg per 10⁶ cells.

The levels of both PGE₃ and PGE₂ increased in the conditioned medium from the transcellular synthesis model, when compared to MC38 ASA and EPA treated and MC39 AA and AA treated cells respectively (Figure 72A and B). The reason for this is likely due to the non-acetylated COXs in the RAW264.7 allowing conversion of the remaining AA/ EPA through to PGE_{2/3} respectively. No aspirin triggered-LXA₄ was detected in the RAW26.7 cell conditioned medium that was received from the aspirin and AA treated MC38 mouse CRC cells (Figure 73).

In conclusion this transcellular synthesis model could not synthesise detectable RvE1 under these *in vitro* conditions.

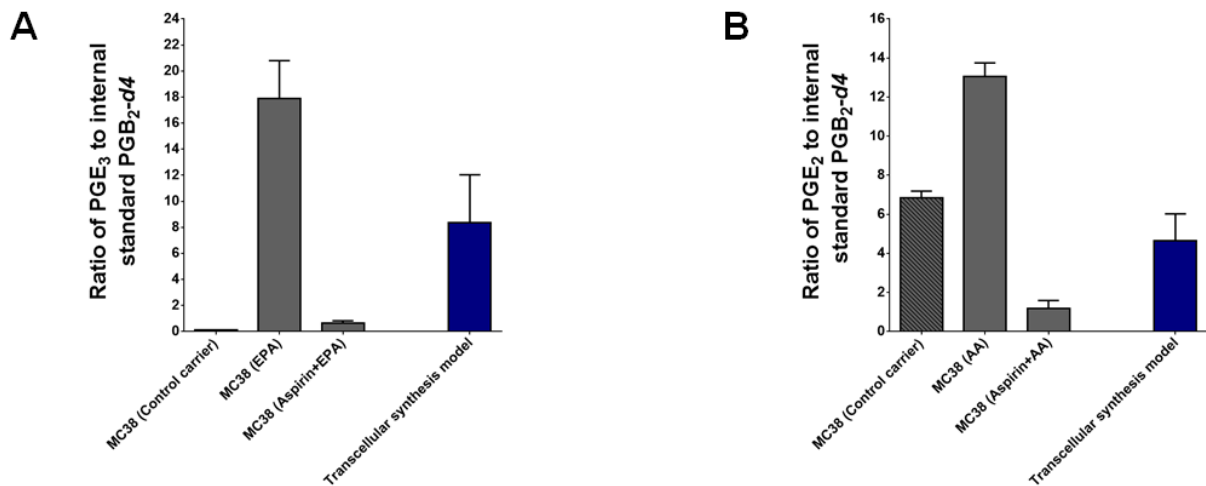


Figure 72. Analysis of the cell cultured medium from the transcellular synthesis model for PGE₂ and PGE₃.

MC38 cells were treated with aspirin and EPA (or aspirin and AA), as appropriate. The cell conditioned medium was then placed on RAW264.7 cells for three hours. The cell conditioned medium was then analysed for PGE₂ and PGE₃ by LC-ESI-MS/MS analysis. (A) PGE₃ synthesis. (B) PGE₂. Results from three independent experiments and shown as mean with standard error of the mean, the control AA alone sample represents data from one experiment. The lipid mediator exceeded the upper limit of the standard calibration curve the data and are shown as a ratio against the internal standard.

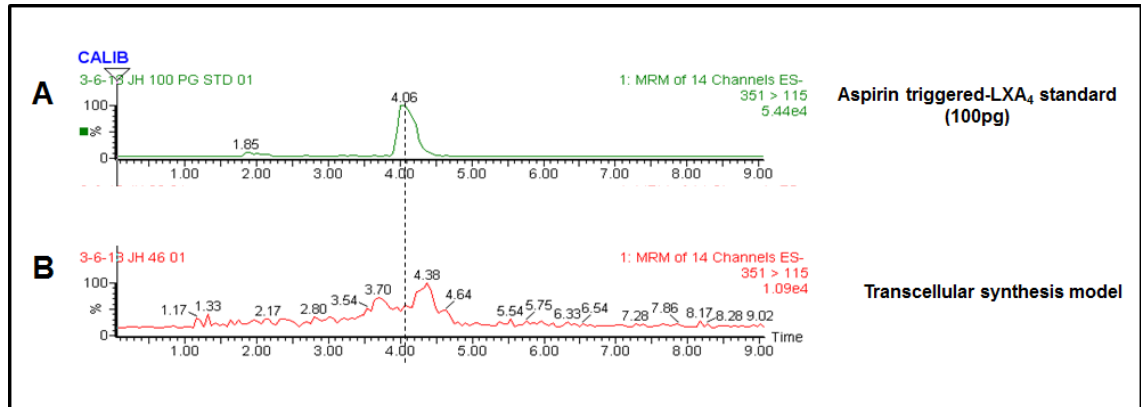


Figure 73. Analysis of the cell conditioned medium from the transcellular synthesis model for aspirin triggered-LXA₄.

MC38 cells were treated with aspirin and AA. The cell conditioned medium was then placed on RAW264.7 cells for three hours. The cell conditioned medium was then analysed for aspirin triggered-LXA₄ by LC-ESI-MS/MS analysis. (A) Aspirin triggered-LXA₄ chromatogram for the standard (Cayman Chemical). (B) Aspirin triggered-LXA₄ for the conditioned medium from the transcellular synthesis model. The dotted line represents the expected retention time for RvE1 and 18-HEPE as appropriate.

4.6 Discussion

The biosynthesis of RvE1 in the context of CRC has not been investigated to date. To address this, a panel of seven human CRC cell lines were characterized for COX-2 and 5-LOX expression by WB, and for COX- and 5-LOX-derived lipid mediator synthesis by LC-ESI-MS/MS.

On identifying a suitable COX-2 expressing cell line(s), the *in vitro* conditions required to successfully acetylate the COXs and allow the synthesis of the acetylated COX-2 product 15R-HETE was determined. The dose of aspirin used and duration of treatment on the cells were taken from published evidence (Serhan *et al.*, 2002), supported by cell viability data that determined that aspirin was not cytotoxic to the cells (discussed later).

Serhan and colleagues (2000) have reported that RvE1 is synthesised through transcellular synthesis (two different cell types, discussed in section 1.9). The candidate initially looked to determine whether human CRC cells alone could synthesise RvE1, when the CRC cell line was treated with EPA in the presence of aspirin. A mouse CRC cell line (MC38) and mouse macrophage (RAW264.7) cell line were also investigated for RvE1 biosynthesis. The use of two mouse cell lines would facilitate the development of an *in vitro* transcellular synthesis experiment without having to use cell lines from different species.

To establish that the LC/ESI-MS/MS system used by the candidate could identify RvE1, a human neutrophil-based experiment was initially performed replicating as closely as possible the experimental protocols published by Serhan *et al.*, 2000; Tjonahen *et al.*, 2006; Oh *et al.*, 2011.

4.6.1 Resolvin E1 synthesis by human polymorphonuclear leukocytes

Published *in vitro* studies have used up to 100 μ M of 18-HEPE standard (Tjonahen *et al.*, 2006, Oh SF *et al.*, 2011) to synthesise RvE1 from human PMNs, which is concerning as to whether RvE1 can be synthesised *in vivo*. The candidate sought to replicate these same *in vitro* conditions to confirm that RvE1 could be synthesised in this cell system and detected by the LC/ESI-MS/MS used in the candidate's lipidomic experiments. Using calcium ionophore activated 18-HEPE treated human PMNs RvE1 was detected. This confirmed that RvE1 synthesis could be replicated in an *in vitro* cell model and detected by the LC/ESI-MS/MS used by the candidate. RvE1 synthesis outside Professor Serhan's group had not been identified in the published literature at the time of writing this report.

4.6.2 Human HCA7 colorectal cancer cell lipidomic experiments

COX-2 expression was identified in HCA7, HRT18, HT29 and Caco2 human CRC cell lines under high sensitivity chemiluminescence, with highest expression clearly seen in the HCA7 human CRC cell line. High COX-2 protein expression in the HCA7 human CRC cell line is in keeping with the published literature (Shao *et al.*, 2000 and Sharma *et al.*, 2001). Using LC/ESI-MS/MS the simultaneous profiling and quantitative analysis of 23 different COX derived lipid mediators was carried out in the same panel of human CRC cell lines, in the presence or absence of AA. The HCA7 CRC cell line produced the highest amounts of COX derived lipid mediators from AA. In respect to the HCA7 AA supplemented cells there was no clear increase found, or the other human cell lines. Reasons for the lack of a clear increase in AA derived lipid mediators could be due to a problem with the AA dosing, such as failure to dose the cells with the correct amount of AA. Another possibility is that the cells were unable to synthesise increased levels of AA derived mediators as the absence of FBS in the culture medium may have placed the cells under too much stress over the 24 hour culture period. However the principal aim of this experiment was to identify a high COX-2 expressing cell line, which was achieved.

As RvE1 synthesis requires 5-LOX enzymatic activity, the presence of 5-LOX lipid mediator 5-HETE was determined in the cell conditioned medium by LC-ESI-MS/MS. Whilst 5-HETE was detected only in the AA supplemented LoVo supernatants, the 5-HETE peak only had a signal-to-noise (S/N) ratio of three, which was below the limit of quantification, (S/N ratio of 10). The WB studies examining for 5-LOX protein expression detected several protein bands, so conclusions on 5-LOX expression could not be made. These additional bands in part could be explained by other isoforms of 5-LOX. Five different human isoforms have previously been identified in PMNs, THP-1 cells and Raji cells, with predicted MWs of 78, 76, 72, 62 and 56 kDa (Boudreau *et al.*, 2011). The authors also showed that in their *in vitro* cell model, expression of alternative 5-LOX isoforms decreased the synthesis of 5-LOX products. The expression of alternative isoforms by the human CRC cell lines may account for low detectable levels of 5-HETE. As 5-LOX is subject to a regulatory control method in that it requires interaction with FLAP. FLAP is believed to play a role in presenting the substrate to 5-LOX, investigation into whether the human CRC cell lines express FLAP was carried out. A clear resolved protein band was evident at the predicted MW of FLAP in all cell lines. Therefore FLAP protein is unlikely to be a limiting factor for 5-HETE production in the cell lines. It is clear that under these *in vitro* conditions used that the human CRC cell lines are not producing quantifiable levels of 5-HETE. Published work also supports the role of a number of factors that are required in order

for 5-LOX to be active. They include calcium, which has been shown to stimulate 5-LOX translocation to the membrane and induce cellular leukotriene synthesis (Noguchi *et al.*, 1994) and adenosine triphosphate (ATP) which also has been shown to stimulate 5-LOX activity and require the presence of calcium (Noguchi *et al.*, 1996). Thus the calcium *in vitro* conditions used here may be affecting 5-LOX activity in the cell systems and preventing its activation.

As the COX-2 enzyme requires acetylation in order to produce 18-HEPE from EPA, the conditions required to acetylate COX-2 were replicated from the literature by the candidate. The Serhan group (Serhan *et al* 2002) published that they had dosed HUVECs with 500 μ M aspirin for 30 minutes prior to DHA treatment. They showed that these *in vitro* conditions allowed production of novel DHA derived bioactive products. This aspirin dosing regimen therefore served as the benchmark in establishing the *in vitro* conditions that could generate 15R-HETE in the human CRC cell line HCA7. The HCA7 human CRC cell line was chosen due to its favourable COX-2 profile on WB and high production of COX derived lipid mediators. After confirming that 500 μ M aspirin for 30 minutes was not irreversibly cytotoxic to the HCA7 cells, HCA7 cells were treated with aspirin with and without AA supplementation in order to amplify any aspirin induced COX effect. Successful acetylation of COX was confirmed by a clear reduction in PGE₂ production in the HCA7 CRC cell conditioned medium in the presence of aspirin, and the switch in chirality of 15-HETE from S in the AA supplemented cells to R in the aspirin and AA supplemented cells. This experiment confirmed the *in vitro* conditions required for successful synthesis of an aspirin acetylated COX-2 product by HCA7 human CRC cells.

The HCA7 cell line was unable to synthesise detectable RvE1 in cell conditioned medium after aspirin and EPA treatment. COX activity on EPA was established in these cells, through PGE₃ detection in the cell conditioned medium. Successful COX-2 acetylation by aspirin was confirmed by a reduction in both PGE₂ and PGE₃ in the presence of aspirin. Interestingly whilst there was an induction in 15-HETE levels in the presence of aspirin, this was not the case for 18-HEPE in the HCA7 cell line. However in this experiment no chiral analysis was performed on the 15-HETE or 18-HEPE to confirm chiral change in the 15-HETE or 18-HEPE product in the presence of aspirin. Additionally 18-HEPE and 15-HETE were present in the no cell EPA and AA control respectively suggesting a degree of non-enzymatic AA oxidation. This control had not been included in the initial 15-HETE chiral analysis experiment. However the increase in 15-HETE detected when AA treated cells were also dosed with aspirin compared to the AA treated cells supports a cell driven process of 15-HETE above that of non-cellular 15-HETE synthesis. Expectations from the literature from human clinical

samples would be that 18-HEPE levels would have increased in the EPA treated aspirin dosed HCA7 cells compared to the EPA treated cells (Serhan *et al.*, 2000, Oh SF, *et al.*, 2011). This suggests that whilst the HCA7 acetylated COX-2 enzyme and can use AA as a substrate it may not be able to use EPA in a similar fashion. Furthermore there is a potential that both 18-HEPE and 15-HETE were already present in the EPA and AA stock solution controls which were not analysed as controls included EPA and AA stock solutions placed in the culture medium. Additional controls including culture medium and AA and EPA stock solution would assist in establishing cell driven synthesis of 18-HEPE and 15-HETE. Interestingly the published methodology from Professor Serhan's group does not comment whether AA and EPA (no cell) controls were included in their experiments to rule out non cell driven lipid oxidation.

No 5-HETE was identified in any cell conditioned media samples from the HCA7 human CRC cells, neither was LTB₄ or EPA derived LTB₅, in either AA or EPA supplemented experimental conditions. The lack of 5-HETE and LTB_{4/5} indicates the probable absence of functional 5-LOX activity in this cell line, with LTA₄H activity uncertain. Therefore the lack of RvE1 was likely secondary to an absence of functional 5-LOX activity in these cells. Further support for a lack of 5-LOX activity comes from the absence of aspirin triggered LXA₄ which also requires a functional 5-LOX to act on the substrate 15-HETE.

The published literature treated human PMNs with doses of up to 100 μ M (Tjonahen *et al.*, 2006, Oh *et al.*, 2011), the candidate dosed 1 μ M 18-HEPE on the CRC and macrophage cells. This emphasises the high concentrations of 18-HEPE required in order to produce detectable RvE1 in the PMN studies when compared to that used by the candidate. Whether this high dose of 18-HEPE would have generated RvE1 by the CRC cells is uncertain. The cost of purchasing 18-HEPE would have been high and made experiments impractical from a costing view point. Whether there was RvE1 produced below the limit of detection for this experiment is difficult to establish as Tjonahen *et al.*, (2006) and Oh *et al.*, (2011) published RvE1 chromatograms alone and did not comment on the amount of RvE1 produced by their cell models. Additionally the relevance of whether RvE1 could be genuinely produced *in vivo* when such large amounts of 18-HEPE are required *in vitro* should not be ignored.

4.6.3 Murine transcellular metabolism experiments

To avoid species cross-reactivity in a transcellular synthesis model, a mouse CRC and macrophage cell line was used. The candidate successfully confirmed that LPS stimulated COX mediated PGE₂ production in RAW264.7 mouse macrophage cells.

MC38 mouse CRC cells and RAW264.7 mouse macrophage were shown to produce AA and EPA derived COX products through the detection of COX derived PGE₂ and PGE₃. Further successful aspirin acetylation of COX was confirmed through the inhibition of both PGE₂ and PGE₃ in the AA and EPA treated cells respectively. However like the HCA7 human CRC cells they were unable to synthesise detectable RvE1 in the cell conditioned medium. The absence of 5-HETE and LTB₄ in the cell conditioned medium supports an absence of a functional 5-LOX plus or minus LTA₄H activity, despite AA and EPA substrate dosing to the cells. The absence of detectable aspirin triggered LXA₄ supports this.

A limitation of the study was that 18-HEPE, 15-HETE and PGE₂ and PGE₃ levels exceeded the upper limit of quantification as set by the calibration curve used for each respective lipid mediator (100 pg/ µL). Whilst the samples could have been diluted and re-analysed for accurate quantification, this was not practical due to the time and financial costs that would have been incurred. In the case where levels exceeded those for accurate quantification, the values were presented as a ratio against the known internal sample. An internal standard was included in every sample analysed, thus allowing the candidate to identify a qualitative increase or decrease in amounts through fold changes in the lipid mediators analysed.

The MC38 and RAW264.7 cells produced increasing levels of 18-HEPE in the conditioned medium when treated with aspirin and EPA, compared to EPA treated cells, mirroring the induction seen for AA-derived 15-HETE. Whilst the AA and EPA controls produced 15-HETE and 18-HEPE respectively there was difficulty in establishing how much 15-HETE and 18-HEPE was derived from cell driven oxidation versus non-cellular oxidation. However there was the trend seen for an increase in both 15-HETE and 18-HEPE in the presence of aspirin for both the MC38 and RAW26.7 cells. Despite ionomycin treatment of the RAW264.7 cells no 5-LOX derived synthesis of 5-HETE could be detected, nor LTB₄ or LTB₅. The ionomycin was used with the purpose of increasing intracellular calcium levels in the RAW264.7 cells, through 5-LOX activation. Ionomycin has been reported to stimulate 5-LOX activity in RAW264.7 cells and the candidate replicated the dose and length of treatment of ionomycin applied to these cells (Buczynski *et al.*, 2007). The candidate established COX activity in these cells but found no 5-LOX activity.

No RvE1 was detected in the cell conditioned medium from the transcellular synthesis model. There was a reduction in the amount of both AA derived 15-HETE and EPA derived 18-HEPE, when compared to matched cell conditioned medium samples from aspirin (+AA), and aspirin (+ EPA) treated MC38 cells. This reduction could be due to cell driven breakdown by the RAW264.7 cells or secondary to RAW264.7 uptake of 15-

HETE and 18-HEPE intracellularly. It could be that the RAW264.7 cells in the transcellular model are synthesising the RvE1 intracellularly. Interestingly in the human PMN based experiments utilised by the Serhan group the PMNs and experimental solution were analysed as one. Indeed on replicating the conditions used by Serhan in the PMN model, RvE1 was detected. In this model the PMNs were lysed with ice cold methanol and the lysed product was analysed for RvE1. Therefore an explanation for a lack of RvE1 synthesis in the candidate's *in vitro* cell models could be that the RvE1 is being synthesised within the cells. Future experiments looking to examine for RvE1 production should address this by analysing both the cell conditioned medium and cell pellets for RvE1 (or lysing the cells in the cell conditioned medium) before immediate storage at -80°C, before lipid mediator analysis.

Furthermore the absence of detectable RvE1 in these experiments could be due to its rapid breakdown. It is known that RvE1 undergoes metabolic inactivation by dehydrogenation (Arita *et al.*, 2006, Hong *et al.*, 2008). Breakdown products such as 19-hydroxy-, 20-hydroxy-, 20-carboxy-,10,11-dihydro-, 18-oxo-RvE1 were not investigated for in the cell conditioned medium, and such mediators could be investigated for in future experiments.

It is likely that the *in vitro* calcium/ ATP conditions used in the experiments to date will need further optimisation in order to see if 5-LOX activity can be induced *in vitro*. Experimentation to establish LTB₄ production in the *in vitro* cell model would confirm 5-LOX/ LTA₄H enzymatic activity, a crucial pathway required in RvE1 synthesis. Lipidomic analysis of the intracellular contents of cells should also be examined as previous published work has lysed the cells within the reaction when RvE1 has been identified.

It is of note that Gleissman *et al.*, (2010) found no D-series resolvins in their neuroblastoma tumour model when tumours were supplemented with DHA. The authors proposed that the lack of D-series resolvins in the neuroblastoma cell line may represent a survival strategy by these cells. Whilst the authors state that these cells express 5-LOX they did not confirm the production of a 5-LOX derived lipid mediator in their study. Therefore a second cell type may be needed in order to synthesise RvE1.

There is evidence that supports an active 5-LOX pathway in fibroblasts (James *et al.*, 2006) as well as PMNs (as discussed previously). The candidate's work has identified PMN type cells in human CRC tissue as well as fibroblast type cells. Future *in vitro* cell culture modelling should consider using PMNs or fibroblasts in transcellular synthesis models with CRC epithelial cells.

4.7 Summary

In vitro production of RvE1 by CRC cells and macrophages separately and using a transcellular synthesis model was not found by the candidate. COX enzymatic activity was proven in the CRC cells and macrophage cell lines. No 5-LOX enzymatic activity was identified in any of the cell lines. However the intermediate 18-HEPE lipid mediator was identified in EPA supplemented cells. Conclusions on whether the 18-HEPE identified was cell or non-enzymatic driven could not be concluded. A second cell type with 5-LOX and LTA₄H activity is likely to be needed alongside the CRC cells for RvE1 synthesis *in vitro*. Establishing whether RvE1 is present within human CRC samples or colorectal samples should be considered important before further *in vitro* RvE1 synthesis studies are performed.

5 Effect of Resolvin E1 on human colorectal cancer cell viability and apoptosis

5.1 Introduction

The candidate has confirmed expression of both ChemR23 and BLT1 in human CRC tissue. The presence of these receptors in human CRC tissue provides a means by which RvE1 might have anti-CRC activity. In order to establish any *in vitro* activity that RvE1 has on CRC cells, the candidate performed cell viability and apoptosis assays.

To confirm that the RvE1 used in the cell viability and apoptosis assays was biologically active, the candidate looked to replicate RvE1 mediated *in vitro* effects from the literature. RvE1 has been shown to induce ALPI expression by ChemR23 mediated signalling (Campbell *et al.*, 2010). Increased epithelial expression of ALPI has been shown to be protective against dextran sodium sulphate (DSS) induced colitis in a mouse model. RvE1 has also been shown to induce the expression of CD55. This induction via ChemR23 in CD55 expression was shown to promote the clearance of PMNs across the epithelial surface thus facilitating the resolution of inflammation (Campbell *et al.*, 2007). As RvE1 has been shown to induce ALPI expression in the ChemR23 expressing human CRC cell line Caco2 (Campbell *et al.*, 2010) and induce the expression of CD55 in the ChemR23 transfected KB oral epithelial cell line *in vitro*, and human CRC cell lines Caco2 and T84, the candidate sought to replicate these findings using these human CRC cell lines. RvE1 has also been shown to induce intracellular calcium levels in human PBMCs this experimental model was also utilised in establishing the biological activity of the Cayman Chemical RvE1 (Arita *et al.*, 2007).

The Cayman Chemical RvE1 product used in the cell viability and apoptosis assays, was analysed by ESI-MS/MS.

5.2 Hypothesis

RvE1 can inhibit CRC cell proliferation, and induce cancer cell apoptosis, through ChemR23 and/ or BLT1 receptor signaling.

5.3 Aims

1. To check the chemical identity and stability of the Cayman Chemical RvE1 standard at 37°C.
2. To establish whether RvE1 affects human CRC cell viability and apoptosis.

3. To investigate whether RvE1 induces ALPI and CD55 expression in human CRC cells and induces intracellular calcium levels in human PMNs

5.4 Materials and Methods

5.4.1 Experimental solutions

5.4.1.1 Resolvin E1 preparation

RvE1 standard (Cayman Chemical, Ann Arbor, MI, US; Cat.No 10007848) was supplied as a stock solution in ethanol at 25 µg in 500 µL (143 µM; stored in 20 µL aliquots at -80°C until use). RvE1 experimental solutions were made in culture medium (RPMI 1640 GlutaMAX™) free of FBS for the cell viability and gene expression assays but in culture medium (RPMI 1640 GlutaMAX™+10% FBS) for the apoptosis assay at a v/v dilution of 0.1%. Cayman Chemical was the sole commercial supplier of RvE1 (at the time of the candidate's period of study). Permission was sought in order to obtain it from Cayman Chemical, as RvE1 was not commercially available.

5.4.1.2 Etoposide preparation

Etoposide was supplied as a powder from Sigma-Aldrich® (4'-Demethylepipodophyllotoxin 9-(4, 6-O-ethylidene-β-D-glucopyranoside), VP-16-213; e1383-25mg). Etoposide was solubilised in DMSO at a concentration of 10 mg/ mL. Experimental solutions were made in culture medium (RPMI 1640 GlutaMAX™+10% FBS) at a v/v dilution of less than 0.1%.

5.4.2 Western blotting

Human cell lines were grown to 50-70% or 100% cell confluency, and protein extracted and as for detailed in section 3.2.2.

5.4.3 Cytotoxicity assay

HCA7, Caco2 and HT29 human CRC cells were seeded in sterile tissue culture treated non-pyrogenic 96-well plates (Corning Incorporated costar®, NY, UK; Cat. No. BC019) at a density of 1000 cells/ well for HCA7 and HT29 cells and 2000 cells/well for Caco2 cells in cell type specific culture medium containing 10% FBS.

After 24 hours of incubation eight replicates (RvE1 0.06 nM to 1000 nM) were added to the culture medium (without FBS so as to prevent lipid binding to the RvE1). Controls included cells cultured in medium containing carrier control and culture medium alone. The experimental solutions were made up in 50 mL falcon tubes before being dispensed from sterile solution basins (Scientific Laboratory Supplies, UK; Cat.No.746180-2), to facilitate dosing of the cells by a multi-channel pipette. After three

hours the RvE1 solution was removed and the cells washed gently three times before culture medium containing FBS was placed on the cells to prevent adverse effects on cell viability secondary to the lack of FBS. Twenty-one hours later the culture medium was removed and cells washed gently three times with sterile DPBS before the experimental RvE1 solutions (without FBS) were placed on the cells for three hours. This cycle was repeated until the cells had been incubated for a total of 72 hours. After 96 hours 20 μ L of 3-(4,5-Dimethylthiazol-2-yl)-2,5-diphenyltetrazolium bromide (MTT), (Sigma-Aldrich, Poole, UK; Cat.No M2128-1G) at a prepared concentration of 5mg/ml (in DPBS) was added to each well and left in the dark at a temperature of 37°C for three hours. The solution was then aspirated off, and 150 μ L of DMSO was added to the formazan crystals left in the wells. The plate was then read at 570 nm using a microplate reader (Opsys MR™ Dynex technologies Ltd, UK) to give an optical density value for each well. The mean OD of a minimum of six wells was taken and a percentage cell growth value calculated by dividing the mean OD value for each individual experimental condition by the mean OD control value for each plate (as cells were visualised pre and post dosing, any wells that had been affected by mechanical trauma to the cells from pipetting were excluded by the candidate). The mean blank well value was subtracted from the cell well OD values. Results are shown as a mean values with SEM from three independent experiments.

5.4.4 Apoptosis assay

Apoptosis was measured using the fluorescein isothiocyanate (FITC) Annexin V propidium iodide (PI) apoptosis detection kit I (BD Pharmingen™; Cat. No.556547), which was used as per manufacturer's instructions. In brief the assay utilises the plasma membrane disruption that occurs in early apoptosis. The assay uses a vital dye called PI, which is excluded by cells with intact plasma membranes; however damaged or dead cells are unable to exclude PI. The membrane phospholipid phosphatidylserine (PS) translocates from the inner to the outer leaflet of the plasma membrane during early apoptosis (Bossy-Wetzel & Green., 2000). Consequently PS is exposed to the external cellular environment. Annexin V is calcium dependent binding protein that that can bind to PS. Therefore this assay uses both PI and Annexin V to identify early and late apoptotic cells; in summary viable cells exclude PI and prevent binding of Annexin V, early apoptotic cells are PI negative but Annexin V positive, and those cells in late apoptosis or dead are both Annexin V and PI positive. In this assay the Annexin V is bound to a flurochrome (FITC) which allows it to be probed by flow cytometry.

Etoposide was used as a pro-apoptotic drug for the apoptosis assay. Etoposide interacts with DNA to form a ternary complex along with the enzyme topoisomerase II. This complex serves to inhibit DNA re-ligation. This ultimately leads to DNA breaks

which cannot pass into the mitotic phase of cell division and subsequently cell death. For the HCA7 cell line 20 μM of etoposide had been shown by others within the research group to be pro-apoptotic over a 24 hour period, so this dose and duration was confirmed by the candidate before the RvE1 experiments were performed. However when Caco2 cells were dosed with 20 μM of etoposide over 24 hours there was no clear apoptosis induction. The candidate subsequently performed an experiment over 72 hours using 50 μM of etoposide, in order to determine reproducible apoptotic experimental conditions in the Caco2 cells before the RvE1 experiments were carried out.

HCA7 and HT29 were grown to 80% confluency and Caco2 cells grown to 100% confluency (in order to maximize ChemR23 expression in the Caco2 cells, see section 3.4.1.2). Cells were grown on sterile tissue culture treated non-pyrogenic 6-well plates. Cells were then washed three times in sterile DPBS. The cells were then dosed with either etoposide 20 μM (HAC7 cells) or 50 μM (Caco2 cells) (positive apoptosis inducing control) or 1 μM RvE1 for 24, 48 or 72 hours, with appropriate carrier controls (DMSO or ethanol carrier), (0.1% v/v). Cells were harvested by trypsinisation (see section 3.1.2) and then centrifuged at 400 x g for five minutes prior to re-suspension in 50 μL DPBS and counted using a haemocytometer. The cells were then prepared for flow cytometry analysis using the FITC Annexin V PI apoptosis detection kit I (BD Pharmingen™; Cat. No.556547), which was used as per manufacturer's instructions. In brief, the cell pellet was washed twice with cold DPBS and then re-suspended in 1X Binding Buffer at a concentration of 1 x10⁶ cells/ mL. A volume of 100 μL cell suspension (1 x10⁵ cells) was transferred into a 5 mL tube. Then 5 μL of FITC Annexin V and 5 μL PI was added to the cell suspension, before gently vortexing and incubating for 15 minutes at room temperature (25°C) in the dark. A further 400 μL of 1X Binding Buffer was then added to each tube before the sample was analysed. Staining controls with no FITC and no PI, PI alone, or FITC alone were included. The samples were run on a Beckton Dickinson LSRII 3 laser flow cytometer and analysed using BD FACS Diva software (v5.0.2). Three independent cultured experiments were completed for the HCA7 cell line and one for the Caco2 cell line. The candidate performed all data analyses.

When carrier control treated Caco2 and HCA7 human CRC cells were analysed by the flow cytometry, two distinct populations on the forward and side scatter dot blots were seen, (labeled as 1 and 2 in Figure 74A (Caco2), Figure 75A (HCA7)). Population 1 was made up of cellular debris (PI positive or FITC Annexin V and PI positive (late apoptotic cells or cell debris) and Population 2 on analysis was a cell population that was viable (FITC Annexin V and PI negative). As the aim of this experiment was to

identify apoptosis occurring as a result of RvE1 population 2 was gated for the subsequent apoptosis analysis.

5.4.5 Gene expression analysis

5.4.5.1 Sample preparation

Caco2 cells were grown to 100% cell confluency, T84 cells were grown to 80% cell confluency in sterile tissue culture treated non-pyrogenic six well plates. The cells were then dosed with either carrier control (ethanol) or RvE1 for between 0-24 hours (time course specific to the experiment), the cells were then washed three times with sterile PBS (1X) before being trypsinised (see section 3.2.1.2). Cell incubations with carrier control or RvE1 were carried out in specific cell culture medium without FBS.

For the ALPI experiment a time course was initially performed over eight hours (0, 4 and 8 hour time points) using a 100 nM RvE1 dose. This replicated as closely as possible the conditions published by Campbell *et al.*, (2010). Who showed a five to six fold induction in ALPI mRNA expression in RvE1 (100 nM) dosed Caco2 cells after four hours with induction still evident after eight hours (2-3 fold) and 12 hours (2 fold). A further experimental condition was included investigating for ALPI gene induction after six hours of 500 nM RvE1 treatment to the Caco2 cells, looking for a concentration dependent effect.

For the CD55 study the candidate performed a time course experiment over 24 hours before completing a dose study at six hours, thus including the published experimental conditions used by Campbell *et al.*, (2010), who showed a three fold and two fold induction in CD55 protein expression in T84 and Caco2 cells respectively.

5.4.5.2 Ribonucleic acid extraction

As per section 3.2.2.2.

5.4.5.3 First strand complementary deoxyribonucleic acid synthesis

As per section 3.2.2.3.

5.4.5.4 Amplification of complementary deoxyribonucleic acid by quantitative polymerase chain reaction

Primers for qPCR were designed by TaqMan gene expression assays (Life Technologies, UK). Target genes were ALPI and CD55 and the housekeeping gene control was β -actin, details shown in Table 1.

PCR reaction mixes were prepared according to manufacturer's instructions as per section 3.2.2.4. In brief a one in two dilution of cDNA to nuclease free water (Severn Biotech Ltd, Cat.No. 20-9000-01) was prepared for both ALPI and CD55 studies. Each 10 μ L reaction volume was therefore made up of 5.5 μ L (Universal MM II and TaqMan gene expression assay) and 4.5 μ L (cDNA and Nuclease free water), (summarised Table 9).

PCR reaction mix	Single 10 μ L reaction
20X Taqman gene expression assay	0.5
2X Taqman gene expression master mix	5
cDNA template	2.25
RNase-free water	2.25

Table 9. TaqMan gene expression assay reaction contents for the ALPI and CD55 studies

5.4.6 Intracellular calcium influx assay

5.4.6.1 Sample preparation

5.4.6.1.1 Human peripheral blood monocytes

Human plasma samples were collected from healthy volunteers who had not taken medication for at least two weeks prior to the samples being taken. Approval for the blood sampling was undertaken under the approval of the Leeds East Research Ethics Committee (REC reference 07/Q1206/47) Multidisciplinary Research Tissue Bank (Dr. Gina Doody).

A total of 10 mL of blood was taken from one volunteer in two six mL VACUTTE[®] coagulation sodium citrate 3.2% tubes. The Lymphoprep (Stemcell Technologies, Cat No;07801) was mixed thoroughly before use. Twenty millilitres of Lymphoprep was added to a 50 mL plastic falcon tube. The 10 mL of blood collected was then mixed with an equal volume of PBS containing 2% FBS. This then was carefully layered on top in order to reduce mixing of the blood with the Lymphoprep. The sample was then centrifuged at 800 \times g for 20 minutes at room temperature. The upper plasma layer was then removed and discarded. The mononuclear cell layer at the plasma-Lymphoprep interface was then carefully removed. The mononuclear cells were then re-suspended in 10 mL in isotonic PBS (without CaCl₂ and MgCl₂) and then centrifuged

at 200 x *g* for 10 minutes. The cells were then resuspended in sterile PBS containing 10% FBS and a viability count as in section 3.2.1.3. The PBMCs cells were then used for the intracellular influx assay, detailed below.

5.4.6.1.2 THP-1 cells

THP-1 human acute monocytic leukaemia cell line was grown in suspension in cell culture medium (RPMI 1640 GlutaMAX™+10% FBS) to a cell concentration of 1×10^6 cells/mL. The cells were then centrifuged at 400 x *g* for five minutes. The cells were then re-suspended in sterile DPBS and counted, in preparation for the calcium influx assay.

5.4.6.2 Intracellular calcium measurement

Fura-2 is a ratiometric calcium indicator dye that allows the measurement of intracellular calcium. The acetoxymethyl ester (AM) form is membrane permeable and once inside the cell the AM group is cleaved by non-specific esterases to produce the charged and active form (Fura-2) that is able to bind calcium with a high affinity. Upon binding calcium there is a spectral shift in fura-2 absorption which is proportional to the concentration of calcium causing this ratio to change (340/380 nm ratio or ΔF Ratio). This allows the measurement of intracellular calcium.

Thapsigargin belongs to an enzyme group of sarco/ endoplasmic reticulum calcium ATPases. Thapsigargin causes an increase in intracellular calcium, by blocking the cell's ability to pump calcium back into the sarcoplasmic and endoplasmic reticulum. ATP has been shown to increase intracellular calcium levels in *in vitro* (Bandyopadhyay *et al.*, 2000). Both the Thapsigargin and ATP experimental solutions were provided to the candidate by the Beech group. As RvE1 has been shown to induce intracellular calcium levels (Arita *et al.*, 2007), and block subsequent intracellular calcium levels in human PBMCs, then LTB₄ (Cayman Chemical 100 nM) was used as a positive control in this assay.

PBMCs and THP-1 human acute monocytic leukaemia cells were counted and the cells pelleted by centrifugation at 300 x *g* for five minutes. The PBMCs and THP-1 human cells were then loaded with 2 μ M Fura-2 AM, 0.01% pluronic acid (5% v/v double distilled water) in standard bath solution (SBS), (130 mmol/ L sodium chloride (NaCl), 5 mmol/ L potassium chloride (KCl), 8 mmol/ L D-glucose, 10 mmol/ L HEPES, and 1.2 mmol/ L magnesium chloride (MgCl₂), 1.5 mmol/ L calcium chloride (CaCl₂) titrated to pH 7.4 with sodium hydroxide (NaOH) at 37°C for one hour. The PBMCs and THP-1 cells were then centrifuged at 300 x *g* for five minutes. The pelleted cells were washed once with SBS at room temperature. The PBMCs and THP-1 cells were then re-

suspended at 1×10^6 /ml in SBS. Then 200,000 cells of the cell suspension was added to each well of a 96 well plate. The cells were then centrifuged in a 96 well plate at 300 x g for five minutes, in order to let cells the form a monolayer at the bottom of each well. All test compounds were prepared at five times the wanted final test concentration in a 96 well plate; this is referred to as the compound plate, as addition to the test plate meant they underwent a 1 in 5 dilution.

The 96 well plate containing the cells was then placed in FlexStation II³⁸⁴ (Molecular Devices, California). The FlexStation II is an automated device that adds compounds from a compound plate onto a prepared 96 well cell plate and measures the subsequent changes in fluorescence. The FlexStation II uses the Softmax Pro 4.7.1 software (Molecular Devices) to measure excitation wavelengths (340 nm, 380 nm) and emission wavelengths (510 nm). All experiments were conducted at room temperature. The FlexStation II³⁸⁴ was programmed to add 50 μ L of compound solution to the 200 μ L in the cell plate thus producing the chosen concentration. Compound solutions included carrier control (ethanol), Thapsigargin (positive assay control), ATP (positive assay control), LTB₄ (positive control) and RvE1.

5.4.7 High performance liquid chromatography electrospray ionisation tandem mass spectrometry analysis of Resolvin E1 standard

5.4.7.1 Sample preparation for Resolvin E1 identification

Aliquots of RvE1 in a volume of 10 μ L were stored at -80°C (25 μ g/ 500 μ L in ethanol) ahead of analysis. These aliquots were taken from the supplied Cayman Chemical RvE1 standard. Fresh aliquots were used for each new experimental stock solution in the gene expression, cell viability and apoptosis assays.

In brief the sample was analysed on a Waters Alliance 2695 electrospray (ESI) triple quadrupole Quattro Ultima mass spectrometer (MS) (Waters, Elstree, Hertfordshire, UK), (LC/ESI-MS/MS). Instrument control and data acquisition were performed using the MassLynx™ version 4.0 software. The ESI-MS/MS was performed by the Nicolaou group. The sample was placed in a clean test tube and the solvent (ethanol) was evaporated under a stream of nitrogen. The residue was then dissolved in 100 μ L of ethanol. The extracted sample was then analysed by LC-ESI-MS/MS and the mass spectrum collected. The MS collected was then compared to a published mass spectrum for RvE1.

5.4.7.2 Sample preparation for Resolvin E1 stability experiment

For the RvE1 stability experiment, sample preparation and subsequent data analysis post the LC/ESI-MS/MS analysis was performed by the candidate. In summary three 100 nM solutions were prepared in culture medium (RPMI 1640 GlutaMAX™ without FBS). The samples were then incubated at 37°C for zero, one or 24 hours, then placed at -80°C until analysis. Prior to lipid extraction samples were thawed on ice and adjusted to 15% (v/v) methanol solution by adding 100% methanol (HPLC-grade, Fisher Scientific, Cat. No. M/4056/17). The internal standard 12-HETE-*d8* (2 ng/ μ L) was added to each at a final concentration of 800 pg/ μ L. The samples were acidified with 0.1M hydrochloric acid (HCl; ACS reagent; Cat.No 320331) to pH 3.0 and applied to separate activated solid-phase extraction cartridges (SPE) cartridges C18-E (500 mg, 6 mL; Cat. No 8B-S001-HCH) as below. The STRATA SPE cartridges were preconditioned with 20 mL of methanol followed by 20 mL of de-ionised water. The extraction procedure was performed using a vacuum manifold (Phenomenex). After the samples were applied, the cartridges were washed with 20 mL 15% Methanol, 20 mL de-ionised water (ELGA system, 18.2 M Ω -cm purity, Model Ultra Ionic, Part No.PRIPLB0450, High Wycombe, UK) and 10 mL Hexane (HPLC-grade, Fisher Scientific, Cat. No. H/0406/17), in succession. The lipid mediators were then eluted in 15 mL methyl formate (HPLC-grade, Fisher Scientific, Cat. No.12682-0025). The fraction was collected in a clean test tube and the solvent was evaporated under a stream of nitrogen. The residue was dissolved in 100 μ L ethanol and stored at -20°C prior to analysis. Peak integrations and calculations of S/N ratios were performed using the MassLynx™ v4.0 software (Waters). The peak-area ratio of the RvE1 against 12-HETE-*d8* (IS) was calculated.

5.4.7.3 Statistical analysis

ALPI and CD55 mRNA expression changes in human CRC cells were tested using the Mann-Whitney U test and Kruskal-Wallis one-way analysis of variance (ANOVA) as appropriate. Statistical significance was assumed if the *P* value was less than 0.05.

5.5 Results

5.5.1 Mass spectrometry analysis of the Resolvin E1 Cayman Chemical standard and stability at 37°C

As RvE1 mediated biological activity was being investigated via cell viability and apoptosis assays it was important that the candidate validated that the Cayman Chemical's RvE1 product actually contained RvE1. In order to investigate this two different experimental objectives were performed, they were:

1. Does the Cayman Chemical's RvE1 product contain RvE1?
2. Does the Cayman Chemical's RvE1 product remain stable in aqueous solution?

5.5.2 Does the Cayman Chemical Resolvin E1 product contain chemically recognisable Resolvin E1?

In order to confirm that the Cayman Chemicals RvE1 standard contain RvE1 an ESI-MS/MS analysis was performed on the product. ESI-MS/MS analysis confirmed the presence of RvE1 in the Cayman Chemical sample as shown in the mass spectrometry spectrum (Figure 74). Whilst both spectra show the same diagnostic peaks there are some differences in the relative abundance of fragmented ions and this is likely due to the fact that two different instruments have been used to record the spectra (Candidate used triple quadrupole, Lu et al., 2007 used an ion trap).

5.5.3 Does synthetic Resolvin E1 remain stable in aqueous solution?

The Cayman Chemical RvE1 was incubated in culture medium at 37°C over a 24 hour period and was subsequently analysed by LC/ESI-MS/MS. LC/ESI-MS/MS analysis of the RvE1 confirmed that RvE1 was present in each of the samples analysed over the 24 hour period (Figure 75A), when compared to the RvE1 standard used by the Nicolaou Group. Furthermore the levels in the samples incubated remained stable, as shown by the area ratio which was calculated by dividing the peak area for RvE1 by the peak area of the internal standard(12-HETE-*d8*) over time (Figure 75B). However only one sample was used for each experimental condition.

In summary the RvE1 remained stable when incubated in culture medium at 37°C over a 24 hour period.

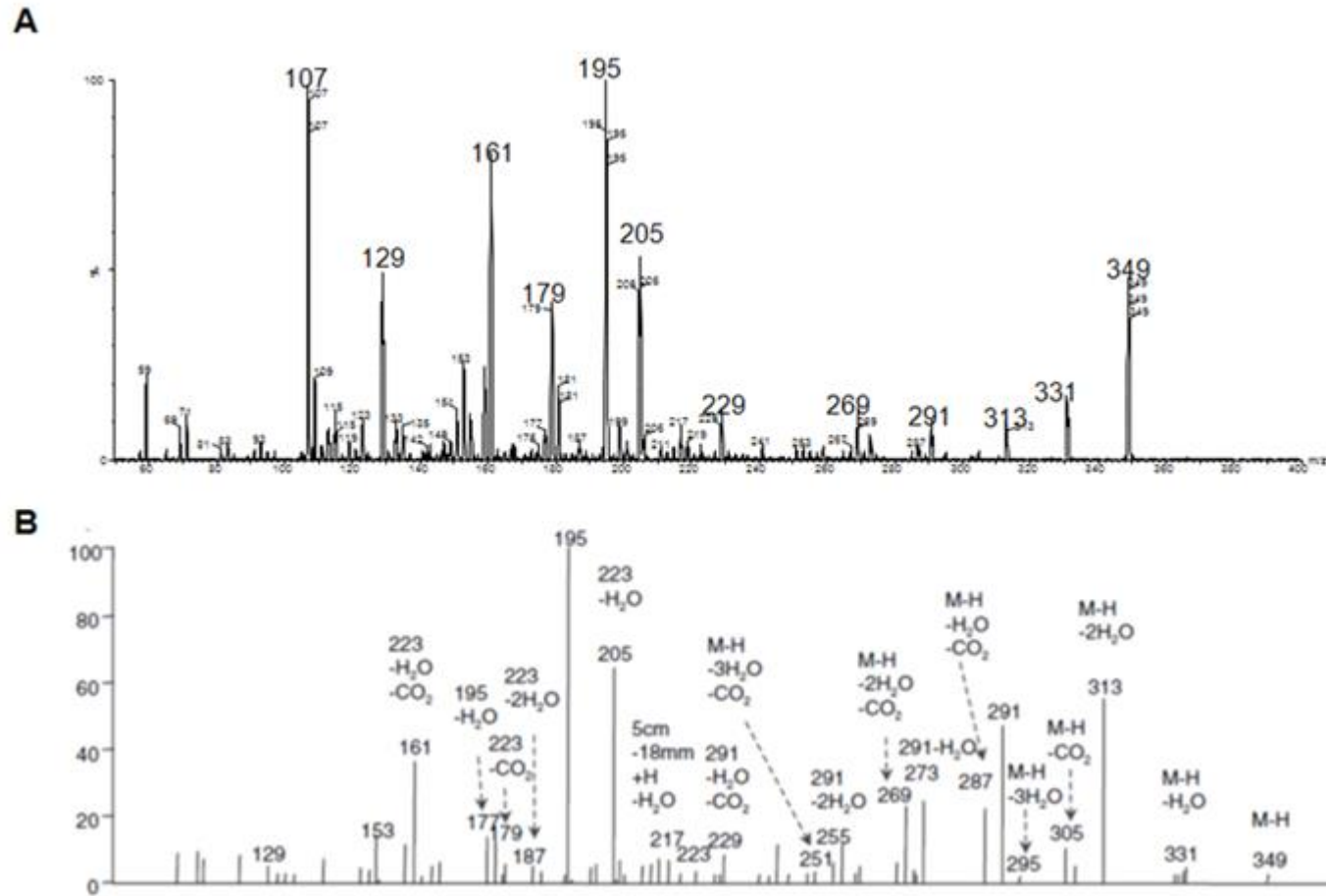


Figure 74. Electro spray ionization product ion spectrum for RvE1.

(A) Product ion spectra obtained from synthetic RvE1 used in the cell viability, apoptosis and gene expression assays. (B). Product ion spectra obtained from the analysis of synthetic RvE1, taken from Lu *et al.*, 2007. The candidate's RvE1 product spectra identified characteristic and stable ions consistent with other published mass spectra (Lu *et al.*, 2007)

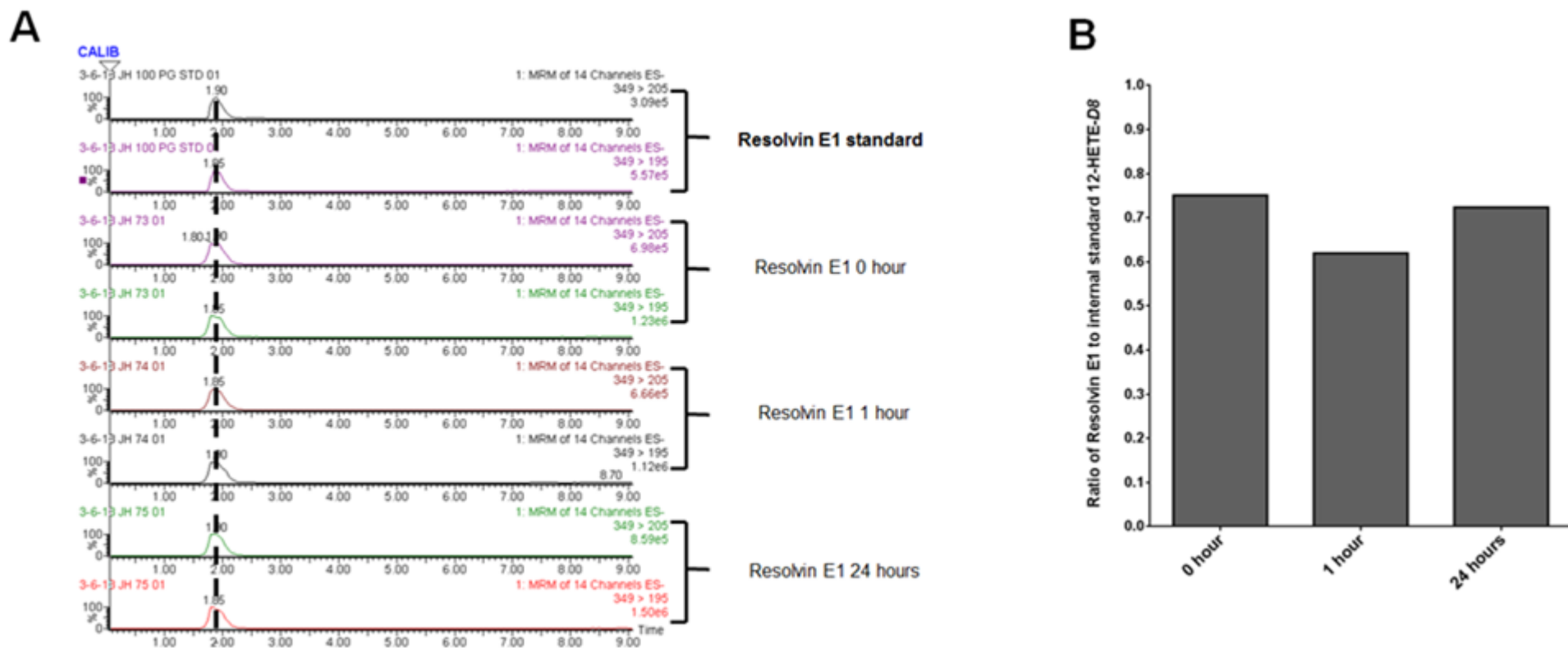


Figure 75. RvE1 identification and stability when incubated at 37°C for 24 hours.

RvE1 (Cayman Chemical) was placed in culture medium and incubated at 37°C for up to 24 hours. RvE1 was then analysed by LC/ESI-MS/MS at 0 hour, 1 hour and 24 hour incubation time point. (A) Comparison of the chromatogram at 0, 1 and 24 hours against RvE1 standard used by the Bradford Group. Two different multiple reaction monitoring (MRM) were used (349>205 and 349>195). (B) Ratio of RvE1 to internal standard (12-HETE-*d8*) at 0, 1, 24 hour time points. MRM 349>195 was used to quantify RvE1 in the three samples. Data shown as a ratio of the peak area for RvE1 by that of the internal standard (12-HETE-*d8*). Data from one experiment.

5.5.4 Effect of Resolvin E1 on human colorectal cancer apoptosis

When control Caco2 and HCA7 human CRC cells (culture medium and ethanol carrier v/v dilution 0.1%) were analysed by the flow cytometry two distinct populations of cellular events, on the forward and side scatter dot blots, were seen, (labeled as 1 and 2 in Figure 76A for the Caco2 cells and Figure 77A for the HCA7 cells).

On analysis of cell population one, it was shown to be predominantly late apoptotic or dead cells for both the Caco2 and HCA7 cells (under control conditions at 24 hours). For the Caco2 and HCA7 cells this gated cell population consisted of principally late apoptotic or dead cells (Table 10 & 11 respectively).

Cell status	Percentage (%) of cell population
Viable	6.3
Early apoptotic	1.5
Late apoptotic/ dead	88.4
Necrotic bodies	3.8

Table 10. Caco2 human CRC cell viability in gated cell population 1 on flow cytometry.

Cell status	Percentage (%) of cell population
Viable	3.4
Early apoptotic	7.2
Late apoptotic/ dead	88.8
Necrotic bodies	0.6

Table 11. HCA7 human CRC cell viability in gated cell population 1 on flow cytometry

On analysis of population two, the cell population was predominantly viable cells for both the Caco2 and HCA7 cells under control conditions at 24 hours (Table 12&13 respectively).

Cell status	Percentage (%) of cell population
Viable	89.3
Early apoptotic	6.7
Late apoptotic/ dead	3.3
Necrotic bodies	0.7

Table 12. Caco2 human CRC cell viability in gated cell population 2 on flow cytometry.

Cell status	Percentage (%) of cell population
Viable	87.4
Early apoptotic	7.6
Late apoptotic/ dead	4.9
Necrotic bodies	0.1

Table 13. HCA7 human CRC cell viability in gated cell population 2 on flow cytometry.

As the aim of this experiment was to identify apoptosis occurring as a result of RvE1 treatment on the CRC cells (and positive control pro-apoptotic drug etoposide) then population two was included in the gated population analysed (Figure 74B; Caco2 cells and Figure 75B; HCA7 cells). This gating protocol was used for all further etoposide and RvE1 treated experiments when Caco2 and HCA7 human CRC cells were used.

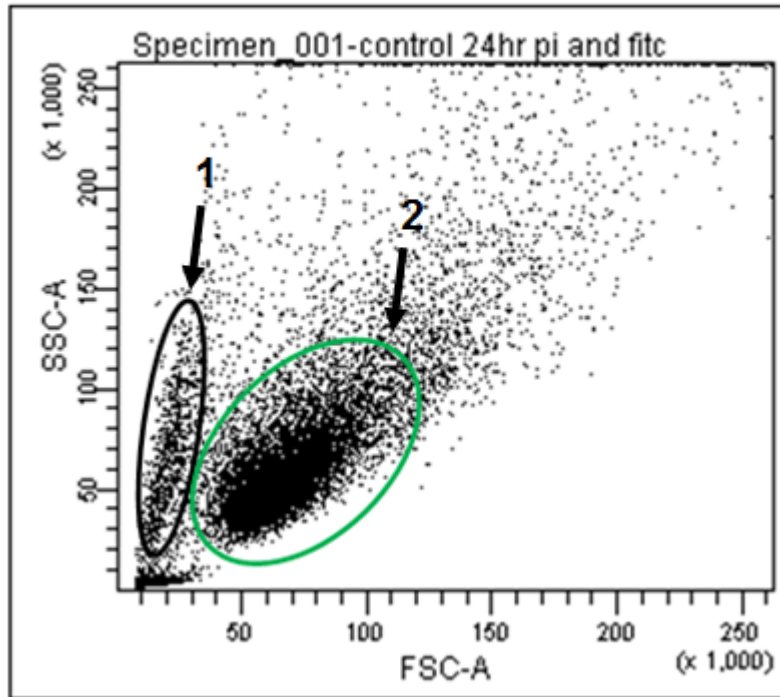
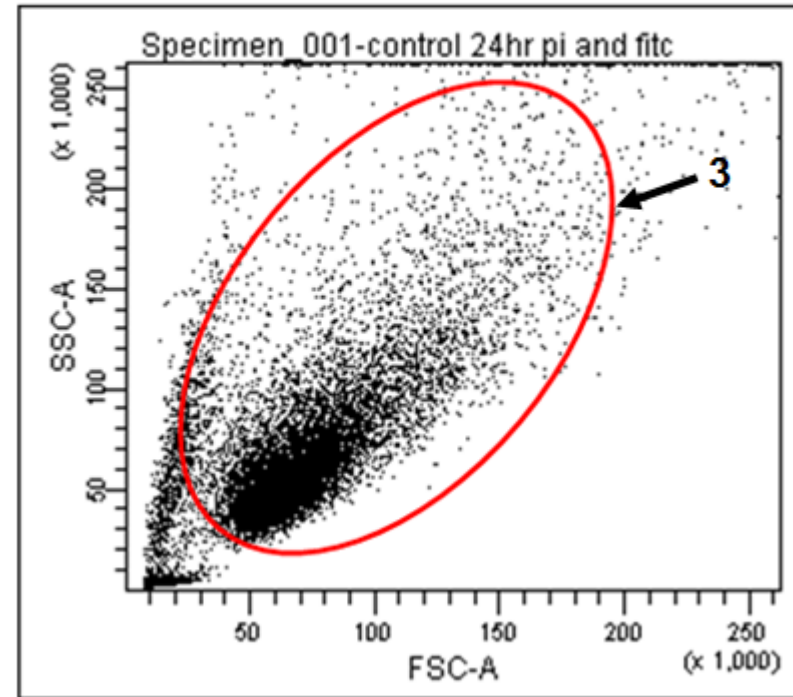
A**B**

Figure 76. Flow cytometry forward and side scatter dot plot for the analysis of the Caco2 human CRC cell line.

Untreated Caco2 human CRC cells were grown to 100% confluency where analysed by flow cytometry for apoptosis using a FITC Annexin V PI apoptosis assay. (A) Two distinct populations of cellular events are seen when Caco2 cells are analysed, defined by black line (1) and green line (2). (B) The cellular event population gated for the analysis is defined by the representative red line (3).

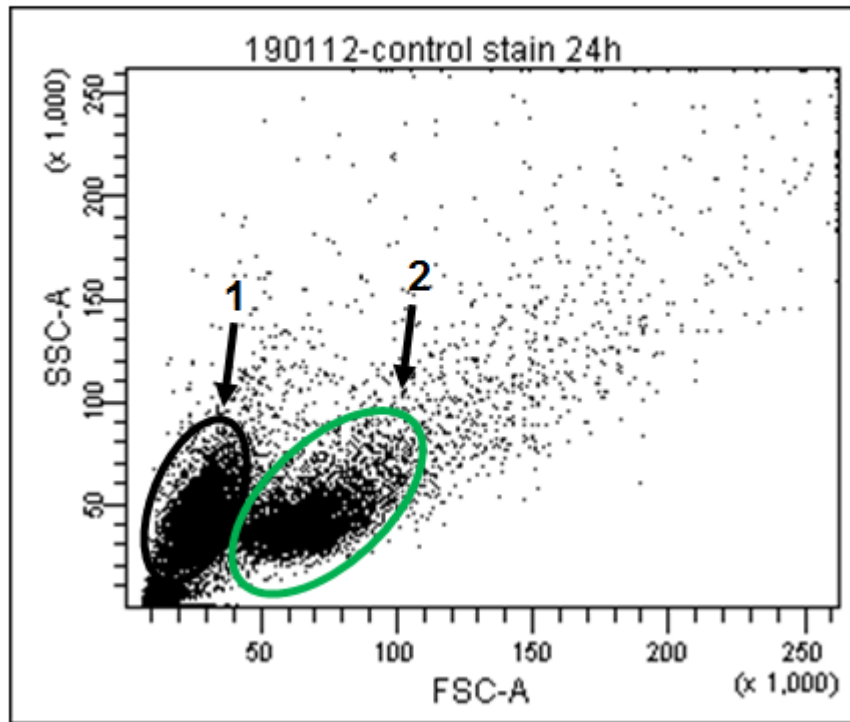
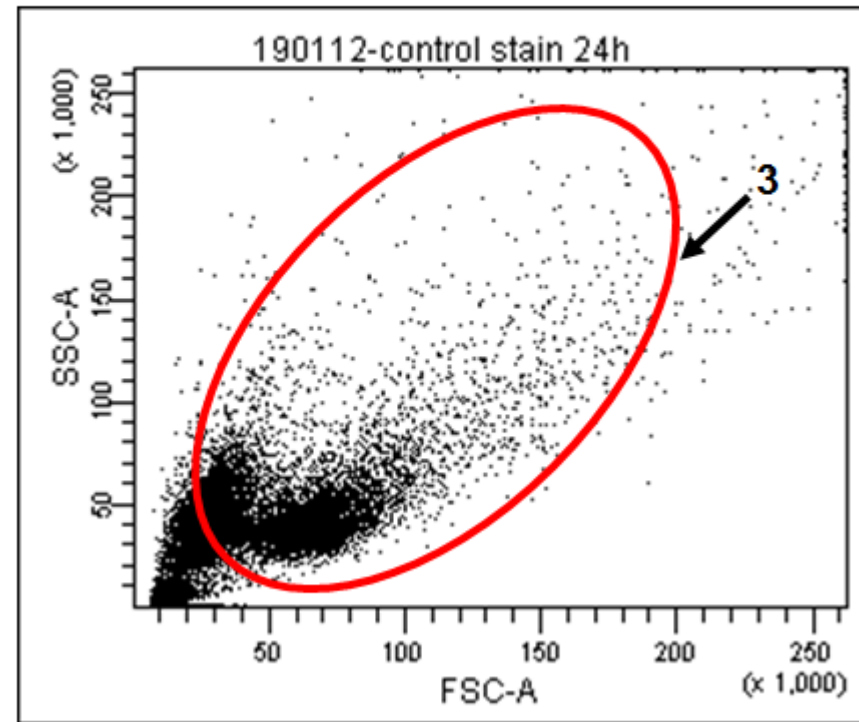
A**B**

Figure 77. Flow cytometry forward and side scatter dot plot for the analysis of the HCA7 human CRC cell line.

Untreated HCA7 human CRC cells were grown to 70% confluency where analysed by flow cytometry for apoptosis using a FITC Annexin V PI apoptosis assay. (A) Two distinct populations of cellular events are seen when HCA7 cells are analysed, defined by black line (1) and green line. (A). (B) The cellular event population gated for the analysis is defined by the representative red line (3).

The dose of etoposide needed to induce apoptosis and the length of time required to induce apoptosis in Caco2 was examined, in order to establish positive control conditions for apoptosis. Initially Caco2 human CRC cells were treated with either carrier control or 50 μ M etoposide over 72 hours with apoptosis assessed at 24, 48 and 72 hour time points. There was approaching 90% cell viability at 24 hours which was maintained at 48 hours and 72 hours in the untreated human CRC cells. In the etoposide treated cells the apoptosis effect on these cells was more clearly seen at 48 hours with a reduction in cell viability and increase in cells in late apoptosis/ dead compared to the control, with further reduction in cell viability at 72 hours (Table 14).

Clear induction in apoptosis was seen in etoposide treated Caco2 cells at 48 hours, so that this time point was utilised as a positive pro-apoptotic control in the RvE1 experiments. The flow cytometry cellular event plots (FITC vs. PI) for the control and etoposide experiments are shown in Figure 78.

A

Cell status	Percentage (%) of cell population (Control 24 hours)	Percentage (%) of cell population (Control 48 hours)	Percentage (%) of cell population (Control 72 hours)
Viable	89.3	91.7	90.3
Early apoptotic	6.7	2.8	0.7
Late apoptotic/ dead	3.3	5.1	7.7
Necrotic bodies	0.7	0.4	1.3

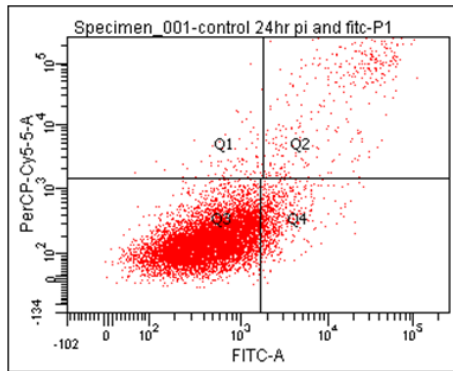
B

Cell status	Percentage (%) of cell population (Etoposide 24 hours)	Percentage (%) of cell population (Etoposide 48 hours)	Percentage (%) of cell population (Etoposide 72 hours)
Viable	86.1	68.9	39.2
Early apoptotic	3.9	6.3	5.9
Late apoptotic/ dead	6.9	23.0	53.0
Necrotic bodies	3.1	1.8	1.9

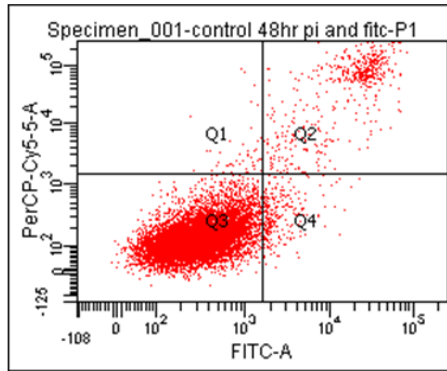
Table 14. Caco2 human CRC cell apoptosis secondary to etoposide.

(A) Control treated Caco2 cell data over 72 hours. (B) Etoposide treated Caco2 cell data over 72 hours. Data taken from one experiment.

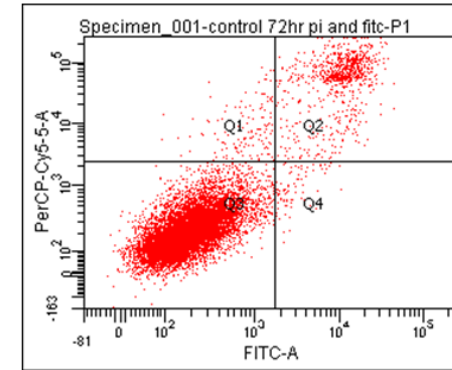
Caco2 cells
(Carrier control)



24 hours



48 hours



72 hours

Caco2 cells
(Etoposide 50µM)

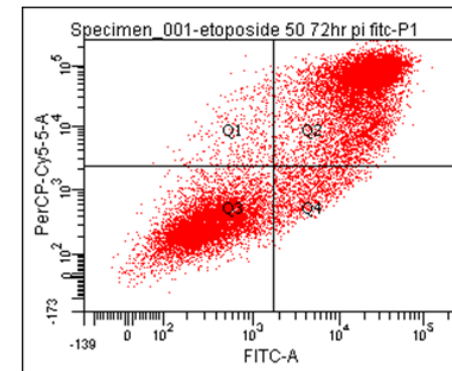
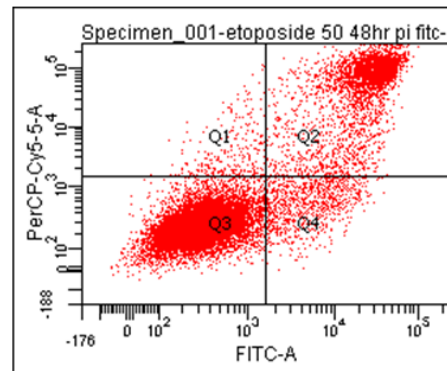
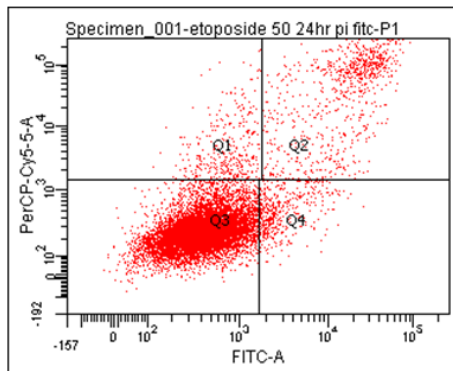


Figure 78. Apoptosis in etoposide treated Caco2 human CRC cells (flow cytometry scatter plots).

Caco2 cells were treated with DMSO carrier or etoposide 50 µM for 72 hours and then analysed for apoptosis by flow cytometry. On the flow cytometry dot plots quadrant 3 (Q3) represents viable cells (FITC Annexin V and PI negative), Q4 represents early apoptotic cells (FITC Annexin V positive and PI negative), Q2 late apoptotic/ dead cells (FITC Annexin V and PI positive) and Q1 necrotic bodies (FITC Annexin V negative and PI positive). The data is shown from one cell cultured experiment.

HCA7 cells were treated with either carrier control or 20 μM etoposide over 48 hours with apoptosis assessed at 24 and 48 hours. There was clear induction in apoptosis at 48 hours in the HCA7 human CRC cells (Data taken from one experiment Table 15; Figure 77 for the flow cytometry cellular event plots (FITC vs. PI) from a representative experiment). Etoposide at a concentration of 20 μM for 48 hours was therefore used a positive control for the HCA7 experiments. (Appendix 43 for graphical data). Data taken from one experiment.

A

Cell status	Percentage (%) of cell population (Control 24 hours)	Percentage (%) of cell population (Control 48 hours)
Viable	81.7	85.1
Early apoptotic	10.4	7.8
Late apoptotic/ dead	7.1	6.9
Necrotic bodies	0.8	0.2

B

Cell status	Percentage (%) of cell population (Etoposide 24 hours)	Percentage (%) of cell population (Etoposide 48 hours)
Viable	72.2	32.8
Early apoptotic	14.2	14.0
Late apoptotic/ dead	13.1	49.4
Necrotic bodies	0.5	3.8

Table 15. HCA7 human CRC cell apoptosis secondary to etoposide.

(A) Control treated HCA7 cell data over 72 hours. (B) Etoposide treated HCA7 cell data over 72 hours.

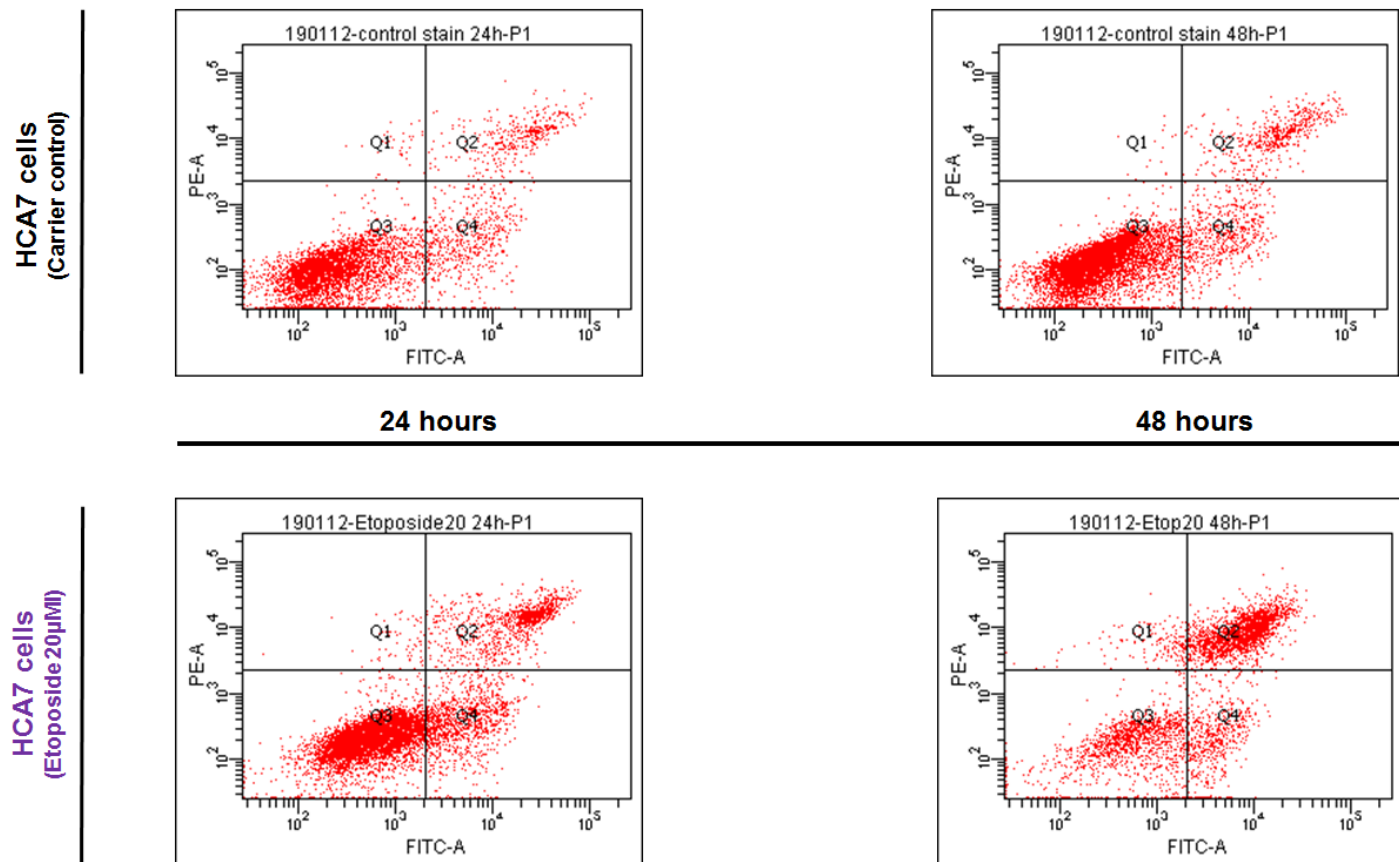


Figure 79. Apoptosis in etoposide treated HCA7 human CRC cells (flow cytometry scatter plots).

HCA7 human CRC cells were treated with DMSO carrier or etoposide 50 μM for 48 hours and then analysed for apoptosis by flow cytometry. On the flow cytometry dot plots quadrant 3 (Q3) represents viable cells (FITC Annexin V and PI negative), Q4 represents early apoptotic cells (FITC Annexin V positive and PI negative), Q2 late apoptotic/ dead cells (FITC Annexin V and PI positive) and Q1 necrotic bodies (FITC Annexin V negative and PI positive). The data is shown from one cell cultured experiment.

RvE1 (1 μ M) treatment of Caco2 and HCA7 human CRC cells over a 72 hour period did not induce apoptosis in these cells. The control CRC cells remained stably viable over the 72 hour period as did the RvE1 treated cells. There was no change in the percentage population of cells in the early apoptotic or late apoptotic cells when the RvE1 treated cells were compared with their respective control (Data for Caco2 human CRC cells Figure 80, and HCA7 human CRC cells Figure 82). The flow cytometry cellular event plots (FITC vs. PI) for the Caco2 cells are shown in Figure 81 and representative plots for the HCA7 cells is shown in Figure 83. These plots show visually that the cell population gated are not progressing differently through the different stages of cell apoptosis when the cells were treated with RvE1.

Clear induction in apoptosis was established in the etoposide positive control. With etoposide treated Caco2 human CRC cells and HCA7 human CRC (Figure showing reduced cell viability with increased apoptotic cells after 48 hours of treatment (Caco2 Figure 84; HCA7 Figure 85). The candidate also investigated whether RvE1 induced apoptosis in the HT29 human CRC cells line (low ChemR23 protein expression). No RvE1 mediated induction of apoptosis was found (data not shown).

In conclusion no RvE1 mediated induction in apoptosis was identified in either the Caco2 or HCA7 human CRC cell lines, using these *in vitro* conditions.

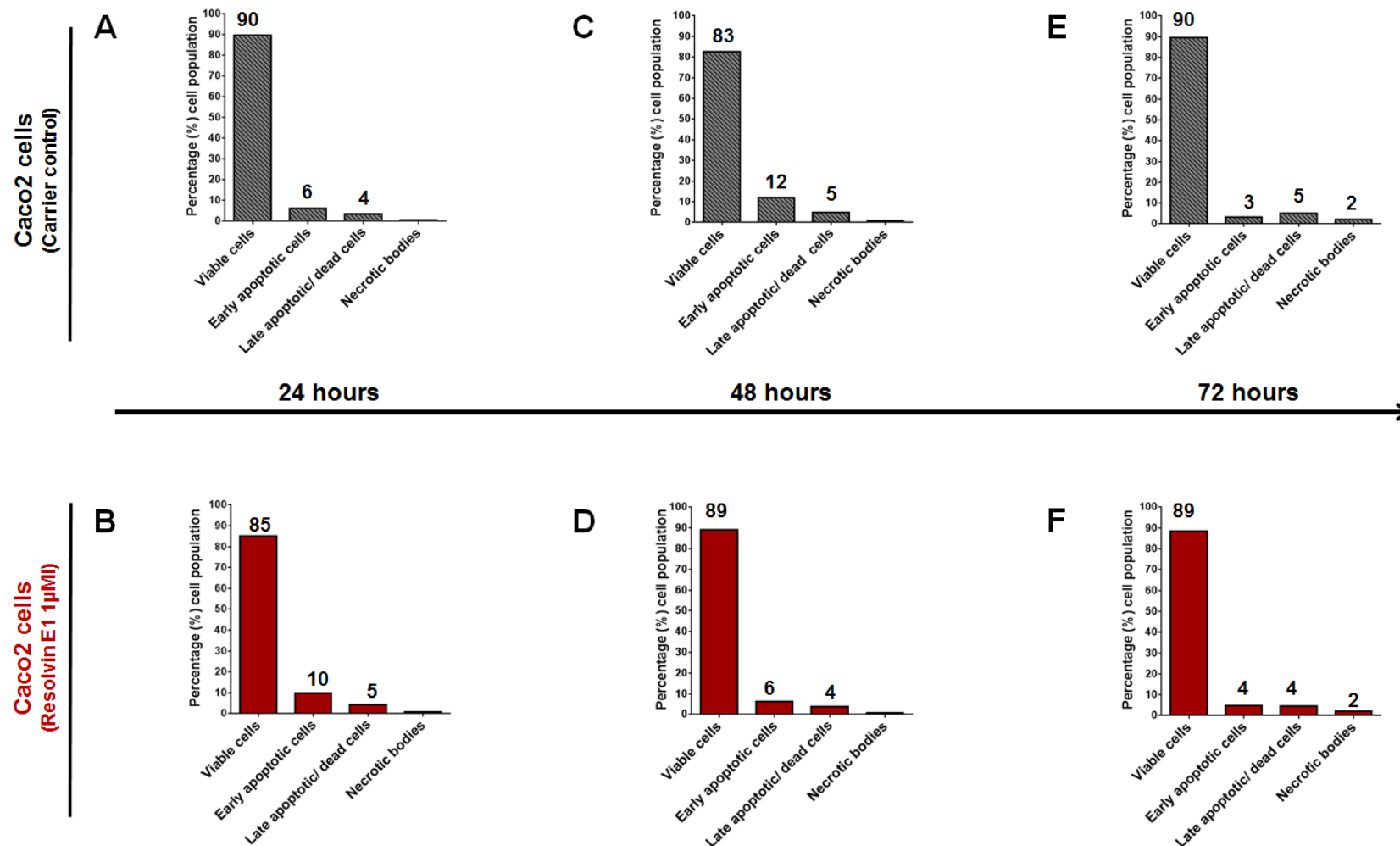


Figure 80. Apoptosis in RvE1 treated Caco2 human CRC cells.

Caco2 human CRC cells were treated with control carrier or RvE1 (1 µM) and then analysed for apoptosis by flow cytometry at 24, 48 and 72 hour time points. (A) Caco2 human colorectal cancer (CRC) cells were treated control carrier (ethanol) for 24 hours. (B) RvE1 1 µM for 24 hours. (C) Control carrier (ethanol) for 48 hours. (D) RvE1 1 µM for 48 hours. (E) Control carrier (ethanol) for 72 hours. (F) RvE1 1 µM for 72 hours. Number above bar represents percentage of cell population. Data from one experiment.

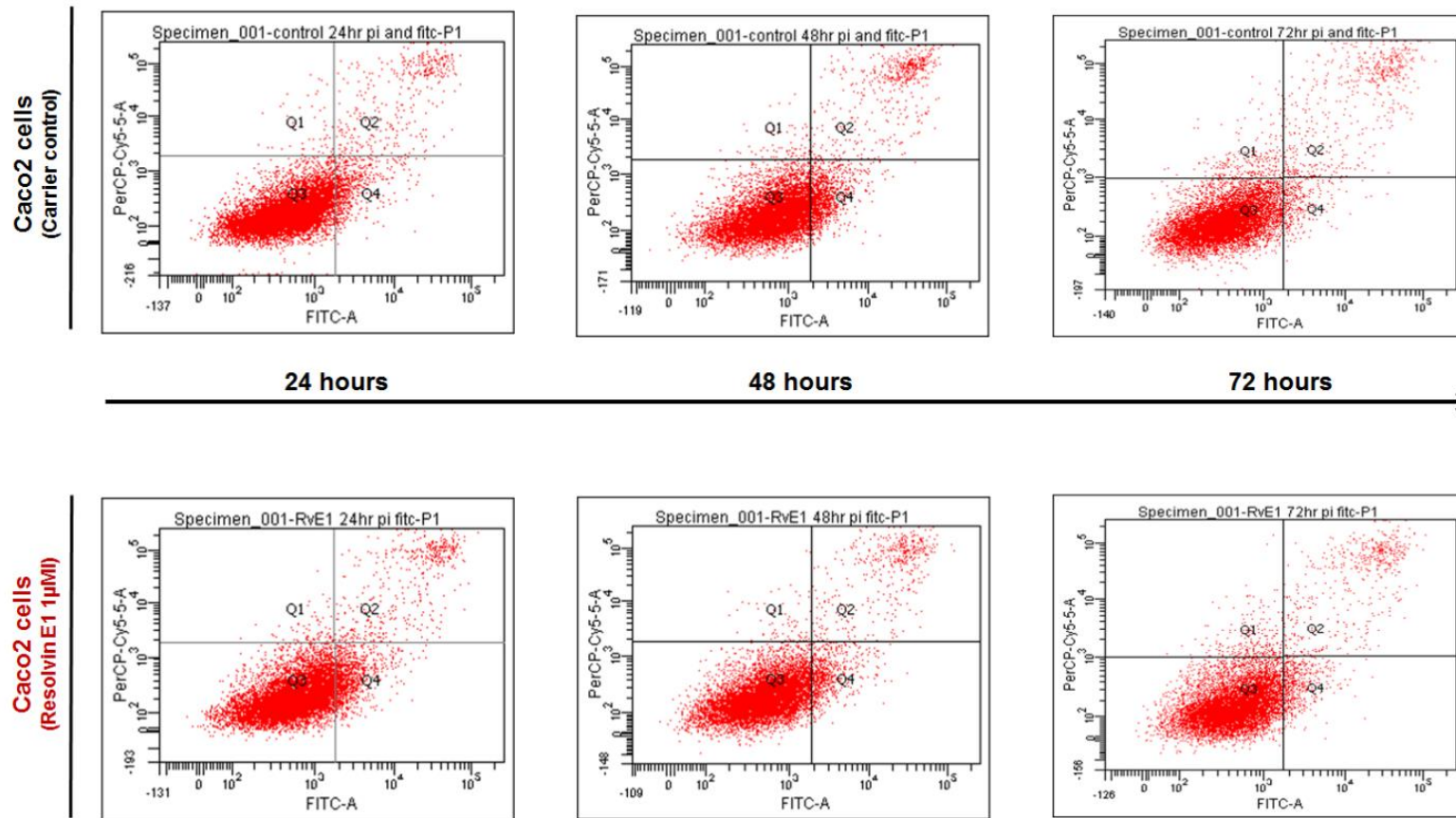


Figure 81. Apoptosis in RvE1 treated Caco2 human CRC (flow cytometry scatter plots).

Caco2 human CRC cells were treated with control carrier or RvE1 (1 μM) and then analysed for apoptosis by flow cytometry at 24, 48 and 72 hour time points. This data is the original flow cytometry dot plots. On the flow cytometry dot plots quadrant 3 (Q3) represents viable cells (FITC Annexin V and PI negative), Q4 represents early apoptotic cells (FITC Annexin V positive and PI negative), Q2 late apoptotic/ dead cells (FITC Annexin V and PI positive) and Q1 necrotic bodies (FITC Annexin V negative and PI positive)

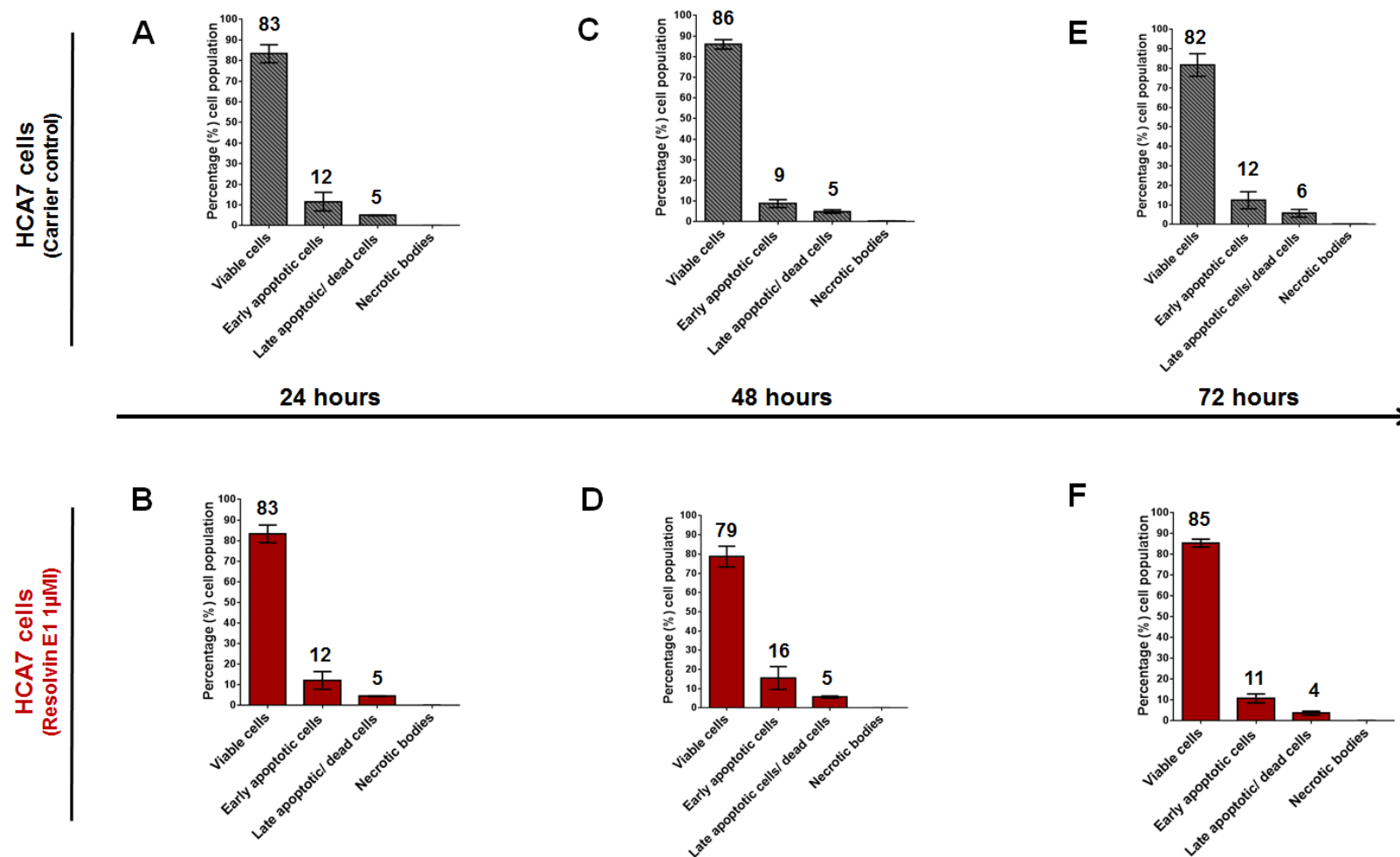
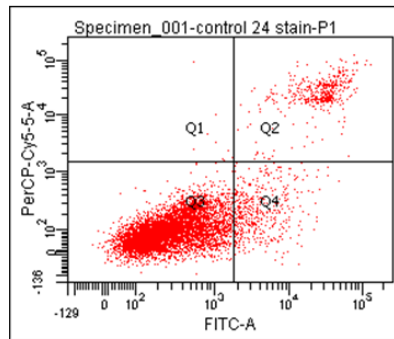


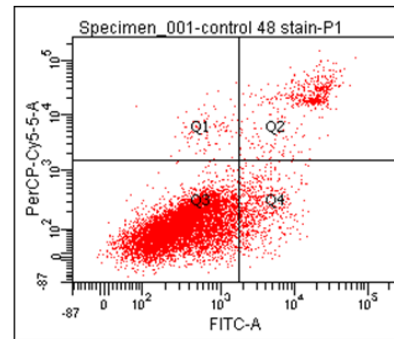
Figure 82. Apoptosis in RvE1 treated HCA7 human CRC cells.

HCA7 human CRC cells were treated with control carrier or RvE1 (1 μM) and then analysed for apoptosis by flow cytometry at 24, 48 and 72 hour time points. (A) HCA7 human colorectal cancer (CRC) cells were treated control carrier (ethanol) for 24 hours. (B) RvE1 1 μM for 24 hours. (C) Control carrier (ethanol) for 48 hours. (D) RvE1 1 μM for 48 hours. (E) Control carrier (ethanol) for 72 hours. (F) RvE1 1 μM for 72 hours. D Number above bar represents mean percentage of cell population. The data was collected from three independent cell cultured experiments, and shown as mean with standard error of the mean.

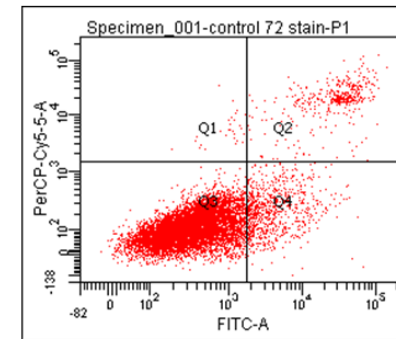
HCA7 cells
(Carrier control)



24 hours



48 hours



72 hours

HCA7 cells
(ResolvinE1 1µM)

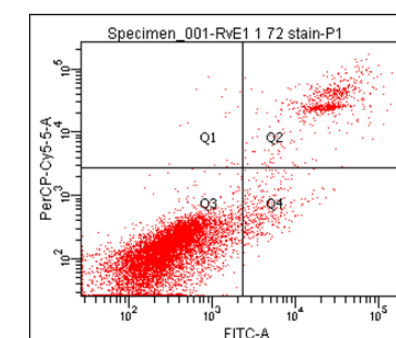
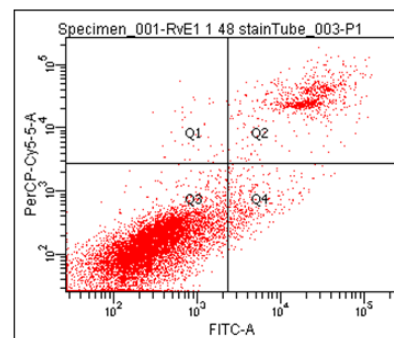
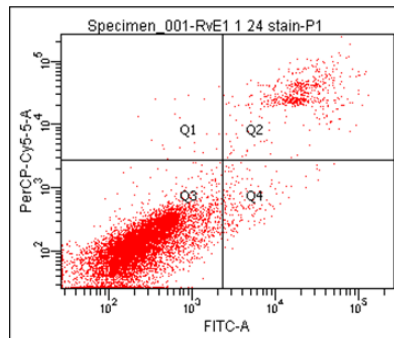


Figure 83. Apoptosis in RvE1 treated HCA7 human CRC cells (flow cytometry scatter plots).

HCA7 human CRC cells were treated with control carrier or RvE1 (1 µM) and then analysed for apoptosis by flow cytometry at 24, 48 and 72 hour time points. This data is the original flow cytometry dot plots. On the flow cytometry dot plots quadrant 3 (Q3) represents viable cells (FITC Annexin V and PI negative), Q4 represents early apoptotic cells (FITC Annexin V positive and PI negative), Q2 late apoptotic/ dead cells (FITC Annexin V and PI positive) and Q1 necrotic bodies (FITC Annexin V negative and PI positive). The data is shown from one cell cultured experiment that is representative of the dot plots obtained from three independently cultured cell experiments.

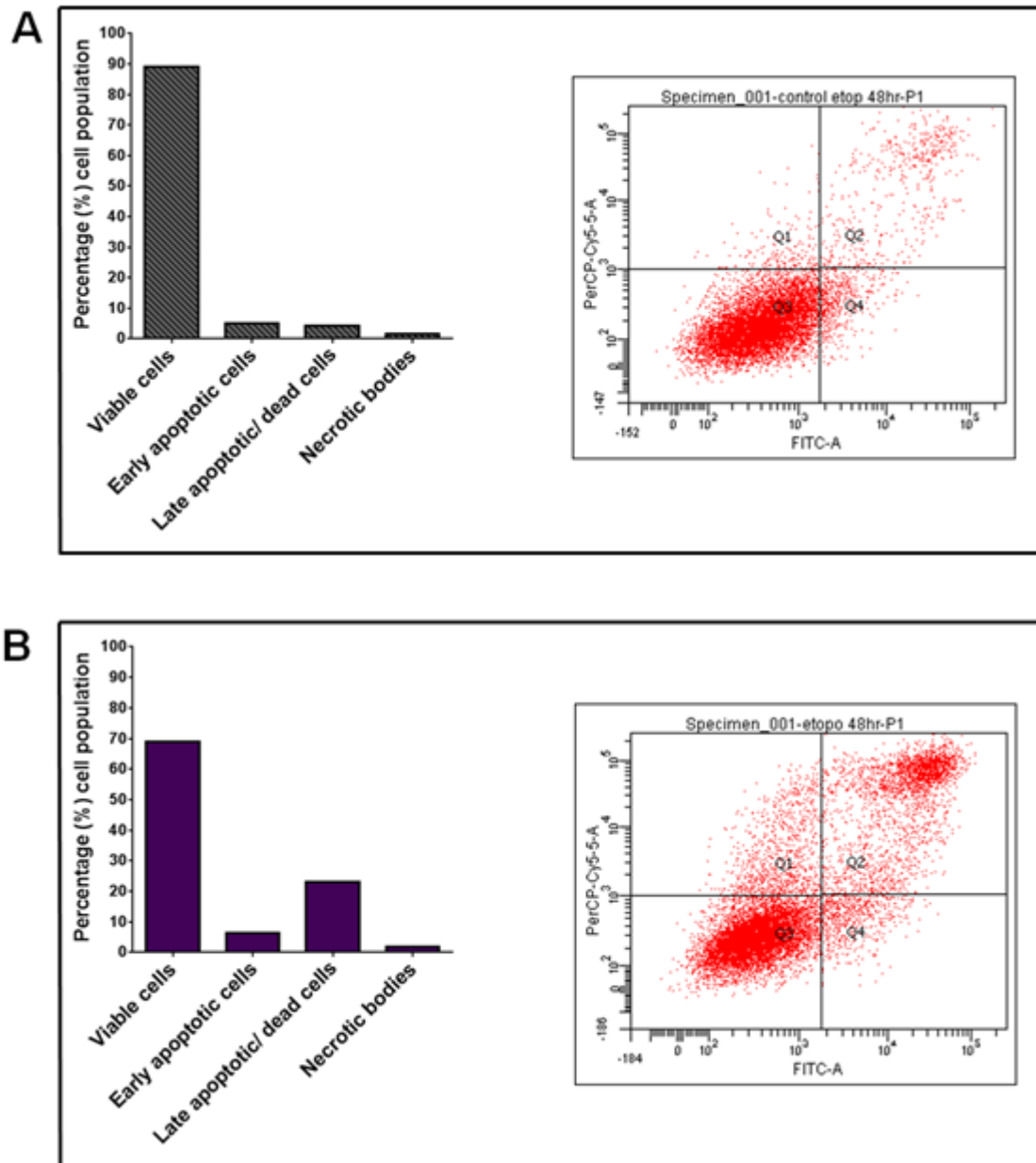


Figure 84. Apoptosis in etoposide treated Caco2 human CRC cells.

Caco2 human CRC cells were grown to 90% cell confluency before being treated with 50 μM etoposide for 48 hours. Apoptosis was measured by flow cytometry using a FITC Annexin V PI assay. (A) Apoptosis results for Caco2 cells treated with carrier control (DMSO). (B) Apoptosis results for Caco2 cells treated with etoposide 50 μM for 48 hours.

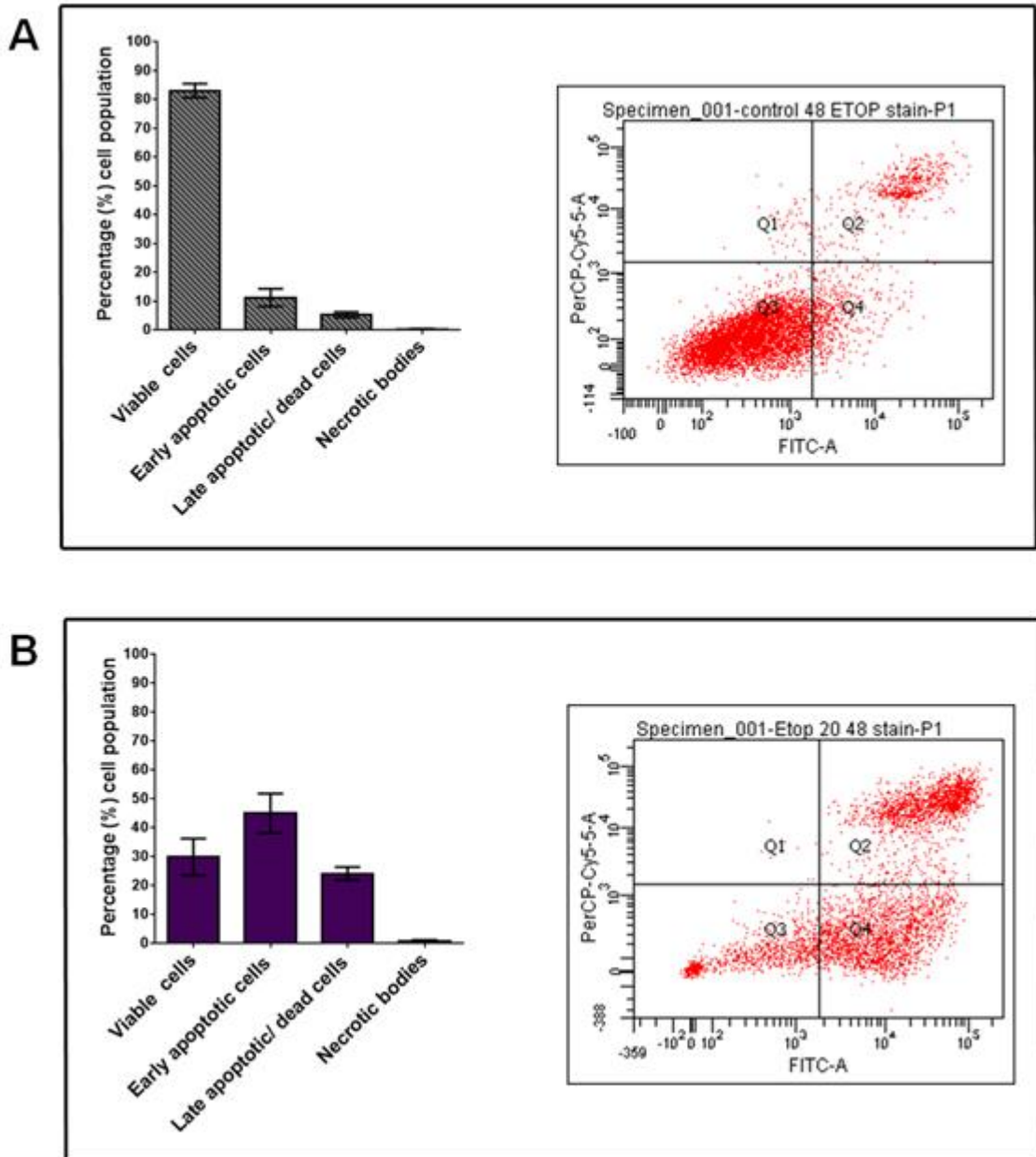


Figure 85. Apoptosis in etoposide treated HCA7 human CRC cells.

HCA7 human CRC cells were grown to 80% cell confluency before being treated with 20 μ M etoposide for 48 hours. Apoptosis was measured by flow cytometry using a FITC Annexin V PI assay. (A) Apoptosis results for HCA7 cells treated with carrier control (DMSO). (B) Apoptosis results for HCA7 cells treated with etoposide 20 μ M for 48 hours.

5.5.5 Effect of Resolvin E1 on human colorectal cancer cell viability

Caco2 human CRC cells were chosen as they expressed the highest levels of ChemR23 protein and HCA7 human CRC cells as they had low ChemR23 expression (see Figure 19). As the candidate had found ChemR23 induction at 100% cell confluency in Caco2 cells (see 3.4.1.2). Cell viability assays were performed when the Caco2 cells were fully confluent. As discussed there was at least a four fold increase in ChemR23 in Caco2 cells.

In the cell viability assays Caco2 and HCA7 cells were dosed with RvE1 daily for a total of 72 hours at a range of concentrations up to 1 μ M. This range encompassed the doses used in the published literature showing RvE1 mediated effects (10-100 nM), (Serhan *et al.*, 2000, Arita *et al.*, 2005, Campbell *et al.*, 2007). The RvE1 was dosed daily in culture medium free of FBS to avoid protein binding of the RvE1 in the serum.

There was no clear effect on cell viability identified when RvE1 was dosed on either Caco2 (Figure 86A) or HCA7 (Figure 86B) human CRC cells when compared to carrier control treated cells.

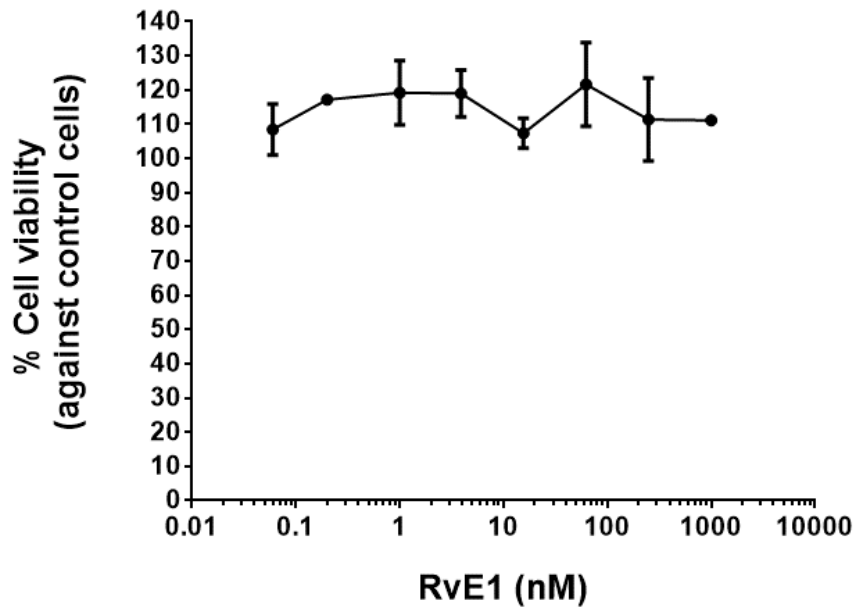
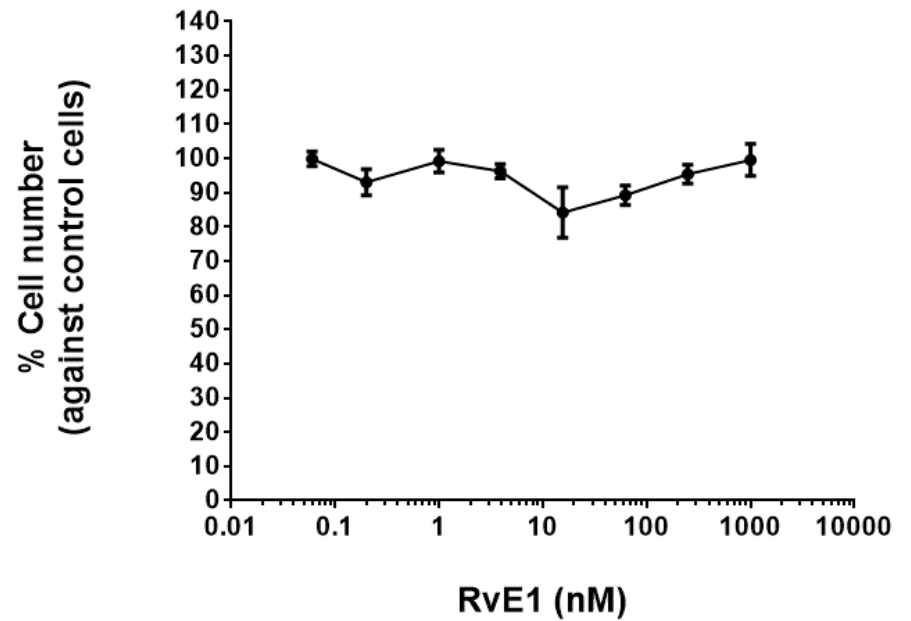
A**B**

Figure 86. Determination of the cytotoxicity of RvE1 by MTT assay in the human CRC cell lines Caco2 and HCA7.

Caco2 and HCA7 human CRC were treated with a range of RvE1 concentrations (as defined above in the graphs). (A) RvE1 treated Caco2 human CRC cell viability. (B) RvE1 treated HCA7 human CRC cell viability. Data shown from three independent cell cultured experiments, shown as mean with standard error of the mean.

5.5.6 Measurement of intestinal alkaline phosphatase expression in Resolvin E1 treated human colorectal cancer cells

As no RvE1 mediated effect was found on human CRC cell survival and apoptosis assays, the candidate sought to confirm the biological activity of the Cayman Chemical RvE1, used in these assays. As RvE1 has been confirmed in the published literature to induce ALPI mRNA expression in Caco2 cells, the candidate replicated the experimental conditions used by Campbell *et al.*, (2010).

Caco2 human CRC cells at 100% cell confluency were treated with 100 nM RvE1 over eight hours. No clear induction in ALPI mRNA was identified, when compared to control cell expression (Figure 87). There was no clear change in Δ -Ct between the control and RvE1 treated cells. The expectation would have been reduction in the Δ -Ct value for the RvE1 treated cells compared to the control, which would have signified increased expression of ALPI. However this was not seen over the eight hour time period. The individual Ct values for β -actin and ALPI with respective Δ -Ct values are shown in Table 16.

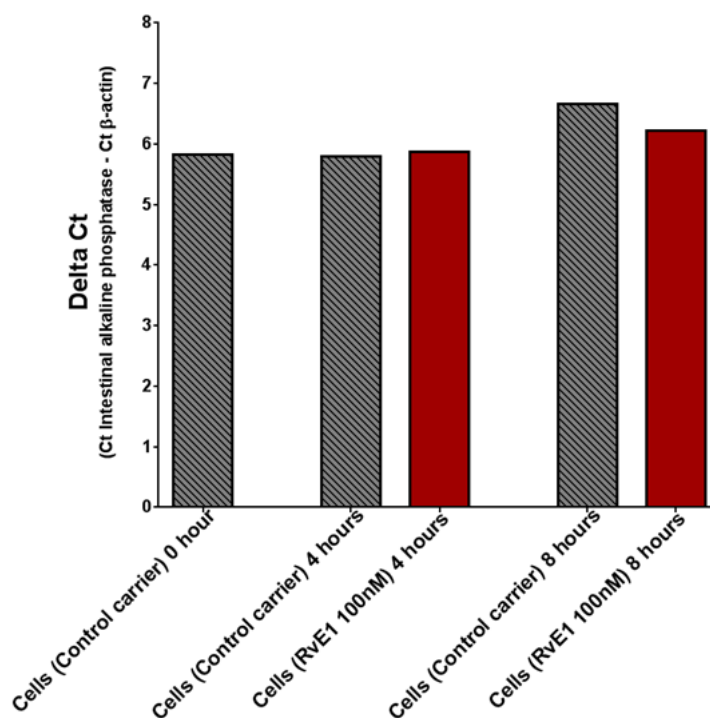


Figure 87. Time dependent expression of ALPI mRNA expression in RvE1 treated Caco2 human CRC cells.

Caco2 human CRC cells were grown to 100% cell confluency. The cells were then treated with RvE1 over an eight hour period, before mRNA was quantified for intestinal alkaline phosphatase (ALPI) expression. ALPI mRNA expression shown as a Δ -Ct value in RvE1 treated Caco2 human CRC cells over eight hours, one independent experiment.

As no induction of ALPI was found, the candidate increased the RvE1 dose used from 100 nM to 500 nM, looking for a dose mediated effect. A six hour time point was used to collect the samples for mRNA analysis as Campbell *et al.*, (2010) had found maximal ALPI induction at this time point. No significant increase in ALPI was identified, when compared to control cell expression (Figure 88), Kruskal-Wallis Test $P = 0.909$. The Δ -Ct was 8.0 (SEM 0.8) for the control, 5.3 (SEM 0.4) for the RvE1 (100 nM) treated cells, 8.8 (SEM 0.2) for the RvE1 (200 nM) treated cells, 8.4 (SEM 0.1) for the RvE1 (500 nM) treated cells. The individual Ct values for β -actin and ALPI are shown in Table 17. No ALPI induction was seen when the RvE1 time course and dose response experiments were carried out in T84 human CRC cells (Appendix 44 and 45, respectively).

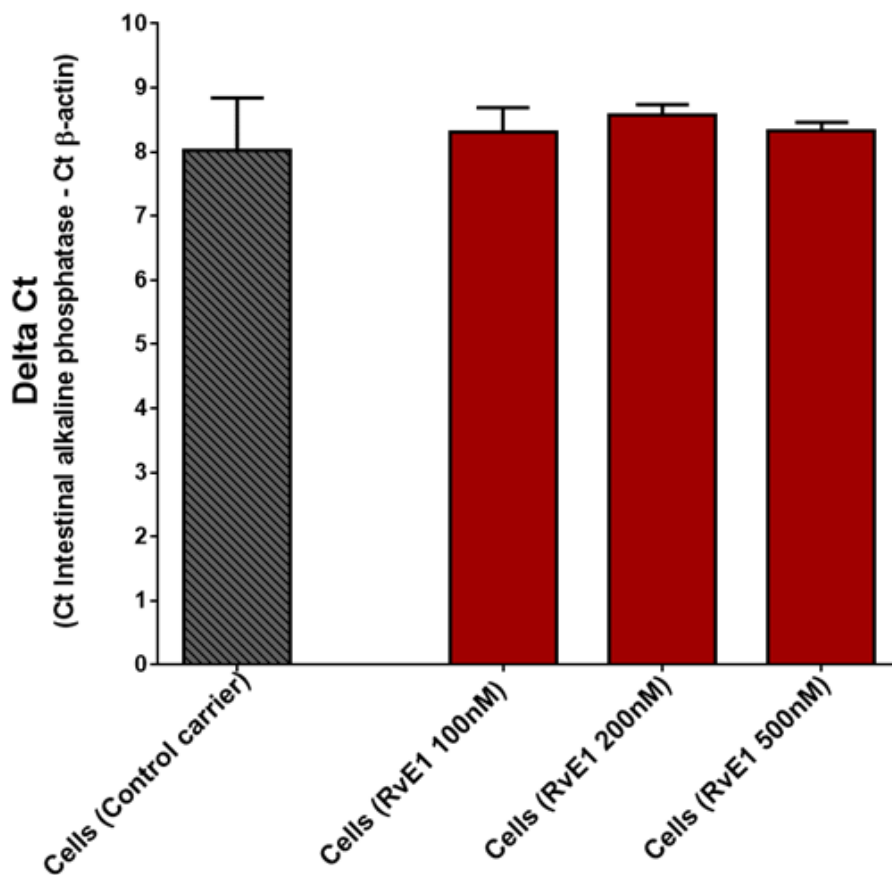


Figure 88. Dose dependent expression of ALPI mRNA in RvE1 treated Caco2 human CRC cells.

Caco2 human CRC cells were grown to 100% cell confluency. The cells were then treated with a range of RvE1 doses, before mRNA was quantified for ALPI expression. ALPI expression in 100 nM, 200 nM, and 500 nM RvE1 treated Caco2 human CRC cells after 6 hours, three independent experiments. Data presented as mean Δ -Ct with standard error of the mean, data analysed using SPSS (Kruskal-Wallis Test, $P = 0.909$).

Condition	β -actin Ct value	ALPI Ct value	Δ -Ct
Control (0 hour)	18.4	24.2	5.8
Control (4 hours)	19.4	25.1	5.7
RvE1 (4 hours)	17.1	23.6	6.5
Control (8 hours)	17.9	24.6	6.7
RvE1 (8 hours)	18.5	24.7	6.2

Table 16. Cycle threshold (Ct) values for β -actin and ALPI for the RvE1 treated Caco2 time course experiment.

Condition	β -actin Ct value	ALPI Ct value	Δ -Ct Experiment 1	β -actin Ct value	ALPI Ct value	Δ -Ct Experiment 2	β -actin Ct value	ALPI Ct value	Δ -Ct Experiment 3
	Experiment 1	Experiment 1		Experiment 2	Experiment 2		Experiment 3	Experiment 3	
Control	21.9	28.2	6.3	17.3	26.3	9.0	21.0	29.7	8.7
RvE1 100nM	21.0	28.7	7.7	17.3	25.7	8.4	22.1	30.2	8.1
RvE1 200nM	18.7	27.1	8.4	19.4	27.8	8.4	18.8	27.7	8.9
RvE1 500nM	19.3	27.5	8.2	20.0	28.2	8.2	21.3	29.9	8.6

Table 17. Cycle threshold (Ct) values for β -actin and ALPI for the RvE1 treated Caco2 dose response experiment.

5.5.7 Measurement of CD55 (decay accelerating factor) expression in Resolvin E1 treated human colorectal cancer cells

As no RvE1 mediated effect on ALPI expression in the Caco2 or T84 human CRC cells, the candidate examined for an RvE1 mediated effect in CD55 mRNA expression in the same CRC cell lines. As discussed, RvE1 has been confirmed in the published literature (Campbell *et al.*, (2010)) to induce CD55 expression in T84 cells. The authors had shown a three fold induction in CD55 in T84 cells and a two fold induction in Caco2 cells (RvE1 100 nM for 24 hours).

The Caco2 cells were initial investigated by the candidate. On dosing 100% confluent Caco2 cells with 100 nM RvE1 over an eight hour time period, no clear induction in CD55 mRNA was identified (Figure 89). The individual Ct and Δ -Ct values are shown in Table 18. There was no reduction in the Δ -Ct in the RvE1 treated cells compared to their respective control, which would be expected if CD55 mRNA expression was induced in these cells by RvE1.

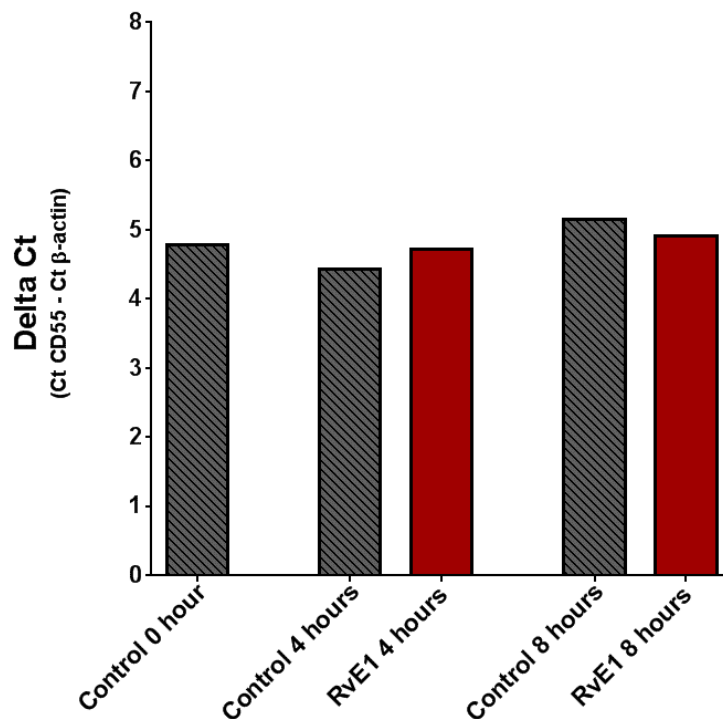


Figure 89. CD55 mRNA expression in RvE1 treated Caco2 human CRC cells.

Caco2 human colorectal cancer (CRC) cells were grown to 100% cell confluency. The cells were then treated with RvE1, before mRNA was quantified over an eight hour period. Data shown from one experiment, shown as a delta Ct values.

As no time dependent effect was established by the candidate on the CRC cells by RvE1, the dose of RvE1 was then increased to investigate for a dose dependent effect on these CRC cells, the six hour time point was chosen. No significant increase in CD55 was identified (Figure 90), Kruskal-Wallis Test $P = 0.210$. No CD55 induction was identified at any of the doses of RvE1 used by the candidate as evidenced by an absence of Δ -Ct reduction in the RvE1 treated compared to their corresponding control (see Table 19 for individual Ct and Δ -Ct values).

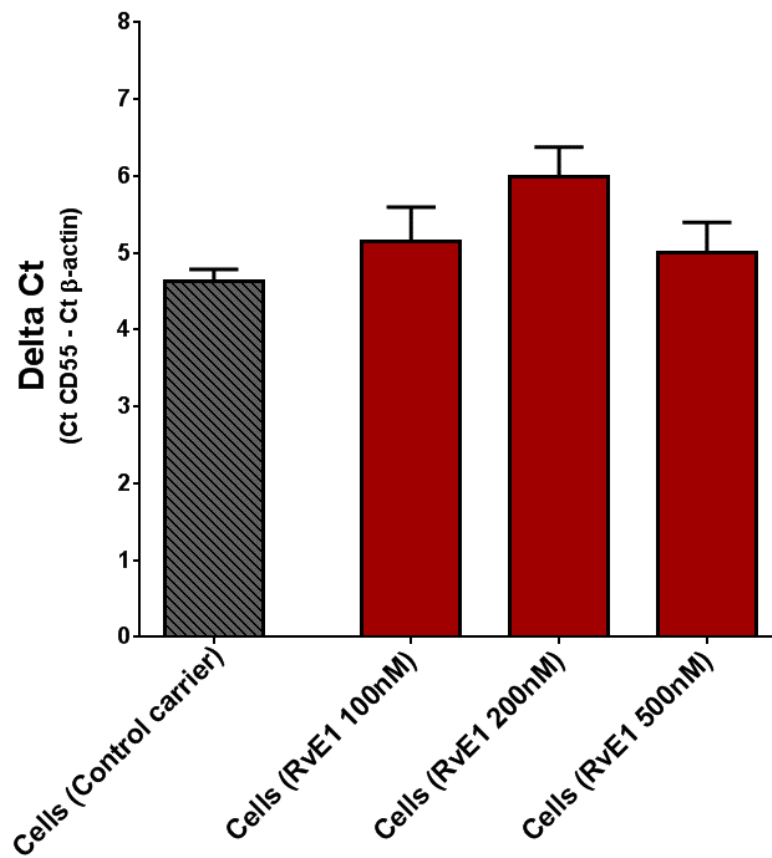


Figure 90. CD55 mRNA expression in RvE1 treated Caco2 human CRC cells.

Caco2 human colorectal cancer (CRC) cells were grown to 100% cell confluency. The cells were then treated increasing doses of RvE1 for six hours, before mRNA was quantified. Data is shown as mean delta Ct values with standard error of the mean, from three independently cell cultured experiments, data analysed using SPSS (Kruskall-Wallis Test, $P = 0.210$).

Condition	β -actin Ct value	CD55 Ct value	Δ -Ct
Control (0 hour)	17.9	22.7	4.8
Control (4 hours)	18.8	23.3	4.5
RvE1 (4 hours)	17.3	22.0	4.7
Control (8 hours)	17.3	22.5	5.2
RvE1 (8 hours)	18.5	23.5	5.0

Table 18. Cycle threshold (Ct) values for the time course CD55 RvE1 treated Caco2 cells experiments.

Condition	β -actin Ct value	CD55 Ct value	Δ -Ct Experiment 1	β -actin Ct value	CD55 Ct value	Δ -Ct Experiment 2	β -actin Ct value	CD55 Ct value	Δ -Ct Experiment 3
	Experiment 1	Experiment 1		Experiment 2	Experiment 2		Experiment 3	Experiment 3	
Control	21.0	25.7	4.7	20.8	25.2	4.4	21.0	25.4	4.4
RvE1 100nM	21.0	25.7	4.7	18.8	24.8	6.0	19.5	24.2	4.7
RvE1 200nM	18.7	25.0	6.3	21.0	26.2	5.2	19.2	25.7	6.5
RvE1 500nM	19.6	25.1	5.5	21.9	26.1	4.3	20.2	25.5	4.3

Table 19. Cycle threshold (Ct) values for CD55 in RvE1 treated Caco2 dose response experiments.

No CD55 mRNA induction was identified in RvE1 treated Caco2 cells by the candidate. RvE1 treatment of T84 human CRC cells had been shown to induce CD55 mRNA by Campbell *et al.* (2010). The candidate then investigated whether RvE1 treatment of T84 cells induced CD55 expression *in vitro*.

There was no significant induction in CD55 found in the treated cells at four hours. The Δ -Ct was 8.0 (SEM 0.1) in the control cells and 7.9 (SEM 0.1) in the RvE1 treated cells (Mann-Whitney U Test, $P = 0.900$). After eight hours there was still no CD55 induction found with a Δ -Ct of 7.8 (SEM = 0.1) in the control cells and 8.0 (SEM 0.1) in the treated cells (Mann-Whitney U Test, $P = 0.700$). Whilst after the 12 hour and 24 hour time points there was a fall in the Δ -Ct values compared to their respective controls this did not reach statistical significance. The Δ -Ct in the control cells after 12 hours was 7.9 (SEM 0.1) and 7.5 (SEM 0.1) in the RvE1 treated cells (Mann-Whitney U Test, $P = 0.100$); 7.5 (SEM 0.1). After 24 hours the Δ -Ct in the control cells was 7.5 (SEM 0.1) and 7.2 (SEM 0.1) in the treated cells (Mann-Whitney U Test, $P = 0.100$). Therefore on dosing the T84 human CRC cells with 100 nM RvE1 over a 24 hour time period, no significant induction in CD55 mRNA was identified (Figure 91). Table 20 shows the individual Ct values for β -actin and CD55 and respective Δ -Ct values.

In order to examine for a dose dependent response in CD55 expression in RvE1 treated T84 cells the candidate increased the RvE1 dose to 500 nM and examined for CD55 mRNA expression at 6 hours. No significant increase in CD55 was identified (Figure 92), Kruskal-Wallis Test $P = 0.640$. The Δ -Ct was 7.2 (SEM 0.2) for the control, 6.8 (SEM 0.3) for the RvE1 (100nM) treated cells, 6.7 (SEM 0.8) for the RvE1 (200 nM) treated cells, 6.4 (SEM 0.3) for the RvE1 (100 nM) treated cells. The individual Ct values for β -actin and CD55 are shown in Table 21.

In conclusion, no RvE1 mediated induction in CD55 was identified in Caco2 or T84 human CRC cells.

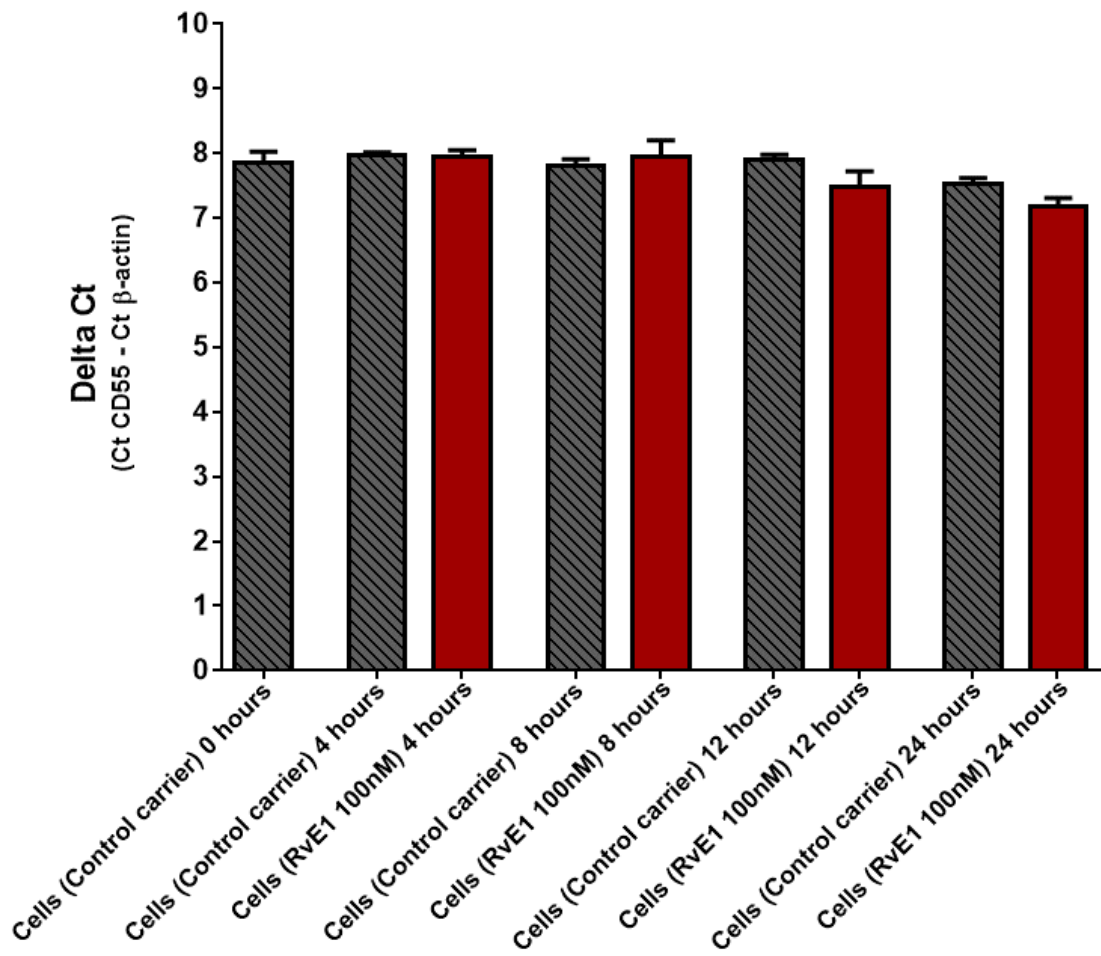


Figure 91. CD55 mRNA expression in RvE1 treated T84 human CRC cells (100nM, 24 hours).

T84 human CRC cells were grown to 100% cell confluency. The cells were then treated with RvE1 (in cell culture medium without FBS), before mRNA was quantified. CD55 expression in 100 nM RvE1 treated T84 cells over 24 hours Figure represents data from three independent experiments, data is shown as mean delta Ct (calculation by Ct value of CD55 minus Ct value of β -actin) with standard error of the mean.

Condition	β -actin	CD55	Δ -Ct	β -actin	CD55	Δ -Ct	β -actin	CD55	Δ -Ct
	Ct value	Ct value	Experiment 1	Ct value	Ct value	Experiment 2	Ct value	Ct value	Experiment 3
	Experiment 1	Experiment 1		Experiment 2	Experiment 2		Experiment 3	Experiment 3	
Control (0 hour)	19.9	27.7	7.8	20.0	27.8	7.8	19.9	28.0	8.1
Control (4 hours)	18.8	26.7	7.9	18.7	26.7	8.0	18.8	26.8	7.9
RvE1 (4 hours)	18.8	27.1	8.3	19.1	27.0	7.9	18.9	26.8	7.9
Control (8 hours)	18.8	26.2	7.4	18.4	26.4	8.0	18.4	26.1	7.7
RvE1 (8 hours)	18.4	26.7	8.3	18.6	26.8	8.2	18.6	26.3	7.7
Control (12 hours)	18.9	26.8	7.9	19.0	26.8	7.8	18.9	26.9	8.0
RvE1 (12 hours)	20.2	27.8	7.6	20.3	27.9	7.6	20.3	27.5	7.2
Control (24 hours)	21.2	28.6	7.4	21.2	28.7	7.5	21.2	28.8	7.6
RvE1 (24 hours)	22.5	29.8	7.3	22.5	29.7	7.2	22.6	29.6	7.0

Table 20. Cycle threshold (Ct) values for β -actin and CD55 for RvE1 treated T84 cells over 24 hours.

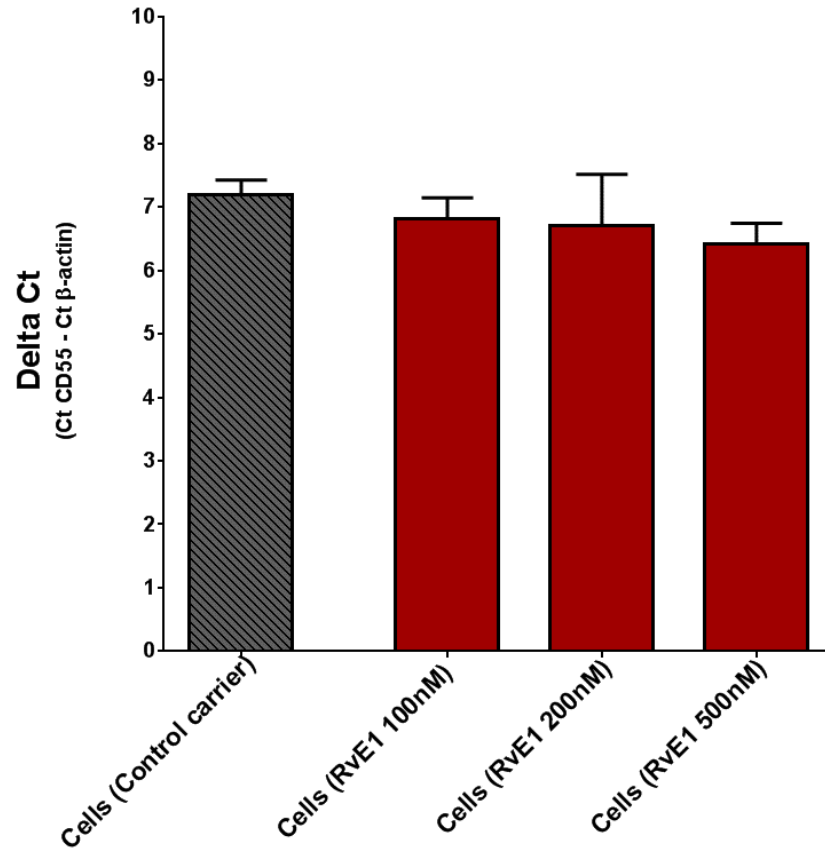


Figure 92. CD55 mRNA expression in RvE1 treated T84 human CRC cells (0-500 nM, 6 hours).

T84 human CRC cells were grown to 100% cell confluency. The cells were then treated with RvE1 for eight hours (in cell culture medium with FBS), before mRNA was quantified. ALPI expression in 100 nM, 200 nM, 500 nM. Figure represents data from one experiment, figure B data is shown as mean delta Ct value (calculation by Ct value of CD55 minus Ct value of β -actin) with standard error of the mean, from three independently cell cultured experiment, data analysed using SPSS (Kruskall-Wallis Test, $P = 0.640$).

Condition	β -actin	CD55	Δ -Ct Experiment 1	β -actin	CD55	Δ -Ct Experiment 2	β -actin	CD55	Δ -Ct Experiment 3
	Ct value	Ct value		Ct value	Ct value		Ct value		
	Experiment 1	Experiment 1		Experiment 2	Experiment 2		Experiment 3	Experiment 3	
Control	16.7	24.2	7.5	18.2	24.9	6.7	17.5	25.0	7.5
RvE1 100nM	17.4	24.8	7.4	18.6	24.8	6.2	17.7	24.4	6.7
RvE1 200nM	17.6	25.5	7.9	20.4	25.5	5.1	18.5	26.4	7.9
RvE1 500nM	18.3	24.6	6.3	18.8	24.6	5.8	18.4	25.3	6.9

Table 21. Cycle threshold (Ct) values for β -actin and CD55 for the RvE1 treated T84 dose response experiment.

5.5.8 Investigation of Resolvin E1 mediated induction of intracellular calcium in human peripheral blood monocytes and the THP-1 human acute monocytic leukaemia cells

The candidate could not establish any RvE1 mediated effect on ALPI or CD55 mRNA expression. The concern was that the RvE1 used was not authentic. The candidate then sought to replicate other published work detailing RvE1 mediated effects. The candidate investigated for an RvE1 mediated effect on human PBMCs, where RvE1 has been shown to increase intracellular calcium (Arita *et al.*, 2007). The authors proposed that RvE1 increased intracellular calcium levels through the GPCR BLT1. The candidate replicated the experimental conditions used by Arita *et al.*, (2007) in order to establish the biological activity of the RvE1 used in the experimentation to date.

Human PBMCs were collected and dosed with RvE1 (100 nM and 200 nM). No rise in intracellular calcium levels was identified in the RvE1 treated PBMCs (see Figure 93A). A clear increase in intracellular calcium is seen in the thapsigargin treated cells confirming that the assay was sensitive to an intracellular calcium induction. No increase in calcium was found with ATP, so was not used in the next experiment. The candidate then increased the concentration of RvE1 up to 2 μ M. Again no RvE1 mediated effect was found in the PBMCs (THP-1, Figure 93B). Furthermore, no LTB₄ mediated increase was seen in either experiment.

As the candidate had shown that there was BLT1 protein expression by the THP-1 cells (section 3.3.1.2) these cells were also investigated for RvE1 mediated induction in intracellular calcium. Despite using doses of RvE1 up to 2 mM no RvE1 mediated induction was found. There was an induction found in the thapsigargin and ATP controls (see Figures 94A & B). Moreover, no LTB₄ mediated increase was identified either.

In conclusion, no RvE1 mediated rise in intracellular calcium was observed in human PBMCs or by the BLT1 protein expressing human acute monocytic leukaemia THP-1 cell line. Therefore the biological activity of Cayman Chemical RvE1 could not be proven.

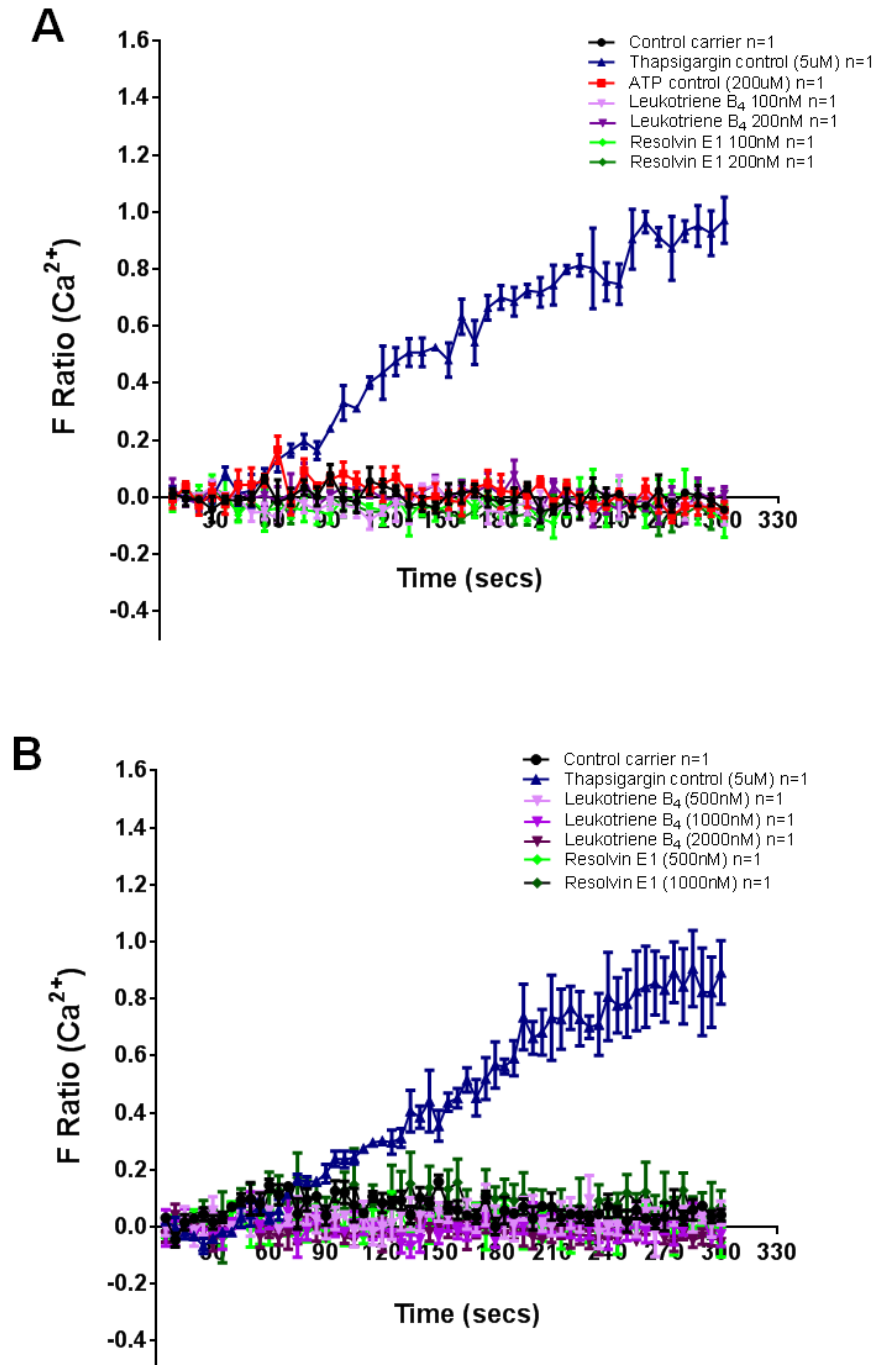


Figure 93. Measurement of intracellular calcium levels in RvE1 treated human PBMCs.

Human PBMCs were loaded with fura 2 and then treated with either thapsigargin, ATP, LTB₄ or RvE1. (A) PBMCs were treated with LTB₄ (100-200 nM) or RvE1 (100-200 nM). (B) PBMCs were treated with LTB₄ (500-2000 nM) or RvE1 (500-1000 nM). Data shown as mean with standard error of the mean from triplicate values obtained at each time point from one experiment.

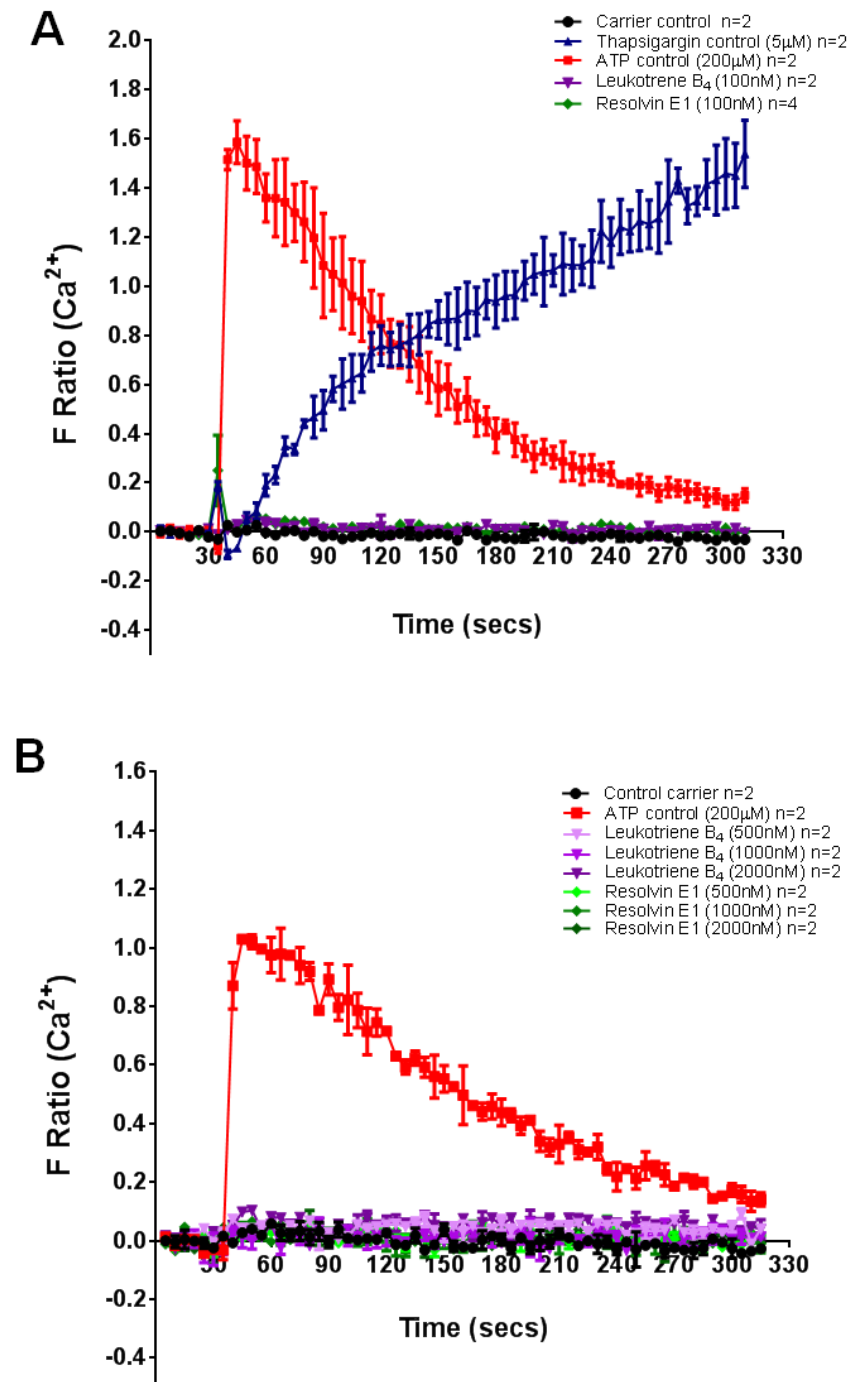


Figure 94. Measurement of intracellular calcium levels in RvE1 treated human THP-1 acute monocytic leukaemia cells.

THP-1 cells were loaded with fura 2 and then treated with either: (A) LTB₄ (100 nM) or RvE1 (100 nM). (B) LTB₄ (500-2000 nM) or RvE1 (500-1000 nM). Data shown as mean with standard error of the mean from triplicate values obtained at each time point from one experiment.

5.6 Discussion

Confirmation that the Cayman Chemical RvE1 product contained chemically recognisable RvE1 was then sought by the candidate. ESI-MS/MS analysis confirmed that the Cayman Chemical product contained RvE1. The ESI-MS/MS product spectra identified characteristic and stable ions consistent with other published mass spectra (Lu Y *et al.*, 2007). The slight differences that were seen in the spectra are due to the fact two different methods to obtain the ion spectral pattern were used, as discussed. Another possibility is that the RvE1 is being rapidly broken down in the experimental solution ahead. Therefore the candidate aimed to confirm that the RvE1 remained stable at 37°C in aqueous solution, thus reflecting the cell conditions at which RvE1 would be placed in the gene expression, cell viability and apoptosis assays. Overall the findings supported that the Cayman Chemical RvE1 remained stable in aqueous solution at a time point that exceeded the length of time that the RvE1 was dosed on the CRC cells in the cell viability, gene expression and intracellular calcium assays. Whilst accurate quantification could not be made there was no clear reduction in RvE1 when presented as a ratio against the IS over the 24 hour period, however the concern was that there was rapid breakdown of the RvE1 is doubtful. Another limitation would be the fact that this experiment was only performed once by the candidate.

RvE1 has been shown to be a potent anti-inflammatory lipid mediator through effects on the synthesis of proinflammatory cytokines and inflammatory cell migration (Serhan *et al.*, 2000 & 2002; Arita *et al.*, 2005b; Campbell *et al.*, 2007). The candidate aimed to establish whether RvE1 exerts any *in vitro* effects on CRC cell survival.

Confirmation of both the presence and stability of RvE1 provided evidence that the absence of an RvE1 mediated CD55 or ALPI mRNA is unlikely to be due to an absence of RvE1, or secondary to rapid non-enzymatic breakdown in solution. However as there was no positive control used for these qPCR studies one cannot exclude the possibility that the primers used were not specific. Further studies should look to optimise or identify a reliable positive control that results in clear ALPI or CD55 induction.

The candidate used the confluency dependent ChemR23 induction in Caco2 CRC cells when exploring for an RvE1 mediated effect on cell viability and apoptosis assays. The rationale being that any biological mediated effect of RvE1 through the ChemR23 receptor would be most likely seen when the Caco2 cells are at full cell confluency. The candidate could not detect RvE1 mediated effects on cell growth and apoptosis. The apoptosis assays required that the CRC cells were grown in culture medium containing FBS. Absence of FBS in the medium over the course of the assay would have resulted

in nutritional deprivation of the cells and subsequent cell death which would have made interpretation of the cell viability and apoptosis impossible. Interestingly the candidate had shown during the EPA viability assays on a number of different cell lines that EPAs negative effect on cell viability was enhanced when made up in culture medium free of FBS (see Appendix 46). Therefore something is limiting the EPA effects on cell viability when made up in culture medium containing FBS. Therefore a reason for a lack of affect on apoptosis in this experimental design may be the presence of FBS in the culture medium. The candidate attempted to limit any RvE1 protein interaction (in FBS) in the cell viability assays by dosing the cells with RvE1 in culture medium without FBS for three hours in each 24 hour cell culture period. However any small effect of RvE1 on cell viability may have been lost as a consequence of the repeated cell washings that were required before and after RvE1 dosing, as outlined in the methods section (5.4.3.1). Another reason for an absence of RvE1 mediated effects on cell viability could lie in the fact that the candidate did not have biologically active RvE1. It has been shown that the chirality of the 18-hydroxyl group with RvE1 has effects on the potency of RvE1 as discussed. However this is unlikely to be a factor as biological activity has been established in both R and S chiral forms (Oh *et al.*, 2011).

To confirm that the RvE1 standard contained biologically active RvE1 and substantiate the *in vitro* cell viability and apoptosis assay findings, two different gene expression assays were examined. As RvE1 has been shown to induce CD55 protein over 24 hours (> three fold) and ALPI mRNA expression (> five fold) via ChemR23 CRC cells (Campbell *et al.*, 2010), these experiments were replicated. When the candidate treated T84 and Caco2 CRC cells RvE1, no significant CD55 mRNA induction was found. When confluent Caco2 cells were treated with 100 nM RvE1 over 8 hours no ALPI mRNA induction was identified. The lack of a positive control condition in the assays, prevented firm conclusions being made on the gene expression findings. Chemerin, a known agonist of the ChemR23 receptor, has been shown to induce ALPI expression and could be used as future positive control, if this assay was to be repeated. The ALPI gene induction identified by Campbell *et al.* (2010) may have been as a consequence of higher endogenous levels of ChemR23 protein expression in the *in vitro* cell lines they used. Future studies could look to overexpress ChemR23 in a CRC cell line, aiming to maximise any RvE1 mediated CD55 or ALPI induction that may be occurring. The candidate performed the gene expression assays in culture medium without 10% FBS, thus removing any potential inhibition of RvE1 through the proteins and lipids contained within the FBS, thus replicating the culture conditions used by Campbell *et al.*, 2010.

As no RvE1 mediated CD55 and ALPI gene expression was identified, a further assay aimed at establishing the RvE1 activity was sought by the candidate. Previous work had shown that RvE1 increased intracellular calcium levels in PBMCs (Arita *et al.*, 2007). The candidate replicated as closely as possible the experimental methodology of Arita and colleagues (2007). Using human PBMCs and the BLT1 expressing cell line THP-1 (section 3.3.1.2) no RvE1 mediated effect on intracellular calcium levels was identified in either cell. Furthermore no LTB₄ mediated induction in PBMCs or THP1 cells was identified, with LTB₄ being used as a positive cell control. LTB₄ had been used by Arita and colleagues (2007) and shown to induce intracellular calcium in human PBMCs. Reasons for the absence of any RvE1 or LTB₄ mediated induction in intracellular calcium could include issues with the chemical integrity of the lipid products both of which were purchased from Cayman Chemical. Problems with possible concentration issues were addressed in that concentrations used in the Arita and colleagues (2007) study were mirrored by the candidate for both LTB₄ and RvE1. Furthermore concentrations exceeded that used by Arita and colleagues (2007), being (20X higher for both LTB₄ and RvE1, and despite this no mediated rise in calcium was found. However no LC-ESI-MS/MS analysis was performed on the LTB₄ to confirm its chemical integrity. The absence of BLT1 in the human PBMCs may also account for a lack of intracellular calcium response to RvE1, and the BLT1 expression status of PBMCs was not commented upon by Arita and colleagues. (2007) and indeed the authors then went on to use human PMNs to confirm BLT1 mediated RvE1 signalling in the same paper. A recent study did however confirm BLT1 mRNA expression by human PBMCs, but it was unclear from this study whether they confirmed BLT1 protein expression in PBMCs from the WB image shown (Galet *et al.*, 2013). The human PBMCs used in this thesis were not examined for BLT1 mRNA or protein expression.

Further published RvE1 mediated biological activities that could be used to confirm biological activity in the Cayman Chemical RvE1 could include;

1. RvE1 inhibition of TNF- stimulated NF- κ B activation in ChemR23 transfected HEK293 cells (Arita *et al.*, 2005).
2. RvE1 inhibition of PMN migration (Serhan *et al.*, 2000, 2002 & 2005).
3. RvE1 stimulated phagocytosis of apoptotic neutrophils (Hong *et al.*, 2008).
4. RvE1 increased phosphorylation of ERK/ MAPK in peripheral blood monocytes and ChemR23 transfected HEK293 cells (Arita *et al.*, 2005).

It remained that the Cayman Chemical RvE1 product was not verified biologically active by the candidate. In the future other sources of RvE1 should be sought if further assays are going to be investigated.

5.7 Summary

No effect of RvE1 on human CRC cell viability, apoptosis or gene expression (ALPI & CD55) was detected in these series of experiments. It remains unclear as to whether the Cayman Chemical RvE1 supplied to the candidate was biologically active. Furthermore the chirality of the RvE1 supplied was unknown.

To date there has been no publications outside Professor Serhan's group that have shown RvE1 activity on GPCRs BLT1 and ChemR23, indeed reference was made to this by Bondue and colleagues (2011) in their comprehensive review detailing the role of chemerin and its receptors. Serhan and colleagues comment in publications investigating the biological activity of RvE1 that they produce it themselves by total organic synthesis (Serhan *et al.*, 2000, Arita *et al.*, 2006, Oh *et al.*, 2011). Therefore their RvE1 source is not the same as that used by the candidate.

If future exploratory experiments examining for a role of RvE1 in colorectal carcinogenesis are to be carried out then robust reproducible *in vitro* assays need to be established. At present the role of chemerin in CRC has not been examined and future studies should not only look to characterise any RvE1 activity on CRC but also look to examine for any that chemerin may have.

6 Final discussion and future work

At the time of writing this thesis, ChemR23 expression in human CRC clinical samples has not been investigated, with just one study investigating BLT1 expression by human CRC tissue (Ihara *et al.*, 2007). Ihara and colleagues showed that inhibition of the LTB₄-BLT1 pathway induced CRC cell apoptosis *in vitro*. Interestingly RvE1 has been shown to have partial agonist activity at the BLT receptor. Future studies should aim to identify a human CRC cell line that expresses BLT1. This would allow investigation into RvE1-BLT1 signaling. If a cell line could not be established transfection of a cell line with BLT1 could be considered.

The candidate established that ChemR23 and BLT1 expression is up regulated in CRC tissue. This induction in expression has not been previously described in CRC or any cancer to date. Whilst ChemR23 and BLT1 were shown to be expressed by normal colorectal and CRC epithelium expression was also identified in the stroma associated with both the CR and CRC epithelium. Immune cells, myofibroblasts and endothelial cells expressed ChemR23 and BLT1. BLT1 expression by CRC epithelium in the human CRC clinical samples and the absence of BLT1 expression *in vitro* may be secondary to the loss of paracrine signaling with the stroma. The increased expression of BLT1 in CRC associated stroma in CRCs distal to the splenic flexure is interesting. There has been reported pathogenetic differences between CRCs at different locations, with proximal CRC being associated with MSI, Lynch syndrome, and distal CRCs being associated with FAP, and rectal tumours with related increased *TP53*, *COX-2* and *APC/β-catenin* signaling.

The adenoma-carcinoma sequence for CRC development through genetic and epigenetic mutations (discussed section 1.5) poses the question as to whether ChemR23 and BLT1 are expressed by human colorectal adenomas. Ethical approval for a study examining human adenoma tissue for ChemR23 had been obtained by the candidate (REC reference: 11/YH/0157). Unfortunately time restraints prevented this study from being performed. Whilst the candidate found that human CRC tissue expressed more ChemR23 and BLT1 when compared to matched histologically normal CR tissue, the tissue examined resided on the same tissue block. Therefore a concern would be that the receptor expression in the normal CR tissue may not be an accurate representation. The use of matched histologically normal tissue blocks ideally should be used in order to reduce any direct effects that the CRC tissue may be having on receptor expression. The candidate was also keen to determine whether patient's disease free survival and mortality correlated with ChemR23 and or BLT1 expression.

RvE1 was first identified in the exudates murine dorsal pouches treated with omega-3 fatty acids and aspirin (Serhan *et al.*, 2000). The authors then went on to show that when aspirin was dosed on human vascular endothelial cells with upregulated COX-2 then EPA was converted to 18R-HEPE. When the 18R-HEPE was then placed on human PMNs, RvE1 was generated (Serhan *et al.*, 2000). 18-HEPE has also been shown to be present in the plasma of healthy volunteers supplemented with fish oil (1g EPA), (Oh *et al.*, 2011). Human PMNs have also been shown to biosynthesise RvE1 directly from 18-HEPE (Tjonahen *et al.*, 2006, Oh *et al.*, 2011). Oh and colleagues (2011) also showed RvE1 detection in incubations from recombinant 5-LOX/ LTA₄H and 18-HEPE. RvE1 has been identified *in vivo* within the colitic colons of *fat-1* transgenic mice (Hudert *et al.*, 2006). RvE1 has also been detected and quantified in the plasma of patients treated with EPA (0.1 and 0.4 ng/ mL; six participants; Arita *et al.*, 2005). Whilst there are several studies supporting the generation of RvE1 from EPA or 18-HEPE, the generation of RvE1 in CRC has not been investigated. The generation of a potent anti-inflammatory, pro-resolving lipid mediator such RvE1 in the cancer microenvironment could offer a novel means of inhibiting pro-carcinogenic signalling, particularly as *in vitro* work has that NK-κB signalling is inhibited by RvE1 (Arita *et al.*, 2005).

The candidate therefore looked to establish whether RvE1 could be biosynthesised by human CRC cells *in vitro*. Importantly the candidate established that activated human PMNs generated detectable RvE1 by LC/ESI-MS-MS. One worry raised from the human PMN study was that 50 µM of 18-HEPE was utilised to generate detectable RvE1, which casts doubt as to whether RvE1 could be biosynthesised in an *in vitro* CRC model, when such a concentration of 18-HEPE was required. RvE1 biosynthesis was not detected by LC/ESI-MS/MS in the *in vitro* CRC or transcellular synthesis cell models. Published *in vitro* studies have used up to 100 µM of 18-HEPE to synthesise RvE1 (Tjonahen *et al.*, 2006, Oh SF *et al.*, 2011), compared to the 1 µM used in this study. However the cost implications of using 100 µM concentrations would have been large and made appropriately controlled reproducible experiments such as those performed by the candidate impossible. Published human PMN studies and the PMN experiment performed by the candidate analysed both the PMN conditioned medium and the methanol lysed contents of the PMNs for RvE1. An experimental shortcoming of CRC and transcellular models is that RvE1 LC/ESI-MS/MS analysis was on the cell conditioned medium and did not include the cells. A question remains that RvE1 may have been biosynthesised intracellularly. Future studies should look to address this through analysis of lysed cells and the cell conditioned medium. Interestingly two separate recent studies have failed to identify RvE1 in the plasma of healthy human volunteers supplemented with fish oil (Dawczynski *et al.*, 2013, Sharke *et al.*, 2015).

Interestingly Dawczynski also treated their volunteer's intravenously with endotoxin (LPS) alongside fish oil supplementation in order to provoke an inflammatory response. Recruitment is currently underway for a randomized, double-blind placebo controlled trial is looking to determine whether EPA prevents colorectal adenomas, either alone or in combination with aspirin. It will be valuable to know whether RvE1 is detected in the CR mucosa of the trial participants.

Whilst the candidate identified 18-HEPE *in vitro*, the candidate was unable to conclude as to whether this was cell driven due to the presence of 18-HEPE in the EPA containing culture medium controls, thus suggesting 18-HEPE synthesis by auto-oxidation. However in the mouse cell models there was a reproducible induction in 18-HEPE biosynthesis between the EPA treated and EPA and aspirin treated cell samples. This increase in 18-HEPE with aspirin is in keeping with that found in human plasma (Oh SF *et al.*, 2011). Oh SF and colleagues showed aspirin increased the S chiral form of 18-HEPE (EPA only R: S ratio 3.4:1 and EPA with aspirin 1.4:1). Chiral studies on the 18-HEPE generated by the EPA supplemented cells would be important in identifying any chiral change in the 18-hydroxyl group when aspirin is used and importantly any change when compared to the EPA control culture medium. Chirality change between cell and no cell conditions would support cell mediated 18-HEPE synthesis.

The absence of a 5-LOX/ LTA₄H hydrolase generated lipid mediator supports the assumption that the RvE1 was not biosynthesised in any of the CRC cell models or macrophage cell line due to the lack of 5-LOX and or LTA₄H enzymatic activity. Activation of both calcium (by ionomycin) and Toll-like receptor (TLR)-4 pathways has been shown to have synergistic effects on the activation of the 5-LOX pathway in macrophages (Buczynski *et al.*, 2007) an effect that not has been examined to date in human CRC cells. The candidate looked to replicate these conditions and treated the macrophage cell line (RAW264.7) with both LPS and ionomycin. Whilst a clear induction was identified in the COX pathway, no 5-LOX/ LTA₄H derived lipid mediator was identified. The rationale for using macrophages alongside CRC epithelial cells is supported by the presence of macrophages within CRC (Mantovani *et al.*, 2002, Forsell *et al.*, 2007, Bailey *et al.*, 2007, Kang *et al.*, 2010), however the ability of these CRC associated cells to produce a 5-LOX/ LTA₄H product is not. Confirmation that these cells have functional a 5-LOX/ LTA₄H would provide a plausible pathway for RvE1 biosynthesis in CRC, through a possible transcellular route, such as between the COX-2 expressing CRC epithelium and associated 5-LOX/ LTA₄H expressing macrophages/ other immune cells. There has been literature published in respect to 5-LOX expression in cancer (discussed previously), however 5-LOX/ LTA₄H activity in human

CRC had not been investigated at the time of writing. Future studies should look to determine the 5-LOX/ LTA₄H expressional and functional status within CRC. PMNs and fibroblasts have both been reported to have active 5-LOX enzymatic pathway, therefore PMNs and fibroblasts along with macrophages could therefore potentially an important role in the biosynthesis RvE1.

To conclude the candidate has shown that human CRC tissue expresses the RvE1 receptors ChemR23 and BLT1, and that these receptors appear to be upregulated between matched colorectal tissue and CRC. Future studies should look to establish whether ChemR23 and BLT1 receptor expression is associated with clinical outcomes. Such studies should establish whether either or both of these receptors could serve as potential human CRC biomarkers, or therapeutic targets.

The candidate was unable to identify an RvE1 mediated effect on human CRC cell viability, apoptosis, and ALPI or CD55 gene expression. Whilst the chirality of RvE1 has been shown to effect potency this is unlikely to be the cause of the negative findings, as both chiral forms of RvE1 have been shown to be biologically active. The use of long acting RvE1 analogue would be useful, at the time of writing such an analogue was not readily available. However a RvE1 analogue is currently being investigated in a phase III clinical trial in patients with dry eye syndrome (Safety and Efficacy Study of RX-10045 NCT0079952; www.clinicaltrials.gov). The candidate went to great lengths to confirm the biological activity of the RvE1 used in the cell viability and apoptosis assays, through a series of gene expression and intracellular calcium assays. The candidate also utilised the reproducible, confluence dependent induction, in ChemR23 expression, in Caco2 human CRC cells, however no biological effect was identified. Further reason for the lack of biological activity of RvE1 on the human CRC may be due to an absence in BLT1 expression or RvE1 interactions with protein within the FBS containing culture medium. As no biological activity was established using the Cayman Chemical RvE1 the candidate was unable to conclude on the negative *in vitro* findings.

Whether RvE1 can be generated *in vitro* by CRC remains unanswered at present. Further research should look to establish whether RvE1 can be detected in human CRC samples. If detected in human colorectal or CRC samples, establishing whether it has a role to play in EPA's anti-cancer effects should be pursued. Establishing the presence of other specialised pro-resolving mediators in CRC such as the D-series resolvins also warrants investigation. The D-series resolvins are derived from DHA via a similar transcellular route to RvE1, these D-series resolvins also have well established pro-resolatory and anti-inflammatory actions (Serhan *et al.*, 2002, Duffield *et al.*, 2006, Sun *et al.*, 2007). Mention should also be made to chemerin, which is an

agonist at the ChemR23 receptor. Levels of chemerin have recently been shown to be elevated in plasma of patients with CRC (Erdogan *et al.*, 2015). At present the significance of raised chemerin levels is unknown and future studies are needed in order to determine its significance. Whether RvE1 could block any pro-tumorigenic actions that chemerin may have through ChemR23 remains purely hypothetical.

Whilst RvE1 was not detected in the supernatant of CRC *in vitro* models the candidate did establish that RvE1 could be generated by human PMNs and also importantly confirm that the ESI-MS/MS method used in these studies could detect RvE1.

7 References

- Abe, M., Havre, P.A., Urasaki, Y., Ohnuma, K., Morimoto, C., Dang, L.H., and Dang, N.H. (2011). Mechanisms of confluence-dependent expression of CD26 in colon cancer cell lines. *BMC Cancer* 11, 51.
- Aliberti, J., Serhan, C.N., and Sher, A. (2002a). Parasite-induced lipoxin (A4) is an endogenous regulator of IL-12 production and immunopathology in toxoplasma gondii infection. *J Exp Med* 196, 1253-1262.
- Aliberti, J., Hieny, S., Reis, E., Sousa, C., Serhan, C.N., and Sher, A. (2002b). Lipoxin-mediated inhibition of IL-12 production by DCs: a mechanism for regulation of microbial immunity. *Nat Immunol* 3, 76-82.
- Alexander, D.D., and Cushing, C.A. (2011). Red meat and colorectal cancer: a critical summary of prospective epidemiologic studies. *Obes Rev* 12, e472-93.
- Altenburg, J.D., and Siddiqui, R.A. (2009). Omega-3 polyunsaturated fatty acids down-modulate CXCR4 expression and function in MDA-MB-231 breast cancer cells. *Mol Cancer Res* 7, 1013-1020.
- Alvaro-Gracia, J.M. (2004). Licofelone--clinical update on a novel LOX/COX inhibitor for the treatment of osteoarthritis. *Rheumatology (Oxford)* 43, Suppl 1, i21-5.
- Anti, M., Marra, G., Armelao, F., Bartoli, G.M., Ficarelli, R., Percesepe, A., De Vitis, I., Mari, G., Sofo, L., and Rapaccini, G.L. (1992). Effect of omega-3 fatty acids on rectal mucosa proliferation in subjects at risk for colon cancer. *Gastroenterology* 103, 883-891.
- Arber, N., and Levin, B. (2005). Chemoprevention of colorectal cancer: ready for routine use? *Recent results in cancer research* 166, 213-230.
- Arita, M., Bianchini, F., Aliberti, J., Sher, A., Chiang, N., Hong, S., Yang, R., Petasis, N.A., and Serhan CN. (2005). Stereochemical assignment, anti-inflammatory properties, and receptor for the omega-3 lipid mediator resolvin E1. *The Journal of Experimental Medicine* 201, 713-722.
- Arita, M., Oh, S.F., Chonan, T., Hong, S., Elangovan, S., Sun, Y.P., Uddin, J., Petasis, N.A., and Serhan, C.N. (2006). Metabolic inactivation of resolvin E1 and stabilization of its anti-inflammatory actions. *J Biol Chem* 281, 22847-22854.
- Arita, M., Ohira, T., Sun, Y-P., Elangovan, S., Chiang, N., and Serhan, C.N. (2007). Resolvin E1 selectively interacts with leukotriene B4 receptor BLT1 and ChemR23 to regulate inflammation. *Journal of Immunology* 178, 3912-3917.

- Arnold, M., Sierra, M.S., Laversanne, M., Soerjomataram, I., Jemal, A., and Bray, F. (2016). Global patterns and trends in colorectal cancer incidence and mortality. *Gut*. Published online ahead of print 27th January 2016.
- Backlund, M.G., Mann, J.R., Holla, V.R., Buchanan, F.G., Tai, H.H., Musiek, E.S., Milne, G.L., Katkuri, S., and DuBois, R.N. (2005). 15-Hydroxyprostaglandin dehydrogenase is down-regulated in colorectal cancer. *J Biol Chem* 280, 3217-3223.
- Bagga, D., Wang, L., Farias-Eisner, R., Glaspy, J.A., and Reddy, S.T. (2003). Differential effects of prostaglandin derived from ω -6 and ω -3 polyunsaturated fatty acids on COX-2 expression and IL-6 secretion. *PNAS* 4, 1751-1756.
- Bailey, C., Negus, R., Morris, A., Ziprin, P., Goldin, R., Allavena, P., Peck, D., and Darzi, A. (2007). Chemokine expression is associated with the accumulation of tumour associated macrophages (TAMs) and progression in human colorectal cancer. *Clin Exp Metastasis* 24, 121-130.
- Bamba, H., Ota, S., Kato, A., Adachi, A., Itoyama, S., and Matsuzaki, F. (1999). High expression of cyclo-oxygenase-2 in macrophages of human colonic adenoma. *Int J Cancer* 83, 470-475.
- Bandeira-Melo, C., Serra, M.F., Diaz, B.L., Cordeiro, R.S., Silva, P.M., Lenzi, H.L., Batchle, Y.S., Serhan, C.N., and Martin, M.A. (2000). Cyclooxygenase-2 derived prostaglandin E₂ and lipoxin A₄ accelerate resolution of allergic oedema in *Angiostrongylus costaricensis*-infected rats: relationship with concurrent eosinophilia. *J Immunol* 164, 1029-1036.
- Bandyopadhyay, A., Shin, D.W., Kim, D.H. (2000). Regulation of ATP-induced calcium release in COS-7 by calcineurin. *Biochem J* 348 173-181.
- Bannenberg, G., and Serhan, C.N. (2010). Specialised pro-resolving lipid mediators in the inflammatory response: an update. *Biochimica et Biophysica Acta* 1801, 1260-1273.
- Barker, N., van Es, J.H., Kuipers, J., Kujala, P., van den Born, M., Cozijnsen, M., Haegebarth, A., Korving, J., Begthel, H., Peters, P.J., and Clevers, H. (2007). Identification of stem cells in small intestine and colon by marker gene Lgr5. *Nature* 449, 1003-1007.
- Baron, J.A., Sandler, R.S., Bresalier, R.S., Quan, H., Ridell, R., Lanas, A., Bolognese, J.A., Oxenius, B., Horgan, K., Loftus, S., and Morton, D.G. (2006). A randomised trial of rofecoxib for the chemoprotection of colorectal adenomas; APPROVe Trial Investigators. *Gastroenterology* 131, 1674-1682.

- Barresi, V., Grosso, M., Vitarelli, E., Tuccari, G., and Barresi, G. (2007). 5-Lipoxygenase is co-expressed with COX-2 in sporadic colorectal cancer: a correlation with advanced stage. *Diseases of the Colon and Rectum* 50, 1576-1584.
- Bellenger, J., Bellenger S., Bataille, A., Massey, K., Nicolaou, A., Rialland, M., Tessier, C., Kang, J.X., and Narce, M. (2010). High pancreatic n-3 fatty acids prevent STZ-induced diabetes in fat-1 mice: inflammatory pathway inhibition. *Diabetes* 60, 1090-1099.
- Bellizzi, A.M. and Frankel, W.L. (2009). Colorectal cancer due to deficiency in DNA mismatch repair function: a review. *Advances in Anatomic Pathology* 16, 405-417.
- Berg, V., Sveinbjörnsson, B., Bendiksen, S., Brox, J., Meknas, K., and Figenschau, Y. (2010). Human articular chondrocytes express ChemR23 and chemerin; ChemR23 promotes inflammatory signalling upon binding the ligand chemerin. *Arthritis & Therapy* R228.
- Bonnans, C., Vachier, I., Chavis, C., Godard, P., Bousquet, J., and Chanez, P. (2002). Lipoxins are potential endogenous anti-inflammatory mediators in asthma. *Am J Resp Crit Care Med* 165, 1531-1535.
- Bondue, B., Wittamer, V., and Parmentier, M. (2011). Chemerin and its receptors in leukocyte trafficking, inflammation and metabolism. *Cytokine Growth Factor Rev* 22, 331-338.
- Bonizzi, G., Piette, J., Schoonbroodt, S., Greimers, R., Havard, L., Merville, M-P., and Bours, V. (1999). Reactive oxygen intermediate-dependent NF- κ B activation by interleukin-1 β requires 5-lipoxygenase or NADPH oxidase activity. *Molecular and Cellular Biology* 19, 1950-1960.
- Borthwick, G.M., Johnson, A.S., Partington, M., Burn, J., Wilson, R., and Arthur, H.M (2006). Therapeutic levels of aspirin and salicylate directly inhibit a model of angiogenesis through a COX-independent mechanism. *The Journal of the Federation of American Societies for Experimental Biology* 20, 2009-2016.
- Bosetti, C., Rosato, V., Gallus, S., Cuzick, J., and La Vecchia, C. (2012). Aspirin and cancer risk: a quantitative review to 2011. *Annals of Oncology* 23, 1403-1415.
- Bossy-Wetzel, E., and Green, D.R. (2000). Detection of apoptosis by Annexin V labeling. *Methods Enzymol* 322, 15-18.
- Botteri, E., Iodice, S., Bagnardi, V., Raimondi, S., Lowenfels, A., and Maisonneuve, P. (2008). Smoking and colorectal cancer: a meta-analysis. *JAMA* 300, 2765-2778.

Boudreau, L.H., Bertin, J., Robichaud, P.P., Laflamme, M., Ouellette, R.J., Flamand, N., and Surette, M.E. (2011). Novel 5-lipoxygenase isoforms affect the biosynthesis of 5-lipoxygenase products. *The Journal of the Federation of American Societies for Experimental Biology* 25, 1097-1105.

Breivik, J., Lothe, R.A., Meling, G.I., Rognum, T.O., Børresen-Dale, A.L., and Gaudernack G. (1997). Different genetic pathways to proximal and distal colorectal cancer influenced by sex-related factors. *Int J Cancer* 74, 664-669.

Browning, L.M., Walker, C.G., Mander, A.P., West, A.L., Madden, J., Gambell, J.M., Young, S., Wang, L., Jebb, S.A., and Calder, P.C. (2012). Incorporation of eicosapentaenoic and docosahexaenoic acids into lipid pools when given as supplements providing doses equivalent to typical intakes of oily fish. *Am J Clin Nutr* 96, 748-758.

Buczynski, M.W., Stephens, D.L., Bowers-Gentry, R.C., Grkovich, A., Deems, R.A., and Dennis, E.A. (2007). TLR-4 and sustained calcium agonists synergistically produce eicosanoids independent of protein synthesis in RAW264.7 cells. *The Journal of Biological Chemistry* 282, 22834-22847.

Burdge, G, C. (2006). Metabolism of linolenic acid in humans. *Prostaglandins, Leukotrienes and Essential Fatty Acids* 75, 161-168.

Calviello, G, Di Nicolol, F., and Gragnoli, S., (2004). n-3 PUFA reduce VEGF expression in human colon cells modulating COX-2/PGE2 induced ERK-1 and -2 and HIF-1 alpha induction pathway. *Carcinogenesis* 25, 2303-2310.

Calviello, G., Serini, S., and Piccioni, E., (2007). n-3 polyunsaturated fatty acids and the prevention of colorectal cancer: molecular mechanisms involved. *Current Medicinal Chemistry* 14, 3059-3069.

Campbell EL, Louis NA, Tomassetti SE, Canny GO, Arita M, Serhan CN, and Colgan SP.(2007). Resolvin E1 promotes mucosal surface clearance of neutrophils: a new paradigm for inflammatory resolution. *FASEB J.* 2007;21, 3162-3170.

Campbell, E.L., MacManus, C.F., Kominsky, D.J., Keely, S., Glover, L.E., Bowers, B.E., Scully, M., Bruyninckx, W.J., and Colgan, S.P. (2010). Resolvin E1-induced intestinal alkaline phosphatase promotes resolution of inflammation through LPS detoxification. *Proceedings of the National Academy of Sciences of the United States of America* 107, 14298-14303.

Calder, P.C. (2006). Polyunsaturated fatty acids and inflammation. *Prostaglandins Leukotrienes Essent Fatty Acids* 75, 273-278.

Canavan, C., Abrams, K.R., and Mayberry, J.F. (2007). Meta-analysis: mortality in Crohn's disease. *Aliment Pharmacol Ther* 25, 861-870.

Cancer Research UK. About cancer: Cancer statistics. <http://www.cancerresearchuk.org> accessed 17/09/12.

Cao, Y., and Prescott, S.M. (2002). Many actions of cyclooxygenase-2 in cellular dynamics and in cancer. *Journal of Cellular Physiology* 190, 279-286.

Capdevila, J.H., Wei, S., Helvig, C., Falck, J.R., Belosludtsev, Y., Truan, G., Graham-Lorence, S.E., and Peterson, J.A. (1996). The highly stereoselective oxidation of polyunsaturated fatty acids by cytochrome P450BM-3. *The Journal of Biological Chemistry* 271, 22663-22671.

Capone, M.L., Tacconelli, S., Di Francesco, L., Sacchetti, A., Sciulli, M.G., and Patrignani, P. (2007). Pharmacodynamic of cyclooxygenase inhibitors in humans. *Prostaglandins Other Lipid Mediat* 82, 85-94.

Cash, J.L., Hart, R., Russ, A., Dixon, J.P., Colledge, W.H., Doran, M.B., Hendrick, A.G., Carlton, M.B., and Greaves D.R. (2008). Synthetic chemerin-derived peptides suppress inflammation through ChemR23. *J Exp Med* 205, 767-775.

Castellone, M.D., Termoto, H., and Gutkind, J.S. (2006). Cyclo-oxygenase-2 and colorectal cancer chemoprevention: the beta-catenin connection. *Cancer Research* 66, 11085-11088.

Cha, Y.I., and Dubois, R.N. (2007). NSAIDs and cancer prevention: targets downstream of COX-2. *Annu Rev Med* 58, 239-252.

Chan, AT., Ogino, S., and Fuchs, C.S. (2007). Aspirin and the risk of colorectal cancer in relation to the expression of COX-2. *New England Journal of Medicine* 356, 2131-2142.

Chandrasekharan, N.V., Dai, H., Roos, L.T., Evanson, N.K., Tomsik, J., Elton, T.S., and Simmons, D.L. (2002). COX-3, a cyclooxygenase-1 variant inhibited by acetaminophen and other analgesic/ antipyretic drugs: Cloning, structure, and expression. *PNAS* 99, 13926-13931.

Chen, C., Eldelstein, L.C., and Gelinas, C. (2000). The Rel/ NF- κ B family directly activates expression of apoptosis inhibitor Bcl-x(L). *Molecular and Cellular Biology* 20, 2687-2695.

Chen, C., Gaudreau, R., Le Gouill, C., Rola-Pleszczynski, M., and Stankova, J. (2004). Agonist-induced internalization of leukotriene B₄ receptor 1 requires G-protein coupled receptor kinase 2 but not arrestins. *Molecular Pharmacology*, 66, 377-386.

- Chen, G., Gharib, T.G., Huang, C.C., Taylor, J.M., Misek, D.E., Kardia, S.L., Giordano, T.J., Iannettoni, M.D., Orringer, M.B., Hanash, S.M., and Beer, D.G. (2002). Discordant protein and mRNA expression in lung adenocarcinomas. *Mol Cell Proteomics*, 1, 304-13.
- Cherukuri, D.P., Chen, X.B.O., Goulet, A.C., Young, R.N., Han, Y., Heimark, R.L., Ryan, J.W., Meuillet, E., and Nelson, M.A. (2007). The EP₄ receptor antagonist, L-161,982, blocks prostaglandin E₂-induced signal transduction and cell proliferation in HCA7 colon cancer cells. *Experimental Cell Research* 313, 2969-2979.
- Chiang, N., Takano, T., Clish, C.B., Petasis, N.A., Tai, H-H., and Serhan, C.N. (1998). Aspirin-triggered 15-epi-lipoxin A₄ (ATL) generation by human leukocytes and murine peritonitis exudates: development of a specific 15-epi-LXA₄ ELISA. *J Pharmacol Exp Ther* 287, 779-790.
- Chiang, N., Gronert, K., Clish, C.B., O'Brien J.A., Freeman, M.W., and Serhan, C.N. (1999). Leukotriene B₄ receptor transgenic mice reveal novel protective roles for lipoxins and aspirin triggered lipoxins in reperfusion. *J Clin Invest* 104, 309-316.
- Chiang, N., Bermudez, E.A., Ridker, P.M., Hurwitz, S, and Serhan, C.N. (2004). Aspirin triggers anti-inflammatory 15-epi-lipoxins A₄ and inhibits thromboxane in a randomised human trial. *Proc Natl Acad Sci USA* 101, 15178-15183.
- Chiang, N., Arita, M., and Serhan, C.N. (2005). Anti-inflammatory circuitry: lipoxins, aspirin-triggered lipoxins and their receptor ALX. *Prostaglandins, Leukotrienes, and Essential Fatty Acids* 73, 163-177.
- Christensen, J. (1991). Gross and microscopic anatomy of the large intestine. *Physiology, Pathophysiology and Disease. Section 1, Structure and Function of the large intestine*, ed Phillips, S.F., Pemberton, J.H., Shorter, R.G. 13-36.
- Choo, M.K., Sakurai, H., Kim, D.H., and Saik, I. (2008). A ginseng saponin metabolite suppresses tumour necrosis factor- α -promoted metastasis by suppressing nuclear factor- κ B signaling in murine colon cancer cells. *Oncology Reports* 19, 595-600.
- Clària, J., Lee, M.H., and Serhan, C.N. (1996). Aspirin-triggered lipoxins (15-epi-LX) are generated by the human lung adenocarcinoma cell line (A549)-neutrophil interactions and are potent inhibitors of cell proliferation. *Mol Med* 2, 583-596.
- Clària, J., and Serhan, C.N (1995). Aspirin triggers previously undescribed bioactive eicosanoids by human endothelial cell-leukocyte interactions. *Proc Natl Acad Sci U S A* 10; 92, 9475-9479.
- Cockbain, A.J., Volpato, M., Race, A.D., Munarini, A., Fazio, C., Belluzzi, A., Loadman, P.M., Toogood, G.J., and Hull, M.A. (2014). Anticolorectal cancer activity of the omega-

3 polyunsaturated fatty acid eicosapentaenoic acid. *Gut* published online first 27th January 2014.

Cole, B.F., Logan, R.F., Halabi, S., Benamouzig, R., Sandler, R.S., Grainge, M.J., Chaussade, S., and Baron, J.A. (2009). Aspirin for the chemoprevention of colorectal adenomas: meta-analysis of the randomized trials. *J Natl Cancer Inst* 101, 256-266.

Colotta, F., Allavena, P., Sica, A., Garlanda, C., and Mantovani, A. (2009). Cancer-related inflammation, the seventh hallmark of cancer: links to genetic instability. *Carcinogenesis* 30, 1073-1081.

Courtney, E.D., Matthews, S., Finlayson, C., Di Pierro, D., Belluzzi, A., Roda, E., Kang, K.J., and Leicester, R.J. (2007). Eicosapentaenoic acid (EPA) reduces cypt proliferation and increases apoptosis in normal colonic mucosa in subjects with a history of colonic adenomas. *Int J Colorectal Dis* 22, 765-776.

Cunningham, D., Atkin, W., Lenz, H.J., Lynch, H.T., Minsky, B., Nordlinger, B. and Starling, N. (2010). Colorectal cancer. *Lancet* 375, 1030-1047.

Cunningham, J.M., Christensen, E.R., Tester, D.J., Kim, C.Y., Roche, P.C., Burgart, L.J. and Thibodeau, S.N. (1998). Hypermethylation of the hMLH1 promoter in colon cancer with microsatellite instability. *Cancer Research* 58, 3455-3460.

Dasari, V.R., Jin, J., and Kunapuli, S.P. (2000). Distribution of leukotriene B4 receptors in human hematopoietic cells. *Immunopharmacology* 48, 157-163.

Dawczynski, C., Massey, K.A., Ness, C., Kiehntopf, M., Stepanow, S., Platzer, M., Grun, M., Nicolaou, A., and Jahreis, G. (2013). Randomised placebo-controlled intervention with n-3 LC-PUFA-supplemented yoghurt: effects on circulating eicosanoids and cardiovascular risk factors. *Clin Nutr* 32, 686-696.

Delattre, O., Law, D.J., Remvikos, Y., Sastre, X., Feinberg, A.P., Olschwang, S., Melot, T., Salmon, R.J., Validire, P., and Thomas, G. (1989). Multiple genetic alterations in distal and proximal colorectal cancer. *The Lancet* 334, 353-355.

Demoor, T., Bracke, K.R., Dupont, L.L., Plantinga, M., Bondue, B., Roy, M.O., Lannoy, V., Lambrecht, B.N., Brusselle, G.G., and Joos, G.F. (2011). The role of ChemR23 in the induction and resolution of cigarette smoke-induced inflammation. *J Immunol* 186, 5457-5467.

Deng, L., Hu, S., Baydoun, A.R., Chen, J., Chen, X., and Cong, X. (2009). Aspirin induces apoptosis in mesenchymal stem cells requiring Wnt/beta-catenin pathway. *Cell Proliferation* 42, 721-730.

Dias, V.C., Wallace, J.L., and Parsons H.G. (1992). Modulation of cellular phospholipid fatty acids and leukotriene B4 synthesis in the human intestinal cell (Caco2). *Gut* 33, 622-627.

Di Francesco, L., Totani, L., Dovizio, M., Piccoli, A., Di Francesco, A., Salvatore, T., Pandolfi, A., Evangelista, V., Dercho, R.A., Seta, F., and Patrignani, P. (2009). Induction of prostacyclin by steady laminar shear stress suppresses tumour necrosis factor-alpha biosynthesis via heme oxygenase-1 in human endothelial cells. *Cir Res* 104, 506-513.

Dorsam, R.T., and Gutkind, J.S. (2007). G-protein-coupled receptors and cancer. *Nature Reviews Cancer* 7, 79-94.

Dovizio, M., Bruno, A., Tacconelli, S., and Patrignani, P. (2012). Mode of action of aspirin as a chemopreventative agent. *Recent Results Cancer Res* 191, 39-65.

Dovizio, M., Tacconelli, S., Ricciotti, E., Bruno, A., Maier, T.J., Anzellotti, P., Di Francesco, L., Sala, P., Signoroni, S., Bertario, L., Dixon, D.A., Lawson, J.A., Steinhilber, D., FitzGerald, G.A., and Patrignani, P. (2012). Effects of celecoxib on prostanoid biosynthesis and circulating angiogenesis proteins in familial adenomatous polyposis. *J Pharmacol Exp Ther* 341, 242-50.

Dona, M., Fredman, G., Schwab, J.M., Chiang, N., Arita, M., Goodarzi, A., Cheng, G., von Andrian, U.H., and Serhan, C.N. (2008). Resolvin E1, an EPA-derived mediator in whole blood, selectively counterregulates leukocytes and platelets. *Blood* 112, 848-855.

Duffield, J.S., Hong, S., Vaidya, V.S., Lu, Y., Fredman, G., Serhan, C.N., and Bonventre, J.V. (2006). Resolvin D series and protectin D1 mitigate acute kidney injury. *J Immunol* 177, 5902-2911.

Duque, J., Díaz-Muñoz, M.D., Fresno, M., and Iñiguez, M.A. (2006). Up-regulation of cyclooxygenase-2 by interleukin-1beta in colon carcinoma cells. *Cell Signal* 18, 1262-1269.

Eaden, J.A., Abrams, K.R., and Mayberry, J.F. (2001). The risk of colorectal cancer in ulcerative colitis: a meta-analysis. *Gut* 48, 526-535.

Eberhart, C.E., Coffey, R.J., Radhika, A., Giardiello, F.M., Ferrenbach, S., and DuBois, R.N. (1994). Up-regulation of cyclooxygenase 2 gene expression in human colorectal adenomas and adenocarcinomas. *Gastroenterology* 107, 1183-1188.

El Kebir, D., Gjorstrup, P., and Filep, J.G. (2012). Resolvin E1 promotes phagocytosis-induced neutrophil apoptosis and accelerates resolution of pulmonary inflammation. *Proc Natl Acad Sci U S A* 109, 14983-14988.

Erdogan S., Yilmaz, F.M., Yazici, O., Yozgat, A., Sezer, S., Ozdemir, N., Uysal, S., Pumak, T., Sendur, M.A., and Ozasian, E. (2015). Inflammation and chemerin in colorectal cancer. *Tumour Biol* December 1st [Epub ahead of print].

Ferlay, J., Parkin, D.M. and Steliarova-Foucher, E. (2010a). Estimates of cancer incidence and mortality in Europe in 2008. *European Journal of Cancer* 46, 765-781.

Ferlay, J., Shin, H.R., Bray, F., Forman, D., Mathers, C. and Parkin, D.M. (2010b). GLOBOCAN 2008: Cancer Incidence and Mortality Worldwide in 2008 [online]. [Accessed 15th August 2011]. Available from: <http://globocan.iarc.fr>.

Ferrández, A., Piazuolo, E., and Castells, A. (2012). Aspirin and the prevention of colorectal cancer. *Best Pract Res Clin Gastroenterol* 26, 185-195.

Fini L, Piazzzi G, Ceccarelli C, Daoud Y, Belluzzi A, Munarini A, Graziani G, Fogliano V, Selgrad M, Garcia M, Gasbarrini A, Genta RM, Boland CR, and Ricciardiello L. (2010). Highly purified eicosapentaenoic acid as free fatty acids strongly suppresses polyps in *Apc(Min/+)* mice. *Clin Cancer Res* 16, 5703-5711.

Fiorucci, S., De Lima Jr, O.M., Mencarelli, A., Palazzetti, B., Distrutti, E., McKnight, W., Dickey, M., Ma, L., Romano, M., Morelli, A., and Wallace, J.L. (2002). Cyclooxygenase-2-derived lipoxin A4 increases gastric resistance to aspirin-induced damage. *Gastroenterology* 123, 1598-1606.

Fiorucci, S., Santucci, E., Wallace, J.L., Sardina, M., Ronano, M., Soldato, P.D., and Morelli, A. (2003). Interaction of a selective cyclooxygenase-2 inhibitor with aspirin in the human gastric mucosa. *Proc Natl Acad Sci USA* 100, 10937-10941.

Fitzpatrick, F.A. (2004). Cyclooxygenase enzymes: regulation and function. *Curr Pharm Des* 10, 577-588.

Flossman, E., and Rothwell, P.M. (2007). Effect of aspirin on long-term risk of colorectal cancer: consistent evidence from randomised and observational studies. *Lancet* 369, 1603-1613.

Ford-Hutchinson, A.W., Bray, M.A, Doig, M.V., Shipley, and M.E., Smith, M.J. (1980). Leukotriene B, a potent chemokinetic and aggregating substance released from polymorphonuclear leukocytes. *Nature* 286, 264-265.

Forsell, J., Oberg, A., Henriksson, M.L., Stenling, R., Jung, A., and Palmqvist, R. (2007). High macrophage infiltration along the tumour front correlates with improved survival in colon cancer. *Clin Cancer Res* 13, 1472-1479.

Fredman, G., Van Dyke, T.E., and Serhan, C.N. (2010). Resolvin E1 regulates adenosine diphosphate activation of human platelets. *Arterioscler Thromb Vasc Biol* 30 2005-2013.

Funk, C.D. (2001). Prostaglandins and leukotrienes: advances in eicosanoid biology. *Science* 294, 1871-1879.

Galet, C., Gollapudi, K., Stepanian, S., Byrd, B., Henning, S.M., Grogan, T., Elashoff, D., Heber, D., Said, J., Cohen, P., and Aronson, W.J. (2013). Effect of a low-fat fish oil diet on pro-inflammatory eicosanoids and cell cycle progression score in men undergoing radical prostatectomy. *Cancer Prevention Research* 7, 97-104.

Gardner, S.H., Hawcroft, G., and Hull, M.A. (2004). Effect of nonsteroidal anti-inflammatory drugs on β -catenin protein levels and catenin-related transcription in human colorectal cancer cells. *British Journal of Cancer* 91, 153–163.

Gay, L.J., and Felding-Habermann, B. (2011). Contribution of platelets to tumour metastasis. *Nat Rev Cancer* 11, 123-134.

Geelen, A., Schouten, J.M., Kamphuis, C., Stam, B.E., Burema, J., Renkema, J.M.S., Bakker, E-J., Veer, P.V., and Kampan, E. (2007). Fish consumption, n-3 fatty acids, and colorectal cancer: A meta-analysis of prospective cohort studies. *Am J Epidemiol* 166, 1116-1125.

Gerber, M. (2012). Omega-3 fatty acids and cancers: systematic update review of epidemiological studies. *British Journal of Nutrition* 107, 228-239.

Glaser, C., Heinrich, J., and Koletzko, B. (2010). Role of FADS₁ and FADS₂ polymorphism in polyunsaturated fatty acid metabolism. *Metabolism* 59, 993-999.

Gleissman, H., Yang, R., Martinod, K., Lindskog, M., Serhan, C.N., Johnsen, J.I., and Kogner, P. (2010). Docosahexaenoic acid metabolome in neural tumors: identification of cytotoxic intermediates. *FASEB J* 24, 906-915.

Goel, A., Chang, D.K., Ricciardiello, L., Gasche, C., and Boland, C.R. (2003). A novel mechanism for aspirin-mediated growth inhibition of human colon cancer cells. *Clin Cancer Res* 9, 383-390.

Gorjão, R., Azevedo-Martins, A.K., Rodrigues, H.G., Abdulkader, F., Arcisio-Miranda, M., Procopio, J., and Curi, R. (2009). Comparative effects of DHA and EPA on cell function. *Pharmacol Ther* 122, 56-64.

Goralski, K.B., McCarthy T.C., Hanniman, E.A., Zabel, B.A., Butcher, E.C., Parlee, S.D., Murunganandan, S., and Sinal, C.J. (2007). Chemerin, a novel adipokine that regulates

adipogenesis and adipocyte metabolism. *The Journal of Biological Chemistry* 38, 28175-28188.

Greene, E.R., Huang, S., Serhan, C.N., and Panigrahy, D. (2011). Regulation of inflammation in cancer by eicosanoids. *Prostaglandins & Other Lipid Mediators* 96, 27-36.

Greten F.R., Eckmann, L., Greten, T.F., Park, J.M., Li, Z.W., Egan, L.J., Kagnoff, M.F., and Karin, M. (2004). IKKbeta links inflammation and tumorigenesis in a mouse model of colitis-associated cancer. *Cell* 118, 285-296.

Groden, J., Thliveris, A., Samowitz, W., Carlson, M., Gelbert, .L, Albertsen, H., Joslyn, G., Stevens, J., Spirio, L., Robertson, M., Sargeant, L., Krapcho, K., Wolff, E., Burt, R., Hughes, J.P., Warrington, J., McPherson, J., Wasmuth, J., Le Paslier, D., Abderrahim, H., Cohen, D., Leppert, M. and White, R. (1991). Identification and characterization of the familial adenomatous polyposis coli gene. *Cell* 66, 589-600.

Guillen-Ahlers, H., Tan, J., Castellino, F.J., and Ploplis, V.A. (2011). Effect of sulindac sulfide on metallohydrolases in the human colon cancer cell line HT29. *PLoS One* 6 e25725.

Guttridge, D.C., Albanese, C., Reuther, J.Y., Pestell, R.G., and Baldwin, A.S. (1999). NF- κ B controls cell growth and differentiation through transcriptional regulation of cyclin D1. *Molecular Cell Biology* 19, 5785-5799.

Haas-Stapleton, E.J., Lu, Y., Hong, S., Arita, M., Favoreto, S., Nigam S., Serhan, C.N., and Agabian, N. (2007). *Candida albicans* modulates host defence by biosynthesising the pro-resolving mediator resolvins E1. *PLoS one* 12, e1316.

Hall, M.N., Chavarro, J.E., Lee, I.M., Willet, W.C., and Ma, J. (2008). A 22-year prospective study of fish, n-3 fatty acid intake, and colorectal cancer risk in men. *Cancer Epidemiology Biomarkers & Prevention* 17, 1136-1143.

Hamberg, M., and Samuelsson, B. (1967). Oxygenation of unsaturated fatty acids by the vesicular gland of sheep. *The Journal of Biological Chemistry* 242, 5344-5354.

Hamilton, S.R., Vogelstein, B., Kudo, S., Riboli, E., Nakamura, S., Hainaut, P., Rubio, C.A., Sobin, L.H., Fogt, F., Winawer, S.J., Goldgar, D.E. and Jass, J.R. (2000). Carcinoma of the colon and rectum. In *Pathology and Genetics of Tumours of the Digestive System*. ed. Hamilton, S.R. & Aaltonen, L.A., , pp. 105-143. IARC Press, Lyon.

Hanahan, D., and Weinberg, R.A. (2000). The hallmarks of cancer. *Cell* 100, 57-70.

- Hanahan, D., and Weinberg, R.A. (2011). Hallmarks of cancer: the next generation. *Cell*. 144, 646-674.
- Hanif, R., Pittas, A., Feng, Y., Koutsos, M.I., Qiao, L., Staiano-Coico, L., Shiff, S.I., and Rigas, B. (1996). Effects of nonsteroidal anti-inflammatory drugs on proliferation and on induction of apoptosis in colon cancer cells by a prostaglandin-independent pathway. *Biochem Pharmacol*. 52, 237-245.
- Hardcastle, J.D., Chamberlain, J. O., Robinson, M.H., Moss, S.M., Amar, S.S., Balfour, T.W., James, P.D., and Mangham, C.M. (1996). Randomised controlled trial of faecal-occult-blood screening for colorectal cancer. *Lancet* 348, 1472-1477.
- Hashidate, T., Murakami, N., Nakagawa, M., Ichikawa, M., Kurokawa, M., Shimizu, T., and Nakamura, M. (2010). AML1 enhances the expression of leukotriene B4 type-1 receptor in leukocytes. *The Journal of the Federation of American Societies for Experimental Biology* 24, 3500-3510.
- Hawcroft, G., Loadman, P.M., Belluzzi, A., and Hull, M.A. (2010). Effect of eicosapentaenoic acid on E-type prostaglandin synthesis and EP4 receptor signaling in human colorectal cancer cells. *Neoplasia* 12, 618-627.
- Henry, L.R., Leem H.O., Lee, J.S., Klein-Szanto, A., Watts, P., Ross, E.A., Che, W.T., and Cheng, J.D. (2007). Clinical implications of fibroblast activation protein in patients with colon cancer. *Clin Cancer Res* 13, 1736-1741.
- Hernandez, Y., Sotolongo, J., Breglio, K., Conduah, D., Chen, A., Xu, R., Hsu, D., Ungaro, R., Hayes LA., Pastorini, C., Abreu, MT., and Fukata, M. (2010). The role of prostaglandin E2 (PGE₂) in toll-like receptor 4 (TLR4)-mediated colitis associated neoplasia. *BMC Gastroenterology* 10, 82.
- Herová, M., Schmid, M., Gemperle, C., and Hersberger, M. (2015). ChemR23, the receptor for chemerin and resolving E1, is expressed and functional on M1 but not M2 macrophages. *J Immunol* 194, 2330-2337.
- Hewitson, P., Glasziou, P., Watson, E., Towler, B and Irwig, L. (2008). Cochrane systematic review of colorectal cancer screening using the faecal occult blood test (hemoccult): an update. *American Journal of Gastroenterology* 103, 1541-1549.
- Hofmann, B., Rödl, C.B., Kahnt, A.S., Maier, T.J., Michel, A.A., Hoffmann, M., Rau, O., Awwad, K., Pellowska, M., Wurglics, M., Wacker, M., Živković, A., Fleming, I., Schubert-Zsilavec, Stark, H., Schneider, G., and Steinhilber, D. (2012). Molecular pharmacological profile of a novel thiazolinone-based direct and selective 5-lipoxygenase inhibitor. *BJP* 165, 2305-2313.

Holtzman, M.J, Turk, J and Shornick L.P. (1992). Identification of a pharmacologically distinct prostaglandin H synthase in cultured epithelial cells. *Journal of Biological Chemistry* 267, 21438-21445.

Hong, S., Porter, T.F, Lu, Y., Oh, S.F., Pillai, P.S and Serhan CN. (2008). Resolvin E1 metabolome in local inactivation during inflammation-resolution. *Journal of Immunology* 180, 3512-3519.

Hoshino, R., Chatani, Y., Yamori, T., Tsuruo, T., Oka, H., Yoshida, O., Shimada, Y., Ari-i S, Wada, H., Fujimoto, J., and Kohno, M. Constitutive activation of the 41-/43-kDa mitogen-activated protein kinase signaling pathway in human tumors. *Oncogene* 18, 813-822.

Huang, R.Y., Guilford, P., and Thiery, J.P. (2012). Early events in cell adhesion and polarity during epithelial-mesenchymal transition. *J Cell Sci* 125, 4417-4422.

Hubbard, W.C., Litterst, C.L., Liu, M.C., Bleecker, E.R., Eggleston, J.C., McLemore, T.L., and Boyd, M.R. (1986). Profiling of prostaglandin biosynthesis in biopsy fragments of human lung carcinomas and normal lung by capillary gas chromatography-negative ion chemical ionisation mass spectrometry. *Prostaglandins* 32, 889-906.

Hudert, C.A., Weylandt, K.H., Lu, Y., Wang, J., Hong, S., Dignass, A., Serhan, C.N., and Kang, J.X. (2006). Transgenic mice rich in endogenous omega-3 fatty acids are protected from colitis. *Proceedings of the National Academy of Sciences of the United States of America* 103, 11276-11281.

Hull, M.A., Sandell, A.C., Montgomery, A.A., Logan, R.F., Clifford, G.M., Rees, C.J., Loadman, P.M., and Whitham, D. (2013). A randomized controlled trial of eicosapentaenoic acid and/or aspirin for colorectal adenoma prevention during colonoscopic surveillance in the NHS Bowel Cancer Screening Programme (The seAFood Polyp Prevention Trial): study protocol for a randomized controlled trial. *Trials* 14, 237.

Illemann, M., Bird, N., Majeed, A., Sehested, M., Laerum, O.D., Lund, L.R., Danø, K., and Nielsen, B.S. (2006). MMP-9 is differentially expressed in primary human colorectal adenocarcinomas and their metastases. *Mol Cancer Res* 4, 293-302.

Ihara, A., Wada, K., Yoneda, M., Fujisawa, N., Takahashi, H., and Nakajima, A. (2007) Blockade of Leukotriene B4 Signalling Induces Apoptosis and Suppresses Cell Proliferation in Colon Cancer. *Journal of Pharmacological Sciences* 103, 24-32.

Ishida, T., Yoshida, M., Arita, M., Nishitani, S., Masuda, A., Mizuno, S., Takagawa, T., Morita, Y., Kutsumi, H., Inokuchi, H., Serhan, C.N., Blumberg, R.S., and Azuma, T (2010). Resolvin E1, an endogenous lipid mediator derived from eicosapentaenoic

acid, prevents dextran sulphate sodium induced colitis. *Inflammatory Bowel Disease* 16, 87-95.

Isobe, Y., Arita, M., Matsueda, S., Iwamoto, R., Fujihara, T., Nakanishi, H., Taguchi, R., Masuda, K., Sasaki, K., Urabe, D., Inoue, M., and Ara, H. (2012). Identification and structure determination of novel anti-inflammatory mediator resolvin E3, 17, 18-dihydroxyeicosapentaenoic acid. *J Biol Chem* 287, 10525-10534.

Jame, A.J., Penrose, J.F., Cazaly, A.M., Holgate, S.T., and Sampson, A.P. (2006). Human bronchial fibroblasts express the 5-lipoxygenase pathway. *Respiratory Research* 7, 1-11.

Jass JR. Classification of colorectal cancer based on correlation of clinical, morphological and molecular features. *Histopathology* 50, 113-130.

Jeong, C-H., Borde, A.M., Pugliese, A., Cho, Y.Y., and Kun, H-G. (2009). [6]-Gingerol suppresses colon cancer growth by targeting leukotriene A₄ hydrolase. *Cancer Research* 69, 5584-5591.

Jiang, J.G., Chen, C.L., Card, J.W., Yang, S., Chen, J.X., Fu, X.N., Ning, Y.G., Xiao, X., Zeldin, D.C., and Wang, D.W. (2005). Cytochrome P450 2J2 promotes the neoplastic phenotype of carcinoma cells and is up-regulated in human tumors. *Cancer Res* 65, 4707–4715.

Kabadere, S., Kus, G., Uyar, R., and Oztopcu-Vatan, P. (2014). Licofelone abolishes survival of carcinogenic fibroblasts by inducing apoptosis. *Drug Chem Toxicol* 37, 1-7.

Kanaoka, S., Taki, T., and Yoshida, K. (2007). Cyclooxygenase-2 and tumour biology. *Advances in Clinical Chemistry* 43, 59-78.

Kang, J.X., Wang, J., Wu, L., and Kang, Z.B. (2004). Transgenic mice: fat-1 mice convert n-6 to n-3 fatty acids. *Nature* 427, 504.

Kang, J.C., Chen, J.S., Lee, C.H., Chang, J.J., and Shieh, Y.S. (2010). Intratumoral macrophage counts correlate with tumour progression in colorectal cancer. *J Surg Oncol* 102, 242-248.

Kansal, S., Bhatnagar, A., and Agnihotri, N. (2014). Fish oil suppresses cell growth and metastatic potential by regulating PTEN and NF- κ B signalling in colorectal cancer. *PLoS One* 9, e84627.

Karp, C.L., Flick, L.M., Park, K.M., Softic, S., Greer, T.M., Keledjian, R., Yang, R., Uddin, J., Guggino, W.B., Atabani, S.F., Belkaid, Y., Xu, Y., Whitsett, J.A., Accurso, F.J., Wills-Karp, M., and Petasis, N.A. (2004). Defective lipoxin-mediated anti-inflammatory activity in the cystic fibrosis airway. *Nat Immunol* 5, 388-392.

- Kawamori, T., Kitamura, T., Watanabe, K., Uchiya, N., Maruyama, T., Narumiya, S., Sugimura, T., and Wakabayashi, K. (2005). Prostaglandin E receptor subtype EP (1) deficiency inhibits colon cancer development. *Carcinogenesis* 26, 353-357.
- Kebir, E.D., Gjorstrup, P., and Filep, J.G. (2012). Resolvin E1 promotes phagocytosis-induced neutrophil apoptosis and accelerates resolution of pulmonary infiltration. *Proceedings of the National Academy of Sciences of the United States of America* 109, 14983-14988.
- Kong, D., Li, Y., Wang, Z., and Sarkar, F.H. (2011). Cancer stem cells and epithelial to mesenchymal transition (EMT) - phenotypic cells: are they cousins or twins? *Cancer* 3, 716-729.
- Konkel, A., and Schunck, W.H. (2011). Role of the cytochrome P450 enzymes in the bioactivation of polyunsaturated fatty acids. *Biochim Biophys Acta* 1814, 210-222.
- Kew, S., Mesa, M.D., Tricon, S., Buckley, R., Minihane, A.M., and Yaqoob, P. (2004). Effects of oils rich in eicosapentaenoic and docosahexaenoic acids on immune cell composition and function in healthy humans. *Am J Clin Nutr.* 79, 674-681.
- Kinzler, K.W., Nilbert, M.C., Su L.K., Vogelstein, B., Bryan, T.M., Levy, D.B., Smith, K.J., Preisinger, A.C., Hedge, P., McKechnie, D., et al. (1991). Identification of FAP locus genes from chromosome 5q21. *Science* 253, 661-5.
- Kinzler KW, and Vogelstein B. (1996). Lessons from hereditary colorectal cancer. *Cell* 87, 159-170.
- Knüpfner, H., and Preiss, R. (2010). Serum interleukin-6 levels in colorectal cancer patients - a summary of published results. *Int J Colorectal Dis* 25, 135-140.
- Konishi, K., Fujii, T., Boku, N., Kato, S., Koba, .I, Ohtsu, A., Tajiri, H., Ochiai, A., and Yoshida, S. (1999). Clinicopathological differences between colonic and rectal carcinomas: are they based on the same mechanism of carcinogenesis? *Gut.* 1999 45, 818-21.
- Koyama, Y., and Kotake, K. (1997). Overview of colorectal cancer in Japan: report from the Registry of the Japanese Society for Cancer of the Colon and Rectum. *Diseases of the Colon and Rectum* 40, supplement, S2-S9.
- Kroeze, W.K., Sheffler, D.J., and Roth, B.L. (2003). G-protein-coupled receptors at a glance. *Journal of Cell Science* 116, 4867-4869.
- Kronborg, O., Fenger, C., Olsen, J., Jørgensen, O.D., and Søndergaard, O. (1996). Randomised study of screening for colorectal cancer with faecal-occult-blood test. *Lancet* 348, 1467-1471.

Kure, I., Nishiumi, S., Nishitani, Y., Tanoue, T., Ishida T., Mizuno, M., Fujita, T., Kutsumi, H., Arita, M., Azuma, T., and Yoshida, M. (2010). Lipoxin A (4) reduces lipopolysaccharide-induced inflammation in macrophages and intestinal epithelial cells through inhibition of nuclear factor-kappaB activation. *J Pharmacol Exp Ther* 332, 541-548.

Langman, J. (1985). *Medical embryology*. 5th Edition Baltimore: Williams & Wilkins 235-243.

Lecomte, M., Laneuville, O., Ji, C., DeWitt, D.L., and Smith, W.L. (2007). Acetylation of human prostaglandin endoperoxide synthase-2 (cyclooxygenase-2) by aspirin. *The Journal of Biological Chemistry* 269, 1307-13215.

Leggett B, and Whitehall V. (2010). Role of the serrated pathway in colorectal cancer pathogenesis. *Gastroenterology* 138, 2088-2100.

Lengauer, C., Kinzler, K.W., and Vogelstein, B. (1997). Genetic instability in colorectal cancers. *Nature* 386, 623-627.

Levy, B.D., Bonnans, C., Silverman, E.S., Palmer, L.J., Marigowda, G., and Israel, E. (2005). Severe Asthma Research Program National Heart, Lung, and Blood Institute Diminished lipoxin biosynthesis in severe asthma. *Am J Respir Crit Care Med* 172:824– 830.

Lewis, R.A., Austen, K.F., and Soberman, R.J. (1990), *Leukotrienes and Other Products of the 5-Lipoxygenase Pathway — Biochemistry and Relation to Pathobiology in Human Diseases*. *The New England Journal of Medicine*, 323, 645-655.

Lin, W.W., and Karin, M. (2007). A cytokine-mediated link between innate immunity, inflammation, and cancer. *J Clin Invest* 117, 1175-83.

Lind, D.S., Hochwald, and S.N., Malaty, J. (2001). Nuclear factor- κ B is upregulated in colorectal cancer. *Surgery* 130, 363-369.

Lipkin, M. (1974). Phase 1 and phase 2 proliferative lesions of colonic epithelial cells in diseases leading to colonic cancer. *Cancer* 34, 878-888.

Louis, N.A., Hamilton, K.E., Kong, T., and Colgan, S.P. (2005). HIF-dependent induction of apical CD55 coordinates epithelial clearance of neutrophils. *The FASEB Journal* 19, 950-959.

Lu, Y, Hong, S., Yang, R., Uddin, J., Gotlinger, K.H., Petasis, N.A., and Serhan CN. (2007). Identification of endogenous resolvin E1 and other lipid mediators derived from eicosapentaenoic acid via electro-spray low-energy tandem mass spectrometry:

spectra and fragmentation mechanisms. *Rapid Communications in Mass Spectrometry* 21, 7-22.

Luangsay, S., Wittamer, V., Bondue, B., De Henau, O., Rouger, L., Brait, M., Franssen, J.D., de Nadai, P., Huaux, F., and Parmentier, M. (2009). Mouse ChemR23 is expressed in dendritic cell subsets and macrophages, and mediates an anti-inflammatory activity of chemerin in a lung disease model. *Journal of Immunology* 183, 6489-6499.

Lundeen, K.A., Sun, B., Karlsson, L., and Fourie, A.M. (2006). Leukotriene B4 receptors BLT1 and BLT2: Expression and function in human and murine mast cells. *Journal of Immunology* 177, 3439-3447.

Lynch, H.T., and de la Chapelle, A. (2003). Hereditary colorectal cancer. *N Engl J Med* 348, 919-932.

Mancini, J., Abramovitz, M., Cox, M.E., Wong, E., Charleson, S., Perrier, H., Wang, Z., Prasit, P., and Vickers, P.J. 1993. 5-Lipoxygenase-activating protein is an arachidonate binding protein. *FEBS Lett* 318, 277-281.

Mancini, J.A., O'Neill, G.P., Bayly, C., and Vickers, P.J. (1994). Mutation of serine-516 in human prostaglandin G/H synthase-2 to methionine or aspirin acetylation of this residue stimulates 15R-HETE synthesis. *FEBS Letters* 342, 33-37.

Mandel, J.S., Bond, J.H., Church, T.R., Snover, D.C., Bradley, G.M., Schuman, L.M., and Ederer, F. (1993). Reducing mortality from colorectal cancer by screening for fecal occult blood: Minnesota Colon Cancer Control Study. *New England Journal of Medicine* 328, 1365-1371.

Mani, S.A., Gou, W., Liao, M-J., Eaton, E.N., Ayyanan, A., Zhou, A.Y., Brooks, M., Reinhard, F., Zhang, C.C., Shipitsin, M., Campbell, L.L., Polyak, K., Brisken, C., Yang, J., and Weinberg, R.A. (2008). The epithelial mesenchymal transition generates cells with properties of stem cells. *133*, 704-715.

Mantovani, A., Sozzani, S., Locati, M., Allavena, P., and Sica, A. (2002). Macrophage polarization: tumour-associated macrophages as a paradigm for polarized M2 mononuclear phagocytes. *Trends Immunol* 23, 549-555.

Masoodi, M., and Nicolaou, A. (2006). Lipidomic analysis of twenty-seven prostanoids and isoprostanes by liquid chromatography/ electrospray tandem mass spectrometry. *Rapid Communications in Mass Spectrometry* 20, 3023-3029.

Masoodi, M., Mir, A.A., Petasis, N.A., Serhan, C.N., and Nicolaou, A. (2008). Simultaneous lipidomic analysis of three families of bioactive lipid mediator's leukotrienes, resolvins, protectins and related hydroxy-fatty acids by liquid

chromatography/ electrospray ionization tandem mass spectrometry. *Rapid Communications in Mass Spectrometry* 22, 3023-3029.

Melstrom, L.G., Bentrem, D.J., Salabat, M.R., Kennedy, T.J., Ding, X.Z., Strouch, M., Rao, S.M., Witt, R.C., Ternent, C.A., Talamonti, M.S., Bell, R.H, and Adrian, T.A. (2008) Overexpression of 5-lipoxygenase in colon polyps and cancer and the effect of 5-LOX inhibitors in vitro and in a murine model. *Clin Cancer Res* 14, 6525-6530.

Mengeaud, V., Nano, J.L., Fournel, S., and Rampal, P. (1992). Effects of eicosapentaenoic acid, gamma-linolenic acid and prostaglandin E1 on three human colorectal cancer cell lines. *Prostaglandins Leukot Essent Fatty Acids* 47, 313-319.

Midgley, R. and Kerr, D. (1999). Colorectal cancer. *Lancet* 353, 391-399.

Miles, E.A., Banerjee, T., and Calder, P.C. (2004). The influence of different combinations of gamma-linolenic, stearidonic and eicosapentaenoic acids on the fatty acid composition of blood lipids and mononuclear cells in human volunteers. *Prostaglandins Leukot Essent Fatty Acids* 70, 529-538.

Miller, P.E., Lazarus, P., Lesko, S.M., Cross, A.J, Sinha, R., Laio, J., Zhu, J., Harper, G., Muscat, J.E., and Hartman, T.J. (2013). Meat-related compounds and colorectal cancer risk by anatomical subsite. *Nutr Cancer*. 65, 202-226.

Mobraten, K., Haug, T.M., Kleiveland, C.R., and Lea, T. (2013). Omega-3 and omega-6 PUFAs induce the same GPR120-mediated signalling events, but with different kinetics and intensity in Caco-2 cells. *Lipids in health and disease* 12, 101.

Mohammed, A., Janakiram, N.B., Li, Q., Choi, C.I., Zhang, Y., Steele, V.E., and Rao, C.V. (2011). Chemoprevention of colon and small intestinal tumorigenesis in APC (Min/+) mice by licoferone, a novel dual 5-LOX/COX inhibitor: potential implications for human colon cancer prevention. *Cancer Prev Res (Phila)* 12, 2015-2026.

Munger, K.A., Montero, A., Fukunaga, M., Uda, S., Yura, T., Imai, E., Koneda, Y., Valdivielso, J.M., and Badr, K.F. (1999). Transfection of rat kidney with human 15-lipoxygenase suppresses inflammation and preserves function in experimental glomerulonephritis. *Proc Natl Acad Sci USA* 96, 13375-13380.

Muruganandan, S., Parlee, S.D., Rourke, J.L., Ernst, M.C., Goralski, K.B., and Sinal, C.J. (2011). Chemerin, a novel peroxisome proliferator-activated receptor gamma (PPARgamma) target gene that promotes mesenchymal stem cell adipogenesis. *J Biol Chem* 286, 23982-23995.

Muto, T., Bussey, H.J.R and Morson, B.C. (1975). The evolution of cancer of the colon and rectum. *Cancer* 36, 2251-2270.

- Naugler, W.E., and Karin, M. (2008). NF-kappaB and cancer-identifying targets and mechanisms. *Curr Opin Genet* 18, 19-26.
- Nakajima, H., Nakajima, K., Nagano, Y., Yamamoto, M., Tarutani, M., Takahashi, M., Takahashi, Y., and Sano, S. (2010). Circulating level of chemerin is upregulated in psoriasis. *J Dermatol Sci* 60, 45-47.
- Nelson, D.R. (2009). The cytochrome p450 homepage. *Hum Genomics* 4, 59-65.
- Nicosia, S., Vigano, T., and Folco, G.C. (1992). Eicosanoids in allergic reactions: quantitative determination by enzyme immunoassay. *Pharmacol Res* 26, 116-117.
- Noguchi, M., Miyano, M., Matsumoto, T., and Noma, M. (1994). Human 5-lipoxygenase associates with phosphatidylcholine liposomes and modulates LTA4 synthetase activity. *Biochim Biophys Acta*; 1215, 300-306.
- Noguchi, M., Miyano, M., and Matsumoto, T. (1996). Physicochemical characterization of ATP binding to human 5-lipoxygenase. *Lipids*.31, 367-371.
- Norat, T., Bingham, S., Ferrari, P., Slimani, N., Jenab, M., Mazuir, M., Overvad, K., Olsen, A., Tjønneland, A., Clavel, F., Boutron-Ruault, M.C., Kesse, E., Boeing, H., Bergmann, M.M., Nieters, A., Linseisen, J., Trichopoulou, A., Trichopoulos, D., Tountas, Y., Berrino, F., Palli, D., Panico, S., Tumino, R., Vineis, P., Bueno-de-Mesquita, H.B., Peeters, P.H., Engeset, D., Lund, E., Skeie, G., Ardanaz, E., González, C., Navarro, C., Quirós, J.R., Sanchez, M.J., Berglund, G., Mattisson, I., Hallmans, G., Palmqvist, R., Day, N.E., Khaw, K.T., Key, T.J., San Joaquin, M., Hémon, B., Saracci, R., Kaaks, R. and Riboli, E. (2005). Meat, fish, and colorectal cancer risk: the European Prospective Investigation into cancer and nutrition. *Journal of the National Cancer Institute* 97, 906-916.
- Norris, P.C., and Dennis, E.A. (2012). Omega-3 fatty acids cause dramatic changes in the TLR4 and purinergic eicoasanoid signaling. *PNAS* 109, 8517-8522.
- Ogino, S., Kirkner, G.J., Nosho, K., Irahara, N., Kure, S., Shima, K., Hazra, A., Chan, A.T., Dehari, R., Giovannucci, E.L., and Fuchs, CS. (2008). Cyclooxygenase-2 expression is an independent predictor of poor prognosis in colon cancer. *Clinical Cancer Research* 14, 8221-8227.
- Oh, S.F., Pillai, P.S., Recchiutu, A., Yang, R., and Serhan, C.N. (2011). Pro-resolving actions and stereoselective biosynthesis of 18S E-series resolvins in human leukocytes and murine inflammation. *The Journal of Clinical Investigation* 121, 569-581.
- Ohira, T., Arita, M., Omori, K., Recchiuti, A., Van Dyke, T.E., and Serhan, C.N. (2010). Resolvin E1 receptor activation signals phosphorylation and phagocytosis. *The Journal of Biological Chemistry* 285, 3451-3461.

- Ong, S.M., Tan, Y.C., Beretta, O., Jiang, D., Yeap, W.H., Tia, J.J.Y., Wong, W.C., Yang, H., Schwarz, H., Lim, K.H., Koh, P.K., Ling, K.L., and Wong, S.C. (2012). Macrophages in human colorectal cancer are pro-inflammatory and prime T cells towards an anti-tumour type-1 inflammatory response. *Eur J Immunol* 42, 89-100.
- Ota, S., Bamba, H., Kato, A, Kawamoto, C., Yoshida, Y., and Fujiwara, K. (2002). COX-2, prostanoids and colon cancer. *Aliment Pharmacol Ther* 16, 102-106.
- Pachynski, R.K., Zabel, B.A., Kohrt, H.E., Tejada, N.M., Monnier, J., Swanson, C.D., Holzer, A.K., Gentles, A.J., Sperinde, G.V., Edalati, A., Hadeiba, H.A., Alizadeh, A.A., and Butcher, E.C. (2012). The chemoattractant chemerin suppresses melanoma by recruiting natural killer cell antitumour defenses. *The Journal of experimental medicine* 209, 1427-1435.
- Palozza, P., Calviello, G., Maggiano, N., Lanza, P., Ranelletti, F.O., and Bartoli, G.M. (2000). Beta-carotene antagonises the effects of eicosapentaenoic acid on cell growth and lipid peroxidation in WiDr adenocarcinoma cells. *Free Radic Biol Med* 28, 228-234.
- Panigrahy, D., Kaipainen, A., Greene, E.R., and Huang, S. (2010). Cytochrome P450-derived eicosanoids: the neglected pathway in cancer. *Cancer Metastasis Rev* 2010 29, 723-735.
- Parolini, S., Santoro, A., Marcenaro, E., Luini, W., Massardi, L., Facchetti, F., Communi, D., Parmentier, M., Majorana, A., Sironi, M., Sironi, M., Tabellini, G., Moretta, A., and Sozzani, S. (2007). The role of chemerin in the co-localisation of NK and dendritic cell subsets into inflamed tissues. *Blood* 109, 3625-3632.
- Patrono, C., Collier, B., FitzGerald, G.A., Hirsch, J., and Roth, G. Platelet-active drugs: the relationship among dose, effectiveness, and side effects: the Seventh ACCP Conference on Antithrombotic and Thrombolytic Therapy. *Chest* 126, 234S-2364S.
- Pawlosky, R.J., Hibbein, J.R., Novotny, J.A., and Salem, N. (2001). Physiological compartmental analysis of α -linolenic acid metabolism in adult humans. *J Lipid Res* 42, 1257-1265.
- Perreti, M., Chiang N., La, M., Fierro, I.M., Marullo, S., Getting, S.J., Solito, E., and Serhan, C.N. (2002). Endogenous lipid- and peptide-derived anti-inflammatory pathways generated with glucocorticoid and aspirin treatment activate the lipoxin (A4) receptor. *Nat Med* 8, 1296-1302.
- Pesole, G., Mignone, F., Giss, C., Grillo, G., Licciulli, F., and Liuni, S. (2001). Structural and functional features of eukaryotic mRNA untranslated regions. *Gene* 276, 73-81.
- Peters-Golden, M., and Brock, T.G. (2003). 5-Lipoxygenase and FLAP. *Prostaglandins, Leukotrienes and Essential Fatty Acids* 69, 99-109.

Peterson, J., Garges, S., Giovanni, M., McInnes, P., Wang, L., Schloss, J.A., Bonazzi, V., McEwen, J.E., Wetterstrand, W.A., Deal, C., Baker, C.C., Di Francesco, V., Howcroft, T.F., Karp, R.W., Lunsford, R.D., Wellington, C.R., Belachew, T., Wright, M., Giblin, C., David, H., Mills, M., Salomon, R., Mullins, C., Akolkar, B., Begg, L., Davis, C., Grandison, L., Humble, M., Khalsa, J., Little, A.R., Peavy, H., Pontzer, C., Portnoy, M., Sayre, M.H., Starke-Reed, P., Zakhari, S., Read, J., Watson, B., and Guyer, M. (2009). The NIH Human Microbiome Project. *Genome Res* 19, 2317-2323.

Pettersson, A., Boketoft, A., Sabirish, A., Nilsson, N.E., Kotarsky, K., Olde, B., and Owman, C. (2000). First-generation monoclonal antibodies identifying the human leukotriene B4 receptor-1. *Biochemical and Biophysical Research Communications* 279, 520-525.

Pham, N.M., Mizoue, T., Tanaka, K., Tsuji, I., Tamakoshi, A., Matsuo, K., Wakai, K., Nagata, C., Inoue, M., Tsugane, S., and Sasazuki, S; Research Group for the Development and Evaluation of Cancer Prevention Strategies in Japan.(2013). Fish consumption and colorectal cancer risk: an evaluation based on a systematic review of epidemiologic evidence among the Japanese population. *Jpn J Clin Oncol* 43, 935-941.

Pidgeon, G.P., Lysaght, J., Krishnamoorthy, S., Reynolds, J.V., O'Byrne, K., Nie, D., and Honn, K.V. (2007). Lipoxygenase metabolism: roles in tumour progression and survival. *Cancer Metastasis Reviews* 26, 503-524.

Peinado, H., Olmeda, D., and Cano, A. (2007). Snail, Zeb and bHLH factors in tumour progression: an alliance against the epithelial phenotype? *Nature Rev Cancer* 7, 415-428.

Planagumà, A., Kazani, S., Marigowda, G., Haworth, O., Mariani, T.J., Israel, E., Blecker, E.R., Curran-Everett, D., Erzurum, S.C., Calhoun, W.J., Castro, M., Chung, K.F., Gastron, B., Jarjour, N.N., Busse, W.W, Wenzel, S.E, and Levy, B.D. (2008) Airway lipoxin A₄ generation and lipoxin A₄ receptor expression are decreased in severe asthma. *Am J Respir Crit Care Med* 178:574–582.

Popivanova BK, Kitamura K, Wu Y, Kondo T, Kagaya T, Kaneko S, Oshima M, Fujii C, and Mukaida N. (2008). Blocking TNF-alpha in mice reduces colorectal carcinogenesis associated with chronic colitis. *J Clin Invest* 118, 560-570.

Pouliot, M., Clish, C.B., Petasis, N.A., Van Dyke, T.E., and Serhan, C.N. (2000). Lipoxin A₄ analogues inhibit leukocyte recruitment to *Porphyromonas gingivalis*: a role for cyclooxygenase-2 and lipoxins in periodontal disease. *Biochemistry* 39, 4761-4768.

Pradono, P., Tazawa, R., Maemondo, M., Tanaka, M., Usui, K., Saijo, Y., Hagiwara, K., and Nukiwa, T. (2002). Gene transfer of thromboxane A₂ synthase and prostaglandin

I(2) synthase antithetically altered tumor angiogenesis and tumor growth. *Cancer Res.* 62, 63-66.

Qu, X., Zhang, X., Yao, J., Song, J., Nikolic-Paterson, D.J., and Li, J. (2012). Resolvins E1 and D1 inhibit interstitial fibrosis in the obstructed kidney via inhibition of local fibroblast proliferation. *Journal of Pathology* (Epub ahead of print 18/05/12).

Qui, H., Johansson, A.S., Sjöström, M., Wan, M., Schröder, O., Palmblad, J., and Haeggström, J.Z. (2006). Differential induction of BLT receptor expression on human endothelial cells by lipopolysaccharide, cytokines, and leukotriene B4. *Proceedings of the National Academy of Sciences of the United States of America* 103, 6913-6918.

Rama, D., Esendagli, G., and Guc, D. (2011). Expression of chemokine-like receptor 1 (CMKLR1) on J744A.1 macrophages co-cultured with fibroblast and/ or tumour cell: modeling the influence of the microenvironment. *Cellular Immunology* 271, 134-140.

Renehan, A.G., Tyson, M., Egger, M., Heller, R.F., and Zwahlen, M. (2008). Body-mass index and incidence of cancer: a systematic review and meta-analysis of prospective observational studies. *Lancet* 371, 569-578.

Revermann, M., Mieth, A., Popescu, L., Paulke, A., Wurglics, M, Pellowaska, M., Fischer, A.S., Steri, R., Maier, T.J., Schermuly, R.T., Geisslinger, G., Schuberts-Zsilavec, M., Brandes, R.P., and Steinhilber, D. (2011). A pirinixic acid derivative (LP105) inhibits murine 5-lipoxygenase activity and attenuates vascular remodeling in a murine model of aortic aneurysm. *BJP* 163, 1721-1732.

Ricciotti, E., and FitzGerald, G.A. (2011). Prostaglandins and Inflammation. *Arterioscler Thromb Vasc Biol* 31, 986-1000.

Rigas, B., Goldman, I.S., and Levine, L. (1993). Altered eicosanoid levels in human colon cancer. *J Lab Clin Med* 122, 518-523.

Rothwell, P.M., Wilson, M., Elwin, C.E., Norrving, B., Algra, A., Warlow, C.P., and Meade, T.W. (2010). Long term effect of aspirin on colorectal cancer incidence and mortality: 20-year follow-up of five randomised trials. *Lancet* 376, 1741-1750.

Sakamoto, K., Maeda, S., Hikiba, Y., Nakagawa, H., Hayakawa, Y., Shibata, W., Yanai, A., Ogura, K., and Omata, M. (2009). Constitutive NFκB activation in colorectal carcinoma plays a key role in angiogenesis promoting tumor growth. *Clinical Cancer Research* 15, 2248-58.

Samowitz, W.S., Albertsen, H., Herrick, J., Levin, T.R., Sweeney, C., Murtaugh, M.A., Wolff, R.K., and Slattery, M.L. (2005). Evaluation of a large, population-based sample supports a CpG island methylator phenotype in colon cancer. *Gastroenterology* 129, 837-845.

Sanders, L.M., Henderson, C.E., Hong, M.Y., Barhoumi, R., Burghardt, R.C., Wang, N., Spinka, C.M., Carroll, R.J., Turner, N.D., Chapkin, R.S., and Lupton, J.R. (2004). An increase in reactive oxygen species by dietary fish oil coupled with the attenuation of antioxidant defenses by dietary pectin enhances rat colonocyte apoptosis. *J Nutr* 134, 2333-2338.

Sano, H., Kawahito, Y., Wilder, R.L., Hashiramoto, A., Mukai, S., Asai, K., Kimura, S., Kato, H., Kondo, M., and Hla, T. (1995). Expression of cyclooxygenase-1 and-2 in human colorectal cancer. *Cancer Research* 55, 3785-3789.

Savage, D.C. (1977). Microbial ecology of the gastrointestinal tract. *Annu Rev Microbiol* 31, 107-133.

Schley, P.D., Brindley, D.N., and Field, C.J. (2007). (n-3) PUFA alter raft lipid composition and decrease epidermal growth factor receptor levels in lipid rafts of human breast cancer cells. *J Nutr* 137, 548-553.

Schwab, J.M., Chiang, N., Arita, M., and Serhan, C.N. (2007). Resolvin E1 and protectin D1 activate inflammation-resolution programmes. *Nature* 447, 869-74.

Sell, H., Laurencikiene, J., Taube, A., Eckardt, K., Cramer, A., Horrichs, A., Arner, P., and Eckel, J. (2009). Chemerin is a novel adipocyte-derived factor inducing insulin resistance in primary human skeletal muscle cells. *Diabetes* 58, 2731-2740.

SEER Cancer Statistics Review, 1975-2002. http://seer.cancer.gov/archive/csr/1975_2002/results_merged/sect_06_colon_rectum.pdf. Accessed 5th December 2013.

Serhan, C.N. (1997). Lipoxins and novel aspirin-triggered 15-epi-lipoxins (ATL). *Prostaglandins* 53, 107-137.

Serhan, C.N. (2005). Lipoxins and aspirin-triggered 15-epi-lipoxins are the first lipid mediators of endogenous anti-inflammation and resolution. *Prostaglandins Leukot Essent Fatty Acids* 73, 141-162.

Serhan, C.N., Clish, C.B., Brannon, J., Colgan, S.P., Chiang, N., and Gronert, K. (2000). Novel functional sets of lipid-derived mediators with anti-inflammatory actions generated from omega-3 fatty acids via cyclooxygenase 2-nonsteroidal anti-inflammatory drugs and transcellular processing. *Journal of Experimental Medicine* 192, 1197-1204.

Serhan, C.N., Hong, S., Gronert, K., Colgan, S.P., Devchand, P.R., Mirick, G., and Moussignac, R.L. (2002). Resolvins: a family of bioactive products of omega-3 fatty acid transformation circuits initiated by aspirin treatment that counter proinflammation signals. *Journal of Experimental Medicine* 196, 1025-1037.

- Serhan, C.N., and Savill, J. (2005). Resolution of inflammation: the beginning programs the end. *Nat Immunol* 6, 1191-1197.
- Serhan, C.N., Yacoubian, S., and Yang, R. (2008). Anti-inflammatory and pro-resolving lipid mediators. *Annual Review of Pathology: Mechanisms of Disease* 3, 279-312.
- Shacter, E., and Weitzman, S.A. (2002). Chronic inflammation and cancer. *Oncology (Williston Park)* 16, 217-226.
- Shao, J., Sheng, H., Inoue, H., Morrow, J.D., and DuBois, R.N. (2000). Regulation of constitutive cyclooxygenase-2 expression in colon carcinoma cells. *The Journal of Biological Chemistry* 275, 33951-33956.
- Sharma, R.A., Gescher, a., Plataras, J.P., Leuratti, C., Singh, R., Gallacher-Horley, B., Offord, E., Marnett, L.J., Steward, W.P., and Plummer, S.M. (2001). Cyclooxygenase-2, malondialdehyde and pyrimidopurine adducts of deoxyguanosine in human colon cells. *Carcinogenesis* 22, 1557-1560.
- Sheehan, K.M., Sheahan, K., O'Donoghue, D.P., MacSweeney, F., Conroy, R.M., Fitzgerald, D.J., and Murray, F.E. (1999). The relationship between cyclooxygenase-2 expression and colorectal cancer. *The Journal of the American Medical Association* 282, 1254-1257.
- Shen, X.J., Rawls, J.F., Randall, T., Burcal, L., Mpande, C.N., Jenkins, N., Jovov, B., Abdo, Z., Sandler, R.S., and Keku, T.O. (2010). Molecular characterisation of mucosal adherent bacteria and associations with colorectal adenomas. *Gut Microbes* 1, 138-147.
- Sheng, H., Shao, J., Washington, M.K., and Dubois, R.N. (2001). Prostaglandin E2 increases growth and motility of colorectal carcinoma cells. *J Biol Chem* 276, 18075-18081.
- Shoji, Y., Takahashi, M., Kitamura, T., Watanabe, K., Kawamori, T., Maruyama, T., Sugimoto, Y., Negishi, M., Narumiya, S., Sugimura, T., and Wakabayashi, K. (2004). Downregulation of prostaglandin E receptor subtype EP3 during colon cancer development. *Gut* 53, 1151-1158.
- Skarke, C., Alamuddin, N., Lawson, J.A., Ferguson, J.F., Reilly, M.P., and FitzGerald, G.A. (2015). Bioactive products formed in humans from fish oils. *J Lipid Res* 2015, published ahead of print.
- Smith, W.L., DeWitt, D.L., and Garavito, R.M. (2000). Cyclooxygenases: structural, cellular, and molecular biology. *Ann. Rev. Biochem* 69, 145-182.

Sobhani, I., Tap, J., Roudot-Thoraval, F., Roperch, J.P., Letulle, S., Langella, P., Corthier, G., Van Nhieu, J.T., and Furet, J.P. Microbial dysbiosis in colorectal cancer (CRC) patients. *PLoS One* 6, e16393.

Sobin, L.H., and Wittekind, C. (1997). TNM classification of malignant tumours. Edition 5, 66-69. Wiley-Liss, New York.

Soslow, R.A., Dannenberg, A.J., Rush, D., Woerner, B.M., Khan, K.N., Masferrer, J., and Koki, A.T. (2000). COX-2 is expressed in human, pulmonary, colonic, and mammary tumors. *Cancer* 89, 2637-264.

Soumaoro, L.T., Lida, S., Uetake, H., Ishiguro, M, Takagi, Y., Higuchi, T., Yasuno, M., Enomoto, M., and Sugihara., K (2006). Expression of 5-lipoxygenase in human colorectal cancer. *World Journal of Gastroenterology* 12, 6355-6360.

Soumaoro, L.T., Uetake, H., Higuchi, T., Takagi, Y., Enomoto, M., and Sugihara, K. (2004). Cyclooxygenase-2 expression: a significant prognostic indicator for patients with colorectal cancer. *Clinical Cancer Research* 10, 8465-8471.

Sun, Y., Tang, X.M., Half, E., Kuo, M.T., and Sinicrope, F.A. (2002). Cyclo-oxygenase-2 overexpression reduces apoptotic susceptibility by inhibiting the cytochrome c-dependent apoptotic pathway in human colon cancer cells. *Cancer Res* 62, 6323-6328.

Sun, Y.P., Oh, S.F., Uddin, J., Yang, R., Gotlinger, K., Campbell, E., Colgan, S.P., Petasis, N.A., and Serhan, C.N. (2007). Resolvin D1 and its aspirin-triggered 17R epimer. Stereochemical assignments, anti-inflammatory properties, and enzymatic inactivation. *J Biol Chem* 282, 9323-9334.

Tager, A.M., and Luster, A.D. (2003). BLT1 and BLT2: the leukotriene B₄ receptors. *Prostaglandins, Leukotrienes and Essential Fatty Acids* 69, 123-134.

Takeda, H., Sonoshita, M., Oshima, H., Sugihara, K., Chulada, P.C., Lagenbach, R., Oshima, M., and Taketo, M.M. (2003). Cooperation of cyclooxygenase 1 and cyclooxygenase 2 in intestinal polyposis. *Cancer Res* 63, 4872-4877.

Tang, X., Jin, R., Qu, G., Wang, X., Li, Z., Yuan, Z., Zhao, C., Siwko, S., Shi, T., Wang, P., Xiao, J., Liu, M., and Luo, J. (2013). GPR116, an adhesion G-protein-coupled receptor, promotes breast cancer metastasis via the Gαq-p63Rho GTPase pathway. (2013). *Cancer Research* 73, 6206-6218.

Tang, Y., Chen, Y., Jiang, H., Robbins, T.G., and Nie, D. (2010). G-protein-coupled receptor for short-chain fatty acids suppresses colon cancer. *International Journal of Cancer* 128, 847-856.

- Tatsuno, I., Saito, H., Chang, K.J., Tamura, Y., and Yoshida, S. (1990). Comparison of the effect between leukotriene B4 and leukotriene B5 on the induction of interleukin 1-like activity and calcium mobilizing activity in human blood monocytes. *Agents Actions* 29, 324-327.
- Tavolari, S., Bonafé, M., Marini, M., Ferreri, C., Bartolini, G., Brighenti, E., Manara, S., Tomasi, V., Laufer, S., and Guarnieri, T. (2008). Licofelone, a dual COX/5-LOX inhibitor, induces apoptosis in HCA7 colon cancer cells through the mitochondrial pathway independently from its ability to affect arachidonic acid cascade. *Carcinogenesis* 29,371-380.
- Tavolari, S., Munarini, A., Storci, G., Laufer, S., Chieco, P., and Guarnieri, T. (2012). The decrease of cell membrane fluidity by the non-steroidal anti-inflammatory drug Licofelone inhibits epidermal growth factor receptor signalling and triggers apoptosis in HCA-7 colon cancer cells. *Cancer Lett* 321, 187-194.
- Terano, T., Salmon, J.A., and Moncada, S. (1984). Biosynthesis and biological activity of leukotriene B5. *Prostaglandins* 27, 217-232.
- Terzić, J., Grivennikov, S., Karin, E., and Karin M. (2010). Inflammation and Colon Cancer. *Gastroenterology* 138, 2101-2214.
- Thuault, S., Valcourt, U., Petersen, M., Manfioletti, G., Heldin, C.H., and Moustakas, A. (2006). Transforming growth factor-beta employs HMGA2 to elicit epithelial-mesenchymal transition. *J Cell Biol* 174, 175-183.
- Thiery, J.P. (2002). Epithelial-mesenchymal transitions in tumour progression. *Nat Rev Cancer* 2, 442-454.
- Titos, E., Chiang, C., Serhan, C.N., Romano, M., Gaya, J., Pueyo, G., and Claria, J (1999). Hepatocytes are a rich source of novel aspirin-triggered 15-epi-lipoxin A4 (ATL). *Am J Physiol* 277, C870-C877.
- Tjonahen, E., Oh, S.F., Siegelman, J., Elangovan, S., Percapio, K.B., Hong, S., Arita, M., and Serhan, C.N. (2006). Resolvin E2: Identification and anti-inflammatory action: Pivotal role of human lipoxygenase in resolvin E series biosynthesis. *Chemistry & Biology* 13, 1193-1202.
- Thuresson, E.D., Lakkides, K.M., and Smith, W.L. (2000). Different catalytically competent arrangements of arachidonic acid within the cyclooxygenase active site of prostaglandin endoperoxide H synthase-1 lead to the formation of different oxygenated products. *J Biol Chem* 275, 8501-8507.

- Tommelein, J., Verset, L., Bolterberg, T., Demetter, P., Bracke, M., and De Wever, O. (2015). Cancer associated fibroblasts connect metastasis promoting communication in colorectal cancer. *Front Oncol* 5, article 63.
- Tomozawa, S., Tsuno, N.H., Sunami, E., Hatano, K., Kitayama, J., Osada, T., Saito, S., Tsuruo, T., Shibata, Y., and Nagawa, H. (2000). Cyclooxygenase-2 over-expression correlates with tumour recurrence, especially haematogenous metastasis, of colorectal cancer. *British Journal of Cancer* 83, 324-328.
- Topper, J.N., Cai, J., Falb, D., and Gimbrone Jr, M.A. (1996). Identification of vascular endothelial genes differentially responsive to fluid mechanical stimuli: cyclooxygenase-2, manganese superoxide dismutase, and endothelial cell nitric oxide synthase are selectively up-regulated by steady laminar shear stress. *PNAS* 93, 10417-10422.
- Toyoda Y., Nakayama T., Ito Y., Ioka A., and Tsukuma H. (2009). Trends in colorectal cancer incidence by subsite in Osaka, Japan. *Jpn J Clin Oncol* 39, 189-191.
- Toyota M, Ahuja N, Ohe-Toyota M, Herman JG, Baylin SB, and Issa JP. (1999). CpG island methylator phenotype in colorectal cancer. *Proc Natl Acad Sci U S A* 96, 8681-8686.
- Tsukamoto, H., Hishinuma, T., Mikkaichi, T, Nakamura, H., Yamazaki, T., Tomioka, M., and Mizugaki, M. (2002). Simultaneous quantification of prostaglandins, isoprostane and thromboxane in cell-cultured medium using gas-chromatography-mass spectrometry. *J Chromatogr B Analyt Technol Biomed Life Sci* 774, 205-214.
- Turk, H.F., and Chapkin, R.S. (2013). Membrane lipid raft organisation is uniquely modified by n-3 polyunsaturated fatty acids. *Prostaglandins Leukot Essent Fatty Acids* 88, 43-47.
- Ueno, N., Takegoshi, Y., Kamei, D., Kudo, I., and Murakami, M. (2005). Coupling between cyclooxygenases and terminal prostanoid synthases. *Biochem Biophys Res Commun* 338, 70-76.
- Vargas AJ, and Thompson PA. (2012). Diet and nutrient factors in colorectal cancer risk. *Nutr Clin Pract* 27, 613-623.
- Vermi, W., Riboldi, E., Wittamer, V., Gentil, F., Luini, W., Marrelli, S., Vecchi, A., Franssen, J.D., Communi, D., Massardi, L, Sironi, M., Mantovani, A., Parmentier, M., Facchetti, F., and Sozzani, S. (2005). Role of ChemR23 in directing the migration of myeloid and plasmacytoid dendritic cells to lymphoid organs and inflamed skin. *The Journal of Experimental Medicine* 201, 509-515.
- Vilar E, and Gruber SB. (2010). Microsatellite instability in colorectal cancer-the stable evidence. *Nat Rev Clin Oncol*.7, 153-162.

Vogelstein, B., Fearon, E.R., Hamilton, S.R., Kern, S.E., Preisinger, A.C., Leppert, M., Nakamura, Y., White, R., Smits, A.M., and Bos, J.L. (1988). Genetic alterations during colorectal-tumor development. *New England Journal of Medicine* 319, 525-532.

Wada, M., DeLong, C., Hong, Y.H., Rieke, C.J., Song, I., Sidhu, R.S., Yuan, C., Warnock, M., Schamaier, A.H., Yokoyama, C., Smyth, E.M., Wilson, S.J., FitzGerald, G.A., Garavito, R.M., Sui, D.X., Regan, J.W., and Smith, W.L. (2007). Enzymes and receptors of prostaglandin pathways with arachidonic acid-derived versus eicosapentaenoic acid-derived substrates and products. *The Journal of Biological Chemistry* 282, 22254-22266.

Waghray, A., Feroze, F., Schober, M.S., Yao, F., Wood, C., Puravs, E., Krause, M., Hanash, S., and Chen, Y.Q. (2001). Identification of androgen-regulated genes in the prostate cancer cell line LNCaP by serial analysis of gene expression and proteomic analysis. *Proteomics* 1, 1327-1338.

Wang, D., and Dubois, R.N. (2006). Prostaglandins and cancer. *Gut* 55, 115-122.

Wang, D., and DuBois, R.N. (2010). The role of COX-2 in intestinal inflammation and colorectal cancer. *Oncogene* 29, 781-788.

Wang, D, Wang, H., and Shi, Q., (2004). Prostaglandin E(2) promotes colorectal adenoma growth via transactivation of the nuclear peroxisome proliferator-activated receptor delta. *Cancer Cell* 6, 285-295.

Wasilewicz, M.P., Kołodziej, B., Bojułko, T., Kaczmarczyk, M., Sulzyc-Bielicka, V., Bielicki, D., and Ciepiela, K. (2010). Overexpression of 5-lipoxygenase in sporadic colonic adenomas and a possible new aspect of colon carcinogenesis. *International Journal of Colorectal Disease* 25, 1079-1085.

Wassall, S.R., and Stillwell, W. (2009). Polyunsaturated fatty acid-cholesterol interactions: domain formation in membranes. *Biochim Biophys Acta* 1788, 24-32.

Weigert, J., Obermeier, F., Neumeier, M., Wanninger, J., Filarsky, M., Bauer, S., Aslanidis, C., Rogler, G., Ott, C., Schäffler, A., Schölmerich, J., and Buechler, C. (2010). Circulating levels of chemerin and adiponectin are higher in ulcerative colitis and chemerin is elevated in Crohn's disease. *Inflamm Bowel Dis* 16, 630-637.

West, N.J., Clark, S.K., Phillips, R.K.S., Hutchinson, J.M., Leicester, R.J., Belluzzi, A., and Hull, M.A. (2010). Eicosapentaenoic acid reduces rectal polyp number and size in familial adenomatous polyposis. *Gut* 59, 918-925.

Weylandt, K.H., Krause, L.F., Gomolka, B., Chiu, C.Y., Bilal, S., Nadolny, A., Waechter, S.F., Fischer, A., Rothe, M., and Kang, J.X. (2011). Suppressed liver tumorigenesis in

fat-1 mice with elevated omega-3 fatty acids is associated with increased omega-3 derived lipid mediators and reduced TNF- α . *Carcinogenesis* 32, 897-903.

Winawer, S.J., Zauber, A.G., Fletcher, R.H., Stillman, J.S., O'Brien, M.J., Levin, B., Smith, R.A., Lieberman, D.A., Burt, R.W., Levin, T.R., Bond, J.H., Brooks, D., Byers, T., Hyman, N., Kirk, L., Thorson, A., Simmang, C., Johnson, D., and Rex, D.K. (2006). Guidelines for colonoscopy surveillance after polypectomy: a consensus update by the US Multi-Society Task Force on Colorectal Cancer and the American Cancer Society. *Gastroenterology* 130, 1872-1885.

Wong, W.M., and Wright, N.A. (1999). Cell proliferation in gastrointestinal mucosa. *J Clin Path* 52, 321-333.

Wittamer, V., Jean-Denis Franssen, J.D., Vulcano, M., Jean-François Mirjolet, J-F., Emmanuel Le Poul, E., Migeotte, I., Brézillon, S., Tyldesley, R., Blanpain, C., Detheux, M., Mantovani, A., Sozzani, S., Gilbert Vassart, G., Parmentier, M., and David Communi. (2003). Specific recruitment of antigen presenting cells by chemerin, a novel processed ligand from human inflammatory fluids. *JEM* 198, 977-985.

Wittamer, V., Gregoire, F., Robberecht, P., Vassart, G., Communi, D., and Parmentier, M. (2004). The C-terminal nonapeptide of mature chemerin activates the chemerin receptor with low nanomolar potency. *Journal of Biological Chemistry* 279, 9956-9962.

Wittekind, C., and Oberschmid, B. 2010. TNM classification of malignant tumours. *Pathologie*, 31, 333-338.

World Cancer Research Fund/ American Institute for Cancer Research. <http://www.dietandcancerreport.org>. accessed 10th December 2013.

Wu, S., Feng, B., Li, K., Zhu, X., Liang, S., Liu, X., Han, S., Wang, B., Wu, K., Miao, D., Liang, J., and Fan, D. (2012). Fish consumption and colorectal cancer risk in humans: a systematic review and meta-analysis. *Am J Med* 125, 551-559.

Wu, X., Ye, Y., Rosell, R., Amos, C.I., Stewart, D.J., Hildebrandt, M.A.T., Roth, J.A., Minna, J.D., Gu, J., Lin, J., Buch, S.C., Nukui, T., Serrano, J.L.R., Taron, M., Cassidy, A., Lu, C., Chang, J.Y., Lippman, S.M., Hong, W.K., Spitz, M.R., Romkes, M., and Yang, P. (2011). Genome-wide association study of survival in non-small cell lung cancer patients receiving platinum-based chemotherapy. *Journal of the National Cancer Institute* 103, 817-825.

Xie, L., Law, B.K., Chtil, A.M., Brown, K.A., Aakre, M.E., and Moss, H.L. (2004). Activation of the Erk pathway is required for TGF- β induced EMT *in vitro*. *Neoplasia* 6, 603-610.

Ye, Y.N., Liu, E.S., Shin, V.Y., Wu, W.K., Luo, J.C., and Cho, C.H. (2004). Nicotine promoted colon cancer growth via epidermal growth factor receptor, c-src, and 5-lipoxygenase-mediated signal pathway. *The Journal of Pharmacological Experimental Therapeutics* 308, 66-72.

Yokomizo, T., Kato, K., Terawaki, K., Izumi, T., and Shimizu, T. (2000). A second leukotriene B(4) receptor, BLT2. A new therapeutic target in inflammation and immunological disorders. *J Exp Med* 192, 421-432.

Yu, W., Chen, L., Yang, Y.Q., Falck, J.R., Guo, A.M., Li, Y., and Yang, J. (2011). Cytochrome P450 ω -hydroxylase promotes angiogenesis and metastasis by upregulation of VEGF and MMP-9 in non-small cell lung cancer. *Cancer Chemother Pharmacol* 68, 619-29.

Yu, H.G., Huang, J.A., Yang, Y.N., Huang, H., Luo, H.S., Yu, J.P., Meier, J.J., Schrader, H., Bastian, A., Schmidt, W.E., and Schmitz, F. (2002). The effects of acetylsalicylic acid on proliferation, apoptosis, and invasion of cyclooxygenase-2 negative colon cancer cells. *Eur J Clin Invest* 32, 838-46.

Zabel BA, Ohyama T, Zuniga L, Kim JY, Johnston B, Allen SJ, Guido DG, Handel TM, and Butcher EC. (2006) Chemokine-like receptor 1 expression by macrophages in vivo: regulation by TGF-beta and TLR ligands. *Exp Hematol* 34, 1106-1114.

Zhang H and Sun XF. (2002). Overexpression of cyclooxygenase-2 correlates with advanced stages of colorectal cancer. *American Journal of Gastroenterology* 97, 1037-1041.

Zhang, L., Yu, J., Park, B.H., Kinzler, K.W., and Vogelstein, B. (2000). Role of BAX in the apoptotic response to anticancer agents. *Science* 290, 989-992.

Zhang, Z., and DuBois R.N. (2000). Par-4, a proapoptotic gene, is regulated by NSAIDs in human colon carcinoma cells. *Gastroenterology* 118, 1012-1017.

8 Appendices



National Research Ethics Service

NRES Committee Yorkshire & The Humber - Leeds Central

Yorkshire and Humber REC Office
 First Floor, Millside
 Mill Pond Lane
 Meanwood
 Leeds
 LS6 4RA

Telephone: 0113 3050127

02 June 2011

Professor Mark Hull
 Professor of Molecular Gastroenterology
 University of Leeds
 Leeds Institute of Mol. Medicine
 St James's University Hospital
 Leeds
 LS9 7TF

Dear Professor Hull

Study title: ChemR23 and BLT1 receptor expression in colorectal tumours
REC reference: 11/YH/0157

The Research Ethics Committee reviewed the above application at the meeting held on 20 May 2011. Thank you for attending to discuss the study.

Ethical opinion

The Committee advised you that a lay summary of the study is required.

The members of the Committee present gave a favourable ethical opinion of the above research on the basis described in the application form, protocol and supporting documentation, subject to the conditions specified below.

Conditions of the favourable opinion

The favourable opinion is subject to the following conditions being met prior to the start of the study.

Management permission or approval must be obtained from each host organisation prior to the start of the study at the site concerned.

Management permission ("R&D approval") should be sought from all NHS organisations involved in the study in accordance with NHS research governance arrangements.

Guidance on applying for NHS permission for research is available in the Integrated Research Application System or at <http://www.rdforum.nhs.uk>.

Where a NHS organisation's role in the study is limited to identifying and referring potential participants to research sites ("participant identification centre"), guidance should be sought from the R&D office on the information it requires to give permission for this activity.

This Research Ethics Committee is an advisory committee to the Yorkshire and The Humber Strategic Health Authority
 The National Research Ethics Service (NRES) represents the NRES Directorate within
 the National Patient Safety Agency and Research Ethics Committees in England

Appendix 1. Research ethics committee approval letter.

Committee approval letter, for the ChemR23 and BLT1 receptor expression in colorectal tumours study. REC reference 11/YH/0157. Meeting attended by candidate.

For non-NHS sites, site management permission should be obtained in accordance with the procedures of the relevant host organisation.

Sponsors are not required to notify the Committee of approvals from host organisations

1. A lay summary of the study is required.

It is responsibility of the sponsor to ensure that all the conditions are complied with before the start of the study or its initiation at a particular site (as applicable).

You should notify the REC in writing once all conditions have been met (except for site approvals from host organisations) and provide copies of any revised documentation with updated version numbers. Confirmation should also be provided to host organisations together with relevant documentation

Approved documents

The documents reviewed and approved at the meeting were:

<i>Document</i>	<i>Version</i>	<i>Date</i>
Covering Letter		18 April 2011
Investigator CV		08 April 2011
Other: CV - John Hutchinson (student)		12 April 2011
Protocol	1	18 April 2011
REC application	1	18 April 2011
Referees or other scientific critique report		06 April 2011

Membership of the Committee

The members of the Ethics Committee who were present at the meeting are listed on the attached sheet.

Statement of compliance

The Committee is constituted in accordance with the Governance Arrangements for Research Ethics Committees (July 2001) and complies fully with the Standard Operating Procedures for Research Ethics Committees in the UK.

After ethical review

Now that you have completed the application process please visit the National Research Ethics Service website > After Review

You are invited to give your view of the service that you have received from the National Research Ethics Service and the application procedure. If you wish to make your views known please use the feedback form available on the website.

The attached document "After ethical review – guidance for researchers" gives detailed guidance on reporting requirements for studies with a favourable opinion, including:

- Notifying substantial amendments
- Adding new sites and investigators
- Progress and safety reports
- Notifying the end of the study

Research ethics committee approval letter.

Committee approval letter, for the ChemR23 and BLT1 receptor expression in colorectal tumours study. REC reference 11/YH/0157. Meeting attended by candidate.

Page 2 of 3.

The NRES website also provides guidance on these topics, which is updated in the light of changes in reporting requirements or procedures.

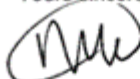
We would also like to inform you that we consult regularly with stakeholders to improve our service. If you would like to join our Reference Group please email referencegroup@nres.npsa.nhs.uk.

11/YH/0157

Please quote this number on all correspondence

With the Committee's best wishes for the success of this project

Yours sincerely



ML Dr Margaret L Faulk
Chair

Email: nicola.mallender-ward@nhs.net

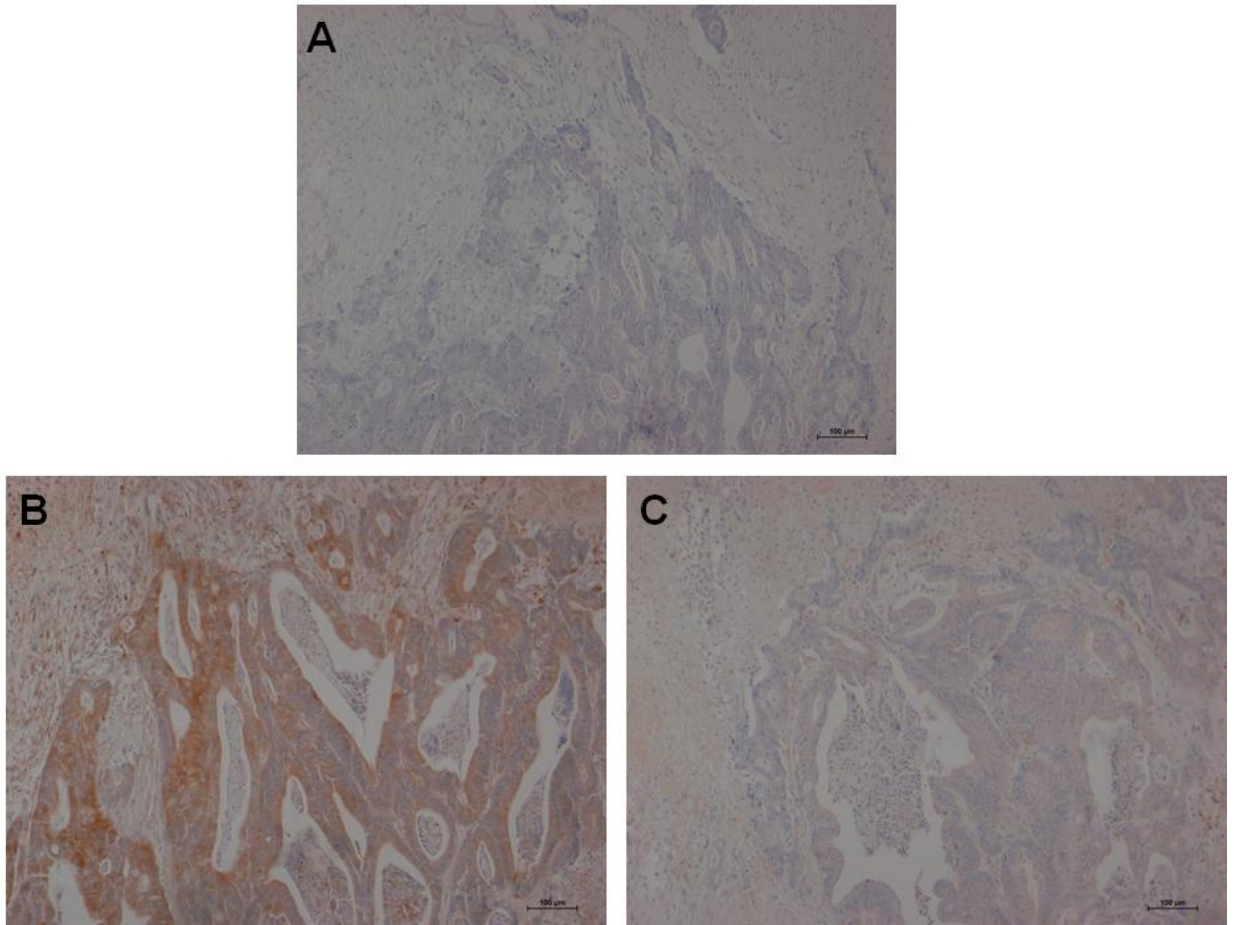
Enclosures: *List of names and professions of members who were present at the meeting and those who submitted written comments*

"After ethical review – guidance for researchers"

Copy to: *Mrs Rachel E De Souza, University of Leeds*
Mrs Anne Gowing, Leeds Teaching Hospitals NHS Trust

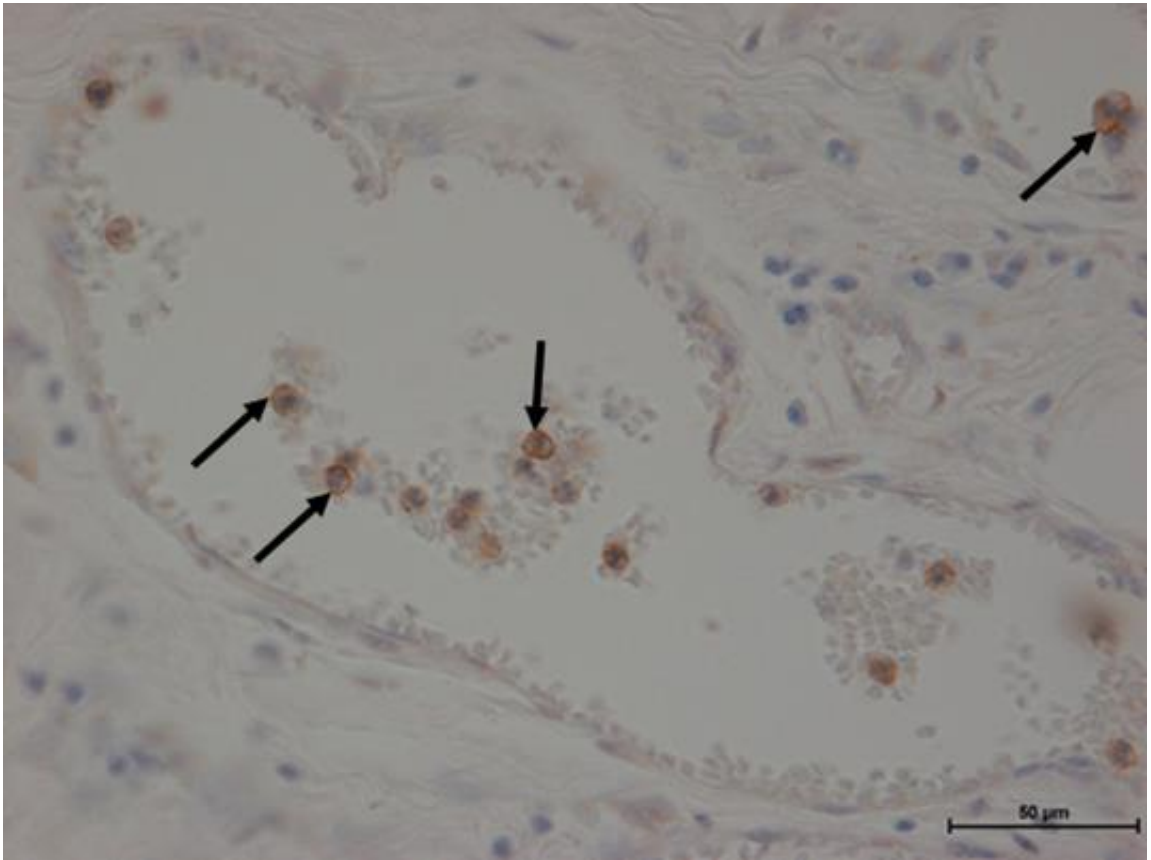
Research Ethics Committee approval letter.

Committee approval letter for the ChemR23 and BLT1 receptor expression in colorectal tumours study. REC reference 11/YH/0157. Meeting attended by candidate. Page 3 of 3.



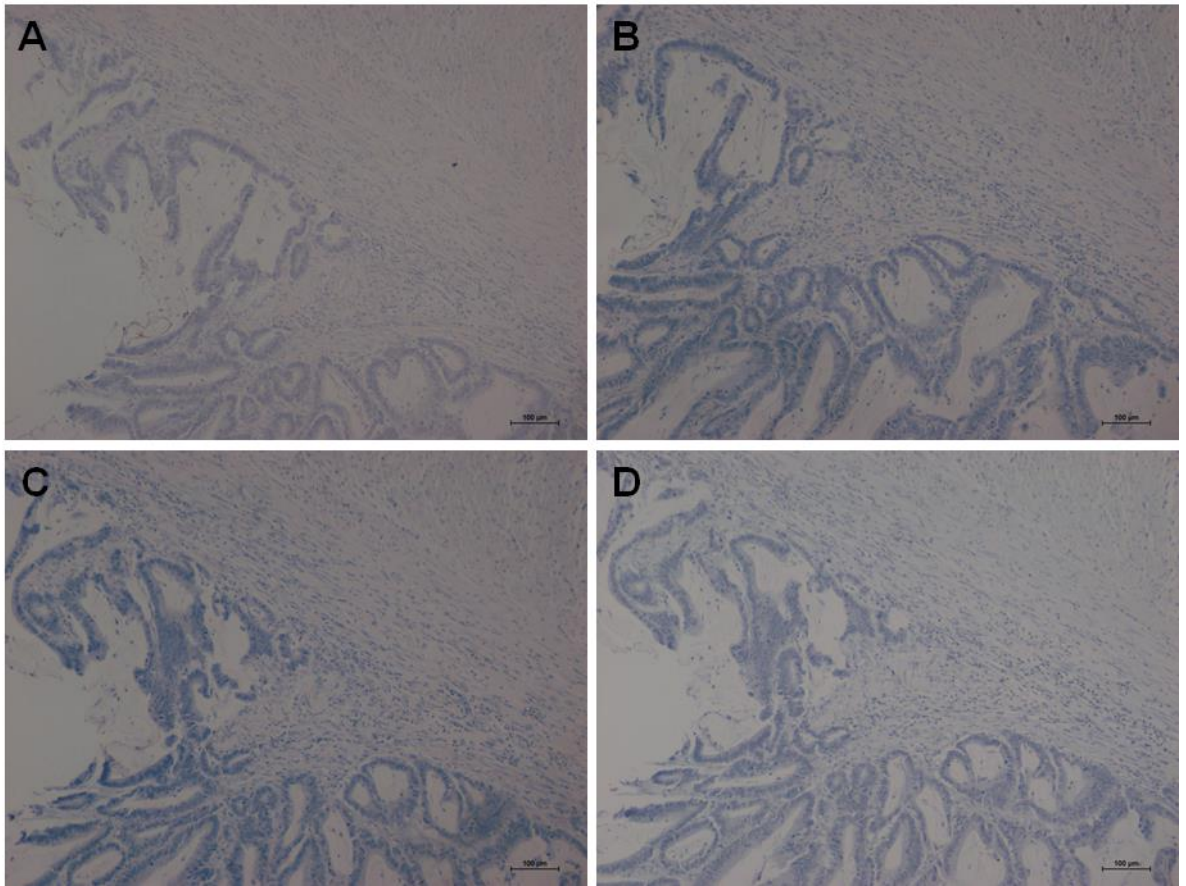
Appendix 2. BLT antibody optimisation for immunohistochemistry.

Human CRC tissue was probed for BLT1 expression using a rabbit polyclonal anti-BLT antibody (Cayman Chemicals) by IHC. Three sections were taken from the same FFPE human CRC tissue sample, two sections were probed for BLT1 using two different antibody concentrations and one section was used as a control (no primary antibody). A: No primary control. B: 1 in 1500 dilution. C: 1 in 2500 dilution. (Scale bars 100 µm).



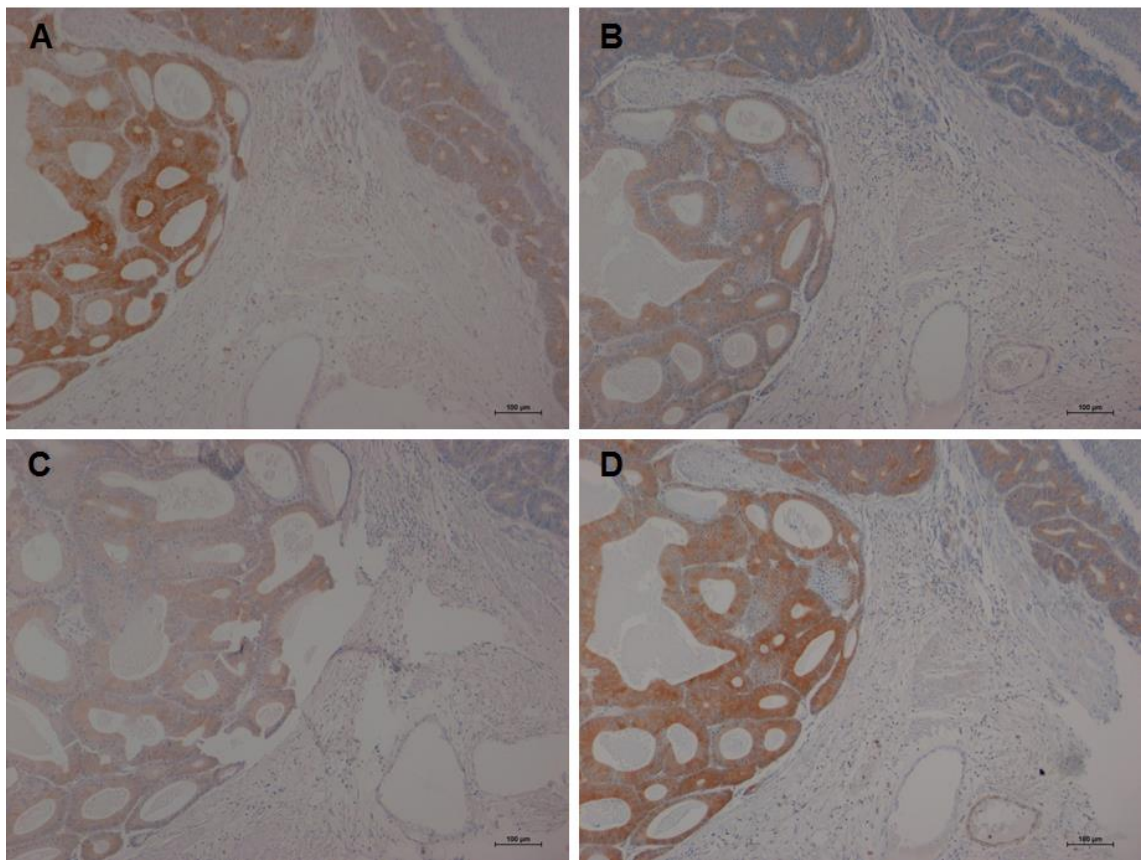
Appendix 3. Membranous BLT1 protein expression by human immune type cell.

Image taken from one of the FFPE human CRC tissue samples, which was probed for BLT1 expression by IHC (Cayman Chemical rabbit polyclonal antibody 1 in 1500 dilution). The arrow points to an immune cell. Further staining of the cells for specific immune cell markers would be needed to clarify the type of immune cell that is showing clear membranous staining. (Scale bar 50 μm).



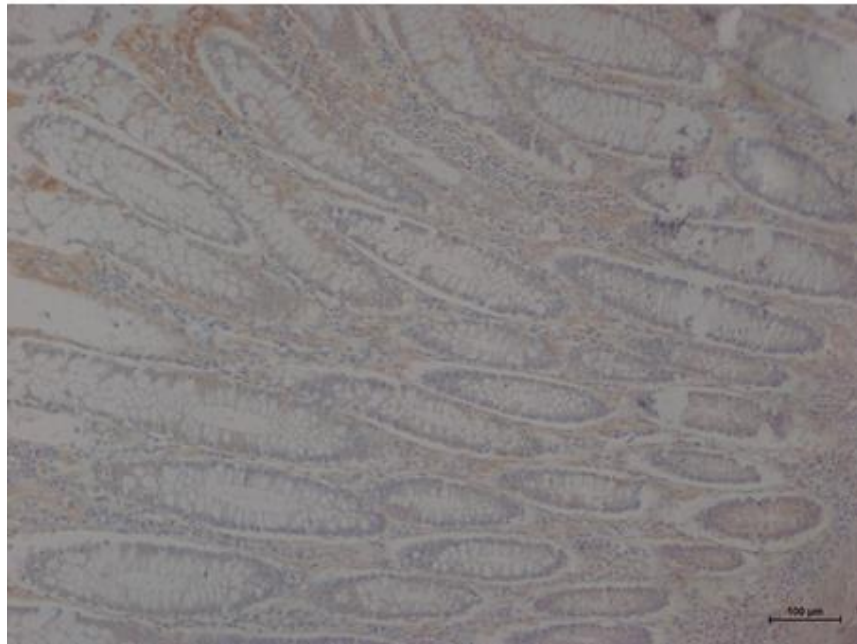
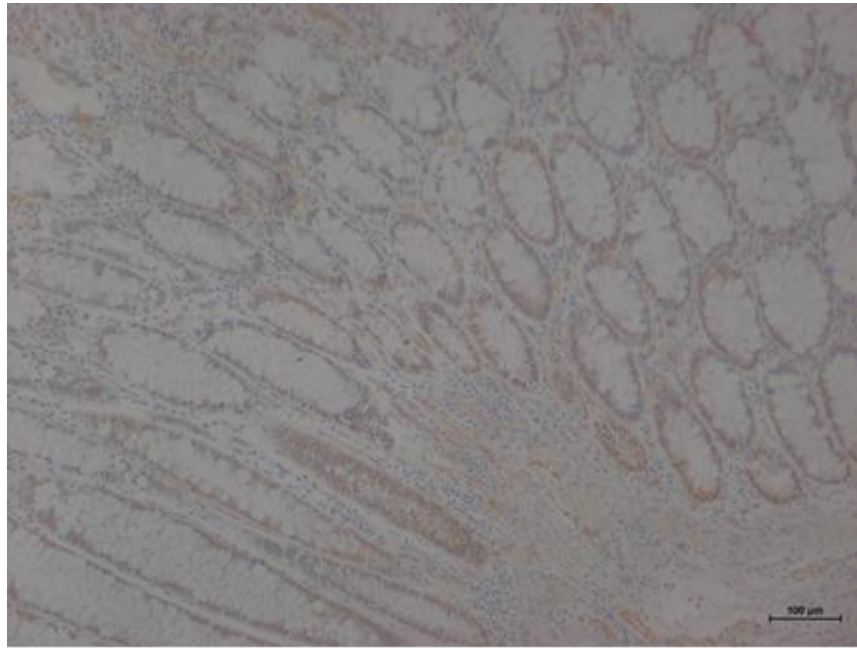
Appendix 4. No primary control images between different BLT1 immunohistochemistry runs.

The candidate stained 78 different FFPE human CRC tissue samples for BLT1 expression. Four different IHC runs were performed by the candidate. In each run a no primary antibody control slide was included (taken from the same CRC tissue sample). These images represent the no primary control in each of the four different IHC runs. A: Run 1. B: Run 2. C: Run 3. D: Run 4. (Scale bars 100 μm).



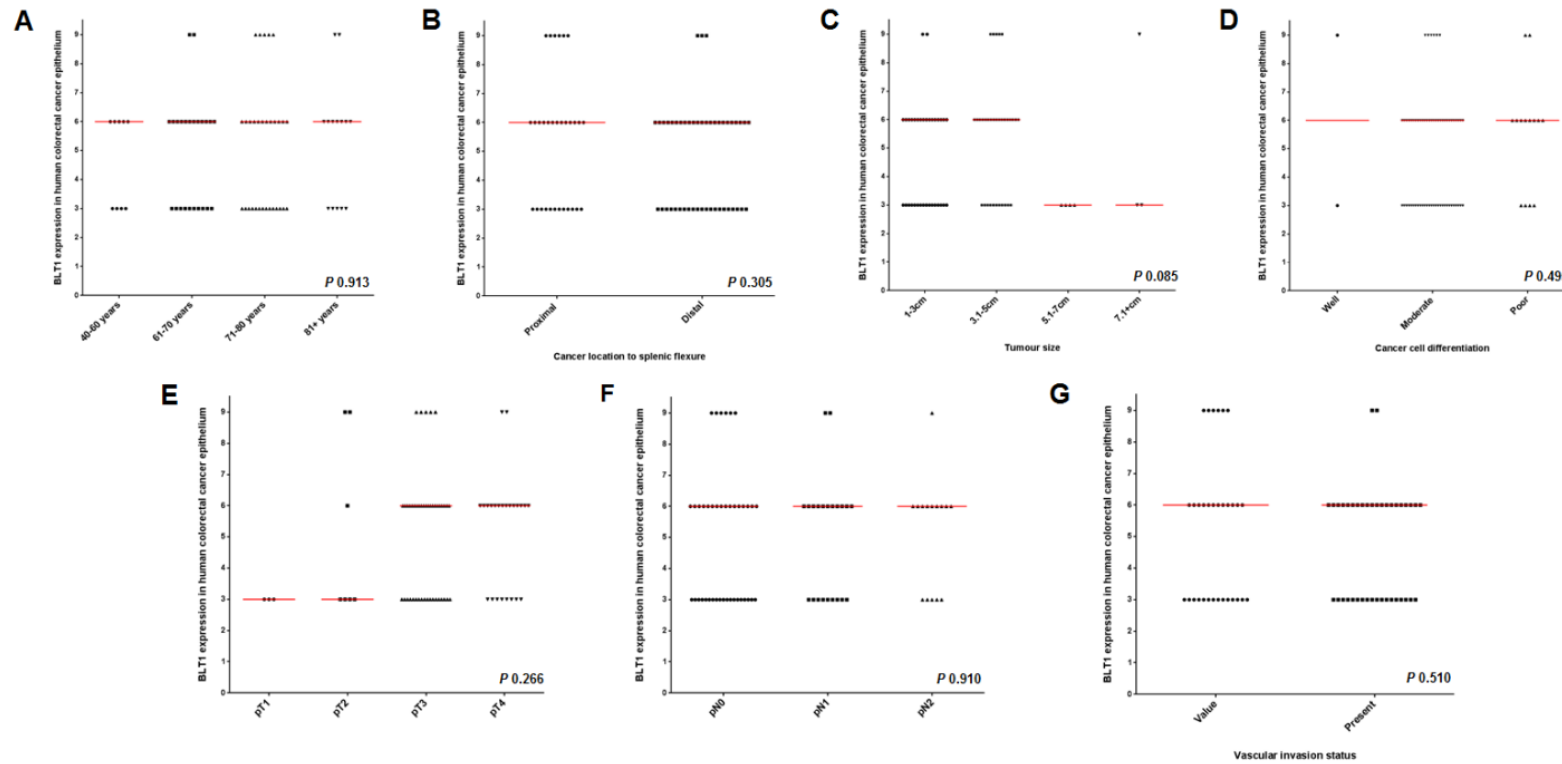
Appendix 5. BLT1 immunohistochemistry inter-run variability in a human CRC tissue sample.

The candidate stained 78 different FFPE human CRC tissue samples for BLT1 expression. Four different IHC runs were performed by the candidate. In each run a primary antibody control was included (taken from the same CRC tissue sample). These images represent the primary control in each of the four different IHC runs. A: Run 1. B: Run 2. C: Run 3. D: Run 4. (Scale bars 100 µm).



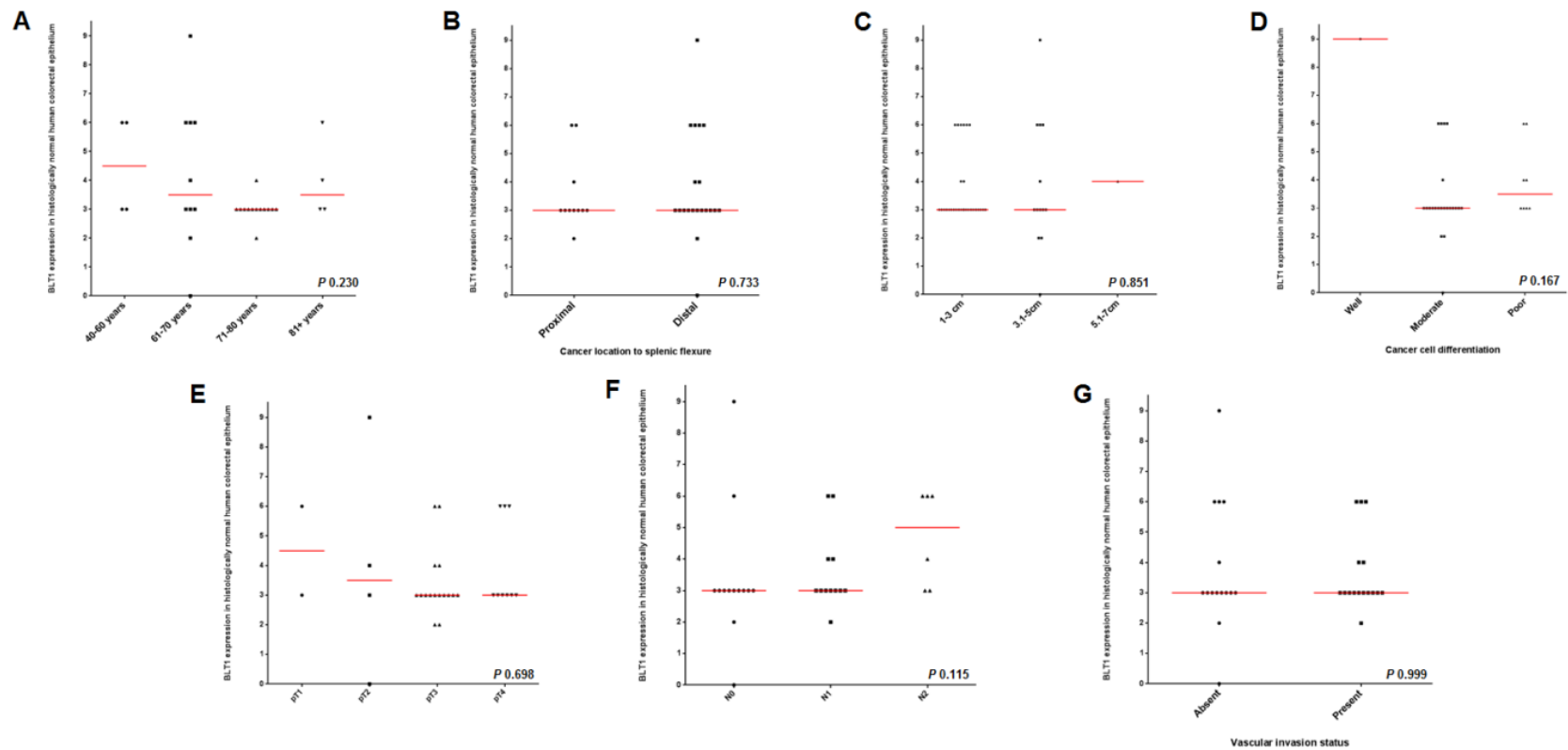
Appendix 6. BLT1 human CR epithelial and associated stromal expression by immunohistochemistry in two different human CRC tissue samples.

The candidate stained 78 different FFPE human CRC tissue samples for BLT1 expression (Cayman Chemicals rabbit polyclonal antibody; 1 in 1500 dilution). The above are presentative images of the human CR epithelium and associated stroma identified in the CRC tissue, from 31 of the 78 tissue samples examined by IHC. The candidate appreciates that the close proximity of this CR epithelium and associated stroma to the CRC tissue means that the epithelium and stroma does not truly represent normal CR epithelium and stroma as discussed in Chapter 3. (Scale bars 100 μm).



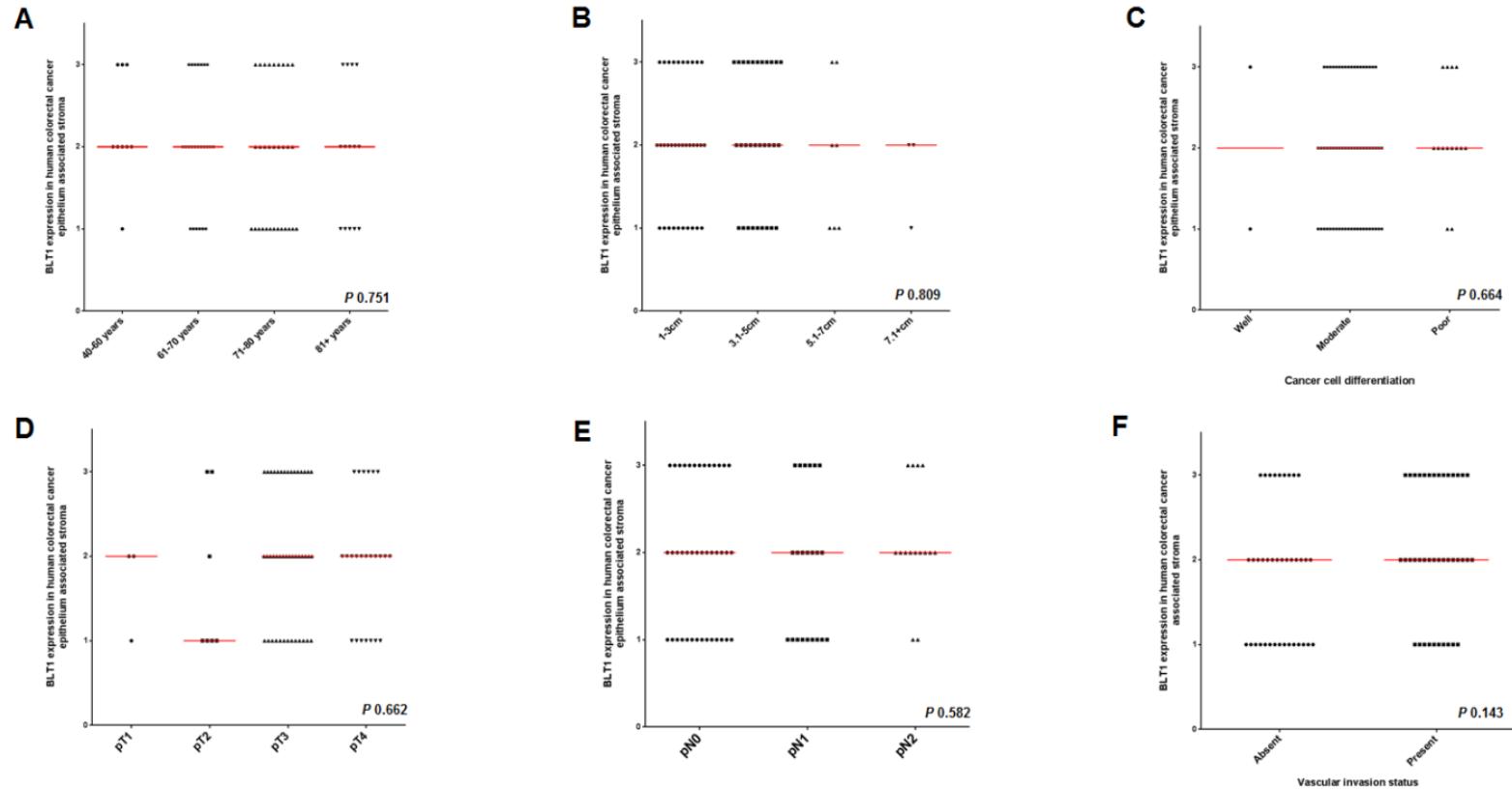
Appendix 7. Correlation of BLT1 expression in human CRC epithelium with age, cancer location, cancer size, cancer cell differentiation, pT, pN stage and vascular invasion status.

There were 78 different FFPE human CRC epithelium scored samples. Statistical analysis was performed on the total BLT1 expression score (I x P) for all samples. Statistical analysis was performed using SPSS. Correlation between BLT1 expression and age ($P = 0.913$, Kruskal-Wallis) (A). Correlation between BLT1 expression and cancer location to splenic flexure ($P = 0.305$, Mann-U Whitney) (B). Correlation between BLT1 expression and cancer size ($P = 0.085$, Kruskal-Wallis) (C). Correlation between BLT1 expression and cancer cell differentiation ($P = 0.495$, Kruskal-Wallis) (D). Correlation between BLT1 expression and cancer pT stage ($P = 0.266$, Kruskal-Wallis) (E). Correlation between BLT1 expression and cancer pN stage ($P = 0.910$, Kruskal-Wallis) (F). Correlation between BLT1 expression and cancer vascular invasion status ($P = 0.510$, Mann-U Whitney) (G). There was no statistically significant correlation ($P < 0.05$) between BLT1 expression and the clinic-pathological data.



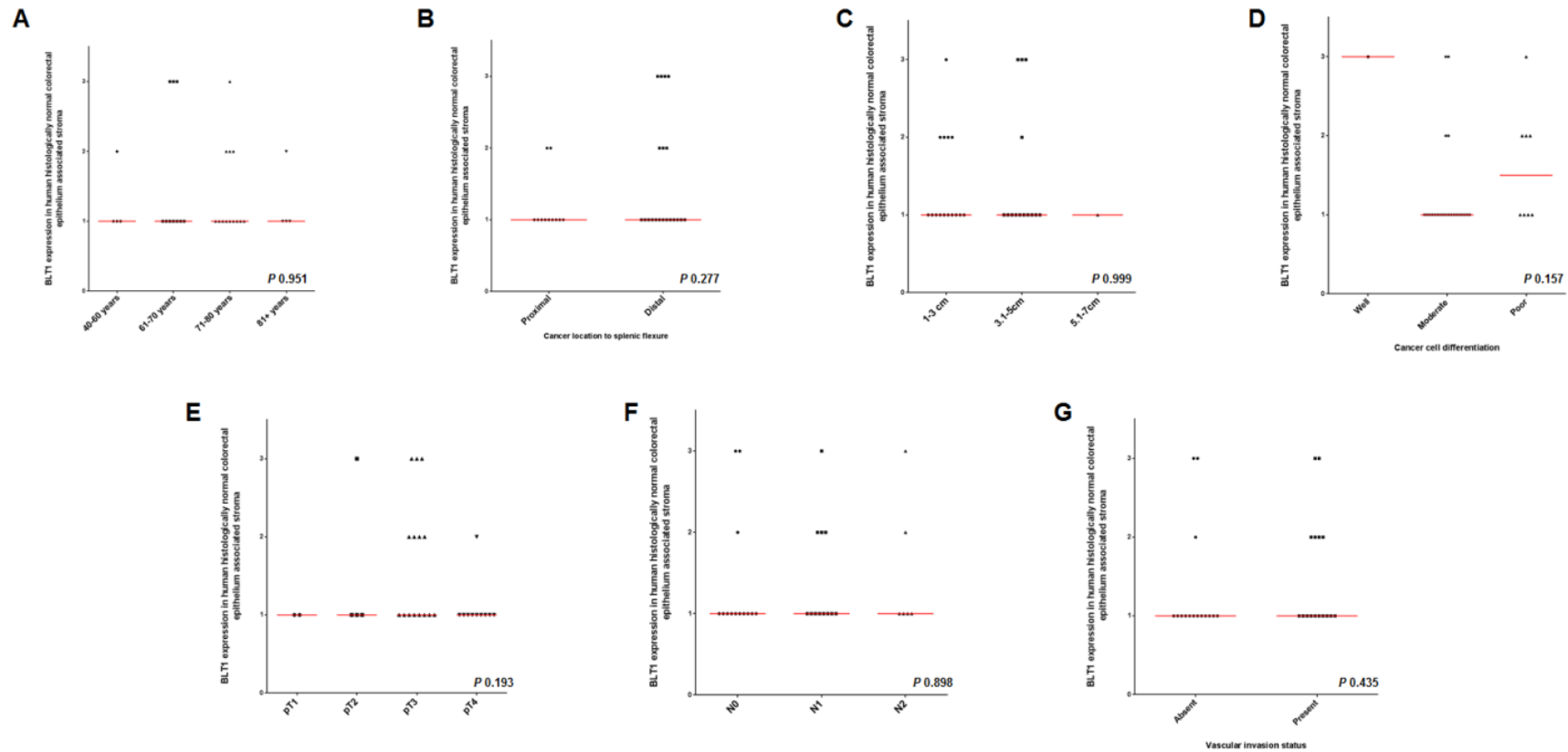
Appendix 8. Correlation of BLT1 expression in human histologically normal colorectal epithelium with age, cancer location, cancer size, cancer cell differentiation, pT, pN stage and vascular invasion status.

There were 31 different formalin fixed paraffin embedded human colorectal cancer samples containing histologically normal epithelium. Statistical analysis was performed on the total BLT1 expression score (I x P) for all samples. Statistical analysis was performed using SPSS. Correlation between BLT1 expression and age ($P = 0.230$, Kruskal-Wallis) (A). Correlation between BLT1 expression and cancer location to splenic flexure ($P = 0.733$, Mann-U Whitney) (B). Correlation between BLT1 expression and cancer size ($P = 0.851$, Mann-U Whitney) (C). Correlation between BLT1 expression and cancer cell differentiation ($P = 0.167$, Mann-U Whitney) (D). Correlation between BLT1 expression and cancer pT stage ($P = 0.698$, Kruskal-Wallis) (E). Correlation between BLT1 expression and cancer pN stage ($P = 0.115$, Kruskal-Wallis) (F). Correlation between BLT1 expression and cancer vascular invasion status ($P = 0.999$, Mann-U Whitney) (G). There was no statistically significant correlation ($P < 0.05$) between BLT1 expression and the clinic-pathological data.



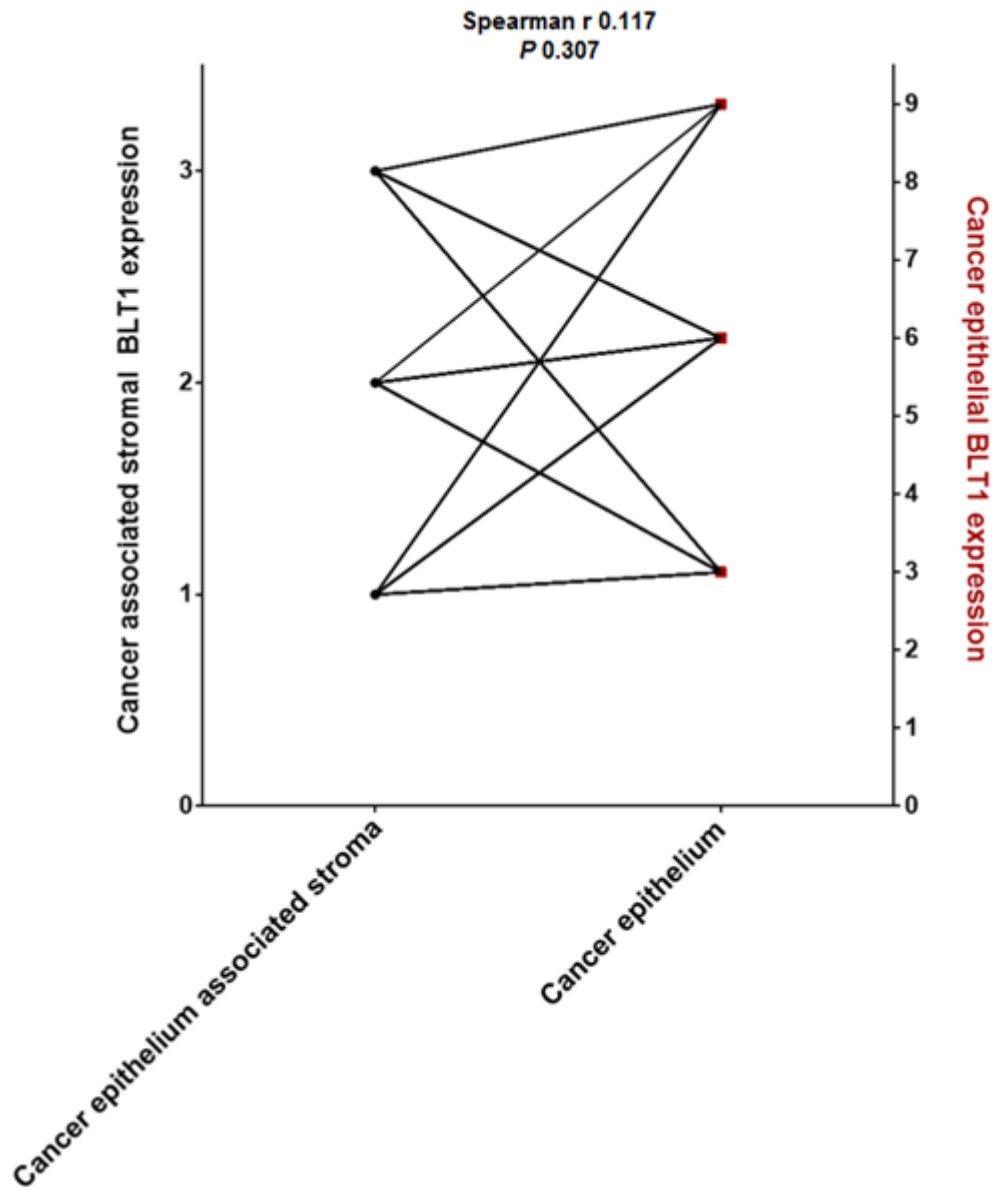
Appendix 9. Correlation of BLT1 expression in human CRC associated stroma with age, cancer size, cancer cell differentiation, pT, pN stages and vascular invasion status.

Statistical analysis was performed on the BLT1 expression score (I) for all 78 samples. Statistical analysis was performed using SPSS. Correlation between BLT1 expression and age ($P = 0.639$, Kruskal-Wallis) (A). Correlation between BLT1 expression and cancer size ($P = 0.809$, Mann-U Whitney) (B). Correlation between BLT1 expression and cancer cell differentiation ($P = 0.664$, Mann-U Whitney) (C). Correlation between BLT1 expression and cancer pT stage ($P = 0.662$, Kruskal-Wallis) (D). Correlation between BLT1 expression and cancer pN stage ($P = 0.582$, Kruskal-Wallis) (E). Correlation between BLT1 expression and cancer vascular invasion status ($P = 0.143$, Mann-U Whitney) (F). There was no statistically significant correlation ($P < 0.05$) between BLT1 expression and the clinic-pathological data shown.



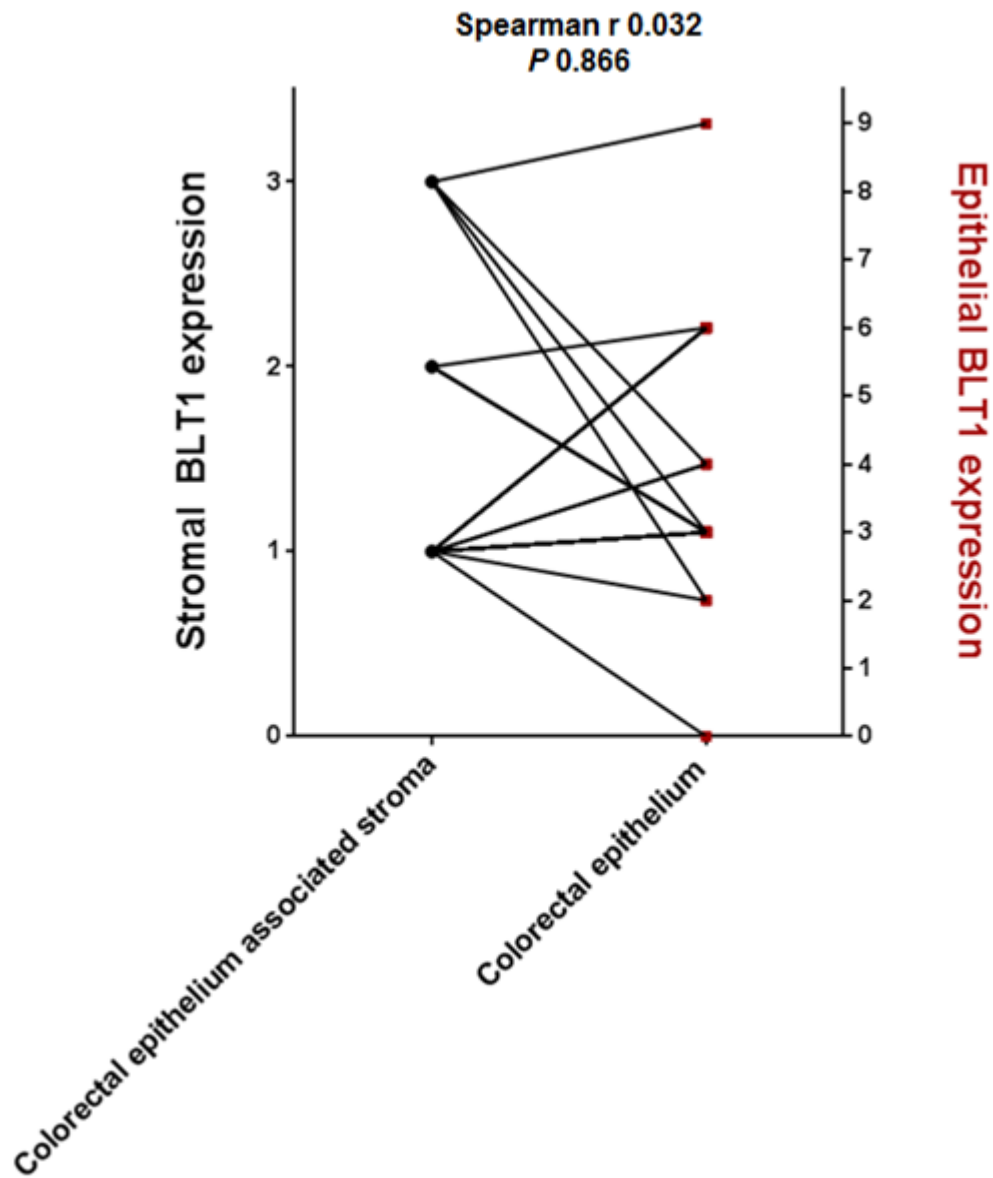
Appendix 10. Correlation of BLT1 expression in human histologically normal CR epithelium associated stroma with age, cancer location, cancer size, cancer cell differentiation, pT, pN stages and vascular invasion status.

Statistical analysis was performed on the BLT1 expression score (I) for all 78 samples. Statistical analysis was performed using SPSS. Correlation between BLT1 expression and age ($P = 0.951$, Kruskal-Wallis) (A). Correlation between BLT1 expression and cancer location ($P = 0.277$, Mann-U Whitney) (B). Correlation between BLT1 expression and cancer size ($P = 0.999$, Kruskal-Wallis) (C). Correlation between BLT1 expression and cancer cell differentiation ($P = 0.157$, Mann-U Whitney) (D). Correlation between BLT1 expression and cancer pT stage ($P = 0.193$, Kruskal-Wallis) (E). Correlation between BLT1 expression and cancer pN stage ($P = 0.898$, Kruskal-Wallis) (F). Correlation between BLT1 expression and cancer vascular invasion status ($P = 0.435$, Mann-U Whitney) (G). There was no statistically significant correlation ($P < 0.05$) between BLT1 expression and the clinic-pathological data shown.



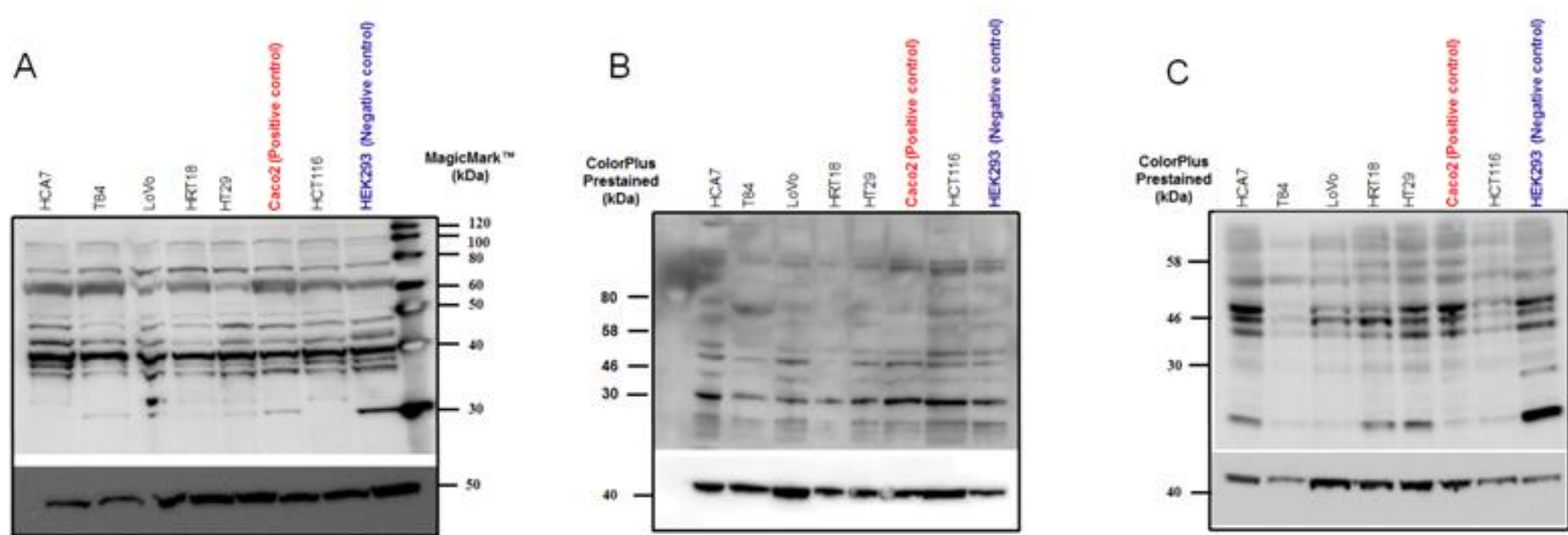
Appendix 11. Correlation of BLT1 expression between human CRC associated stroma and CRC epithelium.

Human CRC samples were probed for BLT1 expression. The samples were scored for BLT1 expression in the CRC epithelium associated stroma 0-3 and in the CRC epithelium 0-9 as described. Statistical analysis was performed using SPSS and spearman r correlation coefficient test. The spearman r value = 0.117 (95% confidence interval -0.115 to 0.337), $P = 0.307$.



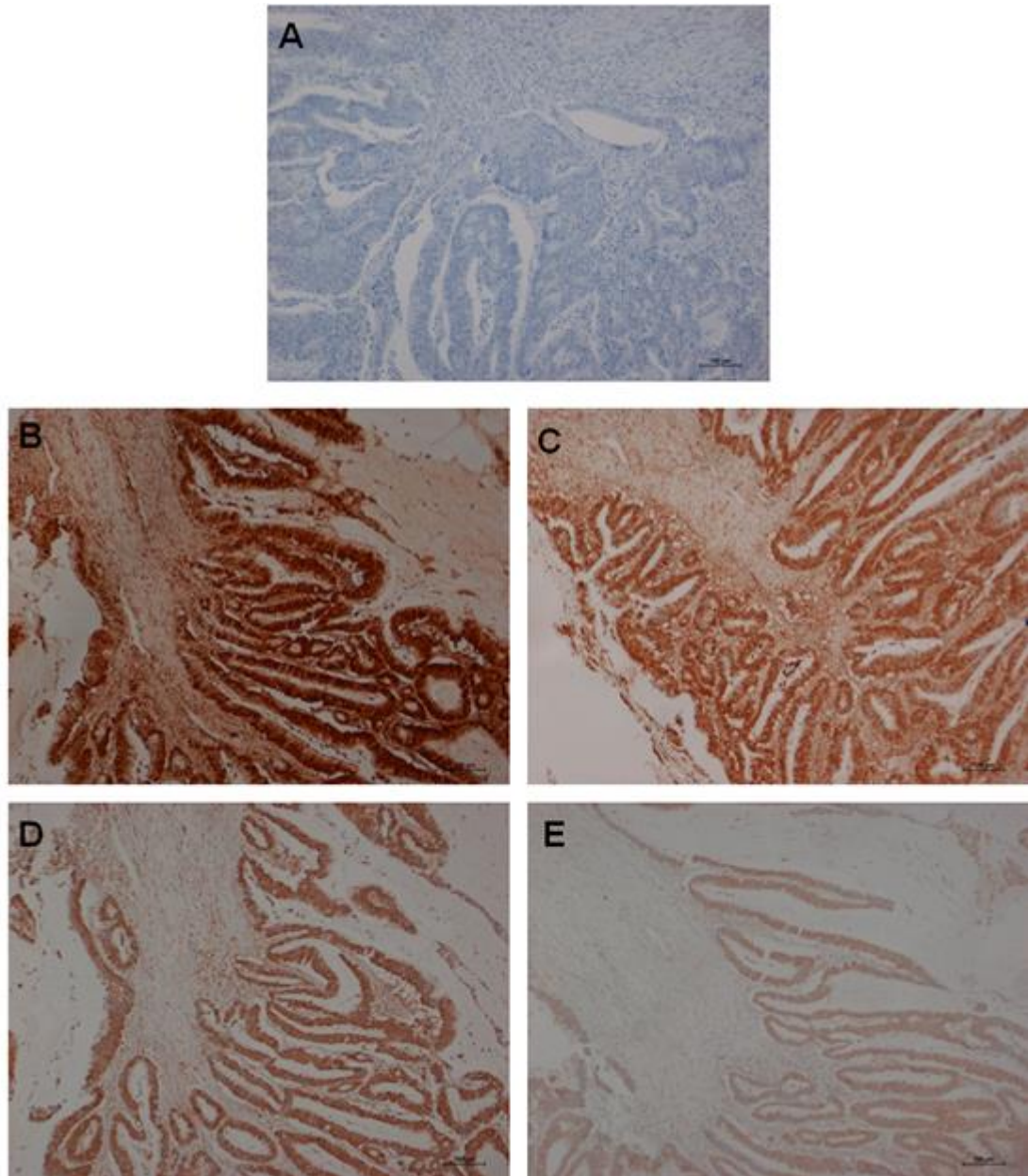
Appendix 12. Correlation of BLT1 expression between histologically normal human CR epithelium associated stroma and CR epithelium.

Thirty-one different FFPE human CRC samples were probed for BLT1 expression. The samples were scored for BLT1 expression in the histologically normal CR epithelium associated stroma 0-3 and in the CR epithelium 0-9 as described. Statistical analysis was performed using SPSS and spearman r correlation coefficient test. The spearman *r* value was 0.032 (95% confidence interval -0.336 to 0.391), *P* = 0.866.



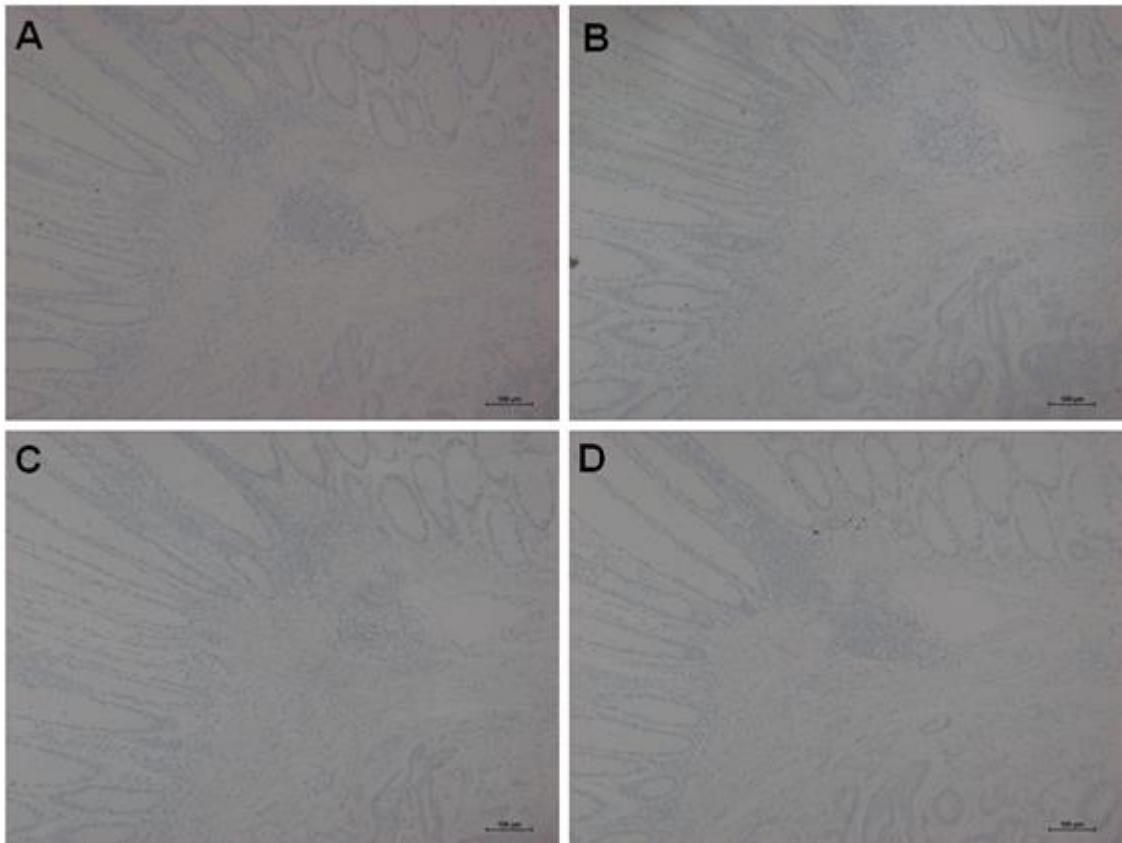
Appendix 13. Western blot analysis of ChemR23 receptor protein expression by three different commercially available anti-ChemR23 antibodies in a panel of seven different human CRC cell lines.

Thirty micrograms of human lysate was probed with either Novus Biologicals (rabbit polyclonal), R&D Systems (mouse monoclonal) or Abcam (rabbit polyclonal) anti-human ChemR23 antibodies, and probed with a secondary conjugated HRP antibody (1:2000). (A) Protein expression in a panel of human colorectal cancer cell lines and the negative control HEK293 cell line under high sensitivity chemiluminescence (30 seconds) using the Novus Biologicals anti-ChemR23 antibody (1:1000) with protein loading image using α -tubulin (1:5000), image under standard chemiluminescence (30 seconds). (B) Protein expression in a panel of human colorectal cancer cell lines and the negative control HEK293 cell line under high sensitivity chemiluminescence (15 seconds) with image using the R&D Systems anti-ChemR23 antibody (1:1000) with protein loading image using β -actin (1:5000), image under standard chemiluminescence (10 seconds). (C) Protein expression in a panel of human colorectal cancer cell lines and the negative control HEK293 cell line under high sensitivity chemiluminescence (90 seconds) with image using the Abcam anti-ChemR23 antibody (1:1000) with protein loading image using β -actin (1:5000), image under standard chemiluminescence (10 seconds).



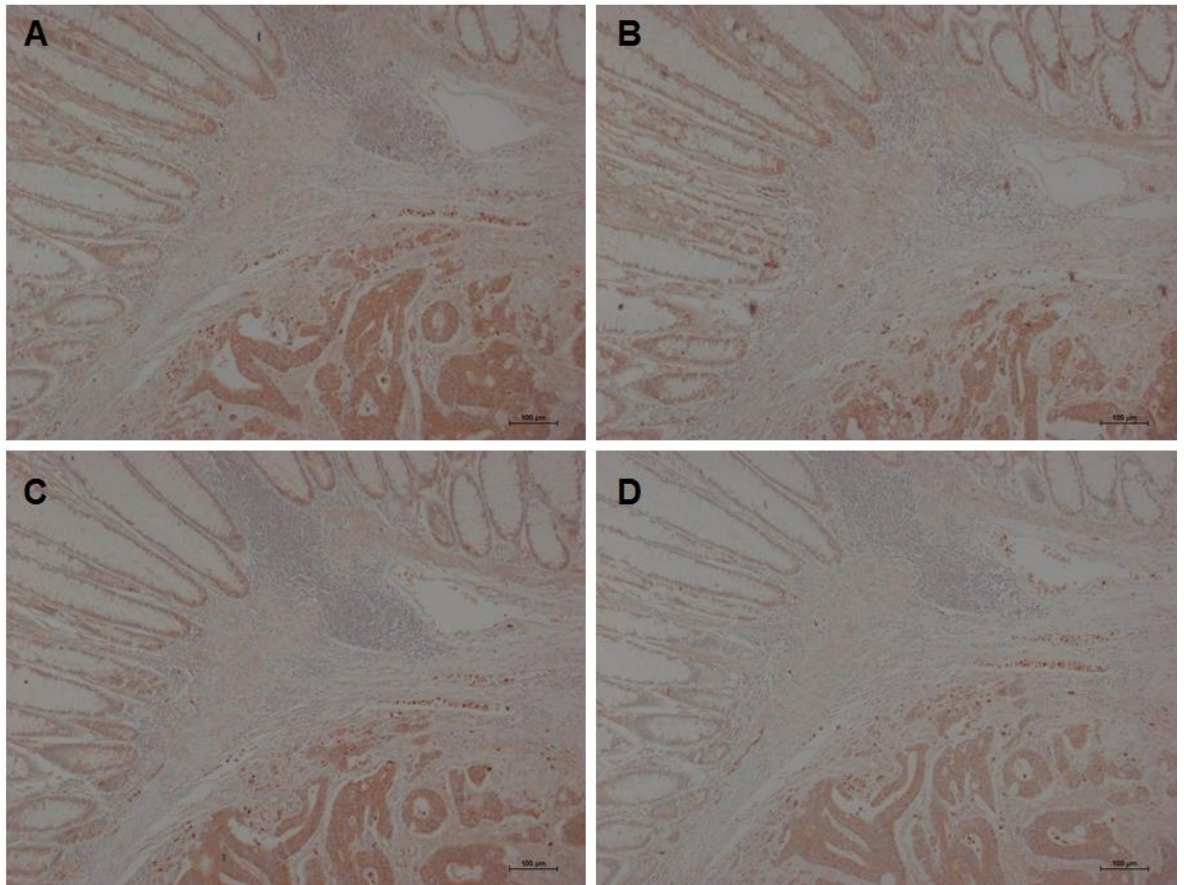
Appendix 14. ChemR23 antibody optimisation for immunohistochemistry.

Five sections were taken from the same FFPE human CRC tissue sample. The sections were probed for ChemR23, using a heat retrieval step (Bioss polyclonal anti-rabbit antibody) by IHC. A: No primary control. B: 1 in 50 dilution. C: 1 in 200 dilution. D: 1 in 500. C: 1 in 2000. (Scale bars 100 μ m).



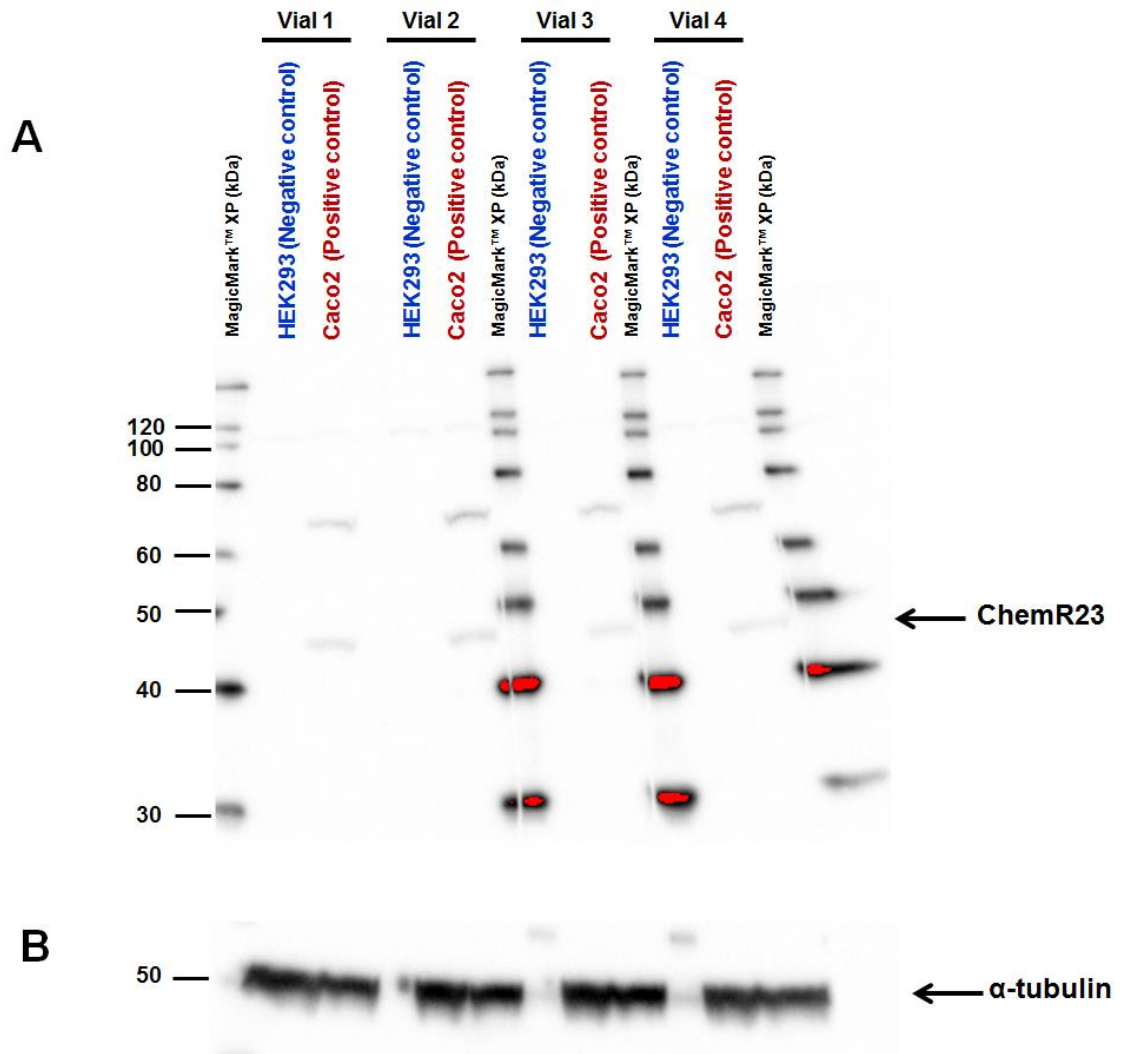
Appendix 15. No primary control images between different ChemR23 immunohistochemistry runs.

The candidate stained 73 different FFPE human CRC tissue samples for ChemR23 expression. Four different IHC runs were performed by the candidate. In each run a no primary antibody control was included (taken from the same CRC tissue sample). These images represent the no primary control in each of the four different IHC runs. A: Run 1. B: Run 2. C: Run 3. D: Run 4. (Scale bars 100 μm)



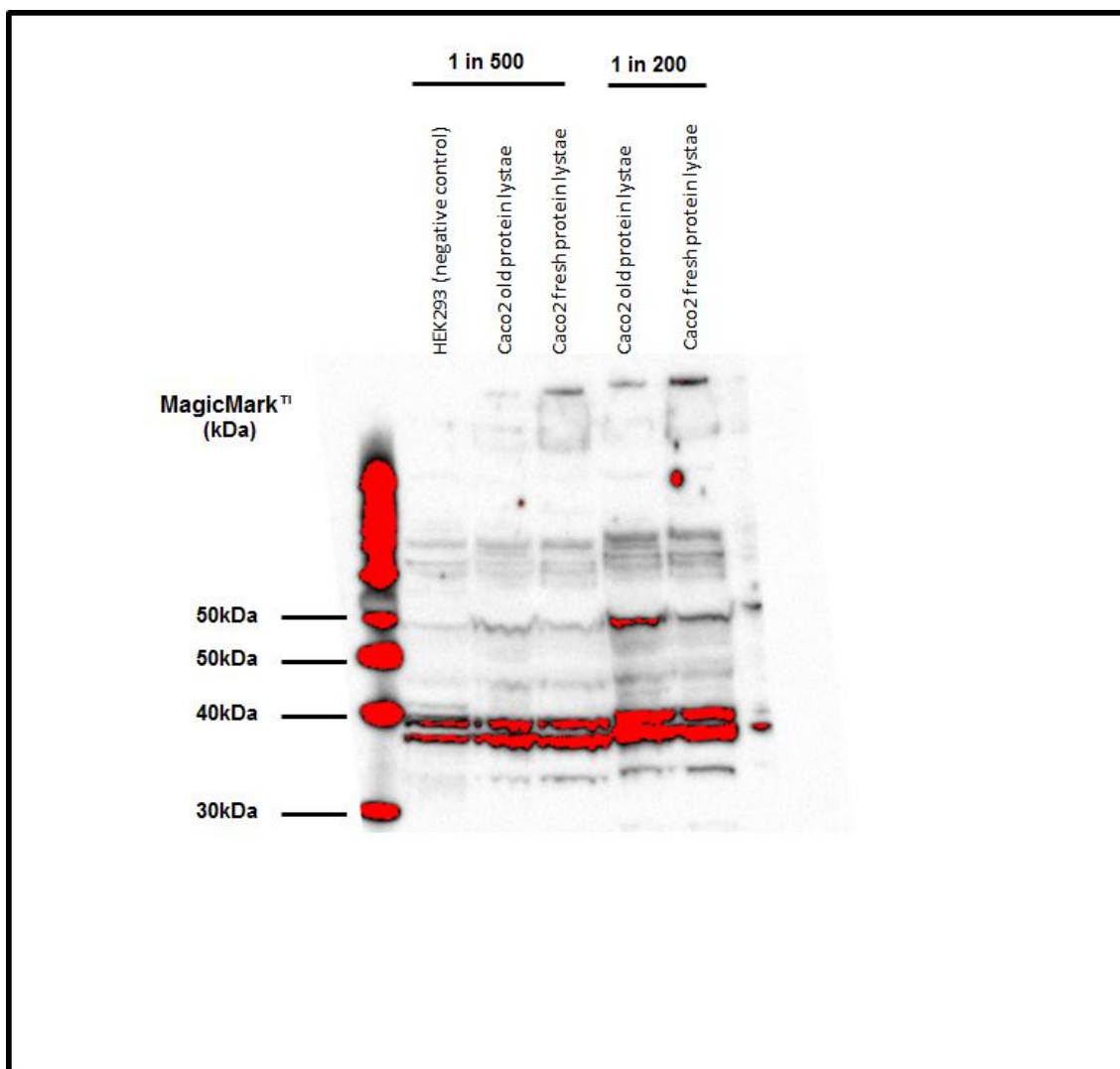
Appendix 16. ChemR23 immunohistochemistry inter-run variability in a human CRC tissue sample.

The candidate stained 73 different FFPE human CRC tissue samples for ChemR23 expression (Bioss polyclonal anti-rabbit antibody). Four different IHC runs were performed by the candidate. In each run a primary antibody control was included (taken from the same CRC tissue sample). These images represent the primary control in each of the four different IHC runs. A: Run 1. B: Run 2. C: Run 3. D: Run 4. (Scale bars 100 μm).



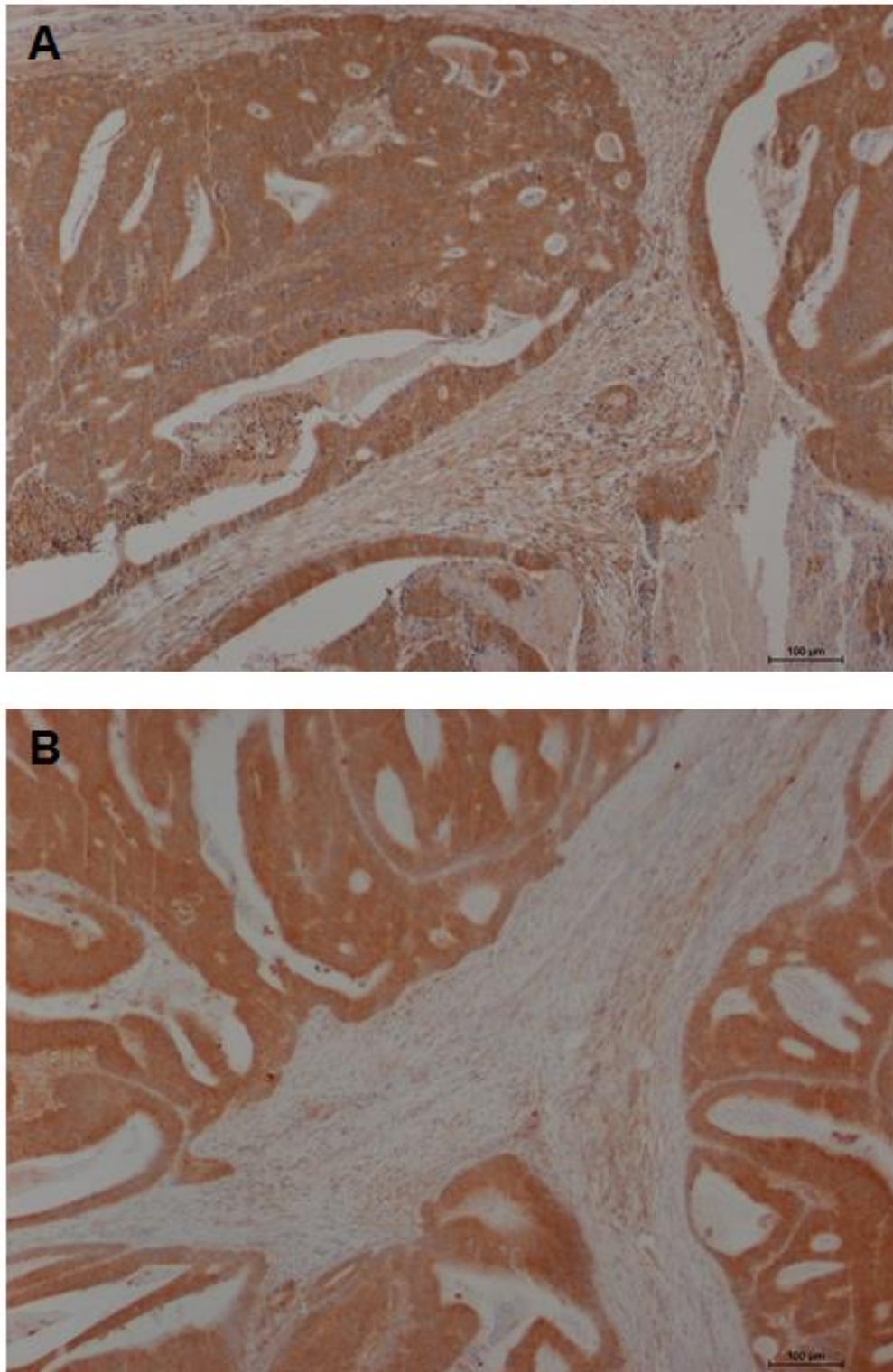
Appendix 17. Bioss anti-ChemR23 antibody sensitivity and specificity consistency between four different vials of antibody (bs-2530R.LOT 130320).

Human CRC protein lysate (HEK293 negative control; Caco2 positive control) was probed with Bioss anti-ChemR23 (BS2530R. lot 130320) from four separate vials at 1 in 500 dilution, then probed with a secondary conjugated HRP antibody (1:2000), equal protein loading was confirmed using α -tubulin (1:5000). (A) ChemR23 protein expression under standard chemiluminescence (five seconds). (B) Alpha-tubulin expression under standard chemiluminescence (one second). The specificity and sensitivity of all vials of Bioss anti-ChemR23 antibody were consistent between each vial. The vials were then mixed and this antibody master mix was used in the IHC ChemR23 expression study detailed in this thesis.



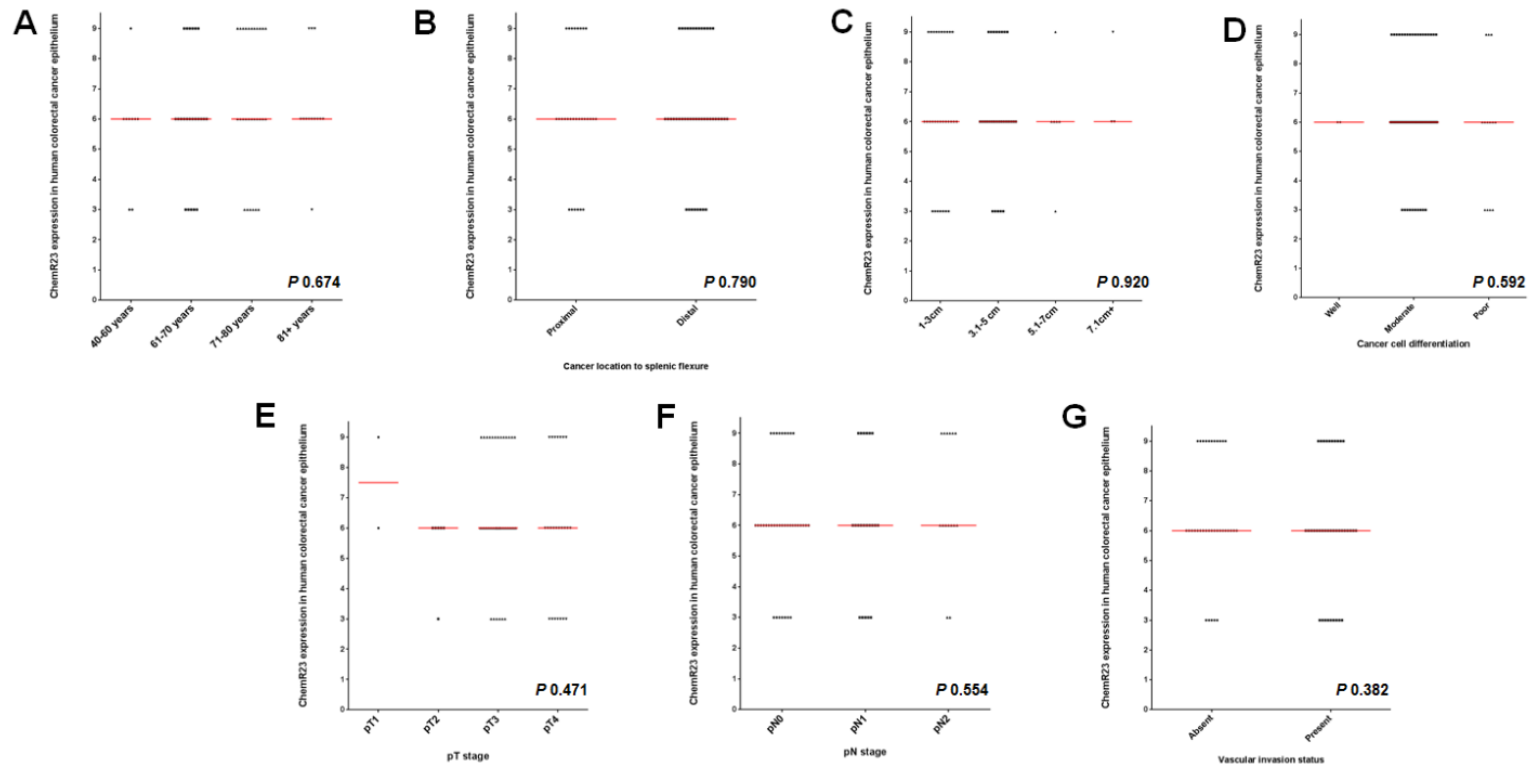
Appendix 18. Bioss anti-ChemR23 antibody sensitivity and specificity inconsistency between different LOTS (example shown BS2530R. lot YE1027W).

Human CRC protein lysate (HEK293 negative control; Caco2 positive control) was probed with Bioss anti-ChemR23, then probed with a secondary conjugated HRP antibody (1:500 or 1:200), equal protein loading was confirmed using α -tubulin (1:5000). Image taken under high sensitivity chemiluminescence.



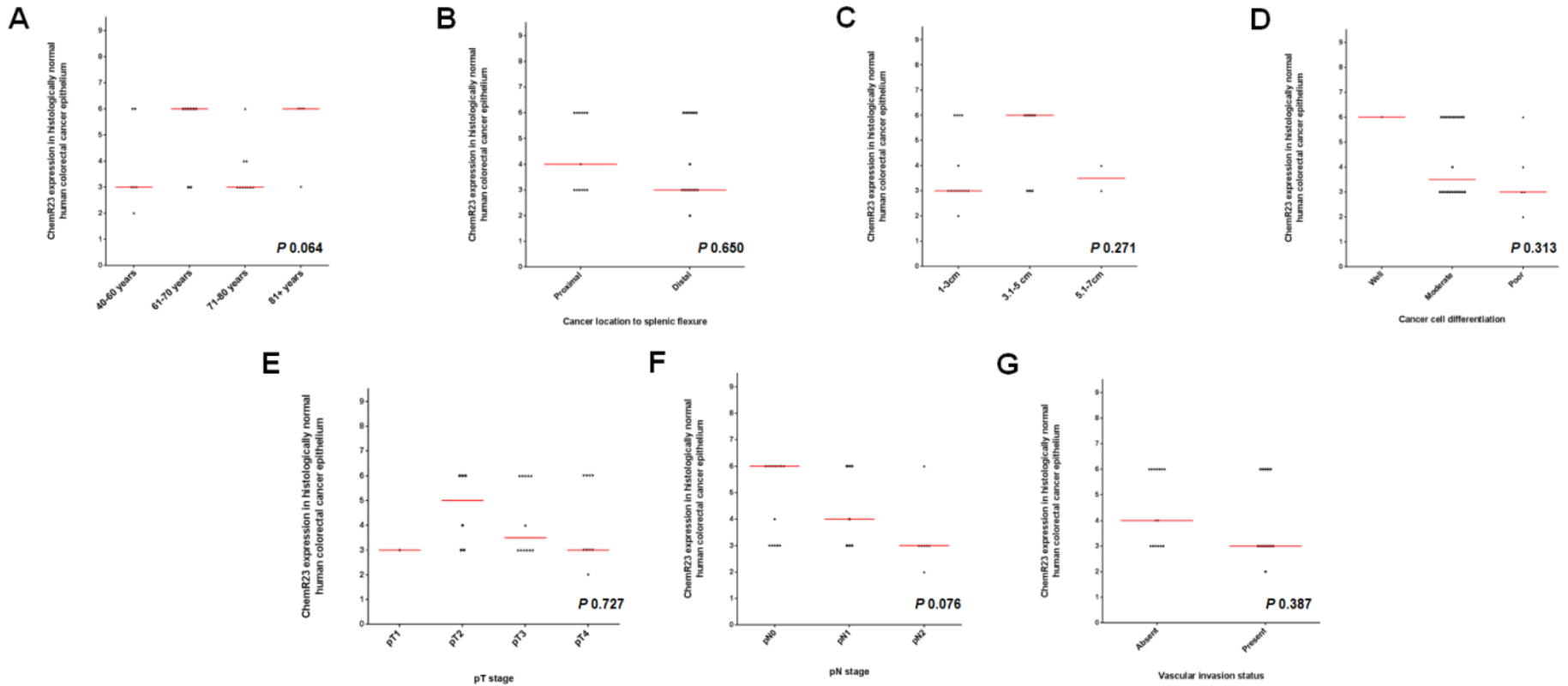
Appendix 19. ChemR23 expression in human CRC between two different batches of the same Bioss anti-ChemR23 antibody.

The same human CRC tissue was used for both batches of the anti-ChemR23 antibody. (A). Bioss anti-ChemR23 bs-2530R (lot: YE1215W), used initially then batch became unavailable (1:2000; Heat Retrieval). (B). Bioss anti-ChemR23 bs-2530R (lot: 130320), used for IHC study (1:25; Heat Retrieval). (Scale bars 100 µm).



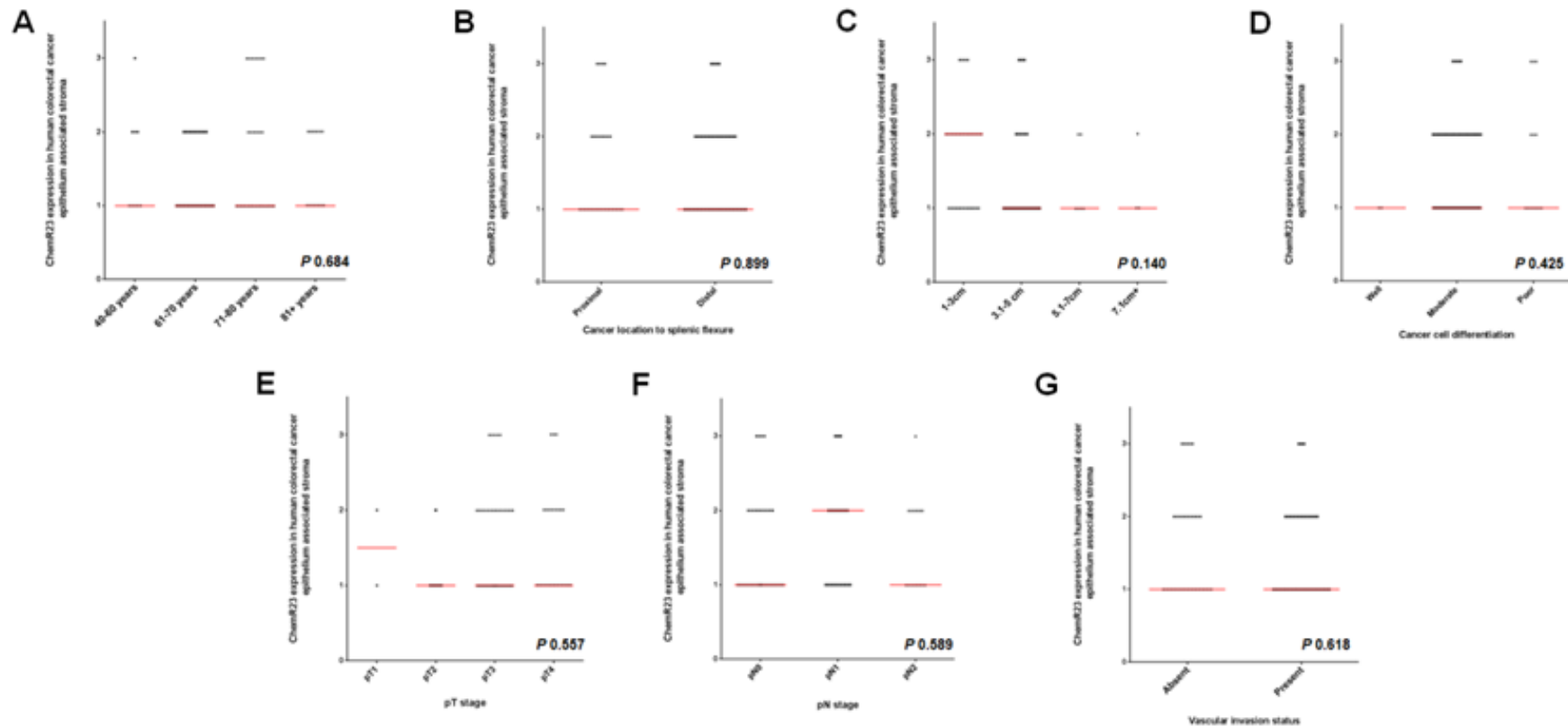
Appendix 20. Correlation of ChemR23 expression in human CRC epithelium with age, cancer location, cancer size, cancer cell differentiation, pT, pN stage and vascular invasion status.

There were 73 different FFPE human CRC epithelium scored samples. Statistical analysis was performed on the total ChemR23 expression score (I x P) for all samples. (A) Statistical analysis was performed using SPSS. Correlation between ChemR23 expression and age ($P = 0.674$, Kruskal-Wallis). (B) Correlation between ChemR23 expression and cancer location to splenic flexure ($P = 0.790$, Mann-U Whitney). (C) Correlation between ChemR23 expression and cancer size ($P = 0.920$, Kruskal-Wallis). (D) Correlation between ChemR23 expression and cancer cell differentiation ($P = 0.592$, Kruskal-Wallis). (E) Correlation between ChemR23 expression and cancer pT stage ($P = 0.471$, Kruskal-Wallis). (F) Correlation between ChemR23 expression and cancer pN stage ($P = 0.554$, Kruskal-Wallis). (G) Correlation between ChemR23 expression and cancer vascular invasion status ($P = 0.382$, Mann-U Whitney). There was no statistically significant correlation ($P < 0.05$) between ChemR23 expression and the clinic-pathological data.



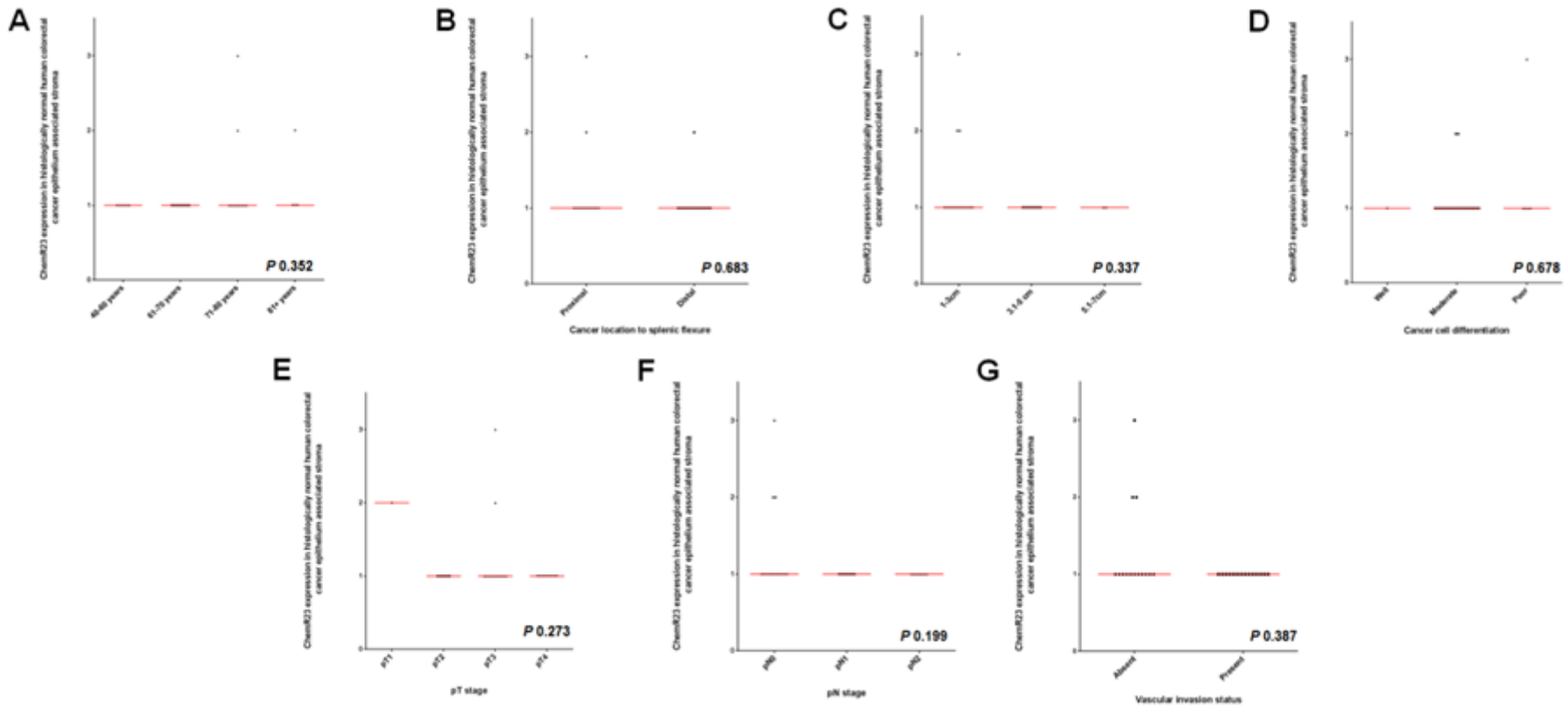
Appendix 21. Correlation of ChemR23 expression in histologically normal human CRC epithelium with age, cancer location, cancer size, cancer cell differentiation, pT, pN stage and vascular invasion status.

There were 28 different FFPE human CRC epithelium scored samples. Statistical analysis was performed on the total ChemR23 expression score (I x P) for all samples. Statistical analysis was performed using SPSS. Correlation between ChemR23 expression and age ($P = 0.064$, Kruskal-Wallis) (A). Correlation between ChemR23 expression and cancer location to splenic flexure ($P = 0.650$, Mann-U Whitney) (B). Correlation between ChemR23 expression and cancer size ($P = 0.271$, Kruskal-Wallis) (C). Correlation between ChemR23 expression and cancer cell differentiation ($P = 0.313$, Kruskal-Wallis) (D). Correlation between ChemR23 expression and cancer pT stage ($P = 0.727$, Kruskal-Wallis) (E). Correlation between ChemR23 expression and cancer pN stage ($P = 0.076$, Kruskal-Wallis) (F). Correlation between ChemR23 expression and cancer vascular invasion status ($P = 0.387$, Mann-U Whitney) (G). There was no statistically significant correlation ($P < 0.05$) between ChemR23 expression and the clinic-pathological data.



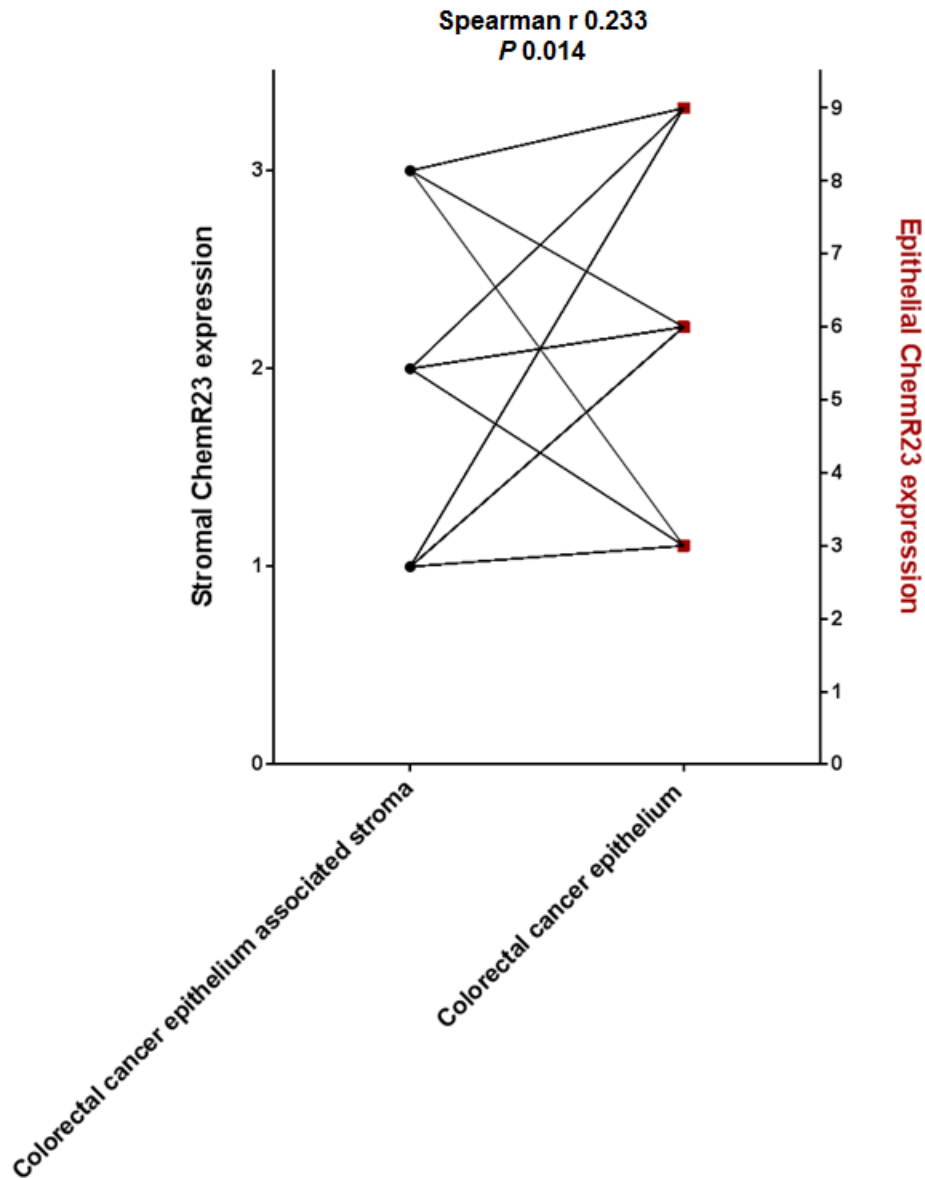
Appendix 22. Correlation of ChemR23 expression in human CRC epithelium associated stroma with age, cancer location, cancer size, cancer cell differentiation, pT, pN stage and vascular invasion status.

There were 73 different FFPE human CRC epithelium scored samples. Statistical analysis was performed on the total ChemR23 expression score (I x P) for all samples. (A) Statistical analysis was performed using SPSS. Correlation between ChemR23 expression and age ($P = 0.684$, Kruskal-Wallis). (B) Correlation between ChemR23 expression and cancer location to splenic flexure ($P = 0.899$, Mann-U Whitney). (C) Correlation between ChemR23 expression and cancer size ($P = 0.140$, Kruskal-Wallis). (D) Correlation between ChemR23 expression and cancer cell differentiation ($P = 0.425$, Kruskal-Wallis). (E) Correlation between ChemR23 expression and cancer pT stage ($P = 0.557$, Kruskal-Wallis). (F) Correlation between ChemR23 expression and cancer pN stage ($P = 0.589$, Kruskal-Wallis). (G) Correlation between ChemR23 expression and cancer vascular invasion status ($P = 0.618$, Mann-U Whitney). There was no statistically significant correlation ($P < 0.05$) between ChemR23 expression and the clinic-pathological data.



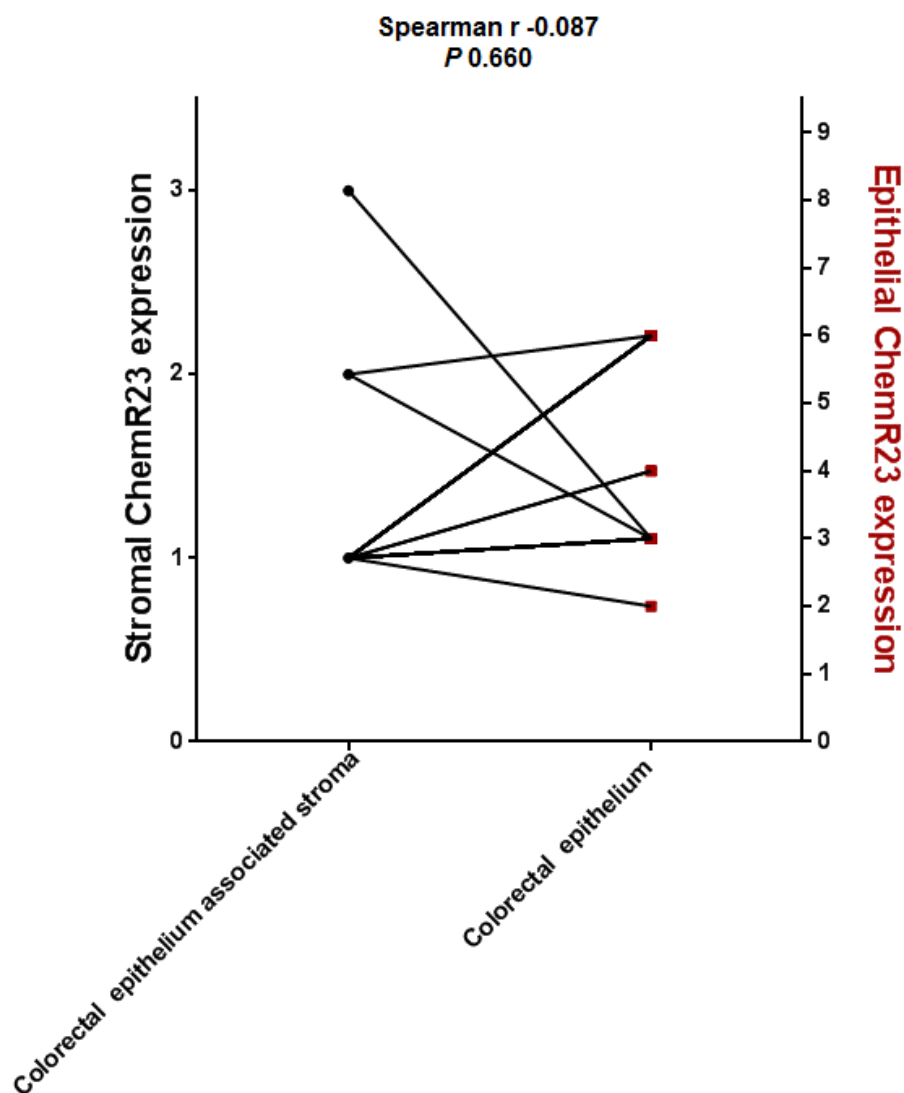
Appendix 23. Correlation of ChemR23 expression in histologically normal human CR epithelium associated stroma with age, cancer location, cancer size, cancer cell differentiation, pT, pN stage and vascular invasion status.

There were 28 different FFPE human CRC epithelium scored samples. Statistical analysis was performed on the total ChemR23 expression score (I x P) for all samples. Statistical analysis was performed using SPSS. Correlation between ChemR23 expression and age ($P = 0.352$, Kruskal-Wallis) (A). Correlation between ChemR23 expression and cancer location to splenic flexure ($P = 0.683$, Mann-U Whitney) (B). Correlation between ChemR23 expression and cancer size ($P = 0.337$, Kruskal-Wallis) (C). Correlation between ChemR23 expression and cancer cell differentiation ($P = 0.678$, Kruskal-Wallis) (D). Correlation between ChemR23 expression and cancer pT stage ($P = 0.273$, Kruskal-Wallis) (E). Correlation between ChemR23 expression and cancer pN stage ($P = 0.199$, Kruskal-Wallis) (F). Correlation between ChemR23 expression and cancer vascular invasion status ($P = 0.387$, Mann-U Whitney) (G). There was no statistically significant correlation ($P < 0.05$) between ChemR23 expression and the clinic-pathological data.



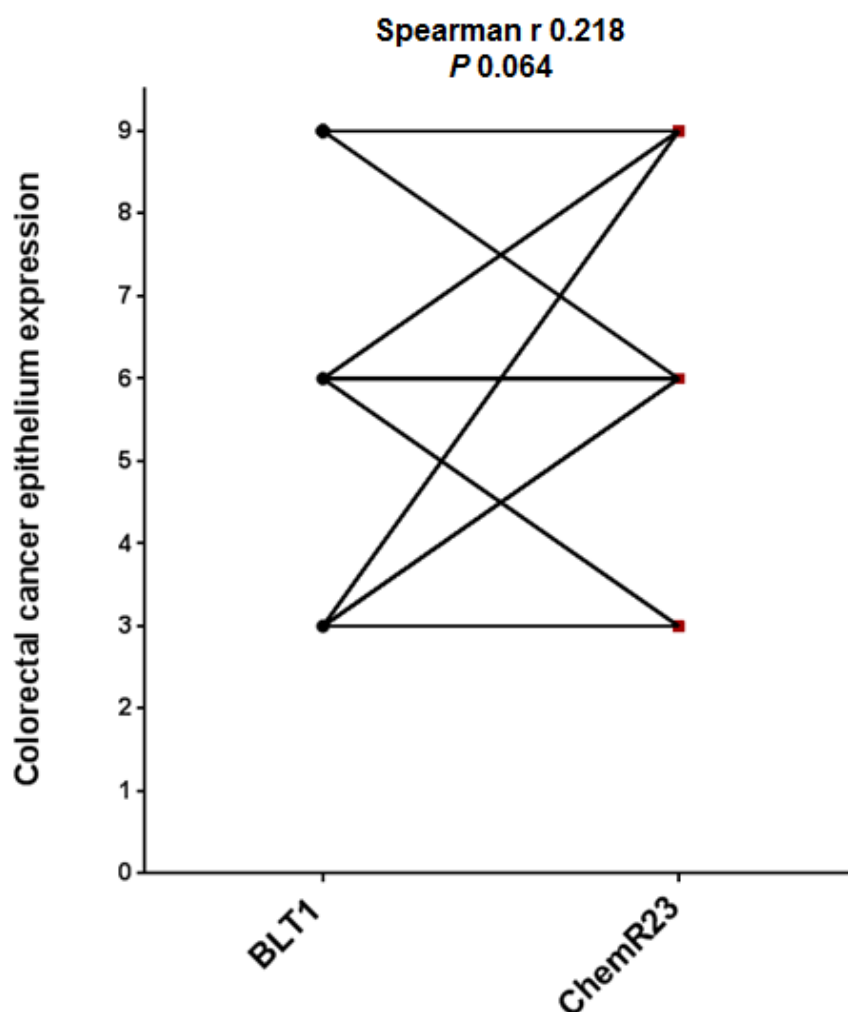
Appendix 24. Correlation of ChemR23 expression in human CRC associated stroma with matched CRC epithelium.

There were 73 different FFPE human CRC samples examined. Statistical analysis was performed on matched samples for ChemR23 expression in the CRC epithelium associated stroma (0-3) and CRC epithelium (0-9). Statistical analysis was performed using SPSS. A Spearman's rank correlation coefficient was calculated. Spearman's r was 0.233 (95% confidence interval 0.044-0.406, $P = 0.014$). There was a weak correlation between ChemR23 expression in the CRC epithelium associated stroma and CRC epithelium.



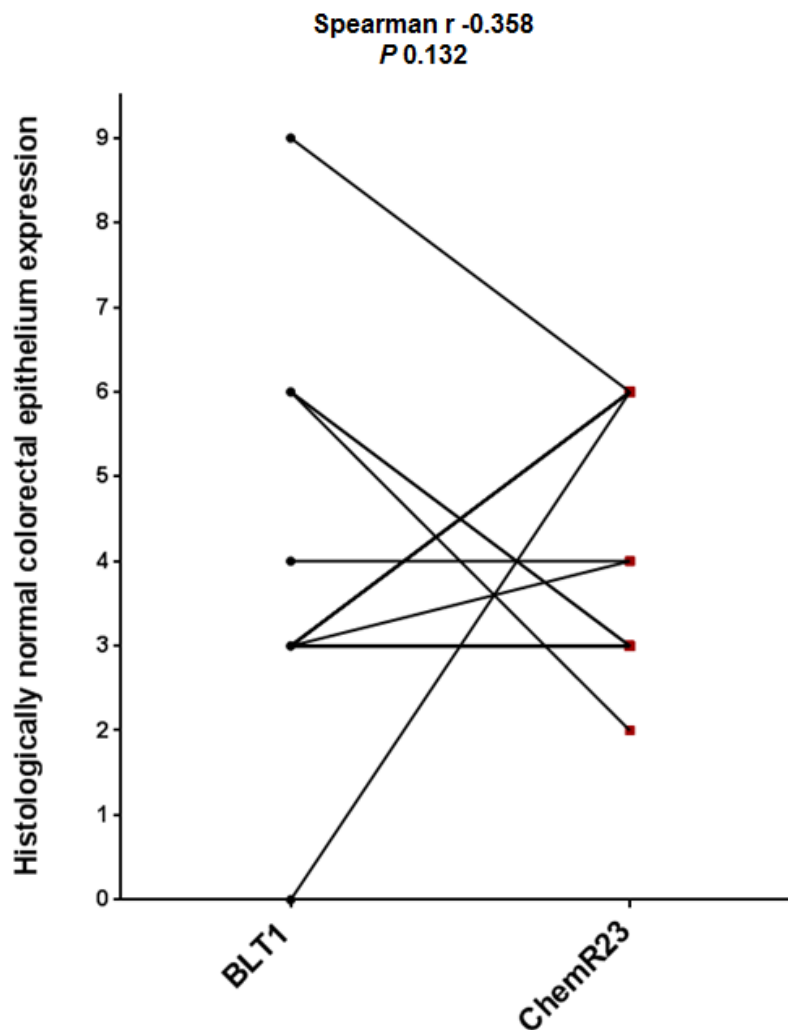
Appendix 25. Correlation of ChemR23 expression between matched histologically normal human CR epithelium associated stroma and CR epithelium.

Twenty-eight different FFPE human CRC samples were probed for ChemR23 expression. The samples were scored for ChemR23 expression in the histologically normal colorectal epithelium associated stroma 0-3 and in the colorectal epithelium 0-9 as described. A spearman's rank correlation coefficient was calculated. Spearman's r was -0.087 (95% confidence interval -0.455 to 0.306, $P = 0.660$). There was no correlation found between ChemR23 expression in the histologically normal CR epithelium associated stroma and CR epithelium.



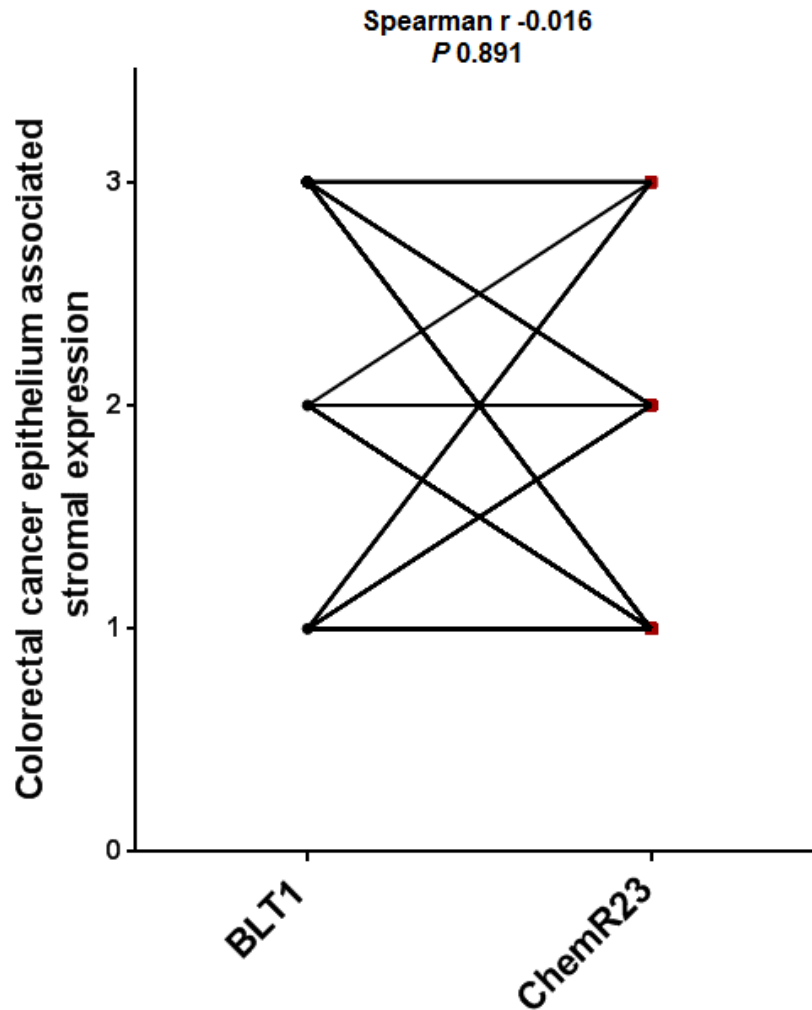
Appendix 26. Correlation of BLT1 and ChemR23 expression in matched human CRC epithelial samples.

Seventy-three different FFPE human CRC samples were matched for BLT1 and ChemR23 correlation. The samples were scored for BLT1 and ChemR23 expression in the epithelium 0-9 as described. A spearman's rank correlation coefficient was calculated. Spearman's r was 0.218 (95% confidence interval -0.019 to 0.433, $P = 0.064$). There was no correlation found between BLT1 and ChemR23 expression in the CRC epithelium.



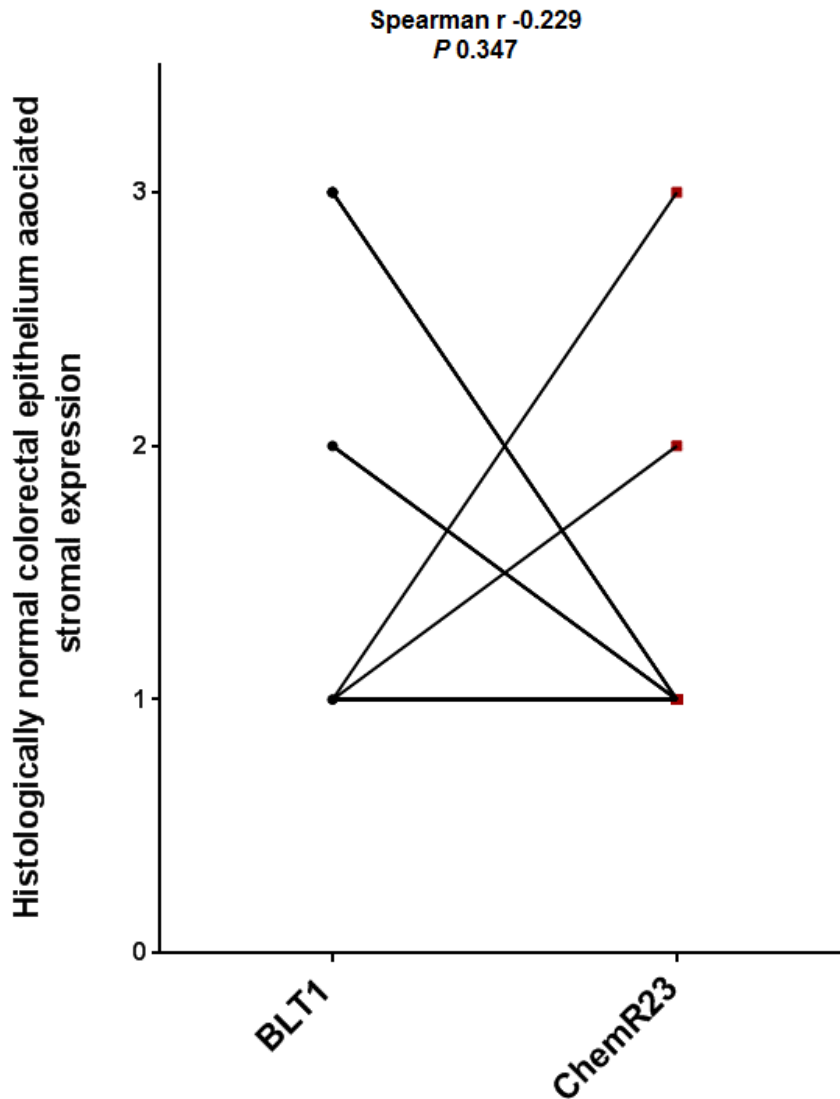
Appendix 27. Correlation of BLT1 and ChemR23 expression in matched histologically normal human CR epithelium samples.

Nineteen different FFPE human matched CRC samples were correlated for BLT1 and ChemR23 expression. The samples were scored for BLT1 and ChemR23 expression in the epithelium 0-9 as described. A spearman's rank correlation coefficient was calculated. Spearman's r was -0.358 (95% confidence interval -0.706 to 0.129, $P = 0.132$). There was no correlation found between BLT1 and ChemR23 expression in matched histologically normal CR epithelium samples.



Appendix 28. Correlation of BLT1 and ChemR23 expression in matched human CRC epithelium associated stromal samples.

Seventy-three different FFPE human CRC samples were probed for BLT1 and ChemR23 expression. The samples were scored for BLT1 and ChemR23 expression in the epithelium 0-3 as described between matched specimens. A spearman's rank correlation coefficient was calculated. Spearman's r was -0.016 (95% confidence interval -0.252 to 0.221, $P = 0.891$). There was no correlation found between BLT1 and ChemR23 expression in the CRC epithelium associated stroma.



Appendix 29. Correlation of BLT1 and ChemR23 expression in matched histologically normal human CR epithelium associated stromal samples.

Nineteen different FFPE human CRC samples were probed for BLT1 and ChemR23 expression. The samples were scored for BLT1 and ChemR23 expression in the stroma 0-3 as described. A spearman's rank correlation coefficient was calculated. Spearman's r was -0.229 (95% confidence interval -0.623 to 0.266, $P = 0.347$). There was no correlation found between BLT1 and ChemR23 expression in matched histologically normal CR epithelium associated stromal samples.

5' end ctggtctcgg gtgtggggaa gaaaggccat caaggtagat gcgggtgggg aacagctga gagaggaggc aaggacaacc
 cagttctgt ctgaaggggc ctctgggtga cctggagtt tctgtccca aacacagggc tcacgggatt cttctgtcc tcatgactg ggcagaggt 181
 ccttaactc cttgttga cattgccatt ctctcacatc cgtgcgggc aggaagccct tcctgaactc tgactcagt tctgtctg gttctgcc
 atttttca taccctga cagctgcgag gtcactctg ctctggctt tctcaagca gaacaagtgg gggctctgga aaggtaagg gacctcagt
 gccaccatta tacttgcac ctctctgag aagtgagagt tgaaggaa gcaggaaggc ccatggtcag attgaaggaa ggactttta gttctttt
 tttttttt ttttttgag atggagtctc gctctgtcat tcaggctgga gtgcagtgt gcgatctcag ctactgcag cctccactc ctgggtcac
 atgattctcc tgcctcagcc tccaagtag ctgagactac aggcacatgc cactacacc agctatctt tgtatttta gtgagacgg ggtttacca
 tgttggccag gctgtctca aactgtaac atcaagtgat ctgtccctc cagcctccca aagtgtctgg attaccgga tgaaccacca caacctgcca
 ggaatttta gttttagct tttcaggag actcaagga aaggagacat tcctctgctc aggaaacggg taaggggacc atttctcat tctgtgttc
 cctctggc aggggtggca tgaggcatca ctgtctgc tcctcactc ctgtctca tctcagct gccagctcg cctcaactt gtgtctca
 agtggaaactg aatagtaggc tgtgagaaga taggaaagag gtagtccaa tctctgcc cagatcata atccagactc agcagggtaa
 cccatgggc aagcacaagg taggtctg gggaaaggg aagtaattg cattctgt gataccaagg agaccattg gattttgct
 tctaccaag agaattgaga attggtgac ctaaaggaa ccagtcctt taagtaaggg gaggaaggg ggtgctgaa gatggcctc
 ttcccacc ctatgata gctgaactg aagccaagga cagagtctg cccctcgg cactactga tgtccctt ttaaatcatg atgtatca
 acccaaac agaccagga ctatgcaca gctcaact acacttcta ttaactta acaaaagca acaaaacaa aaagatatca
 gcaattgac ctcaactg agccattc cttctctg ctaccatac tctctctc atatgatac atccactt ttttcaat atccagctc
 gacctgac ttagggccac acccagctt ctactccc acaccctt tctctctc actgctct cctgtctt tctcatctg ccccactc
 aaggagtct cctgctct ggggtccct ggaaacaga ctatcccc tctagtga gggagtggg aggggttca gccccct
 caggaagat cgtctctt gctctgct ctgtgtact tctctctg ctgattagc aaacagcacc tagacctgg gccagcct tggcagggg
 acagatccag gtagggta caccacctg cctgacct **gggattggca tcagctcca accagttct gccaagctt**
gtaagctc cgcaggcca tgaactac atctctgca gcacccct cactaggtg agagtctc
tctctctg ctatctct gctgtcagtg gcgtggctg tggggctcc cggcaacagc tttgtggtg
ggagtatct gaaaaggatg cagaagcgt ctgtcactgc cctgatggg ctgaacctgg cctggccga
cctggccgta ttgctactg ctccctttt cttcactc ctggcccaag gcacctggag tttggactg
gctggtgcc gctgtgtca ctatgtctg ggagtcagca tgtacgccag cgtcctgct atcagggcca
tgagtctaga ccgtcactg gcgggtggcc gccctttgt gtcccagaag ctacgcacca agcgatggc
ccggcgggtg ctggcaggca tctgggtgt gctctctg ctggccacac ccgtcctgc gtaccgaca
gtagtccct gaaaacgaa catgagcctg tctctccc gcgtaccag cgaagggc cgggctcc
atcaatct cgaggctgc acgggctcc tctgcccct cctggctgt gtggcagct actcggacat
agggcgtcct ctacaggccc ggcgctcc cgcagccc cgcaccggc gctgggtgt gctatctc
ctgacctcg ccgctctg gctgccctc cagtggtga acctggctga ggcggccgc gcgtggccg
gccaggccc cgggttagg ctctgggga agcggctgag cctggcccgc aactgctca tgcactgc
ctctgagc agcagcgtga acccgtgt gtagcgtgc gccggcggc gctgctgctg ctggcggg
gtggctctg tgcacaagct gctggagggc acgggctcc aggcgtccag cagcggccgc gggggcagcc
tggccagac cgctaggag gcccccgc ctctggagcc cggccctcc gagacctca ctgctccag
ccctcaag taaacgaac tgaactagc ctggtggaag gaggcact tctctctg cagaatgta gctctgacc agtctcagc
 ctggaggag agcagggggc tggagggcgt ggagggcgt ggagcgtgg agcgggaggt ggagtgaag aagagggaga ggtggagca
 agtggggcc gtaggagagc gtgtccagc ctggctcca caggcact taaccataa aactgaagc tgaatttg tcaactgt
 gagtgggta catgtctgt ggtatcgg gtgtctgtg ggcctgtt gggcccctc tggtagtg agagtacgt ctttagtc ccatgatt
 acaatttg aaggacaca aagaacata gactcccc atccagatg attccagta catagtct agataact tagcaaacg
 cagtctac actcctaaag cagctgtct aggaagaca ccatgtgg ctatcactc cagttctgt gacccgggac ctctgagaa aacagactg
 ctgtgaaata tctctga agcctgtat agtctctt gtagaata ctcaactc ctccaataa tcttctct ctccatagga gatgtctag
 gggatcct cttccctc attcaca gggccagac ttgaggacta agtcttaga tctatctct tagaatttg catatcagca tctgtaacc
 tccacaac accctggcac aggggtggc tggggccc aggaacaaa gattccaaa agtgagagg atgagctt attcctaga
 gatgactgt gtttagaga acctgttc aactgttc tgacaaggt ttaggaagat ggcaacaaca tggcagcag tctacttt ggtctct
 cataaaaa caaaagagca agtaagagag ggaacaaaa tatccatg caacatccg acaaatcta gtagtcaag gttgacata
 ctccatgga ccccaagta tgaccagtg agaagatc atcaatct caagacct ataccagat ctgtcagaa gtagcagaa
 ggaagcaag gtagtggga tggacctaa aagaggat ccccaagct tctacagat ctactggaa gtagtgtg accaattga
 gaacagcag tgaactgg agggacctaa cggagtatt cccagctc tgcaccatc ttagtggta gcacataa ggtactat tagtgggt
 cgaattaata aagtcaaat gacattccc tggaaaaaaa aaaaaaaaa **3' end**

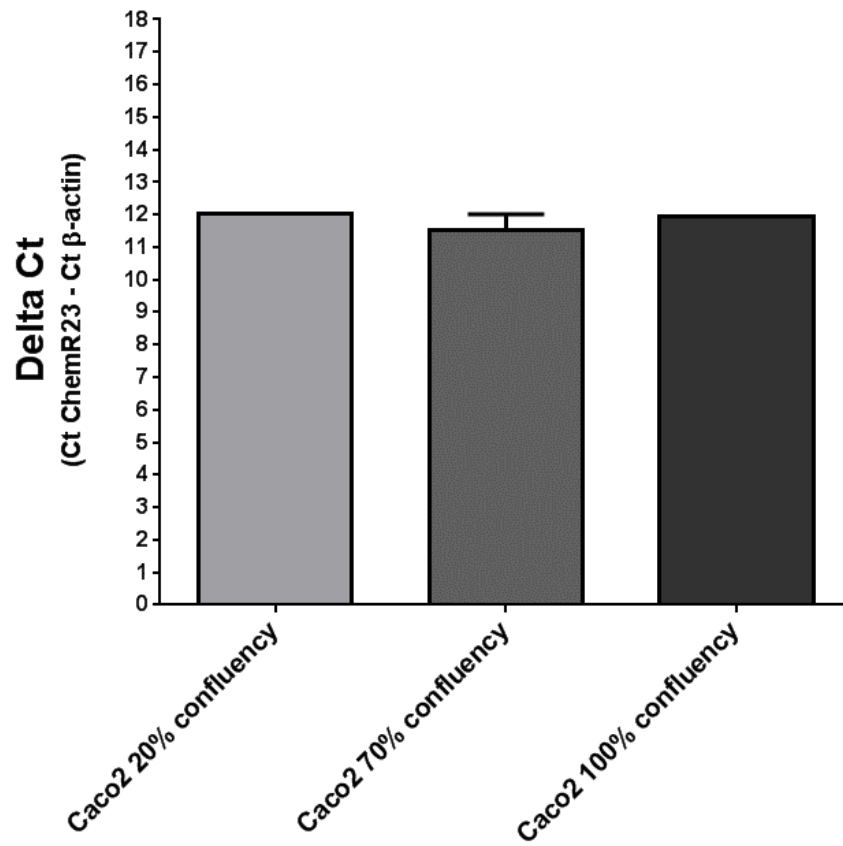
Appendix 30. Nucleotide sequence for BLT1 with TaqMan assay target.

Nucleotide sequence in black bold codes for the BLT1 protein. Nucleotide sequence in red bold is the context sequence that is targeted by the TaqMan gene expression assay.

5' end agtcccaatc agggagacag ccccgccggc cagcaggagag ctaggacag agcaggctcc ctgggaagcc tccgggtgat aggggtgtc cagctcggc
gctctggggg ttcagagggg gatcttgaat gaacaaatga atgaactgt tctgggcaa acagccacag ccagaggagc ctgtgattg cagaagaag ccagggtgtg
caagtctccc caacagctc gagtggcctg cagtcacagg gaacctcag gaagacctc cgggcagaga ccagagggaa gccactctc ccagcagaac tctgttgatt
ttctaccag gaggctcagg gctdgaac aatgataga gaagctgat gcatctagag atctaggctg ggactagcac agcatcact ctaccactt ctgttgta
cagcaactca ccatgccagt gcagattcaa ggggaggaga aatagagctc actctgat gggaggctg acatgtgtt ctgctgtgt acagggactg atggctgag
gactcacatt ggagagctgc agacaacata acggtaagt agaatggagg **atgaagatta caacactcc atcagttac gtgatgaata cctgattat**
ttagactcca ttgtggttt ggaggactta tcccccttg aagccagggt gaccaggatc ttctgtgtg ttggtacag catcgtctgc
ttctcggga ttctgggcaa tggctgtgt atcatcttg ccacctcaa gatgaagaag acagtgaaca tggctgtgtt
cctcaactg cgagtggcag atttctgtt caactctc tccccatcc atatcacta tgcggccatg gactaccact gggtttcgg
gacagcctg tcaagatca gcaactctc tctcatccac aacatgttca ccagcgtct cctgtgacc atcatcagct
ctgaccctg tcatctgtg ctctcctg tctgttccca gaaccaccg agcgttcgct tggcttaccat ggctcctg
gtcactgtgg tctgtgctt ctcttgagt tccccctc tctgttccg ggacacagcc aacctgcatg ggaaaatc ctgctcaac
aactcagcc tctccacacc tgggtcttc tctgtgcca ctaactcca aatggacct gtgggtata gccggacat
ggtgtgact gtcaccgct tctctgtg ctctgtgct ccagctcctc tcatcagc ttgctactc accatctgt gcaactgca
gccaaccg ctggccaaga ccaagaagcc ctcaagatt atgtgacca tcatcattc ctctctc tctgtgtg
ctaccacac actcaactc ctgagctcc accacactg catgctggc tctgttca gctgggtt gccctggc
actgcctg ctaattgcaa cagctgcat aaccactc tgtatgtt ctgggtcag gacttcaaga agtcaagg ggcctctc
tctcctgt caatgtct aagtgaagt acggcact ctctacc cagccataga agcttacca agatgtcat
aatgaatg aggacttca tgaatgag ggagaccgg atgcttga cctcactg gaaccctca atgactct tcaaccagg
gacaccaag gatattct ctgaagatc agccaagaac ctcttagca tccaccaat tctactgat ttgcatgg atgaacagt ttatgtg gaaactagg
gcttgaacc 1861 ctctctct agtgacaga acatgtgt tccatcag ccttgacta gcaattatg **ctcttggga gccagcctt** gactgacta
aagcaaaaa ggaagaatc tcaaaagat tgcatgaac tgggattgc atagggcgt gggattaagc tgcctattg tgtgcccc gaaatgacac tctcaaggt
ccattctgg tgtgagcagt gaggggtca gagcaaac agtgtgatc agatcacact tggcctgt atatatata tcaatgctg gccagaaaa cctacctc
agtactgt ctgtttaa gtatgtgaa atgcatagt gatctgggag aggaagtgta catatcagcc catgaactcc atagccatg aatttggct tggatcagc
taggaagaca gagaactgt cctgagagt cctgtggct ctgtcaagg gcaagacaag tgaggatgc aacgaggact tgagattgg caaagaatg agaaaggaga
aaagaacct taaaggatgc aggcattgg cagctacc tagaacatc aggcctgat gtccttag ctggagctat ttggggctc aggggtgtc cagccctga
tctcctg cctcttcc ctgggggtg ggtgtgca ggcactca ccagcagcc tccccatc acagggatt ttctgct tctcaatc actcagct gctggagg
gcttgaata aaactctg ggtgggtct ctactctg ttaattct caagcctt ggagacagt caaaaatga gcttgggaa gcaactcgg agagtccct
gggaagaaga gtatgtcca gactcagc actgagaca gactctgg ctggactct tgaactgt tctgagct cagacacaa atacctctg gatacaggt
ctggatg ctcttcat caatactga cagctctg tggccaca gtgctagc ccaattca aatgacatg ctgagccca gatgggaaa gtaactgcc
cagcatcaca cagtaata gtggcagat taagatga actgctcc gctggctc agaaactct tctctat tgaattat ctgtggat tattctaga tattgatg
ctacttat ttgacttt ttatattg cacttcat atgttctc attaatat tacagcaac ctgagttag tatgtata actcctt tacataggag gaatctgag
cttagaggg taaagtaact tccccaaagg taccagctc gctctgct gagctggat tgaactca gttgctgg ctcaaatgag gctcagat tgggaaggac
ttaaagtt tggagatt ttccataat atgatttt ctgcaaatg ggaatgaac cttaatgccc ttaagaac ttgcaaaa gtttcaaaa atgatcaac atggcagaga
aaatgact ggtctcagc tcccaaca gccaltaca gctctacc gttgctcca ctctatgt ctccagat caaggaatg gggaggaaa gctggcaga
ggcagctct tgtggcctg aggccttgg gctcctaagt gtcacact tgtctctc caagctct cattgtaag ctgattcc aacaagatc aatgaacaga tcaatgtct
accctgct gggcagct cggaggcat gggctgtg gaatcacat tcaatgaag acaactgt ctctctta ttgtctta atgtatga caaggcagct
ctgaattgt ccaagctg agcctgaa tctttaaag agttgaata tagagctt gagacaaa agggagctt aaatattgt cagtgcccc catctctc
ctcccat ttactgagc acgagatgg atggacct tcccgtca cagcagct ctgagctc ttggcctc tggctgtg gatctgt tctctggct
tctggcagc cagccagga tggggagcc aggaaltcat gttgtctg gaaaagctga taaacaggag caaatca accgctgt tctctta gatctggc
tctctctc tggctgct gtggctc ctgtctgac ttaggctc gcaagatc taaatgac cttaactcc catacagct ttgtccaca gctcatgt aactctca
tggctatc atatatctc ctgagatg gcaagatg ctacctca ctgctgca ggcaacca atactatg ccagagct tctctggt cccaggact
agtgtggg cctacttag cctgctcc tgggtgggt gggggagct agggatctg aggacaagag gtgagggaa aagaagaaga gatgtgtt gaggatagg
gaggacag agagggaca gaaagctcc agagcatg gatgaaggaa aggatctg calcatgaa gcacctca tggctcagc acaactct
aaactcaaa ttggcctg cagaagggga ccatcatagc aaggtgggg ggggtgag aaagtatgt tctgttca gaaacagct cactgctca gatgtgca
gctagtgg tatggagct ggcttgaat caggtcagct gctgaatc ccaactct cagccctg agggaggg tggggaga aagaaggaaa agacaaggaa
gaaagaaga agagagaagg ggagaggaat ggaagtcaa agagtggag gaattgat tcaagaacct ctccagctc ccttgacc agcaaggaca
gggagaagg aagagcaaga acagagggg cctcaagcag cgggatgct ttgcagct tagataatc ccagagcga cagagccct caggtctg ggtctctc
cagagaag gcacagat tctggcagca agttcagaa ggggtgaga aactggcag tcacaagg agggatgg ctcaattc acccagat cagctgtg
gggtggga gctggatg gtggagaag atagaatca atctgaaaa ccataaggga cctcaaac catctgccc agatgtcc cattcag atgaggaac
tgaggttg agagctcc ctgagact tcaaaaac ggtgtgtct gtttgatg aaagtgtg gttactc aactctgccc ctgctctc ctctgtcc tctcaaat
gtatgct tgtgggtg ggtgtcct aggcccaagg ttacaaatc ctgggttg aaaaatgct ctgggggtg tatctaggac cagagaggaa tctactat
ctactgaa ataactcagc aggggtct ctactct ccttgagg acaagttc tctgaataa agagactgaa gcaaga **3' end**

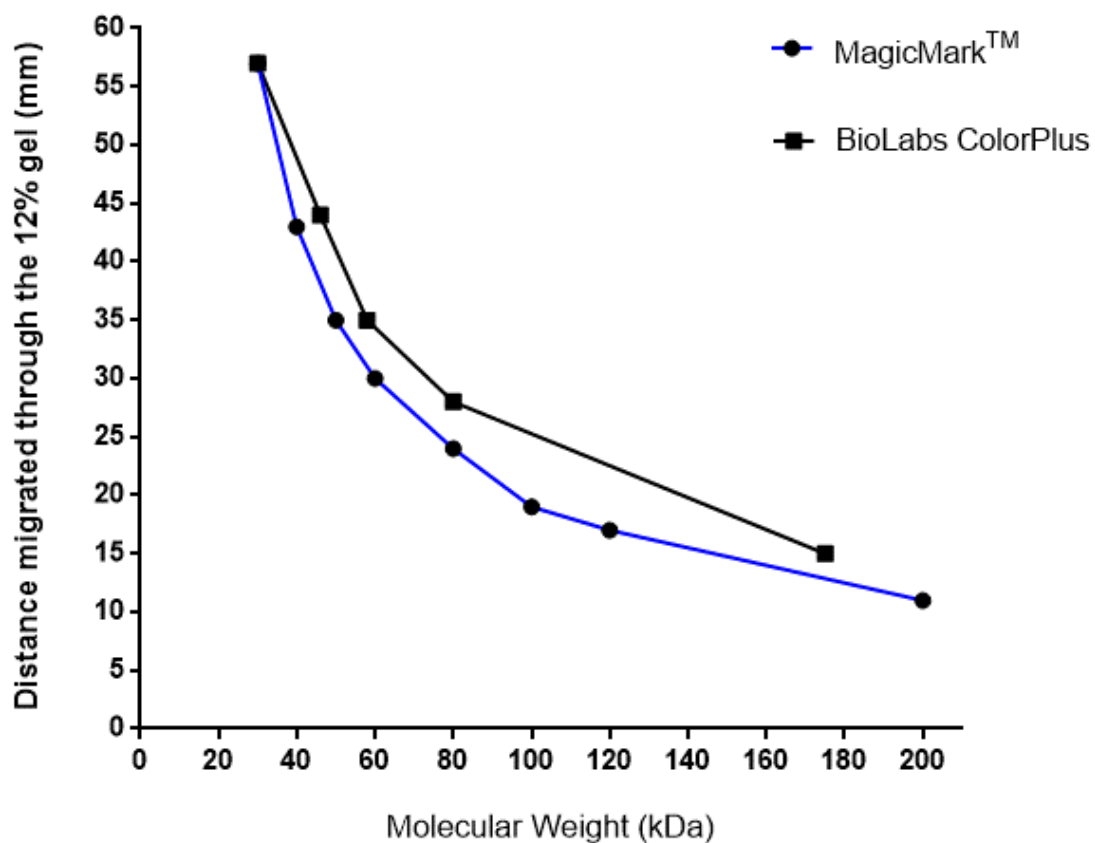
Appendix 31. Nucleotide sequence for ChemR23 with TaqMan assay target.

Nucleotide sequence in black bold codes for ChemR23 protein. Nucleotide sequence in red bold is sequence targeted by the TaqMan gene expression assay.



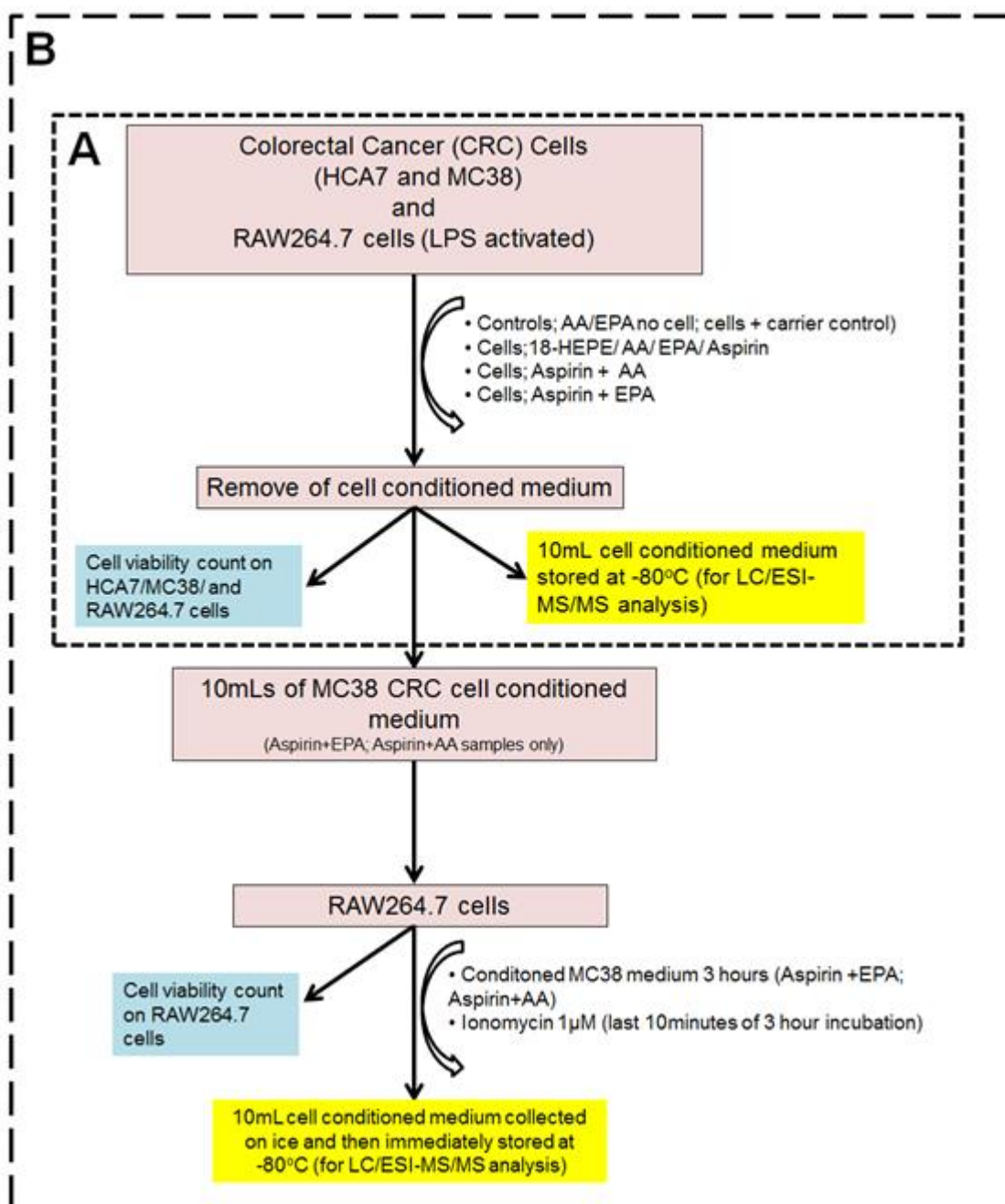
Appendix 32. ChemR23 mRNA expression in Caco2 human CRC cells at increasing cell confluency.

Caco2 human CRC cells were grown to either 20, 70 or 100% cell confluency. Messenger RNA was then quantified by qPCR. Figure represents data from one (20 and 100%) and three (70%) independent experiments, data is shown as mean with standard error of the mean. No ChemR23 mRNA induction was identified in the Caco2 human CRC cell line at increasing cell confluency under these experimental conditions.



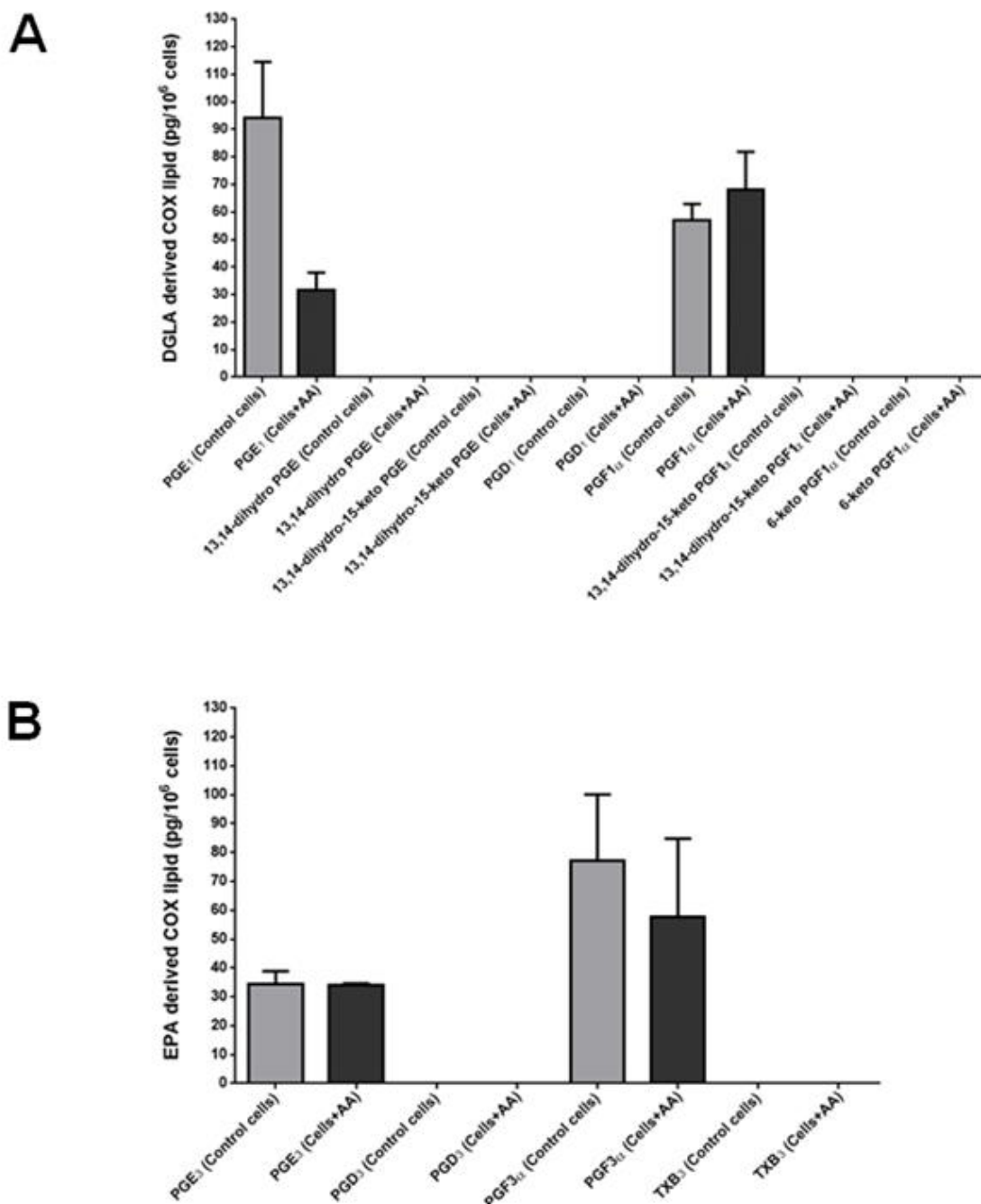
Appendix 33. The migration of two commercially available protein standards through a 12% SDS-PAGE gel.

The Invitrogen MagicMark™ XP standard (LC5603) and BioLabs ColorPlus Prestained Protein Marker were used.



Appendix 34. Detailed experimental schematic for the CRC and macrophage RvE1 biosynthesis experiment.

Diagram illustrating the experimental set up for the *in vitro* RvE1 synthesis experiment. (A) Single cell type synthesis experiment. (B) Transcellular synthesis experiment. Discussed in detail in Chapter 4.



Appendix 35. COX derived DGLA and EPA lipid mediators from the HCA7 human CRC cell line.

HCA7 cell conditioned medium was analysed for: (A) Seven different COX derived DGLA and (B) Four different COX derived EPA lipid mediators by LC/ESI-MS/MS, in the presence and absence of supplementary AA treatment. Lipid mediators are shown as pg per million ($\times 10^6$ cells). The lighter coloured bars are the control samples and the darker coloured bars are the AA treated cell samples. Data shown as mean and standard error of the mean (two independently cell cultured experiments).

A

AA derived	Experiment 1	Experiment 2
PGE ₂ (Control cells)	5.8	5.3
PGE ₂ (Cells+AA)	4.4	6.8
13,14-dihydro-15-keto PGE ₂ (Control cells)	0	0
13,14-dihydro-15-keto PGE ₂ (Cells+AA)	0	12.7
8-iso-15-keto PGE ₂ (Control cells)	0	0
8-iso-15-keto PGE ₂ (Cells+AA)	0	0
PGB ₂ (Control cells)	19.2	11.6
PGB ₂ (Cells+AA)	16.6	14.1
PGD ₂ (Control cells)	0	0
PGD ₂ (Cells+AA)	0	0
PGF _{2α} (Control cells)	0.2	0.2
PGF _{2α} (Cells+AA)	0.4	0.6
8-iso-PGF _{2α} (Control cells)	0	0
8-iso-PGF _{2α} (Cells+AA)	0	0
13,14-dihydro PGF _{2α} (Control cells)	0	0
13,14-dihydro PGF _{2α} (Cells+AA)	0	0
PGJ ₂ (Control cells)	97.3	72.2
PGJ ₂ (Cells+AA)	130.7	121.9
Δ 12-PGJ ₂ (Control cells)	0	0
Δ 12-PGJ ₂ (Cells+AA)	0	0
15-deoxy- Δ 12,14PGJ ₂ (Control cells)	0	0
15-deoxy- Δ 12,14PGJ ₂ (Cells+AA)	0	0
TXB ₂ (Control cells)	1	0.9
TXB ₂ (Cells+AA)	1.2	1.8

B

DGLA derived	Experiment 1	Experiment 2
PGE ₁ (Control cells)	114.5	73.6
PGE ₁ (Cells+AA)	25.1	37.9
13,14-dihydro PGE ₁ (Control cells)	0	0
13,14-dihydro PGE ₁ (Cells+AA)	0	0
13,14-dihydro-15-keto PGE ₁ (Control cells)	0	0
13,14-dihydro-15-keto PGE ₁ (Cells+AA)	0	0
PGD ₁ (Control cells)	0	0
PGD ₁ (Cells+AA)	0	0
PGF _{1α} (Control cells)	62.9	51.1
PGF _{1α} (Cells+AA)	53.9	81.9
13,14-dihydro-15-keto PGF _{1α} (Control cells)	0	0
13,14-dihydro-15-keto PGF _{1α} (Cells+AA)	0	0
6-keto PGF _{1α} (Control cells)	0	0
6-keto PGF _{1α} (Cells+AA)	0	0

C

EPA derived	Experiment 1	Experiment 2
PGE ₃ (Control cells)	38.8	29.7
PGE ₃ (Cells+AA)	33.5	34.6
PGD ₃ (Control cells)	0	0
PGD ₃ (Cells+AA)	0	0
PGF _{3α} (Control cells)	100.1	53.8
PGF _{3α} (Cells+AA)	30.5	84.8
TXB ₃ (Control cells)	0	0
TXB ₃ (Cells+AA)	0	0

Appendix 36. COX derived AA/ DGLA and EPA lipid mediator synthesis by HCA7 human CRC cells.

(A) AA derived lipid mediators. (B) DGLA derived lipid mediators. (C) EPA derived lipid mediators. Values represented as pg of lipid mediator per million ($\times 10^6$) cells. The PGE₂, PGF_{2 α} and TXB₂ values are represented as a ratio against internal standard (PGB2-*d4*), as the values exceeded the standard calibration curve ($> \text{pg}/\mu\text{L}$).

A

AA derived	Experiment 1	Experiment 2
PGE ₂ (Control cells)	0	0
PGE ₂ (Cells+AA)	0	0
13,14-dihydro-15-keto PGE ₂ (Control cells)	0	0
13,14-dihydro-15-keto PGE ₂ (Cells+AA)	0	32.1
8-Iso-15-keto PGE ₂ (Control cells)	0	0
8-Iso-15-keto PGE ₂ (Cells+AA)	0	0
PGB ₂ (Control cells)	0	0
PGB ₂ (Cells+AA)	25.1	0
PGD ₂ (Control cells)	0	30.8
PGD ₂ (Cells+AA)	0	0
PGF _{2α} (Control cells)	0	0
PGF _{2α} (Cells+AA)	0	0
8-Iso-PGF _{2α} (Control cells)	0	0
8-Iso-PGF _{2α} (Cells+AA)	0	0
13,14-dihydro PGF _{2α} (Control cells)	0	0
13,14-dihydro PGF _{2α} (Cells+AA)	0	0
PGJ ₂ (Control cells)	0	0
PGJ ₂ (Cells+AA)	0	0
Δ12-PGJ ₂ (Control cells)	0	0
Δ12-PGJ ₂ (Cells+AA)	0	0
15-deoxy-Δ12,14PGJ ₂ (Control cells)	0	0
15-deoxy-Δ12,14PGJ ₂ (Cells+AA)	0	0
TXB ₂ (Control cells)	0	0
TXB ₂ (Cells+AA)	0	0

B

DGLA derived	Experiment 1	Experiment 2
PGE ₁ (Control cells)	0	0
PGE ₁ (Cells+AA)	0	0
13,14-dihydro PGE ₁ (Control cells)	0	0
13,14-dihydro PGE ₁ (Cells+AA)	0	0
13,14-dihydro-15-keto PGE ₁ (Control cells)	0	0
13,14-dihydro-15-keto PGE ₁ (Cells+AA)	0	0
PGD ₁ (Control cells)	0	0
PGD ₁ (Cells+AA)	0	0
PGF _{1α} (Control cells)	0	0
PGF _{1α} (Cells+AA)	0	0
13,14-dihydro-15-keto PGF _{1α} (Control cells)	0	0
13,14-dihydro-15-keto PGF _{1α} (Cells+AA)	0	0
8-keto PGF _{1α} (Control cells)	0	0
8-keto PGF _{1α} (Cells+AA)	0	0

C

EPA derived	Experiment 1	Experiment 2
PGE ₃ (Control cells)	0	0
PGE ₃ (Cells+AA)	0	0
PGD ₃ (Control cells)	0	0
PGD ₃ (Cells+AA)	0	0
PGF _{3α} (Control cells)	153.5	154.7
PGF _{3α} (Cells+AA)	145.7	152.9
TXB ₃ (Control cells)	0	0
TXB ₃ (Cells+AA)	0	0

Appendix 37. COX derived AA/ DGLA and EPA lipid mediator synthesis by LoVo human CRC cells.

(A) AA derived lipid mediators. (B) DGLA derived lipid mediators. (C) EPA derived lipid mediators. Values represented as pg of lipid mediator per million ($\times 10^6$) cells.

A

AA derived	Experiment 1	Experiment 2
PGE ₂ (Control cells)	0	0
PGE ₂ (Cells+AA)	0	0
13,14-dihydro-15-keto PGE ₂ (Control cells)	0	0
13,14-dihydro-15-keto PGE ₂ (Cells+AA)	0	0
8-iso-15-keto PGE ₂ (Control cells)	0	0
8-iso-15-keto PGE ₂ (Cells+AA)	0	0
PGB ₂ (Control cells)	12.4	0
PGB ₂ (Cells+AA)	0	23.83
PGD ₂ (Control cells)	0	0
PGD ₂ (Cells+AA)	0	0
PGF _{2α} (Control cells)	11.7	13.5
PGF _{2α} (Cells+AA)	24.4	0
8-iso-PGF _{2α} (Control cells)	0	0
8-iso-PGF _{2α} (Cells+AA)	0	0
13,14-dihydro PGF _{2α} (Control cells)	0	0
13,14-dihydro PGF _{2α} (Cells+AA)	0	13.5
PGJ ₂ (Control cells)	0	0
PGJ ₂ (Cells+AA)	0	0
Δ12-PGJ ₂ (Control cells)	0	0
Δ12-PGJ ₂ (Cells+AA)	0	0
15-deoxy-Δ12,14PGJ ₂ (Control cells)	0	0
15-deoxy-Δ12,14PGJ ₂ (Cells+AA)	0	0
TXB ₂ (Control cells)	0	0
TXB ₂ (Cells+AA)	0	0

B

DGLA derived	Experiment 1	Experiment 2
PGE ₁ (Control cells)	0	0
PGE ₁ (Cells+AA)	0	0
13,14-dihydro PGE ₁ (Control cells)	0	0
13,14-dihydro PGE ₁ (Cells+AA)	0	0
13,14-dihydro-15-keto PGE ₁ (Control cells)	0	0
13,14-dihydro-15-keto PGE ₁ (Cells+AA)	0	0
PGD ₁ (Control cells)	0	0
PGD ₁ (Cells+AA)	0	0
PGF _{1α} (Control cells)	0	0
PGF _{1α} (Cells+AA)	0	0
13,14-dihydro-15-keto PGF _{1α} (Control cells)	0	0
13,14-dihydro-15-keto PGF _{1α} (Cells+AA)	0	0
8-keto PGF _{1α} (Control cells)	0	0
8-keto PGF _{1α} (Cells+AA)	0	0

C

EPA derived	Experiment 1	Experiment 2
PGE ₃ (Control cells)	0	0
PGE ₃ (Cells+AA)	0	0
PGD ₃ (Control cells)	0	0
PGD ₃ (Cells+AA)	0	0
PGF _{3α} (Control cells)	44.5	29.4
PGF _{3α} (Cells+AA)	50.8	42.9
TXB ₃ (Control cells)	0	0
TXB ₃ (Cells+AA)	0	0

Appendix 38. COX derived AA/ DGLA and EPA lipid mediator synthesis by T84 human CRC cells.

(A) AA derived lipid mediators. (B) DGLA derived lipid mediators. (C) EPA derived lipid mediators. Values represented as pg of lipid mediator per million ($\times 10^6$) cells.

A

AA derived	Experiment 1	Experiment 2
PGE ₂ (Control cells)	0	0
PGE ₂ (Cells+AA)	0	0
13,14-dihydro-15-keto PGE ₂ (Control cells)	0	0
13,14-dihydro-15-keto PGE ₂ (Cells+AA)	0	0
8-iso-15-keto PGE ₂ (Control cells)	0	0
8-iso-15-keto PGE ₂ (Cells+AA)	0	0
PGB ₂ (Control cells)	0	0
PGB ₂ (Cells+AA)	0	0
PGD ₂ (Control cells)	0	0
PGD ₂ (Cells+AA)	0	0
PGF _{2α} (Control cells)	0	0
PGF _{2α} (Cells+AA)	0	0
8-iso-PGF _{2α} (Control cells)	0	0
8-iso-PGF _{2α} (Cells+AA)	0	0
13,14-dihydro PGF _{2α} (Control cells)	0	12.8
13,14-dihydro PGF _{2α} (Cells+AA)	0	0
PGJ ₂ (Control cells)	0	0
PGJ ₂ (Cells+AA)	0	0
Δ ¹² -PGJ ₂ (Control cells)	0	0
Δ ¹² -PGJ ₂ (Cells+AA)	0	0
15-deoxy-Δ ^{12,14} PGJ ₂ (Control cells)	0	0
15-deoxy-Δ ^{12,14} PGJ ₂ (Cells+AA)	0	0
TXB ₂ (Control cells)	0	0
TXB ₂ (Cells+AA)	0	0

B

DGLA derived	Experiment 1	Experiment 2
PGE ₁ (Control cells)	0	0
PGE ₁ (Cells+AA)	0	0
13,14-dihydro PGE ₁ (Control cells)	0	0
13,14-dihydro PGE ₁ (Cells+AA)	0	0
13,14-dihydro-15-keto PGE ₁ (Control cells)	0	0
13,14-dihydro-15-keto PGE ₁ (Cells+AA)	0	0
PGD ₁ (Control cells)	0	0
PGD ₁ (Cells+AA)	0	0
PGF _{1α} (Control cells)	13.6	0
PGF _{1α} (Cells+AA)	0	0
13,14-dihydro-15-keto PGF _{1α} (Control cells)	0	0
13,14-dihydro-15-keto PGF _{1α} (Cells+AA)	0	0
8-keto PGF _{1α} (Control cells)	0	0
8-keto PGF _{1α} (Cells+AA)	0	0

C

EPA derived	Experiment 1	Experiment 2
PGE ₃ (Control cells)	14.9	0
PGE ₃ (Cells+AA)	12.7	0
PGD ₃ (Control cells)	0	0
PGD ₃ (Cells+AA)	0	0
PGF _{3α} (Control cells)	18.9	0
PGF _{3α} (Cells+AA)	0	18.9
TXB ₃ (Control cells)	0	0
TXB ₃ (Cells+AA)	0	0

Appendix 39. COX derived AA/ DGLA and EPA lipid mediator synthesis by HRT18 human CRC cells.

(A) AA derived lipid mediators. (B) DGLA derived lipid mediators. (C) EPA derived lipid mediators. Values represented as pg of lipid mediator per million ($\times 10^6$) cells.

A

AA derived	Experiment 1	Experiment 2
PGE ₂ (Control cells)	0	0
PGE ₂ (Cells+AA)	15.7	10.9
13,14-dihydro-15-keto PGE ₂ (Control cells)	0	0
13,14-dihydro-15-keto PGE ₂ (Cells+AA)	0	0
8-Iso-15-keto PGE ₂ (Control cells)	0	0
8-Iso-15-keto PGE ₂ (Cells+AA)	0	0
PGB ₂ (Control cells)	33.1	0
PGB ₂ (Cells+AA)	17.7	13.3
PGD ₂ (Control cells)	0	0
PGD ₂ (Cells+AA)	0	0
PGF _{2α} (Control cells)	0	0
PGF _{2α} (Cells+AA)	0	0
8-Iso-PGF _{2α} (Control cells)	0	0
8-Iso-PGF _{2α} (Cells+AA)	0	0
13,14-dihydro PGF _{2α} (Control cells)	0	0
13,14-dihydro PGF _{2α} (Cells+AA)	0	0
PGJ ₂ (Control cells)	0	0
PGJ ₂ (Cells+AA)	0	0
Δ ¹² -PGJ ₂ (Control cells)	0	0
Δ ¹² -PGJ ₂ (Cells+AA)	0	0
15-deoxy-Δ ^{12,14} PGJ ₂ (Control cells)	0	0
15-deoxy-Δ ^{12,14} PGJ ₂ (Cells+AA)	0	0
TXB ₂ (Control cells)	0	0
TXB ₂ (Cells+AA)	0	0

B

DGLA derived	Experiment 1	Experiment 2
PGE ₁ (Control cells)	0	0
PGE ₁ (Cells+AA)	0	0
13,14-dihydro PGE ₁ (Control cells)	0	0
13,14-dihydro PGE ₁ (Cells+AA)	0	0
13,14-dihydro-15-keto PGE ₁ (Control cells)	13.9	0
13,14-dihydro-15-keto PGE ₁ (Cells+AA)	0	0
PGD ₁ (Control cells)	0	0
PGD ₁ (Cells+AA)	0	0
PGF _{1α} (Control cells)	0	0
PGF _{1α} (Cells+AA)	0	0
13,14-dihydro-15-keto PGF _{1α} (Control cells)	0	0
13,14-dihydro-15-keto PGF _{1α} (Cells+AA)	0	0
8-keto PGF _{1α} (Control cells)	0	0
8-keto PGF _{1α} (Cells+AA)	0	0

C

EPA derived	Experiment 1	Experiment 2
PGE ₃ (Control cells)	9.3	0
PGE ₃ (Cells+AA)	0	0
PGD ₃ (Control cells)	9.4	0
PGD ₃ (Cells+AA)	12.6	0
PGF _{3α} (Control cells)	0	0
PGF _{3α} (Cells+AA)	0	0
TXB ₃ (Control cells)	0	0
TXB ₃ (Cells+AA)	0	0

Appendix 40. COX derived AA/ DGLA and EPA lipid mediator synthesis by HT29 human CRC cells.

(A) AA derived lipid mediators. (B) DGLA derived lipid mediators. (C) EPA derived lipid mediators. Values represented as pg of lipid mediator per million ($\times 10^6$) cells.

A

AA derived	Experiment 1	Experiment 2
PGE ₂ (Control cells)	0	0
PGE ₂ (Cells+AA)	23.8	0
13,14-dihydro-15-keto PGE ₂ (Control cells)	0	0
13,14-dihydro-15-keto PGE ₂ (Cells+AA)	0	0
8-Iso-15-keto PGE ₂ (Control cells)	0	0
8-Iso-15-keto PGE ₂ (Cells+AA)	0	0
PGB ₂ (Control cells)	33.9	20.5
PGB ₂ (Cells+AA)	0	0
PGD ₂ (Control cells)	0	0
PGD ₂ (Cells+AA)	0	0
PGF _{2α} (Control cells)	0	0
PGF _{2α} (Cells+AA)	165.19	62.06
8-Iso-PGF _{2α} (Control cells)	0	0
8-Iso-PGF _{2α} (Cells+AA)	0	0
13,14-dihydro PGF _{2α} (Control cells)	0	0
13,14-dihydro PGF _{2α} (Cells+AA)	0	0
PGJ ₂ (Control cells)	0	0
PGJ ₂ (Cells+AA)	0	0
Δ12-PGJ ₂ (Control cells)	0	0
Δ12-PGJ ₂ (Cells+AA)	0	0
15-deoxy-Δ12,14PGJ ₂ (Control cells)	0	0
15-deoxy-Δ12,14PGJ ₂ (Cells+AA)	0	0
TXB ₂ (Control cells)	0	0
TXB ₂ (Cells+AA)	0	0

B

DGLA derived	Experiment 1	Experiment 2
PGE ₁ (Control cells)	0	0
PGE ₁ (Cells+AA)	0	0
13,14-dihydro PGE ₁ (Control cells)	0	0
13,14-dihydro PGE ₁ (Cells+AA)	0	0
13,14-dihydro-15-keto PGE ₁ (Control cells)	0	0
13,14-dihydro-15-keto PGE ₁ (Cells+AA)	0	0
PGD ₁ (Control cells)	0	0
PGD ₁ (Cells+AA)	0	0
PGF _{1α} (Control cells)	0	0
PGF _{1α} (Cells+AA)	0	0
13,14-dihydro-15-keto PGF _{1α} (Control cells)	0	0
13,14-dihydro-15-keto PGF _{1α} (Cells+AA)	36.8	0
8-keto PGF _{1α} (Control cells)	0	0
8-keto PGF _{1α} (Cells+AA)	0	0

C

EPA derived	Experiment 1	Experiment 2
PGE ₃ (Control cells)	0	0
PGE ₃ (Cells+AA)	0	0
PGD ₃ (Control cells)	0	0
PGD ₃ (Cells+AA)	0	0
PGF _{3α} (Control cells)	63.3	84.7
PGF _{3α} (Cells+AA)	116.4	0
TXB ₃ (Control cells)	0	0
TXB ₃ (Cells+AA)	0	0

Appendix 41. COX derived AA/ DGLA and EPA lipid mediator synthesis by Caco2 human CRC cells.

(A) AA derived lipid mediators. (B) DGLA derived lipid mediators. (C) EPA derived lipid mediators. Values represented as pg of lipid mediator per million ($\times 10^6$) cells.

A

AA derived	Experiment 1	Experiment 2
PGE ₂ (Control cells)	0	0
PGE ₂ (Cells+AA)	0	0
13,14-dihydro-15-keto PGE ₂ (Control cells)	0	0
13,14-dihydro-15-keto PGE ₂ (Cells+AA)	0	0
8-Iso-15-keto PGE ₂ (Control cells)	0	0
8-Iso-15-keto PGE ₂ (Cells+AA)	0	0
PGB ₂ (Control cells)	6.3	0
PGB ₂ (Cells+AA)	0	0
PGD ₂ (Control cells)	0	0
PGD ₂ (Cells+AA)	0	0
PGF _{2α} (Control cells)	0	0
PGF _{2α} (Cells+AA)	0	0
8-Iso-PGF _{2α} (Control cells)	0	0
8-Iso-PGF _{2α} (Cells+AA)	0	0
13,14-dihydro PGF _{2α} (Control cells)	0	0
13,14-dihydro PGF _{2α} (Cells+AA)	0	0
PGJ ₂ (Control cells)	0	0
PGJ ₂ (Cells+AA)	0	0
Δ12-PGJ ₂ (Control cells)	0	0
Δ12-PGJ ₂ (Cells+AA)	0	0
15-deoxy-Δ12,14PGJ ₂ (Control cells)	0	0
15-deoxy-Δ12,14PGJ ₂ (Cells+AA)	0	0
TXB ₂ (Control cells)	0	0
TXB ₂ (Cells+AA)	0	0

B

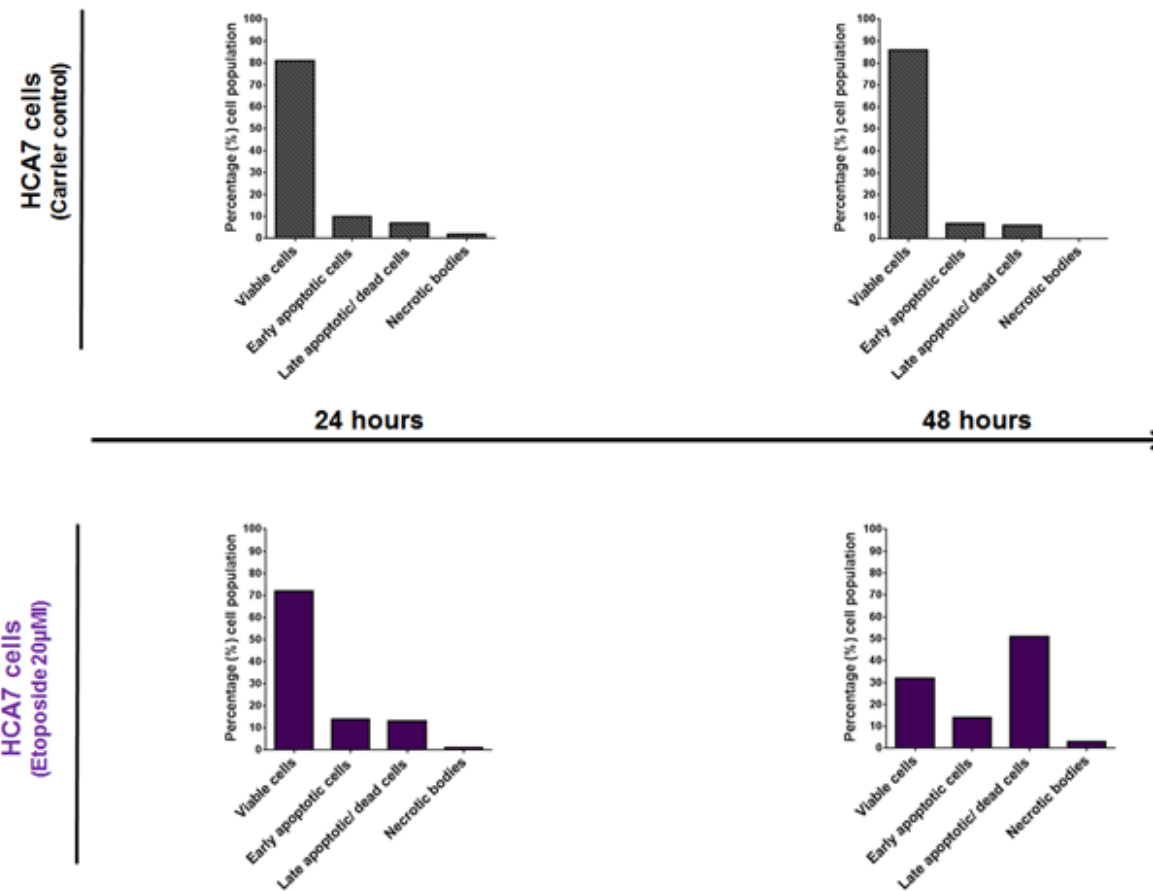
DGLA derived	Experiment 1	Experiment 2
PGE ₁ (Control cells)	0	0
PGE ₁ (Cells+AA)	0	0
13,14-dihydro PGE ₁ (Control cells)	0	0
13,14-dihydro PGE ₁ (Cells+AA)	0	0
13,14-dihydro-15-keto PGE ₁ (Control cells)	0	0
13,14-dihydro-15-keto PGE ₁ (Cells+AA)	0	0
PGD ₁ (Control cells)	0	0
PGD ₁ (Cells+AA)	0	0
PGF _{1α} (Control cells)	10.2	7
PGF _{1α} (Cells+AA)	6.3	6.1
13,14-dihydro-15-keto PGF _{1α} (Control cells)	45.5	32.9
13,14-dihydro-15-keto PGF _{1α} (Cells+AA)	46.5	0
8-keto PGF _{1α} (Control cells)	0	0
8-keto PGF _{1α} (Cells+AA)	0	0

C

EPA derived	Experiment 1	Experiment 2
PGE ₃ (Control cells)	0	0
PGE ₃ (Cells+AA)	0	0
PGD ₃ (Control cells)	0	0
PGD ₃ (Cells+AA)	0	0
PGF _{3α} (Control cells)	10.5	0
PGF _{3α} (Cells+AA)	0	0
TXB ₃ (Control cells)	0	0
TXB ₃ (Cells+AA)	0	0

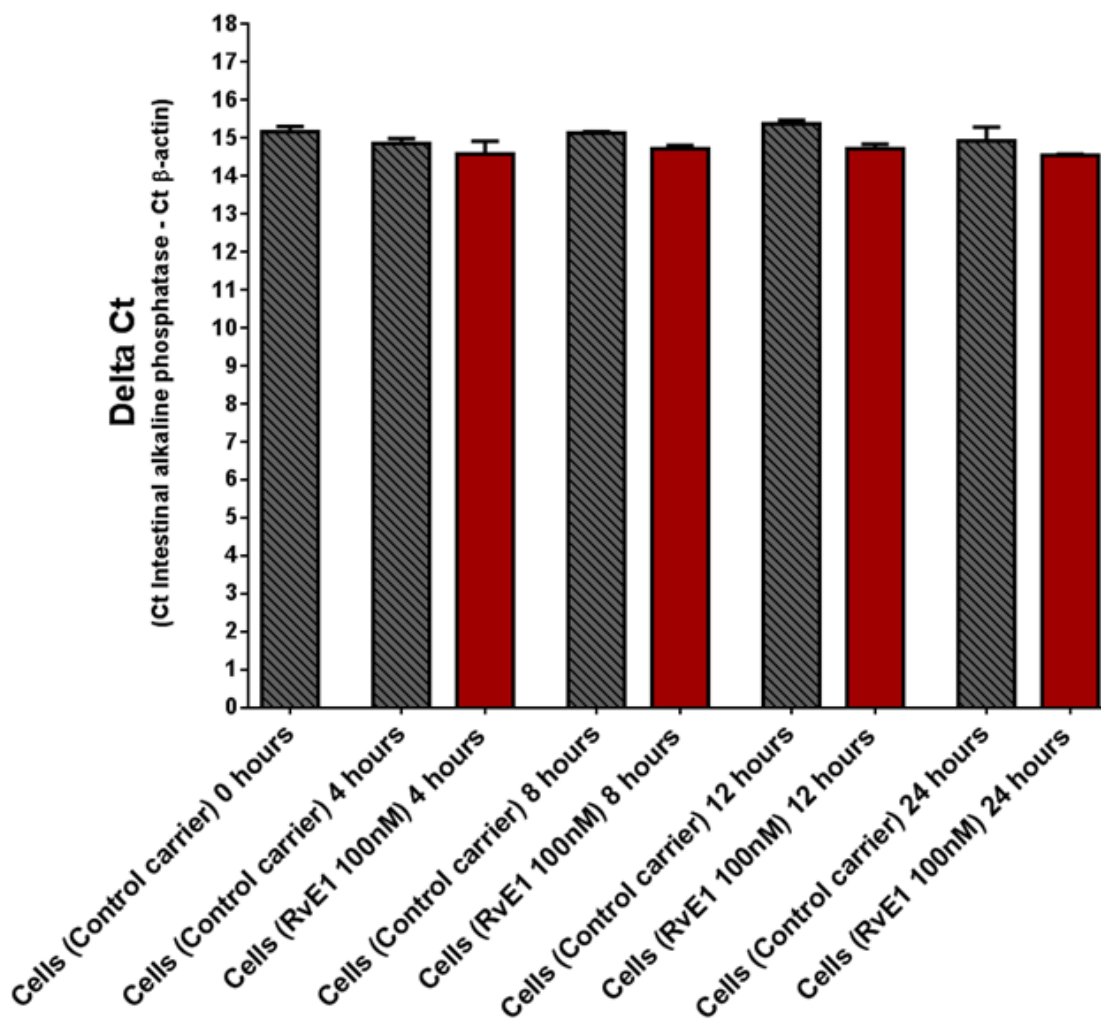
Appendix 42. COX derived AA/ DGLA and EPA lipid mediator synthesis by HCT116 human CRC cells.

(A) AA derived lipid mediators. (B) DGLA derived lipid mediators. (C) EPA derived lipid mediators. Values represented as pg of lipid mediator per million ($\times 10^6$) cells.



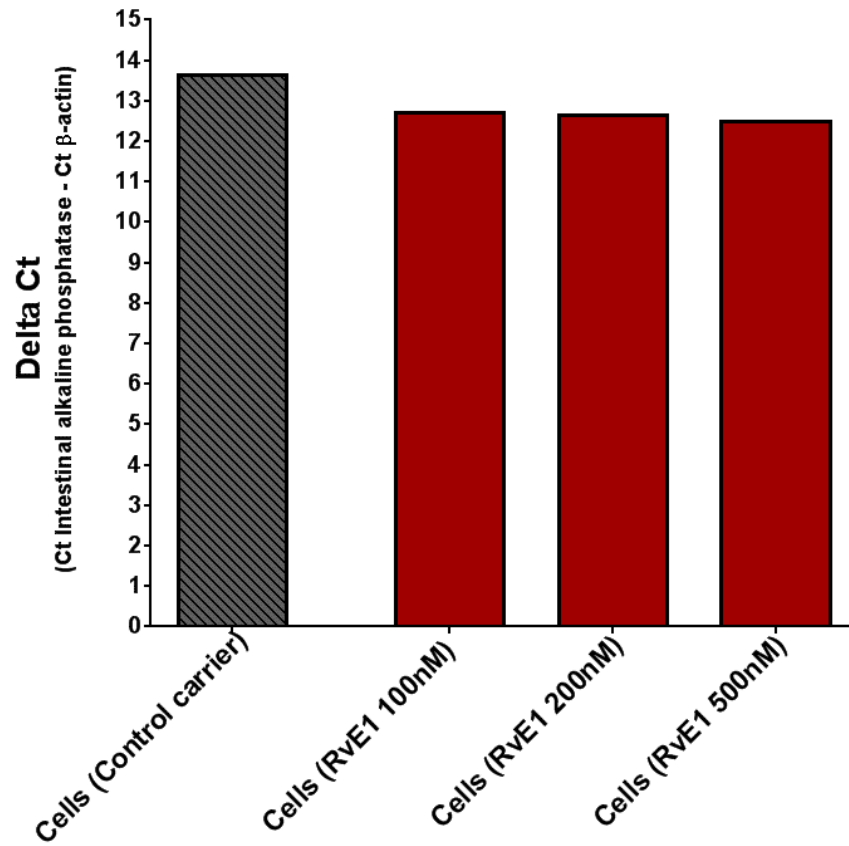
Appendix 43. Apoptosis in etoposide treated HCA7 human CRC cells.

HCA7 human CRC cells were treated with DMSO carrier or etoposide 20 μM for 48 hours and then analysed for apoptosis by flow cytometry. The graphs detail the percentage of cells that are either viable, early apoptotic, late apoptotic/dead or necrotic. The data is shown from one experiment.



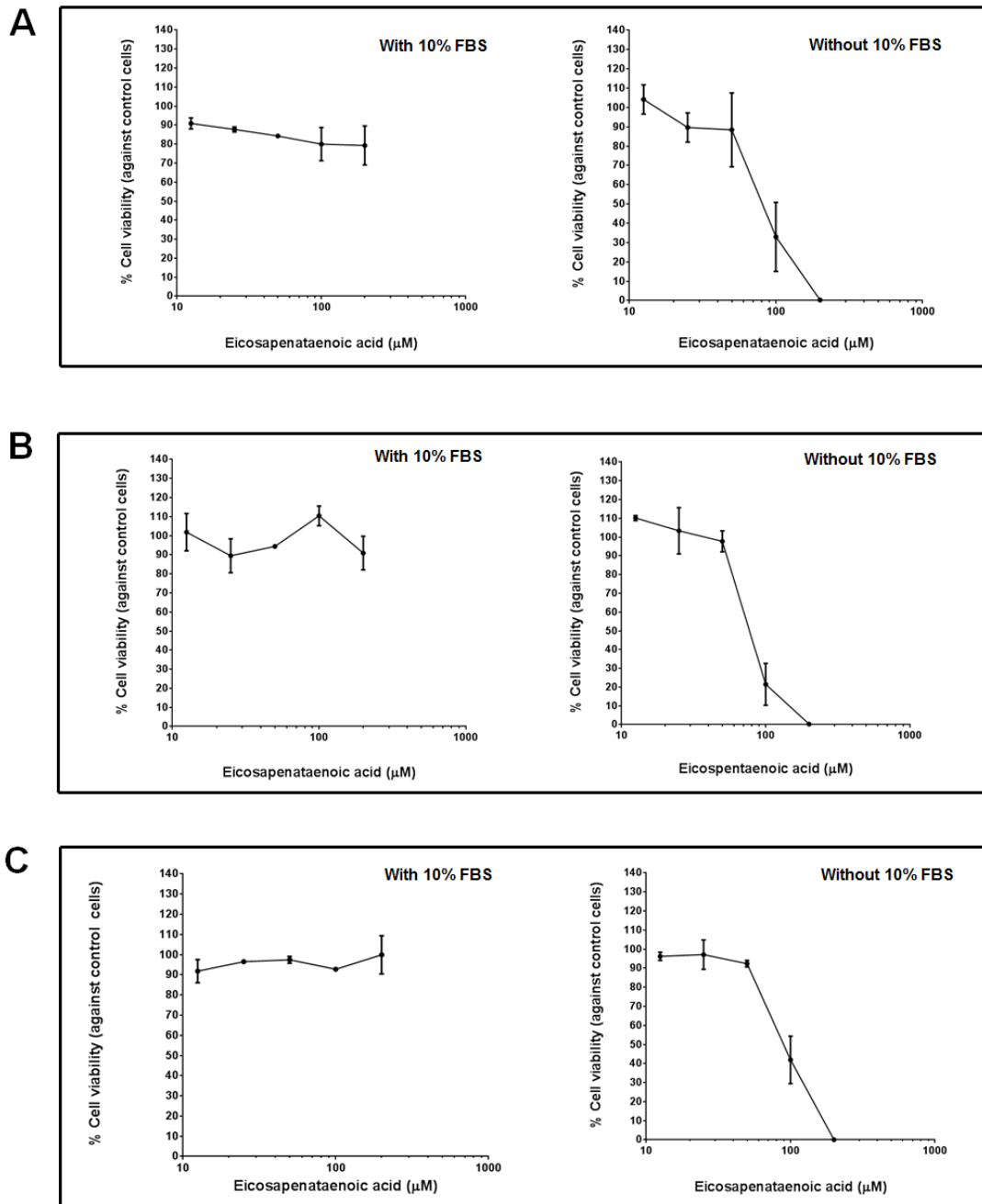
Appendix 44. ALPI mRNA expression in RvE1 treated T84 human CRC cells over 24 hours.

T84 human CRC cells were grown to 70-80% cell confluency. The cells were then treated with 100 nM RvE1 (in cell culture medium without FBS), before ALPI mRNA was quantified at specific time points over a 24 hour period for ALPI expression. The figure represents data from three independent experiments, data is shown as mean with standard error of the mean.



Appendix 45. ALPI mRNA expression in T84 human CRC cells treated for six hours with range of RvE1 doses (0-500 nM).

T84 human CRC cells were grown to 70-80% cell confluency. The cells were then treated with a range of doses of RvE1 (in cell culture medium with FBS), before ALPI mRNA was quantified after six hours. The figure represents data from one experiment.



Appendix 46. The effect of the cytotoxicity of EPA on cells *in vitro* when made up in cell culture medium with and without 10% FBS.

HCA7 human CRC, MC38 mouse CRC cells and RAW264.7 mouse macrophage cells were exposed to a range of EPA (as defined above in the graphs) in cell medium with and without 10% FBS for three hours before fresh solution was then placed on the cells and left for a further 96 hours at an incubation temperature of 37°C, before the cell viability assay was performed. (A) HCA7 cells. (B) MC38 cells. (C) RAW264.7 cells. Data shown from three independent cell cultured experiments, shown as mean with standard error of the mean.